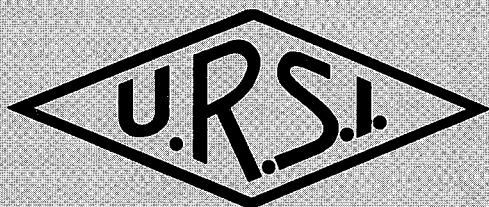


1985 NORTH AMERICAN  
RADIO SCIENCE MEETING

International Union of Radio Science



L'Union Radio-Scientifique Internationale

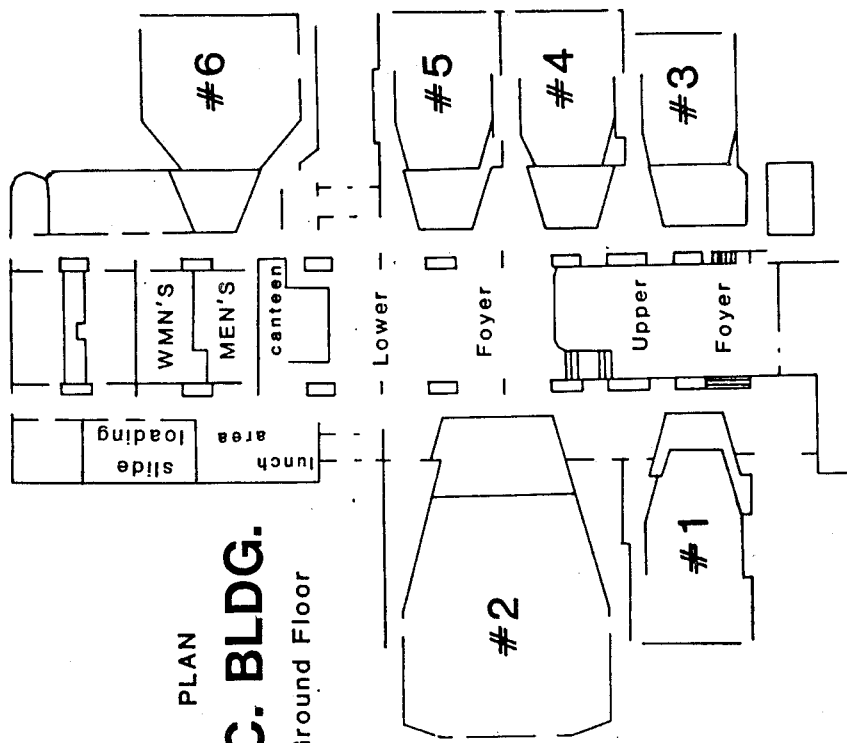
RÉUNION RADIO-SCIENTIFIQUE

NORD-AMÉRICAINNE 1985

June/juin 17-21, 1985

University of British Columbia  
Vancouver, Canada

PLAN  
**IRC. BLDG.**  
Ground Floor



National Academies of Science and Engineering  
National Research Council  
of the  
United States of America  
and/et

The National Research Council of Canada/  
Le conseil national de recherches du Canada

1985 NORTH AMERICAN  
RADIO SCIENCE MEETING

RÉUNION RADIO-SCIENTIFIQUE  
NORD-AMÉRICAINNE 1985

PROGRAM AND ABSTRACTS  
PROGRAMME ET RÉSUMÉS

Sponsored by/Parrainée par  
The United States National Committee for URSI  
and/et

The Canadian National Committee for URSI/  
Le comité national canadien de l'URSI

University of British Columbia  
Vancouver, Canada  
June/juin 17-21, 1985

# ORGANIZATION/ORGANISATION

## ORGANIZING COMMITTEE

K.S. McCormick, Chairman/Président  
A.T. Adams  
K. Charbonneau  
T.N.R. Coyne  
G.Y. Delisle  
L.H. Doherty

## COMITÉ DE DIRECTION

A. Ishimaru  
E.V. Jull  
S.J. Kubina  
A.R. Webster  
J.Y. Wong

## TECHNICAL PROGRAM

## PROGRAMME TECHNIQUE

### AP-S

S.J. Kubina, Chairman/Président  
N.G. Alexopoulos  
Y.M.M. Antar  
P. Bhartia  
Y.L. Chow  
J.A. Cummins  
G.Y. Delisle  
A. Hendry  
A. Hurd  
S. Mishra  
T.J.F. Pavlasek  
T. K. Sarkar  
A. Simons  
W. Ross Stone  
P. J. Wood

### URSI

T.N.R. Coyne, Chairman/Président  
Commission USNC/URSI CNC/URSI  
A N.S. Nahman J. Vanier  
B A. Ishimaru L. Shafai  
C J.W. Schwartz W.F. McGee  
E J.M. Morris T.N.R. Coyne  
F R.K. Moore A.R. Webster  
G K.C. Yeh R. Horita  
H K.J. Harker H.G. James  
J W.J. Welch J.L. Yen  
C.M. Butler

HF RADAR (Special Session/Séance spéciale)  
J.F.R. Gower and G.L. Holland

## LOCAL ARRANGEMENTS

## ORGANISATION LOCALE

E.V. Jull, Chairman/Président  
F.G. Berry  
E.J. Fraser  
H. Gruenberg  
M. Lopianowski  
N. Smith-Gander  
G. Valde  
M. Wlodyka

# WELCOME TO VANCOUVER

The 1985 North American Radio Science Meeting and International IEEE/AP-S Symposium are jointly sponsored by the United States and Canadian National Committees for the International Union of Radio Science (URSI) and the Institute of Electrical and Electronics Engineers Antennas and Propagation Society (IEEE/AP-S). All commissions of URSI have been invited to participate. The technical sessions will be held from Monday June 17 to Friday June 21, 1985 on the campus of the University of British Columbia, Vancouver, Canada.

For many years Canadian radio scientists and AP-S members have found a welcome forum for their work at the annual meetings of the USNC/URSI and IEEE/AP-S and on a few previous occasions they have been hosts. Joint US/Canadian URSI meetings were held in Ottawa in 1961 and 1967. IEEE/AP-S co-sponsored an URSI symposium on Electromagnetic Wave Theory in Toronto in 1959. Only once before has the annual joint meeting between USNC/URSI and IEEE/AP-S been held in Canada; at Laval University, Quebec, in 1980.

Canadian radio scientists and regional members of IEEE/AP-S take this opportunity to extend a warm welcome to their colleagues from the U.S. and abroad. We hope your visit to the Canadian west coast will be useful and enjoyable.

## BIENVENUE À VANCOUVER

La Réunion radio scientifique nord-américaine et le Symposium de la Société antennes et propagation de l'IEEE (1985) sont conjointement parrainés par les comités nationaux américain et canadien de l'Union radio scientifique internationale (URSI) et la Société antennes et propagation (AP-S) de l'Institute of Electrical and Electronics Engineers (IEEE). Toutes les commissions de l'URSI ont été invitées à participer. Les séances techniques se tiendront du lundi 17 juin au vendredi 21 juin 1985 sur le campus de l'Université de la Colombie-Britannique, à Vancouver (Canada).

Les scientifiques canadiens spécialistes de la radio et les membres de la société AP-S présentent depuis de nombreuses années leurs travaux à la réunion annuelle du Comité national américain de l'URSI et de la Société antennes et propagation de l'IEEE; ils ont déjà eu quelquefois l'occasion d'être les hôtes de la conférence. Les réunions mixtes des comités nationaux américain et canadien de l'URSI ont eu lieu à Ottawa en 1961 et 1967. La Société AP-S a co-parrainé un symposium de l'URSI sur la théorie des ondes électromagnétiques; ce dernier a été tenu à Toronto en 1959. La réunion annuelle mixte du Comité national américain de l'URSI et de la Société antennes et propagation de l'IEEE ne s'est tenue qu'une seule fois au Canada; elle avait été organisée en 1980 à l'Université Laval (Québec).

Les scientifiques canadiens spécialistes de la radio et les membres régionaux de la Société antennes et propagation de l'IEEE profitent de cette occasion pour souhaiter la bienvenue à leurs collègues des États-Unis et d'autres pays. Nous espérons que votre séjour sur la Côte Ouest du Canada sera à la fois utile et agréable.

# TABLE DES MATIÈRES

SESSION	Page
A -1	Métrologie des antennes ..... 1
A -2	Calculs du champ proche et du champ lointain ..... 11
A -3	Mesures du champ électromagnétique ..... 21
A -4	Métrologie dans le domaine temporel ..... 29
A -5	Effets biologiques des hyperfréquences ..... 39
AJ -1	Etalons de fréquence et du temps en radioastronomie ..... 47
B -1	Éléments d'antennes ..... 53
B -2	Techniques numériques I ..... 63
B -3	Propagation des ondes dans les milieux aléatoires ..... 75
B -4	Antennes microlignes I ..... 87
B -5	Convergence et minimisation des erreurs dans les méthodes numériques ..... 99
B -6	Les ondes près de l'interface ..... 105
B -7	Transitoires I ..... 117
B -8	Méthodes spectrales pour la propagation des ondes ..... 129
B -9	Diffusion ..... 135
B -10	Transitoires II ..... 147
B -11	Techniques numériques II ..... 159
B -12	Ondes guidées ..... 171
B -13	Antennes microlignes II ..... 183
B -14	Architecture d'ordinateurs aux fins de calculs efficaces en électromagnétique ..... 193
B -15	Champs électromagnétiques I ..... 199
B -16	Guides d'ondes ouverts ..... 211
B -17	Diffraction ..... 223
B -18	Réflecteurs et cornets ..... 235
B -19	Champs électromagnétiques II ..... 247
B -20	Théorie des antennes ..... 257
B -21	Diffusion inverse et multiple ..... 269
C -1	Réseaux de radio ..... 281
C -2	Traitement numérique des signaux ..... 289
C -3	Théorie et codage de l'information ..... 295
C -4	Communications à spectre dispersé ..... 301
C -5	Théorie de filtrage analogiques et numériques et leurs applications ..... 307
E -1	Mesure et modélisation des bruits radio-électriques ..... 315
E -2	Performance des récepteurs en présence de bruits radio-électriques ..... 325
F -1	Théorie de la diffusion ..... 335
F -2	Radio mobile et propagation urbaine ..... 347
F -3	Mesures météorologiques par micro-ondes ..... 355
F -4	Propagation en temps clair I ..... 365
F -5	Téledétection par radar I ..... 375
F -6	Propagation en temps clair II ..... 387
F -7	Téledétection par radar II ..... 395
F -8	Atténuation de la pluie ..... 405
G -1	Propagation HF ..... 415
G -2	Modélisation et dynamique de l'ionosphère ..... 427
G -3	Études ionosphériques au moyen des ondes radio-électriques ..... 437
G -4	Ionosphère aux latitudes élevées ..... 449
G -5	Propagation des ondes - simulation et expériences ..... 461
G -6	Diffusion-non cohérente ..... 471

# TABLE OF CONTENTS

SESSION	Page
A -1 Antenna Metrology .....	1
A -2 Near Field and Far Field Computations .....	11
A -3 EM Field Measurements .....	21
A -4 Time Domain Metrology .....	29
A -5 Health and Microwave Frequencies .....	39
AJ -1 Time and Frequency Standards for radio astronomy .....	47
B -1 Antenna Elements .....	53
B -2 Numerical Techniques I .....	63
B -3 Waves in Random Media .....	75
B -4 Microstrip Antennas I .....	87
B -5 Error Minimization and Convergence in Numerical Methods .....	99
B -6 Waves Near Interface .....	105
B -7 Transients I .....	117
B -8 Spectral Methods for Wave Propagation .....	129
B -9 Scattering .....	135
B -10 Transients II .....	147
B -11 Numerical Techniques II .....	159
B -12 Guided Waves .....	171
B -13 Microstrip Antennas II .....	183
B -14 Computer Architecture for Efficient Computation in Electromagnetics .....	193
B -15 Electromagnetic Fields I .....	199
B -16 Open Waveguides .....	211
B -17 Diffraction .....	223
B -18 Reflectors and Horns .....	235
B -19 Electromagnetic Fields II .....	247
B -20 Antenna Theory .....	257
B -21 Inverse and Multiple Scattering .....	269
C -1 Radio Networks .....	281
C -2 Digital Signal Processing .....	289
C -3 Information Theory and Coding .....	295
C -4 Spread Spectrum Communication .....	301
C -5 Analog and Digital Filtering Techniques and Applications .....	307
E -1 Radio Noise Measurements and Modeling .....	315
E -2 Receiver Performance in Radio Noise .....	325
F -1 Scattering Theory .....	335
F -2 Mobile Radio and Urban Propagation .....	347
F -3 Microwave Meteorological Measurements .....	355
F -4 Clear Air Propagation I .....	365
F -5 Radar Remote Sensing I .....	375
F -6 Clear Air Propagation II .....	387
F -7 Radar Remote Sensing II .....	395
F -8 Rain Attenuation .....	405
G -1 HF Propagation .....	415
G -2 Modeling and Dynamics of the Ionosphere .....	427
G -3 Ionospheric Studies Using Radio Waves .....	437
G -4 High Latitude Ionosphere .....	449
G -5 Wave Propagation - Simulation and Experiments .....	461
G -6 Incoherent Scatter .....	471

GH -1	Échauffement et modification de l'ionosphère au moyen des ondes radio-électriques I .....	481
GH -2	Programme Alouette-ISIS I .....	491
GH -3	Programme Alouette-ISIS II .....	499
GH -4	Échauffement et modification de l'ionosphère au moyen des ondes radio-électriques II .....	507
H -1	Expériences actives avec des véhicules spatiaux I .....	515
H -2	Expériences actives avec des véhicules spatiaux II .....	525
H -3	Effets des précipitations de particules induites par des ondes I .....	535
H -4a	Effets des précipitations de particules induites par des ondes II .....	543
H -4b	Sources d'ondes dans les plasmas spatiaux I .....	549
H -5	Sources d'ondes dans les plasmas spatiaux II .....	553
J -1	Interférométrie à très longue ligne de base .....	563
J -2	Sources primaires de radiotélescope .....	569
J -3	Radar et radioastronomie .....	575
SS -1	Vue d'ensemble des systèmes radar HF et des applications des ondes ionosphériques .....	583
SS -2	Radar HF et mesures océaniques: courants .....	593
SS -3	Radar HF et mesures océaniques: vagues et glace .....	605
AP-S/URSI	COMMISSION F	
	Propagation des ondes / systèmes mobiles .....	617

GH -1	Ionospheric Modification and Heating - I	481
GH -2	Alouette-ISIS Program I	491
GH -3	Alouette-ISIS Program II	499
GH -4	Ionospheric Modification and Heating II	507
H -1	Active Experiments Using Space Vehicles I	515
H -2	Active Experiments Using Space Vehicles II	525
H -3	Wave-Induced Particle Precipitation Effects I	535
H -4a	Wave-Induced Particle Precipitation Effects II	543
H -4b	Sources of Waves in Space Plasmas I	549
H -5	Sources of Waves in Space Plasmas II	553
J -1	Very Long Baseline Interferometry	563
J -2	Radiotelescope Feeds	569
J -3	Radar and Radio Astronomy	575
SS -1	Overview of HF Radar Systems and Skywave Applications	583
SS -2	HF Radar and Ocean Measurements: Currents	593
SS -3	HF Radar and Ocean Measurements: Waves and Ice	605
AP-S/URSI COMMISSION F		
	Wave Propagation/ Land Mobile	617

## SUMMARY OF TECHNICAL PROGRAM

ROOM	MONDAY, June 17		TUESDAY, June 18		WEDNESDAY, June 19		THURSDAY, June 20		FRIDAY, June 21
	AM	PM	AM	PM	AM	PM	AM	PM	AM
IRC-1	B-1 antenna Elements	APS-4 Array Analysis, Design and Synthesis	B-6 Waves Near Interface	B-9 Scattering		APS-13 Scattering and Diffraction I	APS-17 Scattering and Diffraction II	B-17 Diffraction	APS-23 Remote Sensing
IRC-2	APS-1 Phased Arrays I	APS-5 Reflector Antennas	APS-7 Phased Arrays II	APS-10 Dual Reflector Antennas	Plenary Session	APS-14 Phased Arrays III  APS-15 Satellite Antennas	APS-18 Lens/Horn Antennas	B-18 Reflectors and Horns	B-20 Antenna Theory
IRC-3	APS-2 Electro- magnetic Theory	APS/URSI Comm. F Wave Propa- gation/Land Mobile	B-7 Transients I	B-10 Transients II		B-12 Guided Waves	B-15 Electro- magnetic Fields I	APS-20 Polarizers and Frequency Selective Surfaces	B-21 Inverse and Multiple Scattering
IRC-4	B-2 Numerical Techniques I	APS-6 Antenna Theory	B-8 Sprectral Methods for Wave Propagation	APS-11 Sp. Session in honor of Prof. C.T. Tai		B-14 Computer Architecture for Efficient Computation in Electromagnetics	B-16 Open Waveguides	B-19 Electro- magnetic Fields II	APS-24 Special Topics
IRC-5	APS-3 Printed and Microcircuit Antennas	B-5 Error Minimi- zation and Convergence in Numerical Methods	APS-8 Numerical Techniques	B-11 Numerical Techniques II		APS-16 Measurement Techniques I	APS-19 Aircraft, Spacecraft and Vehicle Antennas	APS-21 Measurement Techniques II	AMTA Workshop 8:30 am.- 3:00 p.m.
IRC-6	B-3 Waves in Random Media	B-4 Microstrip Antennas I	APS-9 Feeds	APS-12 Microstrip Antennas		B-13 Microstrip Antennas II		APS-22 Microstrip Arrays	APS-25 Conformal/ Adaptive Antennas

ROOM	MONDAY, June 17		TUESDAY, June 18		WEDNESDAY, June 19		THURSDAY, June 20		FRIDAY, June 21
	AM	PM	AM	PM	AM	PM	AM	PM	AM
LAW-101	F-1 Scattering Theory		F-3 Microwave Meteorological Measurements	F-4 Clear Air Propagation I		F-5 Radar Remote Sensing I	F-6 Clear Air Propagation II	F-7 Radar Remote Sensing II	F-8 Rain Attenuation
LAW-102	F-2 Mobile Radio and Urban Propagation		SS-1 Overview of HF Radar Systems & Skywave App.	SS-2 HF Radar and Ocean Meas.: Currents			SS-3 HF Radar and Ocean Meas.: Waves & Ice	SS-4 HF Radar: Panel Discussion	
LAW 201	G-1 HF Propagation		G-3 Ionospheric Studies Using Radio Waves	G-4 High Latitude Ionosphere		GH-1 Ionospheric Modification and Heating I	G-5 Wave Propagation — Simulation and Experiments	G-6 Incoherent Scatter	GH-4 Ionospheric Modification and Heating II
LAW-157		G-2 Modeling and Dynamics of the Ionosphere		J-1 Very Long Baseline Interferometry			J-2 Radiotelescope Feeds	J-3 Radar and Radio Astronomy	
LAW-169	H-1 Active Experiments Using Space Vehicles I	H-2 Active Experiments Using Space Vehicles II	H-3 Wave-Induced Particle, Precipitation Effects I	H-4(a) Wave-Induced Particle ... II H-4(b) Sources of Waves I		H-5 Sources of Waves II	GH-2 Alouette- ISIS Program I	GH-3 Alouette- ISIS Program II	
LAW-177			AJ-1 Time and Frequency Standards for Radio Astronomy	A-1 Antenna Metrology		A-2 Near Field and Far Field Computations	A-3 EM Field Measurements	A-4 Time Domain Metrology	A-5 Health and Microwave Frequencies
LAW-178		C-1 Radio Networks	E-1 Radio Noise Measurements and Modeling	E-2 Receiver Performance in Radio Noise		C-2 Digital Signal Processing	C-3 Information Theory and Coding	C-4 Spread Spectrum Communications	C-5 Analog Digital Filtering Techniques and Applications

# SOMMAIRE DU PROGRAMME TECHNIQUE

Salle	Le lundi 17 juin		Le mardi 18 juin		Le mercredi 19 juin		Le jeudi 20 juin		Le vendredi 21 juin	
	matinée	après midi	matinée	après midi	matinée	après midi	matinée	après midi	matinée	
IRC-1	B-1 Eléments d'antennes	APS-4 Analyse, conception et synthèse des antennes réseaux	B-6 Les ondes près de l'interface	B-9 Diffusion		APS-13 Diffusion et diffraction I	APS-17 Diffusion et diffraction II	B-17 Diffraction	APS-23 Télé-détection	
IRC-2	APS-1 Antennes réseaux à commande de phase I	APS-5 Antennes à réflecteur	APS-7 Antennes réseaux à commande de phase II	APS-10 Antennes à réflecteur double	Séance plénière	APS-14 Antennes réseaux à commande de phase III	APS-18 Antennes réseaux à cornets et à lentille	B-18 Réflecteurs et cornets	B-20 Théorie des antennes	
						APS-15 Antennes de satellites				
IRC-3	APS-2 Théorie électromagnétique	APS/URSI Comm. F. Propagation des ondes/systèmes mobiles	B-7 Transitoires I	B-10 Transitoires II		B-12 Ondes guidées	B-15 Champs électromagnétiques I	APS-20 Polariseurs et surfaces de sélectivité en fréquences	B-21 Diffusion inverse et multiple	
IRC-4	B-2 Techniques numériques I	APS-6 Théorie des antennes	B-8 Méthodes spectrales pour la propagation des ondes	APS-11 Session spéciale en l'honneur du prof. C.T. Tai		B-14 Architecture d'ordinateurs aux fins de calculs efficaces en électromagnétique	B-16 Guides d'ondes ouverts	B-19 Champs électromagnétiques II	APS-24 Sujets spéciaux	
IRC-5	APS-3 Antennes imprimées et antennes micro-circuits	B-5 Convergence et minimisation des erreurs dans les méthodes numériques	APS-8 Techniques numériques	B-11 Techniques numériques II		APS-16 Techniques de mesures I	APS-19 Antennes d'aéronefs et d'engins spatiaux et de véhicules	APS-21 Techniques de mesure II	Atelier de l'AMTA 8h30 à 15h	
IRC-6	B-3 Propagation des ondes dans les milieux aléatoires	B-4 Antennes microlignes I	APS-9 Sources primaires	APS-12 Antennes microlignes		B-13 Antennes microlignes II		APS-22 Antennes à réseaux microlignes	APS-25 Antennes conformes/ auto-adaptables	

Salle	Le mardi 17 juin		Le mercredi 18 juin		Le jeudi 19 juin		Le vendredi 20 juin		Le samedi 21 juin	
	matinée	après midi	matinée	après midi	matinée	après midi	matinée	après midi	matinée	après midi
LAW-101	F-1 Théorie de la diffusion		F-3 Mesures météorologiques par micro-ondes	F-4 Propagation en temps clair I		F-5 Télé-détection par radar I	F-6 Propagation en temps clair II	F-7 Télé-détection par radar II	F-8 Atténuation de la pluie	
LAW-102	F-2 Radio mobile et propagation urbaine		SS-1 Vue d'ensemble des systèmes radar HF et les appl. des ondes ionosphériques	SS-2 Radar HF et mesures océaniques: courants			SS-3 Radar HF et mesures océaniques: vagues et glace	SS-4 Radar HF: Table ronde		
LAW-201	G-1 Propagation HF		G-3 Études ionosphériques au moyen des ondes radio-électriques	G-4 Ionosphère aux latitudes élevées		GH-1 Échauffement et modification de l'ionosphère au moyen de ondes radio-électriques I	G-5 Propagation des ondes - simulation et expériences	G-6 Diffusion non-cohérente	GH-4 Échauffement et modification de l'ionosphère au moyen des ondes radio-électriques II	
LAW-157		G-2 Modélisation et dynamique de l'ionosphère		J-1 Interférométrie à très longue ligne de base			J-2 Sources primaires de radio-télescope	J-3 Radar et radio astronomie		
LAW-169	H-1 Expériences actives avec des véhicules spatiaux I	H-2 Expériences actives avec des véhicules spatiaux II	H-3 Effets des précipitations de particules induites par des ondes I	H-4(a) Effets des précipitations ... II H-4(b) Sources d'ondes I		H-5 Sources d'ondes II	GH-2 Programme Alouette-ISIS I	GH-3 Programme Alouette-ISIS II		
LAW-177			AJ-1 Étalons de fréquence et du temps en radio-astronomie	A-1 Métrologie des antennes		A-2 Calculs du champ proche et du champ lointain	A-3 Mesures du champ électromagnétique	A-4 Métrologie dans le domaine temporel	A-5 Effets biologiques des hyperfréquences	
LAW-178		C-1 Réseaux de radio	E-1 Mesure et modélisation des bruits radio-	E-2 Performance des récepteurs en présence de bruits radio-		C-2 Traitement numérique des signaux	C-3 Théorie et codage de l'information	C-4 Communications à spectre dispersé	C-5 Théorie de filtrage analogiques et	



## URSI COMMISSION A - SESSION A1

**Antenna Metrology**1:30 - 5:00  
LAW 177**Métrieologie des antennes**Chairperson/Président: **D.W. Hees**, Scientific-Atlanta, Atlanta, GA, USA

- 1 SPHERICAL NEAR-FIELD MEASUREMENTS FROM A "COMPACT-RANGE" VIEWPOINT. **A.C. Ludwig**, General Research Corporation, Santa Barbara, CA, USA; **F. Holm Larsen**, Technical University of Denmark, Electromagnetics Institute, Lyngby, Denmark
- 2 MEASUREMENT OF THE SCATTERED FIELD FROM A SATELLITE STRUCTURE. **J. Hau Lemanczyk**, **F. Holm Larsen**, Technical University of Denmark, Electromagnetics Institute, Lyngby, Denmark
- 3 EVALUATION OF SPHERICAL NEAR-FIELD MEASUREMENTS. **F. Jensen**, TICRA A/S, Copenhagen, Denmark
- 4 COMPARISON BETWEEN MEASUREMENTS AND SIMULATIONS OF INACCURACIES IN SPHERICAL NEAR-FIELD MEASUREMENTS. **A. Frandsen**, TICRA A/S, Copenhagen, Denmark
- 5 INNOVATIONS AND EXPANDED CAPABILITIES IN ANTENNA MEASUREMENTS FROM SPHERICAL NEAR-FIELD SCANNING. **D.W. Hess**, **J.R. Jones**, **C. Green**, **B. Melson**, Scientific-Atlanta, Atlanta, GA, USA
- 6 SPHERICAL NEAR FIELD MEASUREMENTS AND TEST FACILITIES IN EUROPE. **P.J. Wood**, Canadian Astronautics Limited, Ottawa, ON
- 7 THE DEVELOPMENT OF PROBE CORRECTION IN SPHERICAL NEAR-FIELD MEASUREMENTS. **F. Holm Larsen**, Technical University of Denmark, Electromagnetics Institute, Lyngby, Denmark
- 8 SYMMETRY AND NEAR FIELD SCANNING. **P.F. Wacker**, Torrance, CA, USA
- 9 K-CORRECTION. AN EFFICIENT METHOD TO COMPENSATE FOR PROBE POSITIONING ERRORS IN AN ANTENNA NEAR FIELD TEST FACILITY. **P.K. Agrawal**, RCA Corporation, Government Systems Division, Moorestown, NJ, USA

## A-1-1

### SPHERICAL NEAR-FIELD MEASUREMENTS FROM A "COMPACT-RANGE" VIEWPOINT

A.C. Ludwig, General Research Corporation  
F. Holm Larsen, Technical University of Denmark

For a conventional near-field measurement, the field is sampled on a sphere surrounding the antenna under test. The far-field pattern can then be found by a spherical wave near-field to far-field transformation. An alternative to this approach has been suggested at University of Sheffield [Bennett and Schoessow, Proc. IEE, 1978] where a plane wave is synthesized in a region around the antenna by numerically combining the fields from an array of probes distributed over the spherical measurement surface. Although the implementation is quite different, the concept is basically the same as a compact range.

It is not the intent of this paper to suggest that a full spherical array should be used to test antennas. However, analyzing spherical near-field probing from this viewpoint provides useful results. For the conventional analysis of the accuracy of spherical near-field probing, it is necessary to select a specific antenna to be tested; near-field data for the antenna are then generated analytically, processed using a spherical wave transformation to the far field, and the results compared with far-field data generated analytically for the same antenna [Jensen 1970, 1978]. This conventional method has the advantage that very specific results are obtained in regard to the errors in gain, beam-width, etc., but the disadvantage that the results apply only to the particular antenna being modeled. The viewpoint adopted in this paper, in which the quality of the plane wave is evaluated, has the advantage of applying to any antenna under test, but the disadvantage that the results are not easily translated into specific errors in gain, etc. Therefore, the two methods are in fact quite complementary. Another complementary feature is that creating a plane wave with weights produced by a processing technique for spherical near-field probing is a very convincing check that the processing is numerically valid.

Weights were computed, including probe compensation, using an algorithm described elsewhere [Larsen, 1979]. The probes were on a 67 wavelength radius sphere at  $6^\circ$  increments in  $\theta$  and  $\psi$ . This is appropriate for measuring a 4.8 wavelength radius antenna. The conjugates of the weights for computing the field in the z direction were used as element excitations for a spherical array, and the exact fields calculated inside the sphere. Deviations in amplitude and phase from a perfect plane wave were then evaluated, for all polarizations of the E and H field. As an example, the phase error in one plane is less than  $0.1^\circ$  within a 4-wavelength radius, and the amplitude error less than 0.001 dB.

MEASUREMENT OF THE SCATTERED FIELD  
FROM A SATELLITE STRUCTURE

J. Hau Lemanczyk and F. Holm Larsen  
Electromagnetics Institute, Technical University of Denmark

One of the recent major measurement projects carried out at the TUD-ESA spherical near field test facility (ref. J. Hansen, European Space Agency publication BR-19, April 1984) has been on the telemetry and telecommand (TM/TC) antenna on the German Communication Satellite DFS. The antenna was to be measured on the satellite structure complete with solar panels. However, due to its size, measurements were carried out on a scaled model (1:2.5) which measured over six meters in total length. At a measurement frequency of 5.534 GHz, this dimension is almost 115 wavelengths. This necessitated a measurement density on the spherical surface of  $0.5^\circ$  in both theta and phi equalling 260281 sample points, each consisting of two orthogonal field components in amplitude and phase. A description of the antenna and results of the measurements have been presented recently (ref. Fasold et al., ICAP 85, Warwick, England).

The construction of the model was such that the boom on which the TM/TC antenna was mounted also served as the main bearing structure for the model. Thus the satellite body and panels could be removed. The location of the antenna in the spherical coordinate system could thus be precisely maintained. Measurements were carried out with and without the presence of the satellite body and solar panels. The availability of amplitude and phase over the entire sphere for these measurements meant that the fields from the cases with the satellite body and solar panels present and not present could be subtracted. The difference field is the scattered field of the satellite and solar panels.

## A-1-3

### EVALUATION OF SPHERICAL NEAR-FIELD MEASUREMENTS

Frank Jensen  
TICRA A/S, DK-1114 Copenhagen, Denmark

During the last decade the requirements to antenna testing have increased concurrently with the demands for antenna performance. From early stages measuring simple spot beam antennas, the antenna testing today comprises measurements of complex systems as antenna farms on modern communications satellites. For such systems not only the usual beam parameters shall be measured but also parameters for electromagnetic compatibility between different antennas and different beams must be determined with high accuracy.

The mathematical background for determining antenna far-field parameters on the basis of near-field measurements is now well established, and reliable and fast software codes have been applied for this purpose throughout several years. New near-field test ranges have therefore been built on this basis, and several are believed to be constructed within the next years.

For the design of a test range it is important to know the tolerances, mechanical as well as electrical, which are required for the various parts of the set-up. Such tolerances may conveniently be determined by computer simulations of the complete test set-up.

The paper describes design procedures for near-field test ranges, with special emphasis on the spherical technique. The performances are evaluated by the software package FACSIM/SNIFTD. Different mechanical solutions are discussed

- elevation over azimuth rotation in antenna tower
- probe guidance with gantry arm(s)/robotic arm
- modulated dipole array scattering,

and various ways of scanning are considered:

- full sphere/truncated measurement surface,
- polar grid/equatorial grid.

Qualitative as well as quantitative considerations are presented.

COMPARISON BETWEEN  
MEASUREMENTS AND SIMULATIONS OF INACCURACIES  
IN SPHERICAL NEAR-FIELD MEASUREMENTS

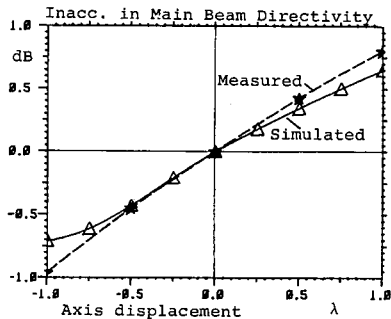
A. Frandsen  
TICRA A/S, DK-1114 Copenhagen, Denmark

**Abstract.** Since its inception in the mid seventies, the spherical near-field antenna test facility at Electromagnetics Institute, Technical University of Denmark (TUD), has gone through several refinements and improvements, so that the facility has now reached a mature stage of an automated near-field range for accurate testing of spacecraft antennas.

As a part of this development TICRA has undertaken to develop a computer program, FACSIM, for simulation of mechanical and electrical inaccuracies in spherical near field set-ups. The need for numerical simulations and error analysis was recognized at an early stage, since it would facilitate the identification of critical items in a measurement set-up. As for the facility itself, the development of FACSIM has undergone several improvements, and it appears now as a highly flexible program for simulating errors in spherical near-field test facilities. Extensive simulations have previously been carried out to evaluate the TUD-facility. In the present paper the results of simulations are verified by comparisons to measurements. Since it is imperative for a sound comparison that the error sources are easily identified and - preferably - dominating over other, less controllable errors, it was decided to introduce large mechanical errors in the measurements, so that the effects of these would prevail.

Two series of measurements were carried out by TUD, one with an initial offset error in the definition of  $\theta=0$ , and one with a displacement of the horizontal axis away from the vertical axis. The test antenna was the OTS Spotbeam reflector antenna, a  $30\lambda$ -diameter rotationally symmetric paraboloid with 4 struts carrying the feed. It was mounted with its nominal boresight towards the probe for  $\theta=0$ , and the antenna was scanned in  $\phi$  and stepped in  $\theta$ . The frequency was 11.7 GHz, and the measurement distance was  $64.2\lambda$ ,  $\sim 3.6\%$  of the Rayleigh distance. Accurate reference fields were also obtained. A Potter horn with known probe-coefficients were used to measure the near fields and probe correction was applied in the transformation to far fields.

For the same range of errors, simulations were carried out for an idealized model of the OTS antenna, where the effects of blockage were neglected. The results of comparisons for typical pattern parameters will be presented, showing in general good agreement between measurements and simulations, thus validating the usefulness of error analysis by computer simulations. An example is shown in the figure to the right.



The present work was carried out for Electromagnetics Institute under ESA Contract No. 4682/81/NL/MS.

## A-1-5

### INNOVATIONS AND EXPANDED CAPABILITIES IN ANTENNA MEASUREMENTS FROM SPHERICAL NEAR-FIELD SCANNING

Doren W. Hess, John R. Jones, Curtis Green, Bruce Melson  
Scientific-Atlanta, P.O. Box 105027, Atlanta, GA 30348

Over the past twenty years research and development efforts have led to implementation of spherical near-field antenna measurement ranges. These facilities provide the capability to determine the far-field radiation pattern and gain of microwave antennas from near-field measurements. The essential features that the control systems and computer systems possess are: automatic data acquisition, near-field to far-field computation, and automatic data display. The early development efforts were focussed on these items.

Recently, more sophisticated features have been shown to be useful and have been added to modern systems. The additional items include: automatic gain comparison measurement, probe antenna polarization correction, probe antenna pattern correction, automatic thermal drift correction, and output format selection. These features significantly enhance the accuracy and versatility of near-field antenna measurements.

More importantly however, as by products of the development of spherical near-field scanning, certain additional capabilities have been brought into the realm of conventional antenna measurement technology. These features were previously utilized only in research laboratories as specialized procedures. They are now available as industrial technology. They are: three antenna polarization measurement, two antenna polarization transfer, spherical wave modal analysis, and near-field to near-field radial transforms.

In this paper we describe these innovations and present measurement results which illustrate their use.

**SPHERICAL NEAR FIELD MEASUREMENTS AND  
TEST FACILITIES IN EUROPE**

Peter J. Wood  
Canadian Astronautics Limited  
Ottawa, Canada

In comparison to the well established "far field test range" method of antenna testing, near field measurements offer improved accuracy of characterisation, freedom from Rayleigh range restrictions on antenna size, and the possibility of indoor testing of quite large antennas. They can also obviate the need for rotation of a fragile spacecraft antenna.

In the spherical near field system, a conventional antenna positioner may be used. With the present trend of antenna measurement instrumentation to full digital automation for "conventional" measurements, the cost of a near field facility need not greatly exceed that of its "conventional" counterpart. The near field facility can actually be used in "conventional" mode when required simply by disabling the processing algorithm. In relation to a planar probing near field system, the spherical version is useful and accurate over a wider range of test antennas, and can be operated with a smaller number of field samples, reducing the measurement time needed for a test.

A spherical near field facility uses a NFFF (near field/far field transformation) using vector spherical waves. Matrix algorithms were developed by Wacker (NBS), and Larsen (TUD), giving a rigorous correction for the measurement probe characteristic. The orthogonality formulation developed by Wood at MRC (Marconi Research Centre, UK) permits a wide range of test geometries in that the test antenna does not need to lie over the centre of rotation to realize full measurement accuracy. It is particularly well suited to the measurement of shaped beam reflector antennas.

Spherical near field facilities have been constructed at MRC in the UK and the Technical University of Denmark. The MRC facility (Marconi Review 204 and 205) has been used extensively for spacecraft antenna measurements. It has an absolute accuracy of 0.07 dB, as has been verified by independent far field (MRC) and cylindrical probing (British Aerospace Dynamics Group) measurements.

## A-1-7

### THE DEVELOPMENT OF PROBE CORRECTION IN SPHERICAL NEAR-FIELD MEASUREMENTS

Flemming Holm Larsen  
Electromagnetics Institute  
Technical University of Denmark  
DK-2800 Lyngby, Denmark

During the last fifteen years spherical near-field measurements have been developed into a highly accurate method of antenna far-field determination. Although good accuracy in many cases can be obtained by assuming the probe antenna to measure the near field at a single point, use of a directive probe and correction for the probe receiving pattern offers the possibility of increased accuracy. The reason for this is that a directive probe suppresses reflections from the surroundings, gives a larger signal, and has polarization characteristics which are more independent of the structure behind the probe than a low-gain probe.

The theoretical foundation for probe correction in spherical near-field measurements was given in the Ph.D. thesis by Jensen, 1970. In the equations with probe correction, the signal received by the probe is described in terms of rotation coefficients for spherical waves rather than the spherical vector waves used to describe the E and H field. Wacker [NBS IR 75-809, 1975] pointed out that the use of orthogonality integrals is greatly facilitated by restricting the probe to have spherical waves with  $m = \pm 1$  only. In addition, he showed that the integrals can be calculated efficiently from the Fourier transform of the measured data not only in  $\phi$  but also in  $\theta$ . The first spherical measurements with probe correction were described in [Larsen, Electronics Letters, 1977]. [Larsen and Hansen, IEEE AP-S, 1979] demonstrated that by restricting the  $m = \pm 1$  probe further to have rotational symmetry, it is possible to correct for different axial ratios of the two ports of a dual-polarized probe. From the beginning it has been clear that measurements without probe correction, i.e. with a small dipole as probe, is a special case of the formulation involving the rotation coefficients. However, it has recently been demonstrated that measurements with the rotationally symmetric probes also can be described in terms of the spherical vector modes themselves [Yaghjian, IEEE AP-S, 1984].

In measurements of reflector antennas, the probe correction compensates for a taper of the probe pattern over the test antenna aperture. In addition it can correct for cross polarization of the probe, which can be important in measurements of frequency reuse satellite antennas.

Since the probe correction amplifies the field coming from the edge of the test antenna aperture, one could ask whether unwanted reflections from the surroundings are amplified as well. This question has been addressed in the paper [P.C. Hansen and Larsen, T-AP, Feb. 1984]. It is shown here that when the probe taper over the test zone is not too strong and provided the spherical wave spectrum for the test antenna is truncated properly, then unwanted amplification does not take place. Therefore the suppression of reflected signals by the probe in the near field is maintained in the calculated far field.

## SYMMETRY AND NEAR FIELD SCANNING

Paul F. Wacker  
 4421 Pacific Coast Highway E107  
 Torrance, CA 90505

Symmetries of Maxwell's equations and of the propagation medium, with the theory of group representations, provide essentially all the tools needed for practical near field scanning analysis. These include a) the exact solutions (modes) for Cartesian, circular cylindrical, and spherical coordinates, b) natural orthogonalities between the modes on the measurement surfaces, c) natural orthogonalities with respect to summation and so the measurement lattices, d) near to far field transformations, e) transformations of the modal expansions under change of coordinate values and f) natural orthogonalities between the transformation coefficients on the measurement lattices. (Correction for the patterns of the probes requires e) and f).) The mode sets provided are mathematically complete with respect to the solutions and the procedures are approximation free except for truncation of the infinite sets of modes and, for planar and circular cylindrical scanning, truncation of the measurement surfaces.

The preceding is based upon the fact that an infinite number of symmetry operations yields an infinite number of symmetry types (each like even or odd) and, for each type, an infinite number of defining constraints (each like  $f(-x) = -f(+x)$  for an odd function). The constraints yield the transformations of e). Given a large enough symmetry group, the pertinent functions and modes are completely defined. Thus: The rotations  $C_\infty$  about an axis define the functions  $\exp(im\phi)$  and lead to Fourier series analysis. The translations  $T_1$  along the real line yield the functions  $\exp(-i\omega t)$  and  $\exp(ik_x x)$  and Fourier transform theory. The addition of reflections in planes containing the axis or in planes perpendicular to the line yields the corresponding sines and cosines. The three dimensional rotation group  $O_3$  yields  $P_n^m(\cos \theta)$   $\exp(im\phi)$  and the theory of spherical harmonics. The two dimensional Euclidean (translation-rotation) group  $E_2$  yields  $J_m(k_R R)$   $\exp(im\phi)$  and the analogous expressions with cylindrical Neumann and Hankel functions. The three dimensional Euclidean group  $E_3$  yields  $P_n^m(\cos \theta)$   $\exp(im\phi)$   $j_n(k_R r)$  and the analogous expressions with spherical Neumann and Hankel functions. With few exceptions, there are three linearly independent three-vector functions for each of the preceding symmetry types. However, addition of gauge invariance reduces the number of independent polarizations to two in the EM cases and the addition of inversion separates the TM and TE modes into different symmetry types and defines them. The group  $C_M$  of rotations by  $2\pi m/M$  ( $m=0$  to  $M-1$ ) separates the terms of a Fourier series into  $M$  types with an infinite number in each type, providing the FFT as an approximation-free symmetry decomposition.

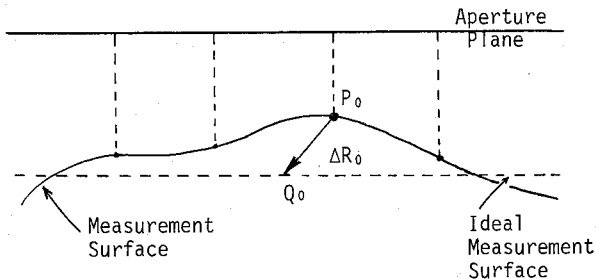
## A-1-9

### K-CORRECTION, AN EFFICIENT METHOD TO COMPENSATE FOR PROBE POSITIONING ERRORS IN AN ANTENNA NEAR FIELD TEST FACILITY

Pradeep K. Agrawal  
RCA Corporation  
Government Systems Division  
Missile and Surface Radar  
Moorestown, New Jersey 08057

In an antenna near field test facility, the electric field is measured at points in a plane which is in front of and is parallel to the antenna aperture. The measured near field data are Fourier transformed to compute the far field spectrum. The Fourier transformation is performed generally through a Fast Fourier Transformer (FFT) scheme. For FFT algorithms to be applicable, the data to be transformed should be known at points on a perfectly planar rectangular lattice. However, no mechanical and/or optical scheme can guarantee that the electric field measurements are made at points that are precisely along a planar rectangular lattice. As a result, a method is needed to compute a modified value of the electric field corresponding to each measurement such that the modified electric field value is a close equivalent of the electric field at ideal measurement point.

Let  $P_0$  be a point of measurement on the non-planar surface, and  $Q_0$  be the corresponding point on the planar rectangular lattice such that  $\Delta R_0$  is a position error vector. Also, let  $\hat{k}$  represent a unit vector in the direction of the main beam. The approximate value of electric field at  $Q_0$  is then the measured electric field value at  $P_0$  with a phase correction equivalent to  $\Delta R_0 \cdot \hat{k}$ . The results will be presented showing the application of k-correction.



## URSI COMMISSION A - SESSION A2

<b>Near Field and</b>	1:30 - 5:00	<b>Calculs du champ</b>
<b>Far Field Computations</b>	LAW 177	<b>proche et du champ lointain</b>

Chairperson/Président: **G.Y. Delisle**, Université de Laval, Québec, PQ

- 1 EVALUATION OF TRANSLATED PROBE COEFFICIENTS IN SPHERICAL NEAR-FIELD SCANNING. **R.C. Wittmann**, National Bureau of Standards, Antenna Systems Metrology, Boulder, CO, USA
- 2 A SIMPLIFIED APPROACH TO PLANE-POLAR SCANNING. **R.L. Lewis**, National Bureau of Standards, Electromagnetic Fields Division, Boulder, CO, USA
- 3 IMPROVED ALGORITHMS FOR SPHERICAL AND HEMISPHERICAL SCANNING. **R.L. Lewis, R.C. Wittmann**, National Bureau of Standards, Electromagnetic Fields Division, Boulder, CO, USA
- 4 AN EFFICIENT AND ACCURATE METHOD FOR CALCULATING AND REPRESENTING POWER DENSITY IN THE NEAR-ZONE OF MICROWAVE ANTENNAS. **A.C. Newell, R.L. Lewis**, National Bureau of Standards, Electromagnetic Fields Division, Boulder, CO, USA
- 5 GAIN OPTIMIZATION OF A NEAR-FIELD FOCUSING ARRAY. **J. Loane, S.W. Lee**, University of Illinois, Electromagnetics Laboratory, Urbana, IL, USA
- 6 PLANAR NEAR-FIELD ANALYSIS OF FREQUENCY RE-USE CONTOURED MULTI-BEAM REFLECTOR ANTENNAS FOR COMMUNICATIONS SATELLITES. **W. Bornemann**, INTELSAT, Washington, DC, **R. Jørgensen, P. Balling**, TICRA, Copenhagen, Denmark
- 7 INFLUENCE OF SOURCE ANTENNA DIRECTIVITY ON THE REFLECTIVITY LEVEL OF MICROWAVE ANECHOIC CHAMBERS. **M.C. Chandra Mouly, N.V. Vani, N.R. Devi, K. Sujata**, VRS Engineering College, Electronics and Communication Engineering Dept., Vijayawada, India
- 8 THE RECEIVING ANTENNA AS A LINEAR DIFFERENTIAL OPERATOR. **A.D. Yaghjian**, Rome Air Development Center, Electromagnetic Sciences Division, Hanscom Air Force Base, MA, USA; **R.C. Wittmann**, National Bureau of Standards, Electromagnetic Fields Division, Boulder, CO, USA
- 9 EFFECTS OF RMS SURFACE DEVIATIONS ON REFLECTOR ANTENNA RADIOMETRIC PERFORMANCE. **L.P. Anderson Jr., T.-K. Wu**, Hughes Aircraft Company, Space and Communications Group, Los Angeles, CA, USA

EVALUATION OF TRANSLATED PROBE COEFFICIENTS IN  
SPHERICAL NEAR-FIELD SCANNING

Ronald C. Wittmann 723.05  
Antenna Systems Metrology  
National Bureau of Standards  
Boulder, Colorado 80303

In spherical near-field scanning the nature of the probe is taken into account by specification of appropriate translated probe coefficients. These coefficients, which depend on the scan radius, are basically the response of the probe in some reference orientation to each elementary multipole excitation in a complete set of basis functions.

The formulas that relate the translated probe coefficients to the receiving function of the probe (or to the far-field if the probe is reciprocal) are usually derived from complicated translation formulas for vector spherical harmonics. In this paper we show how these expressions may also be derived in terms of mode-mode coupling integrals. In addition to avoiding use of the cumbersome translation formulas, this method is largely founded on the familiar plane-wave coupling formalism.

## A SIMPLIFIED APPROACH TO PLANE-POLAR SCANNING

Richard L. Lewis  
Electromagnetic Fields Division  
National Bureau of Standards  
Boulder, Colorado

Planar near-field scanning is an established procedure for obtaining measured far-field antenna patterns. For this, one needs a large, two dimensional, precision probe-transport mechanism for making measurements. By contrast, plane-polar scanning merely requires a linear probe-transport mechanism for making measurements along a radial line while the antenna under test rotates in azimuth (the probe also rotates in synchronism with the test antenna to preserve field alignment). In many cases, one may take advantage of azimuthal symmetry of the measured radiation to greatly reduce the necessary number of azimuth-angle steps. Thus, plane-polar scanning can have significant advantages over plane cartesian scanning in terms of simpler probe transport and reduced data requirements.

In this paper we present a new formulation for plane-polar scanning. In this approach, we expand the received signal as a double series which is readily shown to be mathematically complete. In this representation, the azimuthally symmetric portion is expanded as a series of terms of the form  $(1 - \rho^2)^n$ , where  $\rho$  is normalized radial distance in the measurement plane and  $n$  is the summation index. Such a representation approximates typical excitations for many actual dish antennas. Also, aperture blockage effects can be simulated. Accordingly, determination of the symmetric portion of the measurement plane field may provide useful design feedback, while good aperture-excitation modeling may reduce the number of terms needed for accurate representation.

Our measurement plane representation for the received signal is readily integrated analytically term by term to obtain the spectral coupling product which can then be corrected for probe effects to determine the radiated far-field. The result is simpler (with a simpler derivation) than the Jacobi-Bessel series plane-polar formulation [Rahmat-Samii et al., IEEE/AP Tran., 28, pp. 216-230, March 1980]. Moreover, when the polar angle  $\theta$  is large our formulation appears to converge more rapidly. Accordingly, ease of numerical computation is expected.

## A-2-3

### IMPROVED ALGORITHMS FOR SPHERICAL AND HEMISPHERICAL SCANNING

Richard L. Lewis and Ronald C. Wittmann  
Electromagnetic Fields Division  
National Bureau of Standards  
Boulder, Colorado

A probe corrected spherical-scanning algorithm has been developed which is applicable when the antenna under test radiates negligibly into its rear hemisphere. Compared to an efficient version of the best previously published full-sphere scanning algorithm, it is found that our hemispherical scanning algorithm is over three and a half times more efficient. Improvements have also been made to full-sphere scanning, with the result that our new spherical scanning algorithm is twice as efficient as the best previous full-sphere algorithm. We also show that our new formulations constitute an exact inversion of the band-limited spherical-coordinate expression for the received signal (i.e., no aliasing errors are introduced).

An Efficient and Accurate Method For Calculating and Representing  
Power Density in the Near-Zone of Microwave Antennas

Allen C. Newell and R. L. Lewis  
National Bureau of Standards  
Boulder, Colorado

There are a number of situations related to safety and interference where it is desirable to have a reliable and concise method of estimating the power density levels radiated by microwave antennas. A new technique for predicting near-zone field intensities has recently been developed at NBS using Plane Wave Scattering Matrix Theory to produce accurate calculations along with a highly efficient method of graphically representing the results. Using this technique, comparisons of predicted and measured near fields were carried out for selected antennas and found to be in excellent agreement.

The input to the calculations is the aperture illumination of the antenna obtained from either measured near-field data, design specifications or theoretical assumptions. From this input, programs based on the plane wave theory were developed to calculate the field on a series of x-y planes parallel to the aperture. Then the power-density values in the x-z and y-z planes are obtained and graphically represented on two contour plots. The ordinate of these graphs covers the range  $\pm 4D$  in units of  $D$  and the abscissa extends from just in front of the antenna out to  $D^2/\lambda$  in units of  $D^2/\lambda$ . This choice of scaling means that a single graph will apply without approximation to all antennas with the same  $D/\lambda$  ratio and relative aperture distribution. Different input power levels can be accounted for by scaling. When small structure effects such as those caused by struts and aperture blockage are ignored, it was further found for  $D/\lambda > 30$  that a single graph may be used with appropriate amplitude scaling for all antennas with the same relative aperture distribution regardless of the  $D/\lambda$  ratio.

With the further assumption of pattern symmetry about the antenna axis, a very few graphs can be used to predict near-zone power densities for any  $D/\lambda$  ratio, any input power level, and generally encountered aperture distributions. The program can also be run to produce contours for specific cases where symmetry or assumed distributions may not apply.

## GAIN OPTIMIZATION OF A NEAR-FIELD FOCUSING ARRAY

J. Loane and S. W. Lee  
Electromagnetics Laboratory  
University of Illinois  
Urbana, Illinois 61801

A new variation of the array gain optimization problem has arisen in the study of microwave arrays used for hyperthermia, the heating of biological tissue. For a given array configuration and arbitrary medium it is desired to maximize the power deposition at the observation point in the near field of the array, analogous to the lossless case of radiation maximization in a particular direction. In this formulation the medium need be neither homogeneous nor lossless, and the array elements need not be identical.

For a given array and desired focus, this paper shows how the optimum excitation may be found to produce maximum  $|E|^2$  at a focus in the near field of the array for unit input power. This is a generalization of the far-field formulation of Lo et al. (*Proc. IEEE*, 54, pp. 1033-1045, 1966) in which only one received polarization is maximized. Some practical cases are simulated with both lossy and lossless media showing that the formulation of Lo et al. gives results that closely follow the optimum when the dominant polarization from linearly polarized radiators is maximized. The close correspondence between optimum and dominant-polarization solutions holds even for extreme supergain situations, i.e., high currents with an antiphase distribution. A comparison is also made with the conjugate-field or time-reversal excitation, a scheme which is slightly less efficient in most cases and which causes significantly higher focal shifts for some off-axis scan situations. The Q-factor and sensitivity variations are also included in the study, both of which depend on the excitation and array geometry. Experimental results are also reported, showing the focusing ability of a 7-element array in water.

PLANAR NEAR-FIELD ANALYSIS OF FREQUENCY RE-USE CONTOURED  
MULTI-BEAM REFLECTOR ANTENNAS FOR COMMUNICATIONS SATELLITES

Wilfried Bornemann, INTELSAT, Washington, D.C. (USA)

Rolf Jørgensen and Peter Balling, TICRA, Copenhagen (Denmark)

Commercial communications satellites have increasingly utilized larger and more complex antenna systems employing frequency re-use by spatial and polarization isolation to achieve increases in channel capacity and beam contour flexibility. The large diameter reflector antennas utilized on INTELSAT satellites have historically required the use of far-field ranges of several kilometers length ( $R \geq 10D^2/\lambda$ ) in conjunction with large radome or enclosure facilities. Near-field antenna test techniques, where the antenna system amplitude, phase and polarization response are sampled in the immediate vicinity of the antenna for immediate diagnostic analysis and subsequently computer transformed to the far-field offer an attractive means of reducing multi-path and transportation problems as well as the advantage of a totally enclosed and controlled test environment.

The paper will describe the results of computer calculations on planar near-field analysis for circularly polarized contoured multi-beam INTELSAT reflector antennas. The use of untransformed near-field data for diagnostic and design assistance purposes will be demonstrated and it will be shown, e.g. by examining differences between calculated and measured near-field data, that valuable insights can be derived prior to undertaking FFT processing. Finally, conclusions will be drawn from the comparison between computer far-field data and FFT processed computer near-field data on near-field measurement parameters like distance, scan range and sampling criteria.

## A-2-7

### INFLUENCE OF SOURCE ANTENNA DIRECTIVITY ON THE REFLECTIVITY LEVEL OF MICROWAVE ANECHOIC CHAMBERS

M.C.Chandra Mouly, N.V.Vani, N.R.Devi and K. Sujata  
Electronics and Communication Engineering Department  
VRS Engineering College, Vijayawada-520 006, India

This paper seeks to establish the nexus between the source antenna directivity and the reflectivity levels (RLL) at the center of the quiet zone of both Rectangular Anechoic Chamber (RAC) and Tapered Anechoic Chamber (TAC). For a comparative assessment of the chambers' performance, the RLL at the center of the quiet zone would be adequate. On the same count, the analysis considering only one reflected ray along with the direct ray would suffice. This analysis would provide a quick insight into the relative merits of the chambers. Hence this analytical method would be of great avail in a comparative study of the chambers offered by the manufacturer before having one such installed.

The RLL is evaluated from the field components arriving in the quiet zone one directly and the other after reflection at the wall. A source horn of the pyramidal type is assumed. The walls are presumed to be adorned with VHP-NRL-8 absorbers. Interpolation of the values of reflection coefficient for the actual angles of incidence is done. For the purpose of variation of source antenna directivity four different horns are considered. The frequency of operation is 9 GHz.

In general, the TAC is superior to the RAC due to reduced path difference and low angles of arrival realised in the former. But an increase in source antenna directivity can make the TAC inferior to RAC due to enhanced side wall illumination arising out of wide angle departure of the ray from the source on to the side wall. The results reveal that while attempting to improve the performance of the chamber via greater source antenna directivity, the possibility of stronger side wall illumination in a TAC has to be given due consideration.

## THE RECEIVING ANTENNA AS A LINEAR DIFFERENTIAL OPERATOR

Arthur D. Yaghjian  
Electromagnetic Sciences Division  
Rome Air Development Center  
Hanscom Air Force Base, MA 01731

Ronald C. Wittmann  
Electromagnetic Fields Division  
National Bureau of Standards  
Boulder, CO 80303

The general receiving antenna is represented as a linear differential operator converting the incident field and its spatial derivatives at a single point in space to an output voltage. The differential operator is specified explicitly in terms of the multipole coefficients of the antenna's complex receiving pattern. When the linear operator representation is applied to the special probes used in spherical near-field measurements, a probe-corrected spherical transmission formula is revealed that retains the form, applicability, and simplicity of the nonprobe-corrected equations. The new spherical transmission formula is shown to be consistent with the previous transmission formula derived from the rotational and translational addition theorems for spherical waves.

## A-2-9

### EFFECTS OF RMS SURFACE DEVIATIONS ON REFLECTOR ANTENNA RADIOMETRIC PERFORMANCE

Louis P. Anderson and Te-Kao Wu  
Hughes Aircraft Company  
Space and Communications Group  
Post Office Box 92919  
Los Angeles, California 90009

In this paper, analytical studies were conducted on the effects of RMS surface deviations on the radiometric performance of a 5.9 m diameter offset reflector antenna. Primary radiometric parameters such as beam efficiency, sidelobe levels and cross polarization levels are all investigated as a function of RMS surface deviations with edge illumination as a parameter.

The computer model developed is based on the physical optics current integration approach, wherein a two dimensional surface integration is evaluated on an offset reflector surface. Grid points addressed in the associated numerical integration process are assigned a "path phase error" which simulates the surface distortion relative to the ideal parabolic surface. This is implemented by referencing the defined set of surface points to a uniformly distributed random number generator. A corresponding set of errors, deviating axially from the ideal surface is produced normalized to an input RMS value. Axial deviations from the ideal parabolic shape are assumed to be less than one wavelength of the incident wave. The procedure yields information sufficient to identify the co-polarized and cross-polarized performance in the far field.

Results are presented for an X-band offset reflector design optimized for low cross polarization ( $< 20$  dB) and high beam efficiency ( $> 90\%$ ) for a non distorted surface. Here the beam efficiency is defined as the ratio of the radiated power contained in the main beam of the reflector and the total radiated power from the feed horn.

Conclusions derived from computed results indicate that for the design under consideration an upper limit for RMS surface distortions can be established. Beam efficiencies and sidelobe levels degrade as a function of increasing RMS distortions as expected. Variation of edge illumination proved that high edge tapers can compensate for this performance degradation slightly. In addition, it was found that cross polarization levels in the secondary pattern are unaffected by surface errors.

## URSI COMMISSION A - SESSION A3

EM Field  
Measurements8:30 - 12:00  
LAW 177Mesures du champ  
électromagnétiqueChairperson/Président: **M. Kanda**, National Bureau of Standards, Boulder, CO, USA

- 1 MULTIPLE-SOURCE, MULTIPLE-FREQUENCY ERROR OF AN ELECTRIC FIELD METER. **J. Randa, M. Kanda**, National Bureau of Standards, Electromagnetic Fields Division, Boulder, CO, USA
- 2 AN EXPERIMENTAL INVESTIGATION OF ANTENNA CONFIGURATIONS WHICH ARE NEAR TO OR PASS THROUGH AN AIR-WATER INTERFACE. **C.E. Smith, K.A. Michalski**, University of Mississippi, Dept. of Electrical Engineering, University, MS, USA; **C.M. Butler**, University of Houston, Dept. of Electrical Engineering, Houston, TX, USA; **C.A. Harrison**, University of Southern Mississippi, Dept. of Industrial Technology, Hattiesburg, MS, USA
- 3 MEASUREMENTS OF THE ELECTROMAGNETIC BACKSCATTERING MATRIX ELEMENTS OF A SINGLE BODY. **L.E. Allan, Y.M.M. Antar, A. Hendry**, National Research Council of Canada, Division of Electrical Engineering, Ottawa, ON
- 4 OPTIMIZING THIN MAGNETIC MATERIAL FOR THE THERMOGRAPHIC DETECTION OF MICROWAVE INDUCED SURFACE CURRENTS. **R.M. Sega, G.D. Wetlaufer**, University of Colorado, Dept. of Electrical Engineering, Colorado Springs, CO, USA
- 5 ARRAY ELEMENT PATTERN CORRECTION IN A DIGITAL BEAMFORMING ARRAY - AN EXPERIMENTAL STUDY. **J.S. Herd**, Rome Air Development Center, Electromagnetic Sciences Division, Hanscom AFB, MA, USA
- 6 RADAR CLUTTER SIMULATION AND MTI IMPROVEMENT FACTOR STATISTICS. **J.K. Hsiao**, Naval Research Laboratory, Radar Division, Washington, DC, USA

## A-3-1

### MULTIPLE-SOURCE, MULTIPLE-FREQUENCY ERROR OF AN ELECTRIC FIELD METER

J. Randa and M. Kanda  
Electromagnetic Fields Division  
National Bureau of Standards  
Boulder, Colorado 80303

Electric field meters (EFM's) are typically calibrated using single-frequency, single-source standard fields; but in practice they are not always used in such simple environments, and their response to more complex fields can be different than for the calibrating fields. We have recently completed a study of EFM errors in multiple-source and/or frequency (MSF) environments, and this paper summarizes the results. The analysis concentrated on new errors peculiar to complex environments and not previously analyzed. It also was restricted almost exclusively to periodic fields with periods of about  $10^{-6}$  s or less, much shorter than the time scale ( $\sim 10^{-4}$  s) set by the probe considered.

The MSF errors can be divided into two classes. There are errors in the average and/or peak electric field actually read by the meter when the field being measured does not have a simple sinusoidal time dependence. We investigated these meter errors for a common probe configuration consisting of electrically short dipole antennas with diode loads, connected to the metering unit by an RF filter transmission line. The particular features responsible for the errors will be identified, in order to extract problems which are relevant to other types of meters as well. In addition there are what could be called errors of inference. These are user, rather than meter, errors. Although EFM's measure electric fields only, they are sometimes used as hazard meters or energy-density meters (EDM's). In such applications one assumes that the magnetic field energy density is equal to the measured electric field energy density, as is the case for a monochromatic plane wave. For other field configurations this equality does not hold, and the inferred electromagnetic (EM) energy density is incorrect.

For both types of error the typical size is about one to three dB, but in some cases the error can exceed 10 dB.

AN EXPERIMENTAL INVESTIGATION OF ANTENNA  
CONFIGURATIONS WHICH ARE NEAR TO OR PASS THROUGH  
AN AIR-WATER INTERFACE

Charles E. Smith and  
Krzysztof A. Michalski  
Dept. of Electrical Engineering  
University of Mississippi  
University, MS 38677

Chalmers M. Butler  
Dept. of Electrical Engineering  
University of Houston  
Houston, TX 77004

and

Cecil A. Harrison  
Dept. of Industrial Technology  
University of Southern Mississippi  
Hattiesburg, MS 39401

Three different antennas structures are investigated experimentally. These structures are (1) two parallel antennas parallel to a lossy medium interface, (2) two parallel antennas close to an air-water interface with driven element in water, and (3) a loop antenna which passes through an air-water interface. Input admittance is measured for the driven antennas in or above the water and a normalized current distribution is measured for other related elements. The properties of the water used for these experiments have been measured and are presented (tapwater and water with NaCl where the salinity was 10.7 g/kg and 5.35 g/kg).

All measurements were made with an automated network analyzer using an existing ground, or image, plane facility developed earlier [C.A. Harrison and C.M. Butler, *IEEE Trans. AP*, vol. AP-32, no.4, pp. 397-390]. This facility consists of a large water tank that has dimensions of 16 ft. by 16 ft. along the exterior perimeter and is 4 ft. in depth which is surrounded by anechoic material. The image plane, which is mounted vertically along one wall of the tank, is 13 ft. high and 15 ft. wide and is constructed from 125-mil aluminum. Antennas were physically positioned in the center of image plane at appropriate heights. The measurement of the properties of water used in the experiments employed a coaxial waveguide apparatus to measure amplitude and phase constants from which the constitutive parameters are determined [R.W.P. King and G.S. Smith, *Antennas in Matter*, MIT Press, 1981]. Independent checks of the accuracy and the quality of the measurement range were made by comparison to numerical solutions of wire antenna models. Measured and computer results agreed very favorably, even in the low frequency range.

Measured data are presented for the three antenna configurations referred to before which appear to be in good agreement with existing theory and related numerical results. Results should be adequate for future verification of analytic and numerical solution for such antenna structures near air-water interfaces.

### A-3-3

#### MEASUREMENTS OF THE ELECTROMAGNETIC BACKSCATTERING MATRIX ELEMENTS OF A SINGLE BODY

L.E. Allan, Y.M.M. Antar and A. Hendry  
Division of Electrical Engineering  
National Research Council of Canada  
Montreal Road, Ottawa, Ontario, Canada  
K1A 0R8

Scattering characteristics of a single object in the resonance region are important in fields such as meteorology and remote sensing. These characteristics are represented by the scattering matrix elements related to orthogonal base vectors. Computational techniques have appeared in recent years, but published experimental results were restricted to amplitude measurements, i.e. backscatter radar crosssections, with no phase information available. For a complete description of the polarization response of a target, both amplitude and phase of the backscattered fields are needed.

Concurrent with dual-channel polarization diversity radar observations at NRCC, a single body backscattering measurement program was started. Measurements of the backscattering matrix elements have been performed at 2.86 GHz and are now being conducted at 9.6 GHz on single bodies of various sizes, shapes, and dielectric constants. Measurements are being performed at circular polarization, and results for any elliptical base vectors can be obtained by basic transformations.

The measurement facility comprises a dual-mode horn antenna, a turnstile junction and associated microwave circuitry. The two-channel radar receivers, with phase detection capability, are used. The facility provides a wide dynamic range, high isolation between opposite sense channels, and allows for accurate amplitude and phase calibration, nulling and level-setting procedures.

Various aspects of the measuring facility, the measurement procedure, and a sample of the results will be described in this paper.

OPTIMIZING THIN MAGNETIC MATERIAL FOR THE THERMOGRAPHIC  
DETECTION OF MICROWAVE INDUCED SURFACE CURRENTS

Ronald M. Sega and Gary D. Wetlaufer  
University of Colorado at Colorado Springs

This paper discusses the recent theoretical and experimental advances made toward understanding the material properties necessary for optimizing a thin screen detector for the infrared (IR) detection of surface currents on metal plates in the 2 to 4 GHz frequency range. Surface current density determination can be accomplished through measuring the magnetic field (H) strength at the surface of a good conductor. Magnetic field detection via IR employs a thin material of select imaginary permeability ( $\mu''$ ) which when placed on the surface of a conductor heats via  $\omega\mu''H^2$  coupling. Optimization implies a material much less than a skin depth thick while absorbing sufficient energy to produce a temperature rise (nominally 2K) detectable and resolvable with an IR system.

Understanding the microwave induced heating in magnetic field (H) detection screens is needed so optimum screens can be designed for the IR detection of surface currents. The surface temperature of a detector screen is a function of the absorbed microwave power within the medium. By Poynting's theorem, the absorbed power in a given volume is a function of the electric (E) and H field magnitudes as shown by the equation

$$P_{\text{abs}} = \int_V (\sigma E^2 + \omega \epsilon'' E^2 + \omega \mu'' H^2) dv$$

where  $\sigma$  is the conductivity,  $\epsilon''$  is the imaginary permittivity,  $\mu''$  is the imaginary permeability of the detector, and  $\omega$  is the angular frequency of the incident microwave. Thus, it becomes possible to relate surface temperature variations to H and E field intensities. As shown by the above equation, the detector screen can absorb power via E and/or H field coupling. As the application discussed in this paper requires the detector screen to be placed directly on a highly conductive surface, the primary mechanism for absorbing power is the  $\omega\mu''H^2$  term, for boundary conditions force the E field to or near zero at the surface of a good conductor. Using IR thermographic techniques, H, and hence the magnitude of the surface current density (J), can be measured on an irradiated metal object quickly and relatively easily.

The electromagnetic problem is solved as functions of thickness and  $\mu''$  for a normally incident plane wave on three phase stratified media where a phase of finite thickness (detector) is sandwiched between two other phases of infinite extent (one is free space, the other is metal). An approximate solution of the thermal problem relating surface temperature to absorbed microwave power is then obtained. Empirical IR and probe results using a ferrite-loaded material will be presented. The infrared technique should prove to be efficient for measurement of currents on complex structures.

## A-3-5

### ARRAY ELEMENT PATTERN CORRECTION IN A DIGITAL BEAMFORMING ARRAY

#### AN EXPERIMENTAL STUDY

Jeffrey S. Herd  
Electromagnetic Sciences Division  
Rome Air Development Center  
Hanscom AFB, MA 01731

A digital beamformer is a multichannel receive network which performs an A/D conversion of the complex RF signal at each element of an array prior to beam formation. This digitization in amplitude and phase makes it possible to synthesize versatile beam patterns and digitally correct for element channel imbalances.

The element patterns in an array environment are perturbed by the inter-element coupling. The pattern perturbations are most significant for the outer elements of a finite array where the coupling is asymmetric. The differences between element patterns will introduce phase and amplitude errors which impose a limitation on the minimum attainable sidelobe level and will degrade the open loop nulling performance of a digital beamforming array.

This paper presents an experimental study of a technique to measure and compensate for the effects of aperture coupling in a digital beamforming array. The  $N$  channels of a DBF array form an element signal vector which includes the influence of aperture coupled fields. The complex array element pattern of each of the  $N$  channels can be measured, and an inverse Fourier transform of each pattern to the corresponding element locations at the aperture will give  $N$  effective complex aperture coupling coefficients. A set of these coefficients for each array element pattern forms an  $N \times N$  matrix which describes the effective inter-element aperture coupling. The inverse of this matrix can be multiplied by the element signal vector to correct for the presence of aperture coupling. The corrected element signal vector can then be weighted and summed to give a desired array pattern.

Experimental results will be shown for an eight element digital beamforming array operating at X-band.

RADAR CLUTTER SIMULATION AND MTI IMPROVEMENT  
FACTOR STATISTICS

James K. Hsiao

Radar Division  
Naval Research Laboratory  
Washington, DC

A radar return from a patch of clutter usually consists of a large number of echoes from individual scatterers. Each of these scatterers moves randomly and introduces a randomly distributed doppler spectrum. Therefore, to simulate the performance of a MTI system, we must sum a large number of randomly distributed samples from each radar pulse return. The computer-time required in this case is very lengthy, and therefore it is not feasible for us to use this approach in a large-scale simulation. In this paper we propose to use a simplified version of the clutter model. Such a model, as we will show, will generate a correlation function and a spectral density function which are experimentally measured. Such a model reduces the required computer-time a great deal.

The second problem we will investigate is the improvement factor of the MTI system. This improvement factor is a function of the clutter output and will be used as a base for the design of an MTI system and its required performance. The clutter output is the weighted summation of a number of delayed radar returns. Since the spectral distribution of these radar returns is random, the improvement factor is also a random function. In the past, the expected value of this improvement factor was used for the MTI design; therefore it is possible that it accounts for the fact that a well-designed MTI system may not be adequate to eliminate clutter noises at all times. In this paper, we investigate the probability distribution of the improvement factor for a MTI system.

The clutter output is a summation of random variables. Usually we can assume that such a function has a normal distribution if the summed random variables are independent. Unfortunately, the clutter output is the summation of many MTI pulse returns which, because of long clutter correlation time, cannot be treated as independent. The assumption of a normal distribution is therefore invalid. There is no known probability density function to describe such a process; therefore, the statistic distributions of the MTI improvement factor presented in this paper are based on computer simulations.



## URSI COMMISSION A - SESSION A4

**Time Domain  
Metrology**

1:30 - 5:00  
LAW 177

**Métrologie dans le  
domaine temporel**

Chairperson/Président: **T.K. Sarkar**, Rochester Institute of Technology, Rochester, NY, USA

- 1 IMPULSE RESPONSE DETERMINATION FROM A GIVEN TIME LIMITED INPUT AND OUTPUT UTILIZING THE CONJUGATE GRADIENT METHOD. **T.K. Sarkar, S.A. Dianat, S.M. Rao, F-I. Tseng**, Rochester Institute of Technology, Dept. of Electrical Engineering, Rochester, NY, USA
- 2 AN OPTICALLY COUPLED SAMPLING SYSTEM WITH 4 GHZ BANDWIDTH. **S.B. Samaan**, Beavertown, OR, USA; **L. Wilson Pearson**, McDonnell Douglas Research Labs., Saint Louis, MO, USA; **C.E. Smith**, University of Mississippi, Electrical Engineering Dept., University, MS, USA
- 3 SYNTHETIC ARRAY PROCESSING OF PROBE DATA FOR SPURIOUS SCATTERING STUDIES OF A COMPACT RCS MEASUREMENT RANGE. **E.K. Walton, D.R. Koberstein**, Ohio State University ElectroScience Laboratory, Dept. of Electrical Engineering, Columbus, OH, USA
- 4 APPLICATIONS OF TIKHONOV AND ARSEININ DECONVOLUTION TECHNIQUES TO PICOSECOND PULSE MEASUREMENTS AT NBS. **W.L. Gans**, National Bureau of Standards, Electromagnetic Fields Division, Boulder, CO, USA
- 5 PARAMETERIZATION OF AN ELECTROMAGNETIC TRANSIENT FACILITY AND TEST ANTENNAS FROM TRANSIENT DATA. **R.M. Bevensee, J.V. Candy, G.A. Clark, L.C. Martin, J.K. Breakall, R.J. King**, Lawrence Livermore National Laboratory, Livermore, CA, USA
- 6 A MICROPROCESSOR CONTROLLED DIRECTION FINDER. **W.D. Rawle**, Technical University of Nova Scotia, Dept. of Electrical Engineering, Halifax, NS
- 7 DIELECTRIC SPECTROSCOPY USING OPEN-CIRCUITED COAXIAL LINES OF GENERAL LENGTH. **W.R. Scott Jr., G.S. Smith**, Georgia Institute of Technology, School of Electrical Engineering, Atlanta, GA, USA
- 8 A SIX-PORT SWEPT FREQUENCY CALIBRATION TECHNIQUE USING A NEW SIX-PORT CHART METHOD. **L. Kaliouby, R.G. Bosisio**, Ecole Polytechnique, Electrical Engineering Dept., Montreal, PQ

**IMPULSE RESPONSE DETERMINATION FROM A GIVEN  
TIME LIMITED INPUT AND OUTPUT UTILIZING THE  
CONJUGATE GRADIENT METHOD**

Tapan K. Sarkar  
Soheil A. Dianat  
Sadasiva M. Rao  
Fung - I. Tseng

Department of Electrical Engineering  
Rochester Institute of Technology  
Rochester, New York - 14623  
Phone: (716) 475-2143

**ABSTRACT:** The input and the output of a system are related by the well known convolution integral. The solution for the impulse response from the convolution integral is a well-known, ill-posed problem. Since the conjugate gradient method can solve iteratively any operator equations, including singular operator equations, we now apply it for the solution of the deconvolution problem. It is also well known that if the conjugate gradient method is terminated properly, then it provides a good approximate solution even for ill-posed problems. Computed impulse response utilizing this technique will be presented and it will be shown that for most of our experimental data the method converged in just one iteration.

AN OPTICALLY COUPLED SAMPLING  
SYSTEM WITH 4 GHZ BANDWIDTH

Samie B. Samaan\*, P.O. Box 231, Beaverton, OR 97075, U.S.A. ;  
L. Wilson Pearson, McDonnell Douglas Research Labs, P.O. Box 516,  
Saint Louis, Mo 63166, U.S.A. ; Charles E. Smith, Electrical  
Engineering Department, University of Mississippi, University,  
MS 38677, U.S.A.

\*Previously with the University of Mississippi.

A new approach to the design of an optically coupled multi-gigahertz sampling system with improved bandwidth for use in time domain scattering measurements is reported. The system utilizes the Tektronix S-6 sampling head, the Tektronix 7S12 TDR/Sampler plug-in unit, and a Tektronix 7000 series oscilloscope. Three fiber optic links replace existing hardwired conductors which convey the vertical error and feedback signals and the horizontal sampling command signal between the sampling head and the oscilloscope sampling plug-in. The remote sampling head and its associated fiber optic interfacing circuits are powered using a rechargeable battery pack. The dielectric fiber pigtailed allow placing the sampling head inside a metallic scatterer without the distortion of the outside electromagnetic fields usually caused by the metallic connecting conductors. Replacing the metallic conductors by the fiber pigtailed also eliminates electromagnetic interference (EMI) with the sampling system operation.

Two commercial fiber optic links are used in the analog mode to convey the error and feedback signals between the S-6 head and the 7S12 sampler. The sampling command signal issued by the 7S12 sampler is used to trigger a pulsed laser diode driver circuit. The laser diode produces a fast-rise infrared laser pulse of several hundred milliwatts. This laser pulse is used to trigger the avalanche transistor in the sampling head strobe generator circuit by coupling the infrared energy directly to the reverse biased collector-base junction of the transistor.

Qualitative and Quantitative tests were carried out to evaluate the optically coupled system performance. The test results show that the error and feedback links cause only a small distortion of acquired waveforms. The noise introduced by these links is significant only for small sampled signals on the order of 10 mV. The sampling command link is shown to introduce strobe jitter with a standard deviation of 28 ps. The overall system bandwidth is shown to be 4 GHz. Improvements in the noise and bandwidth performance are possible, and recommendations are made to this effect for implementation in a future version of the system.

## A-4-3

### SYNTHETIC ARRAY PROCESSING OF PROBE DATA FOR SPURIOUS SCATTERING STUDIES OF A COMPACT RCS MEASUREMENT RANGE

E. K. WALTON AND D. R. KOBERSTEIN  
The Ohio State University  
ElectroScience Laboratory  
Electrical Engineering Department  
Columbus, Ohio

The OSU compact radar backscatter cross section (RCS) measurement range consists of a 3.6 meter radius offset parabolic-section reflector illuminated by a broadband microwave feed at the focus. The resultant plane wave reflected from the parabolic surface scatters from the target under test and the signal is received at the focus of the parabola. The processed data gives the measured far field RCS of the target. The entire system is installed in a 6.1 by 12.2 by 18.3 meter room. In such a system, spurious scattering terms exist which must be properly treated. Such terms as the scattering from the edge of the parabolic surface, bistatic scattering from the (absorber coated) walls, ceiling, and floor of the room or from the feed and feed support structure and target support structure can become critically important for certain test target orientations.

In order to quantitatively study these spurious scattering terms, a computer controlled system consisting of a microwave probe (antenna) attached to a linear probe positioner was implemented. The received signal amplitude and phase was measured as a function of probe antenna position for a number of frequencies and polarizations. (including a number of cross polarized cases) Of particular interest was the change in performance induced by reshaping of the top edge of the reflector from a serrated shape to a rolled edge. The probe positioner was located so as to scan 1.7 m. vertically near the top of the test target zone.

The amplitude and phase data from the probe antenna as well as the probe position were used to generate a range focused synthetic aperture image of the distribution of scattering sources in the room. Forward scattering "hot spots" due to the feed and feed support structure as well as the top edge and ceiling scattering terms can be seen in the resultant image. Example images will be shown, and quantitative comparisons will be given for the various spurious scattering terms.

APPLICATIONS OF TIKHONOV AND ARSEININ DECONVOLUTION  
TECHNIQUES TO PICOSECOND PULSE MEASUREMENTS AT NBS.WILLIAM L. GANS  
ELECTROMAGNETIC FIELDS DIVISION  
NATIONAL BUREAU OF STANDARDS  
BOULDER, COLORADO 80303

The Electromagnetic Fields Division at the National Bureau of Standards, Boulder, Colorado, is tasked with the accurate measurement of fast (picosecond-nanosecond range) electrical pulse parameters. The primary system used to perform these measurements, referred to as the NBS Automatic Pulse Measurement System (APMS), consists essentially of a wideband (dc - 18 GHz) equivalent-time sampling oscilloscope interfaced to a minicomputer. It operates in such a manner that under computer control repetitive fast electrical pulse waveforms can be acquired and recorded into the computer memory for subsequent processing and analysis. Along with such pulse parameters as pulse transition duration (rise/fall time), pulse duration (width), pulse amplitude and pulse time delay, this system can also measure such frequency domain parameters as microwave scattering parameters and impulse spectrum amplitude by employing the fast Fourier transform (FFT) operator on the time domain waveform data.

The measurement accuracy of the APMS is limited by two major sources of error. The first source is the deterministic distorting effect of the sampling oscilloscope wideband sampling head. The pulse waveform recorded by the APMS is really the convolution of the true waveform and the impulse response function of the sampling head,  $h_1(t)$ . An estimate of  $h_1(t)$  has been derived at NBS from sampling head circuit models and measurements.

The other major source of error is the presence of noise in the measurement system, both in the form of voltage additive noise and sample timing jitter. The use of simple additive signal averaging allows the errors due to voltage additive noise to be made arbitrarily small. Such is not the case with timing jitter, however. It can be shown that the distorting effect of timing jitter under additive signal averaging conditions is analogous to passing the signal through a low-pass filter whose time domain equivalent impulse response function is simply the probability density function (PDF) of the timing jitter noise. Thus, a second measurement system impulse response function,  $h_2(t)$ , due to timing jitter can be obtained by measuring the PDF of the timing jitter noise.

These two system impulse responses,  $h_1(t)$  and  $h_2(t)$ , may then be combined by convolution to yield a total system impulse response,  $h_t(t)$ . Then, the deconvolution techniques of Tikhonov and Arsenin may be used to remove the distorting effects of  $h_t(t)$  from the measured waveform. Satisfactory estimates of the true waveform are thus obtained with estimated uncertainties approaching  $\pm 1\%$ .

## A-4-5

### PARAMETERIZATION OF AN ELECTROMAGNETIC TRANSIENT FACILITY AND TEST ANTENNAS FROM TRANSIENT DATA

R. M. Bevensee, J. V. Candy, G. A. Clark, L. C. Martin,  
J. K. Breakall, and R. J. King  
Lawrence Livermore National Laboratory

The Lawrence Livermore National Laboratory is characterizing antennas in their environments from transient reflectometry and scatter data taken on an Electromagnetic Transient Facility (EMTF). This paper discusses the linear system ARMAX (autoregressive, moving-average with exogenous input) modeling of the entire, recently-upgraded EMTF and its use in obtaining the frequency-domain equivalent circuit impedance and effective height of a test antenna at its load port.

The EMTF is decomposed into blocks and model identification of each is achieved by data pre-processing, model-order testing, parameter estimation, prediction error tests for "fit" validation, and finally ensemble data tests on a well-understood electromagnetic dipole for overall EMTF model validation. The details of the dipole model validation by various prediction and output error modeling algorithms are explained. Once the EMTF model is validated the equivalent circuit of any test antenna can be similarly modeled with confidence.

The antenna modeling of equivalent circuit impedance by time-domain reflectometry (TDR) measurements and effective height by scatter measurements is discussed. The disadvantages of several types of ARMAX modeling are noted, compared to the advantages of using an off-line Nonlinear Iterative Least Squares (NLS) method. Data processing rules are given. Finally the procedures for characterizing impedance and effective height are discussed and these spectra as obtained by several models for a 30 cm monopole antenna are compared with the spectra obtained by frequency-domain division.

It will be shown how the transient parameterization of a test antenna enables accurate prediction of the output response for an arbitrary load, particularly the short circuit current without need of awkward current probes which often exhibit inferior frequency response.

Conclusions emphasize the need for proper data pre-processing, anti-aliasing filters, and avoidance of models with too high a model order. ARMAX modeling with NLS so as to include the modeling of input noise appears to be the most promising technique.

\*Work performed under the auspices of the U. S. Department of Energy by the Lawrence Livermore National Laboratory under contract number W-7405-ENG-48.

**A MICROPROCESSOR CONTROLLED DIRECTION FINDER**

W.D. Rawle  
Technical University of Nova Scotia  
Department of Electrical Engineering  
Halifax, NS

A simple, low cost microprocessor controlled direction finding system is presented. The system, based upon a phase comparison technique represents a significant departure from conventional direction finding system technology. An angular resolution of 1 degree is easily obtainable with an eight bit microprocessor implementation. The advantages of this system are accuracy, reliability, simplicity, and lightweight implementation.

**DIELECTRIC SPECTROSCOPY USING OPEN-CIRCUITED  
COAXIAL LINES OF GENERAL LENGTH**

**Waymond R. Scott, Jr. and Glenn S. Smith**  
School of Electrical Engineering  
Georgia Institute of Technology  
Atlanta, Georgia 30332

**Abstract**

The open-circuited coaxial line of general length is studied in detail as a sample cell for broadband measurements of the dielectric permittivity. This cell is a section of transmission line with the center conductor abruptly terminated. The dielectric material to be measured fills the coaxial section of the cell and extends beyond the center conductor into the tube formed by the outer conductor of the transmission line.

The inverse function for obtaining the permittivity of the sample from the measured input admittance of the cell is multivalued. The error in the measured permittivity caused by passage onto the wrong branch of the inverse function is analyzed, and a procedure that can prevent passing onto the wrong branch is developed. The errors in the measured permittivity due to the inaccuracies in the instrumentation are also analyzed. Contour graphs are constructed that quantify the effects of this error on the measured permittivity. This error is shown to be largest when the combination of frequency, sample length, and sample permittivity place the measured normalized admittance near a branch point of the inverse function.

A time-domain measurement system was constructed, calibrated, and used with an open-circuited sample cell to measure the permittivities of several primary alcohols over the frequency range  $50 \text{ MHz} < f < 2 \text{ GHz}$ . The measured relaxation spectra for these alcohols are in good agreement with those determined by previous investigators.

A Six-Port Swept Frequency Calibration Technique  
 Using a New Six-Port Chart Method  
 L. Kaliouby, R.G. Bosisio  
 Ecole Polytechnique, Electrical Engineering Department  
 Montreal, Canada

Six-port automatic network analysis allows complete measurement of reflection coefficient, by means of four output power readings. However, due to the complex calibration procedure and lengthy calculations of  $\Gamma$  from the power readings, its use has been limited to point-by-point measurements. Recently, the authors have developed a real-time swept frequency measurement technique, using a new six-port chart method (Fig.1). However, to guarantee proper interpretation of results in swept frequency measurement, it's necessary to first calibrate the six-port in a swept frequency mode. It will be shown that this can be done by comparing experimented measurements of a fixed short (Fig.2 curve #4), between  $f_1$  and  $f_2$ , with the theoretical calibration charts at  $f_1$  and  $f_2$  (Fig.2, curves #1 and 2). Intermediate calibration (curve #3) has to be carried out until the experimental curve corresponds with the theoretical charts in this interval. Afterwards, measurement of a DUT can be carried out in swept frequency mode (Fig.3), with the guarantee of a correct interpretation, of the results.

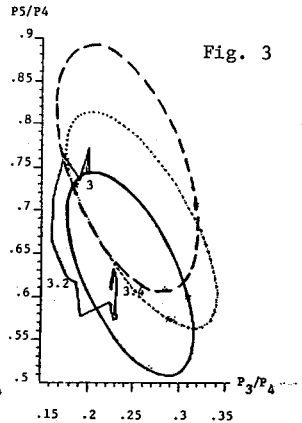
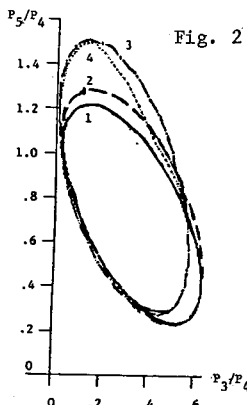
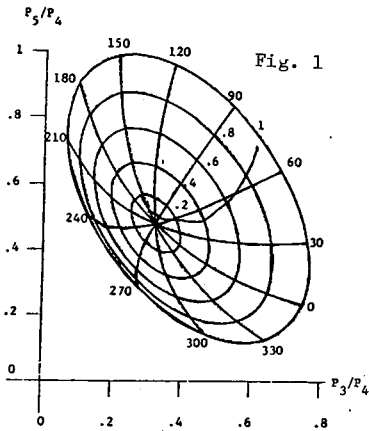


Fig. 1: Real-time measurement using six-port chart.  
 Fig. 2: Swept frequency calibration between  $f = 3$  GHz (---) and 3.4 GHz (- - -). Measurement with fixed short (.....) shows need for calibration at 3.2 GHz (-.-.-).  
 Fig. 3: Swept frequency measurements of a DUT between 3 GHz (---) and 3.4 GHz (.....), including calibration at 3.2 GHz (- - -).



## URSI COMMISSION A -SESSION A5

Health and Microwave  
Frequencies

8:30 - 12:00  
LAW 177

Effets biologiques  
des hyperfréquences

Chairperson/Président: **M.A. Stuchly**, University of Ottawa, Ottawa, ON

- 1 (8:40) NCRP-SC53 REPORT ON BIOLOGICAL EFFECTS AND EXPOSURE CRITERIA FOR RADIO FREQUENCY EM FIELDS. **A.W. Guy**, University of Washington, Bioelectromagnetics Research Laboratory, Seattle, WA, USA
- 2 (9:20) EXPERIMENTAL DOSIMETRY IN THE NEARFIELD-RECENT ADVANCES. **S.S. Stuchly, M.A. Stuchly, A. Kraszewski, G.W. Hartsgrrove**, University of Ottawa, Dept. of Electrical Engineering, Ottawa, ON
- 3 (9:40) BIOLOGICAL EFFECTS OF RADIOFREQUENCY RADIATION: A 1985 PERSPECTIVE. **J.A. Elder**, U.S. Environmental Protection Agency, Cellular Biophysics Branch, Research Triangle Park, NC, USA
- 4 (10:00) INTERNATIONAL ACTIVITIES AND RECOMMENDATIONS IN NON-IONIZING RADIATION PROTECTION. **A. Duchêne**, International NIR-Committee Secretariat, Institut de Protection et de Sécurité Nucléaire - DPS, Fontenay-aux-Roses, France
- 5 (10:20) SOME PROBLEMS IN COMPARING EXTERNAL SIGNALS TO INTERNALLY GENERATED BIOLOGICAL SIGNALS AND NOISE. **F.S. Barnes, M.S. Seyed-Madani**, University of Colorado, Dept. of Electrical and Computer Engineering, Boulder, CO, USA
- 6 (10:40) CELL MEMBRANES AND MICROWAVE FIELDS IN MODELS OF TUMOR PROMOTION. **W.R. Adey, C.V. Byus, D.B. Lyle**, VA Medical Center, Loma Linda, CA, USA

NCRP-SC53 Report on Biological Effects and Exposure Criteria for  
Radio Frequency EM Fields

Reviewed by  
Arthur W. Guy  
University of Washington  
Seattle, Washington

The lack of quantitative data on biological effects of radiofrequency electromagnetic (RFEM) fields has resulted in widespread concern that exposure poses the risk of injury to health regardless of intensity. Although there are more than 6,000 scientific papers, books, articles and newspaper reports of widely varying scientific quality that report data and opinion on the biological response to RFEM radiation, no consensus has emerged regarding mechanisms and thresholds of injury. The wide variation in RFEM-radiation exposure standards around the world reflects this absence of consensus. An objective analysis of the scientific literature and recommendations for exposure limits by qualified and unbiased group of experts are sorely needed. To address this need, the NCRP decided in 1973 to extend its scope of activities to the publication of reports that provide evaluations of the biological effects on non-ionizing radiation and recommendations for exposure limits. The report reviewed in this paper addresses the biological effects of exposure to RFEM fields that range in frequency from  $3 \times 10^5$  to  $10^{11}$  Hz beginning with the discussion of fundamental studies at the molecular level. The discussion continues to progressively larger values or scales of interaction including macromolecular and cellular effects, chromosomal and mutagenic effects, and carcinogenic effects. The scope of the subject matter is then expanded to include systemic effects such as reproduction, growth and development, hematopoiesis and immunology, endocrinology and autonomic nervous function, cardiovascular effects, and cerebrovascular effects. The nervous system and special senses including the more interesting and controversial effects have received wide attention. Neural effects are discussed with specific reference to peripheral and neuromuscular systems. Some of the more sensitive biological endpoints, performance and behavior, contrast greatly with the apparently insensitive biological endpoint of cataractogenesis. The thermoelastic mediated interaction, which has had widespread attention over the past two decades as a possible auditory neural effect, is a phenomenon that deserves special attention. Probably of greatest importance in terms of effects of non-ionizing radiation on human populations are the epidemiological studies. Thermoregulation is an especially important subject since its failure can result in hyperthermia, which is responsible for many reported effects, some well accepted as thermal and others seemingly non-thermal in nature. Hyperthermia, as such, is also extremely important since it is the basis for the use of non-ionizing radiation as an adjunct for the treatment of cancer, which is reviewed in detail in the report. Because the major purpose of the report was to interpret the literature in terms of safety and health in an electromagnetic environment, the results are summarized in the form of human exposure criteria and rationale. Exposure criteria recommended by the committee for the occupational population was similar to the American National Standards Institute C95.1-1982 Standard. However, the committee recommended that the exposure levels for the general population be reduced by a factor of 5 from that of the occupational recommendation. Also, the practical problems relating to partial and whole-body exposures and to the use of low-power radio devices, essential to the quality of life and public safety had to be dealt with by recommending maximum energy absorption levels in addition to the exposure levels.

## EXPERIMENTAL DOSIMETRY IN THE NEARFIELD-RECENT ADVANCES

S.S. Stuchly, M.A. Stuchly\*, A. Kraszewski and G.W. Hartsgrove  
Dept. of Electrical Engineering, University of Ottawa  
Ottawa, Ontario, Canada, K1N 6N5  
\*also Radiation Protection Bureau, Health & Welfare Canada.

It is recognized that biological effects due to exposure to radiofrequency fields depend on the spatial distribution of the electric field inside the exposed body. The specific absorption rate (SAR) has been commonly used as a dosimetric quantity. The SAR is directly proportional to the square of the electric field and inversely proportional to the tissue conductivity, and indicates the rate at which the electromagnetic energy is imparted into the exposed biological body.

Humans are frequently exposed in the near-field of radiators as in the case of portable and mobile transmitters or leaky transmitter cabinets. Theoretical evaluation of the spatial distribution of the SAR resulting from these exposures is, at present, rather difficult and of limited accuracy. As an alternative approach an experimental method has been developed. In this method an implantable electric field probe of small dimensions is used to measure the electric field strength in a full-scale, anatomically correct model of man. The model is filled with a phantom material having the electrical properties of the human tissue. The probe positioning, data acquisition, processing display and recording are performed under computer control. The measurement system developed is capable of obtaining SARs in hundreds of locations within the model with an uncertainty better than  $\pm 1$  dB.

The SAR distributions were measured at frequencies of 160, 350 and 915 MHz for the models exposed in the near field (at distances less than  $0.1 \lambda$ ) of resonant dipoles, resonant dipoles with reflectors and resonant slots with various polarizations. In all situations investigated highly non-uniform spatial distribution of the SAR with large spacial gradients was observed. The local SARs (averaged over 1 g of tissue) are usually a few hundred times greater than the whole-body average SAR for a given exposure. For some antennas, fed with powers larger than 1 W, the local SARs exceed the peak limit of 8 W/kg recommended by the current ANSI exposure standard.

## A-5-3

### BIOLOGICAL EFFECTS OF RADIOFREQUENCY RADIATION: A 1985 PERSPECTIVE

Joe A. Elder  
Cellular Biophysics Branch  
Experimental Biology Division  
Health Effects Research Laboratory  
U.S. Environmental Protection Agency  
Research Triangle Park, NC 27711

A critical review of the literature on the biological effects of radiofrequency radiation (500 kHz - 100 GHz) was published in September 1984 (Biological Effects of Radiofrequency Radiation, J. A. Elder and D. F. Cahill, editors, EPA-600/8-83-026F, 268 pages). The reported consequences of the interaction between radiofrequency radiation and biological systems were examined from two perspectives: whole-body-averaged specific absorption rate (SAR) and radiofrequency-energy-induced core-temperature increase. It was concluded that biological effects occur at an SAR of about 1 W/kg and that some of the effects may be significant under certain environmental conditions. The report is a critical review of the literature published through 1980 and, in addition, includes some 1981-1984 references. In this presentation, the more recent literature is reviewed and the summary statements and conclusion of the 1984 report are reevaluated based on current information of the effects of radiofrequency radiation on cellular and subcellular systems, hematology, immunology, reproduction, nervous system, behavior, special senses, endocrine system, genetics, and thermal physiology.

INTERNATIONAL ACTIVITIES AND RECOMMENDATIONS IN  
NON-IONIZING RADIATION PROTECTION

A. DUCHÈNE, International NIR-Committee Secretariat  
Institut de Protection et de Sûreté Nucléaire - DPS  
B.P. N° 6 - 92260 FONTENAY-AUX-ROSES (France)

With the expanding use of high frequency and microwave emitting equipment, the health authorities of an increasing number of countries become involved in the development of protection standards and look for some guidance in this respect. During the last decade, several international organizations have attempted to answer this request. These are more particularly : the World Health Organization (WHO), the International Labour Organization (ILO), the International Electrotechnical Commission (IEC), the International Union of Radio Science (URSI) and the International Radiation Protection Association (IRPA). The IRPA specifically set up the International Non-Ionizing Radiation Committee (INIRC) with the commitment to lay down general principles of non-ionizing radiation (NIR) protection, including internationally acceptable exposure limits, and to explore with other international organizations ways of furthering protection in this field.

The WHO, through its Environmental Health Criteria Programme financed by the United Nations Environment Programme (UNEP), collaborates with IRPA/INIRC to produce Environmental Health Criteria documents for the different types of NIR. Five documents have been issued among which EHC 16 for *Radiofrequency and Microwaves* (UNEP/WHO/IRPA, Geneva 1981) and EHC 35 for *Extremely Low Frequency Fields* (1984). An EHC document on *Static and Slowly Varying Magnetic Fields* is in preparation. WHO's own programme also includes the establishment of collaborating Centres on NIR and the publication of a manual on *Non-Ionizing Radiation Protection* by the WHO Regional Office for Europe (M.J. Suess, Ed., Copenhagen 1982).

The ILO and IRPA/INIRC cooperate in the preparation of a Code of practice for the *Protection of workers against radiofrequency radiation*.

On the basis of the data collected in the EHC documents, the IRPA/INIRC develops guidelines on protection standards. The *Interim guidelines on limits of exposure to radiofrequency electromagnetic fields in the frequency range from 100 kHz to 300 GHz* were approved in July 1983 (Health Phys., 46, n° 4, 975-984). These differ somewhat from the 1982 Safety Levels recommended by ANSI. For occupational exposure, in the frequency range from 10 MHz to 300 GHz, the guidelines recommend a basic SAR limit of 0.4 W/kg when averaged over the whole body and 4 W/kg when averaged over one gramme of tissue, and derived working limits expressed as root mean square electric and magnetic field strengths or equivalent plane-wave power densities. All values are averaged over any 6 minutes. In the frequency range from 0.1 to 10 MHz, the limits are expressed only as effective E and H field strengths and based mainly on the shock and burn hazards. Exposure limits for the public incorporate an additional safety factor of 5 compared to those for workers.

## A-5-5

### SOME PROBLEMS IN COMPARING EXTERNAL SIGNALS TO INTERNALLY GENERATED BIOLOGICAL SIGNALS AND NOISE

Dr. Frank S. Barnes and M.S. Seyed-Madani, Department of Electrical and Computer Engineering, University of Colorado, Boulder, CO 80309

For reasons ranging from setting safety standards to generating invasive signals for medical intervention in biological processes, it is important to be able to estimate the strength of externally generated signals at a variety of locations inside the body. This problem is complicated by the complex shape and inhomogeneous nature of the body, as well as nonlinearities.

Our particular interest has been in trying to compare the noise from internally generated signals such as nerve impulses and EEGs, with signals received from outside sources. At low frequency, the problem is one of estimating induced current density, in order to change electric and magnetic fields so that they can be compared to biologically generated currents or current densities. This calculation is complicated by the frequency dependence of the coupling coefficient, scattering and attenuation, which may change pulse shapes or the frequency composition of externally generated signals by the time they arrive at the site of interest, such as the surface of a brain cell, a bone break or a heart muscle. For frequencies outside the biological signaling bands, the conversion of modulation signals by weak nonlinearities to signals inside the natural signaling bands where amplifying processes exist, may make the modulation frequencies more important than the carrier.

Quantitative estimates of signal strengths needed to generate current densities at the surface of brain cells will be presented and related to the  $\text{Ca}^{++}$  efflux experiments, EEG signals and noise generated in nerve cells. This work is part of an on-going study to try to estimate the lowest electromagnetic signals which may be biologically significant.

## CELL MEMBRANES AND MICROWAVE FIELDS IN MODELS OF TUMOR PROMOTION

W.R. Adey, C.V. Byus and D.B. Lyle, VA Medical Center, Loma Linda, CA 92357 USA and University of California, Riverside, CA 92521 USA

Cell membranes are prime sites of interaction with ELF electromagnetic fields and with "athermal" RF/microwave fields sinusoidally amplitude modulated at ELF frequencies (Adey, 1981, 1984). Imposed fields have revealed both the sequence and the energetics of cell membrane transductive coupling, and nonlinear and nonequilibrium aspects of the coupling sequence. These fields appear to perturb normal transductive processes by which extracellular signals from binding of hormone, antibody and neurotransmitter molecules at cell surface receptor sites are transmitted to the cell interior.

We have tested sensitivity of human lymphocyte protein kinases to 450 MHz fields (1.5 mW/cm<sup>2</sup> peak envelope power), sinusoidally amplitude-modulated at frequencies from 3 to 100 Hz (Byus, et al., 1984). Approximately 20 percent of the total kinase activity was due to cAMP-dependent protein kinase (a measure of the action of membrane-bound adenylate cyclase in producing cAMP from ATP). This was not altered by exposure to fields modulated at 16 or 60 Hz for 15, 30, or 60 min. However, total cAMP-independent kinase activity was reduced by more than 50 percent 15 and 30 min. after onset of exposure to a 16 Hz modulated fields, but returned to control levels after 60 min. despite continued field exposure. In addition to this "window" in time, there was a "window" with respect to modulation frequency, with maximum effects at 16 Hz.

Protein kinase enzymes form a major messenger system to intracellular organelles, including the nucleus. A major class of tumor promoters (phorbol esters) have as a cell membrane receptor a specific protein kinase (phosphatidylserine calcium-dependent kinase, kinase C) (Nishizuka, 1984). This kinase is also activated by diacylglycerol, formed by breakdown of inositol phospholipid at membrane receptor sites. One molecule of diacylglycerol may activate every molecule of protein kinase C, and one molecule of phorbol ester can combine directly with one molecule of kinase C, irreversibly activating the enzyme.

We are testing the hypothesis that nonionizing electromagnetic fields play a role in tumor promotion via the cell membrane by action on cAMP-independent protein kinases, including kinase C. (supported by DOE, ONR, and Southern California Edison Company).



## URSI COMMISSION AJ - SESSION AJ1

**Time and Frequency**

8:30 - 12:00

**Etalons de fréquence et****Standards for radio astronomy**

LAW 177

**du temps en radioastronomie**Chairperson/Président: **J.R. Fisher**, NRAO, Greenbank, WV, USA

- 1 LONG-TERM ROTATIONAL STABILITY OF THE MILLISECOND PULSAR PSR 1937+21. **D.C. Backer**, University of California, Radio Astronomy Laboratory, Berkeley, CA, USA; **M.M. Davis**, Arecibo Observatory, Arecibo, PR, USA; **J.H. Taylor**, Princeton University, Physics Dept., Princeton, NJ, USA; **J.M. Weisberg**, Carleton College, Dept. Physics and Astronomy, Northfield, MN, USA; **R.W. Hellings**, **E.M. Standish**, Jet Propulsion Laboratory, Pasadena, CA, USA
- 2 COHERENCE LIMITS IN VLBI OBSERVATIONS. **J.M. Moran**, Harvard Smithsonian Center for Astrophysics, Cambridge, MA, USA; **A.E.E. Rogers**, Massachusetts Institute of Technology, Haystack Observatory, Westford, MA, USA; **A.T. Moffet**, California Institute of Technology, Owens Valley Radio Observatory, Pasadena, CA, USA; **D.C. Backer**, University of California, Radio Astronomy Laboratory, Berkeley, CA, USA
- 3 TIME AND POLAR MOTION: CALIBRATION FOR LONG TERM DRIFTS. **K.J. Johnston**, Naval Research Laboratory, Washington, DC, USA
- 4 THE STATUS OF SUPERCONDUCTIVITY CAVITY STABILIZED OSCILLATORS. **A.T. Moffet**, California Institute of Technology, Owens Valley Radio Observatory, Pasadena, CA, USA
- 5 A HIGHLY STABLE HYDROGEN MASER CLOCK SYSTEM FOR LONG-TERM APPLICATIONS IN SPACE. **R.F.C. Vessot**, **E.M. Mattison**, **G.U. Nystrom**, Smithsonian Astrophysical Observatory, Cambridge, MA, USA

## AJ-1-1

### LONG-TERM ROTATIONAL STABILITY OF THE MILLISECOND PULSAR PSR 1937+21

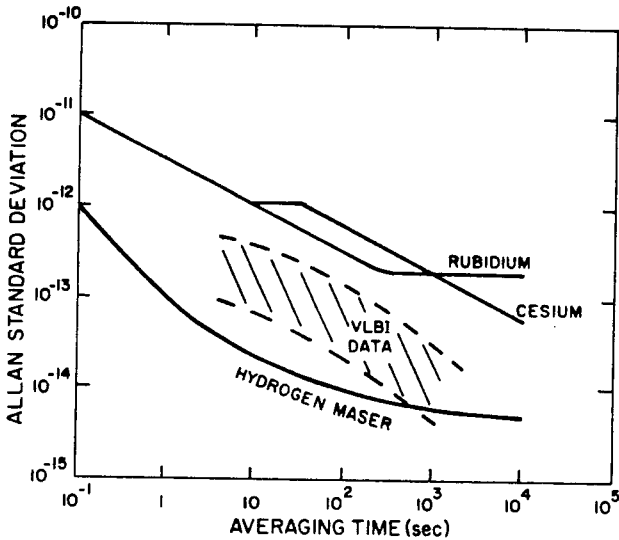
D. C. Backer, Radio Astronomy Laboratory, University of California, Berkeley, CA, 94720; M. M. Davis, Arecibo Observatory, Arecibo, PR, 00612; J. H. Taylor, Physics Department, Princeton University, Princeton, NJ, 08544; J. M. Weisberg, Department of Physics and Astronomy, Carleton College, Northfield, MN 55057; R. W. Hellings and E. M. Standish, Jet Propulsion Laboratory, Pasadena, CA, 91103.

Pulsars are rotating neutron stars with a large dipole moment which are detected by their emission of intense beams of microwave radiation. A pulsar with a 1.6-millisecond period, PSR 1937+21, was detected in 1982. Comparison of the arrival times of the pulsed microwaves from this pulsar with international atomic time over the past two years indicates that the long-term stability of its rotation is comparable to that of the best atomic clocks. The Allen standard deviation for the arrival-time residuals from a simple model is close to  $10^{-11}/T$  with  $T$  in days up to 256. In this comparison a deceleration of the neutron star rotation of  $4.3 \times 10^{-14} \text{ s}^{-2}$  is removed; the origin of this deceleration is electromagnetic dipole radiation at the pulsar rotation frequency and its harmonics. One of the limits to this comparison has been Loran C time transfer of UTC from USNO to the Arecibo Observatory. This limit has been reduced by the introduction of a NBS-supported GPS time transfer system. The comparison requires accurate knowledge of the location of the observatory in the inertial reference frame of the solar system barycenter. Results from use of planetary ephemerides from the Center for Astrophysics (740-R) and the Jet Propulsion Laboratory (DE118 and DE200) will be compared. Other limits to the accuracy of the pulsar observation such as interstellar propagation effects will be discussed.

## COHERENCE LIMITS IN VLBI OBSERVATIONS

J. M. Moran, Harvard Smithsonian Center for Astrophysics, Cambridge, MA 02138, A. E.E. Rogers, Haystack Observatory, Westford, MA 01886, A. T. Moffet, Owens Valley Radio Observatory, California Institute of Technology, Pasadena, CA 91125, D. C. Backer, Radio Astronomy Laboratory, University of California, Berkeley, CA 94720

VLBI observations at frequencies above 1 GHz using rubidium and cesium standards are severely limited by the performance of those standards, while observations using hydrogen masers are limited by tropospheric and ionospheric phase fluctuations except on time scales shorter than one second or longer than 1000 seconds. Typical coherence times for VLBI using hydrogen masers under good observing conditions range from 1000 seconds in the microwave range down to 100 seconds at 100 GHz. The Allan standard deviations are shown below for tropospheric phase fluctuations and the rubidium, cesium and hydrogen maser frequency standards.



**AJ-1-3**

**TIME AND POLAR MOTION  
CALIBRATION FOR LONG TERM DRIFTS**

K.J. Johnston  
Naval Research Laboratory  
Washington, DC

Abstract not available at time of printing/  
Le résumé n'était pas disponible lors de l'impression

**THE STATUS OF SUPERCONDUCTIVITY  
CAVITY STABILIZED OSCILLATORS**

A.T. Moffet  
California Institute of Technology  
Owens Valley Radio Observatory  
Pasadena, CA, USA

Abstract not available at time of printing/  
Le résumé n'était pas disponible lors de l'impression

## AJ-1-5

### A HIGHLY STABLE HYDROGEN MASER CLOCK SYSTEM FOR LONG-TERM APPLICATIONS IN SPACE

R.F.C. Vessot, E.M. Mattison and G.U. Nystrom

Smithsonian Astrophysical Observatory

Cambridge, Ma 02138

Orbiting Very Long Baseline Interferometry Terminal and extremely high accuracy orbiting time and frequency comparison systems [D.W. Allan et.al, IEEE Trans. on Geoscience, GE-20, 321-324, 1982) will require clocks of very high stability capable of long-term operation in space. We describe the design and performance expectations of a spaceborne atomic hydrogen maser clock based on the successful 1976 rocket borne clock used in the SAO-NASA gravitational Redshift experiment [R.F.C. Vessot et.al, Phys. Rev. Lett., 45, 2081-2084, 1980]. We have tested radically different design concepts for the atomic hydrogen dissociator, the thermal control system for the maser cavity-belljar assembly, and the cavity resonator structure, which improve the weight, power and performance capability of the maser under conditions of long-term exposure in the vacuum of space. The expected physical dimensions are 19.6 inches in diameter, 36 inches long; weight is 60 pounds; power ~35 watts (depending on thermal environment). The stability performance expected is given by the Allan Variance,  $\sigma(\tau)$ , as follows:  $\sigma(1 \text{ sec}) \leq 1 \times 10^{-13}$ ,  $\sigma(10 \text{ sec}) \leq 2 \times 10^{-14}$ ,  $\sigma(100 \text{ sec}) \leq 8 \times 10^{-14}$ ,  $\sigma(1000 \text{ sec}) \leq 2 \times 10^{-14}$ ,  $\sigma(10,000 \text{ sec}) \leq 8 \times 10^{-16}$ . Long-term drift is expected to be less than  $2 \times 10^{-15}$  per day and predictable to better than  $3 \times 10^{-16}$  per day. The design of this maser will be described and possible space applications in VLBI and time synchronization will be discussed.

This work was supported by the N.A.S.A. Marshall Space Flight Center under Contract No. NAG-8006 and the U.S. Naval Research Laboratory under Contract No. N00014-85-K-2001.

## URSI COMMISSION B - SESSION B1

Antenna Elements

8:30 - 12:00  
IRC-1

Éléments d'antennes

Chairperson/Président: **G. Thiele**, University of Dayton, Dayton, OH, USA

- 1 A NUMERICAL SOLUTION OF THE COUPLED INTEGRAL EQUATIONS WHICH DESCRIBE THE SYMMETRIC MODES OF THE CIRCULAR DIFFRACTION ANTENNA WITH A RECESSED CENTER POST. **D.J. Riley**, Sandia National Laboratories, Electromagnetic Applications Division, Albuquerque, NM, USA
- 2 A METHOD FOR EXACT INTEGRATION OF VECTOR POTENTIALS OF THIN DIPOLE ANTENNAS. **P.L. Overfelt**, Naval Weapons Center, Physics Division, China Lake, CA, USA
- 3 A COAXIAL WAVEGUIDE OPENING INTO A GROUND PLANE AND COVERED BY A DIELECTRIC HEMISPHERE. **R.D. Nevels, J.E. Wheeler**, Texas A&M University, Dept. of Electrical Engineering, College Station, TX, USA
- 4 A NEW SIMPLE LEAKY WAVE ANTENNA FOR MILLIMETER WAVES. **A.A. Oliner**, Polytechnic Institute of New York, Brooklyn, NY, USA; **P. Lampariello**, University of Rome "La Sapienza", Rome, Italy
- 5 ANALYSIS OF A FINITE LENGTH TUBULAR MONOPOLE ANTENNA DRIVEN BY A COAXIAL LINE AND PRECISION ADMITTANCE MEASUREMENTS. **M.E. Morris**, Sandia National Laboratories, Electromagnetic Analysis Division 7553, Albuquerque, NM, USA
- 6 LOW ORDER POLES OF A LINEAR ANTENNA USING DIAKOPTIC THEORY. **H. Smith, E. Niver, G. Whitman**, New Jersey Institute of Technology, Electrical Engineering Dept., Newark, NJ, USA
- 7 OPTIMUM MULTIPLE FEED OF A DIPOLE ANTENNA. **S. Saoudy, M. Hamid**, University of Manitoba, Dept. of Electrical Engineering, Winnipeg, MB
- 8 FOLDED DIPOLE ANTENNAS ON A METALLIC MAST. **H.A. Kalhor, A.R. Mallahzadeh**, Shiraz University, Electrical Engineering Dept., Shiraz, Iran

## B-1-1

### A NUMERICAL SOLUTION OF THE COUPLED INTEGRAL EQUATIONS WHICH DESCRIBE THE SYMMETRIC MODES OF THE CIRCULAR DIFFRACTION ANTENNA WITH A RECESSED CENTER POST

Douglas J. Riley  
Sandia National Laboratories  
Electromagnetic Applications Division, 2322  
Albuquerque, New Mexico 87185

The circular diffraction antenna with a recessed center post, shown in Figure 1, represents a simplified model for multiwire umbilical connectors used on aircraft. It is of interest to predict power levels received by the load  $Z_1$ , over a wide frequency range, for arbitrary angle of plane wave incidence and recession depth of the center post. To obtain a complete solution, one must examine all TE and TM modes within the waveguides. The solution considered in this paper represents a partial solution since only the symmetric excited modes are considered. However, in the low frequency regime when only a TEM mode propagates within the coaxial line, the power delivered to the load is completely given by the solution presented here. In the high frequency regime, the power delivered to the load by each propagating symmetric mode is determined by using multimode transmission line theory. Examples are presented in this paper which depict the variation of the coaxial effective height, coaxial aperture admittance, and delivered load power as a function of frequency and also recession depth of the center post.

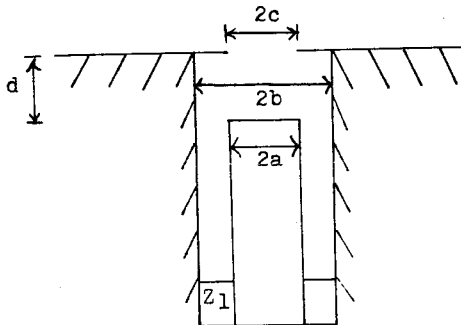


Figure 1: The circular diffraction antenna with a recessed center post.

A METHOD FOR EXACT INTEGRATION OF VECTOR POTENTIALS  
OF THIN DIPOLE ANTENNAS

P. L. Overfelt

Michelson Laboratory, Physics Division  
Naval Weapons Center, China Lake, California 93555

Radiation or far-field approximate expressions for the vector potentials of thin dipole antennas with various current distributions are well known. Less familiar are expressions which are valid in the induction and near-fields of such antennas. One such expression can be found assuming a sinusoidal current distribution (Stratton, Electromagnetic Theory, 454-457, 1941), but a general method for deriving exact vector potentials for arbitrary current distributions does not appear available.

In this paper, we derive vector potentials based on constant, sinusoidal, triangular, and polynomial (of any degree) current distributions by performing the integrals exactly. Several variable transformations are used to express the integrand as an infinite series of Bessel functions, the arguments of which do not depend on the variable of integration. The integration is easily done, and the solution is transformed back to the original variables. Such solutions are completely general and independent of the usual restrictions involving the wavelength, distance to the observation point, and dipole length. In particular, the solution for a constant current distribution is shown to reduce to its far-field form under appropriate conditions. Convergence properties are discussed, and numerical results comparing the exact solutions to their far-field forms are presented.

## B-1-3

### A Coaxial Waveguide Opening into a Ground Plane and Covered by a Dielectric Hemisphere

Robert D. Nevels and J. Edward Wheeler  
Department of Electrical Engineering  
Texas A&M University  
College Station, Texas, 77843

A coaxial waveguide opening into a ground plane and covered by a dielectric hemisphere is investigated. Two configurations are considered, a coax with a flat center conductor (figure 1) and one with a hemispherical center conductor extension (figure 2). Both are excited by an incident TEM wave and the frequency is chosen for single mode operation.

The field equivalence principle and image theory are used to separate the cylindrical and spherical geometries of the problem and analytic Green's functions are derived for the fields. By requiring continuity of the tangential magnetic field in the waveguide aperture an integral equation is obtained. Using the method of moments the integral equation is solved for the aperture magnetic current. The electric and magnetic fields can then be obtained using the Green's functions.

Results are presented for selected values of the hemisphere dielectric constant. Impedance as a function of the device dimensions (or frequency of excitation) is presented. Near field power flow from the aperture is presented graphically and the far field power density patterns are also presented.

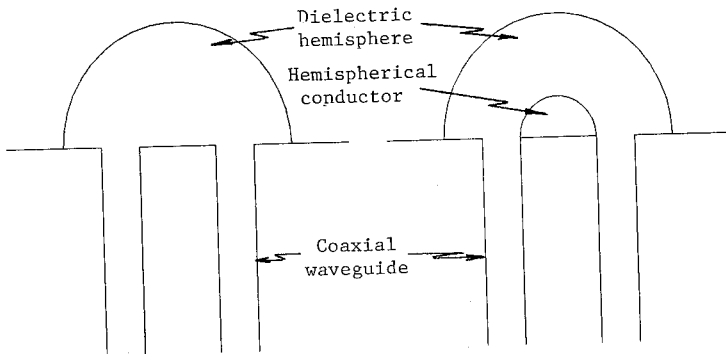


figure 1

figure 2

A NEW SIMPLE LEAKY WAVE ANTENNA  
FOR MILLIMETER WAVES

A. A. Oliner  
Polytechnic Institute of New York  
Brooklyn, New York, USA

and

P. Lampariello  
University of Rome "La Sapienza"  
Rome, Italy

Traveling wave antenna structures at millimeter wavelengths must be simple in form, to minimize fabrication difficulties, and be based on a low-loss waveguide, so that the radiation per unit length does not have to compete with the waveguide attenuation. We here propose and analyze a new leaky wave antenna structure that addresses both of these considerations, and is particularly simple in form.

The new structure consists of groove guide that is bisected with a metal wall along the long axis of its cross section. The cross section then looks like a length of parallel plate guide with a short tee stub near its center but on one side only. One end of the parallel plate section is short-circuited (at an optimum location) so that radiation occurs from one end only.

An accurate analysis in equivalent circuit form has been conducted for the tee stub configuration based on a variational formulation, and then this equivalent circuit was employed in a transverse resonance procedure to yield a simple but accurate dispersion relation for the phase and leakage constants of the leaky wave antenna structure. The structure is found to be versatile in that it can furnish either narrow beams or relatively wide beams, depending on the design. Optimization considerations relating to the relative dimensions of the cross section are also presented in the context of some numerical results.

## B-1-5

### Analysis of a Finite Length Tubular Monopole Antenna Driven by a Coaxial Line and Precision Admittance Measurements

Marvin E. Morris  
Electromagnetic Analysis Division 7553  
Sandia National Laboratories  
Albuquerque, NM 87185

In this paper, the problem of a coaxially-driven, finite length tubular monopole antenna over an infinite ground plane is formulated as a rigorous boundary value problem. The resulting coupled pair of singular integral equations is numerically solved for the electric field in the end of the coaxial line and for the total current on the antenna. The electric field is used to compute the admittance of the antenna. The admittance, electric field, and current are presented for a wide range of experimentally useful parameters. Precision admittance measurements are presented for a range of drive frequencies, antenna lengths, and drive geometry configurations.

LOW ORDER POLES OF A LINEAR ANTENNA  
USING DIAKOPTIC THEORY

Howard Smith, Edip Niver and Gerald Whitman  
Electrical Engineering Department  
New Jersey Institute of Technology  
Newark, N.J. 07102

The diakoptic theory (1), which has been successfully applied to the analysis of multielement antennas in free space, is extended to obtain a frequency dependent expression for the input impedance of a dipole. This expression is used to determine the lower order poles of the radiating structure.

The thin linear antenna is diakopted into electrically short segments. Each segment is treated as a two-port network. An impedance matrix is found which characterizes coupling between segments. By expanding the free space Green's function in a power series in wavenumber  $k$  each entry in the resultant impedance matrix is obtained as a function of frequency (2). Enforcement of continuity of currents and equality of scalar potentials at the nodes of the diakopted structure yield a system of linear equations. It's solution yields the current distribution and hence, a frequency dependent admittance expression. The poles of this function are determined using a numerical scheme. Lower order poles are observed to be in a good agreement with the reference solution obtained using the Singularity Expansion Method (3).

References

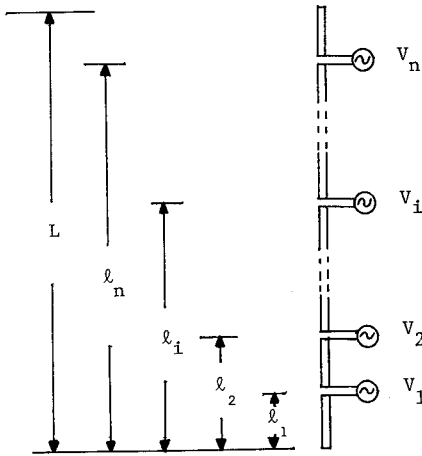
- (1) G. Goubau, N.N. Puri and F.K. Schwing, "Diakoptic Theory for Multielement Antennas", IEEE Trans. Antennas and Propagat., vol., AP-30, pp. 15-26, 1982.
- (2) H. Smith, E. Niver and G. Whitman, "Frequency Dependent Input Impedance Function of a Thin Linear Antenna", submitted for a presentation in International Symposium on Antenna and EM Theory, Beijing, China, August 24-26, 1985.
- (3) F.M. Tesche, "On the Analysis of Scattering and Antenna Problems Using the Singularity Expansion Technique", IEEE Trans. Antennas and Propagat., vol. AP-21, pp. 52-59, 1973.

## OPTIMUM MULTIPLE FEED OF A DIPOLE ANTENNA

*S. Saoudy and M. Hamid*  
 Antenna Lab., Elec. Eng. Dept.  
 University of Manitoba  
 Winnipeg, Canada, R3T 2N2

### ABSTRACT

The gain of a dipole antenna of any length ( $L$ ) and wire radius ( $a$ ) is computed by the method of moments for an arbitrary number ( $n$ ) and location of voltage sources along the dipole. An optimization routine is also employed to maximize the gain for any given number of sources and antenna length in order to determine the optimum complex amplitude and location ( $l_i, i=1,2,\dots,n$ ) of each voltage source. The results are presented for a wide range of antenna length and number of sources. It is shown that the gain and beamwidth are improved by this technique at the expense of a more complicated feed network.

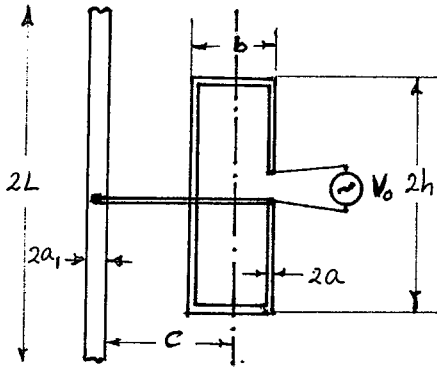


Schematic diagram of the multiply fed dipole.

FOLDED DIPOLE ANTENNAS ON A METALLIC MAST

H. A. Kalhor and A. R. Mallahzadeh  
 Electrical Engineering Department, Shiraz University  
 Shiraz, Iran

Most of development work on these antennas which find application in VHF and UHF bands are done by antenna manufacturers and technical details do not appear in the public literature. We have studied stacked folded dipoles mounted on metallic masts and electrically connected to them. The figure shows such antenna with one folded element.



An integral equation of Hallen type is derived for the current distribution on the antenna and the mast. Numerical solution of this integral equation gives the current distribution from which the radiation pattern and the input impedance are calculated. Numerical results are compared against experimental results and good agreement is observed. For one folded element with parameters  $\ln \frac{2h}{a} = 5, b = 10a, a_1 = 4a, L = 2h$  and different  $c/b$  ratios the input impedance of  $\frac{\lambda}{2}$  antenna is as shown:

$c/b$	$Z_{in}$	$c/b$	$R_{in}$ (resonance)	$h/\lambda$ (resonance)
2.5	171.061 + j214.45	2.5	112.50	0.2240
2.75	192.18 + j226.22	2.75	123.80	0.2234
3.0	217.70 + j235.52	3.0	135.10	0.2225

The input impedance and the radiation resistance depart significantly from those of a folded dipole in free space. The reduction is due to shorting effect of the mast.



## URSI COMMISSION B - SESSION B2

## Numerical Techniques I

8:30 - 12:00  
IRC-4

## Techniques numériques I

Chairperson/Président: **D.R. Wilton**, University of Houston, Houston, TX, USA

- 1 INTEGRAL EQUATION FORMULATION FOR IRREGULAR BOUNDARIES: NOVEL APPLICATION OF GALERKIN EXPANSIONS. **L.N. Medgyesi-Mitschang, J.M. Putnam**, McDonnell Douglas Research Laboratories, St. Louis, MO, USA
- 2 HYBRID SOLUTIONS FOR SCATTERING FROM IMPERFECTLY CONDUCTING BODIES. **D.-S. Wang, L.N. Medgyesi-Mitschang**, McDonnell Douglas Research Laboratories, St. Louis, MO, USA
- 3 A HYBRID EQUATION APPROACH FOR THE SOLUTION OF ELECTROMAGNETIC SCATTERING PROBLEMS INVOLVING TWO-DIMENSIONAL INHOMOGENEOUS DIELECTRIC CYLINDERS. **Z. Gong, A.W. Glisson**, University of Mississippi, Dept. of Electrical Engineering, University, MS, USA
- 4 BEHAVIOR OF SOLUTIONS OF THE COMBINED FIELD INTEGRAL EQUATION FORMULATION OF ELECTROMAGNETIC SCATTERING AND ITS GENERALIZATION. **P.L. Huddleston, L.N. Medgyesi-Mitschang, J.M. Putnam**, McDonnell Douglas Research Laboratories, St. Louis, MO, USA
- 5 QUASI-TEM ANALYSIS OF ISOLATED AND COUPLED MICROWAVE TRANSMISSION LINES BY THE FINITE ELEMENT METHOD. **Z. Pantic, R. Mittra**, University of Illinois, Electromagnetic Communication Laboratory, Urbana, IL, USA
- 6 TRIANGULAR ELEMENT ANALYSIS OF SCATTERING BY ARBITRARY PLANAR PERIODIC SURFACES. **J.P. Montgomery, E.J. Kuster**, Georgia Institute of Technology, Georgia Tech Research Institute, Atlanta, GA, USA
- 7 ELECTROMAGNETIC SCATTERING FROM ELECTRICALLY LARGE COATED STRIPS. **J.M. Putnam, L.N. Medgyesi-Mitschang**, McDonnell Douglas Research Laboratories, St. Louis, MO, USA
- 8 RADIATION AND SCATTERING FROM ELECTRICALLY SMALL CONDUCTING BODIES OF ARBITRARY SHAPE. **E. Arvas**, Rochester Institute of Technology, Rochester, NY, USA; **R.F. Harrington, J.R. Mautz**, Syracuse University, Syracuse, NY, USA
- 9 PHASE ESTIMATION IN TWO DIMENSIONAL NUMERICAL INTEGRATION. **R.J. Pogorzelski**, TRW Space and Technology, Redondo Beach, CA, USA
- 10 EFFICIENT NUMERICAL TECHNIQUES FOR SOLVING ELECTROMAGNETIC FIELD PROBLEMS. **T.K. Seshadri, K. Rajaiah, B.K. Sinha**, Centre for Electromagnetics, Department of Electronics, Madras, India

## B-2-1

### INTEGRAL EQUATION FORMULATION FOR IRREGULAR BOUNDARIES: NOVEL APPLICATION OF GALERKIN EXPANSIONS

L. N. Medgyesi-Mitschang and J. M. Putnam  
McDonnell Douglas Research Laboratories  
P. O. Box 516  
St. Louis, MO 63166

Electric or magnetic integral equation (EFIE or MFIE) formulations have been used to represent the scattering processes for objects not conforming to separable geometries. Method of moments (MM) solutions offer great flexibility in geometries that may be treated. Entire domain Galerkin expansions are often analytically convenient and computationally highly efficient in implementing solutions for classes of one-, two-, and three-dimensional scatterers and can be used for surfaces with irregular boundaries. In EFIE or MFIE formulations of such bodies, the boundary irregularities are embedded in the integro-differential operators. The structure of the MM solutions are examined for these cases, with emphasis on the EFIE formulation. The concepts are illustrated in detail for one class of three-dimensional problems, namely finite circular cylinders with irregular edges. Entire domain Galerkin representations are used for the axial and circumferential currents. The coupling of these currents are examined as a function of the boundary irregularity (stochastic or deterministic) and compared with previous results for finite cylinders. Extensions of these concepts to the MFIE formulation will be discussed.

HYBRID SOLUTIONS FOR SCATTERING  
FROM IMPERFECTLY CONDUCTING BODIES

D.-S. Wang and L. N. Medgyesi-Mitschang  
McDonnell Douglas Research Laboratories  
P. O. Box 516  
St. Louis, MO 63166

An extension of the hybrid method, originally developed for perfectly conducting and partially coated bodies (IEEE Antennas Propagation, Vol. AP-31, No. 4, 570, 1983 and Vol. AP-32, No. 7, 717, 1984), is presented for electromagnetic scattering from electrically large bodies, coated or consisting of lossy material. An integral equation arising from the impedance (Leontovich) boundary condition is solved by incorporating physical optics (PO) and Fock Ansatzes for the surface currents into a method of moments (MM) solution. High-frequency methods are used to evaluate the currents on the smooth convex part of the scatterer so that the number of unknowns required in the MM is substantially reduced; hence, electrically large scatterers can be treated. The use of the MM technique enables the treatment of irregular surfaces, such as geometric/material discontinuities and edges, not amenable to the geometric or physical theories of diffraction.

The formulation is particularized to axisymmetric scatterers. Numerical results for spheres, compared with the Mie solution, illustrate the range of validity of the impedance boundary condition as to the material properties and geometry of the scatterers. Representative results are presented for bodies of revolution with and without surface discontinuities and edges. For body dimensions near the resonance region, the results are correlated with MM solutions; for electrically large scatterers, the results are compared with recently measured data.

**A HYBRID EQUATION APPROACH FOR THE SOLUTION  
OF ELECTROMAGNETIC SCATTERING PROBLEMS INVOLVING  
TWO-DIMENSIONAL INHOMOGENEOUS DIELECTRIC CYLINDERS**

Zhengquan Gong and Allen W. Glisson  
Department of Electrical Engineering  
University of Mississippi  
University, MS 38677

A numerical procedure is presented for the solution of electromagnetic scattering problems involving inhomogeneous dielectric cylinders which have arbitrary cross section. The cases of illumination by both TM and TE plane waves are considered. The scattering problems are formulated via a hybrid integral equation/partial differential equation approach in which the inhomogeneous region is modeled by the partial differential equation for the electric field and the radiation condition is incorporated by enforcing an integral equation at the surface of the inhomogeneous region. The surface integral equation is developed in the usual manner via application of the equivalence principle so that the fields exterior to the body are radiated by equivalent electric and magnetic surface currents  $\underline{J}$  and  $\underline{M}$ . Line segments are used to model the cylinder surface while the interior region is gridded into triangular cells. Appropriate testing functions and basis functions for the unknown surface currents  $\underline{J}$  and  $\underline{M}$  and for the unknown interior electric field are chosen, and the method of moments is applied to produce a system of simultaneous equations which may be solved for the unknown quantities.

The partial differential equation for the interior region and the surface integral equation are coupled in such a manner that existing surface integral equation computer codes for treating problems involving scattering by homogeneous cylinders can be used to generate the block of the matrix corresponding to the surface current interactions. It is necessary only to modify a few elements near the diagonal of this matrix block in a straightforward manner. The remaining blocks of the matrix, which comprise the interior differential equation elements and the elements due to coupling between the surface and the interior region, are very simple to generate and are sparse. The system matrix is therefore largely sparse and should be amenable to specialized matrix solution techniques or iteration. In addition, the procedure has the advantage that more scatterers may be included in the vicinity of the inhomogeneous body with the usual simplicity of moment method formulations, while still retaining the partially sparse nature of the matrix.

BEHAVIOR OF SOLUTIONS OF THE COMBINED FIELD INTEGRAL  
EQUATION FORMULATION OF ELECTROMAGNETIC  
SCATTERING AND ITS GENERALIZATION

P. L. Huddleston, L. N. Medgyesi-Mitschang, and J. M. Putnam  
McDonnell Douglas Research Laboratories  
P. O. Box 516  
St. Louis, MO 63166

Formulations of electromagnetic scattering for closed, perfectly conducting bodies based on the electric field integral equation (EFIE) or the magnetic field integral equation (MFIE) are known to suffer from nonuniqueness of their solutions at frequencies associated with internal cavity resonances. The combined field integral equation (CFIE) formulation, which involves a linear combination of these two integral equations using a coupling parameter has been proved to provide unique solutions at these internal resonances (J. R. Mautz and R. F. Harrington, AEU 32, 159-164, 1978).

An electromagnetic scattering formulation for dielectrically coated, perfectly conducting bodies that treats the conducting surface by either the EFIE or the MFIE approach also leads to nonuniqueness at internal resonances. To remedy this problem, a generalization of the CFIE formulation to treat conductors with layered dielectric coatings is proposed. This generalized formulation is proved to provide unique solutions at all frequencies.

Results on the dependence of the numerical solutions of the CFIE and the generalized CFIE on the coupling parameter are presented for a variety of body-of-revolution configurations.

## QUASI-TEM ANALYSIS OF ISOLATED AND COUPLED MICROWAVE TRANSMISSION LINES BY THE FINITE ELEMENT METHOD

Zorica Pantic\* and Raj Mittra  
Electromagnetic Communication Laboratory  
University of Illinois  
Urbana, Illinois 61801

Accurate prediction of the characteristic impedance, attenuation, coupling, crosstalk, etc., in microstrips, striplines and similar transmission lines is important in digital circuit design, communication and other applications. In this paper a computer-aided analysis of isolated and coupled microwave transmission lines of arbitrary cross section is presented. The analysis is based on a quasi-TEM model that is adequate for typical pulse rise times of interest and is sufficiently accurate for lower microwave frequencies. The characteristics of isolated lines as well as the even- and odd-mode propagation in coupled transmission lines are investigated.

The finite element method employing both the first order and higher order triangular elements is used to solve for the quasistatic potential and the corresponding electric field distribution in the transmission lines. It is shown that the accuracy and efficiency of computation can be significantly enhanced via the use of the high-order elements as compared to the case where only the first-order elements are employed. However, the first-order elements are found to be better suited for modeling boundaries of complex shape. Once the potential distribution is known, the capacitance per unit length of the transmission line is obtainable from the variational expression, and the effective permittivity as well as the characteristic impedance of the line can be readily calculated. Next, the conductor and dielectric losses can be estimated using a perturbational approach.

One of the principal advantageous features of the finite element method is that it is capable of handling transmission lines with rather arbitrary configurations. Lines treatable by the technique described in this paper may contain an arbitrary number of conductors of arbitrary shape and inhomogeneous dielectric regions that can be approximated locally by a number of homogeneous subregions. In contrast, the spectral-domain methods are often restricted to conductors that are thin strips and dielectrics that have planar interfaces.

The paper describes two different computer software packages that have been developed for solving the problem at hand. The first of these is employed for semiautomatic generation of either the first or the high-order triangular element meshes. The second package calculates the potential and field distributions, capacitance per unit length, characteristic impedance, effective permittivity, and attenuation due to conductor and dielectric losses.

The results obtained using the finite element procedure have been compared for various types of isolated and coupled microwave transmission lines and have been found to agree well with the available theoretical and experimental data.

---

\*Visiting Fulbright Scholar from the University of Niš, Yugoslavia.

TRIANGULAR ELEMENT ANALYSIS OF SCATTERING BY  
ARBITRARY PLANAR PERIODIC SURFACES

J. P. Montgomery and E. J. Kuster  
Georgia Tech Research Institute  
Georgia Institute of Technology  
Atlanta, Georgia 30332

The electromagnetic scattering by a planar periodic structure has been discussed for both aperture (C. C. Chen, IEEE Trans. MTT, 627-632, 1970) and conducting (J. P. Montgomery, IEEE Trans. AP, 70-75, 1975) structures. The purpose of this paper is to discuss the application of a triangular patch basis function (S. M. Rao, et. al., IEEE Trans. AP, 409-418, 1982) to these planar periodic structures. The triangular patch lends itself well to very arbitrary shapes, including those not easily analyzed by rectangular patches (B. J. Rubin and H. L. Bertoni, IEEE Trans. AP, 829-836, 1983). The method has been applied to a variety of single and dual layer structures and allows for an arbitrary number of dielectric layers. Lossy conducting elements are also permitted. Input data for the program is conveniently created using interactive graphic techniques.

Several examples have been examined including a comparison with previous computations for a two layer four legged slot array and a single layer Jerusalem cross array.

## B-2-7

### ELECTROMAGNETIC SCATTERING FROM ELECTRICALLY LARGE COATED STRIPS

J. M. Putnam and L. N. Medgyesi-Mitschang  
McDonnell Douglas Research Laboratories  
P. O. Box 516  
St. Louis, MO 63166

Efficient numerical solutions for the electromagnetic scattering for classes of electrically large, coated, perfectly conducting strips, flat or curved, are presented. The formulation is based on the solution of a coupled system of electric and magnetic field integral equations using the method of moments (MM). Entire domain Galerkin representations for the currents are used on the surface of the coating and at the coating-conductor interface. The resulting matrix equation is well conditioned and admits rapid, accurate solutions. Numerical results are presented for various coating thicknesses, strip width, and curvature. The convergence of the Galerkin solution is examined as a function of these parameters. The effect of the edge approximation in the choice of expansion functions is discussed. The analytical results are compared with experimental measurements.

RADIATION AND SCATTERING FROM ELECTRICALLY SMALL  
CONDUCTING BODIES OF ARBITRARY SHAPE

Ercument Arvas  
Rochester Institute of Technology  
Rochester, NY 14623

Roger F. Harrington and Joseph R. Mautz  
Syracuse University  
Syracuse, NY 13210

A simple moment solution is given for low frequency electromagnetic scattering and radiation problems. The problem is approximated by two corresponding electrostatic and magnetostatic problems, and each static problem is then solved using the Method of Moments. The surface of perfectly conducting scatterer is modeled by a set of planar triangular patches. Pulse expansion functions and point matching testing are used to compute the charge density in the electrostatic problem. For the magnetostatic current a set of charge-free vector expansion functions is used. The induced electric and magnetic dipole moments are obtained using the computed electrostatic charge and the magnetostatic current distributions. The scattered field is computed using these dipoles. The problem is formulated assuming the scatterer to be in an unbounded homogeneous region. The scatterer is assumed to be illuminated either by an incident plane wave or by a slowly oscillating electric or magnetic dipole placed nearby. Scatterers of various shapes, such as the circular disc, the sphere, and the cube are studied. Special attention is paid to a conducting box with a narrow slot.

The results of computations are in good agreement with exact results and published numerical results. It is observed that for the same incident plane wave the induced dipole moments for a cube are slightly larger than the ones for a sphere, provided the volumes of the cube and the sphere are equal. When a tangential (perpendicular) magnetic (electric) dipole is placed at the center of a face of a cube, the induced moments are about three times less than those which would result if the dipole were placed on a sphere, irrespective of the sizes of the sphere and the cube. It is also observed that a narrow slot at the center of a face of a cube transmits energy outside less efficiently than a slot close to an edge of the cube.

The quantities involved in the computations (such as the moment matrix elements) are real. We believe that the present method may be more efficient, in terms of computer storage and time, than an EFIE method of solution which uses the same patching scheme. Also the present method gives more accurate results as the frequency gets smaller and smaller.

## B-2-9

### PHASE ESTIMATION IN TWO DIMENSIONAL NUMERICAL INTEGRATION

R. J. Pogorzelski  
TRW Space and Technology  
One Space Park  
Redondo Beach, CA 90278

In an earlier presentation this author discussed a numerical integration algorithm applicable to one dimensional complex integrals wherein the phase function can be approximated by a polynomial. (R. J. Pogorzelski, National Radio Science Meeting, Boston, MA, 1984.) The remainder of the algorithm involves expansion in Chebyshev polynomials via FFT and recursive generation of the constituent integrals. In that presentation a generalization of this algorithm to two dimensional integration was suggested. However, it was remarked that the performance of this generalization was not nearly as impressive as its one dimensional counterpart. In the present work the source of the difficulty is identified and a mitigation is suggested.

In dealing with two dimensional integrals via the above algorithm, one is faced with the necessity of estimating the phase variations associated with the interior integral as continuous functions suitable for approximation by a polynomial in carrying out the outer integration. The difficulty in obtaining such estimates was recognized by earlier workers (J. J. Starnes, et.al., *Optica Acta*, vol. 30, pp. 207-222, 1983) and resulted in their abandonment of a related approach. It is also noted that the method suggested in the previous work of this author embodies a fundamental misconception which is exhibited in the present work.

The difficulty with the previously suggested method of phase estimation centers around the introduction of an extraneous term when one attempts to use the one dimensional algorithm to evaluate the inner integral at its upper limit (or its lower limit) individually. The extraneous term introduced in the upper limit contribution is identical to that introduced in the lower limit contribution so that when the integral is evaluated by subtracting these contributions, this extraneous term cancels resulting in the correct value of the integral. However, when dealing with the two contributions individually, as one might in estimating the phase behavior of the integral, one must properly account for the extraneous term. The present work concerns analytical expression of the offending term and suggestion of means of appropriately dealing with it in the phase estimation process.

**EFFICIENT NUMERICAL TECHNIQUES FOR SOLVING ELECTROMAGNETIC  
FIELD PROBLEMS**

\*T.K. Seshadri, K. Rajalah and \* B.K. Sinha  
\* Centre for Electromagnetics  
Department of Electronics  
283, Anna Salai  
Madras 600 018, India

Several analytical techniques for solving Electro-magnetic field problems by numerical methods have been evolved for obtaining the solutions. This paper discusses in detail about the recently implemented successive integration and least collocation techniques in solving the electromagnetic field problems. The implementation of the above numerical techniques have been quite effective in the characterization of certain field structures of homogeneous and inhomogeneous types as compared to the usual numerical methods. The result of the certain TEM transmission line problems are discussed in detail and compared for its computational efficiency and suitability. Alternate approach for solving the field problems of that kind in conjunction with the pointmatching technique has also been suggested.



## URSI COMMISSION B - SESSION B3

Waves in  
Random Media

8:30 - 12:00  
IRC-6

Propagation des ondes  
dans les milieux aléatoires

Chairperson/Président: **A. Ishimaru**, University of Washington, Seattle, WA, USA

- 1 NONLINEAR STOCHASTIC TRANSPORT THEORY. **I.M. Besieris, M.E. Sockell**, Virginia Polytechnic Institute and State University, Dept. of Electrical Engineering, Blacksburg, VA, USA
- 2 LARGE-ANGLE SCATTERING IN THE CFSB APPROXIMATION. **D.A. de Wolf**, Virginia Polytechnic Institute and State University, Dept. of Electrical Engineering, Blacksburg, VA, USA
- 3 SOLUTION FOR THE FOURTH MOMENT OF WAVES PROPAGATING IN RANDOM MEDIA. **J.L. Codona, D.B. Creamer, S.M. Flatté, R.G. Frehlich, F.S. Henyey**, La Jolla Institute, Center for Studies of Nonlinear Dynamics, La Jolla, CA, USA
- 4 TWO FREQUENCY INTENSITY CORRELATION OF AN EXTENDED SOURCE SEEN THROUGH A STRONGLY SCATTERING PHASE SCREEN. **J.L. Codona, D.B. Creamer, S.M. Flatté, R.G. Frehlich, F.S. Henyey**, La Jolla Institute, Center for Studies of Nonlinear Dynamics, La Jolla, CA, USA
- 5 A TWO-DIMENSIONAL SIMULATION OF WAVE PROPAGATION THROUGH A RANDOM MEDIUM. **W.A. Coles, J.P. Filice**, University of California-San Diego, Dept. of Electrical Engineering and Computer Sciences, La Jolla, CA, USA
- 6 THEORY OF BACKSCATTERING ENHANCEMENT OF RANDOM DISCRETE SCATTERERS BASED ON THE SUMMATION OF ALL LADDER AND CYCLICAL TERMS. **L. Tsang, A. Ishimaru**, University of Washington, Dept. of Electrical Engineering, Seattle, WA, USA
- 7 THE RELATIONSHIP BETWEEN THE FIELD CORRELATION FUNCTION AND THE SPECIFIC INTENSITY. **R.H. Lang, A.M. Ghuniem**, George Washington University, Dept. of Electrical Engineering and Computer Science, Washington, DC, USA
- 8 IMPEDANCE AT A ROUGH WAVEGUIDE BOUNDARY. **J.A. DeSanto**, Colorado School of Mines, Mathematics Dept., Golden, CO, USA
- 9 SCATTERING BY ANISOTROPIC MODELS OF COMPOSITE ROUGH SURFACES-FULL WAVE SOLUTION. **E. Bahar**, University of Nebraska-Lincoln, Dept. of Electrical Engineering, Lincoln, NE, USA
- 10 TRANSMISSION AND REFLECTION OF PULSES IN A RANDOM MEDIUM. **C-M. Chu, H-F. Maa**, University of Michigan, Dept. of Electrical Engineering and Computer Science, Ann Arbor, MI, USA

## B-3-1

### NONLINEAR STOCHASTIC TRANSPORT THEORY

Ioannis M. Besieris and Michael E. Sockell  
Department of Electrical Engineering  
Virginia Polytechnic Institute and State University  
Blacksburg, Virginia 24061

An urgent need has been felt recently for a statistical generalization of the theory of nonlinear electromagnetic waves. The necessity for such an extension has been dictated by specific problems in nonlinear optics, laser physics, etc., which require the investigation of nonlinear effects in a field of random waves.

Our specific aim in this exposition is to motivate a systematic construction of a nonlinear stochastic transport theory starting from the Dyson and Bethe-Salpeter equations. The latter are derived at the level of the direct interaction and ladder approximations, respectively, following a procedure analogous to that used by Kraichman in the case of hydrodynamic turbulence. The transition from the second moment to a nonlinear Boltzmann-like radiative transfer equation for the incoherent field intensity is effected via the Wigner phase-space distribution function.

For the sake of simplicity, our discussion will be limited to scalar cw nonlinear random waves governed by a Helmholtz equation with a randomly perturbed Kerr-like index of refraction.

LARGE-ANGLE SCATTERING IN THE CFSB APPROXIMATION

David A. de Wolf  
Department of Electrical Engineering  
Virginia Polytechnic Institute and State University  
Blacksburg, VA 24061

Recently, new expressions were derived for the electromagnetic power flux scattered at large angles from a bounded medium containing weak but extensive fluctuations of the dielectric permittivity at scale sizes large compared to the wavelength. The results take Cumulative Forward scattering in account, but restrict large-angle scattering to a Single "Backscatter", hence use a "CFSB" approximation to a renormalized wave equation.

In order to make numerical calculations tractable, further approximations are introduced. The most drastic of these reduces the geometry to scattering of plane waves from cylindrical fluctuations in a half space. It is then possible to estimate the ratio of the scattered flux to that of the conventional single-scattering approximation. The power spectrum of the fluctuations is given by a single-scaled power law. Numerical results will be presented.

**SOLUTION FOR THE FOURTH MOMENT OF WAVES  
PROPAGATING IN RANDOM MEDIA**

Johanan L. Codona, Dennis B. Creamer, Stanley M. Flatté, R.G. Frehlich,  
and Frank S. Henyey

Center For Studies of Nonlinear Dynamics  
La Jolla Institute  
La Jolla, California 92037  
Affiliated with the University of California, San Diego.

Using Green's function techniques and the parabolic approximation, a series solution is developed for the fourth moment of a beamed field incident on a random phase screen or extended random medium. Each term of the series generates two expressions for the intensity correlation; one valid at low spatial frequency, the other valid at high spatial frequency. The electric field Green's function for the thin screen problem is the Fresnel kernel. The Green's function for the fourth moment is a product of four Fresnel kernels. This expression is reduced to a series by an expansion in phase structure functions. The Green's function for the field of waves propagating through an extended random medium is a Feynman path integral. The Green's function for the fourth moment is then a product of four path integrals. The Markov approximation, Gaussian refractive index fluctuations and slowly varying statistics in the propagation direction are assumed in order to perform the expectation over the random medium. The resulting expression is very similar to the thin screen derivation. A series solution similar to the thin screen result is produced by an analogous expansion in wave structure functions and a path integral identity. The same result is derived using moment equation methods: thus demonstrating that the two approaches are equivalent. The advantages of the two methods are discussed. The behavior of the leading terms is compared to previous results for plane wave and point source geometries.

**TWO FREQUENCY INTENSITY CORRELATION OF AN EXTENDED SOURCE  
SEEN THROUGH A STRONGLY SCATTERING PHASE SCREEN**

Johanan L. Codona, Dennis B. Creamer, Stanley M. Flatté, R.G. Frehlich,  
and Frank S. Henyey

Center For Studies of Nonlinear Dynamics  
La Jolla Institute  
La Jolla, California 92037  
Affiliated with the University of California, San Diego.

Intensity scintillations caused by waves from an incoherent, extended source passing through a random phase screen are considered. As a starting point, the intensity cross-spectrum of a plane wave incident on a thin screen will be modeled. For monochromatic light, the intensity power spectrum at high spatial frequencies is known to be given by the Fourier transform of the square of the second moment. It is also known that this "fully saturated" approximation is a poor model for the two frequency intensity cross-spectrum due to an exponential factor involving the mean-square phase shift. By considering the two frequency fourth moment, we show that the fully saturated approximation breaks down when the outer scale is large compared with the diameter of the scattering disk. One of the methods for dealing with this problem has been to drop the mean-square phase shift factor entirely. A new approximation is obtained from the two frequency fourth moment which has essentially the same limits of validity as the fully saturated approximation in the monochromatic case. The fully saturated result is recovered at very high spatial frequencies while at lower frequencies the result is equivalent to ignoring the mean-square phase shift factor. The physical significance of the new approximation will be discussed. At very low spatial frequencies a separate approximation is required. This leads to a model for the plane-wave intensity cross-spectrum at all spatial frequencies. The modification to the plane-wave result for an extended, incoherent source will be shown. Scaling laws relating the intensity decorrelation bandwidth, strength of scattering, and the source diameter will be presented.

## B-3-5

### A TWO-DIMENSIONAL SIMULATION OF WAVE PROPAGATION THROUGH A RANDOM MEDIUM

W. A. Coles and J. P. Filice  
Dept. of Electrical Engineering and Computer Sciences  
University of California, San Diego, La Jolla, CA 92093

The problem of the propagation of waves through a random medium is analytically intractable in many cases of practical interest. It is also difficult to study experimentally because of the difficulty of controlling or even characterizing the random medium. We will discuss a digital simulation of this problem for narrow angle forward scatter.

In this simulation a random medium is approximated by a series of phase screens separated by free space. Each phase screen is generated from a sequence of pseudo-random numbers scaled so that the screen is a sample from an ensemble with a specified phase power spectrum. An incident wave of specified geometry is generated and the field at some observing plane is calculated using an integral solution to the parabolic wave equation. Stable estimates of the field statistics can be obtained through repeated calculations.

This technique has many advantages over a direct numerical solution of the equations for the field statistics. It is more comparable to an idealized experiment than a numerical analysis. With this tool one can easily change the spectrum of the medium, the experimental geometry, or the field statistics of interest. The number of grid points required for the discrete approximation increases as the fourth power of the turbulence level; therefore the simulation is limited in practice to cases where the intensity variance calculated in the Born approximation is less than 100. This is convenient because below this limit strong scattering asymptotic approximations break down and the simulation is most needed. The problem of choosing the sampling interval in the phase screens, the number of phase screens required to represent the medium, and determining the effect of these choices on the results is analyzed.

The simulation is applied to the case of a plane wave incident on a thin screen and also that of a point source in a homogeneous random medium. Comparisons with experiments (atmospheric optics and radio propagation in the solar wind) and theory (strong scattering asymptotic theory and weak scattering Born theory) are presented. Finally results are presented for the intensity variance and spatial scales for the case of a power law turbulence spectrum containing an inner scale.

THEORY OF BACKSCATTERING ENHANCEMENT OF RANDOM DISCRETE  
SCATTERERS BASED ON THE SUMMATION OF ALL  
LADDER AND CYCLICAL TERMS

Leung Tsang and Akira Ishimaru  
Department of Electrical Engineering  
University of Washington  
Seattle, Washington 98195

In recent years theoretical and experimental studies have been carried out extensively in relation to remote sensing of the atmosphere and earth terrain such as vegetation, snow, ice-covered land, soil, etc. The radiative-transfer theory has been widely used because it is simpler than the wave theory and has also been shown to be consistent with the wave theory based on the ladder approximation of the Bethe-Salpeter equation. However, the radiative-transfer theory does not account for backscattering enhancement that is a result of multiple-scattering effects. A diagrammatic analysis of the ladder approximation which is consistent with the radiative-transfer theory shows that enhancement of backscattering is not exhibited because the cyclical diagrams which contribute significantly in the backscattering direction have been ignored. Backscattering enhancement of random discrete scatterers was previously investigated by a second-order theory. The theory predicts a sharp peak of angular width of the order  $2K''/K'$  where  $K'$  and  $K''$  are the real and imaginary parts, respectively, of the effective propagation constant. The second-order theory includes first-order scattering, the second-order ladder term, and the second-order cyclical term. However, the second-order solution is not adequate when the albedo and the optical thickness of the scattering medium become appreciable. In this paper, by using the model of isotropic point scatterers, we investigate the multiple-scattering phenomenon by summing all the ladder and cyclical terms. The summation of all the ladder terms leads to the classical Schwarzschild-Milne integral equation with the exponential integral as kernel, the solution of which can be readily calculated. The summation of the cyclical terms leads to a two-variable cyclical-transfer integral equation with a more general kernel. The integral equation is then solved numerically, and the results thus include all the multiple scattering associated with the cyclical terms. Numerical results are illustrated as a function of scattering angle, albedo, and optical thickness. Results differ significantly from the second-order theory for appreciable optical thickness and albedo. The multiple-scattering solution also gives a sharper backscattering peak than the second-order solution. The ability to determine the angular distribution of the bistatic scattering coefficient around the backscattering direction has important applications in remote sensing because receivers generally have a finite angular width in their receiving pattern.

THE RELATIONSHIP BETWEEN THE FIELD CORRELATION  
FUNCTION AND THE SPECIFIC INTENSITY

R. H. Lang and A. M. Ghuniem

Department of Electrical Engineering & Computer Science  
The George Washington University  
Washington, D. C. 20052

The general relation between the two-point correlation function of the field and the specific intensity is obtained for a medium of sparsely distributed discrete random scatterers. Starting from the scalar wave equation, an approximate equation for the correlation function of the field is derived by using the Foldy-Lax-Twersky assumption. By appropriately scaling this equation, the fractional volume is introduced as a small parameter, and a two variable perturbation technique is applied. It is found that the zeroth order approximation to the correlation equation can be represented as an angular transform of a two point specific intensity function. This specific intensity function satisfies a generalized transport equation.

Further analysis shows that this two point specific intensity function can be directly related to the ordinary one point specific intensity function which satisfies the standard transport equation. Combining these two results shows that the two point correlation function of the field is directly related to the specific intensity. The result differs from a similar relation appearing in the literature, however, it reduces to it in the high frequency limit where the particles are pre-dominantly forward scattering.

**IMPEDANCE AT A ROUGH WAVEGUIDE BOUNDARY**

Dr. John A. DeSanto  
Center for Wave Phenomena  
Mathematics Department  
Colorado School of Mines  
Golden, CO 80401

The impedance at the randomly rough upper boundary of an ocean waveguide is derived. The sound speed of the waveguide is an arbitrary function of depth. The boundary surface height is assumed to be a statistically homogeneous Gaussian process. Integral equations for the Green's function and its normal derivative on the boundary are derived. These are solved to second order in the surface interaction. The result is a rational approximation to the impedance in terms of the waveguide Green's function and the statistical properties of the surface. The special cases of small and large roughness as well as that of a constant sound speed profile are presented. For simplicity we restrict the analysis to a semi-infinite waveguide where the waveguide Green's function vanishes at the surface (Dirichlet problem).

**SCATTERING BY ANISOTROPIC MODELS OF COMPOSITE  
ROUGH SURFACES--FULL WAVE SOLUTION**

E. Bahar  
Electrical Engineering Department  
University of Nebraska--Lincoln  
Lincoln, NE 68588

**ABSTRACT**

Various combinations of physical optics theory and perturbation theory have been used to determine the scattering cross sections for composite models of rough surfaces. These solutions are based on a two-scale model of the rough surface. Physical optics accounts for specular point scattering from the large scale surface while perturbation theory accounts for Bragg scattering from the small scale surface. However, the results based on the perturbed-physical optics approach critically depend upon the manner in which the composite surface is decomposed into a large and a small scale surface.

Since the full wave approach accounts for specular point scattering and Bragg scattering in a unified self-consistent manner, the solutions for the scattering cross sections can be derived from a single integral. However, the two-scale model can also be adopted when the full wave approach is used and the results are shown to be independent of the wavenumber  $k_d$  where spectral splitting is assumed to occur, provided that the large scale surface satisfies the criteria for deep phase modulation (E. Bahar, et al., IEEE Trans. on Antennas and Propagation, AP-31, 5, 698-709, 1983).

In this work, the full wave approach is applied to a rough surface characterized by an anisotropic slope probability density function. The full wave solutions based on the unified and two-scale model are presented. Backscatter cross sections for both vertically and horizontally polarized waves are evaluated for all angles of incidence and it is shown that the results are most sensitive to wind direction for angles of incidence around  $40^\circ$ . On examining the individual terms for the total cross sections based on the two-scale model, it is shown that the cross sections become insensitive to wind direction for near grazing incidence.

**TRANSMISSION AND REFLECTION OF PULSES IN A RANDOM MEDIUM**

C-M Chu and Hsiao-Fei Maa  
Radiation Laboratory  
Department of Electrical Engineering and Computer Science  
The University of Michigan  
Ann Arbor, Michigan 48109

**Abstract**

This paper starts with the derivation of a set of coupled partial differential equations governing two frequency mutual coherence functions of the transmitted and reflected waves due to a plane wave normally incident on a layer of random medium. The derivation is based on the parabolic equation formulation of Tatarskii (Zh. Eksp. Teor. Fiz., 56, 2106-2117, 1969), but a backward component is added to include the effect of backscattering and to preserve energy conservation.

Approximate, closed form solutions for the two frequency mutual coherence functions are obtained. The results are expressed in the form of a scattering matrix, relating the two frequency mutual functions of the transmitted and reflected waves to that of the incident plane wave.

Application of the analytical results to the transmission and reflection of high frequency pulses in random layers of various permittivity fluctuations and thicknesses are presented. The conservation of energy in this formulation is demonstrated.



## URSI COMMISSION B - SESSION B4

## Microstrip Antennas I

1:30 - 5:00  
IRC-6

## Antennes microlignes I

Chairperson/Président: **Y.T. Lo**, University of Illinois, Urbana, IL, USA

- 1 SUPERSTRATE EFFECTS ON THE MICROSTRIP PATCH ANTENNA. **S. O'Connor, S. Rengarajan**, California State University-Northridge, Northridge, CA, USA
- 2 STUDY OF THE PROBE FEED FOR MICROSTRIP ANTENNAS. **M. Davidovitz, Y.T. Lo**, University of Illinois at Urbana-Champaign, Dept. of Electrical and Computer Engineering, Urbana, IL, USA
- 3 QUASISTATIC TERMS FOR INTERIOR FIELDS OF MICROSTRIP ANTENNAS. **W.F. Richards**, University of Houston, Dept. of Electrical Engineering, Houston, TX, USA
- 4 NUMERICAL COMPUTATION OF THE GREEN'S FUNCTION FOR INTERIOR FIELDS OF NON-SEPARABLE MICROSTRIP ANTENNAS. **W.F. Richards, C.M. Butler**, University of Houston, Dept. of Electrical Engineering, Houston, TX, USA
- 5 REFINEMENT OF THE RADIATING-SLOT MODEL FOR MICROSTRIP ANTENNAS TO ACCOUNT FOR NEAR-FIELD PHENOMENA. **E.F. Kuester, D.C. Chang, T.M. Martinson**, University of Colorado, Dept. of Electrical and Computer Engineering, Boulder, CO, USA
- 6 ANALYSIS OF TUNABLE CIRCULAR PATCH ANTENNAS. **G.-L. Lan, D.L. Sengupta**, University of Michigan, Dept. of Electrical Engineering and Computer Science, Ann Arbor, MI, USA
- 7 SPECTRAL-DOMAIN ANALYSIS OF MICROSTRIP ANTENNAS USING THE CONJUGATE GRADIENT ALGORITHM. **R. Kastner, A. Sabban**, Rafael, Haifa, Israel; **E. Heyman**, Tel-Aviv University, Dept. of Electrical Engineering, Tel-Aviv, Israel
- 8 AN ASYMPTOTIC EVALUATION OF THE MUTUAL COUPLING BETWEEN 2-D STRIPS ON A DIELECTRIC COATED CIRCULAR CYLINDER. **B.W. Kwan**, Florida State University, Institute of Engineering, Tallahassee, FL, USA; **R.G. Kouyoumjian, E.H. Newman**, Ohio State University ElectroScience Laboratory, Dept. of Electrical Engineering, Columbus, OH, USA
- 9 AN EIGENFUNCTION SOLUTION FOR THE MUTUAL COUPLING BETWEEN MICROSTRIP MODES ON A DIELECTRIC COATED CYLINDER. **B.W. Kwan**, Florida State University, Institute for Engineering, Tallahassee, FL, USA; **E.H. Newman, R.G. Kouyoumjian**, Ohio State University ElectroScience Laboratory, Dept. of Electrical Engineering, Columbus, OH, USA
- 10 ANALYSIS OF APERTURE COUPLED PATCH ANTENNA. **P.L. Sullivan, D.H. Schaubert, D.M. Pozar**, University of Massachusetts, Dept. of Electrical and Computer Engineering, Amherst, MA, USA

## B-4-1

### SUPERSTRATE EFFECTS ON THE MICROSTRIP PATCH ANTENNA

Stephen O'Connor  
Sembiam Rengarajan  
California State University, Northridge  
Northridge, California 91330

A spectral domain analysis of rectangular microstrip patch antennas (Itoh and Menzel, IEEE AP. Trans., 29, 63-68, 1981) provides results on the resonant frequency, radiation pattern, and bandwidth. In this paper, the above analysis has been modified to study the effects of a dielectric superstrate on the resonant frequency, copolar and crosspolar radiation patterns, and bandwidth. In the literature, superstrate effects on printed dipoles have been analyzed in terms of Sommerfeld integrals (soares et al., IEEE AP. Trans., 32, 1149-1153, 1984). The application of such a technique for a microstrip patch is very involved. The spectral domain is an elegant and simple alternative, maintaining the same theoretical rigor. Computed results in this work are compared to similar published results. These results will be useful in evaluating the effects of a dielectric cover or environmental effects like rain or snow on a microstrip patch antenna.

## STUDY OF THE PROBE FEED FOR MICROSTRIP ANTENNAS

M. Davidovitz, Y. T. Lo  
Department of Electrical and Computer Engineering  
University of Illinois at Urbana-Champaign  
Urbana, IL 61801

In order to facilitate the analysis of various microstrip patch antenna problems, the feeding structures have been in most cases simplified by replacing the actual feed by an ideal current probe or ribbon. Such idealized models have been shown to be adequate for calculating the input impedance of the microstrip patches when the thickness of the dielectric substrate is small compared to the wavelength. However, such models fail to predict accurately the input impedance of the microstrip antenna as the substrate thickness increased. In the case of the probe feed, this failure is due primarily to the fact that the boundary conditions on the probe are not satisfied.

In this paper a canonical model for the probe fed microstrip patch is proposed and analyzed. The model consists of a circular patch fed by an arbitrarily located probe of finite radius. The analysis is simplified by assuming that the sides of the patch are enclosed by PMC. The problem is thus reduced to the one of a magnetic wall cavity fed by an eccentrically located probe. An integral equation for the electric field in the aperture of the coaxial feed is solved by the mode-matching method. The addition theorem for Bessel functions is used in constructing the modes of the magnetic wall cavity with an eccentrically placed inner conductor. The cutoff frequencies of this structure are computed by finding the zeros of a determinant, whose elements are transcendental functions of the frequency. The modes of the magnetic wall cavity with an eccentrically placed inner conductor are constructed and shown to satisfy boundary conditions on the probe, as well as the PMC wall. The input impedance of the microstrip antenna is computed and compared with available experimental data.

## B-4-3

### QUASISTATIC TERMS FOR INTERIOR FIELDS OF MICROSTRIP ANTENNAS

William F. Richards  
Department of Electrical Engineering  
University of Houston  
Houston, TX 77004

The field between the patch and ground plane of a microstrip antenna, the interior field, can be attributed to a primary current source driving the antenna and equivalent secondary electric surface currents on a magnetic wall. The magnetic wall is placed on a surface extending from the ground plane to the edge of the patch thus forming a closed cavity. One can write an integral equation in the unknown secondary current. This integral equation involves, among other things, the Green's function for the microstrip cavity. By solving this integral equation, one can determine all important parameters of the antenna. Alternatively, one can assume as an approximation that the secondary electric current is zero and solve directly for the interior field. One also must modify the dielectric loss tangent by introducing an effective dielectric constant to account for the radiated power. This latter approximation is included in the so called cavity model of a microstrip antenna. Whether or not one uses the full-wave analysis mentioned first, or the cavity model approximation, one needs the microstrip cavity Green's function. How to compute this Green's function efficiently is the subject of this paper.

The cavity Green's function can be broken into the sum of a dynamic part, which requires the computation of the first few resonant modes of the cavity, and a quasistatic part. The quasistatic part is a two-term polynomial in frequency. The two coefficients of this polynomial can be expressed as infinite series of the special functions associated with the patch geometry (eg., Bessel functions). These series converge very slowly making their acceleration important for practical applications. A method is presented for analytically obtaining the quasistatic terms for patches separable in one of four cylindrical coordinate systems: rectangular, circular cylindrical, elliptic cylindrical, and parabolic cylindrical systems. The quasistatic terms are obtained from Stevenson's method. The higher-order terms are solutions to differential equations whose forcing functions involve the lower-order terms. By applying these techniques, one can obtain a single-index series for the quasistatic terms involving only exponential and circular functions. Further acceleration of these simpler series results in explicit extraction of the static singularity. In the case of circular-disk elements, the lowest-order term is even obtainable in closed form. Similar techniques can also be applied to non-separable patches, except that the quasistatic boundary-value problems are cast in terms of integral equations which must be solved numerically. This is the subject of a companion paper presented in this symposium (Richards and Butler, "Numerical computation of the green's function for interior fields of non-separable microstrip antennas).

**NUMERICAL COMPUTATION OF THE GREEN'S FUNCTION FOR INTERIOR FIELDS OF NON-SEPARABLE MICROSTRIP ANTENNAS**

William F. Richards and Chalmers M. Butler  
Department of Electrical Engineering  
University of Houston  
Houston, TX 77004

Some techniques, both full-wave and approximate, for the analysis of microstrip antennas require the Green's function for a microstrip cavity. The microstrip cavity consists of two parallel, flat electric walls, joined at their edges by a ribbon of magnetic wall. The required Green's function is the electric field due to a filamentary, uniformly distributed electric current extending from one electric wall to the other along a line perpendicular to the electric walls. The Green's function can be written as the sum of two parts. One is a dynamic part, which accounts for the contribution of the first few resonant modes of the cavity. The remaining part is the quasistatic contribution, which is a first-degree polynomial in the square of the frequency. This representation is particularly efficient in that the resonant modes themselves are frequency independent as are the coefficients of the quasistatic contribution. Thus, they need only be determined once regardless of at how many different frequencies the Green's functions is to be computed.

If the boundary of the patch (the magnetic wall) coincides with the constant-coordinate surfaces of one of the four cylindrical coordinate systems in which the Helmholtz equation is separable, then these frequency-independent quantities can be determined analytically. These systems are rectangular, circular cylindrical, elliptic cylindrical, and parabolic cylindrical systems. Consideration of such separable patches is given in a companion paper (Richards, "Quasistatic terms for interior fields of microstrip antennas") in this symposium. When the patch geometry is not separable, then both the dynamic and the quasistatic parts of the Green's function must be determined numerically. The numerical computation of this Green's function is the topic of this paper.

The dynamic part (the lowest resonant modes) can be determined by applying the moment method to solve a homogeneous integral equation for the unknown source-free magnetic current on the magnetic wall. A more interesting problem is the determination of the quasistatic terms. This requires writing and solving a pair of static integral equations. The solution of the integral equation for the higher-order term requires the solution of the integral equation for the lowest-order term. There are several possible formulations. The one currently being investigated explicitly removes the free-space static singularity and the nearest image term. By image term, we mean the static image of the source with respect to an osculating plane at a point on the boundary nearest the source point. This leaves an unknown field distribution which is relatively smooth.

## B-4-5

### REFINEMENT OF THE RADIATING-SLOT MODEL FOR MICROSTRIP ANTENNAS TO ACCOUNT FOR NEAR-FIELD PHENOMENA

Edward F. Kuester, David C. Chang and  
Thomas M. Martinson  
Electromagnetics Laboratory  
Department of Electrical and Computer Engineering  
University of Colorado, Box 425  
Boulder, CO 80309 USA

A common method for the calculation of the far fields of rectangular microstrip patch antennas is to model the radiating edges by equivalent slots on the top of the substrate which is otherwise covered with metal in this equivalent representation. The field across the narrow dimension of the slot can be assumed constant for the purpose of calculating these far fields [P. Hammer et al., IEEE Trans. Ant. Prop., 27, 267-270, 1979]. When calculating near fields, however, or quantities such as the imaginary part of the slot admittance which depend on the near field, the constant field assumption is inadequate, and does not reproduce the correct results for certain canonical problems which are available from Wiener-Hopf analyses [E.F. Kuester et al., IEEE Trans. Ant. Prop., 30, 910-917, 1982].

In the static problem of the circular disc capacitor with small plate separation, F. Leppington and H. Levine [Proc. Camb. Phil. Soc., 68, 235-254, 1970] showed how knowledge of the exact electric field in the plane of one of the plates when the edge is straight could be used to obtain accurate formulas for the disc capacitor when the edge is slightly curved. In this paper, we will use a similar idea to predict the correct behavior of an electrically thin patch antenna by using a knowledge of the exact electric field (the "slotfield") on the surface of the substrate for the static problem of a semi-infinite upper conductor with a straight edge. This result has been found by others [N.N. Lebedev, Sov. Phys. Tech. Phys., 3, 1234-1243, 1958; W.C. Chew and J.A. Kong, Math. Proc. Camb. Phil. Soc., 89, 373-384, 1981] and reproduces the proper values of edge admittance (or reflection coefficient) for thin substrates with considerably less effort than is required from a dynamic Wiener-Hopf analysis. This more precise use of the equivalent radiating-slot formulation can be extended for use in other shapes of patch antenna by segmenting the edge into a sufficiently large number of slots over which the voltage is substantially constant. The resulting matrix equation involves only edge voltages rather than currents over the entire surface of the patch, and thus yields accurate data on resonant frequency with much less computational effort.

## ANALYSIS OF TUNABLE CIRCULAR PATCH ANTENNAS

Guey-Liou Lan\* and Dipak L. Sengupta  
Radiation Laboratory  
Department of Electrical Engineering and Computer Science  
The University of Michigan  
Ann Arbor, Michigan 48109

## ABSTRACT

The resonant or operating frequency of a circular patch antenna can be varied by placing passive metallic or tuning posts at suitable locations within the antenna's boundary. The present paper discusses a theoretical model developed for the analysis of the input performance of such tunable antennas. The antenna is modelled as a radial waveguide terminated by an admittance appropriate for the radiating aperture; the effects of the tuning posts are accounted for by their equivalent admittances placed at the locations of the posts. The input admittance of the antenna is then obtained from the equivalent radial line considerations. The operating frequency is obtained as that frequency where the input admittance becomes real. Comparison of analytical and measured results seems to establish the validity of the model for the purpose of design of such antennas.

---

\* Now with RCS Laboratories, Princeton, NJ 08540.

## B-4-7

### SPECTRAL-DOMAIN ANALYSIS OF MICROSTRIP ANTENNAS USING THE CONJUGATE GRADIENT ALGORITHM

R. Kastner and A. Sabban  
RAFAEL, P.O.Box 2250/87  
Haifa 31021, Israel.

E. Heyman  
Department of Electrical Engineering  
Tel- Aviv University  
Tel-Aviv 69978, Israel.

The planarity of microstrip structures makes it attractive to employ the spectral representation of fields. For these structures, the method based upon the combination of the spectral representation and the Conjugate Gradient algorithm is shown in this work to be a highly efficient and with good convergence characteristics. Unlike the cavity-model method, this method can handle very general microstrip structures, and it is not restricted by size as much as moment methods are. Current distributions and near fields are obtained both at the antenna and along the nearby feeding structure.

The method uses a closed-form, spectral algebraic Green's function at the presence of dielectric layers and (infinite) ground plane, obtained by transmission-line-equivalence method. A compact and general representation for any number of layers is derived. Next, an "incident field" model is constructed from an elementary source current located on the feeding line at some distance away from the antenna. The antenna problem is thereby transformed into the familiar scattering problem and the Conjugate Gradient is employed in a standard manner (Kastner & Mittra, 1984 Int'l IEEE/AP-S Symposium digest, pp 925-928).

The calculations agree with our experimental results. The method is also capable of handling multiple layers as well as finite ground plane problems.

AN ASYMPTOTIC EVALUATION OF THE MUTUAL COUPLING BETWEEN  
2-D STRIPS ON A DIELECTRIC COATED CIRCULAR CYLINDER

B.W. Kwan  
The Florida St. Univ.  
Inst. for Engineering  
Rm. 106 Education Bldg.  
Tallahassee, FL 32306

R.G. Kouyoumjian, E.H. Newman  
The Ohio State Univ.  
Dept. of Electrical Engr.  
ElectroScience Lab  
1320 Kinnear Rd.  
Columbus, Ohio 43212

A crucial step in the method of moments solution of an integral equation for the current distribution on an array of microstrip antennas on a dielectric coated cylinder is the evaluation of the mutual impedance between the microstrip patch modes. The mutual impedance between two microstrip patch modes on a dielectric coated cylinder can be expanded in terms of the coated cylinder eigenfunctions, using the radially propagating dyadic Green's function. Typically, the eigenfunction expansion is poorly convergent when the coated cylinder is more than a few wavelengths in radius. For large cylinders asymptotic high frequency solutions are preferable, because they are computationally more efficient, and can be interpreted in terms of ray-optics.

For simplicity, we have considered the 2-D problem of the mutual coupling between infinite strips on a dielectric coated cylinder. An essential step in deriving asymptotic solutions is the conversion of the radially propagating Green's dyadic (upon which the eigenfunction solution is based) into a circumferentially propagating type by employing the Poisson summation formula. Thereby two alternative expressions for the mutual impedance between two dipole modes are obtained. The first method is the residue series which converges rapidly provided the strips are not too close. The second method involves an integral representation which is derived by replacing the cylindrical Bessel functions by their Debye approximations, and is applicable when the strips are close. A numerical example is presented which compares the exact eigenfunction solution with the two asymptotic methods. This example illustrates the accuracy of the asymptotic methods, and also their regions of applicability.

## B-4-9

### AN EIGENFUNCTION SOLUTION FOR THE MUTUAL COUPLING BETWEEN MICROSTRIP MODES ON A DIELECTRIC COATED CYLINDER

B.W. Kwan  
The Florida St. Univ.  
Inst. for Engineering  
Rm. 106 Education Bldg.  
Tallahassee, FL 32306

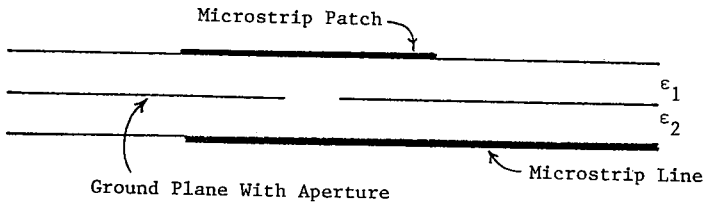
E. H. Newman, R.G. Kouyoumjian  
The Ohio State Univ.  
Dept. of Electrical Engr.  
ElectroScience Lab  
1320 Kinnear Rd.  
Columbus, Ohio 43212

The current distribution on an array of microstrip antennas on a dielectric coated circular cylinder can be found from the solution of an integral equation. The kernel of this integral equation contains the coated cylinder Green's function, which is expanded in terms of the eigenfunctions of the coated cylinder. The moment method is an effective numerical technique to solve these equations for the unknown currents on the microstrip patch antennas. A crucial step in carrying out the moment method solution is the calculation of the elements of the impedance matrix and voltage vector associated with the expansion and weighting modes chosen. Exact expressions for these elements are derived using the above mentioned Green's dyadic. It is found that the self impedance of a microstrip patch mode at the surface of the coated cylinder converges to that of the infinite, planar, grounded, dielectric slab as the radius of the cylinder increases. The major limitation of the eigenfunction solution is that as the cylinder radius increases, one must retain a larger number of terms in the eigenfunction summation, resulting in increased computer run times and some numerical difficulties. Numerical results will be presented for both the self and mutual impedance between microstrip patch modes on dielectric coated cylinders ranging from 0.25 to 10 wavelengths in radius.

## ANALYSIS OF APERTURE COUPLED PATCH ANTENNA

P.L. Sullivan, D.H. Schaubert, and D.M. Pozar  
 Department of Electrical and Computer Engineering  
 University of Massachusetts  
 Amherst, MA 01003

An antenna that consists of a microstrip patch coupled to a microstrip transmission line by means of a small aperture in an intervening ground plane is analyzed. This structure is potentially useful for low-profile, high-performance phased arrays that utilize monolithic circuitry. The current excited on the microstrip line and the patch radiation due to a source on the microstrip line are determined by the moment method. From these currents input impedance and radiation patterns are easily computed. The analysis uses the complete Green's functions for grounded dielectric slabs so that all radiation and surface wave effects are included. Piecewise sinusoidal basis functions are used to expand the unknown electric currents and entire domain sinusoidal basis functions are used for the field in the rectangular aperture. Galerkin testing is employed. The input impedance is evaluated and compared to measurements.





## URSI COMMISSION B - SESSION B5

**Error Minimization and  
Convergence in Numerical Methods**

1:30 - 5:00  
IRC-5

**Convergence et minimisation  
des erreurs dans les méthodes  
numériques**

Chairperson/Président: **D.G. Dudley**, University of Arizona, Tucson, AZ, USA

- 1 (1:40) ERROR MINIMIZATION AND CONVERGENCE IN NUMERICAL METHODS (INTRODUCTION). **D.G. Dudley**, University of Arizona, Dept. of Electrical and Computer Engineering, Tucson, AZ, USA
- 2 (2:10) ERROR MINIMIZATION IN SCATTERING: ITERATIVE SCHEMES. **P.M. van den Berg, A.T. de Hoop**, Delft University of Technology, Dept. of Electrical Engineering, Delft, The Netherlands
- 3 (2:40) ITERATIVE SOLUTION OF ELECTROMAGNETIC BOUNDARY VALUE PROBLEMS IN THE SPECTRAL DOMAIN. **R. Mittra, C.H. Chan**, University of Illinois, Electromagnetic Communication Laboratory, Urbana, IL, USA
- 4 (3:10) ITERATIVE TECHNIQUES APPLIED TO SOME RADIATION AND SCATTERING PROBLEMS. **F. Jouvie, D. Lesselier**, CNRS, Laboratoire des Signaux et Systèmes, Gif-sur-Yvette, France; **D. Vuillet-Laurent**, École Supérieure d'Electricité, Gif-sur-Yvette, France
- 5 (3:40) EVERYTHING YOU WANTED TO KNOW ABOUT NUMERICAL METHODS IN ELECTROMAGNETICS BUT WERE DISCOURAGED TO ASK. **T.K. Sarkar**, Rochester Institute of Technology, Dept. of Electrical Engineering, Rochester, NY, USA
- 6 (4:10) PANEL DISCUSSION/TABLE RONDE. **Members/Membres: L.B. Felsen, (Chairperson/Président), D.G. Dudley, T.K. Sarkar, R. Mittra, D. Lesselier, P.M. van den Berg**

ERROR MINIMIZATION AND CONVERGENCE  
IN NUMERICAL METHODS (INTRODUCTION)

D. G. Dudley  
Electromagnetics Laboratory  
Department of Electrical and Computer Engineering  
University of Arizona  
Tucson, AZ 85721 USA

The solution to most linear electromagnetic boundary value problems involves consideration of a linear second-order partial differential equation. Because of boundary complexity in many problems of practical interest, the researcher must often use numerical methods to obtain an approximation to the solution. Numerical techniques can be applied directly to the differential equation (finite differences, finite elements,...) or to an integral equation (MFIE, EFIE,...) obtained by use of a Green's theorem. In either case, one is faced with inversion of a linear operator equation  $Lu = f$ , where  $L$  is a differential, integral, or integrodifferential operator.

Unfortunately, except in quasistatic limits, the operator seldom has mathematical properties (positive-definiteness, self-adjointness,...) that allow firm statements concerning properties of the solution. In addition, in the numerical process, the operator  $L$  is usually represented by a matrix  $A$  in such a manner that the relationship between the domains of  $L$  and  $A$  is often unclear. The result is that, even if properties of the inversion of  $A$  can be established, it is difficult to relate them to the inversion of  $L$ .

A further complication occurs when the size of the matrix  $A$  is large enough that direct inversion methods become intractable. In this case, iterative methods are attractive, but they can add further uncertainty to attempts to relate the numerical solution to solution of the original problem.

It is the purpose of this special session to consider the present state of numerical methods, with emphasis on convergence, error minimization, and what is meant by problem 'solution.' The speakers will discuss the mathematical issues as well as examples of various techniques. The session will be followed by a panel discussion with audience participation encouraged.

## ERROR MINIMIZATION IN SCATTERING: ITERATIVE SCHEMES

P.M. van den Berg and A.T. de Hoop

Laboratory of Electromagnetic Research  
Department of Electrical Engineering  
P.O. Box 5031, 2600 GA Delft  
The Netherlands

The computation of radiating electromagnetic fields in the presence of complicated bounded configurations that are embedded in a relatively simple medium of infinite extent will be discussed. The unboundedness of the outer medium inevitably requires the handling of the fields in this region in an analytic manner, the fields in the complicated bounded structure being amenable to a computational handling. To handle the integral equation (or other equations) that results from this analysis computationally and at the same time have a measure for the accuracy attained, we introduce the global (i.e. integrated over the domain of the structure) root-mean-square error in the equality signs that have to be satisfied by the exact solution. This error criterion also enables us to develop an iterative technique to solve the problem. In it, variational techniques are employed that enforce a monotonous decrease in the error in each iteration, and thus lead to an iterative improvement of the solution to the problem. Starting with an arbitrary initial guess and a set of arbitrarily chosen correction functions, some iteration schemes are discussed. Some suitably chosen choices for the correction functions are discussed. Some numerical results pertaining to a number of representative problems illustrate the rate of convergence of the different methods.

ITERATIVE SOLUTION OF ELECTROMAGNETIC BOUNDARY VALUE PROBLEMS  
IN THE SPECTRAL DOMAIN

R. Mittra and C. H. Chan  
Electromagnetic Communication Laboratory  
University of Illinois  
Urbana, Illinois 61801

In this paper we discuss the problem of iterative solution of a class of boundary value problems arising in electromagnetics that are conveniently solved using the spectral domain formulation, and present a technique which draws both on the concepts of the Spectral Iterative Technique (SIT) and the Conjugate Gradient Method (CGM), but which differs in detail from either of the above two approaches. The spectral iterative technique is an asymptotic method that has been employed for the solution of a variety of radiation and scattering problems involving both the perfectly conducting and dielectric bodies. This technique, though quite versatile, suffers from the disadvantages that the convergence of the iteration scheme is not guaranteed and no systematic procedure is available to circumvent the divergence problem when it occurs. In contrast, the conjugate gradient method has the distinct advantage of assuring that the solution will not diverge, regardless of how the initial approximation is chosen. However, experience shows that the convergence can often be slow, and the algorithm can require a very large number of iterations to achieve an accurate result. Furthermore, the iteration procedure itself is highly susceptible to machine round-off errors.

In this paper we begin, just as in the CGM method, by casting the iteration problem into one of reducing EBC, the norm of the error in the satisfaction of the boundary condition. We then show that the choice of the direction vector  $a$  la the CGM method is not optimal and better choices are found by following the concepts embodied in the spectral iterative or spectral Galerkin procedures.

Unlike the SIT procedure, however, the proposed iterative method is shown to have an upper bound for the error; hence, the iteration process is guaranteed not to diverge. One can also prove that with  $n$  linearly independent direction vectors that can be chosen a priori, the iteration procedure will converge and yield a solution to the operator equation that is identical to the one that would have been obtained if an  $n \times n$  matrix were inverted using the Galerkin procedure. Note, however, that the storage problem associated with the matrix inversion is circumvented in the iteration procedure.

Extensive numerical studies based on the use of the CGM, related methods and the new iterative approach have been carried out. A comparison of the accuracies, computational efficiencies and the convergence properties of various algorithms will be included in the presentation of the paper.

ITERATIVE TECHNIQUES APPLIED TO SOME  
RADIATION AND SCATTERING PROBLEMS

F. JOUVIE\*, D. LESSELIER\*, D. VUILLET-LAURENT\*\*

\*Groupe d'Electromagnétisme, Laboratoire des Signaux et Systèmes

\*\*Service d'Electromagnétisme, Ecole Supérieure d'Electricité  
Plateau du Moulon - 91190 GIF-sur-YVETTE, FRANCE

Iterative techniques can be powerful tools to solve direct problems in electromagnetics and acoustics. Our aim is to illustrate applicability of such techniques in two particular domains, radiation by large wire-structures, and scattering by inhomogeneous cylindrical targets.

In the radiation problem, integral equations, based upon the thin-wire approximation, are solved using the moments method; the linear systems of equations that are obtained thereby are of large rank and the matrices contain many elements whose values are close to zero (coupling between remote wires). Various computations have been carried-out for typical systems to clear-up the behaviour of several conjugate-gradient inversion algorithms, with respect to direct algorithms; in the case of periodic structures, as such systems present strong symmetries (Bloc Toeplitz matrices), the behaviour of a well-adapted algorithm (Akaiké-Robin's) will be also investigated.

In the scattering problem, iterative algorithms can be derived to directly solve integral operator equations in Hilbert space. Such techniques are readily applied to 2<sup>nd</sup> kind Fredholm equations because of the rich properties of the solution (existence, unicity, well-posedness). The behaviour of gradient-and conjugate-gradient-like algorithms has been investigated in the case of large but weakly refractive fluid targets in acoustics (scalar case), with regards to the well-known Neumann's series algorithm. It will be shown in particular that the latter may appear quite effective, when convergent, compared with the former. Nevertheless, only conjugate-gradient-like algorithms enable us to handle large targets with important variations of their parameters. This shall be confirmed in the em. scattering by a lossy dielectric biological structure illuminated by a set of several wave-guides (vector case).

EVERYTHING YOU WANTED TO KNOW ABOUT NUMERICAL METHODS  
IN ELECTROMAGNETICS BUT WERE DISCOURAGED TO ASK

Tapan K. Sarkar  
Department of Electrical Engineering  
Rochester Institute of Technology  
Rochester, New York - 14623  
Phone: (716) 475-2143

**ABSTRACT:** The objective of this paper is to summarize the contemporary numerical methods (method of moments, spectral iterative method and the conjugate gradient method) and illustrate what error is being minimized for each of the methods and their rates of convergence. Secondly, it will be shown that the conjugate gradient method has the capability of minimizing the error  $X$  (exact) -  $X$  (approximate) at each iteration even though the exact solution is not known. Examples will be presented to illustrate the application of the conjugate gradient method to a wide variety of areas.

**REFERENCES:**

1. Sarkar, T. K., Siarkiewicz, K. R. and Stratton, R. F., "Survey of Numerical Methods for the Solution of Large Systems of Linear Equations for Electromagnetic Field Problems," AP, Vol-29, pp 847-56, 1981.
2. Sarkar, T. K. and Rao, S. M., "An Iterative Method for Solving Electrostatic Problems," AP-30, pp 611-616, 1982.
3. Sarkar, T. K., "A Note on the Variational Method (Raleigh-Ritz), Galerkins Method and the Method of Least Squares," Radio Science, Vol-18, pp 1207-1224, Nov. 1983.
4. Harrington, R. F. and Sarkar, T. K., "Boundary Elements and the Method of Moments," Ed by C. Brebbia in Proc. of the 5th Intl. Conference on Boundary Elements, Hiroshima, Japan, pp 31-40, 1983.
5. Sarkar, T. K. and Rao, S. M., "The Application of the Conjugate Gradient Method for the Solution of Electromagnetic Scattering from Arbitrarily Oriented Wire Antennas," AP, Vol-32, pp 398-403, 1984.
6. Sarkar, T. K., "The Application of the Conjugate Gradient Method for the Solution of Operator Equations Arising in Electromagnetic Scattering from Wire Antennas," Radio Science, Vol- 19, pp 1156-1172, Sept. 1984.
7. Rao, S. M., Sarkar, T. K. and Dianat, S. A., "The Application of the Conjugate Gradient Method to the Solution of Transient Scattering from Thin Wires," Radio Science, Vol-19, pp 1319-1326, Sept. 1984.
8. Sarkar, T. K. and Dianat, S. A., "Adaptive Spectral Estimation by the Conjugate Gradient Method," 1984 Digital Signal Processing Workshop, Chatham.

## URSI COMMISSION B - SESSION B6

Waves Near Interface

8:30 - 12:00

Les ondes près de l'interface

IRC-1

Chairperson/Président: **C.M. Butler**, University of Houston, Houston, TX, USA

- 1 APPLICATION OF EXACT IMAGE THEORY IN ANALYSIS OF ANTENNAS ABOVE THE GROUND. **I.V. Lindell, E. Alanen, K. Mannersalo**, Helsinki University of Technology, Electromagnetics Laboratory, Espoo, Finland
- 2 EXTENSION OF EXACT IMAGE THEORY TO PROBLEMS INVOLVING TRANSMISSION THROUGH INTERFACES AND LAYERED MEDIA. **I.V. Lindell, E. Alanen**, Helsinki University of Technology, Electromagnetics Laboratory, Espoo, Finland
- 3 TIME HARMONIC SOLUTIONS FOR A LONG HORIZONTAL ANTENNA OVER THE GROUND WITH GRAZING INCIDENCE. **K.C. Chen**, Sandia National Laboratories, Albuquerque, NM, USA
- 4 THE RADIATION RESISTANCE OF AN INCLINED DIPOLE ANTENNA IN THE PRESENCE OF A PLANE CONDUCTING EARTH. **G.P.S. Cavalcante, J.T. Pinho**, Universidade Federal do Pará, Depto. de Engenharia Elétrica, Pará, Brazil; **D.A. Rogers**, North Dakota State University, Dept. of Electrical and Electronics Engineering, Fargo, ND, USA
- 5 NUMERICAL SOLUTION FOR AN INSULATED WIRE INCLUDING THE EFFECT OF AN INTERFACE. **G.J. Burke, E.K. Miller**, Lawrence Livermore National Laboratory, Dept. of Electronics Engineering, Livermore, CA, USA
- 6 CREEPING WAVE PROPAGATION CONSTANTS AND MODAL IMPEDANCE FOR A DIELECTRIC COATED CYLINDER. **J.R.J. Paknys, N. Wang**, Ohio State University ElectroScience Laboratory, Dept. of Electrical Engineering, Columbus, OH, USA
- 7 CREEPING WAVES IN THE COATING OF ABSORBER-COVERED CONDUCTORS. **P.J. Moser**, Sperry Corporation, Reston, VA, USA; **A. Nagl, H. Überall**, Catholic University, Physics Dept., Washington, DC, USA
- 8 ELECTROMAGNETIC RESPONSE OF A BURIED SPHERE. **G. Fan**, China Research Institute of Radiowave Propagation, Xinxiang, China
- 9 ON ARRAY OF HORIZONTAL COAXIAL LOOPS ABOVE A FINITELY CONDUCTING HALF-SPACE. **A.S.A. Kassem**, University of Al-Fateh, Dept. of Electrical Engineering, Tripoli, Libya
- 10 ELECTROMAGNETIC WAVE SCATTERING BY OPEN AND CLOSE DIELECTRIC SHELLS. **N. Subramaniam**, University of Malaya, Dept. of Electrical Engineering, Kuala Lumpur, Malaysia

## B-6-1

### APPLICATION OF EXACT IMAGE THEORY IN ANALYSIS OF ANTENNAS ABOVE THE GROUND

I.V. Lindell, E. Alanen and K. Mannersalo  
Helsinki University of Technology, Electromagnetics Laboratory  
Otakaari 5 A, SF-02150 Espoo 15, FINLAND

Exact image theory, as recently developed by the present authors, is applied to the problem of antenna analysis in the presence of imperfectly conducting ground. The effect of the ground in the antenna current integral equation is seen to modify the Green function to take into account the proper antenna image locating in complex space. This in turn leads to a novel variant of the well-known antenna impedance functional which includes the ground effect.

The theory is applied to dipole antenna impedance calculation and comparisons with results given in the literature are made. It is seen that a simple induced emf method is applicable for thin dipoles, and it can also be used for dipoles of finite thickness if the corresponding dipole free space impedance is known. Results are calculated for the horizontal half-wave dipole, for which much data exist in the literature. The theory gives rise to a simple calculation method applicable for a modest microcomputer (the calculations were in fact made on Commodore 64).

Discussion on the validity of the method for low antenna heights shows that the critical height for the simple method depends on the thickness of the dipole with the order relation  $ka = 2kh \exp(-1/kh)$  between the radius  $a$  and the height  $h$  of the antenna. For smaller heights  $h$ , the simple method is no more applicable, but the full functional with the image-induced kernel can still be applied.

EXTENSION OF EXACT IMAGE THEORY TO PROBLEMS INVOLVING  
TRANSMISSION THROUGH INTERFACES AND LAYERED MEDIA

I.V. Lindell and E. Alanen

Helsinki University of Technology, Electromagnetics Laboratory  
Otakaari 5 A, SF-02150 Espoo 15, FINLAND

Exact image theory was developed for the original Sommerfeld problem involving field calculation from sources on the same side of the interface of two media. Here, the method is extended to field calculation on the other side of the interface. The image source is seen to be located in complex space and expressions for its calculation are evaluated.

The method is further extended to problems involving layered media with more than just one planar interface. For this kind of problems, there results an infinite set of continuous image currents in complex space. In some cases, a finite number of these images is sufficient for field calculations at reasonable accuracy. As an example, the field focusing in the skin-flesh problem of human irradiation in hyperthermia treatment is considered.

## B-6-3

### Time Harmonic Solutions for a Long Horizontal Antenna Over the Ground with Grazing Incidence

Kenneth C. Chen  
Sandia National Laboratories  
Division 7553  
Albuquerque, NM 87185

The grazing incidence gives the largest induced current on a long horizontal antenna over the ground. Previous results on this subject are for the continuous waves (CW) and for an infinite antenna extending at both ends. This paper shows the difference in CW responses for a finite horizontal antenna and the responses for an infinite antenna. First, the transmission line theory due to King et al is extended to higher frequencies. Procedures for obtaining numerical values for the transmission line parameters are given. Accurate simple formulas for the line parameters are given. Second, simple formulas for line currents are applied to obtain the antenna currents for frequencies ranging from 10 kHz to 1 MHz; ground conductivities of  $10^{-1}$ ,  $10^{-2}$ ,  $10^{-3}$  S/m; antenna heights of 10, 5, and 1m; different load conditions; and different antenna lengths. In particular, we report the required antenna length so that the long antenna will respond as an infinite antenna. Thirdly, antenna currents for an incident lateral wave are investigated.

THE RADIATION RESISTANCE OF AN INCLINED DIPOLE  
ANTENNA IN THE PRESENCE OF A PLANE CONDUCTING EARTH

Gervásio Protásio S. Cavalcante  
João Tavares Pinho  
Departamento de Engenharia Elétrica  
Universidade Federal do Pará  
Belém, Pará, Brazil

David Anthony Rogers  
Department of Electrical and Electronics Engineering  
North Dakota State University  
Fargo, North Dakota 58105

In this paper it is shown that the induced EMF method can be used to calculate the radiation resistance of an inclined dipole antenna in the presence of a plane conducting earth. Following the procedures of Schelkunoff and Friis (Antennas: Theory and Practice, Wiley, pp. 160-167, 1952) in conjunction with image theory, the radiation resistance as a function of antenna height,  $R(z)$ , can be written as a  $2N$  by  $N$  double summation involving the radiation influence coefficients, the element moments, and the phase difference between elements.

Simple geometric calculations allow  $R(z)$  to be found to reasonable accuracy for  $N < 50$ . The usual results for  $R(z)$  for vertical and horizontal polarizations are obtained using this method. Comparison of the results with those of NBS Technical Note 175 (1963) shows agreement for both polarizations. Similar results for the inclined dipole for a fixed angle of inclination are also obtained. For fixed antenna heights, this method allows the calculation of  $R(z)$  as a function of the inclination angle. For example, for a height-to-wavelength ratio of 0.25,  $R(z)$  decreases from about 100 ohms at vertical polarization to about 86 ohms for horizontal polarization. When the ratio is changed to 2.5, the radiation resistance is independent of the inclination angle.

This elementary method shows itself to be quite useful due to its ease of utilization and to the low required computational time.

## B-6-5

### NUMERICAL SOLUTION FOR AN INSULATED WIRE INCLUDING THE EFFECT OF AN INTERFACE\*

G. J. Burke and E. K. Miller  
Lawrence Livermore National Laboratory

A Method-of-Moments solution for current on an insulated wire in a lossy medium is investigated. The equivalent radial current approach taken by Richmond and Newman (Radio Science, January, 1976) is used with a three-term spline current basis and point matching of the boundary condition. With this current expansion, conditions on the behavior of current and charge are explicitly enforced at junctions between insulated and bare wires. For an insulated wire near an air-earth interface the solution involves Sommerfeld integrals for which values are obtained through table-lookup and parameter estimation.

Results are compared with those from Richmond's Method-of-Moments code and an analytic solution for an infinite insulated wire in a lossy medium. The solution for an insulated wire near an interface is compared with approximations based on transmission line theory.

---

\*Work performed under the auspices of the U. S. Department of Energy by the Lawrence Livermore National Laboratory under contract number W-7405-ENG-48.

CREEPING WAVE PROPAGATION CONSTANTS AND MODAL IMPEDANCE  
FOR A DIELECTRIC COATED CYLINDER.

J.R.J. Paknys and N. Wang  
The Ohio State University ElectroScience Laboratory  
Department of Electrical Engineering  
Columbus, Ohio 43212

The electromagnetic characteristics associated with creeping waves supported by a dielectric coated cylinder is investigated. The propagation constants and wave impedances of the creeping waves are obtained numerically. Higher order modes which are sometimes significant for a thick coating are also investigated. The propagation constants and creeping wave modal impedance are compared with those obtained for a planar dielectric slab backed by a ground plane. It is found that, contrary to the planar configuration, no cutoff frequencies exist for the creeping waves associated with the coated cylinder modes. In fact, the coated cylinder supports an infinite number of modes. However, depending upon the thickness of the coating, only a few Elliot type creeping wave modes with low attenuation can exist. Furthermore, for each of the Elliot type creeping waves, there is a critical radius for the cylinder below which the Elliot type creeping wave cannot exist.

The results are also compared with an impedance boundary cylinder, where the impedance is chosen to be purely imaginary.

## B-6-7

### CREEPING WAVES IN THE COATING OF ABSORBER-COVERED CONDUCTORS

Philip J. Moser, Sperry Corp., Reston, VA 22091, USA  
Anton Nagl and Herbert Überall, Physics Dept., Catholic  
University, Washington, DC 20064, USA

The effects of absorbing coating on a curved conductor will in general reduce the radar cross section; it is known from experiment, however (R. J. Garbacz and D. L. Moffat, *Proceed. IRE*, 49, 1184-1192, 1961), that e.g. the bistatic small-angle scattering can be enhanced in that case. This effect may be attributed to the existence of creeping waves in the coating. In order to assess their effects, we have in addition to our previous studies on conductors with lossless coating (W. E. Howell and H. Überall, *IEEE Trans. AP-32*, 624-627, 1984), carried out an investigation for coated conducting spheres with lossy dielectric coating. A calculation of the complex-frequency poles in the scattering amplitude of such a target provides us with the dispersive phase and group velocity and attenuation curves of the creeping waves as functions of dielectric and magnetic loss factors. Scattering amplitudes were evaluated numerically for the total field and for the field of the generated creeping waves alone; in this way, the magnitude of the creeping-wave effects as compared to the field reflected from the conductor could be obtained for various choices of dielectric and magnetic loss factors of the object's coating. In evaluating the cross section, interference terms between the reflected echo and the creeping waves have been obtained also. It is found that, at least for coatings with small losses, creeping wave effects can be of considerable importance.

## ELECTROMAGNETIC RESPONSE OF A BURIED SPHERE

Fan Guoxin  
China Research Institute of Radiowave Propagation  
P.O. Box 138  
Xinxiang, Henan Province  
China

A series form solution is derived for the scattered fields from two buried concentric spheres with arbitrary electric parameters under the excitation of an arbitrary electromagnetic source above the earth.

The expressions of the primary fields in absence of the spheres are obtained first by means of the dyadic Green's functions for flat earth in terms of the cylindrical vector wave functions. The secondary fields in each region are expanded in spherical vector wave functions and cylindrical vector wave functions. The relations between the two systems of vector wave functions are established for convenience of matching the boundary conditions. The coefficients in the expansions of the secondary fields are found by solving a set of equations which are established by applying the boundary conditions to the field expansions with the help of the orthogonal properties of the vector wave functions.

As a special example, a solution for a single-layered sphere is obtained directly from the above solution. In addition, the problem for a perfectly conducting sphere is solved in the same way and the numerical results are given. In case of plane incident wave, two buried concentric spheres are also considered with the result which can be reduced to the well-known Mie solution of the scattering of a plane wave by a sphere.

It is certain that the method here can be used to calculate the scattered fields from a layered sphere in a layered medium with arbitrary electric parameters under the excitation of an arbitrary source.

withdrawn

B-6-9

ON ARRAY OF HORIZONTAL COAXIAL LOOPS  
ABOVE A FINITELY CONDUCTING HALF-SPACE

By

Ahmed S.A. Kassem

University of Al-Fateh, Faculty of Engineering  
Dept. of Electrical Engineering, P.O. Box 13275  
TRIPOLI - LIBYA

The performance of loop antennas above a finitely conducting half-space is of great importance in geophysical probing, communication in mine tunnels as well as in direction finding. Characteristics of a single horizontal loop antenna above a dissipative half-space or arrays of circular coaxial loop antennas situated in free space were dealt with recently. The problem of an array of horizontal coaxial loops above a dissipative half space is not treated in the open literature. This paper treats, "numerically" the problem of an array consisting of two circular coaxial loops situated above a lossy half space, using Fourier series expansion method and circuit theory to solve for the current on the loops then compute the input admittance of either of the array elements. Results were checked in the case when the two loops were situated above a perfect conductor to simulate an array of four coaxial loops using image theory. Data of input admittance of any of the two elements of the array were computed for perfect conductor and a finitely conducting half-space for two cases:

- 1) The normalized separation  $kd$ , where  $k$  is free space wave number and  $d$  is the metric distance between the two loops, is kept constant and the normalized height  $kh$ ,  $h$  is the lower loop height above the lossy ground in meters, is changed between 0.1 and 1.5. The input admittance was found, as expected, to oscillate around the input admittance of the array when it is situated in an unbounded free space.
- 2) The normalized height  $kh$  of the lower loop antenna was kept fixed at  $kh = 0.2$  and the normalized separation  $kd$  between the loops was changed from  $kd = 0.1$  to  $kd = 2.0$ . The input admittance  $Y_{in}$  oscillates, as expected, around the value of the input admittance of a single loop above the lossy half space, which itself is dependent on the characteristics of this lossy half space.

For both loops the real part of  $Y_{in}$  follows a resonance curve as the separation between the loops is increased. It is sharper for the lower loop. This new information provides better discrimination between different half spaces probed. Such an information is of great importance in geophysical prospecting.

Knowledge of the performance of an array of horizontal coaxial loops is important in studying the more general problem of an array of staggered loops as well as Yagi array type made of loops when taken to be situated very close to a dissipative half space. The analysis of the above mentioned arrays is in progress.

ELECTROMAGNETIC WAVE SCATTERING BY  
OPEN AND CLOSED DIELECTRIC SHELLS

N. Subramaniam  
Electrical Engineering Department  
University of Malaya  
Kuala Lumpur, Malaysia  
and  
L.B. Felsen  
E.E.C.S. Department  
Polytechnic Institute of New York  
Farmingdale, NY, U.S.A.

Paper Withdrawn/  
La communication a été retirée



## URSI COMMISSION B - SESSION B7

Transients I

8:30 - 12:00  
IRC-3

Transitoires I

Chairperson/Président: **D.C. Chang**, University of Colorado, Boulder, CO, USA

- 1 LATE TIME RESPONSE OF THE PROLATE SPHEROIDAL IMPEDANCE ANTENNA. **J.D. Kotulski**, Sandia National Laboratories, Division 2322, Albuquerque, NM, USA
- 2 APPROXIMATE IMPULSE RESPONSE OF THE TIP OF A FLAT CONDUCTING PLATE. **J.D. Young, R.J. Marhefka**, Ohio State University ElectroScience Laboratory, Columbus, OH, USA
- 3 TRANSIENT SCATTERING FROM SOME CANONICAL GEOMETRIES. **W. Leeper, J.D. Young**, Ohio State University ElectroScience Laboratory, Dept. of Electrical Engineering, Columbus, OH, USA
- 4 A TRANSIENT VIEW OF THE SPHERICAL WAVE PROBLEM IN A COMPACT SCATTERING RANGE. **W. Leeper**, Ohio State University ElectroScience Laboratory, Dept. of Electrical Engineering, Columbus, OH, USA
- 5 TIME-DOMAIN FINITE-DIFFERENCE MODELING OF THIN APERTURES. **K.R. Demarest**, University of Kansas Center for Research Inc., Remote Sensing Laboratory, Lawrence, KS, USA
- 6 NUMERICAL EVALUATION OF COMPLEX RESONANCES OF AN ELLIPTIC CYLINDER. **R. Naishadham**, University of Mississippi, Dept. of Electrical Engineering, University, MS, USA; **L. W. Pearson**, McDonnell Douglas Research Laboratories, St. Louis, MO, USA
- 7 CHARACTERIZATION OF OPTICAL FIBERS BY IMPULSE RESPONSE MEASUREMENTS. **G.L. Yip, S. Belkasim, A.B. Puc**, McGill University, Dept. of Electrical Engineering, Montreal, PQ
- 8 COMPARISONS OF BACKGROUND CHARACTERISTICS OF AN RCS MEASUREMENT RANGE USING A CW NULLING TECHNIQUE AND A PULSED-RANGE GATE TECHNIQUE. **B.M. Kent**, Air Force Wright Aeronautical Laboratories, Wright Patterson Air Force Base, OH, USA; **G.R. Simpson, R.J. Jost, A.J. Terzuoli**, Air Force Institute of Technology, Wright Patterson Air Force Base, OH, USA
- 9 MEASUREMENT OF THE IMPULSE TIME DOMAIN SCATTER OF TARGETS IN A SMALL CHAMBER. **T.P. Fontana, K.M. Yon**, Westinghouse Defense and Electronics Center, Advanced Development Division, Baltimore, MD, USA
- 10 EXPERIMENTAL DETERMINATION OF RESONANT FREQUENCIES BY TRANSIENT SCATTERING FROM CONDUCTING SPHERES AND CYLINDERS. **F.I. Tseng, T.K. Sarkar**, Rochester Institute of Technology, Dept. of Electrical Engineering, Rochester, NY, USA

## B-7-1

### LATE TIME RESPONSE OF THE PROLATE SPHEROIDAL IMPEDANCE ANTENNA

J.D. KOTULSKI  
Sandia National Laboratories  
Division 2322  
Albuquerque, N.M. 87185

The prolate spheroidal antenna with an impedance boundary condition is considered. The impedance is either inductive or capacitive and varies with the position on the antenna surface to insure no mode coupling (confocal approximation). The antenna is excited by a  $\phi$ -independent equatorial gap voltage and the expression for the input admittance is derived. An equivalent circuit is obtained for the first two modes of the antenna and the poles of these modes are considered as a function of the impedance and the antenna thickness. The time response is then obtained by Laplace inversion. The applicability of this method for higher order modes and different types of excitation will be discussed.

APPROXIMATE IMPULSE RESPONSE OF THE TIP  
OF A FLAT CONDUCTING PLATE

J. D. Young and R. J. Marhefka  
The Ohio State University  
ElectroScience Laboratory  
1320 Kinnear Road  
Columbus, Ohio 43212

Transient scattering measurements were made on a set of conducting plates for a variety of look angles and polarizations. For those cases where the look angle is not perpendicular to the plate or a plate edge, the tips of the plates are clearly identifiable as scattering centers.

This paper first describes the target set, the measurement system, and the look angles of the data set. Next, it presents some typical time-domain and frequency domain data. The tip-scattering components are identified and discussed.

There are several existing analytical approaches for predicting the approximate impulse response of the tip of a plate. These are identified and discussed. Finally, the theoretical and experimental results are compared.

## B-7-3

### TRANSIENT SCATTERING FROM SOME CANONICAL GEOMETRIES

W. Leeper and J. D. Young  
The Ohio State University ElectroScience Laboratory  
Department of Electrical Engineering  
Columbus, Ohio 43212

The transient scattering responses of some canonical shapes have been measured and compared to broadband hybrid theoretical solutions. The transient responses are obtained from complex spectral information spanning the Rayleigh, resonance, and optics regions with a bandwidth of 100:1, giving an effective time resolution of 0.125 nsec. Measurement error is shown to be approximately 20 dB below the desired return. The waveforms have an accuracy and resolution which permit an examination of local scattering phenomena from curved edges, multiple diffractions, creeping waves, and higher order interactions as a function of polarization and aspect angle. The polarization dependence of the response from a junction discontinuity in surface curvature is displayed graphically for the first time. In addition to local scattering phenomena some low frequency natural resonances are shown. The correlation between the transient waveform and the geometry of the scatterer offers a physically intuitive insight into scattering behavior.

A TRANSIENT VIEW OF THE SPHERICAL WAVE  
PROBLEM IN A COMPACT SCATTERING RANGE

W. Leeper

The Ohio State University ElectroScience Laboratory  
Department of Electrical Engineering  
Columbus, Ohio 43212

The compact range concept has recently been adapted to indoor broadband scattering spectrum measurements. In a compact radar system, which simulates a far field plane wave, the spherical wave scattering caused by diffraction from the edges of the reflector or feed structure interferes with the desired illumination and therefore limits the size of the available plane wave window. An a priori field probe is typically used to insure that this window is large enough to contain the target, since, at a single frequency, it is virtually impossible to detect or extract such error once the measurement is made.

Studies in the transient scattering of canonical shapes have been applied to range diagnostics on two generations of broadband, coherent, stepped CW compact scattering ranges. The transient waveform displays the desired as well as undesired scattered components at time displacements which may be predicted by simple geometry and allows the analyst to isolate, identify, and ultimately reduce error terms. By comparing the measured transient waveforms of several canonical shapes to known theoretical responses obtained from inverse Fourier transforms of exact complex scattering spectra it is possible to identify measurable errors and to trace their origins in a manner which is impossible with a single frequency pattern. The variation of these errors as a function of polarization, frequency, calibration technique, and target size, shape, and orientation has been analyzed and the results have led to a greater understanding of the capabilities of the compact range. It has been found that the spherical wave error depends more on the pattern and gain of the scatterer than on absolute size, and that the error falls in a time frame which is impossible to time gate from the desired signal using a pulsed radar. The error is discussed quantitatively and methods of reducing it, in some cases, to acceptable levels are demonstrated.

## B-7-5

### TIME-DOMAIN FINITE-DIFFERENCE MODELING OF THIN APERTURES

Kenneth R. Demarest  
Remote Sensing Laboratory  
The University of Kansas Center for Research, Inc.  
Lawrence, Kansas 66045-2969

Time-domain finite-difference (TDFD) numerical codes have found increasing application in the modeling of conducting structures which are excited by transient fields, such as from NEMP or lightning. In these codes, space is divided into a three-dimensional rectangular grid and the fields in each cell are advanced in time by the direct application of Maxwell's curl equations. The major advantage of these codes is that they allow the modeling of a broad range of geometries, simply by defining the appropriate cells to be perfectly conducting.

A major shortcoming of these codes is their inability to model surface details that are on the order of the cell size or smaller due to the averaged nature of the calculated fields in each cell. Thus, small apertures, such as those resulting from door seams on an aircraft, cannot be handled directly by these codes. This paper describes a technique of augmenting such a code to calculate the early time responses of cavities, internal to the scatterer, that are coupled to the external scatter surface via long, thin apertures. The excitation source is a direct strike lightning channel which injects a current pulse to the scatterer.

In this technique, Babinet's principle is used to calculate the fields inside the cavity by considering all portions of the external scatterer surface except the portion which contains the aperture to be the source which excites the aperture. The cavity fields are thus found by taking the difference between the incident fields (obtained with the aperture plate removed) and the complementary fields (obtained with the aperture replaced by a magnetic wire). In both cases, the external scatter currents must be forced to be those present when the aperture is present. Since the apertures are thin, these currents can be found by first modeling the external portion of the scatterer with the aperture closed. The magnetic wires are modeled using the dual of a well-known thin wire TDFD technique [R. Holland, L. Simpson, IEEE Trans. on EMC, vol. EMC-23, pp. 88-97, May 1981].

Example calculations will be presented.

NUMERICAL EVALUATION OF COMPLEX RESONANCES  
OF AN ELLIPTIC CYLINDER

Radhakrishna Naishadham  
Electrical Engineering Department  
University of Mississippi  
University, MS 38677

L. Wilson Pearson  
McDonnell Douglas Research Laboratories  
P.O. Box 516  
St. Louis, MO 63166

## Abstract

The time-harmonic Green's function for induced currents on the surface of an infinite cylinder of arbitrary but smooth convex cross-section, excited by a uniform magnetic line source of infinite extent, is representable as an expansion in terms of creeping waves that circumnavigate the cylinder (E. Heyman and L.B. Felsen, IEEE Trans. Antennas Propagat., 31, 426-437, 1983). Computation of this Green's function is important in the numerical implementation of hybrid expansion schemes based on the creeping-wave representation.

The surface current density on the conducting cylinder may be expanded as a series of damped oscillations characterized by the complex natural resonances of the cylinder. This expansion is most effective at intermediate and lower frequencies. The natural resonances may be derived by imposing a self-consistency condition on the phase of the creeping waves which revolve around the cylinder. Numerical implementation of the phase integral expression for the complex resonances on an elliptic cylinder of 3:2 aspect ratio is discussed in the paper.

Complex resonances of the elliptic cylinder are determined independently by contour integration of the determinant of the moment matrix obtained in a homogeneous solution of the electric field integral equation. These resonances compare well with the asymptotic estimates derived from the creeping wave expansion.

## B-7-7

### CHARACTERIZATION OF OPTICAL FIBERS BY IMPULSE RESPONSE MEASUREMENTS

G.L. Yip, S. Belkasim and A.B. Puc  
Dept. of Electrical Engineering, McGill University,  
3480 University Street, Montreal, P.Q., Canada H3A 2A7

In pulse dispersion measurements of optical fibers, convenient, accurate and efficient computational methods are required to process the measured data for fiber characterizations. In particular, it is necessary to perform deconvolution with the measured input and output waveforms. The "Fast Fourier Transform" (FFT) method is widely used, but usually involves considerable amount of computer memory and time. Further, the numerical division of one Fourier spectrum by the other is very sensitive to the errors and inaccuracies in the measured waveforms and their digitization.

We present an alternative method for characterizing an optical fiber in terms of the temporal moments of its impulse response (S. Geckeler, Appl. Optics. 18, 13, pp. 2192-2198, 1979). These moments can be determined through evaluating the central moments of the measured input and output pulses of a fiber in a pulse dispersion experiment. Assuming the impulse response  $h(t)$  deviates but slightly from a Gaussian function and using an infinite series in Hermite polynomials to represent this small departure, an analytical expression for  $h(t)$  can be obtained. The moment method was applied in a pulse dispersion measurement experiment involving several multimode graded-index fiber samples. Moments evaluated to the sixth order were used to calculate  $h(t)$  and such fiber parameters as attenuation ( $\alpha$ ), pulse dispersion ( $\sigma$ ) and 3 dB bandwidth (B). Good agreement was achieved with  $h(t)$  obtained by the FFT method. Results will be presented and discussed.

The moment method is convenient, less sensitive to noise and much faster than the "FFT" method. It is considered ideally suited to industrial applications.

withdrawn

B-7-8

COMPARISONS OF BACKGROUND CHARACTERISTICS OF AN RCS  
MEASUREMENT RANGE USING A CW NULLING TECHNIQUE  
AND A PULSED-RANGE GATE TECHNIQUE

B. M. Kent, Air Force Wright Aeronautical Laboratories  
G. R. Simpson, R. J. Jost, A. J. Terzuoli  
Air Force Institute of Technology  
Wright Patterson Air Force Base, Ohio 45433

This paper deals with a direct comparison between the CW Nulling method and the pulsed-range gate method for radar cross-section measurements on an indoor far-field range. These two methods of obtaining RCS patterns are probably the most common and have been discussed in the past. The ultimate goal of this work is to apply the optimum RCS measurement technique to a new compact RCS measurement range. This newer arrangement has become popular due to its advantages over a far-field range and has been described to some extent in recent articles. A study independent of but similar to the one described here, was undertaken by Whitacre and Burnside at the Ohio State University.

In the CW nulling technique the empty chamber is illuminated and the received signal is added to a portion of the transmitted signal that has been altered such that it is of the same amplitude but opposite in phase to the received signal. This produces a deep null in the received signal. When a target is then placed in the signal path any measurable return is assumed to be target backscatter. The problem with CW nulling are the stringent phase and frequency stability requirements of all components in the RF system. Worse yet are the mechanical stability requirements of the anechoic chamber walls and all waveguiding components. Another problem stems from the constant illumination of the target and chamber. The null in the received signal was originally achieved in an empty chamber under a certain distribution of illuminating energy. By placing a target in the chamber, the energy is scattered and diffracted in various ways changing the distribution of illuminating energy. The possibility then exists that the chamber is no longer in a null and measurable return might not all be target backscatter. For targets with complex shapes it is hard to predict this effect in advance.

In the pulsed-range gate technique, by pulse modulating the transmitted signal and range gating the receiver, the system is capable of isolating the target from the rest of the chamber. Problems associated with this technique are the increased system complexity and inherent increase in internal noise levels. Another problem arises from pulse modulation. Power is distributed over a broadened spectrum as predicted by Fourier analysis, compounding the problem of distinguishing system noise from a low-level backscatter.

To compare the background characteristics of these techniques; RCS measurements of a plate, a cylinder, and a cone-sphere are taken using each method. These results are compared with each other and with numerical RCS predictions for the same shapes.

B-7-9

MEASUREMENT OF THE IMPULSE TIME DOMAIN  
SCATTER OF TARGETS IN A SMALL CHAMBER

Thomas P. Fontana and Kerry M. Yon  
Westinghouse Defense and Electronics Center  
Advanced Development Division  
P.O. Box 746, MS-333  
Baltimore, MD 21203

The Fast Fourier Transform of the spectral backscatter from a target is equivalent to the time domain reflection from a periodic train of pulses. It is customary to measure the spectral data in a large chamber using a precisely milled compact range reflector to simulate a plane wave in the near field. This paper describes measurements and processing techniques used with a small chamber (20 ft. x 10 ft. x 10 ft.) equipped with a standard four foot dish.

After describing the experimental setup, the calibration and processing techniques are presented. A calibration procedure for a small chamber is demonstrated in which the comparisons between a measured standard and modeled response are restricted to a small region about the standard. Windowing the target's time domain response is shown to be a viable technique for reconstructing accurate CW responses. Finally, it is shown that by demodulating the impulse response, some scattering mechanisms display simple phase signatures in their impulse response.

Processed time domain images and CW responses agree well with those obtained at more sophisticated ranges. It is concluded that small targets can be studied reasonably well in small chambers.

EXPERIMENTAL DETERMINATION OF RESONANT  
FREQUENCIES BY TRANSIENT SCATTERING FROM  
CONDUCTING SPHERES AND CYLINDERS

F. I. Tseng and T. K. Sarkar

Department of Electrical Engineering  
Rochester Institute of Technology  
Rochester, New York 14623

This paper presents a new experimental technique to measure resonant frequencies of a target. A Tektronix WP1310 waveform processing system has been employed, which features signal processing software with extensive control over instruments, waveform manipulations, and graphic display. Numerous transient waveforms scattered from spheres and cylinders of various sizes have been recorded. A recently developed data-processing technique has been described and applied to these transient waveforms to extract their resonant frequencies. With the use of a new window designed to have a low near-sidelobe level, the modified FFT is shown to be able to improve the measurement capability of the system.



## URSI COMMISSION B - SESSION B8

**Spectral Methods for  
Wave Propagation**8:30 - 12:00  
IRC-4**Méthodes spectrales pour  
la propagation des ondes**Chairperson/Président: **L.B. Felsen**, Polytechnic Institute of New York, Farmingdale, NY, USA

- 1 (8:40) REAL OR COMPLEX SPECTRA? AN EXAMINATION OF OPTIONS. **L.B. Felsen**, Polytechnic Institute of New York, Dept. of Electrical Engineering and Computer Science, Farmingdale, NY, USA
- 2 (9:10) SPECTRAL METHODS IN NON-DESTRUCTIVE EVALUATION. **K.J. Langenberg**, Theoretische Elektrotechnik, FB 16, Kassel, FRG
- 3 (9:40) TRANSIENT WAVEFIELDS AND CAUSTICS. **M.G. Brown**, University of Miami, Rosenstiel School of Marine and Atmospheric Science, Miami, FL, USA
- 4 (10:10) SPECTRAL SYNTHESIS OF INTRINSIC MODES FOR GENERAL WAVEGUIDING ENVIRONMENT. **J.M. Arnold**, University of Glasgow, Dept. of Electronics and Electrical Engineering, Glasgow, UK
- 5 (10:40) OCEAN ACOUSTIC WAVE PROPAGATION BY THE PARABOLIC EQUATION METHOD. **D. Lee**, Department of the Navy, Naval Underwater Systems Center, New London, CT, USA

## B-8-1

### REAL OR COMPLEX SPECTRA? AN EXAMINATION OF OPTIONS

L.B. Felsen

Department of Electrical Engineering and Computer Science  
Polytechnic Institute of New York  
Route 110, Farmingdale, NY 11735

Wave spectra play a fundamental role in the representation of time-harmonic and transient propagation and scattering phenomena. While rigorously and globally applicable in idealized environments with separability and (or) symmetry constraints, these formulations are extendable, at high frequencies, or "early" observation times, to a considerably more general class of environments since the spectra can then be contracted around their interference maxima and tracked locally along maximal trajectories. The trajectories, the ray paths, are defined by the stationary phase (constructive interference) condition in the spectral integral. Conventional ray theory results from the most drastic spectral shrinkage while various uniformized ray theories retain spectral intervals sufficiently wide to accommodate transition regions where the simple theory fails. The initial synthesis, before contraction, usually involves real spectra in the wave-number and frequency domains. These real spectra are well suited to describe wave processes localized around real stationary points that describe real rays. However, certain collimated wave fields - confined by tapered illumination, medium refraction, or concave surface guiding - have spectral integrands with complex stationary points. The option then exists to retain the distributed real spectra intact in these cases, or to localize, by analytic continuation, around compact complex spectral values. The latter define complex ray trajectories. Examples are presented to illustrate the smeared out real and concentrated complex spectral alternatives.

## SPECTRAL METHODS IN NON-DESTRUCTIVE EVALUATION

K.J. Langenberg  
Theoretische Elektrotechnik, FB 16  
Gesamthochschule Kassel  
D-3500 Kassel, FRG

Presently, non-destructive evaluation (NDE) of flaws and defects in materials by means of ultrasound utilizes two basic approaches: firstly, imaging methods derived from a linearized inversion of Huygens' principles are applied to data collected within a synthetic aperture, and, secondly, identification procedures rely on the information contained in a record of just one scattered transient signal. This transient signal is composed of specific prominent wave fronts and more smoothly varying portions contributed by the so-called penumbra-umbra region of the scatterer. Generally, the wave fronts, according to a theory provided by Felsen and Shirai, can be of inherent or non-inherent types, where the latter ones allow a decomposition into resonances within a complex spectral domain.

The paper presents numerical model computations and experimental results obtained by an NDE-related ultrasonic scattering experiment to illustrate this specific structure of scattered transients and how it can be used for identification purposes.

As a first approach, the underlying scattering model is scalar, referring to longitudinal-longitudinal wave scattering, and the geometries under consideration are infinitely long cylinders with arbitrary elliptical cross-sections, two-dimensional strips, and prolate and oblate spheroids. Interpretation of the results within the context of the Felsen-Shirai theory is intuitive by comparing various techniques of computation (eigenfunction expansions, GTD and Physical Optics). Derivation of appropriate spectral identification methods is then straight forward.

Experimental results are essentially non-scalar; therefore, elastodynamic full-wave solutions of the above kind are presently evaluated to be compared with experiments for a ribbon crack with stressfree boundaries.

## B-8-3

### TRANSIENT WAVEFIELDS AND CAUSTICS

Michael G. Brown  
University of Miami  
Rosenstiel School of Marine and Atmospheric Science  
4600 Rickenbacker Causeway  
Miami, Florida 33149 USA

The propagation of high frequency acoustic waves in inhomogeneous media excited by a point source is considered. The Maslov-WKB technique provides a spectral decomposition of time-harmonic wavefields for both separable and non-separable problems. Transient wavefields are then represented as two-fold integrals over frequency and ray parameter. Chapman's method allows both integrals to be evaluated without approximation. The caustics of high frequency wave propagation may be classified using catastrophe theory: the stationary phase condition (Fermat's principle) establishes the connection between the two subjects. The Maslov-WKB-Chapman wavefield representation combined with the results of catastrophe theory provides a complete description of transient wavefields in the vicinity of caustics. These wavefields are examined in some detail. Waveform distortions as well as travel time curve behavior in the vicinity of caustics are discussed. Both the 'interior catastrophes' (of the Airy, Percy, etc. type) and the 'boundary or constraint catastrophes' (of the Fresnel, etc. type) are considered. Constraints imposed on these wavefields by causality are discussed. Finally, it is shown how constraints on transient wavefields imposed by catastrophe theory can be exploited in the seismic inverse problem.

SPECTRAL SYNTHESIS OF INTRINSIC MODES FOR  
GENERAL WAVEGUIDING ENVIRONMENT

J.M. Arnold  
Department of Electronics and Electrical Engineering  
University of Glasgow  
Glasgow G12 8QQ

The problem of constructing approximate wavefunctions for the description of propagation in weakly nonseparable environments has recently been subjected to intensive investigation. Problems of this type are the rule, rather than the exception, in naturally occurring waveguides such as are found in underwater acoustics or geophysical exploration; they also occur frequently in man-made structures and are particularly important in integrated optics devices, where tapered couplers, lenses, and other components are made from non uniform sections of waveguides.

It has transpired from recent work on weakly nonseparable waveguides that spectral objects, called intrinsic modes, can function in a very similar manner to the normal modes of a separable (translation invariant) waveguide. Intrinsic modes are superpositions, in the form of spectral integrals, of certain basic spectral elements. These spectral basis elements, while being in principle globally extended wavefields throughout the configuration space, are subject to mutual interference. For a fixed observation point in the waveguiding structure, constructive interference of the basis wavefunctions occurs only for a small portion of the spectrum centred around a particular unique spectral basis function, by the principle of stationary phase. If the spectral basis functions are chosen in such a way that they look like local normal modes in neighbourhoods of points where they dominate the spectral integral, then one has a representation for the field in the non uniform guide which is very similar to the conventional adiabatic mode theory; however, the integral also smooths out the non uniformities of adiabatic mode theory where a local normal mode becomes radiative or is reflected due to narrowing of the waveguide.

These ideas originated in a study of a special model problem, the open wedge with planar boundaries (J.M. Arnold and L.B. Felsen; JASA, 75, 1105-1119, 1983; JASA, 76, 850-860, 1984). The generality of intrinsic mode spectra has since been widened to describe general 3-dimensional geometries including curved open boundaries and transverse (as well as lateral) inhomogeneities of refractive index; numerical comparisons with less sophisticated techniques have been conducted, and the connection with ordinary coupled mode theory has been established by means of a renormalisation method. It has thus emerged that the intrinsic mode concept provides the foundation for a comprehensive theory of wave propagation in nonuniform waveguides.

## B-8-5

### OCEAN ACOUSTIC WAVE PROPAGATION BY THE PARABOLIC EQUATION METHOD

Ding Lee  
Naval Underwater Systems Center  
New London, CT 06320, U.S.A.

Most ocean acoustic wave propagations are predicted by the solution of the Helmholtz equation. A class of ocean acoustic wave propagation problems can be solved by a set of partial differential equations other than the Helmholtz equation. These partial differential equations include the parabolic wave equation. Over a decade ago, when the Parabolic Equation (PE) method was introduced, it received a lot of interest. However, during that period of time, the PE method was not fully developed to its capability. Until recent years, the PE method was much refined and its computations enhanced by advances in numerical analysis and availability of supercomputers. The PE approach is an important development and is proved to handle a class of range-dependent problems efficiently. These recent improvements permit the PE model to handle sophisticated ocean environments in realistic and systematic manner. These overall developments are highlighted. The main theme of this talk is centered at one particular contribution - the wide angle capability. The wide angle development involves contributions in applied mathematics, numerical methods, and computational acoustics; most importantly, the capability of handling realistic ocean environments. The theoretical development will be outlined. A benchmark ocean acoustic problem is chosen to discuss the need for the wide angle capability. Then, the wide angle model is used to solve the benchmark problem whose numerical results are used to support the validity of the wide angle development.

## URSI COMMISSION B - SESSION B9

## Scattering

1:30 - 5:00

## Diffusion

IRC-1

Chairperson/Président: **M.A.K. Hamid**, University of Manitoba, Winnipeg, MB

- 1 ROTATIONAL-TRANSLATIONAL ADDITION THEOREMS FOR SPHEROIDAL WAVE FUNCTIONS. **R.H. MacPhie, J. Dalmas, R. Deleuil**, Université de Provence, Laboratoire de Radioélectricité, Marseille, France
- 2 ELECTROMAGNETIC SCATTERING BY TWO PROLATE SPHEROIDS IN PARALLEL CONFIGURATION: EXPERIMENTAL RESULTS. **R. Deleuil, J. Dalmas, R.H. MacPhie**, Université de Provence, Laboratoire de Radioélectricité, Marseille, France
- 3 SCATTERING BY A DIELECTRIC CYLINDER OF RECTANGULAR CROSS SECTION WITH OBLIQUE INCIDENCE. **R.G. Rojas**, Ohio State University ElectroScience Laboratory, Dept. of Electrical Engineering, Columbus, OH, USA
- 4 SCATTERING BY A METAL CYLINDER COATED BY DIELECTRIC LAYERS AND PENETRABLE SHEETS. **J.G. Davis**, Motorola Inc., Schaumburg, IL, USA; **P.L.E. Uslenghi**, University of Illinois at Chicago, Dept. of Electrical Engineering and Computer Science, Chicago, IL, USA
- 5 GEOMETRICAL OPTICS SCATTERING FROM A PENETRABLE WEDGE. **N.J. Damaskos**, Damaskos Inc., Concordville, PA, USA; **P.L.E. Uslenghi**, University of Illinois at Chicago, Dept. of Electrical Engineering and Computer Science, Chicago, IL, USA
- 6 A BACKSCATTERING STUDY OF MUTUAL INTERFERENCE BETWEEN CONDUCTING PLATES. **C.L. Yu**, Pacific Missile Test Center, Electromagnetic Systems Division, Point Mugu, CA, USA
- 7 SCATTERING BY SMALL STEPS ON LARGE PLATES. **W. Hallidy**, General Dynamics-Convair, San Diego, CA, USA
- 8 A RESONANCE EXPANSION FOR THE ELECTROMAGNETIC FIELDS SCATTERED BY CONDUCTING AND NON-CONDUCTING SPHERES. **D.J. Riley**, Sandia National Laboratories, Electromagnetic Applications Division, Albuquerque, NM, USA
- 9 A THREE-DIMENSIONAL, FINITE POISSON TRANSFORMATION AND ITS APPLICATION IN OBTAINING A HYBRID REPRESENTATION OF FIELDS IN AN OVER-MODED RECTANGULAR CAVITY. **D. Wu, D.C. Chang**, University of Colorado, Electrical and Computer Engineering, Boulder, CO, USA
- 10 SIMULATION OF SYNTHETIC APERTURE RADAR IMAGERY OF THREE DIMENSIONAL OBJECTS. **I.J. LaHaie**, Environmental Research Institute of Michigan, Infrared and Optics Division, Ann Arbor, MI, USA

## B-9-1

### ROTATIONAL-TRANSLATIONAL ADDITION THEOREMS FOR SPHEROIDAL WAVE FUNCTIONS

R.H. MacPhie, J. Dalmas and R. Deleuil  
Laboratoire de Radioélectricité  
Université de Provence, Marseille France

An addition series is deduced to represent the scalar spheroidal wave function  $\Psi_{mn}^{(q)}(h_q; \xi_q, \eta_q, \Phi_q)$ , based on an arbitrarily located and oriented cartesian reference frame  $(x_q, y_q, z_q)$ , in terms of scalar spheroidal wave functions  $\Psi_{\mu\nu}^{(j)}(h_r; \xi_r, \eta_r, \Phi_r)$ , based on a second arbitrarily positioned and oriented Cartesian coordinate system  $(x_r, y_r, z_r)$ . The coefficients of the expansion series  $Q_{mn, \mu\nu}^{qr}$  can be expressed as a simple product of two matrices (a rotation matrix and a translation matrix) which are preceded and followed by column matrices which depend respectively only on the spheroid parameters  $h_r$  and  $h_q$ , i.e., on the semiinterfocal distances ( $F = h\lambda/2\pi$ ) of the two spheroidal systems. The extension of the theory to vector wave functions is also discussed.

**ELECTROMAGNETIC SCATTERING BY TWO PROLATE SPHEROIDS  
IN PARALLEL CONFIGURATION : EXPERIMENTAL RESULTS**

R. Deleuil, J. Dalmás and R.H. MacPhie  
Laboratoire de Radioélectricité  
Université de Provence, Marseille France

Experimental data, in the form of monostatic radar cross sections, has been obtained for two prolate conducting spheroids, each with an axial ratio ( $a/b$ ) of 2. Both end-to-end and side-by-side configurations are considered at frequencies that span the so-called resonance region and for a variety of center-of-center separations. The radar cross sections of two spheroids, each with  $a/b = 10$ , are also presented. In both cases ( $a/b = 2$  and  $a/b = 10$ ) the measured data is compared with theoretical results available in the recent literature.

## B-9-3

### Scattering by a Dielectric Cylinder of Rectangular Cross Section with Oblique Incidence

Roberto G. Rojas  
The Ohio State University ElectroScience Laboratory  
Department of Electrical Engineering  
Columbus, Ohio 43212

A Moment Method (MM) solution is developed for the fields scattered by a dielectric cylinder of rectangular cross section. Unlike previous papers [Richmond, IEEE Trans. Vol. AP-13, May 1965, pp. 334-341, Vol. AP-14, July 1966, pp. 460-464], this paper considers the incident plane wave to have oblique incidence with respect to the axis of the cylinder as depicted in Figure 1. Furthermore, the incident plane wave can have arbitrary polarization. For the case of oblique incidence, the TE and TM scattered fields are coupled and the unknown total electric field inside the dielectric cylinder has three nonzero components, i.e.,  $E_x$ ,  $E_y$ , and  $E_z$ . The total electric field inside the dielectric cylinder is the unknown quantity in an integral equation from which a system of linear equations is obtained. The cylinder cross section is divided into square cells which are small enough so that the electric field is nearly constant in each cell, however, all the fields have the same exponential  $z$  dependence as the incident field. The system of linear equations is obtained by enforcing at the center of each cell the condition that the total electric field must be equal to the sum of the scattered and incident fields. Once the total electric field inside the cylinder is computed, the scattered field at any other point in space is easily obtained.

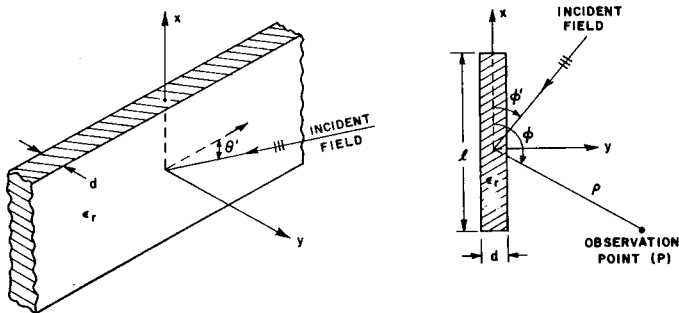


Figure 1. Plane wave incident on a dielectric cylinder of rectangular cross section.

SCATTERING BY A METAL CYLINDER COATED BY  
DIELECTRIC LAYERS AND PENETRABLE SHEETS

J. G. Davis

Motorola Inc., Schaumburg, IL 60196

and

P. L. E. Uslenghi

Department of Electrical Engineering and Computer Science  
University of Illinois at Chicago

The scattering of a plane electromagnetic wave by a coated metallic cylinder is considered. The coating consists of layers of dielectric materials separated by sheets on which an impedance condition holds, implying discontinuity of the tangential magnetic field across each sheet. The sheet impedance may model a resistive layer or a frequency-selective surface and, therefore, is important in such applications as antenna radomes and modification of radar cross-sections.

An exact solution to the scattering problem is obtained, and high-frequency asymptotic results for the far field are derived using well-known techniques. The effectiveness of this type of layered structures on curved surfaces is discussed in detail.

## B-9-5

### GEOMETRICAL OPTICS SCATTERING FROM A PENETRABLE WEDGE

N. J. Damaskos  
Damaskos Inc., P.O. Box 469, Concordville, PA 19331  
and  
P. L. E. Uslenghi  
Department of Electrical Engineering and Computer Science  
University of Illinois at Chicago

The scattering of a plane electromagnetic wave by the edge of a penetrable wedge is considered. The electromagnetic field in air and inside the wedge may be considered, in a first approximation based on geometrical optics (G.O.), as a discrete set of plane waves which are generated by reflection and transmission at the faces of the wedge, and which travel in different directions with different amplitudes and phases that are determined by G.O. considerations. However, these plane waves occupy only certain angular regions of space, and terminate abruptly at G.O. boundaries, where G.O. predicts a discontinuity in the field. The G.O. solution is a good approximation to the exact solution if the observation point is at a distance of at least a few wavelengths from the edge and is not near a G.O. boundary.

The discrete spectrum of plane waves is extracted from an integral equation formulation of the problem, in order to obtain a bound on the error made by taking the G.O. solution. An approximate description of the field near a G.O. boundary is given in terms of Fresnel integrals.

A BACKSCATTERING STUDY OF MUTUAL INTERFERENCE  
BETWEEN CONDUCTING PLATES

C. Long Yu  
Electromagnetic Systems Division  
Pacific Missile Test Center  
Point Mugu, California 93042

The electromagnetic mutual interaction between simple objects such as flat plates or finite cylinders in a backscattering environment is of considerable interest in the study of electromagnetic shadowing effects and mutual interference of scatterers on a modern complex radar target. This mutual interference problem represents higher-order electromagnetic backscattering contributions to the radar cross section (RCS) of a radar target. If realistic backscattering properties of a complex radar target are to be determined analytically, mutual interaction effects must be included in the mathematical simulation calculations. In order to determine and assess the effect and significance of various scattering mechanisms involved in the mutual interaction problem, an experimental approach using high-resolution microwave imaging measurements may be employed. High-resolution measurements are capable of isolating and determining the dominant scattering contributions due to the higher-order reflection and diffraction terms such as reflected-reflected, reflected-diffracted, diffracted-reflected, reflected-diffracted-reflected and diffracted-diffracted terms. Test models, composed of two finite conducting flat plates oriented in various configurations, were used in high-resolution and continuous-wave (CW) RCS measurements to experimentally study the mutual interaction phenomenon as well as the primary scattering mechanisms involved. Interesting results exhibited in CW backscattering patterns, range profile patterns, and two-dimensional image maps will be presented to illustrate the significance of shadowing effects and mutual interference encountered in the measurements.

Withdrawn

**B-9-7**

Scattering by small steps on large plates

William Hallidy  
General Dynamics-Convair  
MZ 416850, P.O. Box 85357  
San Diego, CA 92138

A two dimensional analytical solution is developed for scattering of plane waves by a small step on a perfectly conducting plane. The scattering may be described by an equivalent magnetic current in the TE<sub>z</sub> case or an equivalent magnetic line dipole in the TM<sub>z</sub> case. Thus it is easy to determine diffraction coefficients for use in three dimensional GTD applications. For the backscatter case the solutions possess a remarkable symmetry about the normal to the plane. The complex field viewed step down is the negative of the field viewed step up at the same angle to the plane's normal.

GTD equivalent current techniques are applied to backscatter by a step on an ogive shaped flat plate. Analytical results are presented for this configuration and compared to experimental results obtained at General Dynamics-Convair's Sycamore Canyon test facility.

Applications to steps on appropriately terminated cylindrical surfaces are also mentioned.

A RESONANCE EXPANSION FOR THE ELECTROMAGNETIC FIELDS  
SCATTERED BY CONDUCTING AND NON-CONDUCTING SPHERES

Douglas J. Riley  
Sandia National Laboratories  
Electromagnetic Applications Division, 2322  
Albuquerque, New Mexico 87185

The use of contour integration provides a straightforward method for expanding a function in terms of its singularities. The resulting expansion represents one possible form of the more general Mittag-Leffler expansion theorem. The benefit of using the contour technique is that the expansion is completely determined; an arbitrary (unknown) entire function does not need to be added to ensure the validity of the expansion. However, the method is only applicable to functions which remain suitably bounded within a contour which encompasses all singularities.

In general, the coefficients associated with the Mie series for the electromagnetic fields scattered from both perfectly conducting and dielectric spheres exhibit asymptotic growth within arbitrary contours which encircle the singularities associated with the coefficients. As a consequence, according to the contour method, it is not possible to expand the entire Mie coefficient. However, the contour technique can be used if one expands only a portion of the Mie coefficient; a portion which remains properly bounded within the contour. The resulting expansion is then independent of an unknown entire function, valid for arbitrary scattering angle, and possesses the desired property that the scattered field is specified in terms of the natural resonances associated with the sphere. The theory for applying this technique for representing the fields scattered from both perfectly conducting and homogeneous dielectric spheres in terms of their resonances is presented in this paper. In addition, numerical examples are presented which demonstrate the accuracy and stability of the expansions.

## B-9-9

### A THREE-DIMENSIONAL, FINITE POISSON TRANSFORMATION AND ITS APPLICATION IN OBTAINING A HYBRID REPRESENTATION OF FIELDS IN AN OVER-MODED RECTANGULAR CAVITY

Doris Wu and David C. Chang  
Electrical and Computer Engineering  
University of Colorado, Boulder, CO 80309

In assessing the electromagnetic interference of an equipment-under-test (EUT), it is often sufficient and frequently for sake of expediency to take EMI measurements in a so-called "reverberating chamber" which ideally is capable of producing a randomly-varying field over a time period substantially longer than the system response time of the EUT. In practice, such a chamber is made of an electrically large metallic rectangular cavity with a sufficiently low Q so that a large number of resonant cavity modes can be excited simultaneously at a given frequency. A rotating metallic "mode-stirrer" is then used to provide the mode-conversion function needed for producing the randomly-varying field.

In analyzing the ability of a mode-stirrer to produce the needed mode conversion, one has to deal with the scattering problem of a metallic object placed in an over-mode rectangular cavity. A double-variational formulation is used to find the scattered cavity modes due to a given incident cavity mode, and, as such, one has to deal with the issue of how to develop a numerically desirable expression for the diadic Green function of a rectangle cavity, particularly when the source point is close to the observation point. Being a resonant cavity, the resonant modes clearly should be retained; however, one can ill-afford the exclusive use of a model representation since the convergence of the higher-order, non-resonant modes is notoriously slow from a numerical view point. In the case of a single infinite summation, it is a well-known practice that one may truncate the sum to a finite one, and then evaluate the remainder analytically, albeit approximately. Such a procedure proves to be cumbersome in the three-dimensional case. In this work, a finite, three-dimensional Poisson transformation is developed rigorously and the resultant expression gives rise to a hybrid representation of cavity modes, combined with images produced by the reflecting boundaries of the cavity. Depending upon the composite Q of the cavity, we then judiciously select only those cavity modes that are near resonant and express the remainder field by its image terms. Such a hybrid representation turns out to be particularly effective in dealing with the integration of the Green's function with the current distribution over the surface of the scatterer, since only the self-term plus, at the most, several adjacent images are needed to obtain the desirable numerical accuracy. Using this representation, we have calculated successfully the statistics of the scattered field distribution as a result of a rotating thin-wire mode-stirrer of finite length. Several conclusions regarding its physical location and orientation will be given in the presentation.

**SIMULATION OF SYNTHETIC APERTURE RADAR  
IMAGERY OF THREE DIMENSIONAL OBJECTS**

Ivan J. LaHaie  
Infrared and Optics Division  
Environmental Research Institute of Michigan  
P.O. Box 8618  
Ann Arbor, MI 48107

A computer-based simulation package for generating Spotlight synthetic aperture radar (SAR) imagery of arbitrary, three-dimensional objects is described. The objects are created using a geometrical modeling method based on combinatorial solid geometry techniques, whereby a complex structure is built up via Boolean operations on a set of primitive bodies (spheres, cylinders, cones, etc). The scattering of the radar waveform by the object is modeled by a generalization of the physical optics (PO) approximation. The generalization allows the inclusion of multiple reflections and shadowing, and is achieved through a novel approach to the sampling of the object geometry. A system transfer function technique is used in the calculations, permitting the combined effects of the scattering and SAR image formation processing to be cast into a single input-output relationship for each geometrical sampling point. This is possible because of the local nature of the physical optics scattering process. Perfectly conducting as well as impedance boundary conditions can be specified, and full polarization capability exists within the limits of the PO model. A wide variety of SAR system parameters, such as wavelength, resolution, and collection geometry can be specified. Two modes of image simulation are possible, depending upon whether or not the aspect variation of the object scattering can be ignored. Simulated images of simple scattering objects for both modes are shown.



## URSI COMMISSION B - SESSION B10

## Transients II

1:30 - 5:00  
IRC-3

## Transitoires II

Chairperson/Président: **S.K. Chaudhuri**, University of Waterloo, Waterloo, ON

- 1 SPECTRAL THEORY OF TRANSIENTS: FORMULATION, INTERPRETATION, APPLICATION. **E. Heyman**, Tel Aviv University, Dept. of Electrical Engineering, Tel Aviv, Israel; **L.B. Felsen**, Polytechnic Institute of New York, Dept. of Electrical Engineering and Computer Science, Farmingdale, NY, USA
- 2 ACCELERATION OF FD-TD NUMERICAL MODELING OF RADAR CROSS SECTION VIA FAST FOURIER TRANSFORM COMPUTATION OF FIELD SPATIAL DERIVATIVES. **T.G. Jurgens, K.R. Umashankar**, University of Illinois at Chicago, Dept. of Electrical Engineering and Computer Science, Chicago, IL, USA; **A. Taflove**, Northwestern University, Dept. of Electrical Engineering and Computer Science, Evanston, IL, USA
- 3 FINITE DIFFERENCE-TIME DOMAIN FORMULATION OF AN INVERSE SCATTERING SCHEME FOR REMOTE SENSING OF INHOMOGENEOUS LOSSY LAYERED MEDIA. **S.K. Chaudhuri**, University of Waterloo, Dept. of Electrical Engineering, Waterloo, ON; **K. Umashankar**, University of Illinois at Chicago, Dept. of Electrical Engineering and Computer Science, Chicago, IL, USA; **A. Taflove**, Northwestern University, Dept. of Electrical Engineering and Computer Science, Evanston, IL, USA
- 4 ACOUSTIC PULSE DIFFRACTION BY TILTED HALF-PLANES. **M.J. Yedlin, E.V. Jull**, University of British Columbia, Dept. of Geophysics and Astronomy and Dept. of Electrical Engineering, Vancouver, BC
- 5 ANNIHILATION OF PURELY IMAGINARY SINGULARITIES. **R.K. Ritt**, Illinois State University, Dept. of Mathematics, Normal, IL, USA
- 6 SPECULAR SCATTERING FROM SURFACES WITH A SMALL RADIUS OF CURVATURE. **A.K. Dominek, W.D. Burnside, L. Peters Jr.**, Ohio State University ElectroScience Laboratory, Columbus, OH, USA
- 7 TRANSIENT RESPONSE CALCULATION FOR MULTIPLE CONDUCTOR STRUCTURES ABOVE A HOMOGENEOUS EARTH. **O. Aboul-Atta, G. Bridges**, University of Manitoba, Dept. of Electrical Engineering, Winnipeg, MB
- 8 K-PULSE FOR A THIN CIRCULAR LOOP. **H.T. Kim, N. Wang, D.L. Moffatt**, Ohio State University ElectroScience Laboratory, Dept. of Electrical Engineering, Columbus, OH, USA
- 9 ANALYSIS OF N-CONDUCTOR TRANSMISSION LINE SYSTEMS WITH NON-LINEAR LOADS. **S.P. Castillo, C.H. Chan, R. Mittra**, University of Illinois, Electromagnetic Communication Laboratory, Urbana, IL, USA
- 10 ANALYSIS OF CONDUCTOR LOSSES OF A MULTICONDUCTOR TRANSMISSION LINE SYSTEM. **J. Venkataraman, T.K. Sarkar**, Rochester Institute of Technology, Rochester, NY, USA; **A.R. Djordjevic**, University of Belgrade, Dept. of Electrical Engineering, Belgrade, Yugoslavia

SPECTRAL THEORY OF TRANSIENTS: FORMULATION,  
INTERPRETATION, APPLICATION

E. Heyman

Department of Electrical Engineering  
Tel Aviv University, Israel

and

L.B. Felsen

Department of Electrical Engineering and Computer Science  
Polytechnic Institute of New York  
Route 110, Farmingdale, NY 11735

Spectral synthesis of source-excited strongly dispersive transient wave phenomena usually requires construction of the time-harmonic solution and subsequent Fourier inversion over frequency. However, when wave processes are weakly dispersive, the harmonic spectra can be approximated by local plane waves that are invertable explicitly into the time domain. Subsequent spatial spectral superposition of the constituent transient fields then yields the source-excited response in simple form. This feature has been incorporated into a spectral theory wherein the wave spectra are allowed to be real or complex. Various physical weakly dispersive wave processes are categorized by the singularities (poles or branch points), which they generate in the complex spectral plane, and by the motion of these singularities as a function of time. At early times, "wavefront approximations" yield simple explicit results, but implicit forms are valid at all observation times that do not violate the weakly dispersive assumption. Spectral objects compact in complex space are shown to give rise to distributed, and physically less transparent, objects when the spectra are constrained to be real. Illustrative examples include source excited transient wave fields in configurations giving rise to abrupt or continuous refraction, to multiple reflection-refraction, with associated different species of ray caustics, to lateral waves, and to edge diffraction.

ACCELERATION OF FD-TD NUMERICAL MODELING OF RADAR CROSS SECTION  
VIA FAST FOURIER TRANSFORM COMPUTATION OF FIELD SPATIAL DERIVATIVES

Thomas G. Jurgens and Korada R. Umashankar  
Department of Electrical Engineering and Computer Science  
University of Illinois at Chicago  
Chicago, IL 60680 USA

Allen Taflove  
Department of Electrical Engineering and Computer Science  
Northwestern University  
Evanston, IL 60201 USA

In previous work, the finite-difference time-domain (FD-TD) method was demonstrated by the authors to provide a high numerical modeling accuracy of 1 dB (with respect to measurements) over at least a 40-dB dynamic range of radar cross section values for 9-wavelength size three-dimensional objects exhibiting such scattering physics as edge and corner diffraction, corner reflection, and cavity penetration. It appears that the cases previously studied represent the largest detailed three-dimensional numerical scattering models of any type ever verified wherein a uniformly fine spatial resolution and the ability to treat non-metallic composition is incorporated in the model.

Wider use of the FD-TD approach has been inhibited by the large computer storage and running time requirements of FD-TD, and the general lack of access to supercomputers which can deal with these requirements. The goal of the research described in this paper is the development of efficient algorithms for FD-TD which could ultimately cut its storage and running time requirements for large three-dimensional numerical models by 125:1 and 625:1, respectively. This would permit VAX 11/780 computers to process 10-wavelength size models in about 4 minutes per look angle, and Cray-1S computers to process 50-wavelength size models in about 10 minutes per look angle.

The acceleration of FD-TD numerical modeling in this manner would result from utilizing a spatial discretization approaching the Nyquist sampling limit of 2 points per wavelength, rather than the present sampling of 10 - 11 points per wavelength. Existing local (centered-difference) field derivatives are grossly inaccurate at 2 samples per wavelength. However, a global computation of field spatial derivatives using the fast Fourier transform method (O. G. Johnson, Proc. IEEE, 72, 90-95, 1984) permits approaching the Nyquist limit.

This paper describes initial one and two-dimensional results for FD-TD numerical models of radar cross section using the FFT method for computing field spatial derivatives. Emphasis here is on algorithm accuracy and stability, and avoidance of aliasing.

FINITE DIFFERENCE-TIME DOMAIN FORMULATION OF  
AN INVERSE SCATTERING SCHEME FOR REMOTE  
SENSING OF INHOMOGENEOUS LOSSY LAYERED MEDIA

Sujeet K. Chaudhuri  
Department of Electrical Engineering  
University of Waterloo, Waterloo, Ont., Canada

Korada Umashankar  
Department of Electrical Engineering and Computer Science  
University of Illinois at Chicago, Chicago, IL. USA

Allen Taflove  
Department of Electrical Engineering and Computer Science  
Northwestern University, Evanston, IL. USA

The present paper is concerned with the inverse scattering problem of determining the electromagnetic characteristics (conductivity, permittivity, permeability) of an inhomogeneous layered propagation medium from the knowledge of a time dependent incident wave and the resulting backscattered field response. This situation is often considered as an useful model for many practical situations in applications involving the electromagnetic probing of biological media, and the natural geo-physical media (earth, ice, sea, etc).

Several analytical and numerical methods for this profile inversion based on the integral equation formulation - both in the frequency and in the time domain have been discussed previously. In contrast, to the best of authors' knowledge, very little or no attempt to solve this problem with the differential equation formulation has been made. Here it will be shown that the time domain differential equation formulation is simple to implement and has broad applications compared to previously attempted inversion methods.

The profile inversion technique developed in this paper is based on the differential equation formulation of the direct scattering (interaction and also propagation) problem known as the Finite-Difference Time-Domain (FD-TD) method. FD-TD is a direct solution of Maxwell's time-dependent curl equations for the electric and magnetic fields at a regular lattice of points covering a volume of space that contains a given scatterer. A fully explicit numerical algorithm is used to simulate real-time wave propagation and scattering. Using this direct scattering algorithm in conjunction with the causality of the time-domain response, an iterative optimization routine capable of estimating the electromagnetic characteristic profile in a step by step fashion (layer stripping) is developed. This optimization scheme constructs the conductivity, permittivity and permeability profile of the medium such that the time history of the resulting total field at a given location (outside the medium being probed) fits a given input time-domain field (measured) response in a least-square-error sense.

Results of the numerical simulation of various layered stripping examples will be presented.

## ACOUSTIC PULSE DIFFRACTION BY TILTED HALF-PLANES

M.J. Yedlin and E.V. Jull  
Department of Geophysics and Astronomy and  
Department of Electrical Engineering  
University of British Columbia  
Vancouver B.C. V6T 1W5

The analysis of seismic pulse diffraction by simple underground structures is helpful in time interpretation of recorded data in oil exploration. The boundary conditions for acoustic diffraction are the same as in electromagnetics but the fields are scalar. Shear-wave effects are generally less prominent and can be neglected.

The basic model consists of a point source and receiver on the earth's surface over a half-plane arbitrarily tilted with respect to the plane of the earth's surface. A solution for the total field in terms of Fresnel integrals is used. This requires source and receiver to be far from the edge. However, good numerical results can be obtained for distances as small as a wavelength. This monochromatic solution is evaluated for each frequency in the source pulse bandwidth, so that it must be numerically efficient. The frequency range used is 5 to 60 Hz. with a peak amplitude at 20 Hz. Up to 500 source receiver positions with 512 time sampling intervals have been used.

Previous analyses of this kind of problem in Geophysics have used the Kirchoff method. It is well known that this method fails for source and receiver at large angles from the edge. It also results in a diffacted field amplitude which is incorrectly symmetrical about the normal to the edge. The present method appears to be more efficient numerically, particularly with the use of a diffraction coefficient outside the transition regions about the reflection boundary. More complex structures such as strips and corners can also be analyzed by this combination of asymptotic and spectral methods.

## B-10-5

### ANNIHILATION OF PURELY IMAGINARY SINGULARITIES

R.K. Ritt, Illinois State University

It is well known that for perfectly conducting bounded scatterers, the magnetic field integral equation formulation of the exterior problem, in the  $s$ -plane, results in an operator whose inverse, as a function of  $s$ , is analytic for  $\text{Re } s > 0$ , and is otherwise meromorphic. The singularities in the left half plane are used in the analysis of the time dependent initial value problem; the singularities on the imaginary axis are identified with the characteristic frequencies of a dual interior problem. Since, in the use of numerical methods to estimate these singularities, these latter type emerge, there has been, from time to time, concern expressed as to the relationship of these singularities to the exterior problem.

In this paper we show that for the analogous scalar exterior Neumann problem, in the construction of the resolvent Green function, these singularities are annihilated, and consequently play no role in the exterior scattering problem. Specifically, if  $S$  is a bounded smooth surface, and if  $K(s)$  is the integral operator:

$$[K(s)u](x) = \frac{1}{2}u(x) + \iint_S u(y) \frac{\partial}{\partial n_y} G(s, |x-y|) dS_y, \quad G(s, r) = \frac{e^{-sr}}{4\pi r}$$

then the resolvent Green function, corresponding to a source at  $x_0$  and an observation point at  $x$ , both in the exterior region, is given by:

$$G(s, |x-x_0|) - \iint_S \frac{\partial}{\partial n_y} G(s, |y-x|) [K^{-1}(s)G(s, |x_0-y|)] dS_y.$$

In this last expression, when the integration is completed, the purely imaginary singularities of  $K^{-1}(s)$  no longer appear.

The method of proof does not seem to have an immediate extension to the vector problem.

**SPECULAR SCATTERING FROM SURFACES WITH  
A SMALL RADIUS OF CURVATURE**

A.K. Dominek, W.D. Burnside, L. Peters, Jr.  
The Ohio State University  
ElectroScience Laboratory  
1320 Kinnear Road  
Columbus, Ohio 43212

Specular scattering from smooth, two dimensional conducting bodies with small radii of curvature is discussed. Existing solutions such as the Luneburg-Kline expansion and the Pathak Reflection Coefficient with its asymptotic form are compared to results from a Time Domain Extraction technique (TDE). The TDE procedure first obtains the time domain representation of the scattered fields from the numerical transformation of exact or measured frequency domain fields and then "gates" out the specular contribution to recover the "exact" specular scattered field. This specular field is then transformed back to the frequency domain.

Finally a heuristically developed parabolic based, uniform reflection coefficient is presented. The uniformity is with respect to the electrical size of the radii of curvature at the surface's specular point. This uniformity allows the physically interpreted diffracted fields from an edge to be related to the reflected fields from a smooth surface as the radii of curvature increases. The coefficients are heuristically generated from the exact scattered field for a two dimensional parabolic cylinder with plane wave illumination. The significant variables in this solution are the radius of curvature at the specular point and the distance between the specular point and the incident shadow boundaries.

## B-10-7

### TRANSIENT RESPONSE CALCULATION FOR MULTIPLE CONDUCTOR STRUCTURES ABOVE A HOMOGENEOUS EARTH

O. Aboul-Atta and G. Bridges  
Department of Electrical Engineering  
University of Manitoba  
Winnipeg, Manitoba, Canada R3T 2N2

The case of a single conductor located above a lossy medium has been studied extensively at all frequency ranges. An exact solution for the electromagnetic field is generally derived using Maxwell's equations and treating the situation as a boundary value problem. The Sommerfeld integrals involved in the resulting solution, and caused by the finite conductivity of the earth, prove difficult to evaluate and their importance at higher frequencies has led to various solution techniques and approximations. The results of these studies has provided an insight into the higher frequency behaviour of the single wire case. However, in order to be useful for many practical problems the work for the single wire conductor must be extended to the multiple conductor case.

Power engineers have successfully utilized a multiple conductor solution based on the telegrapher's equations. For this quasi-static solution many low frequency approximations have been assumed, such as the simplification or complete elimination of the Sommerfeld integrals, which is only adequate at power frequencies. When higher frequencies are required for accurately describing transient diagnostics and applications, such as lightning effects, EMP coupling, or system fault studies, the low frequency theory in general is no longer adequate.

A frequency domain approach for the determination of the impulse response of multiple parallel conductors located above a lossy earth will be presented. The conductor current matrix is operated on through convolution by the system transfer function  $[S(z,t)]$  as

$$[I(z,t)] = [S(z,t)] * [I(0,t)]$$

$$\text{where } [S(z,t)] = \mathcal{F}^{-1}[P][D][P]^{-1}$$

$$\text{and } [D] = [\exp(jk_z^m)]$$

For transient studies the characteristic propagation constants of the structure,  $k_z^m$ , as well as the modal surge impedances,  $Z_0^m$ , where  $[v] = [Z_0^m][i]$ , are required. The method of extracting  $k_z^m$  and  $Z_0^m$  for use with this model will be presented. The work is aimed at detection and recognition of faults on long transmission lines and the exactness of the solution required to achieve this goal will also be discussed.

K-PULSE FOR A THIN CIRCULAR LOOP

H.T. Kim, N. Wang and D.L. Moffatt  
The Ohio State University ElectroScience Laboratory  
Department of Electrical Engineering  
Columbus, Ohio 43212

Based on the pole elimination concept ( Gerst and Diamond, Proc. IRE, July, 1961 ), a time-limited input waveform, the K-pulse, is obtained for a thin, conducting, circular loop. The resultant response waveforms are also found to be time-limited. Therefore, by employing the K-pulse input, the resonant ringing associated with the circular loop has been eliminated. This paper will describe the concept and the procedures for deriving the K-pulse. An interpretation will also be given to the impulse response of the thin circular loop to demonstrate the various scattering mechanism involved.

ANALYSIS OF N-CONDUCTOR TRANSMISSION LINE  
SYSTEMS WITH NON-LINEAR LOADS

Steven P. Castillo, Chi H. Chan, and Raj Mittra  
Electromagnetic Communication Laboratory  
University of Illinois  
Urbana, Illinois 61801

In recent years the density of solid state devices that can be placed on a printed circuit board or on a single silicon wafer has increased dramatically. Thus, the problem of estimating the coupling, crosstalk and pulse distortion in an n-conductor transmission line has become an important one.

The miniaturization of solid state devices is of great importance in computer driven phased arrays, telecommunication circuits, and computers themselves. In each of these applications, malfunction of the system could result from false gating due to crosstalk and pulse distortion in the circuitry.

Although the study of n-conductor transmission lines is not new, no satisfactory method exists for treating the case where the loads are nonlinear and complex, as in the case of solid state devices.

This paper presents a time-domain method for numerically solving transient problems on transmission line systems with non-linear complex loads. The loads specifically studied are digital devices, e.g., TTL logic gates, mounted on printed circuit boards.

A general circuit model is used to characterize the device. The circuit model consists of a simple R-C network in parallel with a generator. The values of the resistance and the generator voltage are derived from the V-I curves of the device. Therefore, the model does not have to be modified for different devices. Only the V-I curves and the shunt capacitance of each specific device must be known. Application of boundary conditions at each end of the line results in two nonlinear matrix differential equations. These equations cannot be solved using conventional frequency domain analysis followed by Fourier transformation. Thus, they must be solved directly in the time domain. In this paper the nonlinear differential equations are solved numerically using finite difference algorithms.

The results given are for a typical set of line and device parameters. The numerical results are compared with the experimental data and good agreement is found. A comparison of the cpu times used for different finite difference algorithms is also included in the paper.

ANALYSIS OF CONDUCTOR LOSSES OF A MULTICONDUCTOR  
TRANSMISSION LINE SYSTEM

Jayanti Venkataraman\*, Antonije R. Djordjevic<sup>+</sup> and Tapan K. Sarkar\*

\*Department of Electrical Engineering, Rochester Institute of Technology, Rochester, NY 14623

<sup>+</sup>Department of Electrical Engineering, University of Belgrade, 11001 Belgrade, Yugoslavia

A method is presented for the analysis of a multiconductor transmission line system where the conductors and the ground plane are of large but finite conductivity. Of particular interest here is the frequency behaviour of the inductance and resistance. The conventional approach where the resistance is obtained perturbing the perfect conductor case, it is assumed that the skin effect is fully developed. The resistance thus obtained is inadequate to describe the low frequency behavior of the line where it should be almost frequency independent and equal to the dc value. The inductance obtained by inverting the capacitance matrix yields a frequency independent result while in some cases the dc and high frequency inductance can differ by a few tens percent.

The system under consideration consists of transmission lines infinitely long, rectangular in cross section, arbitrary in size and orientation and immersed in a homogenous, non magnetic lossless dielectric. The current density assumed to be uniform along the length of the line is dependent only on the transverse coordinates. The excitation is by an axially independent TM electromagnetic wave. The total electric field intensity is related to the unknown currents in the transmission line by the magnetic vector potential and the gradient of the scalar electric potential. Since the ground plane is of finite extent with a large but finite conductivity, the arbitrary constant appearing in the two-dimensional Green's function has to be evaluated. A numerical method is presented where the condition has been imposed for the total current to be zero, whereby this constant is eliminated rather than evaluated. The distribution of the unknown currents is approximated by pulses and the amplitude of these pulses are determined by a point matching technique.

The inductance and resistance matrices have been obtained for some typical multiconductor transmission line systems. The frequency behavior of a two wire transmission line illustrates very well the low frequency behavior, below 100 kHz, of the resistance, which tends to the dc resistance; and the inductance where the dc and high frequency values differ by a few tens percent. The stability of the numerical method is also illustrated.



## URSI COMMISSION B - SESSION B11

## Numerical Techniques II

1:30 - 5:00  
IRC-5

## Techniques numériques II

Chairperson/Président: **R.F. Harrington**, Syracuse University, Syracuse, NY, USA

- 1 GRAPHICS APPLICATIONS IN EM COMPUTER MODELING. **E.K. Miller, M.J. Barth, G.J. Burke, R.D. Merrill**, Lawrence Livermore National Laboratory, Livermore, CA, USA
- 2 CONJUGATE GRADIENT ITERATIVE SOLUTION OF AN INTEGRAL EQUATION WITH A SMALL NUMBER OF GREEN'S FUNCTION TERMS: THE FIN-LINE DISCONTINUITY PROBLEM. **K.J. Webb**, University of Maryland, Electrical Engineering Dept., College Park, MD, USA; **R. Mittra**, University of Illinois, Dept. of Electrical and Computer Engineering, Urbana, IL, USA
- 3 ON THE ELECTROMAGNETIC WAVE SCATTERING FROM INFINITE RECTANGULAR CONDUCTING GRIDS VIA THE SPECTRAL DOMAIN CONJUGATE GRADIENT METHOD. **C.G. Christodoulou**, University of Central Florida, Orlando, FL, USA; **J.F. Kauffman**, North Carolina State University, Raleigh, NC, USA
- 4 A NOVEL TECHNIQUE TO THE SOLUTION OF TRANSIENT ELECTROMAGNETIC SCATTERING FROM THIN WIRES. **S.M. Rao**, Osmania University, Research and Training Unit for Navigational Electronics, Hyderabad, India; **T.K. Sarkar**, Rochester Institute of Technology, Dept. of Electrical Engineering, Rochester, NY, USA
- 5 THE CONTRACTION CORRECTOR SPECTRAL ITERATION METHOD. **J.C. Brand**, Motorola Inc., Scottsdale, AZ, USA; **C.G. Christodoulou**, University of Central Florida, Orlando, FL, USA; **J.F. Kauffman**, North Carolina State University, Raleigh, NC, USA
- 6 ON MAKING ITERATIVE ALGORITHMS FOR PLANAR STRUCTURES MORE EFFICIENT. **R. Kastner**, Rafael, Haifa, Israel
- 7 AN ITERATIVE METHOD FOR SCATTERING FROM 2-DIMENSIONAL CONDUCTING BODIES. **M. Kaye**, University of Haifa, Electromagnetics Dept., Haifa, Israel; **P.K. Murthy, G.A. Thiele**, University of Dayton, Graduate Engineering and Research, Dayton, OH, USA
- 8 FINITE ELEMENT ANALYSIS OF ELECTROMAGNETIC APERTURE COUPLING PROBLEMS. **S.L. Ray, N.K. Madsen**, Lawrence Livermore National Laboratory, Livermore, CA, USA; **J.C. Nash**, Verstatc, Santa Clara, CA, USA
- 9 SCATTERING FROM A MULTILAYERED PERIODIC ARRAY OF RESISTIVE STRIPS. **R.C. Hall, R. Mittra**, University of Illinois, Electromagnetic Communication Laboratory, Urbana, IL, USA
- 10 SCATTERING FROM CYLINDRICAL PERIODIC SURFACES. **T. Cwik, R. Mittra**, University of Illinois, Electromagnetic Communication Laboratory, Urbana, IL, USA

## B-11-1

### GRAPHICS APPLICATIONS IN EM COMPUTER MODELING

E. K. Miller, M. J. Barth, G. J. Burke, R. D. Merrill  
Lawrence Livermore National Laboratory

Computational procedures for solving electromagnetic radiation and scattering problems have become increasingly routine. Much progress has been made in broadening the variety and complexity of applications amenable to computer solution using a variety of approaches. The result has been to make available an ever growing amount of data to the EM analyst and designer. Paradoxically, however, this added data may not be as fully exploited as would be beneficial due to its sheer volume. In addition, other kinds of data that computational procedures could provide may not even be utilized because of our inability to interpret it. There is clearly a need to extract more information from these data to obtain a better understanding of the electromagnetic phenomena involved, i.e., to acquire knowledge from the data.

Computer graphics represents a tool that could contribute substantially to analyzing computer-generated data for the information and knowledge it can reveal. Use of computer graphics in EM applications is still in its infancy, although examples can be found which indicate its potential. In this paper we will survey possible uses of graphics in EM computations, emphasizing Moment-Method modeling. Presentation of physical observables will be illustrated, as well as quantities of a more abstract nature, such as the matrices which arise in the Moment Method. We also consider how relationships that graphics presentations reveal might be represented in useful mathematical models. Finally, we discuss and demonstrate how computer-controlled, video-cassette recorders can be used to make graphics movies conveniently available to the modeler.

**CONJUGATE GRADIENT ITERATIVE SOLUTION  
OF AN INTEGRAL EQUATION WITH  
A SMALL NUMBER OF GREEN'S FUNCTION TERMS:  
THE FIN-LINE DISCONTINUITY PROBLEM**

Kevin J. Webb  
Electrical Engineering Department  
University of Maryland  
College Park, Maryland 20742

Raj Mittra  
Department of Electrical  
and Computer Engineering  
University of Illinois  
Urbana, Illinois 61801

**ABSTRACT**

Many electromagnetic problems require the solution of an integral operator equation of the form  $Lf = g$ , where  $f$  is the unknown and  $g$  is due to the incident field. A number of these problems involve the use of a Green's function with a relatively small number of terms. Examples occur in the analysis of millimeter-wave and microwave integrated circuit waveguides, such as fin-line and microstrip, where the Green's function is comprised of the waveguide modes. Numerical methods, for example the moment method, are necessary to find approximate mode functions in these waveguides. However, it is difficult to find accurate modal solutions which satisfy the orthogonality condition. This means that only a small number of modes may be used in the Green's function. Difficulties then result when applying the conjugate gradient iterative method to the discontinuity problem with unknowns in the transverse junction plane.

Consider the specific problem of solving for the scattering parameters of a step discontinuity in fin-line. The unknown in the integral equation is the magnetic current over the transverse junction plane within the shield. The unknown is represented discretely on an  $(m, n)$  grid of points. Data has been obtained using three modes with  $m = 17$  and  $n = 33$ . Good results with rapid convergence are achieved when solving the uniform problem even with a poor initial estimate. However, application to the step discontinuity problem with differing slot widths does not yield satisfactory results. The conjugate gradient method converges to a solution which corresponds to a higher-order waveguide mode than those in the Green's function. This results in  $s_{11}$  for the junction going to one.

Difficulties arise when applying the conjugate gradient method to waveguide discontinuity problems which use a Green's function with a relatively small number of modes. The number of degrees of freedom in the unknown is larger than the number of modes used. It is necessary to have the number of unknowns similar to, or less than the number of modes in the Green's function.

## B-11-3

### ON THE ELECTROMAGNETIC WAVE SCATTERING FROM INFINITE RECTANGULAR CONDUCTING GRIDS VIA THE SPECTRAL DOMAIN CONJUGATE GRADIENT METHOD

C.G.Christodoulou  
University of Central Florida  
P.O.Box 25000  
Orlando,FL. 32816

J.F.Kauffman  
North Carolina State University  
P.O.Box 5275  
Raleigh,NC. 27650

The Conjugate Gradient method in the spectral domain is employed to solve the problem of Electromagnetic wave scattering from infinite gratings and meshes which are made of conducting strips of arbitrary conductivity and width. The equivalent radius principle is applied to the strips to evaluate the reflection coefficient for a circular wire mesh. An internal impedance for the infinite wires is utilized to account for the effects of the finite conductivity of the wires. Another impedance expression is used in the case where the wires are made of different alloys. This technique can be used to solve the problem of scattering from a mesh for all spacings among adjacent wires, whereas, other methods, such as the Spectral Iteration Approach and the Averaged Boundary Condition method are limited to certain spacings. This algorithm can be used to solve for both induced currents and aperture fields. Moreover, it was observed that the convergence rate of the problem depends significantly on the shape of the chosen unit cell. Results for the reflection coefficients, induced currents, and aperture fields are compared with data from other methods to support the validity of the new algorithm.

A NOVEL TECHNIQUE TO THE SOLUTION OF  
TRANSIENT ELECTROMAGNETIC SCATTERING FROM THIN WIRES

Sadasiva M. Rao, Research and Training Unit for  
Navigational Electronics, Osmania University, Hyderabad, India.

Tapan K. Sarkar, Department of Electrical Engineering,  
Rochester Institute of Technology, Rochester, NY 14623

Previous approaches to the problem of transient scattering by conducting bodies have utilized the well-known marching-on-in-time solution procedures. However, these procedures are very dependent on discretization techniques and in most cases lead to instabilities as time progresses. Moreover, the accuracy of the solution procedure cannot be verified easily and usually there is no error estimation. Recently an alternate approach to the solution of transient scattering by thin wires was presented (Rao et al., Journal of Radio Science, Sept. 1984) based on Conjugate gradient method. In this procedure space and time are discretized independently into subintervals and the error is minimized iteratively. Unfortunately, this procedure is very slow and is not easily extendable to other geometries. Moreover, with this procedure most of the advantages of marching-on-in-time procedure are lost. In this paper, again Conjugate gradient method is applied to solve the above problem, this time reducing the error to a desired value at each time step. Since error is reduced at each time step, marching-on-in-time can still be done without error accumulation as the time progresses. Computationally, this procedure is as fast as conventional marching-on-in-time procedure. Thus, this new method retains all the advantages of marching-on-in-time procedure and yet does not introduce instabilities in the late time. It is also possible to apply this procedure to other geometries. Details of the solution procedure along with numerical results will be presented.

## B-11-5

### THE CONTRACTION CORRECTOR SPECTRAL ITERATION METHOD

J.C.Brand  
Motorola Incorporated  
8201 E McDowell Road  
Scottsdale, AZ. 85252

C.G.Christodoulou  
University of Central Florida  
P.O.Box 25000  
Orlando,FL. 32816

J.F.Kauffman  
North Carolina State University  
P.O.Box 5275  
Raleigh,NC. 27650

Strip gratings have been widely used in the construction of polarizers, filters, and artificial dielectrics. Similarly, wire meshes have been used extensively for their good electromagnetic shielding properties. In the past, the Moment method, the Averaged Boundary Condition method, and the Spectral Iteration approach have been employed to tackle the problem of electromagnetic wave scattering from such periodic structures. The Spectral Iteration approach (S.I.T) which is the fastest numerical method of the three, fails to converge for spacings of two wavelengths or less between adjacent strips. Recently, a new algorithm called the "Contraction Corrector Spectral Iteration Method" was developed to alleviate the S.I.T approach from its convergence problems for all spacings. In this method the contraction mapping theory is applied to the basic iterative scheme of the S.I.T to insure convergence in a very rapid manner. The problem is formulated for one and two dimensional problems, (i.e infinite gratings and meshes, respectively). The method can handle the problem of scattering from both perfectly conducting strips and strips with finite conductivity. The regions of applicability of the new algorithm and its limitations are presented and discussed. Furthermore, results and comparisons of this algorithm with other methods are included.

ON MAKING ITERATIVE ALGORITHMS FOR PLANAR  
STRUCTURES MORE EFFICIENT

Raphael Kastner  
RAFAEL, P.O.Box 2250/87  
Haifa 31021, Israel

A major problem in many numerical methods is computer storage requirements which may severely limit the size of analyzable scatterers. Iterative algorithms, such as the conjugate Gradient (CG) algorithm, are no exception. This work is aimed at trying to reduce storage requirements as much as possible, sometimes at the expense of computation time, loss of generality or perhaps uncertain convergence. To this end, certain modifications are introduced to the CG algorithm as applied to planar structures via the spectral representation. The modifications take advantage of the fact that the source-field relationships for planar problems are formulated by an invertible operator which the standard CG does not exploit. The modification results in the elimination of one 2-D vector, namely the previous correction (gradient) term normally used at each CG iteration step except for the first one. At each iteration step, a companion step with the inverse operator is added, making the combined algorithm a succession of "restarts", without going back to the very slow Gradient algorithm. The saving is about 30 percent. Convergence is little affected when certain relaxation measures are taken, and is still achieved when SIT, say, fails.

In addition, it is shown that only one vector for both fields and currents need be stored with another minor modification.

Finally, if the closed-form spectral domain 2-D Green's function is continually re-computed from simple 1-D blocks rather than being stored, the total 2-D storage requirement is reduced to twice the number of samples only. Examples with a few thousand sampling points have been worked out using the method discussed above.

AN ITERATIVE METHOD FOR SCATTERING FROM  
2-DIMENSIONAL CONDUCTING BODIES

M. Kaye, Electromagnetics Department  
Haifa, Israel

P. K. Murthy and G. A. Thiele  
Graduate Engineering and Research  
University of Dayton 45469

An iterative method is developed for computing the current induced by TE plane wave excitation on conducting bodies of arbitrary shape. The scattering body is divided into lit and shadow regions separated by the geometric optics boundary. Further, the induced current at any point on the surface of the scatterer is expressed as the sum of an approximate optics current and a correction current. These currents are then determined by requiring that the induced current satisfies the magnetic field integral equation (MFIE). This requirement leads to a sequence of integral equations for optics and correction currents in the lit and shadow regions. The form of all of these equations is the same and all are Fredholm's integral equations of the second kind. Each of these equations may be solved by iteration. Thus, this technique consists in repeating the same procedure over and over again and, as such, is especially suitable for implementation on a digital computer.

The general theory presented here is applied to scattering from a two-dimensional cylinder of square and circular cross sections. These results are compared with those of method of moments and excellent agreement is obtained. An especially interesting feature of this method is that unique and accurate results are obtained even for resonant-size scatterers.

**FINITE ELEMENT ANALYSIS  
OF ELECTROMAGNETIC  
APERTURE COUPLING PROBLEMS\***

*S. L. Ray and N. K. Madsen*

Lawrence Livermore National Laboratory  
P.O. Box 5504, L-156, Livermore, CA 94550

*J. C. Nash*

Versatec  
2710 Walsh, Santa Clara, CA 95051

A general purpose finite-element computer code for solving non-linear, second-order systems of PDE's is currently under development. This code, FENL, uses a Galerkin procedure to reduce a set of PDE's in two spatial dimensions and one time dimension to a larger system of ODE's in the time variable. The solution is then obtained by integrating the system of ODE's with a standard ODE solver.

FENL is capable of handling a wide class of PDE's with fairly arbitrary boundary conditions. In contrast with earlier 2-D finite-element PDE solvers, this code is not restricted to a rectangular region or grid but rather permits any logically-regular mesh.

This code has been used to obtain solutions for electromagnetic aperture coupling problems. As the finite-element technique is applied to the differential equations, time-domain solutions for the interior fields are determined directly. A simple model of air chemistry has been included to study the effects of an electron distribution on the coupling phenomena.

## SCATTERING FROM A MULTILAYERED PERIODIC ARRAY OF RESISTIVE STRIPS

R. C. Hall and R. Mittra  
Electromagnetic Communication Laboratory  
University of Illinois  
Urbana, Illinois 61801

Periodic arrays of conducting patches have many applications in radomes, frequency selective filters and artificial dielectrics. In this paper the formulation of the array problem is extended to the finitely conducting case where the boundary condition on the patches is the resistive condition, or more precisely the jump condition. Calculated results are presented for single as well as multilayered resistive strip gratings.

The Spectral-Galerkin procedure, which is a particularly efficient procedure for studying periodic structures, has been used. The formulation is carried out in the spectral domain where the convolution form of the integral equation reduces to a product form. The unknown induced current is expanded in a set of entire domain basis functions and a matrix equation is derived for the expansion coefficients. Computation time is minimal since the matrix size is typically small and, in addition, no numerical integration or special functions are required in the computation of the matrix elements.

The Spectral-Galerkin method is extended here to include the analysis of imperfectly conducting thin strips that satisfy the resistive boundary condition. A surface resistance is defined that is constant over a wide frequency range for strips that are thin compared to the attenuation length. The current supported by such a strip is proportional to the tangential E and accounts for a jump in the tangential H across the strip.

Results are presented for a periodic array of resistive strips. The incident field is a plane wave polarized with the E-field parallel to the strips. The reflection and transmission coefficients have been investigated for resistances in the range of  $R=0 \text{ } \Omega/\text{square}$  (perfectly conducting case) to  $R=750 \text{ } \Omega/\text{square}$ .

The Spectral-Galerkin technique applied to a single layer yields its generalized scattering matrix which, in turn, can be cascaded to derive the scattering properties of multilayered structures. Using this approach, the transmission loss and reflected power have been calculated for multilayered resistive strip gratings and are presented in the paper. As expected, the results show that increasing the resistivity of the strips reduced the reflection coefficient and lowered the resonance Q relative to the perfectly conducting case. For other periodic structures we would expect a similar reduced resonance effect if imperfectly conducting materials are used.

## SCATTERING FROM CYLINDRICAL PERIODIC SURFACES

*Tom Cwik and Raj Mittra*  
*Electromagnetic Communication Laboratory*  
*University of Illinois*  
*Urbana, Illinois 61801*

The scattering of fields from planar periodic surfaces has been extensively studied during the past fifteen years. Many techniques have been developed which predict, to various degrees of accuracy, the frequency response of planar periodic surfaces comprising patches and apertures of arbitrary shape. In many applications, the frequency selective surfaces are not planar. Immediate examples are hyperbolic subreflectors, spherical or conical antenna radomes, and cylindrical shielding structures. Because these surfaces are non-planar, their analysis is, in general, exceedingly difficult and, to the best of the knowledge of the authors, no systematic studies of such surfaces have been reported in the literature.

In this paper we investigate a specific type of non-planar frequency selective surface, viz., the circular cylindrical FSS (see Fig. 1). We show that this problem is tractable via a generalization of the approaches commonly employed for planar surfaces. In the cylindrical case, periodicity exists both in  $z$  ( $T_z$ ) and  $\phi$  ( $T_\phi$ ), where  $T_\phi = 2\pi/N$ ,  $N$  being the number of cells around the cylinder. Fields for  $\rho \geq \rho_0$  and  $\rho \leq \rho_0$  are represented by Floquet harmonics subject to a given incident field. An equation is formulated for the unknown induced current, on a patch contained within a periodic cell. From a solution of the induced current scattering characteristics of the surface are found in terms of the reflected and transmitted fields along with their respective coefficients.

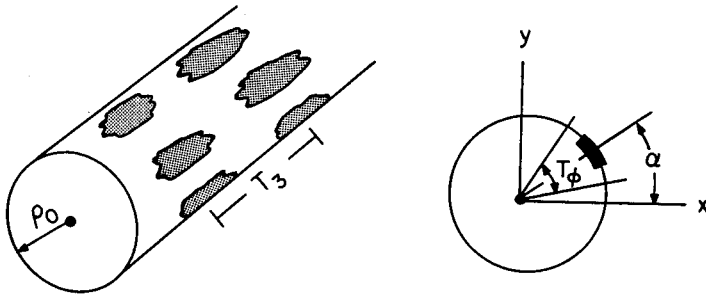


Figure 1. Geometry of cylindrical periodic surface.



## URSI COMMISSION B - SESSION B12

Guided Waves

1:30 - 5:00  
IRC-3

Ondes guidées

Chairperson/Président: **G.L. Yip**, McGill University, Montréal, PQ

- 1 GRADIENT-INDEX FIBER CONFIGURATION FOR A MONOPULSE LIDAR FEED. **S.M.S. Saad** Military Technical College, Cairo, Egypt; **W.K. Kahn**, George Washington University, Washington, DC, USA
- 2 RADIATION PROPERTIES OF A TAPERED DIELECTRIC SLAB WAVEGUIDE. **N.K. Uzunoglu**, National Technical University of Athens, Dept. of Electrical Engineering, Athens, Greece
- 3 A GROUNDED DIELECTRIC SLAB WAVEGUIDE WITH A SMOOTHLY VARYING THICKNESS. **S.R. Seshadri**, University of Wisconsin-Madison, Dept. of Electrical and Computer Engineering, Madison, WI, USA
- 4 THE POSSIBLE EXCITATION OF NOVEL LEAKY WAVES. **T. Tamir, F.Y. Kou**, Polytechnic Institute of New York, Dept. of Electrical Engineering and Computer Science, Brooklyn, NY, USA
- 5 EFFICIENT METHODS TO ANALYZE DIELECTRIC WAVEGUIDE STRUCTURES. **C. Yeh**, University of California at Los Angeles, Dept. of Electrical Engineering, Los Angeles, CA, USA; **A. Johnston**, California Institute of Technology, Jet Propulsion Laboratory, Pasadena, CA, USA
- 6 PROPAGATION CHARACTERISTICS OF WEAKLY GUIDING OPTICAL WAVEGUIDES. **F. Manshadi**, Jet Propulsion Laboratory, Pasadena, CA, USA; **C.W. Yeh**, University of California, Los Angeles, CA, USA
- 7 INTEGRAL EQUATION ANALYSIS OF PROPAGATION IN MICROSTRIP TRANSMISSION LINES. **J.S. Bagby**, University of Texas at Arlington, Dept. of Electrical Engineering, Arlington, TX, USA
- 8 ANALYSIS OF COPLANAR WAVEGUIDE WITH FINITE CONDUCTOR THICKNESS AND A SUBSTRATE WITH A LOSSY LAYER. **C. Tzuang, T. Itoh**, University of Texas, Dept. of Electrical and Computer Engineering, Austin, TX, USA
- 9 REGIMES OF PURELY GUIDED AND LEAKY SURFACE-WAVE MODES ON INTEGRATED DIELECTRIC WAVEGUIDES. **D.P. Nyquist, M.J. Cloud, D.H. Kamm**, Michigan State University, Dept. of Electrical Engineering and Systems Science, East Lansing, MI, USA; **B.C. Drachman**, Michigan State University, Dept. of Mathematics, East Lansing, MI, USA
- 10 WAVE PROPAGATION IN TWO-Dimensionally PERIODIC STRUCTURES. **S.T. Peng**, New York Institute of Technology, Electromagnetics Laboratory, Old Westbury, NY, USA; **T.L. Dong**, Polytechnic Institute of New York, Microwave Research Institute, Brooklyn, NY, USA

GRADIENT-INDEX FIBER CONFIGURATION  
FOR A MONOPULSE LIDAR FEED

Said M. S. Saad  
Military Technical College, Cairo, Egypt and  
George Washington University, Washington, D.C. 20052

Walter K. Kahn  
Department of Electrical Engineering & Computer Science  
George Washington University, Washington, D.C. 20052

A feed comprising two coupled square-law gradient-index (slab) fibers is proposed for a monopulse optical radar, LIDAR application. For the appropriately dimensioned coupling region the magnitude of the coupled field is proportional to the angular target deviation while the transverse form of the coupled wave is characteristic of the sense of the angle deviation. Computed results for the 2-dimensional (cylindrical) case are presented.

The axis of one (slab) gradient-index fiber is coincident with the axis of a cylindrical lens antenna. The input plane of the fiber is located in the focal plane of the lens. Although more general situations could be handled, we will assume apodization (antenna taper), aperture, focal length and fiber parameters chosen so that the focal field approximates the form of the fundamental gaussian beam-mode (displaced fundamental mode) of the fiber.

Using an approximate technique to compute coupling coefficients (M.D.Feit and J. A. Fleck, Jr., J. Opt. Soc.Am. 71, 1361-1372 (1981) in conjunction with the Hamiltonian formalism of W. K. Kahn and S. Yang, Optics Letters 8, 238-240(1983)) we design a coupler with overall length equal to the "beam oscillation suppression length" defined by Kahn and Yang. At this length we find the coupled amplitude (=square root of coupled power) in fiber #2 varies linearly with input beam displacement which is, in turn, proportional to the angular target deviation from the antenna axis. The computed field in fiber #2 closely satisfies the relation

$$F_{2L}(\xi_2) = F_{2R}(-\xi_2)$$

where the subscript L (R) denotes that the initial beam in fiber #1 is deviated to the left (right) and  $\xi_2$  is the normalized transverse coordinate in fiber #2.

RADIATION PROPERTIES OF A TAPERED DIELECTRIC SLAB WAVEGUIDE

Nikolaos K. Uzunoglu  
 Department of Electrical Engineering  
 National Technical University of Athens  
 Athens 10682, Greece

Tapered dielectric rod structures have been used in the past to develop microwave antennas. In these antennas the energy is feed through a hollow tube metallic waveguide or sometimes through a coaxial to waveguide adaptor. In millimeter wave applications there is an increasing interest in using dielectric waveguides because of the achievable lower attenuation figures and lighter weights in comparison with metallic waveguides.

In this paper the radiation from a tapered dielectric slab waveguide is considered for transverse electric(TE) waves. The geometry of the problem is shown in figure 1. Assume an incident guided surface wave from  $z \rightarrow -\infty$  towards  $z=0$  propagating in the dielectric slab waveguide. At  $z=0$  the slab waveguide starts to taper and diminishes at  $z=c$ . In order to analyze the diffraction of the incident wave the tapered region is subdivided into  $N$  sections. A constant thickness is attributed to each section. Then it is possible to describe the field in each section in terms of the well known mixed spectrum eigenwaves of the slab waveguides. According to this in the  $j$ 'th section the electric field can be written as,

$$E^{(j)} = \sum_u (A(u,j)\exp(-jk_{uj}z) + B(u,j)\exp(jk_{uj}z))U_{uj}(x) \quad (1)$$

where  $\sum_u$  is the generalized summation for the mixed spectrum,  $U_{uj}(x)$  are the corresponding eigenwaves,  $k_{uj}$  are the propagation constants and  $A(u,j), B(u,j)$  are the unknown  $u_j$  amplitudes of the forward and backward propagating waves respectively. In the  $j=0$ (semi-infinite dielectric slab waveguide) and  $j=N+1$ (free space) regions eq.(1) is modified appropriately. In order to determine the  $A(u,j), B(u,j)$  amplitudes the terminal conditions on the  $z=0$  and  $z=c$  planes plus the appropriate boundary conditions at the interface planes at  $z=z_1, z=z_2, \dots, z=z_N$ (see fig.1) are employed. Then the field at  $j=1$  section is determined in terms of the amplitudes  $A(u,N+1)(B(u,N+1)=0)$ . Finally the boundary conditions at  $z=0$  are satisfied leading into determination of the  $A(u,N+1)$  and  $B(u,0)$  values which are needed in computing the radiation pattern and input impedance of a given tapered dielectric slab antenna.

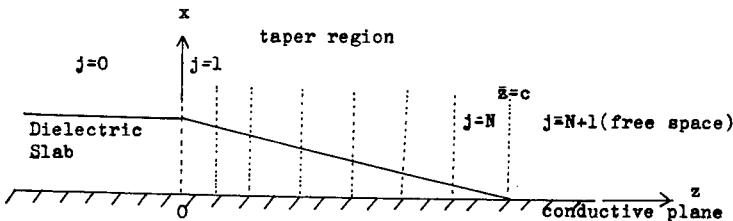


Figure 1. Tapered dielectric slab antenna.

**B-12-3**

**A GROUNDED DIELECTRIC SLAB WAVEGUIDE WITH A  
SMOOTHLY VARYING THICKNESS**

S.R. Seshadri  
Department of Electrical and Computer Engineering  
University of Wisconsin-Madison  
Madison, WI 53706 USA

Paper Withdrawn/  
La communication a été retirée

THE POSSIBLE EXCITATION OF NOVEL LEAKY WAVES

T. Tamir and F.Y. Kou

Department of Electrical Engineering and Computer Science  
Polytechnic Institute of New York, Brooklyn, N.Y. 11201

Recent work on optical waveguides has revealed the presence of novel types of leaky waves along thin-film layers bounded by two open (substrate and cover) regions. The new field varieties include waves that radiate selectively into only one of the two open regions (C.W. Hsue and T. Tamir, *J. Opt. Soc. Amer. A*, 1, 923-931, 1984) and waves having backward propagation characteristics (G.I. Stegeman et al., *Opt. Lett.* 8, 383-385, 1983). However, although a few such novel leaky waves have been identified analytically, the actual excitation of these waves by realistic sources has not yet been reported.

We therefore examine the general problem of exciting a clearly identifiable leaky wave along a dielectric layer bounded by two open regions having different permittivities. For this purpose, we assume the presence of a localized source and describe its field in terms of an integral in a complex wavenumber plane consisting of four Riemann sheets. By using suitable contour deformations, it is possible to express the total field in terms of two continuous wave spectra (given by branch-cut integrals) and a discrete set of leaky waves (given by pole residues). The presence of an experimentally identifiable leaky wave depends on its field being measured as a distinct, and preferably dominant, constituent of the total field. We therefore choose a field representation that clearly separates leaky waves from the continuous wave spectra. With this choice, the excitable leaky waves are those represented by residues due to poles that appear in certain selected portions of the complex Riemann plane. All the other leaky-wave poles yield no residues and therefore they do not represent fields that can be physically identified. We then find that, out of all possible leaky-wave varieties, only a few of them can be excited. However, as some of these excitable fields are of novel types, the results suggest the possibility of field configurations that had not been previously recognized.

## B-12-5

### EFFICIENT METHODS TO ANALYZE DIELECTRIC WAVEGUIDE STRUCTURES

\*C. Yeh  
Electrical Engineering Department  
UCLA  
Los Angeles, CA 90024

A. Johnston  
Jet Propulsion Laboratory  
California Institute of Technology  
Pasadena, CA 91103

It has become increasingly apparent that dielectric-based waveguiding structures are the appropriate waveguides for high-frequency waves in the mm/sub mm or optical wavelength range. Also known is the fact that these waveguides may take on rather unconventional forms (i.e., other than circular cylindrical or rectangular cylindrical shapes). The purpose of this presentation is to summarize the efficient methods that we have developed in the treatment of the general shaped, inhomogeneous dielectric waveguides. Specifically, the finite element approach and the beam propagation (Scalar Wave-Fast Fourier Transform (SW-FFT)) approach will be discussed. Successful numerical examples will also be shown.

PROPAGATION CHARACTERISTICS OF  
WEAKLY GUIDING OPTICAL WAVEGUIDES

F. Manshadi, Jet Propulsion Laboratory, Pasadena, CA.  
C. W. Yeh, University of California, Los Angeles, CA.

This paper presents a powerful technique to treat the problem of wave propagation along a weakly guiding optical waveguide. The shape as well as the three dimensional index variation of the guide may be quite arbitrary as long as its weakly guiding character is preserved. The technique is based on the solution of the scalar wave equation by the forward-marching Fast Fourier Transform method (SW-FFT), which yields the spatial configuration of the field and its power intensity along the guiding structure. A subsequent spectrum analysis performed on the power intensity data provides the modal characteristics of the field such as the propagation constant and the relative amplitude of each mode (M. D. Feit, J. A. Fleck, Jr., Appl. Optics, 19, 1154-1164, 1980). This technique is first applied to several simple optical waveguides such as, step-index circular fiber, graded-index circular fiber, elliptical, triangular, and rectangular dielectric waveguides. The computed dispersion characteristics of these optical guiding structures are then compared with solutions obtained by using other known techniques and an excellent agreement is established. Finally, results are presented for more complex optical waveguides such as circular fiber with arbitrary index variation (other than radial) and dielectric waveguides with longitudinal index variation. The principal purpose of this paper is to show that the SW-FFT technique can be used to solve problems which cannot be handled easily by other approximate or exact techniques and that the field solution of a scalar wave equation for an arbitrarily shaped, inhomogenous dielectric waveguide is easily obtainable.

## B-12-7

INTEGRAL EQUATION ANALYSIS OF PROPAGATION IN  
MICROSTRIP TRANSMISSION LINES: J. S. Bagby,  
Department of Electrical Engineering,  
University of Texas at Arlington, Arlington,  
TX 76019

An exact integral equation is advanced for the analysis of a broad class of microstrip transmission systems. The utility of this formulation is demonstrated by using it to find the complex propagation constant of a rectangular strip transmission line.

The axially transformed surface current,  $\vec{k}(\vec{\rho})$ , associated with a natural mode on an axially uniform microstrip transmission line satisfies the homogeneous integral equation

$$\hat{t} \cdot \oint_{\ell} \vec{g}_e(\vec{\rho}; \vec{\rho}'; \zeta) \cdot \vec{k}(\vec{\rho}') d\ell' = 0$$

where  $\vec{g}_e(\vec{\rho}; \vec{\rho}'; \zeta)$  is the electric Green's dyad for the system. Here  $\zeta$  is the complex propagation constant associated with the mode,  $\hat{t}$  is a unit vector tangential to the transmission line conductor, and  $\ell$  is a closed path around the conductor cross section.

One approximate method of finding  $\zeta$  from this equation is to assume a static potential distribution on the transmission line. Application of the equation of continuity yields an axially directed current density to be used in the integral. Iteration on results in the required root. A more accurate determination of  $\zeta$  is made by implementation of the method of moments to the integral. In this case a more general transversely directed current can be accommodated, yielding improved accuracy for the resultant complex propagation constant.

Numerical results of these methods of solution are presented and compared to measurement and other published results. Further applications of the integral equation are discussed.

ANALYSIS OF COPLANAR WAVEGUIDE WITH FINITE  
CONDUCTOR THICKNESS AND A SUBSTRATE WITH A LOSSY LAYER

C. Tzuang and T. Itoh  
Dept. of Electrical and Computer Engineering  
The University of Texas  
Austin, Texas 78712

A mode-matching method is employed for the analysis of a multi-layer coplanar waveguide integrated circuit including a lossy semiconductor layer and finite thickness of the conductor strips. To incorporate the finite conductor thickness under consideration is important since the aspect ratio of the conductor thickness to the gap between central signal conductor and ground conductors is appreciable in practical integrated circuit design in contrast to other applications.

The coplanar waveguide structure under analysis is subdivided into several regions. In general, these regions fall into two categories: regular layer structure and slot. In terms of hybrid TE and TM mode formulations after matching all the boundary conditions at each region, four coefficients in slot regions and two coefficients at either upper or lower layers are obtained. The final deterministic equation for finding the propagation constant arises from matching the tangential electric and magnetic fields of the slot to those in both upper and lower layers. To match the tangential magnetic fields, the application of the orthogonality property takes place in the slot region. To match the tangential electric field, the orthogonality property is applied in either upper or lower region instead. This automatically matches the required boundary conditions on the conducting strips in both upper and lower layer regions. After the elimination of various types of the coefficients, a  $(2N-1)$  by  $(2N-1)$  homogeneous matrix equation  $ZQ$  is obtained, where  $N$  is the number of modes in the slot regions. Only two of the four types of the coefficients in the slot region remain after elimination process. The complex propagation constant is the root of  $\det(ZQ) = 0$  to yield non-trivial solutions for the remaining two types of the coefficients.

As soon as the propagation constant is found, all the coefficients of both TE and TM expansions in each region can be computed efficiently through matrix multiplications and the characteristics of the coplanar waveguide can be studied effectively.

Accuracy of the method has been confirmed by comparison of the results for a limiting case of infinitely thin conductors and lossless substrate with those in literature.

REGIMES OF PURELY GUIDED AND LEAKY SURFACE-WAVE  
MODES ON INTEGRATED DIELECTRIC WAVEGUIDES

D.P. Nyquist, M.J. Cloud, and D.H. Kamm  
Department of Electrical Engineering and Systems Science  
B.C. Drachman, Department of Mathematics  
Michigan State University, East Lansing, Michigan 48824

Typical integrated (e.g., strip, channel, rib) dielectric waveguides for millimeter and optical wavelengths consist of guiding regions deposited adjacent to or within a planar thin-film layer which is itself deposited upon a substrate and covered by a dielectric overlay. Surface-wave modes of the guiding region are strongly influenced by the substrate/film/cover background environment. When the latter tri-layered background supports TE and/or TM surface waves, i.e., when the film is itself a guiding region, new physical phenomena become evident in surface waves of the integrated guiding region. Conventional approximate analyses are inadequate to expose those new phenomena. Oliner et al. have identified new leakage and resonance effects through elaborate mode-matching solutions for step-index guiding regions with rectangular boundaries. The regimes of purely-guided and leaky surface waves are identified here for graded-index guiding regions of any cross-section shape through an integral-operator description of those modes.

The axial Fourier transform  $\vec{e}(\vec{\rho}, \zeta) = \mathcal{F}_z\{\vec{E}(\vec{\rho}, z)\}$  of the guided-wave-mode electric field satisfies the 2-d electric-field integral equation (EFIE)

$$\vec{e}(\vec{\rho}, \zeta) - (n_c^2 k_0^2 + \nabla \nabla \cdot) \int_{CS} \frac{\delta n^2(\vec{\rho}')}{n_c^2} \vec{g}_\zeta(\vec{\rho}, \vec{\rho}') \cdot \vec{e}(\vec{\rho}', \zeta) dS' = 0$$

for all  $\vec{\rho} \in CS$ , with  $\vec{\rho} = 2$ -d transverse position vector,  $\zeta =$  axial transform variable,  $\delta n^2 =$  contrast of guiding region against refractive index  $n_c$  of cover in which it is immersed,  $\vec{\nabla}_\zeta = \vec{\nabla}_t + z\zeta$ ,  $CS =$  guiding-region cross section where  $\delta n^2 \neq 0$ , and  $\vec{g}_\zeta =$  Hertzian potential Green's dyad descriptive of the layered environment. Integrand in Sommerfeld-integral representations for various components of  $\vec{g}_\zeta$  possess simple-pole singularities at TE and/or TM surface-wave eigenvalues  $\lambda_B$  of the planar, tri-layered background. Complex-plane analysis allows  $\vec{g}_\zeta$  to be expressed as a residue series contributed by those poles augmented by branch-cut integrals arising from branch points of  $\vec{g}_\zeta$ .

Surface waves of the guiding region correspond to those  $\zeta$ -plane poles  $\zeta_B$  leading to non-trivial solutions to the EFIE. The regime of purely-guided surface modes is found to be specified by  $\zeta_B > \lambda_B$ , which leads to transversely-evanescent residue waves. When  $\zeta_B < \lambda_B$ , the residue waves become transversely propagating with resulting leakage from the surface wave of the guiding region. To illustrate these criteria, numerical solutions to the EFIE are obtained for practical guide configurations.

## WAVE PROPAGATION IN TWO-DimensionALLY PERIODIC STRUCTURES

S. T. Peng  
Electromagnetics Laboratory  
New York Institute of Technology  
Old Westbury, NY 11542

and

T. L. Dong  
Microwave Research Institute  
Polytechnic Institute of New York  
Brooklyn, NY 11201

We present here a rigorous analysis of wave propagation in a two-dimensionally (2D) periodic medium of infinite extent, under the most general condition. In the special case of normal propagation, the TE and TM modes had been treated separately as a scalar eigenvalue problem, as perviously reported [S. T. Peng, al. et., 1984 URSI Meeting, Boston, MA]. For the general case of oblique propagation, the Floquet solution of the 2D periodic medium are represented exactly by a double Fourier series and the harmonic amplitudes of the Floquet solution are determined by a five-term recurrence relation in the vector form, properly taking into account the hybrid-mode nature of the propagation problem. More speciafically, the hybrid modes are analyzed in terms of the coupling between the pure TE and TM modes, from which interesting physical phenomena, such as: polarization conversions and the resulting extra stopbands are carefully examined. The characteristic solutions are then applied to the boundary-value problem of multi-layer dielectric waveguides containing a finite layer of 2D periodic medium. Extensive numerical results have been carried out; the dispersion characteristics of 2D periodic structures and their physical significance will be discussed in the presentation.



## URSI COMMISSION B - SESSION B13

## Microstrip Antennas II

1:30 - 5:00  
IRC-6

## Antennes microlignes II

Chairperson/Président: **Y.L. Chow**, University of Waterloo, Waterloo, ON

- 1 ANALYTICAL MODEL AND SCANNING CHARACTERISTICS OF A MEANDERLINE POLARIZER. **R.-S. Chu, K.-M. Lee**, Hughes Aircraft Company, Ground Systems Group, Fullerton, CA, USA
- 2 A COMPUTER-AIDED APPROACH TO REALIZE MICROSTRIP CIRCUITS AND PATCH ANTENNA SYSTEMS. **J.-F. Zürcher, J.R. Mosig**, École Polytechnique Fédérale de Lausanne, Laboratoire d'Electromagnétisme et d'Acoustique, Lausanne, Switzerland
- 3 THEORETICAL INVESTIGATION OF MICROSTRIP PLANAR SHORT-CIRCUITED ANTENNAS. **J.R. Mosig, F.E. Gardiol**, Ecole Polytechnique Fédérale de Lausanne, Laboratoire d'Electromagnétisme et d'Acoustique, Lausanne, Switzerland
- 4 RADIATION FROM IMPERFECTLY CONDUCTING PRINTED CIRCUIT ANTENNAS. **D.M. Schultz, P.L.E. Uslenghi**, University of Illinois at Chicago, Dept. of Electrical Engineering and Computer Science, Chicago, IL, USA
- 5 A LOG-PERIODIC SLOT ANTENNA. **Y.L. Chow, S.K. Chaudhuri**, University of Waterloo, Dept. of Electrical Engineering, Waterloo, ON
- 6 RADIATION CHARACTERISTICS OF RESONANT AND TRAVELLING UNDULATED PRINTED LINE ANTENNAS. **L. Shafai, I.A. Haroun**, University of Manitoba, Dept. of Electrical Engineering, Winnipeg, MB
- 7 THEORY AND EXPERIMENT FOR COUPLED CAVITY-BACKED SLOT ANTENNAS. **D.R. Tanner, P.E. Mayes**, University of Illinois, Dept. of Electrical and Computer Engineering, Urbana, IL, USA
- 8 SCATTERING MATRIX CHARACTERIZATION OF A STRIP LINE Y-JUNCTION. **R. Johnk and D.C. Chang**, University of Colorado, Dept. of Electrical and Computer Engineering, Boulder, CO, USA
- 9 A SINGULAR INTEGRAL EQUATION APPROACH FOR CALCULATING THE CHARACTERISTICS OF A SHIELDED DIELECTRIC IMAGE LINE. **M.D. Abouzahra**, Massachusetts Institute of Technology, Lincoln Laboratory, Lexington, MA, USA; **L. Lewin**, University of Colorado, Dept. of Computer and Electrical Engineering, Boulder, CO, USA

## B-13-1

### ANALYTICAL MODEL AND SCANNING CHARACTERISTICS OF A MEANDERLINE POLARIZER

Ruey-Shi Chu and Kuan-Min Lee

Hughes Aircraft Company, Ground Systems Group, Fullerton, CA 92634

Meanderline polarizer is a well-known device to transform a linearly polarized wave into a circularly polarized wave. The design of a polarizer depends mainly on characterizing the admittance variation with respect to frequency, incident angle, and constitutive dimensions for electric fields perpendicular and parallel to the meanderline axis. In this paper we first will present the analytic-empirical formulas for the admittances of the meanderline panel for the perpendicular and parallel polarizations. Next, we have set up a transmission-line and T-matrix network model for N-layer meanderline polarizer, from which the reflection and transmission coefficients for a plane wave obliquely incident on the meanderline polarizer are obtained. Since for E-type modes all the H-component of the field is along the meanderline axis this mode will see the meanderline panel as capacitive circuit, and for H-type modes all the E-component of the field is along the meanderline axis this mode will see the meanderline panel as inductive circuit, therefore, we have decomposed the incident plane wave into these two orthogonal mode components. We obtain the transmitted field components for these two mode and reconstructed then into an elliptically polarized wave after transmission through the polarizer. The axial ratio for the transmitted wave as functions of frequency, incident angle and incident polarization angle with respect to the meanderline axis, can be obtained. Experimental and analytical results for some meanderline polarizer designs will be presented in this paper.

A COMPUTER - AIDED APPROACH TO REALIZE MICROSTRIP CIRCUITS  
AND PATCH ANTENNA SYSTEMS

Jean-François Zürcher and Juan R. Mosig  
Laboratoire d'Electromagnétisme et d'Acoustique  
Ecole Polytechnique Fédérale de Lausanne  
Ch. de Bellerive 16, CH-1007 Lausanne, Switzerland

Drawing the layout and cutting the mask for a microstrip array of patch antennas and their connecting circuitry are some of the most delicate and time-consuming operations encountered in the design of such assemblies. While automatic design systems have been available for some time, these rely on rather expensive drawing machines, such as coordinatographs and photoplotters.

A new technique was developed, utilizing basic computing equipment, which is available in many microwave laboratories at the present time. The basic idea is to use a standard X-Y recorder (plotter) connected to a desktop computer to actually draw, and then cut the mask directly on the plotter itself. For this purpose, a specially designed microknife was developed, which cuts through the thin soft layer of the Rubylith sheet, but not the underlying mylar. The program was originally designed for the realization of microstrip circuits (J.F. Zürcher, *Mikrowellen Magazin*, 4/81), to draw couplers, filters with connecting transmission lines and bends. With the addition of "user-defined elements", its use is now extended to the layout of patch antenna systems. Square, rectangular and circular patches can be drawn, as well as combinations of these shapes.

The program MICROS runs on Hewlett-Packard desktop computers. It operates in an interactive and self-documented manner, providing maximum facilities for the operator. Circuit elements are calculated, based on substrate dimensions and permittivity, and operating frequency. Patch dimensions, on the other hand, must be specified. Connections with transmission line segments and mitered bends are carried out in a semi-automatic manner, where smooth transitions are ensured. The accuracies obtained on the final masks are of the same order as those provided by much more sophisticated equipment.

## B-13-3

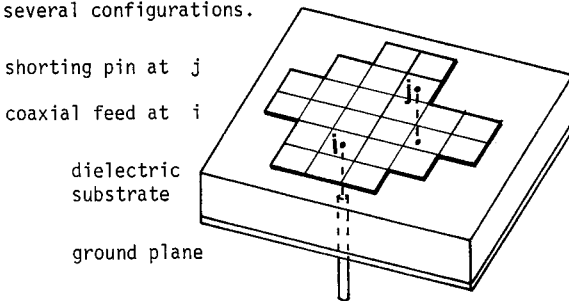
### THEORETICAL INVESTIGATION OF MICROSTRIP PLANAR SHORT-CIRCUITED ANTENNAS

Juan R. Mosig and Fred E. Gardiol  
Laboratoire d'Electromagnétisme et d'Acoustique  
Ecole Polytechnique Fédérale de Lausanne  
Ch. de Bellerive 16, CH-1007 Lausanne, Switzerland

Microstrip antennas with short-circuiting pins, which connect the upper conductor to the ground plane, have been used in an experimental way to improve radiation patterns (E-plane beamwidth), to modify the polarization state or, also, to achieve dual frequency operation (James, Hall and Wood: Microstrip Antennas, Theory and Design, IEE Press, London, 1981).

From a theoretical point of view, the analysis of antennas of this type is uneasy, so that only approximate qualitative models have been available so far. This paper analyzes the microstrip patch by using an integral equation method with a rigorous treatment of the Green's function (Mosig and Gardiol, Proc. IEE, Part H, March 1983). The patch is divided into  $N$  cells, and a two-dimensional method of moments is used. The antenna becomes an  $N$ -port network, with physical connections to the centers of the cells. The element  $z_{ij}$  of the impedance matrix of the network is obtained as the ratio of the calculated voltage in the open-circuited  $i$ -th port to a unit source current entering the  $j$ -th port. In particular,  $z_{ii}$  provides the impedance of the antenna fed by a coaxial probe in the  $i$ -th port. If a shorting pin is placed on the  $j$ -th port the input impedance just becomes  $z_{in} = z_{ii} - z_{ij}^2 / (z_{jj} + z_{pin})$ , where the self-impedance  $z_{pin}$  of the pin has a small inductive component determined through field analysis.

The technique presented provides the characteristics of short-circuited antennas as a by-product of the rigorous analysis of the standard open-circuited patch. The treatment may easily be extended to more than one pin. Theoretical results and measured values will be presented for several configurations.



**RADIATION FROM IMPERFECTLY CONDUCTING  
PRINTED CIRCUIT ANTENNAS**

D. M. Schultz and P. L. E. Uslenghi  
Department of Electrical Engineering and Computer Science  
University of Illinois at Chicago

A printed-circuit antenna located at the interface between air and a dielectric substrate of constant thickness covering a plane metallic ground is considered. The antenna is assumed to be imperfectly conducting; this is important in a variety of applications, including the use of semiconductor materials.

A modified form of Pocklington's integral equation for the surface current is derived, that reduces to a previously known equation for the particular case of a perfectly conducting antenna (see e.g., Alexopoulos and Jackson, IEEE Trans. AP-32, p. 807, August 1984). This integral equation is solved using the method of moments. First, the one-dimensional case of a horizontal dipole antenna is considered; then, the two-dimensional case of patch antennas is studied. Numerical results are given for different dipole lengths, and for various shapes and dimensions of the patch. Finally, several antenna parameters are determined and discussed.

## B-13-5

### A LOG-PERIODIC SLOT ANTENNA

Y. L. Chow and S. K. Chaudhuri  
University of Waterloo  
Waterloo, Ontario N2L 3G1

A direct conversion of a log-periodic dipole antenna to its slot equivalent has two difficulties: (i) the high radiation impedance ( $490\Omega$ ) of a slot antenna makes the construction of the feeding transmission line difficult, (ii) a difficulty is in achieving slot element phase reversals, especially if the feeding transmission line is a co-planar line such that it can be printed on the same supporting dielectric sheet of the log-periodic slot antenna (LPSA).

These problems are overcome by an LPSA shown in the figure: (i) By feeding a slot element away from the center, the radiation impedance is lowered, i.e. to  $245\Omega$  for a resonant element in the figure. A feeding co-planar line of this range of impedance is easy to construct. (ii) By moving the feed points alternatively to the left and right of the slot center, the phase reversals are achieved.

The figure gives an experimental LPSA for 1 to 3 GHz. The experimental results show that an excellent difference endfire pattern is achieved when a finite ground plane for the LPSA is used.

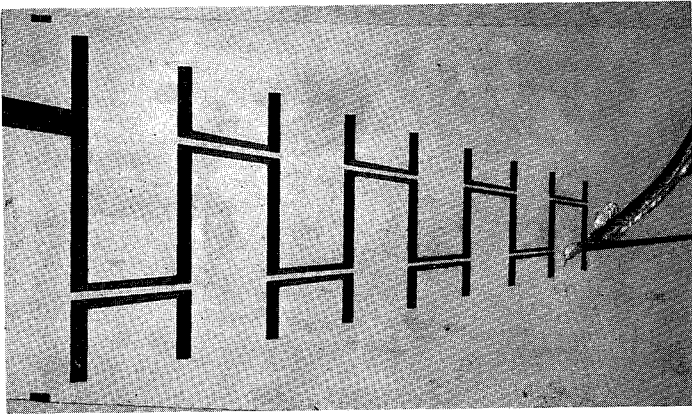


Fig. 1. The log-periodic slot antenna

\* This work was supported by a contract from the Defence Research Establishment Ottawa, through contract No. DSS 03SU.97714-2-1260.

RADIATION CHARACTERISTICS OF RESONANT  
AND TRAVELLING UNDULATED PRINTED LINE ANTENNAS

L. Shafai and I.A. Haroun  
Department of Electrical Engineering  
University of Manitoba  
Winnipeg, Manitoba  
Canada R3T 2N2

A procedure for the design of low sidelobe undulated printed line antennas was described previously (L. Shafai and A.A. Sebak, 1984 IEEE Symposium, pp. 55-57). The method was used to design travelling line antennas for a specified sidelobe level, where the line geometry was determined progressively using the radiation conductance of the line and a selected Taylor distribution. Sidelobe levels, in order of -40dB, were achieved. Because of the travelling nature of the designed geometries, the beamwidth and sidelobe levels were retained over a wide frequency band, but the beam direction tilted with frequency.

Further work on these antennas is conducted to design resonant type configurations. Here the direction of the beam is stationary, but the beamwidth and sidelobe levels deteriorate with frequency. This paper will discuss the design implications and compare the radiation characteristics of resonant printed line configurations with the travelling types. A method for improving the cross-polarization will also be discussed.

**THEORY AND EXPERIMENT FOR COUPLED  
CAVITY-BACKED SLOT ANTENNAS**

D. R. Tanner and P. E. Mayes  
Electromagnetics Laboratory  
Department of Electrical and Computer Engineering  
University of Illinois  
Urbana, Illinois 61801

The cavity-backed slot (CBS) antenna has been used in the past several decades; however, its utility as a low profile microstrip antenna has not been fully exploited. The aspect ratio ( $L/W$ ) of the CBS antenna makes it an attractive alternative to the microstrip patch for linear periodic or log-periodic array applications. With these applications in mind, it was found necessary to develop an analysis for self, mutual and driving point impedances of thin CBS elements. Previous analysis has been limited to self impedance of elements of moderate electrical thickness (K. Itoh and H. Hara, Electronics and Comm. in Japan, Vol. 62-B, No. 4, 1979). This paper describes a moment method analysis for computing the self and mutual impedances of one or more CBS elements. Also, the calculation of driving-point impedance or active reflection coefficient of a CBS element in an infinite-linear-phased array is described.

Using Huygen's theorem, the original problem is converted to an equivalent problem in terms of unknown magnetic currents for each slot due to impressed electric currents representing coaxial feed probes in each cavity. Within an electrically-thin cavity these currents can be assumed  $z$ -independent with little change in the fields. The source-field relations of these currents are formulated by a mode-matching procedure. A Galerkin moment method employing "rooftop" expansion and test functions is used to discretize the problem. The discretized source-field equations for each cavity become a set of generalized-network  $H$ -parameter relations.

In a similar manner the "rooftop" functions are used to expand the magnetic currents in the exterior region. The resulting description of this region is reduced to a set of generalized-network  $Y$ -parameters. For the case of one or two CBS elements the  $Y$ -parameters are found using an exact formulation in the space domain that utilizes an efficient numerical integration technique. The  $Y$ -parameters for an infinite array are computed in the spectral domain by mode matching a field expansion in terms of Floquet-space harmonics.

After discretizing the problem, the desired impedances (self, mutual or driving pt.) are computed from matrix expressions involving the generalized-network  $H$ - and  $Y$ -parameters. Experimental and theoretically-computed data are compared to verify the theory.

## SCATTERING MATRIX CHARACTERIZATION OF A STRIP LINE Y-JUNCTION

Robert Johnk and David C. Chang  
Electrical and Computer Engineering  
University of Colorado, Boulder, CO 80309

In using stripline and microstrip structures for microwave circuit and component design, one frequently encounters the need of bending and branching of the structure in order to achieve a certain circuit configuration. For a low frequency operation, the bending and branching angles are somewhat immaterial since the junction effect is generally negligible, and impedance-matching usually can be accomplished using a conventional transmission line analysis. The same, however, is not true for a high frequency operation, for the junction not only is reactive because of the inductive and capacitive couplings, but also is resistive because of the spurious radiation. A double-variational formulation is developed in this case in order to obtain an explicit expression for each element of the junction scattering matrix. For the special case involving branches with same characteristic impedance, one can make the usual thin-wire assumption, which stipulates that the source current on the strip can be approximately represented by a line current propagating along the axis of the strip, while the observation point for the variational formulation is along the edge of the strip. This approximation leads to a substantial simplification of the result (Chang, 1984 National Radio Science Meeting, Boston, MA, p. 133). However, in the design of a stripline Y-junction, in order to minimize the reflection from the junction, the characteristic impedance and hence the corresponding strip width for each of the branches is likely to be different. The same thin-wire approximation in this case leads to a direct violation of the reciprocity theorem and the scattering matrix elements no longer possesses the symmetrical property it should have. In this work, a distributed current model over the surface of the strip is used, and the correction to the scattering matrix for a stripline structure is explicitly obtained. Issues regarding the dynamic nature of the junction impedances and the extension from a stripline to a microstrip of thick substrate also will be addressed.

## B-13-9

### A SINGULAR INTEGRAL EQUATION APPROACH FOR CALCULATING THE CHARACTERISTICS OF A SHIELDED DIELECTRIC IMAGE LINE

M. D. Abouzahra\*  
Lincoln Laboratory  
Massachusetts Institute of Technology  
Lexington, MA 02173  
Leonard Lewin  
Department of Computer and Electrical Engineering  
University of Colorado, Boulder, CO 80309

The singular integral equation method is used for the exact quasi-static calculation of the field distribution and the propagation constant of a single shielded dielectric image line of rectangular cross-section. In order to solve this boundary value problem the system's transverse cross-section was divided into four partial regions and a complete set of field solutions was derived for each subregion. The boundary conditions at the air-dielectric interfaces were imposed and the problem was reduced to a system of three singular integral equations with respect to the transverse electric and magnetic fields. Exact solutions to these singular integral equations were obtained. The physical properties of the electromagnetic fields at the dielectric edge were used to derive the modal equation. The implementation of the quasi-static approximation introduced a mathematical limitation that restricted the validity of this method to the case where the separation between the parallel plates is twice the height of the rectangular dielectric guide.

Dispersion curves of the waveguide structure are presented and the mode designation procedure is discussed. The results of this approach are compared to those of other existing approximate analytical methods, and numerical methods, known from the literature.

## URSI COMMISSION B - SESSION B14

**Computer Architecture for  
Efficient Computation  
in Electromagnetics**

1:30 - 3:00  
IRC-4

**Architecture d'ordinateurs  
aux fins de calculs  
efficaces en électromagnétique**

Chairperson/Président: **W.R. Stone**, IRC Corporation, La Jolla, CA, USA

- 1 EFFECTS OF MODERN HARDWARE AND SOFTWARE ARCHITECTURE ON NUMERICAL ELECTROMAGNETIC ALGORITHMS. **T.K. Sarkar**, Rochester Institute of Technology, Dept. of Electrical Engineering, Rochester, NY, USA; **A.R. Djordjević**, University of Belgrade, Dept. of Electrical Engineering, Belgrade, Yugoslavia
- 2 SOFTWARE AND HARDWARE ARCHITECTURE ISSUES IN ELECTROMAGNETIC COMPUTATIONS. **E.K. Miller**, **M.J. Barth**, **G.J. Burke**, **R.D. Merrill**, Lawrence Livermore National Laboratory, Livermore, CA, USA
- 3 THE APPLICATION OF ARRAY PROCESSORS TO THE ITERATIVE SOLUTION OF SCATTERING PROBLEMS. **M.P. Hurst**, TRW Space and Technology Group, Redondo Beach, CA, USA; **R. Mittra**, University of Illinois, Dept. of Electrical and Computer Engineering, Urbana, IL, USA
- 4 A REVIEW OF TOEPLITZ MATRIX ALGORITHMS FOR SOLUTIONS TO ELECTROMAGNETIC PROBLEMS. **W. Ross Stone**, IRT Corporation, La Jolla, CA, USA
- 5 PANEL DISCUSSION/TABLE RONDE.

**EFFECTS OF MODERN HARDWARE AND SOFTWARE ARCHITECTURE  
ON NUMERICAL ELECTROMAGNETIC ALGORITHMS**

Tapán K. Sarkar  
Department of Electrical Engineering  
Rochester Institute of Technology  
P.O. Box 9887, Rochester, N.Y. 14623

Antonije R. Djordjević  
Department of Electrical Engineering  
University of Belgrade  
P.O. Box 816, 11001 Belgrade, Yugoslavia

Modern computers offer steadily increasing capabilities for numerical analysis of electromagnetic problems as a result of both large storage space and very fast processing. At the present time we are capable of analysing with high accuracy relatively complex structures, such as three-dimensional systems, consisting of conductors in a piecewise-homogeneous medium. Also, the speed of the modern computers has enabled the computer-aided design, often based on numerical optimization techniques. However, the need for the computer power seems to be growing faster than the computer resources, and new techniques have been developed, such as the conjugate-gradient method combined with the least-squares method and the fast Fourier transform, capable of handling large and complex electromagnetic systems.

Besides the power, the modern computers offer a user-friendly environment for program development, as well as for data handling and presentation. The computer graphics plays an important role in the communication between the human and the machine.

A great impact on the numerical electromagnetics has been made by modern powerful personal computers (PPCs). At the moment these computers offer the power of the classical VAX computers, and this information may easily be obsolete in a few months from now. The PPCs offer a complete workstation, ideal for program development and testing, data handling etc. The speed and storage of such microcomputers are comparable to the performances seen by a user in a multiuser/timesharing environment on a large computer. Their relatively low price makes them affordable both at work and at home. The computational power, their good graphic and text editing capabilities make the PPCs suitable for a serious research work. Thus, for example, on a Digital Professional 350 PPC we were able to solve complex electromagnetic problems, involving as many as 150 linear equations. The application of the new techniques based on the conjugate-gradient method offers the possibility of analysing on a PPC electromagnetic systems with a few thousand unknowns.

There are, however, some hardware architecture innovations that have not yet been implemented in everyday's numerical computations, but which may offer a tremendous improvement of the computer efficiency. Most of all, the parallel processing seems very promising in treating large electromagnetic problems.

SOFTWARE AND HARDWARE ARCHITECTURE ISSUES  
IN ELECTROMAGNETIC COMPUTATIONS

E. K. Miller, M. J. Barth, G. J. Burke, R. D. Merrill  
Lawrence Livermore National Laboratory

Computer application of the Method of Moments (MoM) in electromagnetics is straightforward. Although specific details may vary, there are essentially three steps involved in performing any MoM computation. First is development of the problem description via provision of input data and its possible manipulation. Second is computation of an interaction matrix and its subsequent solution via iteration, factorization or inversion. Last is development and presentation of the desired results as output data. It is tantalizing to speculate on how the architecture of both the formulation and software, and hardware being used for MoM modeling might be made more effective in each of these areas.

In this paper we discuss some aspects of this general question and suggest some specific possibilities for consideration. We begin by examining the basic information needs of computing EM fields from the viewpoint of field propagation and boundary-condition matching. Differential and integral formulations are considered in both the time domain and frequency domain. We continue by considering software-oriented approaches to increasing computational efficiency, such as using interpolation for field evaluation. Finally, some concluding comments are addressed to examining the feasibility of various hardware-oriented approaches to MoM application. These include EPROM storage of previously computed results for PC manipulation, a hybrid approach involving measured and computed models, work-station handling of input/output data, and array and optical processing of MoM matrices.

Emphasis throughout our discussion is not on approaches actually implemented but instead on exploring the trade-offs and potential benefits of alternatives to present practice.

## B-14-3

### THE APPLICATION OF ARRAY PROCESSORS TO THE ITERATIVE SOLUTION OF SCATTERING PROBLEMS

M. P. Hurst  
TRW Space and Technology Group  
One Space Park  
Redondo Beach, CA 90278

R. Mittra  
Department of Electrical and Computer Engineering  
University of Illinois  
Urbana, IL 61801

Recently, considerable interest has been shown in iterative methods for the solution of electromagnetic scattering problems. The primary motivation behind these efforts is the need to circumvent constraints on computer core memory available to an individual user. Direct methods for the solution of linear systems of equations are often precluded by these constraints in problems where the number of unknowns becomes large, because the memory required typically grows as the square of the number of unknowns. With iterative methods this growth is usually linear, but the CPU time required to obtain convergence can be excessive, particularly if the computation is performed on a minicomputer such as a VAX. Computation time can be drastically reduced, however, through the use of an array processor (AP), which is a specialized piece of hardware connected as a peripheral to the host computer. These devices use parallel processing to reduce the time required to do vector arithmetic by orders of magnitude ( $10^7$  32-bit floating point operations/sec is typical). Software is readily available for standard algorithms such as the multi-dimensional FFT.

Although the overhead associated with transferring data between the host computer and the array processor reduces efficiency somewhat, modifying a program to use an array processor for major arithmetic operations can reduce computation time by a factor of 5 to 10 in practical problems.

An iterative method which is particularly well suited to the use of an AP (based on the conjugate gradient method and using the FFT to perform convolutions via the transform domain) was used by the authors to solve for induced currents on resistively loaded flat plates, and round finite cylindrical shells. In the presentation the authors' experience in using an AP in conjunction with a VAX 11/780 to solve such problems with as many as 4,000 unknowns will be discussed and the basics of programming for an AP will be outlined.

**A REVIEW OF TOEPLITZ MATRIX ALGORITHMS FOR SOLUTIONS  
TO ELECTROMAGNETIC PROBLEMS**

W. Ross Stone  
IRT Corporation  
1446 Vista Claridad  
La Jolla, CA 92037

A Toeplitz matrix is a matrix in which the elements  $T_{ij} = f(i-j)$ . Such matrices are completely specified by a single row or column. Most electromagnetic scattering, diffraction, and radiation problems can be readily expressed in discrete, numerical form using Toeplitz matrices, because the Green's function appears as a convolution kernel in the integral formulation of these problems. For such formulations, inversion of a Toeplitz matrix is required to obtain a solution. "Classical" matrix inversion methods would require of the order of  $N^3$  operations (multiplications and additions) for inversion of an  $N$  by  $N$  matrix. Levinson's algorithm, which permits inversion in the order of  $N^2$  operations, has been known since the late 1940s. Recently, a whole new class of algorithms has been derived independently by several groups which permits inversion of Toeplitz matrices in the order of  $N \log^2 N$  operations. Furthermore, these algorithms take advantage of the recursive definition of the matrix and require storage of only order  $N$  for inversion. These features can become particularly significant for modern virtual-memory-based computer architectures. The significance of the availability of such algorithms is that the solution speed rivals FFT techniques, without the requirement for formulating the problem so that FFT techniques can be used. Storage requirements can often be reduced from order  $N^2$  to order  $N$  in going from FFT-based techniques to such a Toeplitz formulation.

Because recent discussions have made it apparent that this new class of algorithms is not well known to workers in numerical electromagnetics, this paper presents a review of these algorithms and their application. Comparisons are presented among formulations of the same problem using the Toeplitz approach, the spectral-iterative (or  $K$ -space) technique, and the spacial-frequency/time-domain (or  $K$ - $T$  space) technique. Comparisons among the several Toeplitz algorithms offering similar performance is made. The tradeoffs and effects of virtual memory computer systems and related issues for the three classes of solution techniques are discussed.



## URSI COMMISSION B - SESSION B15

Electromagnetic Fields I

8:30 - 12:00  
IRC-3

Champs électromagnétiques I

Chairperson/Président: **A.D. Yaghjian**, Rome Air Development Center, Hanscom AFB, MA, USA

- 1 THE W-TRANSFORM IN ANTENNA SYSTEMS, PROPAGATION, AND DIFFRACTION. **F.J. Zucker**, RADC/EEA, Electromagnetic Sciences Division, Hanscom AFB, MA, USA
- 2 THE GREEN'S DYADIC AS AN INVERSE OPERATOR. **R.E. Collin**, Case Western Reserve University, Dept. of Electrical Engineering and Applied Physics, Cleveland, OH, USA
- 3 ADMITTANCE OF APERTURES IN BODIES OF FINITE EXTENT. **R.F. Harrington**, Syracuse University, Dept. of Electrical and Computer Engineering, Syracuse, NY, USA
- 4 SCATTERING FROM A SPHERICAL SHELL WITH A CIRCULAR APERTURE: CROSS-SECTIONS AND ENERGY STORAGE FOR A NORMALLY INCIDENT PLANE WAVE. **R.W. Ziolkowski**, Lawrence Livermore National Laboratory, Electronics Engineering Dept., Livermore, CA, USA
- 5 THE GABOR REPRESENTATION AND APERTURE THEORY. **P.D. Einziger, S. Raz and M. Shapira**, Technion-Israel Institute of Technology, Dept. of Electrical Engineering, Haifa, Israel
- 6 APERTURE FIELD OF A DOUBLE WEDGE. **A.Z. Elsherbeni, M. Hamid**, University of Manitoba, Dept. of Electrical Engineering, Winnipeg, MB
- 7 SURFACE CURRENTS INDUCED ON A CIRCULAR STRIP MOUNTED ON A PERFECTLY CONDUCTING SHEET. **J.T. Williams, D.G. Dudley**, University of Arizona, Dept. of Electrical and Computer Engineering, Tucson, AZ, USA; **C.M. Butler**, University of Houston, Dept. of Electrical Engineering, Houston, TX, USA
- 8 APPLICATION OF AN ITERATIVE TECHNIQUE TO THE PERFECTLY CONDUCTING WEDGE AND SQUARE CYLINDER. **R.P. Penno**, University of Dayton, Graduate Engineering and Research, Dayton, OH, USA
- 9 TM SCATTERING BY A DIELECTRIC CYLINDER IN THE PRESENCE OF A HALF-PLANE. **E.H. Newman**, Ohio State University ElectroScience Laboratory, Dept. of Electrical Engineering, Columbus, OH, USA
- 10 AN APPROXIMATE METHOD FOR INCORPORATING THE WALL THICKNESS INTO APERTURE CALCULATIONS. **G.A. Seely**, Sandia National Laboratories, Electromagnetic Applications Divisions, Albuquerque, NM, USA

## B-15-1

### The W-TRANSFORM IN ANTENNA SYSTEMS, PROPAGATION, AND DIFFRACTION

Francis J. Zucker  
Electromagnetic Sciences Division  
RADC/EEA, Hanscom AFB, MA

Over the past several years, the "W-transform" (in honor of Weyl, Wigner, Walther and Wolf) has been increasingly applied in optics, in such diverse contexts as optical systems theory and radiative transfer. This paper explores applications to antenna systems and to propagation in complex media, while hopefully integrating the diverse aspects of the W-transform into a coherent whole.

The discussion is restricted to coherent fields, since Wolf has recently shown that a large class of partially coherent fields can be composed of them, and since a straightforward transcription allows us to write all W-transform relations for stochastic fields when these are truly needed.

In free space, the W-transform, defined as the Fourier transform of the convolution of the field around a point, describes a signal in space  $\underline{r}$  and wave-number  $\underline{k}$  simultaneously, i.e., it is a compact representation of the usual Fourier transform pair. It is related to the well known ambiguity function as a convolution is to a correlation, and our first task is to demonstrate the W-transform's usefulness in complementing computations based on that function.

We next observe that a plane wave and a point source are duals of each other under the W-transform, which translates into a duality between the "ray spread" and the "wave spread" impulse response of a linear system characterized by input-output W-transforms (Bastiaans). The ray spread function leads to a very practical formulation of first-order lens design, a result that does not, however, imply a necessary tie-in between a W-transform ray and geometric optics; the latter, in fact, turns out to be a mere approximation based on the phase of the ray spread function while neglecting its amplitude. The true significance of the W-transform can therefore be seen to lie in its ability to restore this missing information to geometric optics. In so doing, it furthermore transforms the global wave into a local ray description of fields, thus opening the way to propagation studies in media of great complexity. The greatest contribution of this representation will, I think, come from grafting the full W-transform rays onto the geometric optics rays in Felsen's hybrid (ray-wave) spectral formulation encompassing all of propagation, scattering, and diffraction.

Finally, still using the W-transform, we return to the free-space case (via path-length integrals, or equivalently in the way shown by Sudarshan) while retaining the augmented ray picture. Its superiority over geometric optics becomes evident as we trace such a ray through a caustic. While equivalent rather than superior to the conventional wave picture, the new rays offer information that complements the latter; this will be illustrated with an optimal beam energy-transfer calculation due to T. Wu, and with an example from antenna pattern synthesis.

## THE GREEN'S DYADIC AS AN INVERSE OPERATOR

R. E. Collin

Department of Electrical Engineering and Applied Physics  
Case Western Reserve University  
Cleveland, Ohio 44106

The electric field is a solution of the vector wave equation

$$\nabla \times \nabla \times \vec{E} - k_0^2 \vec{E} = -j\omega\mu_0 \vec{J}$$

It will be shown that the usual free space Green's dyadic  $\vec{G}$  will not be an appropriate inverse operator for this equation if the scalar product is chosen as a principal volume integral. In particular, it is shown that

$$\int_{V-V_0} (\nabla \times \nabla \times \vec{E} - k_0^2 \vec{E}) \cdot \vec{G} dV = -j\omega\mu_0 \int_{V-V_0} \vec{J} \cdot \vec{G} dV$$

after integrating by parts to transfer the operator  $\nabla \times \nabla \times$  onto  $\vec{G}$  and taking the limit as the volume  $V_0$  surrounding the singular point vanishes, will not give a correct solution for the electric field. In order to obtain the correct solution for  $\vec{E}$  using  $\vec{G}$  as the inverse operator it is necessary to integrate over the total volume. This requires a procedure for evaluating the integral

$$\int_V \vec{J} \cdot \vec{G} dV$$

Two techniques are presented for evaluating this integral. One method is the classical integration by parts technique. The other is based on using the limiting form of the Green's dyadic  $\vec{G}$  as deduced from the eigenfunction expansion of  $\vec{G}$  given by C. T. Tai for source points  $\vec{r}'$  that are very close to the origin. This latter method provides new insight into the singular behavior of  $\vec{G}$  and gives a straight forward method for evaluating the above integral.

## B-15-3

### ADMITTANCE OF APERTURES IN BODIES OF FINITE EXTENT

Roger F. Harrington  
Dept. of Electrical and Computer Engineering  
Syracuse University  
Syracuse, New York 13210

An integral equation for the change in the aperture admittance matrix for an aperture in a body of finite extent from that for the same aperture in an infinite conducting plane has been derived. The image of the aperture equivalent magnetic current in the conducting plane problem is used as a pseudo-image in the finite body problem. The difference in the field for the aperture in a finite body from that for the same aperture in a conducting plane is expressed in terms of potential integrals due to a difference current over the finite body. This difference current is nonsingular at the aperture because the proper singularity is accounted for by the pseudo-image. Hence, the difference current is well-behaved and relatively easy to obtain by moment methods.

The behavior of an aperture in a body of finite extent can differ greatly from that for the same aperture in a conducting plane. For a small aperture, the polarizabilities obtained from the Bethe-hole theory are not sufficient to predict the behavior of the same aperture in a finite sized body. If the interior of the finite body is near a natural resonant frequency, the distribution of tangential electric field in the aperture is different from that for the same aperture in a conducting plane. The electric field intensity in a body of finite extent can be orders of magnitude greater than that in free space behind the same aperture in a conducting plane. Some computations for apertures in two dimensional problems will be given to illustrate the concepts.

## SCATTERING FROM A SPHERICAL SHELL WITH A CIRCULAR APERTURE: CROSS-SECTIONS AND ENERGY STORAGE FOR A NORMALLY INCIDENT PLANE WAVE\*

*Richard W. Ziolkowski*

Lawrence Livermore National Laboratory  
Electronics Engineering Department  
P. O. Box 5504, L-156 Livermore, CA 94550

Canonical electromagnetic scattering problems are important from several points of view. They provide basic understanding of scattering processes which can be extrapolated to more general geometries. Moreover, they provide fundamental benchmarks for general purpose scattering codes. However, there are few fully three-dimensional scattering problems for which solutions have been found, especially when the scattering body includes an aperture.

The solution to the scattering of a normally incident plane wave from a perfectly conducting spherical shell having a circular aperture has been obtained by Ziolkowski and Johnson [1984 URSI meeting, paper B-13-4, Boston, MA]. It is based upon an essentially analytic solution of the coupled dual series equations for the TE and TM modal coefficients arising from the enforcement of the electromagnetic boundary conditions over the aperture and the shell. The currents induced on the open shell by the plane wave were calculated and used to validate the predictions of a general purpose Triangular Patch Scattering Code. [Johnson and Ziolkowski, 1984 URSI meeting, paper B-14-4, Boston, MA]

The cross-sections (total, forward and back), the energy density ratio at the origin, and the energy stored in the open shell as functions of  $ka$  ( $2\pi \times$  shell radius / wavelength) for both possible angles of incidence (directly into the aperture and antipodal to the aperture) have been studied with that generalized dual series solution. The results of this investigation will be presented. It will be demonstrated that for small apertures the dominant features of the cross-sections and stored energy results closely correspond to the resonant modes of the closed spherical cavity. The deviation from the closed sphere cross-sections is shown to be more pronounced when the wave is incident on the aperture. An interesting conclusion is that these resonance features are clearly discernible even when the plane wave is incident antipodal to the aperture. This is particularly noticeable in the forward (radar) scattering cross-sections where the features have an "anti-resonance" form. The changes in the resonance features and their locations as the aperture size is increased will also be indicated.

## THE GABOR REPRESENTATION AND APERTURE THEORY

P.D. Einziger, S. Raz and M. Shapira

Dept. of Electrical Engineering, Technion Haifa, Israel.

The objective of this work is to investigate the analytical properties and the computational implications of the so called Gabor representation within the context of aperture theory. Although proposed by Gabor in 1946 (D.Gabor, J. Inst. El. Eng. (London) 93 III, 429-457, 1946), use of this nonorthogonal presentation has been rather limited due to difficulties in computing the series coefficients. These difficulties were partly alleviated due to recent contributions by Bastiaans (M.J. Bastiaans, Proc. IEEE 68, 538-539, 1980) and Janssen. This approach emerges, so we hope to demonstrate, as a powerful mathematical tool having relevance to analysis, synthesis as well as spatial filtering. The Gabor series may be viewed as an extended spectral representation comprising a discrete, two-dimensional superposition of elementary "beam" waves. These "beams", characterized by finite width  $L$ , scan the aperture and subsequently the pertinent half-space ( $(x, z)$ ,  $z > 0$ ) by being linearly shifted with respect to one another along a cartesian axis ( $x$ ), a distance  $L$  and rotated by introduction of linear phase shifts at the rate  $\Omega x = (2\pi/L)x$ , between neighboring "beams". Gabor's representation may indeed be considered a generalization in the sense that the classical, generally continuous, plane wave representation as well as Kirchhoff's spatial convolution form are readily recoverable as the limiting cases  $L \rightarrow \infty$  and  $L \rightarrow 0$ , respectively. The radiation field, represented by a discrete collection of linearly shifted, spatially rotated elementary "beams", falls into two distinct categories, propagating (characterized by real rotation angles) and evanescent beams. This grouping resembles but is by no means identical to the distinction made between the "visible" and the "invisible" plane wave spectral regions. It is observed that evanescent beam contains plane wave spectral constituents within the "visible" range, although characteristically, most of its energy at the aperture plane is confined to the "invisible" (reactive) variety. The dual observation holds true for propagating beams. It is not hard to imagine that selection of a specific elementary "beam" and choice of its open width parameter  $L$  are cardinal decisions, greatly affecting complexity and convergence rate of the Gabor series. The particular choice of the Gaussian beam holds promise towards this end. Firstly, the Gaussian function constitutes an optimal choice as it minimizes the uncertainty described by the product of the spatial and the spectral spreads, an indispensable advantage when dealing with the synthesis problem. Secondly invariance of the Gaussian profile under the Fourier Transform leads to significant analytical simplifications. Thirdly, the asymptotic estimations are simple and interpretable in terms of complex ray theory. Furthermore, the paraxially approximated Gaussian beam can be interpreted as a wave emanating from complex-source-point (G.A. Dechamps, Electron. Lett. 7, 684-685, 1971), thereby assigning a one-to-one correspondence between the Gabor discrete space and the collection of source points spread over a complex grid.

**APERTURE FIELD OF A DOUBLE WEDGE**

*A. Z. Elsherbeni and M. Hamid*  
Antenna Lab., Elec. Eng. Dept.  
University of Manitoba  
Winnipeg, Canada, R3T 2N2

**ABSTRACT**

The diffraction by a double wedge of arbitrary aperture due to an incident plane wave is formulated rigorously as the field diffracted by each wedge in the absence of the other plus interaction terms to account for the multiple diffraction between the two wedges. The latter is expressed using an angular spectrum of the plane waves, where each plane wave is diffracted by the other wedge in the same way as the original incident plane wave. The final solution includes four interaction terms to account for all possible conditions of initial and final diffraction from either wedge. The advantages and disadvantages of this technique over a previous rigorous solution by Clemmow ( *The Plane Wave Spectrum Representation in Electromagnetic Fields*, Pergamon Press, New York, 69, 1956 ) as well as asymptotic solutions by Teague and Zitron ( *Appl. Phys. Res.* , 26, 127, 1972 ), Keller ( *J. Appl. Phys.*, 28, 426, 1957 ), Karp and Russek ( *J. Appl. Phys.*, 27, 886, 1956 ) and Elsherbeni and Hamid ( *IEEE Trans. Ant. and Prop.* AP-32, 11, 1262, 1984 ) for related geometries are discussed.

## B-15-7

### SURFACE CURRENTS INDUCED ON A CIRCULAR STRIP MOUNTED ON A PERFECTLY CONDUCTING SHEET

J.T. Williams<sup>+</sup>, D.G. Dudley<sup>+</sup>, and C.M. Butler<sup>\*</sup>

<sup>+</sup>Electromagnetics Laboratory  
Department of Electrical and Computer Engineering  
University of Arizona  
Tucson, Arizona 85721

<sup>\*</sup>Department of Electrical Engineering  
University of Houston  
Houston, Texas 77004

We present the analysis of the surface currents induced on a thin circular strip, mounted on a perfectly conducting sheet, due to an electric dipole source located at its center. This is intended to be the basis of a forward model of the transient electromagnetic scattering of a simple object with finite dimensions and curvature. Such a model can be used in the development of inverse scattering techniques for applications relating to target identification.

In the formulation of this problem an integral equation for the induced currents on the circular strip is obtained. The appropriate edge condition is included specifically and the singular nature of the integral equation is determined and removed analytically. The remaining equation is then solved numerically using the method of moments with pulse expansion functions and piecewise linear testing functions.

In addition to the numerical solution for the induced surface currents, an analytical solution is obtained in the quasi-static limit in terms of Chebyshev polynomials. A comparison with the numerical solution tests the range of validity of the quasi-static approximation.

APPLICATION OF AN ITERATIVE TECHNIQUE TO THE  
PERFECTLY CONDUCTING WEDGE AND SQUARE CYLINDER

Robert P. Penno  
Graduate Engineering and Research  
University of Dayton  
Dayton, Ohio 45469

An iterative approach to solving the M.F.I.E. for surface current density is applied to the cases of the perfectly conducting wedge (for both TE and TM plane wave incidence) and the square cylinder (TM incidence). As described, [M. Kaye, P. K. Murthy and G. A. Thiele, "An Iteration Method for Complex Scattering Problems," IEEE Trans. Antennas Propagation, (in review)], this technique divides the wedge (or square cylinder) into lit and shadow regions separated by the geometric optics boundary. The total current is equal to the sum of an approximate optics current and a non-uniform (correction) current. After selection of an appropriate initial optics current, both the approximate optics current and non-uniform currents are solved via iteration. In this latter respect, the method differs from the work done by Kim and Thiele ("A Hybrid Diffraction Technique-General Theory and Applications," IEEE Trans. Antennas Propagation, Vol. AP-30, pp. 888-897). The results disclosed here improve upon previous results in that they are uniformly valid for all angles of incidence and wedge angles, while eliminating the moment method patch used previously by Kim and Thiele, (ibid.)

In the case of the TM incidence, the inherent singularity in the current density at the apex of the wedge (or the edges of the square cylinder) require attention in their numerical evaluation. Similarly, in evaluating the zeroeth order current on the shadow side of the wedge, special consideration must be given to the evaluation of the semi-infinite integration involved therein. Specific consideration must be given to cases of (i) grazing incidence and (ii) incidence from the transition region of the diffracted field. The selection of more accurate initial approximations, or rather, closed form representations of the previously mentioned semi-infinite integral provides enhanced accuracy and reduced computer time. Finally, results will be shown which include grazing incidence and incidence from the transition region where these results are seen to be excellent when compared with those of the eigenfunction series solution.

B-15-9

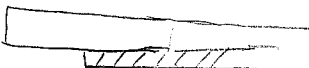
TM SCATTERING BY A DIELECTRIC CYLINDER IN  
THE PRESENCE OF A HALF-PLANE

E.H. Newman  
The Ohio State University  
Dept. of Electrical Engineering  
ElectroScience Lab  
1320 Kinnear Rd.  
Columbus, Ohio 43212

The problem considered is the TM scattering by a dielectric cylinder in the presence of a perfectly conducting half-plane. Since the dielectric cylinder may contact the half-plane, or even completely surround the half-plane edge, this problem is a 2-D model for scattering by a dielectric coated edge. An exact integral equation, involving the half-plane Green's function in it's kernel, is obtained for the equivalent volume polarization currents representing the dielectric cylinder. The integral equation is solved by the method of moments (MM).

The solution can be termed an MM/Green's function technique, and has the advantage that the unknown is limited to the electric field in the dielectric, and does not include the half-plane current. The price one pays for this simplification is that the integrals, which must be evaluated to compute the elements in the MM impedance matrix, involve the half-plane Green's function in the integrand. They are therefore more difficult to evaluate than the corresponding integrals in a conventional MM solution, which would contain the simpler free-space Green's function in the integrand. Methods for avoiding the lengthy numerical integrations, and for treating the singularity associated with the self impedance terms will be described. Numerical data will be compared with measurements for the scattering from a half-plane edge coated with a dielectric slab.

*Pulse basis over trapezoids  
Point matching at centroid of patch*



AN APPROXIMATE METHOD FOR  
INCORPORATING THE WALL THICKNESS  
INTO APERTURE CALCULATIONS

George A. Seely  
Electromagnetic Applications Divisions 2322  
Sandia National Laboratories  
Albuquerque, New Mexico 87185

The effect of finite wall thickness on electromagnetic transmission through an arbitrarily shaped aperture in a conducting ground screen is considered. It is found that an approximate scheme gives reliable results for  $\lambda \geq 6 * T$  where T is wall thickness. Following a brief discussion of the pertinent equations the rationale for choosing this particular approximation is discussed. An existing method of moments triangular patch code is modified to incorporate the effect of wall thickness. Numerical results are presented for a few cases of interest. A brief comparison is made to other numerical results and experimental results.



## URSI COMMISSION B - SESSION B16

## Open Waveguides

8:30 - 12:00

## Guides d'ondes ouverts

IRC-4

Chairperson/Président: **E.F. Kuester** University of Colorado, Boulder, CO, USA

- 1 A GENERAL VARIATIONAL FORMULATION FOR OPEN WAVEGUIDE REFLECTIONS WITHOUT USING THE COMPLETE MODE SPECTRUM. **E.F. Kuester, D.C. Chang**, University of Colorado, Dept. of Electrical and Computer Engineering, Boulder, CO, USA
- 2 REFLECTION OF SURFACE WAVES FROM THE TRUNCATION OF A DIELECTRIC SLAB WAVEGUIDE. **E.F. Kuester, F.S. Quazi**, University of Colorado, Dept. of Electrical and Computer Engineering, Boulder, CO, USA
- 3 SCATTERING OF SURFACE WAVES BY DIELECTRIC TAPERS. **S.T. Peng, S.J. Xu**, New York Institute of Technology, Electromagnetics Laboratory, Old Westbury, NY, USA; **F.K. Schwing**, U.S. Army CECOM, Ft. Monmouth, NJ, USA
- 4 DIFFRACTION OF A PLANE WAVE AT A CORNER COMMON TO P.E.C. AND PENETRABLE QUARTER SPACES. **L.W. Pearson**, McDonnell Douglas Research Laboratories, St. Louis, MO, USA; **A.W. Glisson**, University of Mississippi, Dept. of Electrical Engineering, University, MS, USA
- 5 AN EFFICIENT APPROACH FOR ANALYZING THE EM COUPLING INTO LARGE OPEN-ENDED WAVEGUIDE CAVITIES. **P.H. Pathak, A. Altintas**, Ohio State University ElectroScience Laboratory, Dept. of Electrical Engineering, Columbus, OH, USA
- 6 THE WIENER-HOPF-HILBERT METHOD IN ANALYSIS OF ABRUPT DISCONTINUITIES OF OPEN WAVEGUIDES. **W. Nasalski**, Institute of Fundamental Technological Research, PAS, Warsaw, Poland
- 7 ON THE CONTINUOUS RADIATION-MODE SPECTRUM OF INTEGRATED OPEN-BOUNDARY WAVEGUIDES. **D.P. Nyquist, M.S. Viola**, Michigan State University, Dept. of Electrical Engineering and Systems Science, East Lansing, MI, USA; **B.C. Drachman**, Michigan State University, Dept. of Mathematics, East Lansing, MI, USA
- 8 RADIATION OF AN OPEN-ENDED RECTANGULAR WAVEGUIDE INTO A PLANAR STRATIFIED MEDIUM. **T.M. Habashy, W.C. Chew**, Schlumberger-Doll Research, Electromagnetics Department, Ridgefield, CT, USA
- 9 RADIATION OF A POINT SOURCE IN AN OPEN WAVEGUIDE. **W.C. Chew**, Schlumberger-Doll Research, Electromagnetics Department, Ridgefield, CT, USA; **S.L. Lin**, Massachusetts Institute of Technology, Cambridge, MA, USA
- 10 RADIATION OF A POINT SOURCE IN THE VICINITY OF A MULTI-CYLINDRICALLY LAYERED GEOMETRY. **W.C. Chew, J. Lovell**, Schlumberger-Doll Research, Electromagnetics Department, Ridgefield, CT, USA

## B-16-1

### A GENERAL VARIATIONAL FORMULATION FOR OPEN WAVEGUIDE REFLECTIONS WITHOUT USING THE COMPLETE MODE SPECTRUM

Edward F. Kuester and David C. Chang  
Electromagnetics Laboratory  
Department of Electrical and Computer Engineering  
University of Colorado, Box 425  
Boulder, CO 80309 USA

Variational methods for electromagnetic scattering problems have played an important role in their solution since the 1940's when Schwinger and his co-workers attacked a wide class of hollow waveguide problems using them. To a large extent, V.H. Rumsey [Phys. Rev., 94, 1483-1491, 1954] gave a unified presentation of these methods for scattering by objects in free space; a similar development could well be done for waveguide scattering problems. In a waveguide, the scattering problem is traditionally expressed as an integral equation over the location of the irregularity (junction, aperture, post, etc.) whose kernel is a Green's function consisting of a sum over all the modes supported by the guide or guides in question. While this does not present too much difficulty in the case of a closed guide of simple shape (e.g., rectangular), open waveguides possess a continuous spectrum of radiation modes which can be awkward to deal with, and the mode fields are more difficult to obtain explicitly, if this can be done at all. C.M. Angulo [IRE Trans. Ant. Prop., 5, 100-109, 1957] performed such a variational analysis on the relatively simple problem of a truncated dielectric slab waveguide, and met with very formidable analysis.

In this paper, we present a general variational formulation for problems of scattering by nonuniformities in open waveguides which is based on an integral equation whose kernel is the free-space (or other relatively simple) Green's function and does not require knowledge of the complete mode spectrum of the guide. The germ of the idea is to be found in a little-known paper by H. Levine [J. Acoust. Soc. Amer., 26, 200-211, 1954] dealing with a related problem for acoustic waveguides. In essence, we formulate an integral equation for scattered equivalent currents (induced polarization or conduction currents) in or on the dielectric and metal which make up the waveguide junction. In some portions of space, the scattered currents must add to the incident currents to give zero, if there is no waveguide structure present. A variational expression is then obtained for any desired parameter of the problem (reflection coefficient, etc.) by suitably choosing some reference states of the system. Several illustrations of potential applications will be given.

REFLECTION OF SURFACE WAVES FROM THE TRUNCATION  
OF A DIELECTRIC SLAB WAVEGUIDE

Edward F. Kuester and Fazle S. Quazi  
Electromagnetics Laboratory  
Department of Electrical and Computer Engineering  
University of Colorado, Box 425  
Boulder, CO 80309 USA

In a companion paper presented to this Meeting (Kuester and Chang), a general theory for the treatment of scattering problems in open waveguides using variational techniques has been discussed. In the present paper, we give an application of that theory to the computation of the reflection coefficient of a surface wave from a squarely truncated dielectric slab waveguide. This problem has been attacked by others [C.M. Angulo, IRE Trans. Ant. Prop., 5, 100-109, 1957; T.E. Rozzi and G.H. in't VeId, IEEE Trans. Micr. Theory Tech., 28, 61-73, 1980] using a variational formula involving the aperture field in the plane of truncation. Since this approach needs a Green's function containing a sum over all discrete and continuous spectrum modes, a great deal of additional effort is required.

In our approach, the variational principle involves the fields over the entire length of the waveguide, but only in the core region of the slab. Furthermore, only a simple free-space Green's function is required, so no higher-order modes need to be found. We present results obtained through the use of a single simple trial function (the surface wave with adjustable amplitude) and obtain good comparison with other results available in the literature computed by more exact (and more time-consuming) means. A major advantage of our approach is that the reflection coefficient is obtained directly--it is the functional which is stationary. Therefore, we can hope to achieve increased accuracy with our modest computational expenditure while avoiding any side calculations to find the parameter of interest.

## B-16-3

### SCATTERING OF SURFACE WAVES BY DIELECTRIC TAPERS

S. T. Peng and S. J. Xu  
Electromagnetics Laboratory  
New York Institute of Technology  
Old Westbury, NY 11542

and

Felix K. Schwering  
U.S. Army CECOM  
Ft. Monmouth, NJ 07703

We present here an analysis of the scattering of surface waves by tapered dielectric waveguides. The analysis is carried out by the method of staircase approximation that replaces a continuous taper profile by a piecewise-constant one. Such a method applies to taper structures of any geometrical shape and any material composition; hence, it is particularly suitable for a systematic investigation of the effect of taper profile on radiation characteristics of a taper as an antenna. Furthermore, though approximate, the method contains all essential physical processes involved in the nonuniform dielectric waveguide, such as: multiple internal reflections and mode couplings. Extensive numerical results have been obtained to show the efficiency and radiation pattern of various taper antennas. More specifically, three different taper profiles, namely, linear, parabolic and elliptic profiles, have been considered. In addition, the effects of the thickness and dielectric constant of the feeder waveguide as well as the aspect ratio of the taper are parametrically investigated. Some guidelines for the design of taper antennas are then developed, as will be discussed in the presentation.

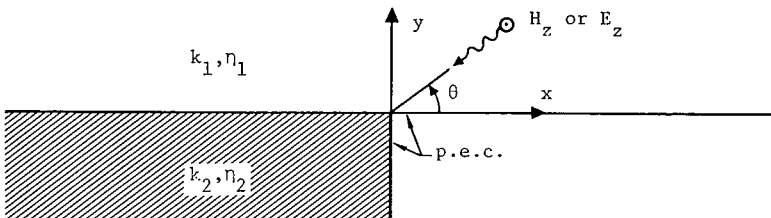
DIFFRACTION OF A PLANE WAVE AT A CORNER  
COMMON TO P.E.C. AND PENETRABLE QUARTER SPACES

L. Wilson Pearson  
McDonnell Douglas Research Laboratories  
P. O. Box 516  
St. Louis, MO 63166

Allen W. Glisson  
Department of Electrical Engineering  
University of Mississippi  
University, MS 30677

The problem of a plane wave incident on the interface geometry pictured below is formulated as a modified Wiener-Hopf equation. The formulation is constructed using an integral equation for the electric field over the aperture defined by  $y = 0, x < 0$ . The Green's function for the lower region contains a term that accounts for the image of the aperture field in the vertical p.e.c. wall in that region. It comprises a Hankel function of argument  $k_2|x + x'|$ . This term precludes a straightforward convolution interpretation of the integral equation and leads to the modified Wiener-Hopf system.

The modified Wiener-Hopf system requires a numerical solution in the spectral domain. Carrying out the spectral-domain numerical solution is attractive compared with solving the original integral equation in the spatial domain, however, because one may construct an asymptotic representation of the diffracted fields from the spectral-domain results in a straightforward fashion.



## B-16-5

### AN EFFICIENT APPROACH FOR ANALYZING THE EM COUPLING INTO LARGE OPEN-ENDED WAVEGUIDE CAVITIES

P.H. Pathak and A. Altintas  
The Ohio State University ElectroScience Laboratory  
1320 Kinnear Road  
Columbus, Ohio 43212

This paper addresses the problem of Electromagnetic (EM) coupling/penetration into open-ended waveguide type cavity structures when illuminated by an external plane wave. Of particular interest is the coupling of EM energy into a duct/cavity at high frequencies where a large number of propagating waveguide modes can be excited and conventional procedures requiring a summation over a large number of propagating modes can become cumbersome and inefficient. It is shown here that the modes which contribute most significantly to the fields coupled into the duct/cavity are those whose corresponding modal ray directions are closely phase matched to the incident ray at the open end. This concept is illustrated by calculating the far-zone EM fields backscattered from a 3-D open-ended rectangular waveguide geometry with a perfectly-conducting planar (short circuit) termination inside. These calculations show that over each small set of aspect angles (or angles of incidence) only a set of approximately 3 consecutive propagating modes (which satisfy the condition described above) are required. The above calculations employ the usual geometrical optics, aperture field and Ufimtsev edge current techniques for analyzing the fields coupled into, and re-radiated from the waveguide for a wide range of aperture dimensions and termination distances. The same calculations are also repeated utilizing all of the propagating modes as a comparison to illustrate the accuracy of the more efficient approach which utilizes extremely few modes. Also included are some experimental results which further verify the accuracy of the above computations. Additional results and implications will be discussed.

THE WIENER-HOPF-HILBERT METHOD IN ANALYSIS  
OF ABRUPT DISCONTINUITIES OF OPEN WAVEGUIDES

W. Nasalski

Institute of Fundamental Technological Research, PAS  
00-049 Warsaw, Świętokrzyska 21, Poland

The problem of guided mode scattering by a junction between two planar, symmetric, dielectric waveguides is considered. Discontinuity is due to sudden changes in the slab thickness (from  $d_1$  to  $d_2$ ) or abrupt refractive index changes. An auxiliary diffraction problem is formulated in a semi-infinite free-space region bounded by a plane, referred to as the impedance plane, placed on or over surfaces of the dielectric slabs. Application of the Wiener-Hopf-Hilbert method (R.A.Hurd, Can.J.Phys, 54, 775-780, 1976) gives the solution to the auxiliary problem. There are some fundamental features of the approach:

1. The longitudinal spectral representation is assumed for the scattered field.
2. Surface impedances  $\eta_1$  and  $\eta_2$  with spatial dispersion are defined on the surfaces of the two slabs.
3. On the impedance plane the continuity relations of tangent field components are replaced by impedance boundary conditions in integral form.
4. For the region above the impedance plane the boundary conditions together with the continuity relations at the junction plane result in a homogeneous Wiener-Hopf equation.
5. The W-H equation is transformed to the Hilbert problem on the contour  $J$  ( $\text{Im}\alpha=0$ ,  $\text{Im}\beta\leq 0$  or  $\geq 0$ ;  $\beta$  and  $\alpha$  are wave numbers in the free space in longitudinal and transverse directions, respectively):

$$V^+(t) = H(t)V^-(t), \quad t \in J,$$

$$H(t) = (\alpha + k\eta_1)(\alpha + k\eta_2)(\alpha - k\eta_1)^{-1}(\alpha - k\eta_2)^{-1} \exp(i\alpha(d_1 - d_2))$$

where  $k$  is a wave number in the free space,  $V$  is the holomorphic function everywhere but  $J$  and  $V^+$ ,  $V^-$  are its limiting values from the two sides of  $J$ .

6. The Plemelj formulae together with the edge condition yield the solution to the problem.

A novel formulation of the problem, applied in this contribution, results in effective factorization of the W-H equation derived.

The solution obtained in such a way can be used in total field synthesis, where the remaining continuity relations at the junction plane and below the impedance plane are to be employed.

ON THE CONTINUOUS RADIATION-MODE SPECTRUM  
OF INTEGRATED OPEN-BOUNDARY WAVEGUIDES

D.P. Nyquist and M.S. Viola  
Department of Electrical Engineering and Systems Science  
B.C. Drachman, Department of Mathematics  
Michigan State University, East Lansing, Michigan 48824

The complete propagation-mode spectrum of integrated, open-boundary waveguides consists of discrete guided-wave modes augmented by a continuous radiation-mode spectrum. While the guided-wave modes of practical microstrip and dielectric waveguide structures have been studied extensively, the radiation modes of such integrated configurations have apparently received little attention. An integral-operator description of the continuous spectrum for integrated open-boundary waveguides is advanced here. Attention is focused on integrated dielectric guides; an analogous (but simpler) formulation is applicable to conducting microstrip lines.

Electric field  $\vec{E}$  excited in the guiding region of a dielectric waveguide integrated adjacent to a layered substrate/film/overlay environment by impressed field  $\vec{E}^1$  is described rigorously by an electric field integral equation (EFIE). The integral operator is convolutional in the axial variable, and Fourier transforming leads to the 2-d EFIE

$$\vec{e}(\vec{\rho}, \zeta) - (n_c^2 k_0^2 + \nabla \cdot \nabla) \int_{CS} \frac{\delta n^2(\vec{\rho}')}{n_c^2} \vec{g}_{\zeta}(\vec{\rho}, \vec{\rho}') \cdot \vec{e}(\vec{\rho}', \zeta) dS' = \vec{e}^1(\vec{\rho}, \zeta)$$

where  $\vec{e}, \vec{e}^1$  are transforms,  $\vec{\rho}$  = transverse position vector,  $\zeta$  = axial transform variable,  $\delta n^2$  = contrast of guiding region against refractive index  $n_c$  of cover in which it is immersed,  $\nabla = \nabla_{\rho} + \hat{z}j\zeta$ , CS = guiding region cross section where  $\delta n^2 \neq 0$ , and  $\vec{g}_{\zeta} = 2$ -d Hertzian potential Green's dyad (Sommerfeld-integral representation) descriptive of the layered environment. Inverse transformation of  $\vec{e}(\vec{\rho}, \zeta)$  is aided by complex  $\zeta$ -plane analysis, leading to discrete surface-wave-mode residues and the radiation field which arises from integration along the branch cuts associated with  $\vec{g}_{\zeta}$ . Since  $\vec{e}^1$  is maintained by  $\vec{J}$  immersed in the layered environment, then that impressed field is given by the spatial superposition of  $\vec{g}_{\zeta} \cdot \vec{J}$  where  $\vec{g}_{\zeta}$  is itself a spectral integral representation. Radiation spectrum  $\vec{e}(\vec{\rho}, \zeta)$  can therefore be uniquely decomposed into elementary contributions associated with point spatial and spectral contributions to  $\vec{e}^1$ . The total radiation field can finally be expressed as a fourfold integral superposition (2 spatial, 2 spectral) over those elementary radiation-mode spectra.

EFIE's for the elementary radiation-mode spectra are developed for a general class of integrated open-boundary waveguides. It is demonstrated that solutions to those EFIE's replicate existing results for the asymmetric-slab and uniformly-clad circular cylindrical guides. Methods for quantifying the continuous spectra of practical integrated structures are investigated.

**RADIATION OF AN OPEN-ENDED RECTANGULAR WAVEGUIDE  
INTO A PLANAR STRATIFIED MEDIUM**

T.M. Habashy and W.C. Chew  
Schlumberger-Doll Research  
Old Quarry Road  
Ridgefield, CT 06877-4108

The radiation of an open-ended rectangular waveguide which is excited by an arbitrary point source or a probe into a planar stratified medium, is investigated analytically. The complexity of analyzing the discontinuity at the waveguide junction arises mainly from the vector nature of the electromagnetic field and the necessity to match discrete modes in the waveguide to the continuum modes in the open space. A vector Fourier transform together with a vector Fourier series are developed and their properties are discussed, which help facilitate the analysis and simplify the process of matching the boundary conditions at the waveguide aperture.

The vector Fourier transform is introduced to express the continuous spectrum of modes in the planar stratified medium whereas the vector Fourier series helps in representing the discrete modal spectrum inside the waveguide. With the help of the orthogonality relationships of these operators, mode matching at the waveguide junction can be carried out in a simple manner and hence allows us to compute the transmission and reflection operators at the discontinuity. These transmission and reflection operators represent the mode conversion physics at the discontinuity. With this canonical problem solved, the problem involving more than one discontinuity can be analyzed by concatenating the physics at each of the discontinuities. Numerical results are presented and discussed.

RADIATION OF A POINT SOURCE IN AN OPEN WAVEGUIDE

W. C. Chew  
Schlumberger-Doll Research  
Old Quarry Road  
Ridgefield, Connecticut 06877-4108

S. L. Lin  
Massachusetts Institute of Technology  
77 Massachusetts Avenue  
Cambridge, Massachusetts 02139

Abstract

The radiation of a point source in the neighborhood of a waveguide discontinuity is well-known, but when the waveguide is terminated in an open space, the solution is not well-known. In this paper, we present the solution to the problem of a point source in the vicinity of a cylindrical waveguide discontinuity where half of the space is an infinite half-space, and the other half a semi-infinite cylinder. The eigenmodes in the cylindrical waveguide are discrete guided modes of the waveguide, while the eigenmodes in the open half-space consist of a continuum of wave or radiation mode. We will show how the mode in the waveguide can be matched to the radiation or continuum modes in the open region. For the non-axial symmetric modes, the bookkeeping is more complicated. However, the use of vector Hankel transforms simplifies the derivation. The use of vector series in the waveguide region and vector Hankel transform in the open region allows the ease of mode watching. Reflection and transmission operators can be derived which represent the physics of transmission, reflection and mode conversion in the discontinuities. The use of reflection and transmission operators easily allow the generalization to any number of discontinuities.

**RADIATION OF A POINT SOURCE IN THE VICINITY  
OF A MULTI-CYLINDRICALLY LAYERED GEOMETRY**

W. C. Chew and J. Lovell  
Schlumberger-Doll Research  
Old Quarry Road  
Ridgefield, Connecticut 06877-4108

**Abstract**

We present here the solution to the radiation of an arbitrary point source in the vicinity of a multi-cylindrically layered geometry. This is essentially the Green's function for a cylindrically layered geometry. We present here a solution where we use only two scalar components of the electric and magnetic field. An off-center point source can be expanded in terms of cylindrical harmonics using Graf's formula. The generalized recursive formulas for the propagation of the waves through the cylindrical layers are derived. The cylindrical boundary couples the two scalar components of the wave, so hybrid modes exist in general. With the solution, we can derive the singularities or the guided modes in the cylindrical structure. The singularities provide physical insight into the physics of wave propagation in such a structure.



## URSI COMMISSION B - SESSION B17

Diffraction

1:30 - 5:00  
IRC-1

Diffraction

Chairperson/Président: **R.G. Kouyoumjian**, Ohio State University, Columbus, OH, USA

- 1 MODIFIED GTD FOR GENERATING COMPLEX RESONANCES FOR FLAT STRIPS AND DISKS. **H. Shirai, L.B. Felsen**, Polytechnic Institute of New York, Dept. of Electrical Engineering and Computer Science, Farmingdale, NY, USA
- 2 SPECTRAL SYNTHESIS OF UNIFORM GTD WAVEFUNCTIONS. **J.M. Arnold**, University of Glasgow, Dept. of Electronics and Electrical Engineering, Glasgow, UK
- 3 UNIFORM DIFFRACTION COEFFICIENTS FOR AN IMPEDANCE HALF-PLANE. **J.L. Volakis, T.B.A. Senior**, University of Michigan, Dept. of Electrical Engineering and Computer Science, Ann Arbor, MI, USA
- 4 DIFFRACTION BY AN ANISOTROPIC IMPEDANCE HALF-PLANE. **R.A. Hurd**, National Research Council of Canada, Division of Electrical Engineering, Ottawa, ON; **E. Lüneburg**, DFVLR, Oberpfaffenhofen, FRG
- 5 SCATTERING BY A CONDUCTING STRIP WITH A RANDOMLY SERRATED EDGE. **C. Eftimiu, P.L. Huddleston**, McDonnell Douglas Research Laboratories, St. Louis, MO, USA
- 6 THE RADIATION FROM SCATTERERS AT THE EDGE OF A WEDGE. **O.M. Buyukdura, R.G. Kouyoumjian**, Ohio State University ElectroScience Laboratory, Dept. of Electrical Engineering, Columbus, OH, USA
- 7 DIFFRACTION BY A DOUBLE CAPPED-WEDGE. **A.Z. Elsherbeni, M. Hamid**, University of Manitoba, Dept. of Electrical Engineering, Winnipeg, MB
- 8 TWO-DIMENSIONAL PLANE WAVE SCATTERING FROM MULTIPLE RADially-DIRECTED STRIPS IN THE PRESENCE OF A CYLINDER. **D.F. Hanson**, University of Mississippi, Dept. of Electrical Engineering, University, MS, USA; **C.M. Butler**, University of Houston, Dept. of Electrical Engineering, Houston, TX, USA
- 9 SCATTERING BY A PERFECTLY CONDUCTING CIRCULAR CYLINDER CUT BY A SINGLE CIRCUMFERENTIAL SLOT. **L.K. Warne**, Sandia National Laboratories, Albuquerque, NM, USA
- 10 THE BACKSCATTERING CROSS SECTION OF THIN WIRE LOOPS. **J.W. Burns**, University of Michigan, Radiation Laboratory, Ann Arbor, MI, USA

## B-17-1

### MODIFIED GTD FOR GENERATING COMPLEX RESONANCES FOR FLAT STRIPS AND DISKS

H. Shirai and L.B. Felsen  
Department of Electrical Engineering and Computer Science  
Polytechnic Institute of New York  
Route 110, Farmingdale, NY 11735

The complex resonance frequencies of a scatterer are important elements in target classification and identification. In the singularity expansion method (SEM), the resonances are defined by a homogeneous integral equation whose numerical solution is feasible in the low, but not in the high, frequency range. At high frequencies, GTD provides an attractive numerical alternative and, furthermore, incorporates an interpretation of the resonance generation process in terms of multiple wavefronts (ray) traversals. Except for extremely simple scatterer configurations, the (damped) complex resonances are known to occupy an entire half of the complex frequency plane. Dominant and higher order creeping wave GTD applied to cylinders and spheres does indeed yield resonances arranged along a sequence of "layers" in that entire half plane, but multiple edge diffracted GTD applied to flat strips and disks furnishes only a single (dominant) layer. By drawing analogies with higher order creeping waves on a smooth object, the conventional edge diffracted GTD field is here augmented by higher order ray fields undergoing higher order "slope diffraction". Each of these higher order ray fields can be made to satisfy its own resonance equation, which is now found to provide the missing layers, with remarkably accurate values for the resonances when compared, where available, with those calculated numerically by the moment and T-matrix methods. The success of higher order ray diffraction in predicting the complex resonance structure suggests that this mechanism may play a corrective role also in other edge dominated scattering phenomena.

SPECTRAL SYNTHESIS OF UNIFORM GTD WAVEFUNCTIONS

J.M. Arnold

Department of Electronics and Electrical Engineering,  
 University of Glasgow,  
 Glasgow G12 8QQ, Scotland.

It is well known that diffraction fields constructed according to the prescription of GTD exhibit a variety of singularities where the method predicts infinite or nondifferentiable fields. These singularities can be classified into caustics, cusps, shadow boundaries and so on, according to type. It is widely believed that GTD cannot be consistently modified directly to smooth these singularities, and that recourse must be made to more complex theories, such as moment methods or surface integral representations or to some 'ansatz' such as UAT or Ludwig's caustics correction.

It has recently been shown that this is not the case; globally uniform wavefunctions for fields diffracted from apertures and curved reflectors can be constructed directly from Keller's GTD, without any 'ansatz' on the nature of the transition functions and without any intervening 'surface current' representation being required. This construction, which proceeds directly from the geometrical ray construction of GTD, is called spectral synthesis.

The fundamental idea of spectral synthesis is the identification of the manifold of diffracted rays with the manifold of plane waves forming a plane wave spectral representation of the field, the identification being that of identical directions of propagation. It turns out that the spectral coefficients of the plane waves can be computed from the GTD amplitude and phase along the rays in a direct geometrical manner. The resulting spectral integral reduces to GTD by the principle of stationary phase away from singularities; near caustics and cusps the correct transition functions are automatically generated by applying the Morse theory of degenerate stationary phase points (catastrophe theory). Near diffraction shadow boundaries a slight modification of the construction is required which can be carried out in a natural geometrical fashion by adding and subtracting a regular reference wave to the wavefunction (a counter-term). The arbitrariness of the reference wave permits the representation of the total field in any of the combinations: physical optics plus edge diffracted wave; Kirchoff-Huyghens plus edge diffracted wave; Fresnel integral plus edge diffracted wave (UAT); or a generalised representation making no reference to any of the conventional ones. It is a transparent feature of the theory that these are all equivalent up to  $O(k^{-3})$  asymptotics, all follow from the same basic geometrical structure of the Keller ray manifold, and all are constructible using only the geometry of this manifold.

The theory is currently being employed to analyse the precise significance of complex rays in diffraction theory, and to investigate cross-polar fields in focussed reflector systems near the focal point, where it is known that none of the conventional asymptotic theories give acceptable results, but where the spectral synthesis method gives a well behaved uniform representation directly from the ray geometry.

## B-17-3

### UNIFORM DIFFRACTION COEFFICIENTS FOR AN IMPEDANCE HALF-PLANE

J. L. Volakis and T.B.A. Senior  
Radiation Laboratory

Department of Electrical Engineering and Computer Science  
The University of Michigan  
Ann Arbor, Michigan 48109

Uniform diffraction coefficients will be presented for the cases of normal and oblique incidence on a half-plane edge associated with impedance boundary conditions. These coefficients are based on the Weiner-Hopf solution by Senior (Radio Science, 1975). Numerical results will also be presented using such uniform solutions.

The dominant parts of the diffraction coefficient are put in a form compatible with the corresponding uniform coefficients for a conducting edge. They are then examined in detail, especially at the shadow and reflection boundaries. At these boundaries, a direct comparison can be made with existing heuristic coefficients. Not surprisingly, the coefficients involve the appropriate split functions of the Weiner-Hopf solution which can be expressed in terms of the Maliuzhinets meromorphic function. In case of real impedances, a simple analytical expression will be given for this function.

The results at normal incidence, using the above uniform solution, are in agreement with recently published patterns employing more involved diffraction coefficients (Tiberio, etc., AP-S/URSI Symposium, 1984). Scattering patterns will also be presented at oblique incidences with real and complex impedances. Finally, a generalization of these coefficients to the case of wedges will be discussed.

## DIFFRACTION BY AN ANISOTROPIC IMPEDANCE HALF-PLANE

R.A. Hurd, Division of Electrical Engineering, National Research Council, Ottawa, Ontario, K1A 0R8, Canada.

E. Lüneburg, Deutsche Forschungs-und Versuchsanstalt für Luft-und Raumfahrt e.V. (DFVLR), 8031 Oberpfaffenhofen, West Germany.

We solve a new diffraction problem: that of a plane electromagnetic wave obliquely incident on a half-plane characterized by anisotropic impedance boundary conditions

$$E_x = \pm Z_1 H_z, \quad E_z = \mp Z_2 H_x$$

where the upper/lower signs are for the top/bottom of the half-plane, and the x/z axes are perpendicular/parallel to the edge of the half-plane.

Following a standard procedure, we are led to the consideration of a matrix Wiener-Hopf equation of the form

$$G(\alpha)L(\alpha) = U(\alpha) + P(\alpha)$$

where  $G(\alpha)$  is a known  $2 \times 2$  matrix,  $P(\alpha)$  a known column vector, and  $L(\alpha)$  and  $U(\alpha)$  are unknown column vectors analytic respectively in lower and upper halves of the complex  $\alpha$ -plane.

The complexity of  $G(\alpha)$  is such that it cannot be diagonalized by pre-and post-multiplication by polynomial matrices, i.e. by introducing new unknowns obtained by polynomial transformations of  $L(\alpha)$ ,  $U(\alpha)$ . On the other hand, by using a combination of new and old factorization techniques (V. Daniele, SIAM J. Appl. Math. 44, 667-680, 1984; A.A. Khrapkov, Prikl. Mat. Mekh. 35, 625-637, 1971), we find that  $G(\alpha)$  can be factorized into  $\overline{G}(\alpha) = G_U(\alpha)G_L(\alpha)$  with  $G_U$  and  $G_L$  analytic respectively in upper and lower half-planes. From this point, the analysis follows standard Wiener-Hopf procedures, leading to a complete solution of the problem.

## B-17-5

### SCATTERING BY A CONDUCTING STRIP WITH A RANDOMLY SERRATED EDGE

C. Eftimiu and P. L. Huddleston  
McDonnell Douglas Research Laboratories  
P. O. Box 516  
St. Louis, MO 63166

The coherent monostatic response of a strip with a randomly serrated edge is evaluated. The serration is assumed to be canonically distributed, and the average response is calculated by using the ergodic theorem. Results are given for various values of the rms width and correlation length of the serrated edge.

THE RADIATION FROM SCATTERERS AT  
THE EDGE OF A WEDGE

O.M. Buyukdura and R.G. Kouyoumjian  
ElectroScience Laboratory  
Department of Electrical Engineering  
The Ohio State University  
1320 Kinnear Road  
Columbus, Ohio 43212

This paper is concerned with the radiation from scatterers positioned at the edge of a perfectly-conducting wedge. The problem is interesting because the guiding effect of the edge causes strong interaction between the scatterers, thereby greatly enhancing the scattered field as compared with that of the scatterers in free space. This configuration also can be used to model the scattering from a rough edge.

As a first step, the dyadic Green's function for a conducting sphere at the edge is obtained. For a small sphere, it is observed that the field close to the edge can be approximated by the sum of two terms: the field in the absence of the sphere, and an edge guided wave due to an equivalent point source placed close to the edge at the position of the sphere.

Next, scattering by an irregularly shaped object at the edge is considered. A generalized T-Matrix formulation is used for this problem. The incident field is defined as the field in the absence of the scatterer but with the wedge present; it is expanded in terms of a set of spherical vector wave functions which satisfy the boundary condition on the surface of the wedge together with the edge condition. The dyadic Green's function used in this formulation is the one previously obtained for the perfectly conducting wedge (R.G. Kouyoumjian and O.M. Buyukdura, Proc. of the 1983 International URSI Symposium, Universidad de Santiago de Compostela, Spain, pp. 151-154). It too is expanded in terms of these vector wave functions. Again, for a small scatterer, the field close to the edge is given by the sum of the field in the absence of the scatterer and an edge wave. The T-Matrix formulation is also used along with a self-consistent method to solve the problem of multiple scatterers located along the edge of the wedge. Numerical results are presented to show the enhanced scattering from small objects positioned at the edge of a wedge.

## DIFFRACTION BY A DOUBLE CAPPED-WEDGE

A.Z. Elsherbeni and M. Hamid  
 Antenna Lab., Elec. Eng. Dept.  
 University of Manitoba  
 Winnipeg, Canada. R3T 2N2

Following a recent asymptotic solution for the diffraction by two conducting sharp-wedges (Elsherbeni and Hamid, IEEE Trans. Ant. and Propag., AP-32, No. 11, pp. 1262-5, 1984), the diffraction of a normally incident plane wave by two cylindrically capped identical wedges is investigated by a generalization of the Karp and Russek technique for a wide slit. The cap is considered to be either a conducting or a dielectric cylinder whose axis coincides with the wedge edge and its radius is much less than the separation between the two wedge edges. The effects of the cap radius, permittivity and wedge angle on the diffraction pattern, transmission coefficient, equivalent line source intensity and edge-edge interaction term are presented. The transmission coefficient of the aperture is increased over the uncapped wedge case for dielectric caps and decreased for conducting caps. Other effects of the caps on the diffraction pattern such as beamwidth, level and position of first sidelobe are also investigated.

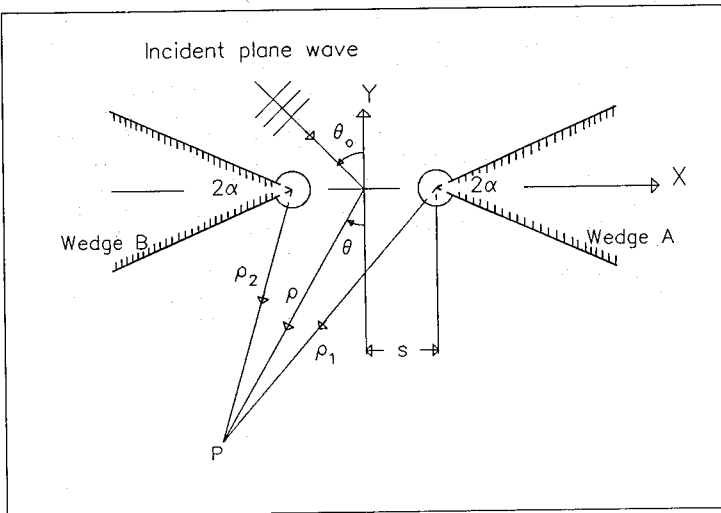


Fig. 1: Double capped-wedge geometry.

TWO-DIMENSIONAL PLANE WAVE SCATTERING FROM MULTIPLE  
RADIALLY-DIRECTED STRIPS IN THE PRESENCE OF A CYLINDER

Donald F. Hanson  
Dept. of Electrical Engineering  
University of Mississippi  
University, MS 38677

Chalmers M. Butler  
Dept. of Electrical Engineering  
University of Houston  
Houston, TX 77004

Two recent papers (Hanson and Butler, 1983 Spring URSI Meeting Digest, Houston, TX, and Karunaratne, Michalski, and Butler, IEEE SOUTHEASTCON '84 Proceedings, Louisville, Kentucky, April 8-11, 1984, pp. 85-89) have examined the cases of a single radially directed conducting strip attached to, penetrating or external to a conducting or dielectric circular cylinder. The incident field is a plane wave.

In this paper, the conducting cylinder case is extended to the multiple strip case. Two or more radially directed strips are in the presence of a conducting circular cylinder. This case is important in view of the interest in modeling of aircraft with wings and missiles with fins. Superposition and symmetry are used to derive a coupled set of integral equations for the current on the fins. These equations are solved numerically. The integral equation kernel contains an infinite series of Bessel functions which is slowly convergent, so an acceleration technique is introduced to limit the number of terms necessary for evaluation. Data are presented for several cases of interest.

## B-17-9

### SCATTERING BY A PERFECTLY CONDUCTING CIRCULAR CYLINDER CUT BY A SINGLE CIRCUMFERENTIAL SLOT

Larry K. Warne  
Sandia National Laboratories, 7553  
Albuquerque, NM 87185

The problem of electromagnetic scattering from a perfectly conducting circular cylinder containing a single circumferential slot (gap) is considered. This problem is a useful canonical example of aperture coupling and as is well known, gives rise to coupling between both axial polarizations.

The incident wave is assumed to be a plane wave impinging at an arbitrary angle of incidence with respect to the cylinder axis. The incident wave has arbitrary polarization and the slot has finite width.

The problem is formulated as a coupled set of integral equations which are subsequently reduced to a pair of series equations. The series equations are then solved numerically. The resulting coefficients are used to generate the interior and exterior fields. An approximation is used when the gap is narrow. This approximate solution is compared with the numerical solution.

## THE BACKSCATTERING CROSS SECTION OF THIN WIRE LOOPS

Joseph W. Burns  
Radiation Laboratory  
University of Michigan  
Ann Arbor, Michigan 48109

An investigation of the high frequency backscattering of circular thin wire loops produced unexpected results which have led to a better understanding of the physical processes involved in loop scattering. In this paper, a caustically matched second order GTD solution for the backscattered field is given, which incorporates ray paths neglected in previous GTD analyses. The backscattering behavior of large circular loops as a function of loop radius and angle of incidence is numerically evaluated and compared to the backscattered field predicted by the GTD formula. The GTD is found to be quite accurate for normal and near normal incidence, but departs significantly from the numerical data at wide angles of incidence. Subsequent analysis of the numerical data suggests that waves propagating on the loop contribute to the backscattering in a manner not described by a GTD solution incorporating only edge-diffracted rays. A qualitative physical model of the wide angle scattering process is described and an accurate approximate formula for the E polarization backscattering at edge-on incidence is given to support the physical model.



## URSI COMMISSION B - SESSION B18

**Reflectors and Horns**1:30 - 5:00  
IRC-2**Réflecteurs et cornets**Chairperson/Président: **R. Mitra**, University of Illinois, Urbana, IL, USA

- 1 ANALYSIS OF REFLECTOR ANTENNAS WITH ELLIPTICAL APERTURES USING JACOBI-BESSEL EXPANSION - A COMPARATIVE STUDY. **Y. Rahmat-Samii**, California Institute of Technology, Jet Propulsion Laboratory, Pasadena, CA, USA
- 2 GTD TECHNIQUES FOR THE DESIGN OF OFFSET DUAL REFLECTOR ANTENNAS. **C.J. Sletten**, GTE Communication Systems, Needham Heights, MA, USA
- 3 FAR-FIELD COMPUTATIONS OF DISTORTED REFLECTOR ANTENNAS BY LEAST SQUARES SURFACE APPROXIMATION. **T.J.F. Pavlasek, R. Pokuls, L. Wegrowicz**, McGill University and Spar Aerospace Ltd., Montreal, PQ
- 4 APERTURE IMPEDANCE OF TE AND TM MODES IN CONICAL AND QUASI-PYRAMIDAL HORNS. **R.E. Collin**, Case Western Reserve University, Dept. of Electrical Engineering and Applied Physics, Cleveland, OH, USA
- 5 RETURN LOSS OF A RECTANGULAR HORN. **A. Kumar**, Spar Aerospace Ltd., Antenna Engineering, Ste-Anne-de-Bellevue, PQ
- 6 NEW CLASSES OF HYBRID MODE ANTENNAS - ALTERNATIVES TO CORRUGATED HORN FEEDS. **E. Lier**, Norwegian Institute of Technology, Electronics Research Lab., Trondheim-NTH, Norway, **T. Schaug-Pettersen, J.A. Aas**, Norwegian Institute of Technology, Division of Telecommunications, Trondheim-NTH, Norway
- 7 COMPACT CORRUGATED POLARISERS FOR DUAL FREQUENCY OPERATION. **J.M. Rebolgar**, E.T.S.I. de Telecomunicacion, Grupo de Electromagnetismo Aplicado, Madrid, Spain
- 8 RADIATION CHARACTERISTICS OF N CIRCULAR CONDUCTING CYLINDERS SIMULATING CYLINDRICAL REFLECTORS. **H.A. Ragheb, M. Hamid**, University of Manitoba, Dept. of Electrical Engineering, Winnipeg, MB
- 9 PHYSICAL OPTICS ANALYSIS OF NASA/JPL DEEP SPACE NETWORK 70-M ANTENNAS. **A.G. Cha**, California Institute of Technology, Jet Propulsion Laboratory, Pasadena, CA, USA
- 10 FOCAL SHIFTS IN PARABOLIC REFLECTORS. **H. Ling**, University of Illinois, Dept. of Electrical and Computer Engineering, Urbana, IL, USA

## B-18-1

### ANALYSIS OF REFLECTOR ANTENNAS WITH ELLIPTICAL APERTURES USING JACOBI-BESSEL EXPANSION -- A COMPARATIVE STUDY

Y. Rahmat-Samii  
Jet Propulsion Laboratory  
California Institute of Technology  
Pasadena, CA 91109

Applications of the Jacobi-Bessel expansion for vector diffraction analysis of reflector antennas with circular apertures have been well-documented and studied. One may refer, for example, to the review paper (Y. Rahmat-Samii, R. Mittra and V. Galindo, *Electromagnetics*, Vol. 1, No. 2, 155-185, 1981). Jacobi polynomials (related to Zernike functions) are orthogonal functions over circular regions; hence, their applications to circular apertures are very natural. Although many reflector antennas possess circular projected apertures, there are many applications for which it is desirable to employ reflectors with elliptical apertures, in order to generate elliptical beams. These reflectors are, in particular, being used considerably in modern satellite communications systems.

Recently, a modification of the Jacobi-Bessel expansion has been reported (D. C. Chang and W. Rusch, *IEEE Antennas and Propagation*, Vol. 32, No. 11, 1230-1236, 1984) for a spherical reflector with a projected elliptical aperture and some numerical results were presented. It is the purpose of this paper to present a further generalization of this modified formulation of the Jacobi-Bessel expansion for reflectors with elliptical apertures and conduct a comparative study between two different analysis algorithms. One algorithm uses the Jacobi-Bessel expansion over a circular region and represents the elliptical projection by introduction of zeros in the area between the circumscribing circular region and the actual elliptical aperture. The second algorithm uses the modified Jacobi-Bessel approach, based on a particular integration parameter transformation, for the elliptical apertures. Elliptical apertures with different eccentricities are studied and results are shown for both parabolic and non-parabolic reflectors. It is shown that, for parabolic reflectors, the first algorithm results in the application of a recursion relation which cannot be used in the second algorithm. However, for elongated elliptical apertures, the second algorithm demonstrates an improved convergence behavior. Numerical results are tailored for many currently designed satellite reflector antenna configurations and, in particular, the generation of cross-polar fields for offset reflectors with circular and elliptical apertures are examined and compared.

GTD TECHNIQUES FOR THE DESIGN OF OFFSET  
DUAL REFLECTOR ANTENNAS

C. J. Sletten  
GTE Communication Systems  
Needham Heights, MA

On very low sidelobe antennas the diffracted radiation from the subreflector edges generally produce objectionably high sidelobe levels. Together with the radiation pattern of the feed horn the subreflector scattering determines the aperture illumination and edge diffraction from the main reflector. To control these edge diffraction and spillover lobes reliable information is needed on the amplitude, phase, and polarization of fields in the near- and far-zones in relation to the subreflector aperture. Using the Uniform GTD techniques of Kouyoumjian, et al, the direct and diffracted fields illuminating the edges of the main reflector are computed and shields designed to reduce sidelobe levels. The relative merits of extending the main reflector rim as a shield, of extending the subreflector rim with a phasing step, and of using absorbing shields or high edge tapers are studied and compared. To achieve precise near-zone patterns on conical corrugated horns formulations due to Clarricoats, et al, are programmed and amplitude and phase on the subreflector computed. Optimum configurations of horn and subreflectors for large bandwidths and low spillover radiation are described.

The analytical procedure and the computer software needed to compute the edge diffraction on tilted Gregorian subreflectors are presented. To improve computational accuracy the slope diffraction coefficients are determined when high edge tapers are encountered. Complete patterns are developed when using metal shielding to make sure scattered energy doesn't generate high sidelobes in the main antenna patterns. The combined effects of horn patterns, subreflector edge diffraction, and main dish rim diffraction are included in the study.

## B-18-3

### FAR-FIELD COMPUTATIONS OF DISTORTED REFLECTOR ANTENNAS BY LEAST SQUARES SURFACE APPROXIMATION

T.J.F. Pavlasek, R. Pokuls, L. Wegrowicz  
McGill University and Spar Aerospace Ltd.  
Montreal, Quebec, Canada

An efficient aperture integration routine has been coupled with a ray-tracing procedure allowing the analysis of non-paraboloidal reflector antennas. This integration routine requires the knowledge of the aperture plane field  $E$  at certain pre-defined points on the plane (usually a rectangular grid). Geometric optics techniques are used to determine  $E$  and hence ray-tracing must be performed. If the pre-determined aperture plane point and feed position are specified, then the reflection point may be found through the use of Fermat's principle. The solution of a set of non-linear equations is required.

Surfaces which are describable by "reasonable" functions (i.e. gored reflectors, spheroids,...) have been examined using this technique and results have been presented elsewhere. If the surface is described by a set of measured points, then difficulties of interpolation and ray-tracing arise because of the possible "bumpiness" of the reflector.

A method of overcoming these difficulties is the overlapping patch method. The method of least squares interpolation is used to approximate segments or "patches" of the reflector surface with the use of a second order surface. Thus, the following surface is passed amongst a subset of the measured surface points contained within a patch:

$$f(x,y) = ax^2 + by^2 + cxy + dx + ey + f$$

A circular patch is associated with each aperture plane point. The patch is centered on the reflector location where the reflection point for an ideal reflector would be. The non-ideal nature of the surface would cause the true reflection point to migrate from this ideal position. The radius of the patch must be sufficiently large such the non-ideal reflection point would still be contained within the perimeter of the patch. However, the radius should be small enough so that the patch may be considered to be a "local" description of the reflector.

An advantage of this method of interpolation is that the reflection points algorithm will always deal with surfaces of a second order nature which converge rapidly. The global reflector may be envisioned as being comprised of smaller, circular reflectors of various orientations, focal lengths, and positions.

Far-field patterns for two reflectors with known distortions were available for the testing of the algorithm. Results comparing calculations and measurements are presented.

APERTURE IMPEDANCE OF TE AND TM MODES  
IN CONICAL AND QUASI-PYRAMIDAL HORNS

R. E. Collin

Department of Electrical Engineering and Applied Physics  
Case Western Reserve University  
Cleveland, Ohio 44106

In the analysis of mutual coupling effects in arrays of conical and pyramidal horns it is necessary to know the wave impedance of the TE and TM modes in the aperture of the horn. For horns with small flare angles Legendre's differential equation is solved by a perturbation technique and the wave impedance is derived in terms of the spherical Hankel functions and their derivatives. It is shown that the wave impedance that is derived from the WKB method is not very accurate and hence it is concluded that the use of the WKB method is inappropriate.

RETURN LOSS OF A RECTANGULAR HORN

A. Kumar  
Antenna Engineering  
Spar Aerospace Ltd.  
21025 Trans-Canada Highway  
Ste-Anne-de-Bellevue,  
Quebec  
Canada H9X 3R2

An accurate prediction of the return loss of a rectangular horn is of great interest for antenna designers. The E-plane and H-plane horns were studied by many authors but no such study has been reported on rectangular horns with both E-plane and H-plane flares.

This paper describes the theoretical and experimental investigations of a linear single or double tapers connecting waveguide and aperture of arbitrary dimensions and propagating a fundamental mode. The impedances for the tapered waveguide and aperture have been analysed separately. The complex reflection coefficient is calculated from the impedances. The reflection coefficients of the tapered section and aperture of the horn have been added vectorially to get the total reflection coefficient. From the total reflection coefficient, the return loss has been calculated. We have assumed that the aperture of the horn is a rectangular open ended waveguide in the theory to calculate the complex impedance.

A good agreement was found between theoretical and measured return loss of a number of rectangular horns. Horn mismatch arises from the tapered section and from the aperture of the horn. The reflection from the tapered section is small compared to that of the aperture. A detailed description on the theory and experiment will be given at the Conference.

**NEW CLASSES OF HYBRID MODE ANTENNAS-  
ALTERNATIVES TO CORRUGATED HORN FEEDS**

E.Lier  
Electronics Research Laboratory (ELAB)  
Norwegian Institute of Technology (NTH)  
N-7034 Trondheim-NTH, Norway

T.Schaug-Pettersen, J.A.Aas  
Division of Telecommunications  
Norwegian Institute of Technology  
N-7034 Trondheim-NTH, Norway

Until now the corrugated horn antenna has been the most frequently used feed element in reflector antennas where low crosspolarization over a wide frequency band is required, for instance in satellite communication. Drawbacks of this antenna are high production costs and high weight. Therefore there is a need for simpler antenna feeds with the same good electrical performance as that of the corrugated horn antenna.

This paper describes three new patent-applied types of horn antennas. The antennas are characterized by dielectric materials combined with conical horn antennas. They are constructed for supporting the hybrid  $HE_{11}$ -mode under balanced hybrid conditions. Therefore, they will in principle exhibit similar radiation characteristics as the corrugated horn, with low crosspolarization and low sidelobes over a wide frequency band. They are cheaper to fabricate than corrugated horns. This will especially be important at high frequencies (millimeter waves) where corrugated horns become extremely expensive. In addition, one of the horn types will have much lower weight than the corrugated horn. The two other types are filled with dielectric materials. This may cause extra attenuation and noise due to dielectric losses and increases the weight.

The new horn antennas have been measured, with crosspolarization lower than -30 dB for all three types. One of the horns has shown crosspolarization better than -30 dB over more than 40% bandwidth, with sidelobes lower than -26 dB and  $VSWR < 1.2$  over almost the entire band.

Further theoretical and experimental development is needed to optimize the new horn antennas and develop better design tools. The results obtained so far show that these horn antennas are attractive alternatives to the corrugated horn feeds.

COMPACT CORRUGATED POLARISERS FOR DUAL  
FREQUENCY OPERATION

J.M. Rebollar  
Grupo de Electromagnetismo Aplicado  
E.T.S.I. de Telecomunicacion  
Ciudad Universitaria, 28040 Madrid. España

Different E-plane corrugations have been used to design polarisers (e.g. single-depth, dual-depth, etc), due to its robust structure and wide frequency band.

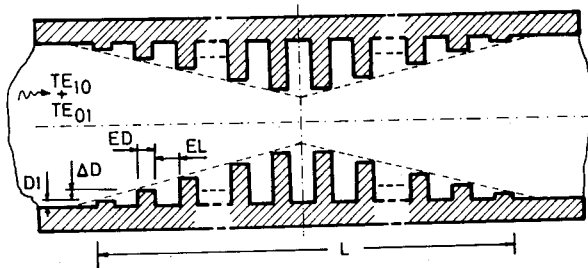
In many applications, often it is not necessary that the polariser work in a continuous wide-band, but it should operate in two or more discrete bands widely separated in frequency.

In this paper we shall present a compact E-plane corrugated square waveguide polariser (figure 1), that can be of interest for dual frequency operation.

An accurate method based on modal Analysis and Scattering Matrix Concept of Discontinuities (H. Patzlet and F. Arndt, IEEE Trans Microw Theory Tech, MTT-30, 771-776, 1982) has been used to calculate the phase and amplitude of the reflection and transmission coefficients of the structure.

Several advantages have been obtained with this polariser. One of them is that it minimizes the reflection of both fundamental modes at the same time, another is that it is shorter than other kind of polarisers for the same allowed magnitude of reflection coefficient, due to the fact that very slow slope is used.

Numerical results for different polarisers will be presented to support the mentioned advantages.



**RADIATION CHARACTERISTICS OF N CIRCULAR  
CONDUCTING CYLINDERS SIMULATING  
CYLINDRICAL REFLECTORS**

*H. A. Ragheb and M. Hamid*

Antenna Lab., Elec. Eng. Dept.  
University of Manitoba  
Winnipeg, Canada, R3T 2N2

*ABSTRACT*

The simulation of conducting scatterers of arbitrary shape by a wire-grid model was introduced by Richmond using the point matching technique (IEEE Trans. Ant. and Prop., AP-14, 6, 782, 1966). In this paper we simulate a cylindrical reflector by circular conducting cylinders of arbitrary number ( $N$ ), radius and distribution along the trajectory of the continuous reflector surface. The resulting radiation pattern of the transmitting reflector is computed as the backscattering pattern of the circular cylinders due to a line source excitation at the center or focal line. The results are compared for large  $N$  with published data for a semi-circular cylindrical reflector by Azarbar and Shafai (IEEE Trans. Ant. and Prop., AP-26, 3, 500, 1978) and a parabolic cylindrical reflector by Kildal (IEEE Trans. Ant. and Prop., AP-32, 6, 541, 1984). It is shown that, contrary to expectation, the gain, beamwidth and level of first and second sidelobes are not necessarily improved by increasing the number of cylinders.

## B-18-9

### PHYSICAL OPTICS ANALYSIS OF NASA/JPL

#### DEEP SPACE NETWORK 70-M ANTENNAS

A. G. CHA

JET PROPULSION LABORATORY, PASADENA, CA

This paper summarizes the RF analysis and performance of the NASA/JPL Deep Space Network (DSN) 70-m shaped dual reflector antenna, using physical optics. This very high gain and ultra low noise antenna (25 K at X-band and 22 K at S-band, at 30° elevation angle) will be operational in time to support the Voyager spacecraft encounter with Neptune in 1989. This antenna is based on a dual shaped reflector design invented by P. D. Potter.

The salient feature of the 70-m antenna RF analysis is the use of a more rigorous and hence presumably more accurate near field approach as compared to the simpler conventional far field analysis approach used in most previous ground station antennas. By way of an example, the 70-m antenna S-band system noise temperature is 22.7 K and 21.3 K, respectively, based on far field and near field analysis. The difference of 1.4 K corresponds to 0.28 dB in system (G/T) performance in this ultra low noise receive system. We will also discuss the ray optics and diffraction characteristics of the high efficiency dual shaped reflector, which are very different from the familiar paraboloid/hyperboloid design. As a result of Potter's work and recent researches at JPL funded by NASA, a much better understanding of the dual shaped reflector characteristics and performance has been acquired.

## FOCAL SHIFTS IN PARABOLIC REFLECTORS

Hao Ling

Electromagnetics Laboratory  
Department of Electrical and Computer Engineering  
University of Illinois  
1406 W. Green Street  
Urbana, IL 61801

## ABSTRACT

Given a parabolic reflector, the maximum directivity is not always achieved by placing the feed at the focal point. Depending on the nature of the feed, the maximum directivity can be obtained by axially displacing the feed either toward or away from the reflector. For low-tapered feeds, the shift should be toward the reflector. This result is similar to an optical phenomenon called the focal shift. We find that this positive shift depends mainly on the Fresnel number of the reflector. For highly tapered feeds, the shift should be away from the reflector. This negative shift becomes significant when the reflector aperture is small, in units of wavelength. A unified view is presented to explain both the positive shift and the negative shift in terms of spillover, aperture illumination efficiency and phase asynchronism. For a system with optimum aperture edge taper, no focal shift can exist.



## URSI COMMISSION B - SESSION B19

Electromagnetic Fields II

1:30 - 5:00  
IRC-4

Champs électromagnétiques II

Chairperson/Président: **D.L. Sengupta**, University of Michigan, Ann Arbor, MI, USA

- 1 CURRENTS INDUCED ON UNINSULATED WIRES WITH FINITE CONDUCTIVITY. **G.C. Sherman, J.L. Gilbert**, Mission Research Corporation, Santa Barbara, CA, USA
- 2 COMPUTATION OF THE NEAR FIELD OF AN INSULATED DIPOLE IN A DISSIPATIVE DIELECTRIC MEDIUM. **J.P. Casey**, Department of the Navy, Naval Underwater Systems Center, New London, CT, USA; **R. Bansal**, University of Connecticut, Dept. of Electrical Engineering and Computer Science, Storrs, CT, USA
- 3 QUANTIFICATION OF INDUCED EM FIELDS IN FINITE HETEROGENEOUS BODIES. **H. Wang, Y.Q. Liang, K.M. Chen**, Michigan State University, Dept. of Electrical Engineering and Systems Science, East Lansing, MI, USA
- 4 INTERACTION OF ELF ELECTROMAGNETIC FIELDS WITH HUMAN BODY. **H.R. Chuang, K.M. Chen**, Michigan State University, Dept. of Electrical Engineering and Systems Science, East Lansing, MI, USA; **C.J. Lin**, University of Detroit, Dept. of Electrical Engineering, Detroit, MI, USA
- 5 THE FIELDS OF A POINT SOURCE RADIATING IN THE PRESENCE OF A LAYERED CYLINDRICAL OBSTACLE. **L.W. Pearson**, McDonnell Douglas Research Laboratories, St. Louis, MO, USA
- 6 ALTERNATIVE SOURCE-FIELD RELATIONS. **P.E. Mayes**, University of Illinois, Dept. of Electrical and Computer Engineering, Urbana, IL, USA
- 7 SPATIAL E-WAVE AND H-WAVE PROPAGATION. **M.R. Havey, T. Koryu Ishii**, Marquette University, Dept. of Electrical Engineering and Computer Science, Milwaukee, WI, USA
- 8 A "LATERALLY INHIBITED" ARRAY ANTENNA FOR LOCATING SOURCES. **S.S. Sandler**, Northeastern University, Dept. of Electrical and Computer Engineering, Boston, MA, USA
- 9 THREE-DIMENSIONAL SCATTERING FROM ANISOTROPIC STRUCTURES. **R.D. Graglia**, Politecnico di Torino, CESPA, Torino, Italy.; **P.L.E. Uslenghi**, University of Illinois at Chicago, Dept. of Electrical Engineering and Computer Science, Chicago, IL, USA

## B-19-1

### CURRENTS INDUCED ON UNINSULATED WIRES WITH FINITE CONDUCTIVITY

George C. Sherman and James L. Gilbert  
Mission Research Corporation  
P.O. Drawer 719  
Santa Barbara, CA 93102

Calculations of the response of very long buried and elevated cables to a localized electromagnetic source have generally been performed using transmission-line theory. That theory is useful when the response is dominated by an approximately TEM mode. Although an uninsulated wire supports such a mode, it is very difficult to excite. Other waves may dominate the response, invalidating the application of transmission-line theory.

This study analyzes the response of an infinitely long, uninsulated wire with finite conductivity in a homogeneous material to a monochromatic voltage-generating source localized near the wire. The mathematical approach is similar to that used in the theory of perfectly conducting long wire antennas, but the analysis and results are changed significantly by the presence of finite wire conductivity. Using Fourier techniques, an exact integral representation of the current induced on the wire is obtained by solving the full electromagnetic scattering problem. The integral is then expressed using contour integration as the sum of pole residues and an integral around a branch cut. The residues represent the contributions of TM modes of the wire. All of these modes damp out immediately except one, known as the principal mode. The principal mode is approximately TEM and hence can be treated by transmission-line theory. The branch-cut integral represents the contribution of an electromagnetic wave (known as a space wave) that radiates out into space. The space-wave can not be treated by standard transmission-line theory.

Numerical comparison of the magnitudes of the space-wave and the principal-mode contributions to the current for representative frequencies and wire resistances shows that the wire response is totally dominated by the space wave. Hence, standard transmission-line theory is not useful. Moreover, the results show that theory based on a perfect-conductor model of the wire is not very useful either. The current in the resistive wire is reduced by a substantial amount (from the perfect-conductor result) that is nearly independent of distance from the source over a very long range along the wire. An analytical approximation for the magnitude of this effect is obtained.

COMPUTATION OF THE NEAR FIELD OF AN INSULATED DIPOLE IN A  
DISSIPATIVE DIELECTRIC MEDIUM

John P. Casey

Naval Underwater Systems Center, New London, CT 06320  
and

Rajeev Bansal

Department of Electrical Engineering and Computer Science  
The University of Connecticut, Storrs, CT 06268

The near field of an insulated dipole antenna in a dissipative dielectric medium is important in microwave hyperthermia and geophysical applications. In this paper the electric field near an insulated dipole has been calculated by the direct numerical evaluation of a surface integral over the insulation. The computed results are compared with those previously obtained by an approximate numerical calculation (King et al., IEEE Trans., MTT-31, July 83). Both approaches produce identical results far away from the insulation. However, in the vicinity of the insulation, the approximations utilized by King et al. are found to be inadequate as indicated by figure 1.

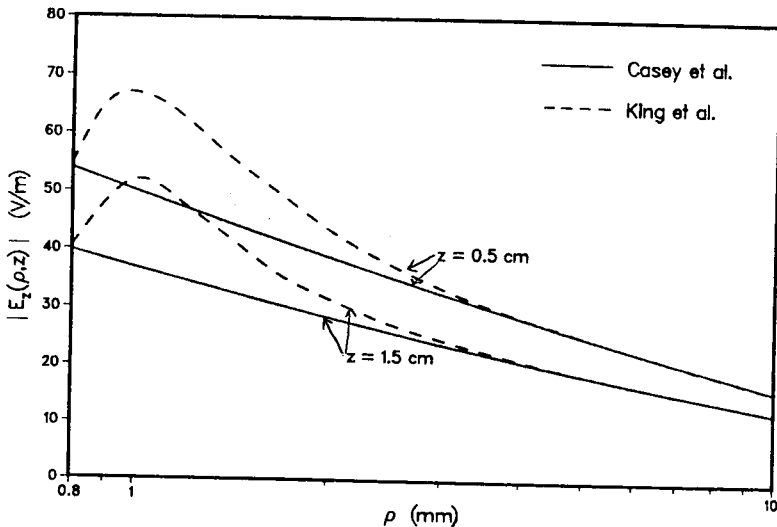


Figure 1. Magnitude of axial electric field in muscle tissue ( $\epsilon_r = 42.5$ ,  $\sigma = 0.88$  mho/m) for an air insulated dipole (half length  $h = 3.1$  cm, insulation radius  $c = 0.8$  mm).

QUANTIFICATION OF INDUCED EM FIELDS  
IN FINITE HETEROGENEOUS BODIES

H. Wang, Y.Q. Liang and K.M. Chen  
Department of Electrical Engineering and System Science  
Michigan State University, E. Lansing, MI 48824

A numerical method for quantifying the interaction between an EM field and a finite, heterogeneous body is investigated. Chen (Research Topics in EM Wave Theory, John Wiley and Sons, 1981) has derived a set of coupled integral equations to express the induced electric field  $\vec{E}$  and the induced magnetic field  $\vec{H}$  inside the body, with arbitrary parameters  $\epsilon(\vec{r})$ ,  $\mu(\vec{r})$  and  $\sigma(\vec{r})$ , in terms of the incident electric field  $\vec{E}^i$  and the incident magnetic field  $\vec{H}^i$ . Recently, we have decoupled this set of coupled integral equations into a separate electric field integral equation (EFIE) for  $\vec{E}$  in terms of  $\vec{E}^i$  and a separate magnetic field integral equation (MFIE) for  $\vec{H}$  in terms of  $\vec{H}^i$ . Advantages and disadvantages for using the coupled integral equations or the separate integral equations are being investigated.

One approach seems to provide advantage in the numerical calculation. This approach is explained as follows. When the body is illuminated by an incident EM wave, the induced electric field inside the body can be divided into the electric mode with a linear type of electric field and the magnetic mode with a circulatory type of electric field. The linear electric mode can be numerically determined without difficulty, but the numerical calculation of the circulatory magnetic mode encounters slow convergence. To overcome this difficulty, the problem is divided into the electric and magnetic modes first. The electric mode is determined with the EFIE in terms of the electric field. The magnetic mode is solved with the MFIE in terms of the magnetic field which is now linear in nature, thus avoiding the slow convergence. After the determination of the magnetic mode, the corresponding electric field is found from the obtained magnetic field using the Maxwell's equation. The total induced electric field is obtained by combining the electric fields of the electric and magnetic modes.

INTERACTION OF ELF ELECTROMAGNETIC FIELDS WITH HUMAN BODY

H.R. Chuang Department of Electrical Engineering  
 and Systems Science  
 K.M. Chen Michigan State University, E. Lansing, MI 48824

C.J. Lin Department of Electrical Engineering  
 University of Detroit, Detroit, MI 48221

The present study develops a numerical method to quantify the interaction of ELF EM fields with human body based on a realistic model of the body situated in a realistic environment. Consider a geometry of a human body standing on the ground being exposed to an ELF electric field of angular frequency  $\omega$ . The contact between the feet (or a part of the body) and the ground is represented by a grounding impedance  $Z$ . Due to the nature of ELF EM fields, the impressed electric field on the body can be assumed to be locally uniform, and the body is assumed to be equi-potential. The ground effect can be taken into account by the method of image. The analysis is simplified by using the quasi-static approximation.

To analyze the problem, the induced surface charge on the body is determined first. The body surface is divided into  $N$  subareas and the induced surface charge  $\eta_n(\vec{r})$  on each subarea  $\Delta S_n$  is assumed to be a unknown constant. The induced equi-potential of the body is assumed to be  $\phi_b$ . The impressed potential on the body at the location of  $\Delta S_n$  is assumed to be  $\phi_{on}$  which is a given quantity. The unknown induced surface charge  $\eta_n$  and the unknown body potential  $\phi_b$  can be determined from the following matrix equation:

$$\begin{bmatrix} M_{11} & M_{12} & \dots & M_{1N} & -1 \\ & & \dots & & \\ M_{N1} & M_{N2} & \dots & M_{NN} & -1 \\ \Delta S_1 & \Delta S_2 & \dots & \Delta S_N & \frac{-i2}{\omega Z} \end{bmatrix} \begin{bmatrix} \eta_1 \\ \vdots \\ \eta_N \\ \phi_b \end{bmatrix} = - \begin{bmatrix} \phi_{o1} \\ \vdots \\ \phi_{oN} \\ 0 \end{bmatrix}$$

where the matrix element  $M_{nm}$  represents the potential at  $\Delta S_n$  due to the induced surface charge  $\eta_m$  at  $\Delta S_m$ . After the induced surface charge is determined, the induced current and electric field inside the body can be quantified.

The validity of the method was checked by first applying it to the idealized bodies of sphere and spheroid. After that it was applied to a realistic model of human body with various body positions and various grounding impedances. The following results are of particular interest: (1) induced surface charge and electric field enhancement factor, (2) short circuit currents for various grounding impedances, including resistive, capacitive and inductive, and (3) induced current density and electric field inside the body.

THE FIELDS OF A POINT SOURCE RADIATING  
IN THE PRESENCE OF A LAYERED CYLINDRICAL OBSTACLE

L. Wilson Pearson  
McDonnell Douglas Research Laboratories  
P. O. Box 516  
St. Louis, MO 63166

The electromagnetic fields of time-harmonic point sources of z-directed electric and magnetic currents are constructed. The source fields are represented by way of the characteristic Green's function method so that the angular propagation regime (creeping wave) is directly revealed. The source fields are augmented with a homogeneous solution that accounts for the layered obstacle. The vehicle of electric and magnetic vector potentials is used in calculating the homogeneous solution and leads to a partitioning of the fields into a superposition of fields that are transverse magnetic (TM) and transverse electric (TE) to the axial direction. The resulting fields in each layer are characterized by four scalar constants.

Because of the axial variation of the fields, the TE and TM fields are coupled at interfaces separating materials of differing constitutive parameters. This coupling can be represented in terms of four-by-four transmission matrices, the cascade of which accounts for multiple layers. The elements of the matrices comprise Hankel functions whose arguments are dependent on the wave numbers of the layers and radii at the interfaces. The zeros of this matrix with respect to the (complex) order of the Hankel functions are shown to yield the angular propagation wave numbers for creeping waves on this structure. It appears feasible to determine these wave numbers numerically.

**ALTERNATIVE SOURCE-FIELD RELATIONS**

Paul E. Mayes  
Electromagnetics Laboratory  
Department of Electrical and Computer Engineering  
University of Illinois  
Urbana, Illinois 61801

Paper moved to AP-S Session 2/  
La communication présenté dans la section AP-S Session 2

**SPATIAL E-WAVE AND H-WAVE PROPAGATION**

Michael R. Havey and T. Koryu Ishii  
Department of Electrical Engineering and Computer Science  
Marquette University  
1515 W. Wisconsin Avenue  
Milwaukee, Wisconsin 53233 U.S.A.

Propagation supporting characteristics of open space for TEM waves are well known, yet, when the open space is excited by either E-waves or H-waves, the behavior of the open space against these waves is little known or documented. In this paper Maxwell's equations are solved in open space for non-TEM wave excitation. The E-waves or H-waves are launched into the space and the propagation support characteristics are studied. The items studied are the impedance and admittance of the space per unit distance of propagation, propagation constant, attenuation constant, phase constant, wave impedance, wavelength and the phase velocity of the propagation.

For E-wave propagation, when compared with the conventional TEM-wave propagation, the impedance per unit distance of propagation is decreased by a factor of the square of the launching parameter and admittance per unit distance of propagation is unchanged, the propagation constant is decreased by a factor of the launching parameter and so are the attenuation constant and the phase constant. Therefore the phase velocity of the propagation increases by the factor of the reciprocal of the launching parameter and the wave impedance decreases by a factor of the square of the launching parameter. The wavelength is longer by the factor of reciprocal of the launching parameter.

For H-wave propagation, when compared with the TEM-wave propagation, the attenuation constant and the phase constant and the propagation constant decrease by a factor of the launching parameter, the impedance of the space per unit distance of propagation is unchanged and the admittance per unit distance of propagation decreased by a factor of square of the launching parameter. The wave impedance increases by a factor of the reciprocal of the launching parameter and so are the phase velocity of propagation and the wavelength.

The launching parameter is a function of the scheme of the launching mechanism of the waves to the open space. In both E- or H-waves in open space, the wavelength is longer, the phase velocity is higher, the attenuation constant and phase constant are smaller and the wave impedance is higher than those for the TEM-wave propagation at the same frequency.

A "LATERALLY INHIBITED" ARRAY  
ANTENNA FOR LOCATING SOURCES

Sheldon S. Sandler  
Department of Electrical  
and Computer Engineering  
Northeastern University  
Boston, MA 02115

This research concerns the application of physiological vision concepts to antenna arrays. The area investigated was the use of lateral inhibition for analysing the field received by an antenna array.

Lateral inhibition appears early in visual processing to efficiently encode a scene. A retinal cell is surrounded by other cells which through lateral connections inhibit the output of the central cells. The lateral inhibition mechanism is also an efficient way of detecting changes in a visual scene, particularly edges. Conversely, when retinal cells are exposed to uniform scene segments, the mechanism only produces small changes.

Image intensives of a visual scene are analogous to either the amplitude or phase of an electromagnetic field quantity. Edges of a visual scene are also analogous to rapid changes in field amplitude or phase. Based on these analogies, a "laterally inhibited" antenna array has been devised to locate sources and to analyse the received field.

THREE-DIMENSIONAL SCATTERING FROM  
ANISOTROPIC STRUCTURES

R. D. Graglia  
CESPA, Politecnico di Torino, Italy  
and

P. L. E. Uslenghi  
Department of Electrical Engineering and Computer Science  
University of Illinois at Chicago

A three-dimensional scatterer characterized by a complex electric susceptibility tensor  $\underline{\epsilon}_{ec}$  and a magnetic susceptibility tensor  $\underline{\chi}_m$  is considered. The integro-differential equations for the unknown electric and magnetic fields previously given by the authors (Graglia and Uslenghi, National Radio Science Meeting, Houston, Texas, May 1983; IEEE Trans. AP, vol. 32, p. 867, August 1984) are solved numerically, by extending to three dimensions the work previously carried out for two-dimensional problems (Graglia and Uslenghi, National Radio Science Meeting, Boston, Massachusetts, June 1984; *ibid.*, 1984 AP Symposium Digest, p. 367).

The three-dimensional computer code is tested on a variety of shapes and materials. Extensive results are shown for anisotropic spheres in free space, for anisotropic spherical shells, and for metallic spheres coated by a layer of anisotropic material; in these examples, different forms for the susceptibility tensors are considered.

## URSI COMMISSION B - SESSION B20

## Antenna Theory

8:30 - 12:00  
IRC-2

## Théorie des antennes

Chairperson/Président: **L. Shafai**, University of Manitoba, Winnipeg, MB

- 1 ON SIDELOBE REDUCTION IN LINEAR ARRAYS USING RANDOM PHASE. **D.G. Dudley**, University of Arizona, Dept. of Electrical and Computer Engineering, Tucson, AZ, USA
- 2 GTD ANALYSIS OF THE COUPLING BETWEEN TWO SLOTS SEPARATED BY AN IMPEDANCE PATCH ON A GROUND PLANE. **R. Tiberio, G. Pelosi, G. Manara**, University of Florence, Dipto. Ingegneria Elettronica, Florence, Italy; **P.H. Pathak, R. Rojas**, Ohio State University ElectroScience Laboratory, Columbus, OH, USA
- 3 A NEARLY FREQUENCY-INDEPENDENT SIDELOBE SUPPRESSION TECHNIQUE FOR PHASED ARRAYS. **G. Monser**, Raytheon Company, Goleta, CA, USA
- 4 NON-UNIFORMLY SPACED ELEMENTS LINEAR ARRAYS WITH WEIGHTED SYNTHESIS ERROR. **D.C. Patel**, University of Surrey, Dept. of Electronic and Electrical Engineering, Guildford, UK
- 5 DESIGN OF A HORIZONTALLY-POLARIZED CIRCULAR ARRAY. **M.R. Schrote**, Westinghouse Defense and Electronic Center, Advanced Development Division, Baltimore, MD, USA
- 6 SURFACE WAVE DIFFRACTION BY A TRUNCATED INHOMOGENEOUS DIELECTRIC SLAB RECESSED IN A CONDUCTING SURFACE. **C.W. Chuang**, Ohio State University ElectroScience Laboratory, Dept. of Electrical Engineering, Columbus, OH, USA
- 7 IMPEDANCE LOADING TECHNIQUE REVISITED. **J.L. Lin, S.A. Haberman**, Boeing Aerospace Company, Electromagnetic Technology, Seattle, WA, USA
- 8 VEHICULAR ANTENNA CONCEPTS FOR LAND MOBILE SATELLITE COMMUNICATION. **L. Shafai, G.B. Neilson**, University of Manitoba, Dept. of Electrical Engineering, Winnipeg, MB
- 9 THE USE OF OPTIMIZATION TECHNIQUES IN COMPUTER-AIDED-DESIGN OF ANTENNAS. **G.B. Neilson, M.A. Barakat**, National Research Council, Winnipeg, MB; **L. Shafai**, University of Manitoba, Dept. of Electrical Engineering, Winnipeg, MB
- 10 EFFECT OF TROPOSPHERIC REFRACTION ON THE PERFORMANCE OF ADAPTIVE ARRAYS. **H.M. Ibrahim**, Assiut University, Electrical Dept., Assiut, Egypt

ON SIDELOBE REDUCTION IN LINEAR ARRAYS  
USING RANDOM PHASE

D. G. Dudley  
Electromagnetics Laboratory  
Department of Electrical and Computer Engineering  
University of Arizona  
Tucson, AZ 85721 USA

In linear array design, the desired sidelobe level is normally obtained by selection of the amplitude distribution from well-known families, such as the Taylor distributions. In some applications, however, it could be desirable to have a uniform distribution in one operational mode and a tapered distribution in another. If the main beam is positioned electronically with phase shifters, it is possible to obtain a reduction in sidelobe level by suitable adjustment of the phase shifters. Indeed, it has been recently proposed (Guo, Y. C. and M. S. Smith, Proc. IEE, v130, pt. H, pp. 343-357, 1983) that this be done with random settings of one-bit or two-bit phase shifters.

In this paper, we explore limitations in sidelobe reduction using random phase. We define a stochastic process, consisting of the difference between the resulting array factor and the desired array factor. Using the central limit theorem, we show that the probability density function of the process real and imaginary parts approaches bivariate Gaussian in the limit as the number of array elements increases. In the sidelobe region, the density of the process magnitude, to an excellent approximation, is Rayleigh, with the approximation exact at the nulls of the desired pattern and in the limit as the normalized angle variable becomes large.

We investigate the applicability of the ergodic hypothesis for equating array ensemble averages and angle variable averages for a single ensemble member. We compare results with computer Monte Carlo experiments. We confirm limitations found in the specific cases investigated by Guo and Smith and also conclude that the limitations are fundamental for this class of problems.

GTD ANALYSIS OF THE COUPLING BETWEEN TWO SLOTS SEPARATED BY AN  
IMPEDANCE PATCH ON A GROUND PLANE

R. Tiberio (\*), G. Pelosi, G. Manara  
Dipartimento Ingegneria Elettronica, University of Florence  
Florence, Italy

and

P. H. Pathak, R. Rojas

(\*) The ElectroScience Laboratory, The Ohio State University  
Columbus, Ohio, USA

In designing conformal arrays, an accurate control of the coupling among the radiating elements is of importance. To this end the separation between two adjacent elements of the array may be properly adjusted and patches of non perfectly conducting materials may be also interposed. A useful canonical problem for a GTD analysis of these configurations is that of the coupling between two line sources on a ground plane separated by a surface impedance strip. In this paper a uniform GTD (UTD) formulation is employed for the diffraction at the edge of a surface impedance discontinuity which is derived from exact integral representations obtained both by Maliuzhinets and by a Wiener-Hopf technique. This high-frequency solution together with a spectral extension of this method provide an efficient tool for a parametric study of this canonical problem.

In a previous paper (Tiberio and Pelosi, IEEE Trans. AP-31, No. 4, pp. 590-596, 1983) a uniform solution was presented for the high-frequency scattering from an impedance strip on a ground plane, illuminated by a plane wave. By employing the plane wave spectrum representation of a line source and by analogy with the UTD formulation for the diffraction at edges in perfectly conducting surfaces, the distance parameters involved in that solution are suitably modified to treat the example considered here. Contributions from the fields of doubly and triply diffracted rays are included in the present analysis. Diffracted field contributions from surface waves are also accounted for, when they are excited at the edges of the impedance strip.

Several numerical results are presented and their accuracy is demonstrated in some examples by comparison with a moment method solution.

A NEARLY FREQUENCY-INDEPENDENT  
SIDELOBE SUPPRESSION TECHNIQUE  
FOR PHASED ARRAYS

George Monser  
Raytheon Company  
P.O. Box 1542  
Goleta, CA 93117

A nearly frequency-independent technique for lowering sidelobes in receive phased-array applications is described. Using phase-matched, broadband attenuators with each array element, the signal outputs are modified to approximate the prescribed illumination. Several illumination functions were then modeled to show sidelobe and beam efficiency trade-offs. Test results for two short, lens-fed, linear arrays ( $N < 20$ ) are included and compared to predicted values. Sidelobes are shown to compare favorably with predicted values (within 1 to 3 dB). Measured efficiencies agreed within 1 to 2 dB to the computed values.

NON-UNIFORMLY SPACED ELEMENTS LINEAR  
ARRAYS WITH WEIGHTED SYNTHESIS ERROR

D.C. Patel  
Department of Electronic and Electrical Engineering  
University of Surrey  
Guildford, GU2 5XH, U.K.

Low sidelobe levels, beamwidth and broad band performance are important characteristics of radiation pattern of an antenna array. Several methods are available to calculate the excitation coefficients of elements for uniformly spaced elements linear arrays; but the problem becomes highly non-linear for non-uniformly spaced elements and analytical solutions in closed form are difficult. Iterative numerical procedures to minimise the error in  $m$ -directions between the computed pattern and the specified pattern have been used to design non-uniformly spaced elements arrays.

A relevant technique for design of non-uniformly spaced elements linear arrays is to apply optimising numerical procedures to minimise errors in a formulation which uses a weighing function between the computed and specified patterns. Results of design of symmetrical linear array using above method for different weighing functions and average inter-element spacing of  $\lambda/2$  and  $2\lambda$ , where  $\lambda$  is the wavelength, have been determined and will be presented.

## B-20-5

### DESIGN OF A HORIZONTALLY-POLARIZED CIRCULAR ARRAY

M. R. Schrote  
Westinghouse Defense and Electronic Center  
Advanced Development Division  
P.O. Box 746, MS-333  
Baltimore, MD 21203

Scanning circular antenna arrays have an inherent advantage over scanning linear arrays in that in a circular array, beam steering in azimuth can be achieved simply by shifting the beamforming weights. Therefore, unlike linear arrays, the antenna pattern of a circular array is not a function of the azimuth beam steering angle. This characteristic applies equally to arc arrays in which circular arrays have been sectored into arcs and beam steering is achieved by weighting the elements of the appropriate arc segment. In addition, by exciting different arcs of the circular array independently, multiple beams may be formed. Other authors have shown that a properly designed arc array is capable of performance nearly as good as a circular array.

This paper describes the design of a horizontally-polarized circular array which has been sectored into three 120 degree arcs. By exciting each arc independently, three main beams are formed. The circular array itself is made up of thirty-three horizontal dipoles which are backed by a parasitic reflector dipole. The element weighting in each of the three 11-element arcs are Chebyshev weights. An additional phase shift is added to each element to cause the pattern of each radiating element in a particular arc to add in phase in the direction normal to that arc.

Prior to any hardware being built, the antenna array was first simulated using a Method of Moments (MM) computer code. Using the MM code, tradeoffs in the design of the circular array were studied rather quickly and inexpensively. In addition, the MM code was used to correct for the mutual coupling effects.

Lastly, patterns measured from the actual hardware are compared to the MM simulations.

SURFACE WAVE DIFFRACTION BY A TRUNCATED INHOMOGENEOUS  
DIELECTRIC SLAB RECESSED IN A CONDUCTING SURFACE

C. W. Chuang

The Ohio State University ElectroScience Laboratory  
Department of Electrical Engineering  
Columbus, Ohio 43212

The study of surface wave diffraction by a truncated dielectric slab recessed in a perfectly conducting surface is of importance in designing flush-mounted dielectric covered antennas. The incident surface wave gives rise to waves diffracted and reflected by the junction at the termination of the dielectric. A strong reflected surface wave is undesirable in certain situations in that it may cause a problem in matching antenna impedances. One way to reduce the surface wave reflection is to use an inhomogeneous dielectric near the junction. If the inhomogeneous dielectric near the junction is lossy, a substantial reduction in the surface wave reflection can be achieved as demonstrated in the present study. Because of the added complexity by including inhomogeneous dielectrics, this diffraction problem is solved using an integral equation numerical approach.

**IMPEDANCE LOADING TECHNIQUE REVISITED****JUANG LU LIN and SCOTT A. HABERMAN**

Electromagnetic Technology  
Boeing Aerospace Company  
P.O. Box 3999, Mail Stop 3A-04  
Seattle, Washington 98124

Impedance loading technique has proven effective in modifying the amplitude and phase of the induced current on a metallic object. This technique is, in turn, applied to the parasitic elements of an array for a desirable transmitting pattern; to a small probe for field or antenna measurements; to a thin and long metallic body for the scattering cross section modifications (K.M. Chen, IEEE Trans. on Antennas and Propagation, AP-14, May 1966; W.P. Hansen, Symposium Record, AF Cambridge Res. Lab., Bedford, MA, Sept. 1964).

A new approach heavily depending on the well-developed numerical technique such as a moment methods was developed to modify the bistatic scattering cross sections of a metallic object illuminated by a plane electromagnetic wave at an arbitrary incidence. As a verification, the case investigated by Chen and Hansen was used and the results were compared. In the course of the comparison, we found that the optimum impedances computed by Chen and measured by Hansen were quite different from our computation. Subsequently, a test body was constructed and a built-in circuitry in the body was implemented to provide the required impedances. A fibre optics cable links the control box and impedance circuit to minimize the inadvertent electromagnetic interference to the metallic body. The computations on the backscattering cross sections are verified by the measurement on the metallic body alone; and on the metallic body with loading. The computed value of optimum impedance is also verified by the measurement.

VEHICULAR ANTENNA CONCEPTS FOR  
LAND MOBILE SATELLITE COMMUNICATION

L. Shafai and G.B. Neilson  
Department of Electrical Engineering  
University of Manitoba  
Winnipeg, Manitoba  
Canada R3T 2N2

Circularly polarized vehicular antennas with  $4\text{dB}_i$  and  $8\text{dB}_i$  gains have been considered for the Canadian coverage zone which falls between  $10^\circ$  to  $50^\circ$  elevation angles. Tentative coverage bands are 821-825 MHz for the downlink and 866-896 MHz for the uplink. For  $4\text{dB}_i$  gain, antennas with omnidirectional azimuth patterns can meet the requirements and several candidates have already been developed. However, higher gains of about  $8\text{dB}_i$  or more cannot be achieved with single antennas of acceptable geometrics for vehicular applications, and an array configuration must be used. To date, attention has focussed mainly on the planar arrays with a beam steering capability. Microstrip antennas have been considered for the array elements, to provide a low cost conformal geometry. The beam scanning is normally achieved using the standard phase shift technology.

The planar array with a beam scanning in azimuth requires a moderately large beam forming network which increases the cost and demands a beacon satellite signal. The coverage requirements may also be met by arrays with omnidirectional patterns, scanning only in the elevation. Such antennas may be adequate for initial phase of the MSAT program, and require a relatively simple beam forming network to achieve the elevation scan. Research is being conducted to develop array configurations and elements for such applications. Their performance and potential for MSAT application will be discussed and compared with the azimuth scanning systems.

## B-20-9

### THE USE OF OPTIMIZATION TECHNIQUES IN COMPUTER-AIDED-DESIGN OF ANTENNAS.

G.B. Neilson, M.A. Barakat  
National Research Council  
214-155 Carleton Street  
Winnipeg, Manitoba, R3C 3H8

L. Shafai  
Department of Electrical Engineering  
University of Manitoba  
Winnipeg, Manitoba, R3T 2N2

Computer simulation using various well-developed numerical analysis routines is an important method of antenna design. The purpose of this paper is to describe how one analysis routine, along with certain optimization techniques can be applied to a practical design situation.

So far, the mathematical basis for the analysis routine has been the moment method, using the Electric Field Integral Equation (EFIE). Rosenbrock's multi-variate minimization algorithm for optimization is used and will be described, along with the considerations for an object function to be minimized.

These techniques have been applied to the design of simple antenna elements for use in the MSAT mobile communications system. The design considerations are included as a set of constraint equations combining with some geometric constraints to form the minimization object function. A turn-key graphics system is used to display antenna geometry and pattern plots, allowing for visual verification by the designer, and providing a method to visually modify the antenna geometry if desired.

The creation of this CAD environment and the judicious application of optimization techniques can lead to the efficient design of antennas. Numerical techniques, because of their flexibility, can be applied to virtually any design situation and can help reduce the emphasis placed on the traditional experimental methods.

EFFECT OF TROPOSPHERIC REFRACTION ON THE PERFORMANCE OF  
ADAPTIVE ARRAYS

Hasny M. Ibrahim

College of Engineering , Electrical Dept.  
Assiut University, Assiut, Egypt

Adaptive antenna arrays have found widespread use in satellite and airborne communications. However, signals utilized in these applications travel a long path through the troposphere before they are received by an adaptive array . The adaptive nulling of jamming or interference signals in these conditions depends mainly on the exact knowledge of the angles of arrival of these signals . Tropospheric refraction will cause these angles to change diurnally according to the state of the troposphere . The well known 4/3- earth radius is usually used to account for standard atmospheric refractions . However, the standard atmospheric conditions prevails only during a short period of the diurnal cycle .

The signal to interference plus noise ratio (SINR) is the most commonly accepted criterion for the study of the steady state performance of an adaptive array and it will be utilized in the present analysis . The degradation in the SINR of a 3-element Applebaum - type adaptive array due to atmospheric refraction is presented . Three atmospheric periods namely; standard, cooling, and heating are considered together with their corresponding SINR. The analysis indicates that the tropospheric refraction is an important factor that has to be taken into account in the design of adaptive arrays .



## URSI COMMISSION B - SESSION B21

Inverse and Multiple  
Scattering

8:30 - 12:00

IRC-3

Diffusion inverse  
et multipleChairperson/Président: **W.-M. Boerner**, University of Illinois, Chicago, IL, USA

- 1 AN INVERSE TRANSMISSION PROBLEM FOR THE HELMHOLTZ EQUATION. **T.S. Angell, R.E. Kleinman**, University of Delaware, Dept. of Mathematical Sciences, Newark, DE, USA; **G.F. Roach**, University of Strathclyde, Dept. of Mathematics, Glasgow, UK
- 2 INVERSE SOLUTION FOR A SLAB OF RANDOM DIELECTRIC DISCS: ORIENTATION AND AREA DISTRIBUTIONS. **R.H. Lang, H.A. Saleh**, George Washington University, Dept. of Electrical Engineering and Computer Science, Washington, DC, USA
- 3 SIGNAL FLOW GRAPHS FOR WAVE PROPAGATION IN INHOMOGENEOUS LOSSY MEDIA. **C.Q. Lee**, University of Illinois at Chicago, Dept. of Electrical Engineering, Chicago, IL, USA
- 4 A VALIDATION ANALYSIS OF THE TARGET-DESCRIPTOR INTERPRETATIONS OF THE MUELLER MATRIX ELEMENTS IN POLARIMETRIC RADAR RETURNS WITH THE KENNAUGH'S PHYSICAL OPTICS IMPULSE RESPONSE FORMULATION. **S.K. Chaudhuri**, University of Waterloo, Dept. of Electrical Engineering, Waterloo, ON; **B.-Y. Foo, W.-M. Boerner**, University of Illinois at Chicago, Dept. of Electrical Engineering and Computer Science, Chicago, IL, USA
- 5 BASIC PROPERTIES OF THE BI-STATIC RADAR TARGET SCATTERING MATRIX. **A.B. Kostinski, W.-M. Boerner**, University of Illinois at Chicago, Dept. of Electrical Engineering and Computer Science, Chicago, IL, USA
- 6 MODULATION TRANSFER FUNCTION AND IMAGE TRANSMISSION THROUGH RANDOMLY DISTRIBUTED SPHERICAL PARTICLES. **Y. Kuga, A. Ishimaru**, University of Washington, Dept. of Electrical Engineering, Seattle, WA, USA
- 7 OPTICAL BEAM PROPAGATION IN RANDOM MEDIA BASED ON RADIATIVE TRANSFER THEORY. **H-W. Chang, A. Ishimaru**, University of Washington, Dept. of Electrical Engineering, Seattle, WA, USA
- 8 THE EFFECTIVE CONSTITUTIVE PARAMETERS OF A FOREST. **M. Abouzahra, L. Lewin, H.X. Lian**, University of Colorado, Dept. of Electrical and Computer Engineering, Boulder, CO, USA
- 9 GEOMETRIC OPTICS IN INHOMOGENEOUS NONSTATIONARY MEDIA WITH SPATIAL AND TEMPORAL DISPERSION. **K. Suchy**, University of Düsseldorf, Institute for Theoretical Physics, Düsseldorf, FRG
- 10 BACKSCATTERING CROSS-SECTION OF N PARALLEL CONDUCTING CIRCULAR CYLINDERS. **H.A. Ragheb, M. Hamid**, University of Manitoba, Dept. of Electrical Engineering, Winnipeg, MB

## B-21-1

### AN INVERSE TRANSMISSION PROBLEM FOR THE HELMHOLTZ EQUATION

T. S. Angell and R. E. Kleinman  
Department of Mathematical Sciences  
University of Delaware  
Newark, DE 19716, U.S.A.

G. F. Roach  
Department of Mathematics  
University of Strathclyde  
Glasgow G1 1XH, Scotland

The problem of determining the shape of a homogeneous bounded penetrable object from a knowledge of the scattered far field (or some functional of the far field such as scattering cross section) due to a known incident field is considered. This inverse transmission problem is reformulated as an optimization problem, specifically, finding the surface in a suitably restricted class of admissible surfaces which minimizes an appropriate functional of the far field generated by the surface through the solution of the direct transmission problem. The admissible surfaces are characterized as smooth deformations of a sphere. Starting with a boundary integral equation formulation of the direct problem this is recast as an integral equation over a sphere with the dependence on the unknown surface shifted to a multiplicative factor in the integrand which is the Jacobian of the transformation of the surface onto a sphere. The restrictions on the class of admissible surfaces guarantee that the optimization problem has a solution. An algorithm for reconstructing the boundary of the scatterer is described.

**INVERSE SOLUTION FOR A SLAB OF RANDOM DIELECTRIC DISCS:  
ORIENTATION AND AREA DISTRIBUTIONS**

R. H. Lang and H. A. Saleh  
Department of Electrical Engineering & Computer Science  
The George Washington University  
Washington, D. C. 20052

The backscattering coefficient from a slab of thin random lossy dielectric discs over a flat ground is used to determine the inclination angle and area distribution of the discs. The slab of random discs can be used to model agricultural crops, such as soybeans, in the microwave region. The direct problem is formulated by computing the backscattering coefficient via the Born approximation for the horizontally polarized case. The reconstruction of the joint probability density function of inclination angle and area distribution leads to a linear Fredholm integral equation of the first kind. The integral equation in question is approximated by a simple numerical quadrature formula. Due to the ill-posedness of the problem, the Phillips-Twomey regularization method with the third difference smoothing condition, is used to obtain an inversion.

The calculation is done first assuming that the inclination and area variables are independent. In this case either the inclination or area distribution is taken as known and the other is computed. Backscattered data is taken at 9 different angles of incidence between 0 to 80 degrees at 2.5 GHz. The solution is found without error and then with 1% and 10% randomly distributed errors in the data. In the case where both inclination and area distributions are assumed to be unknown, back-scattered data is taken at 9 angles of incidence between 0 to 80 degrees for nine different frequencies between 2 and 3 GHz. Again the inverse is found with and without noise in the data.

## B-21-3

### SIGNAL FLOW GRAPHS FOR WAVE PROPAGATION IN INHOMOGENEOUS LOSSY MEDIA

C. Q. LEE

Department of Electrical Engineering and Computer Science  
University of Illinois at Chicago

Using the piece-wise uniform approximation, a time domain solution for one-dimensional wave propagation and profile inversion in an inhomogeneous lossy medium has previously been analyzed (C. Q. Lee, Proc. IEEE, 70, pp219-228, 1982). Based on the results derived, we have developed generalized signal flow graphs for wave propagation through a medium in both time and frequency domains, using incident and reflected waves as dependent variables. Similar signal flow graphs in terms of equivalent distributive voltage and current have also been obtained. Our objective is to seek a better understanding of the wave propagation so that we can improve our inversion procedure.

With incident and reflected waves as dependent variables, the signal flow graph provides a clear physical insight to wave propagation in a medium. By successive transformation of dependent variables from one layer to the next, computer algorithms for wave propagation and profile inversion can be logically developed. Since the signal flow graph for the lossy medium has the same topology as that of the lossless case, many of the existing signal processing techniques and inversion methods for the lossless medium can be used for the lossy medium. From the graph, the reflected wave at the sending end boundary can be decomposed into components which are functions of medium parameters in successive layers. The order of significance in these components can be used to minimize the cumulated errors due to numerical calculation in profile inversion.

In terms of equivalent voltage and current, the signal flow graph takes on a different topology and the inversion procedure based on this graph is complicated. However, this approach can be used to analyze a wide range of problems, including some nonlinear propagations. It also suggests means by which the effect of measurement and numerical errors can be minimized in the inversion solution.

A VALIDATION ANALYSIS OF THE TARGET-DESCRIPTOR INTERPRETATIONS OF THE  
 MUELLER MATRIX ELEMENTS IN POLARIMETRIC RADAR RETURNS WITH THE  
 KENNAUGH'S PHYSICAL OPTICS IMPULSE RESPONSE FORMULATION

Sujeet K. Chaudhuri  
 Department of Electrical Engineering  
 University of Waterloo  
 Waterloo, Ontario, Canada N2L 3G1

and

Bing-Yuen Foo and Wolfgang-M. Boerner  
 Communications Laboratory, Electromagnetic Imaging Division  
 Department of Electrical Engineering & Computer Science  
 University of Illinois at Chicago  
 Chicago, IL 60680

SUMMARY

It is known that high frequency radar interrogation may disclose fine geometrical structures of targets, whereas low frequency interrogation may recover such coarse information as target sizes and volumes. Any target descriptor which is intended to describe the geometry has to be defined on a high frequency basis and thus its validity becomes questionable at low frequencies. In the phenomenological target-descriptor approach of Huynen, the frequency range of validity has not been established, nor have the descriptors been rigorously related to the target geometry by using the electromagnetic theory. In view of these unresolved problems, the main objective of this paper is to show, based on electromagnetic theory, that Huynen's phenomenological target-descriptors, at high frequencies, can be closely related to specular geometry (in particular, specular curvature) and target orientation. Numerical analysis with measured polarimetric backscattering data is shown, and application of the descriptors in radar target discrimination or identification is suggested.

In this work, first the relationship between the elements of the scattering matrix ( $[S]$ ) and the Mueller matrix ( $[M]$ ) are established. Next, by using these expressions along with the first order corrected physical optics impulse response formulation, certain approximate relations between the Mueller matrix elements and scatterer physical characteristics are established. Now it is possible to compare the phenomenological target-descriptor interpretations of these Mueller matrix elements with the above electromagnetically established geometry related expressions.

During the numerical validation studies the experimental backscattering data on ellipsoidal structures are used. These data primarily consist of two contributions: one specular contribution and the other creeping wave contribution. A time-domain scheme is developed to separate these two individual components in the measured frequency-domain broadband backscattered data. It is shown that the validation of the target-descriptor interpretations of the Mueller matrix elements with the isolated specular contribution data is acceptable, whereas the validation of these interpretations with the total backscattered data is doubtful.

## B-21-5

### BASIC PROPERTIES OF THE BI-STATIC RADAR TARGET SCATTERING MATRIX

Alexander B. Kostinski and Wolfgang-M. Boerner  
Communications Laboratory  
Department of Electrical Engineering & Computer Science  
University of Illinois at Chicago

The theory of the bistatic radar target scattering matrix is put on a firm mathematical basis and analyzed in terms of Kennaugh's characteristic polarimetric target operator theory. The developed theory is extended and generalized for treating a variety of cases of specific multistatic transceiver arrangements from a unified point of view.

#### SUMMARY

It is shown that the radar echo maximization-minimization problem is equivalent mathematically to an extremum problem of various bilinear forms defined by the linear target scattering operator  $[S]$  acting on members of a fixed vector space of polarization states, which are related by a class of unitary transformations.

For instance, it is shown that cases of the monostatic arrangement of (i) different receiver-transmitter polarization states, (ii) bistatic arrangements, but identical polarization states, and finally, (iii) monostatic arrangement of identical polarizations, correspond respectively to symmetric bilinear quadratic and symmetric quadratic forms (symmetric in basis coordinates). The general case is, of course, that of a general bilinear (multilinear/multistatic) form.

The above-mentioned degenerate cases are used to demonstrate the existing differences which affect monostatic versus bistatic set-ups, as well as optional polarization null properties of  $[S]$ , which are essential for polarimetric target null signature interpretations.

The theorem about the possibility of simultaneous diagonalization of two quadratic (Hermitian) forms, (one of which is positive definite) is utilized in order to investigate applications to the target vs. clutter discrimination problem.

The possibility of extending the theory to multilinear forms (multistatic set-up) and generalization to partially polarized states are also demonstrated.

Modulation Transfer Function and Image Transmission Through  
Randomly Distributed Spherical Particles

Yasuo Kuga and Akira Ishimaru  
Department of Electrical Engineering  
University of Washington  
Seattle, Washington 98195

Image transmission through a random medium is important in many areas such as millimeter wave applications, optics, radar target identification, and underwater optics. Transmitted images are often affected by the presence of particulate matter and turbulence between the object and the detector. The quality of imaging systems is usually expressed using the Modulation Transfer Function (MTF) which is the ratio of the modulation in the image to that in the object as a function of the spatial frequency (cycles per mm) of the sine wave pattern. The MTF can be used to express the quality of transmitted images through a random medium. In the past some experimental results, such as the MTF measurements through fresh water that contained both refractive index fluctuation and particulate matter, were obtained. However, experimental data obtained in situ in which scattering characteristics of a random medium are difficult to measure are not often useful for comparison with theories. In order to compare the experimental results with theories, it is desirable to obtain experimental data in controlled conditions.

In this paper we will present the experimental results for the MTF through a random distribution of polystyrene microspheres suspended in water. The experimental system consists of the incoherent light source (wavelength =  $0.63 \mu\text{m}$ ), objects with different spatial frequencies, the scattering cell, the image-forming lens, and the 512-elements array detector. Results are obtained for particulate sizes of  $0.109$  and  $5.7 \mu\text{m}$ , densities much less than  $1\%$ , and the optical distances between  $0$  and  $8$ . Our preliminary results show that when the particle size is much larger than the wavelength, the transmitted image is affected by the incoherent intensity, and the cutoff frequency is close to the value obtained using the mutual coherence function with a large particle approximation. It is also observed that the cutoff frequency depends on the optical distance and decreases as the optical distance increases. On the other hand, when the particle size is much smaller than the wavelength, the transmitted image is affected by the reduced coherent intensity, and the cutoff frequency is close to that of the experimental system without particles.

## B-21-7

### OPTICAL BEAM PROPAGATION IN RANDOM MEDIA BASED ON RADIATIVE TRANSFER THEORY

Hung-Wen Chang and Akira Ishimaru  
Department of Electrical Engineering  
University of Washington  
Seattle, Washington 98195

Optical beams are used for communication through the atmosphere and ocean water. However, the atmospheric turbulence and scatterers such as rain, fog, clouds, hail, and snow cause multiple scattering and severely limit the data transmission rate. For optical beam propagation in discrete scatterers such as fog, clouds, and smoke, the radiative-transfer theory has been widely used. Even though extensive studies have been made for a plane wave incident on a slab of scatterers, the complete beam wave solution is not available at present. The first-order solution and the diffusion approximation are applicable only for small and large optical depths and are not applicable to the most practical region where the optical depth is 1 to 30.

The equation of transfer in the cylindrical system is a integral-differential equation with four independent variables. A Fourier-Bessel transform version of the equation of transfer in a cylindrical system is derived. This equation has one less independent variable and fewer differential operators. It contains one additional variable  $\psi$  and one parameter  $\kappa$  the spatial frequency. When  $\kappa$  is set to zero, the new equation becomes identical to the plane wave equation of transfer. At present, closed-form solutions are not available. To obtain the numerical solution, we extend the idea of the Discrete Ordinate Method by using Legendre-Lagrange polynomials as basis functions for spherical harmonics expansion in  $\psi$  and  $\mu$ . The original beam equation of transfer is approximated by a system of differential equations which is then solved by the eigenvalue-eigenvector technique. The final solution is obtained by taking the inverse Fourier-Bessel transformation of the solution to this beam wave equation of transfer.

Numerical results show that for small optical depths all frequency components contribute to the final intensity, but for large optical depths only low frequency components contribute. For a narrow beam, the transmitting flux due to the diffused specific intensity gradually becomes comparable to that of the reduced specific intensity for  $\tau$  near 15 and becomes saturated after  $\tau = 35$ . This beam spreading behavior is consistent with the experimental measurements. The result is significantly different from that of a plane wave solution. Even though the beam wave equation of transfer requires extensive numerical calculations for a complete narrow beam solution, it does provide a better description of the beam wave propagation in the random media in the useful range of optical depths.

The Effective Constitutive Parameters of a Forest

M. Abouzahra, L. Lewin, H.X. Lian, University of Colorado, Boulder. (Dr. Lian was on leave from the Peking Institute of Posts and Telecommunications, Peoples Republic of China)

To the extent that the tree trunks in a forest can be modeled by a uniform array of vertical cylinders, whose permeability is unity and whose permittivity can be found from the properties of the wood, an effective permittivity for the forest medium can be calculated, and used to predict average propagation and surface wave properties. Actually, it is the propagation constant rather than the permittivity that is determined, the effective permeability being assumed to be unity. Because of the occurrence of resonances at the higher frequencies in the trunks, magnetic energy can be stored, and the effective permeability, due to such structural effects, need not be unity. In order to determine whether this effect is significant, a thorough analysis was made of the reflection and transmission of a plane wave obliquely incident on a uniform semi-infinite array of cylinders. For vertically polarized waves, the effective permeability was found to be not significantly different from unity. For horizontal polarization, both the real and the imaginary part of the magnetic susceptibility, in a typical example, was about  $10^{-4}$ . For the electric susceptibility, the imaginary part was about  $10^{-3}$ , and the real part about 0.05. The upper limit of the approximations inherent in this analysis corresponds to a frequency of about 15 MHz, about 10 times lower than the resonant frequency in the trunks, but the conclusion appears to be that the effect on the permeability is relatively small compared to that on the permittivity.

## B-21-9

### GEOMETRIC OPTICS IN INHOMOGENEOUS NONSTATIONARY MEDIA WITH SPATIAL AND TEMPORAL DISPERSION

Kurt Suchy

Institute for Theoretical Physics, University of Düsseldorf,  
Fed. Rep. Germany

Media treated in geometric optics are mostly stationary without spatial dispersion. The results can be conveniently generalized with four-vectors

$$\underline{X} := \underline{x} + \underline{g}_t^t, \quad \frac{\partial}{\partial \underline{X}} := \frac{\partial}{\partial \underline{x}} + \underline{g}_t^t \frac{\partial}{\partial t}, \quad \underline{K} := \underline{k} - \underline{g}_t^t \omega, \quad \frac{\partial}{\partial \underline{K}} := \frac{\partial}{\partial \underline{k}} - \underline{g}_t^t \frac{\partial}{\partial \omega},$$

where  $\underline{g}_t^t \cdot \underline{g}_t^t = 1 = -\underline{g}_t^t \cdot \underline{g}_t^t / c^2 = -c^2 \underline{g}_t^t \cdot \underline{g}_t^t$ . With the 6x6 and 1x6 matrices

$$\underline{M} := \begin{bmatrix} -\omega \underline{\epsilon} + i \underline{\sigma} & -k x \underline{I} \\ +k x \underline{I} & -\omega \underline{\mu} \end{bmatrix}, \quad \underline{C} := \begin{bmatrix} \underline{\epsilon} & 0 \\ 0 & \underline{\mu} \end{bmatrix}, \quad \underline{f} := \begin{bmatrix} \underline{E} \\ \underline{H} \end{bmatrix}$$

(the column matrix  $\underline{f}$  comprises the slowly varying factors of the electric and magnetic wave field), Maxwell's equations in geometric optics approximation are

$$\left[ \underline{M}(i + \overleftrightarrow{\partial}) + \frac{\partial}{\partial t} \underline{C} \right] \cdot \underline{f} = 0 \quad \text{with} \quad \overleftrightarrow{\partial} := \frac{\partial}{\partial \underline{K}} \cdot \frac{\partial}{\partial \underline{X}}.$$

The zeroth approximation  $\underline{M} \cdot \underline{f} = 0$  is an algebraic relation. The factorized determinant of  $\underline{M}$  yields six modal dispersion equations  $D_M = 0$  with  $M = \pm 1, \pm 2, \pm 3$ . For each mode a set of Hamilton equations can be derived:

$$\frac{d\underline{X}}{dt} = - \frac{\partial D}{\partial \underline{K}}, \quad \frac{d\underline{K}}{dt} = \frac{\partial D}{\partial \underline{X}}.$$

The first approximation leads to the transport equation

$$\frac{\partial}{\partial \underline{X}} \cdot a^2 \underline{W} + a^2 \zeta = 0$$

for the complex amplitude  $a$  of  $\underline{f}$  with the transport vector

$$\underline{W} := \frac{d\underline{X}}{dt} = \frac{-\partial D / \partial \underline{K}}{\partial D / \partial \omega} = \frac{\partial \omega}{\partial \underline{k}} + \underline{g}_t^t.$$

BACKSCATTERING CROSS-SECTION OF  
N PARALLEL CONDUCTING CIRCULAR CYLINDERS

H.A. Ragheb and M. Hamid  
Antenna Lab., Elec. Eng. Dept.  
University of Manitoba  
Winnipeg, Canada. R3T 2N2

The scattering pattern and backscattering cross section, due to an E-polarized plane wave incident on N circular parallel conducting cylinders in an arbitrary two-dimensional configuration, is computed by the boundary value method. The results compare favourably for thin cylinders with an approximate solution based on an extension of the Karp-Russek technique for large separation between any two adjacent cylinders relative to the larger diameter. The results indicate that for broadside incidence and fixed radii and separation of an equispaced linear array of cylinders, the maximum backscattering cross section increases monotonically with increasing number of cylinders. On the other hand, for normal incidence and fixed radii, the peak of the maximum backscattering cross section occurs at the same separation between the cylinders regardless of the number of cylinders.

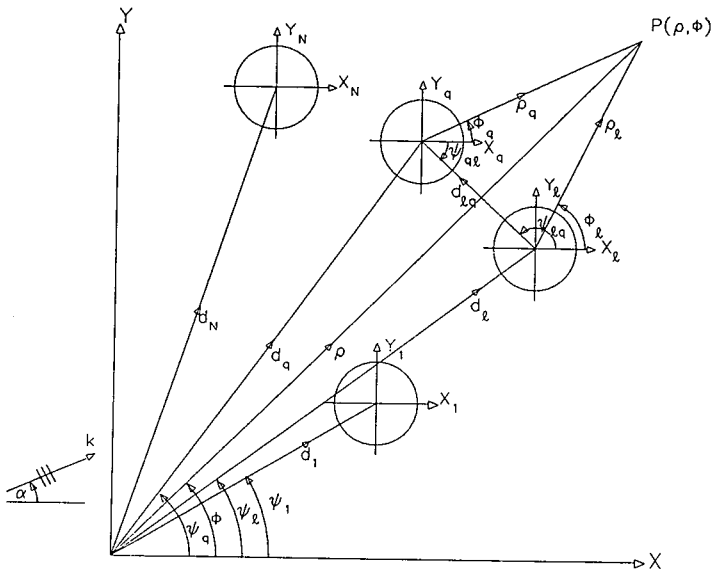


Fig. 1 : Geometry of the problem.



URSI COMMISSION C - SESSION C1

Radio Networks

1:30 - 5:00  
LAW 178

Réseaux de radio

Chairperson/Président: **H.E. de Pedro**, GTE Government Systems Corporation, Needham Heights, MA, USA

- 1 ON HF NETWORKS AND LINK PROTOCOLS. **M. Nesenbergs**, National Telecommunications and Information Administration, Institute for Telecommunication Sciences, Boulder, CO, USA
- 2 ON GROUNDWAVE RADIO NETWORKS. **H.E. de Pedro**, GTE Government Systems Corporation, Communications Systems Division, Needham Heights, MA, USA
- 3 SIGNALLING CONVENTIONS AND PROTOCOLS IN AREA COVERAGE DIGITAL RADIO. **D. Nielson**, SRI International, Menlo Park, CA, USA
- 4 FREQUENCY SHARING BETWEEN ISS AND BSS SYSTEMS NEAR 23 GHz. **C.W. Wang, C.A. Levis**, Ohio State University ElectroScience Laboratory, Dept. of Electrical Engineering, Columbus, OH, USA
- 5 PACKET SWITCHING IN CELLULAR RADIO SYSTEMS. **H.M. Hafez, S. Riordon, S. Aidarous**, Carleton University, Dept. of Systems and Computer Engineering, Ottawa, ON
- 6 EVALUATION OF PILOT SSB SYSTEMS. **M.J. Burke, L. Boucher**, Department of Communications, Communications Research Centre, Ottawa, ON
- 7 RADIO COMMUNICATION AND NAVIGATION IN THE PRESENCE OF LINEARLY DISTRIBUTED NOISE SOURCES. **C.E. Cook**, The MITRE Corporation, Bedford, MA, USA

ON HF NETWORKS AND LINK PROTOCOLS

M. Nesenbergs  
National Telecommunications and Information  
Administration  
Institute for Telecommunication Sciences  
Boulder, Colorado 80303

This paper addresses the capabilities and limitations that high-frequency (HF) radio links impose on HF network structure and performance. When compared to other broadband networks, such as those available via satellite, terrestrial microwave, or optical fibers, the lesser capacity HF radio nets can be viewed as minor adjuncts or as emergency backup. Rapid terminal deployment is supported by easily available and inexpensive shortwave equipments. Broad area coverage for otherwise inaccessible sites has been a historic plus for HF radio.

Depending on geographies involved, the physical phenomena of the ionosphere cause time-varying signal distortions (e.g., fading). Often these distortive characteristics can be identified in near real-time and their influence can then be at least partly counteracted. Techniques, such as frequency forecasting, sounding, multi-frequency management, modulation, error control coding, and special HF link level protocols are all examples of useful networking tools. In particular, the ARQ link protocols that must function full duplex in the BER region between  $10^{-1}$  and  $10^{-4}$  call for unique network tradeoffs between throughput, delay, and perhaps mean times before buffer overflows.

## On Groundwave Radio Networks

Dr. Hugo E. de Pedro  
GTE Government Systems Corporation  
Communication Systems Division  
77 "A" Street  
Needham Heights, MA 02194

This paper discusses issues related to the design of groundwave radio networks. These networks have an important role in military communication systems because of their inherent independence of atmospheric environmental conditions. This characteristic makes them very useful in the performance of functions in stressed environments.

Examples of groundwave radio network designs are presented and discussed. These examples include an MF network design and an LF network design.

The MF network is a spread spectrum network used to provide communications for command and control of ground missile forces. The radio network utilizes a simulcast transmission scheme whereby messages are retransmitted by all nodes upon reception. The average power of the received signal is increased by all the transmitters' contributions but the random phase additions result in a fading signal at the receivers. Computer simulations of network performance have demonstrated that the simulcast power gain more than offsets the degradation due to fading.

Examples of relay network designs are provided for the MF network and for an LF nationwide network. The improvement in network throughput over the simulcast scheme is demonstrated. The effect of interference from other system nodes is minimized by proper selection of time-frequency channel assignments to each node, taking geographic locations into consideration.

SIGNALLING CONVENTIONS AND PROTOCOLS  
IN AREA COVERAGE DIGITAL RADIO

Don Nielson  
SRI International  
Menlo Park, California 94025

ABSTRACT

Packet radio is a technique of providing digital radio networking to a set of mobile users distributed over some geographical area. Information is packetized, with each such packet having some autonomy in wending its way from source to destination. The present design uses line-of-sight frequencies and broadcast and re-transmission strategies to maintain network connectivity. The strategy of applying packet formats to an intermittent (from fading and obscuration) and impulsive-noise channel will be discussed. Since the modulation of packet radio is spread spectrum, channel impact on wide bandwidth signals is also discussed. The frequency of concern is L-band.

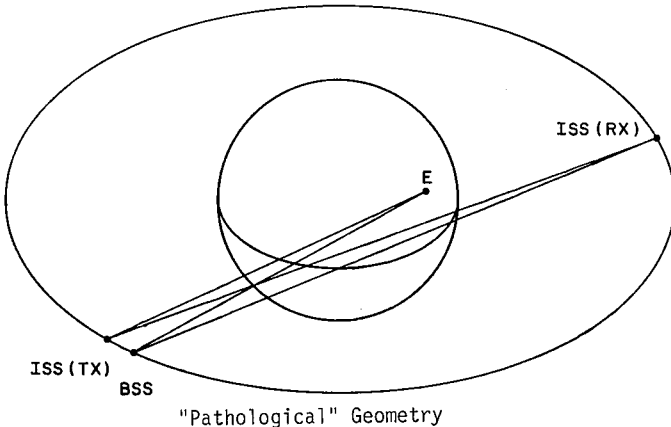
Aside from the modulation and detection design, there are a variety of protocols that serve the mobile user, routing, and network management in general. These elements will be addressed, time permitting.

## FREQUENCY SHARING BETWEEN ISS AND BSS SYSTEMS NEAR 23 GHZ

C. W. Wang and C. A. Levis  
 ElectroScience Laboratory  
 The Ohio State University  
 Department of Electrical Engineering  
 Columbus, Ohio

The 1979 World Administrative Radio Conference (WARC 79) authorized the use of the 22.55-23.55 GHz band by the Inter-Satellite Service (ISS) and the use of the 22.5-23.0 GHz band by The Broadcasting-Satellite Service (BSS) in region 2. This requires frequency sharing between 22.55 and 23.0 GHz. Allowable geometries for such sharing are calculated on a single-entry basis. It is found that sharing is not allowed for a "pathological" geometry in which the intersatellite link approaches  $160^\circ$ , the BSS satellite is located very near the ISS transmitting satellite, and the BSS coverage area includes the part of the Earth nearly in line with the ISS receiver. Thus, if BSS satellites are allowed at low elevations in low or medium latitudes, it will be necessary to restrict very long ISS links to the unshared portion of the band.

Under this restriction it is found, for realistic antenna gains, that the BSS system will always be protected sufficiently if the ISS system protection is sufficient. The required satellite separations are calculated and presented as a series of universal curves, one sheet for each ISS receive antenna gain value under consideration.



PACKET SWITCHING IN CELLULAR RADIO SYSTEMS

by

H. M. Hafez, S. Riordon and S. Aidarous  
Dept. of Systems and Computer Engineering,  
Carleton University,  
Ottawa, Ontario, Canada, K1S 5B6

In cellular mobile radio systems, the radio frequencies (channels) are shared among the mobile telephones by means of circuit switching, hand-off techniques and frequency reuse in space. These conventional techniques are justified for normal telephone calls where the average call duration is about three minutes. However, in many conventional mobile radio applications, the call duration is too short to justify the time wasted in setting up the channel or the complicated hand-off techniques. Examples of the short call applications are: emergency calls, dispatch services and many data communication applications. In order to accommodate these applications in mobile cellular radio systems, new frequency sharing strategies should be considered.

In this paper we propose a novel scheme where mobile terminals with bursty traffic can share a number of radio frequencies on a packet switching basis. The proposed technique does not require hand-off or channel set-up procedures, and it takes advantage of the bursty nature of the traffic and the spatial distribution of the simultaneously active terminals. The proposed system is analyzed. The analysis relates the probability of successful transmission to the traffic density. The proposed system is then simulated.

## EVALUATION OF PILOT SSB SYSTEMS

M.J.Burke and L. Boucher  
Department of Communications, Communications Research Center,  
Ottawa, Canada

A change of modulation system from Frequency Modulation (FM) to a more spectrally efficient modulation mode (Single Sideband - SSB) is considered in order to permit a further growth in the use of civil land mobile radio, particularly in the VHF and UHF bands.

Problems associated with conventional SSB systems have been eliminated by the introduction of 1) a pilot tone transmitted with the voice, and 2) amplitude companding. The pilot tone can take several forms, e.g., pilot carrier, in-band pilot tone, above band pilot tone, or a complex audio sub-carrier containing control information (ex.: Lyncomplex, Syncomplex). Amplitude companding is the amplitude compression/expansion of the audio signal, and is used to reduce the noise floor of the transmitted signal.

Two single sideband systems using amplitude companding and an above band pilot (ACSB) have recently become commercially available, and have been studied for use in Canada. In particular, determination of interference criteria (separation distances between FM & ACSB, co-channel re-use distances, etc.) has been made for assignment purposes. Because of the presence of the pilot tone, special tests had to be developed.

Preliminary results suggest that a 50 dB adjacent channel protection ratio (as given by the commercial ACSB units) is not sufficient to provide adequate interference protection at 5 KHz spacing. Typical FM systems operating at 25 or 30 KHz spacing offer in excess of 70 dB adjacent channel protection to the desired FM signal. In their actual form, the ACSB transceivers would require approximately a 7 KHz channel bandwidth to provide 70 dB isolation between stations.

Intermodulation produced by the non-linearities of the power amplifier is the major cause of spurious emissions into the adjacent channels. In-band pilot, inverted audio, or better linear amplifiers are possible solutions to reduce or limit the spreading of the intermodulation in this kind of system.

Many other techniques such as the ones developed for the Syncomplex systems, or techniques like the speech envelope normalisation, the inversion of the audio signal, transparent tone in-band, and digital signal processing (DSP) of the audio signal are planned to be investigated individually and/or in combination with the others to improve the efficiency of pilot SSB in the VHF and UHF bands. Using DSP, some of the analog sections used for functions such as the insertion of the pilot, preemphasis, amplitude companding, frequency companding, and other analog audio sections could be replaced by a single DSP chip in order to reduce the cost of a pilot SSB system.

All these new developments open the way to many economical alternatives toward a more effective use of the radio spectrum in the UHF and VHF land mobile radio bands.

C-1-7

**RADIO COMMUNICATION AND NAVIGATION IN  
THE PRESENCE OF LINEARLY DISTRIBUTED NOISE SOURCES**

Charles E. Cook  
The MITRE Corporation  
Bedford, MA 01730

Paper withdrawn/  
La communication a été retirée

URSI COMMISSION C - SESSION C2

**Digital Signal  
Processing**

1:30 - 5:00  
LAW 178

**Traitement numérique  
des signaux**

Chairperson/Président: **A.M. Peterson**, Stanford University, Stanford, CA, USA

- 1 REMOTE SENSING OF SEA ICE USING SYNTHETIC APERTURE RADAR. **J.F. Vesecky, R.N. Bracewell, M.P. Smith**, Stanford University, STARLAB, Stanford, CA, USA
- 2 THE MULTI-CHANNEL SPECTRUM ANALYZER. **I. Linscott, K.S. Chen, A.M. Peterson**, Stanford University, STARLAB, Stanford, CA, USA
- 3 HYBRID ANALOG/DIGITAL SIGNAL PROCESSING FOR DATA COMMUNICATIONS IN A MULTIPATH CHANNEL. **J.H. Fischer, J.H. Cafarella**, Massachusetts Institute of Technology, Lincoln Laboratory, Lexington, MA, USA
- 4 150 BPS DIGITAL CHIRP MODEM DESIGN IMPLEMENTED USING NEC 7720 SIGNAL PROCESSOR. **T.J. Kahwa**, Department of Communications, Communications Research Centre, Ottawa, ON
- 5 FILTERING OF DATA IN GEOPHYSICAL TOMOGRAPHY IMAGE RECONSTRUCTION. **J.D. Bentley, C.A. Balanis**, Arizona State University, Dept. of Electrical and Computer Engineering, Tempe, AZ, USA

## C-2-1

### REMOTE SENSING OF SEA ICE USING SYNTHETIC APERTURE RADAR

J. F. Vesecky, R.N. Bracewell and M. P. Smith  
STARLAB, Stanford University, Stanford, CA 94305

Remote sensing using synthetic aperture radar (SAR) images provides an excellent opportunity for both observation and prediction of sea ice motion and deformation. Radar images at 23 cm wavelength can be collected day or night and through clouds. However, tracking sea ice features over a series of co-spatial images separated in time is a tedious and time consuming process to do manually even when computer assisted. Hence, only a very small fraction of the sea ice, SAR images collected by SEASAT have been so analyzed. The objective of the research reported here is to automatically identify and track unique features in sea ice images in order to observe sea ice motion and deformation. It is important to recognize that the desired physical measurement at each point in the ice field is a tensor (movement and distortion) not simply a velocity vector. The sea ice image processing algorithm begins with averaging to make a typical 100 x 100 km image (64,000,000 sample points) more tractable. An algorithm based on lack of correlation with surrounding regions identifies unique 'tie points' at appropriate intervals over the reference image. These points are then located in the next image of the sequence using a guided correlation process. This yields a displacement field over the sea ice image. Movement and distortion of the sea ice are derived from the displacement field. This algorithm has been successfully applied to an ersatz SAR sea ice image. Results for real SAR sea ice images in the Beaufort Sea will be presented and compared with a computer assisted manual analysis.

## THE MULTICHANNEL SPECTRUM ANALYZER

I.R. Linscott, K.S. Chen, A.M. Peterson  
Space, Telecommunications and Radioscience Laboratory  
Stanford University  
Stanford, CA 94305

The MCSA is a special purpose digital signal processor. Its main function is to filter a wide-band signal into many narrower bands, so that each of the output bands has a bandwidth that is a better match to the signal being searched for.

Instead of using a single large Fast Fourier Transform (FFT), the MCSA derives its narrow bands by cascading two stages of digital bandpass filters with moderate-sized Discrete Fourier Transforms (DFT). FFT operations do not yield convenient signals for deriving the intermediate bandwidths that the MCSA delivers. Furthermore, it is possible to provide better RFI rejection with the bandpass filter technique. An FFT has a worst-case sidelobe (adjacent bin) response that is only 13 dB below the response of the main lobe. A bandpass filter can be designed to give more than 70 dB of adjacent channel rejection.

The first bandpass filter splits the input signal into 112 bands, each approximately 74 kHz wide. Each of these 74-kHz-wide signals is then filtered by a second bandpass filter which further subdivides the signal into 72 bands. Each of the resultant bands is about 1024 Hz wide.

The 1024-Hz signals are then fed either to a 36-point DFT or to a 1152-point DFT to form the final 32-Hz or 1-Hz outputs, respectively. Each of these bandwidths (1 Hz, 32 Hz, 1024 Hz, and 74 kHz) is available as a output of the MCSA. The magnitude squared value of each output sample is computed and is available as the square-law-detected power output. Except for the 74-kHz bandwidth, the complex signals from the other bands are also available as outputs.

## C-2-3

### HYBRID ANALOG/DIGITAL SIGNAL PROCESSING FOR DATA COMMUNICATIONS IN A MULTIPATH CHANNEL

J. H. Fischer and J. H. Cafarella\*  
Lincoln Laboratory, Massachusetts Institute of Technology  
Lexington, Massachusetts 02173-0073

The development of a hybrid analog/digital signal processor is described which can provide, in compact equipment, the wide variety of signal processing tasks required to achieve robust network communication links in a diffuse multipath environment. The analog pre-processor and digital post-processor prove to be an ideal combination for performing various signal processing functions required of a distributed communications network. Analog signal processing is performed with surface-acoustic-wave convolvers used as programmable matched filters that provide greater than 30-dB improvement in signal-to-noise ratio. Binary post-processing of the matched-filter outputs extends the overall processing gain to as much as 60 dB. The wideband outputs of the matched filter, which have a 200-MHz instantaneous bandwidth, are applied to a digital integrator/post-processor which performs both coherent and incoherent signal processing for detection, demodulation, and ranging measurements in the presence of a dense multipath profile. The coherent digital processor is desirable in order to optimize the signal-processing gain. When Doppler conditions will not allow the use of the coherent digital processor, an incoherent digital processor, realized at the expense of little additional circuitry, is used. The incoherent processor also allows ranging measurements to be made in the presence of data and allows a wider selection of data rates. The hybrid processor can resolve multipath for demodulation and ranging down to 3 meters. In response to channel conditions, the processing gain (instantaneous time-bandwidth product) can be varied from  $10^3$  to  $10^6$  with the commensurate and nearly ideal tradeoff of data rate from 90 Kbits/sec to 44 bits/sec.

\*Present address: MICRILOR, P.O. Box 624, Swampscott, MA 01907

150 BPS DIGITAL CHIRP MODEM DESIGN  
IMPLEMENTED USING NEC 7720 SIGNAL PROCESSOR

by T.J. Kahwa  
Department of Communication  
Communication Research Centre  
P.O. Box 11490, Station 'H'  
Ottawa, Ontario K2H 8S2

Abstract

Some of the factors that affect good performance of a High Frequency (HF) data modem are frequency selective fading, transmitter-receiver mistuning, intersymbol interference due to multipath, wide dynamic range in received signal strengths and strong co-channel interference. Solution to some of the problems above relies on selecting a good modulation method. Linear frequency modulation (Chirp) has been suggested (G.F. Gott and J.P. Newsome, "HF Data Transmission Using Chirp Signals", Proc. IEE, Sept. 1971) as one possible solution. Earlier reported HF data modem designs used analog components - resulting in designs that were quite sensitive to component value changes.

The presentation and discussion will cover the theory, implementation, and test results of a 150 bit per second (bps) HF data modem. It is implemented almost entirely in software using an NEC 7720 signal processing chip, augmented by A/D, D/A and timing support circuitry.

FILTERING OF DATA IN GEOPHYSICAL TOMOGRAPHY IMAGE  
RECONSTRUCTION

James D. Bentley and Constantine A. Balanis  
Department of Electrical and Computer Engineering  
Arizona State University  
Tempe, AZ 85287

## ABSTRACT

Whenever a picture is copied, imaged, scanned or transmitted, or when attempts are made to reconstruct an image from data, the picture quality may suffer. Various techniques have been examined and utilized to enhance the image quality by designing techniques which compensate for the effects (known, unknown, or estimated) of degradation. This process is generally known as image restoration, and it utilizes extensively filtering methods.

In geophysical tomography image reconstruction can be achieved by transmitting electromagnetic waves and receiving the energy associated with them after it has travelled through the medium which we desire to reconstruct its image. Various iterative reconstruction techniques [such as the Algebraic Reconstruction Techniques (ART) and Simultaneous Iterative Reconstruction Technique (SIRT), and others] have been successfully utilized to reconstruct images in geophysical, medical and other applications. In those both straight-line and refracted paths, obtained using ray-tracing procedures, have been utilized. Although the quality of the restored image is usually acceptable in many applications using such techniques, it has been found that significant improvements in image reconstruction can be attained by attempting to restore the image. Filtering is one process which is extensively used to restore images.

In this paper various types of filters are examined and applied to reconstruct and restore images of objects which are buried within the earth and possess conductivities higher and lower than those of the earth itself. The types of filters considered are the majority filter, median filter, median + 1 filter, mode filter, low- and high-pass filters, and a noise cleaning algorithm. A prime objective of this investigation is to define the boundaries, compared to the surrounding medium, of the buried object. A high-pass filter possesses those desired characteristics which tend to emphasize edges and areas of large variation. The figure-of-merit used to judge the achievement of this process is the minimum variance partitioning. A secondary objective is to determine the relative and absolute contrasts of the anomaly and its surrounding environment. All of the filters examined possess their own strengths and weaknesses. The filter chosen in a given application will depend largely on the desired features of the restored image.

## URSI COMMISSION C - SESSION C3

**Information Theory  
and Coding**8:30 - 12:00  
LAW 178**Théorie et codage  
de l'information**Chairperson/Président: **V.K. Bhargava**, University of Victoria, Victoria, BC

- 1 (8:40) CONVOLUTIONAL CODING AND SEQUENTIAL DECODING. **D. Haccoun**, École Polytechnique de Montréal, Dept. of Electrical Engineering, Montréal, PQ
- 2 (9:10) ON THE UNDETECTED ERROR PROBABILITY OF LINEAR BLOCK CODES. **C. Leung**, University of British Columbia, Dept. of Electrical Engineering, Vancouver, BC
- 3 (9:40) ADAPTIVE FORWARD ERROR CORRECTION TECHNIQUES FOR DIGITAL COMMUNICATIONS BY SATELLITE. **V.K. Bhargava**, University of Victoria, Dept. of Electrical Engineering, Victoria, BC
- 4 (10:10) AN OPTICAL FIBER BASED LOCAL BACKBONE NETWORK. **A. Elhakeem, J.F. Hayes**, Concordia University, Montreal, PQ; **F. Chaya, O. Tanir**, McGill University, Montreal, PQ
- 5 (10:40) CONSTRUCTING SEQUENCES FOR CDMA APPLICATIONS. **G. Séguin**, Université Laval, Département de génie électrique, Québec, PQ

## CONVOLUTIONAL CODING AND SEQUENTIAL DECODING

DAVID HACCOUN

Professor

Department of Electrical Engineering

Ecole Polytechnique de Montréal

C.P. 6079, Succ. "A"

Montréal, Québec, Canada

## Abstract

With the ever increasing use of sophisticated digital communication the problem of providing suitable error control for these systems is of prime importance, and Forward Error Correction (FEC) is becoming an essential component in the system. For discrete memoryless channels (such as the space channel) where the noise is essentially white, systems using convolutional encoding at the transmitting end and sequential decoding at the receiving end are among the most powerful while being readily implementable.

Sequential decoding is a powerful suboptimum decoding technique for tree (or convolutional) codes where only a very small fraction of the encoded tree is explored. The technique attempts to find, one branch at the time, the "best" path through an oriented graph (tree or trellis) in which the branches of the paths are assigned likelihood values or "branch metrics",  $\{\gamma_j\}$ , between the noisy symbols received from the channel and the encoded symbols that may have been transmitted. For a sequence of length  $L$  bits the objective of the decoder is to find that path  $U = (U_1, U_2, U_3, \dots)$  which has the largest total cumulative metric  $\Gamma_L(U) = \sum \gamma_j(U)$  over all possibly transmitted paths, with the highest reliability and the smallest computational effort (V.K. Bhargava, D. Haccoun, R. Matyas, P. Nuspl, "Digital Communications by Satellite", J. Wiley, New York, 1981).

Due to the incomplete exploration of the encoded tree sequential decoding involves a random motion in the tree and consequently the computational effort is on the average very small, but also highly variable, with a cumulative distribution that is asymptotically Pareto. This computational variability is the principal drawback of sequential decoding and several methods for substantially reducing it without degrading the error performance are presented. Using the stack algorithm, in all these methods the exploration of the encoded tree is performed along the  $M$  - most likely paths ( $M \geq 1$ ) rather than along the single most likely path. As a consequence it is shown that the variability of the computational effort may be drastically reduced at a cost of a modest increase in the average decoding effort.

Finally modifications to the stack algorithm with the objective of reducing the required memory storage when decoding high rate codes are presented. Exploiting properties of the codes these modifications are based on the use of a discarding threshold to eliminate a large proportion of the least likely branch extensions at each decoding step.

## ON THE UNDETECTED ERROR PROBABILITY OF LINEAR BLOCK CODES

Cyril Leung  
 Department of Electrical Engineering  
 University of British Columbia  
 2356 Main Mall  
 Vancouver, B.C. V6T 1W5

It is commonly assumed that the probability of undetected error  $P(e)$  for a  $(n,k)$  block code, when used solely for error detection on a binary symmetric channel (BSC) with cross-over probability  $\epsilon < 1/2$ , is upperbounded by  $2^{-P}$ , where  $p = n-k$  is the number of parity-check bits. One argument often used to justify the  $2^{-P}$  bound is as follows. Assume that the  $(n,k)$  code is used over a totally noisy BSC with  $\epsilon = 1/2$ . Then all  $2^n$  possible received sequences are equally likely, and of these only  $2^{k-1}$  are codewords other than the one which was transmitted. The resulting undetected error probability is  $P(1/2) = (2^{k-1})/2^n < 2^k/2^n = 2^{-P}$ . It is then incorrectly argued that for  $\epsilon$  less than  $1/2$ , the undetected error probability should be even smaller.

Although certain codes such as the Hamming and double-error correcting BCH codes obey the  $2^{-P}$  bound, it has been shown that many codes such as single parity-check product codes do not. Cyclic redundancy check codes which are commonly used in many data communication systems do not also generally obey the bound. Therefore, the bound should be used with caution in the design of systems in which the undetected error probability is critical.

### C-3-3

#### ADAPTIVE FORWARD ERROR CORRECTION TECHNIQUES FOR DIGITAL COMMUNICATIONS BY SATELLITE\*

Vijay K. Bhargava  
Department of Electrical Engineering  
University of Victoria  
P. O. Box 1700  
Victoria, B. C., V8W 2Y2

One of the main problems with satellite systems operating at 12/14 GHz frequency band is the attenuation associated with rain-fall. Therefore, significant power margin must be provided to prevent outage due to rain in an adaptive manner.

Two hybrid schemes of time-frequency resource sharing to increase the rain margin of Ku and Ka-band satellite systems are proposed. Scheme 1 requires sharing a small pool of bandwidth for adaptive forward error control coding, small pool of time-frame for rate reduction and a portion of low frequency TDMA back-up frame for downlink transmission to the rain affected stations. Scheme 2 utilizes variable rate modulation and forward error correction, shares a small pool of time frame for rate reduction and a portion of low frequency TDMA back-up frame.

Effective usable capacities of the system using these schemes are calculated. Distribution of resources in order to maximize the effective usable capacity is also analyzed. The results obtained are compared with other adaptive schemes.

Preliminary analysis shows that the utilized capacity of Scheme 1 exceeds 99% of the effective usable capacity possible if it never rains for an outage of 0.05% and fade margin of 2.5 dB. While for Scheme 2 similar performance is achievable at a fade margin of 1.5 dB. For higher outage objectives the loss of effective utilized capacity is higher for Scheme 2.

AN OPTICAL FIBER BASED LOCAL BACKBONE NETWORK

A.Elhakeem and J.F.Hayes - Concordia University

F.Chaya and D.Tanir - McGill University

**Abstract**

In general, Local Area Networks (LAN) are designed to provide a common communication channel among a number of users in the same limited geographical area, usually within a kilometer. A LAN is usually in a protected environment and redundancy in the form of alternative paths is unnecessary. This simplifies the topology since only a single path need be provided between source-destination pairs. In current practice three configurations are prevalent - ring, bus and star.

Optical fiber possesses a number of features that make it attractive as a transmission medium in LANs. It has low transmission loss. A second advantage of optical fiber is high bandwidth. Data rates over 20 Mbps seem to be easily attainable with multimode transmission. Fiber also has the advantage of being immune to electromagnetic interference. Finally optical fibers are small. A bundle of fibers with enormous capacity is about the same size as the standard coaxial cable with several orders of magnitude less capacity.

The capabilities and limitation of the optical fiber medium to some extent shape the implementation of systems and their role in communications. In response to what we see as a changed role of the network, we alter the name of the network calling it a Local Backbone Network (LBN). The function of this new network is to connect a limited number of high volume sources to one another. These high volume sources could be an aggregate of bursty sources such as the output of an Ethernet.

At the present state of development optical fiber has properties which heavily influence the topology which is appropriate. With current technology, fiber is inherently a point-to-point medium, since it is not possible to provide a large number of access points without unacceptable loss. This militates against the bus topology which requires a broadcast capability. In order to provide reliability, it is advisable to bring cable to a central point where the operation of individual stations can be monitored, implying the Daisy Chain form of the ring topology or the star topology.

We have designed and implemented a star system consisting of three components: transmission lines, a Central Switch (CS) and User Access Nodes (UAN). As the name implies the User Access Node (UAN) is the point where traffic enters the system. The UANs act as a concentrator and are connected to the (CS) by means of two fibers enabling full duplex operation. The transmission rate over these lines is 50 Mbps. We call the UAN together with the transmission lines an arm. The basic function of the CS is to route high speed data traffic between arms. Considering the magnitudes of the data rates that are involved and the available effective processing, we do not allow data storage in the Central Switch and the data must be handled on the fly. This is done by means of a form of fast circuit switching. In consideration of the traffic volumes that are involved, the number of arms is limited to sixteen.

## CONSTRUCTING SEQUENCES FOR CDMA APPLICATIONS

Gérald Séguin  
 Département de génie électrique  
 Université Laval  
 Québec, CANADA  
 G1K 7P4

Given two binary  $N$ -tuples  $\underline{a}$  and  $\underline{b}$  the  $K$ -th correlation between them,  $F_K(\underline{a}, \underline{b})$ , is defined as  $\sum_0^{N-K-1} a_j b_{j+K}$  for  $0 \leq K < N$  and  $\sum_0^{N-|K|-1} a_{j+|K|} b_j$  for  $-N < K < 0$ ; and  $F(\underline{a}, \underline{b})$  is defined as  $\max_{-N < K < N} |F_K(\underline{a}, \underline{b})|$  if  $\underline{a} \neq \underline{b}$  and as  $\max_{0 < K < N} |F_K(\underline{a}, \underline{a})|$  if  $\underline{a} = \underline{b}$ . In CDMA applications one seeks a set of

sequences  $(\mathcal{U} = \{a^{(i)} \mid i = 1, 2, \dots, M\})$  ( $M$  being the number of users), such that  $F(a^{(i)}, b^{(j)}) \leq \rho$ ,  $\forall i, j \in \{1, 2, \dots, M\}$  and where  $\rho$  is some real number,  $0 < \rho < N$ . At the moment there exists only ad hoc methods of constructing such sets of sequences (see for example the paper by Sarwate and Pursley, Proc. of the IEEE, Vol. 68, No 5, May 1980). In this paper we propose a method of constructing a set of sequences as described above which is based on cyclic codes. The method is partly constructive; but the final step in the construction involves a computer search. The algorithm is based on the following unpublished result:

**THEOREM:** Let  $V_i$  be a cyclic code of odd block length  $N$ , minimum distance  $d_i > 2$  and maximum distance  $D_i$  for  $i = 1, 2$ . Let  $\rho = \max(|N - 2d_1|, |N - 2d_2|, |N - 2D_1|, |N - 2D_2|)$  and let  $\mathcal{U} = V_1 \cap (V_2 \oplus \underline{Z})$  where  $\underline{Z} = (1010 \dots 101)$ ; then

1. All  $N$ -tuples in  $\mathcal{U}$  have cyclic order  $N$ ,
2. All  $N$ -tuples in  $\mathcal{U}$  are cyclically distinct,
3.  $F(\underline{a}, \underline{b}) \leq \rho \quad \forall$  pair of sequences  $\underline{a}$  and  $\underline{b}$  in  $\mathcal{U}$ .

Simple conditions can be derived to ensure that  $\mathcal{U}$  is non-empty. The algorithm consists in first generating  $\mathcal{U}$  (this is easily done) and then purging  $\mathcal{U}$  of its worst elements. Numerical results will be presented along with the underlying theory.

URSI COMMISSION C - SESSION C4

**Spread Spectrum  
Communication**

1:30 - 5:00  
LAW 178

**Communications  
à spectre dispersé**

Chairperson/Président: **M.K. Simon**, Jet Propulsion Laboratory, Pasadena, CA, USA

- 1 (8:40) TRENDS IN SPREAD SPECTRUM SYSTEMS. **F.D. Natali**, Stanford Telecommunications, Inc., Santa Clara, CA, USA
- 2 (9:10) ON THE DESIGN OF EFFICIENT FHMA SEQUENCES. **U. Cheng, C.L. Weber, G.K. Huth**, University of Southern California, Communication Sciences Institute, Los Angeles, CA, USA
- 3 (9:40) SPECTRAL DETECTION ALGORITHMS FOR FH/LPI SIGNALS. **A. Polydoros**, University of Southern California, Communication Sciences Institute, Electrical Engineering Systems, Los Angeles, CA, USA
- 4 (10:10) PERFORMANCE OF MULTITONE FFH/MFSK SPREAD SPECTRUM SYSTEM IN THE PRESENCE OF MULTITONE JAMMING. **G.E. Atkin, I.F. Blake**, University of Waterloo, Dept. of Electrical Engineering, Waterloo, ON
- 5 (10:40) PERFORMANCE OF CODED FFH/MFSK IN INTERFERENCE AND THERMAL NOISE. **U. Cheng, G.K. Huth, C.L. Weber**, University of Southern California, Communication Research Institute, Los Angeles, CA, USA

TRENDS IN SPREAD SPECTRUM SYSTEMS

Dr. Francis D. Natali  
Stanford Telecommunications, Inc.  
2421 Mission College Blvd.  
Santa Clara, CA 95054

Spread spectrum (SS) techniques are finding wider acceptance in both military and civilian applications. This is due to maturing technologies which are "catching up" with the relatively stringent SS synchronization and processing requirements. This talk discusses the types of SS systems which one may expect to be operational through the rest of this decade. The role of existing and emerging technologies will be commented upon.

A brief introductory discussion of SS techniques will be presented for those not familiar with the subject. Some of the salient characteristics of pseudo-noise (PN) and frequency hopped (FH) systems will be presented and the application of SS signalling will be summarized.

Three SS systems will be discussed briefly. The Global Positioning System (GPS), the Equatorial commercial communications system, and a hypothetical FH communications system. These are representative of systems that will be operational in this decade and the early 1990's.

The GPS system is intended to provide accurate worldwide navigation using satellites. A 1.024 Mbps PN-SS signal is available to civilian users. GPS civilian user equipment is expected to represent a major market in the late 1980's.

Equatorial Communications Company utilizes a 2.45 Mbps PN-SS signal to relay data to terminals which may have more than one satellite in view, due to a small antenna aperture. This is an example of a commercial SS communication system with a large number of users.

The potential of such technologies as gallium arsenide (GaAs), charge-coupled devices (CCD), surface acoustic wave devices (SAW) and LSI for providing smaller, lighter, and less expensive equipment will be discussed.

## ON THE DESIGN OF EFFICIENT FHMA SEQUENCES

U. Cheng, C.L. Weber, G.K. Huth  
University of Southern California  
Communication Sciences Institute  
Los Angeles, CA, USA

The design of a set of frequency hopping multiple access (FHMA) sequences depends upon the choice of frequency hopping signal format, the choice of long sequences versus short sequences, and on the available a priori synchronization. Each of these alters the construction process as well as the measure of performance, namely a correlation bound.

First is the choice of frequency hopping signal format. The choices herein considered are: (i) MFSK (or DPSK) without overlap, (ii) MFSK with partial overlap, (iii) MFSK with maximal partial overlap, (iv) Multi-Level MFSK.

Second is the choice of long sequences versus short sequences. By a short sequence, we mean that one period of the sequence occurs during each information symbol.

Third is the level of available a priori synchronization. We distinguish between three situations. (i) Synchronization Level A represents the broadcast channel, wherein there are  $N$  receivers which operate in a receive only mode, and one transmitter which transmits  $N$  different FH signals; (ii) Synchronization Level B assumes there are  $N$  transmitters and  $N$  receivers all of which are a priori totally synchronized. (iii) Synchronization Level C also has  $N$  transmitters and  $N$  receivers, but exhibits no a priori synchronization at all.

The performance measure is to minimize the number of hits between any pair of FHMA sequences under any relative time shift that may be encountered.

A given operational environment will specify the above hypothetical decisions, for which we have the following bounds and algorithms: (1) For the nonsynchronized (Level C) environment, the Hamming, Plotkin, and Elias block code bounds are extended so that they provide an upper bound on the number,  $N$ , of sequences of period  $L$  over an alphabet of size  $Q$  without overlap, and maximum number of hits,  $H$ , over all out-of-phase autocorrelation values and all cross-correlation values. (2) The Hamming, Plotkin, and Elias bounds can also be extended to sets of sequences employing the maximum partial overlap signal format. These bounds apply for all values of  $M$ , including multi-level MFSK, where  $M=Q$ . (3) A prime candidate for construction of excellent sets of FHMA sequences is to begin with the Reed-Solomon (RS) code. A construction process is described, which applies to both the maximum partial overlap and multi-level MFSK signal formats, as well as all synchronization levels. The number of sequences generated meets the Plotkin bound for the maximum overlap signal format, including the special case of multi-level MFSK; in that sense the resulting sets of FHMA sequences are optimum.

SPECTRAL DETECTION ALGORITHMS FOR FH/LPI SIGNALS

by

Andreas Polydoros  
Communication Sciences Institute  
Electrical Engineering/Systems  
University of Southern California  
Los Angeles, CA 90089-0272

The problem of detecting wideband spread-spectrum signals with unknown parameters in strong noise and/or interference is of current interest. Earlier approaches to this problem capitalized on the difference in the energy level between signal-plus-noise hypothesis ( $H_1$ ) and the noise-only hypothesis ( $H_0$ ), thereby utilizing an energy-measuring device (radiometer) as the key detection unit. Clearly, such a solution overlooks potentially known features of the sought signal and is, therefore, suboptimal.

In this talk, we shall review more advanced methods which clearly improve upon the radiometric approach. These new approaches include (1) optimal composite likelihood-ratio procedures, (2) suboptimal versions thereof, (3) the spectral-maximum or periodogram detector, (4) the recently discussed autocorrelation detector, and (5) certain baseband correlation algorithms, resulting from the AR or ARMA spectral modeling of the underlying process. Performance of each of those schemes is quantified either directly by the associated ( $P_D$ ,  $P_{FA}$ ) pair or, indirectly, via an appropriately defined distance measure. Comparison of the resulting performance curves among themselves and with respect to the lower-bounding radiometric performance allows for certain conclusions to be drawn, depending on the desired region of operation.

PERFORMANCE OF A MULTITONE FFH/MFSK SPREAD SPECTRUM  
SYSTEM IN THE PRESENCE OF MULTITONE JAMMING

G.E. Atkin and Ian F. Blake,  
Department of Electrical Engineering,  
University of Waterloo,  
Waterloo, Ontario.

In a fast frequency hopped (FFH) MFSK spread spectrum communication system, the communicator transmits one of  $M$  possible frequencies of power  $S$ , hopping the carrier frequency at a rate of  $R_H$  hops per second. For the tones to be orthogonal, they must be spaced  $R_H$  Hz apart and in a bandwidth of  $W$  Hz,  $W/MR_H$  slots can be accommodated. Thus to communicate one  $M$ -ary symbol the communicator transmits  $L$  tones, one in each successive chip interval, with the slot of each tone being chosen at random. If the jammer has a total power of  $J$  and jams with tones of power slightly greater than  $S$ , then it has been shown that an optimal strategy is to place one tone per slot in  $J/S$  randomly chosen slots. If one of the tones falls in the slot used by the communicator an incorrect choice by the receiver may result.

With no diversity ( $L=1$ ) the probability of error, either bit or symbol, is inversely proportional to the signal-to-noise ratio on the channel. The use of  $L$  diversity improves the situation and the use of coding restores the exponential dependence of the probability of error on the signal-to-noise ratio. There are some unanswered questions on such systems involving the optimum way to combine information in the diversity chip intervals and effective methods of coding for such channels.

This paper considers the situation when the communicator is allowed to transmit more than one tone in any given chip interval. If  $k$  tones are transmitted per chip, each has power  $S/k$ . Likewise the jammer uses tones of power  $S/k$  and jams with  $k$  times the number of tones used previously. Such an assumption opens a variety of new possibilities for diversity and coding and a few of these are examined in this paper. Particular attention is given to the case where two or three tones are transmitted in each chip interval. Questions such as diversity combining are not considered. For the simplified model assumed it is shown that significant gains over the conventional model can be obtained and the analysis of two particular situations is given.

PERFORMANCE OF CODED FFH/MFSK  
IN INTERFERENCE AND THERMAL NOISE

by

U. Cheng  
G.K. Huth  
C.L. Weber

The performance of fast frequency hopping (FFH) using multiple-frequency-shift-keying (MFSK) modulation and a variety of error-correcting codes is presented. The effect of optimized quantization is compared with linear quadratic detector with and without side-information. It is shown that optimized quantization with clipping acts as a very effective antijam technique. The performance derived in this paper includes the effect of thermal noise, as well as worst case jamming. The results obtained, by taking into account the noncoherent combining losses, are significantly worse than results previously obtained considering only worst case jamming.

The analysis approach used to obtain the probability of bit error derives the exact probability distribution for a single frequency hop, and then determines the overall probability distribution for L hops by taking a discrete convolution.

## URSI COMMISSION C - SESSION C5

**Analog and Digital Filtering  
Techniques and Applications**

8:30 - 12:00  
LAW 178

**Théorie de filtrage  
analogiques et numériques  
et leurs applications**

Chairperson/Président: **A. Antoniou**, University of Victoria, Dept. of Electrical Engineering, Victoria, BC

- 1 (1:40) APPLICATION OF RECURSIVE 2D DIGITAL FILTERS TO IMAGE PROCESSING. **L.T. Bruton**, University of Victoria, Faculty of Engineering, Victoria, BC
- 2 (2:10) DESIGN AND APPLICATION OF SWITCHED-CAPACITOR FILTERS. **A.S. Sedra**, University of Toronto, Dept. of Electrical Engineering, Toronto, ON
- 3 (2:40) DESIGN AND APPLICATION OF ADAPTIVE FILTERS. **W.B. Mikhael**, West Virginia University, Dept. of Electrical Engineering, Morgantown, WV, USA
- 4 (3:10) QUANTIZATION EFFECTS IN DIGITAL FILTERS. **L.E. Turner**, University of Calgary, Dept. of Electrical Engineering, Calgary, AB
- 5 (3:40) DESIGN OF WEIGHTED-CHEBYSHEV NONRECURSIVE DIGITAL FILTERS. **A. Antoniou**, University of Victoria, Dept. of Electrical Engineering, Victoria, BC
- 6 (4:10) PROLATE SPHEROIDAL DIGITAL FILTERING. **B.P. Sinha, V. Neelakantan**, Memorial University of Newfoundland, Faculty of Engineering, St. John's, NF

## C-5-1

### APPLICATION OF RECURSIVE 2D DIGITAL FILTERS TO IMAGE PROCESSING

by L.T. Bruton  
Faculty of Engineering  
University of Victoria

An outstanding problem in the design of recursive 2D digital filters has been to obtain stable algorithms having low quantization errors that meet prescribed frequency response characteristics. In recent years, researchers have developed stable algorithms that yield highly selective 2D frequency response characteristics. However, such algorithms are usually very sensitive to quantization of the coefficients of the 2D difference equation and, in many practical situations, require long multiplier coefficient wordlengths of 32-64 bits. This invariably slows down the calculation and requires extensive hardware. Therefore, it is of interest to search for new 2D algorithms that implement a required stable 2D difference equation using shorter wordlengths.

In this contribution, a 2D integrator-type signal flow graph structure is presented that leads to algorithms having significant reductions in quantization errors and corresponding decreases in the required multiplier coefficient wordlengths. An implementation of this signal flow graph is described that has permitted the construction of a general purpose high speed 2D filter instrument for the enhancement of television images. Experimental results are given to demonstrate the usefulness of this instrument.

Design and Application of Switched-Capacitor Filters\*

Adel S. Sedra  
Dept. of Electrical Engineering  
University of Toronto  
Toronto, Ontario Canada M5S 1A4

Although the principle of generating frequency-selective responses using periodically-switched capacitors has been known since at least the mid 1960s, integrated-circuit (IC) switched-capacitor (SC) filters became a reality only in the late 1970s. Currently, the switched-capacitor technique is the most viable method for implementing precision analog filters in monolithic form. Because they are most suited for MOS technology, SC filters can be fabricated on the same chip together with digital circuitry, thus making possible the realization of mixed analog/digital very-large-scale integrated (VLSI) systems.

Switched-capacitor filters have grown from active-RC filters. The latter utilize op amps together with resistors and capacitors and, depending on production volume, are implemented either on printed circuit boards using IC op amps, metal-film resistors and polystyrene capacitors, or as thick- or thin-film hybrid circuits. Attempts to directly fabricate active-RC filters in monolithic form have not been successful for two reasons: (1) the need for large-valued resistors and capacitors (especially for low-frequency filters), and (2) the need for accurate RC time constants. As shown in this paper, the SC filter technique circumvents both problems.

Switched-capacitor filters are based on the principle that a capacitor C periodically-switched between two circuit nodes at a sufficiently high rate ( $f_c$ ) is approximately equivalent to a resistor  $R = 1/Cf_c$  connecting the two nodes. It is thus possible to realize filter functions using op amps, capacitors and periodically-operated switches. Since MOS technology provides high-quality capacitors, offset-free switches, and moderate-quality op amps it is eminently suited for the realization of SC filters.

Switched-capacitor filters have two other features that make them particularly suited for MOS IC technology: (1) large resistors can be simulated using small-sized capacitors, and (2) the precision of the realized frequency response is dependent on the precision of the clock frequency and the tolerance to which capacitor ratios are implemented.

This paper outlines practical methods for the synthesis and design of switched-capacitor filters. Also, the areas of applicability of such filters are delineated, and predictions are offered on the future development of this highly-promising circuit technique.

## DESIGN AND APPLICATION OF ADAPTIVE FILTERS

W. B. Mikhael  
Department of Electrical Engineering  
West Virginia University  
Morgantown, WV 26506

An adaptive system comprises mainly of three components: the system signals, the adaptive filter (processor or structure) and the adaptive algorithm. In adaptive signal processing, the algorithm examines the system signals periodically and modifies the parameters of the adaptive filter in a manner that minimizes, in some sense, an unwanted signal. This unwanted signal is normally derived or closely related to the signal obtained by subtracting the signal processed by the adaptive filter from a reference process or desired signal.

The areas of adaptive signal processing and adaptive control have grown at a fast rate in recent years. More demanding systems specifications coupled with the spectacular developments in integrated circuits and digital computing motivated the search and design of adaptive systems. These systems employ sophisticated processing algorithms capable of operating in uncertain, time-varying environments. Some of the wide variety of recent applications include noise and echo cancellation, channel equalization for high speed data transmission, spectral estimation, speech processing, ... etc. Most of the work in these areas model the reference process as an output of a finite order discrete-time linear system driven by white noise. Such processes were called autoregressive (AR) corresponding to all pole z-plane system function or autoregressive moving average (ARMA) corresponding to pole zero z-plane system function.

Adaptive techniques can be characterized according to the application, the type of filter, signal processing domain (time or frequency), and mode (continuous or discrete). The filter structure can be classified as recursive or nonrecursive (transversal). Most of the work reported in adaptive filters concentrated on the discrete-time domain. The transversal filter structure received the researchers attention due to its simplicity in implementation and the convergence properties of the available algorithms. Also, several adaptive algorithms were reported. In addition, adaptive signal processing can be classified broadly from the applications point of view as the identification class or the prediction class.

In this talk, the different aspects of adaptive signal processing will be explained briefly and two applications will be discussed, namely, noise cancellation (identification) and pole-zero modeling of speech (prediction).

## QUANTIZATION EFFECTS IN DIGITAL FILTERS

L.E. Turner  
Department of Electrical Engineering  
The University of Calgary  
Calgary, Alberta, Canada T2N 1N4

The design of a digital filter is based on the theory of linear discrete time systems. However, any practical digital filter implementation will be nonlinear. This nonlinear behavior is due to the finite, quantized nature of the digital values which are used to represent signal levels in the digital filter.

Non-ideal factors which must be considered in any practical digital filter implementation are:

- (1) Signal level quantization occurs at the input to the filter and at any internal filter node where the signal is multiplied by a non-integer value. The effect of signal quantization is often modeled as a linear process with additive, uncorrelated, white noise sources.
- (2) Signal overflow occurs whenever the finite digital signal space available is not large enough to represent the level required. This must be avoided by careful choice of a filter structure and/or reducing the input signal level.
- (3) Multipliers in the filter may have coefficients which are quantized. This quantization causes errors in the filter response. The severity of this effect is directly related to the multiplier sensitivity of the filter structure.
- (4) Recursive digital filters may exhibit undesirable oscillations which are known as limit cycles. These limit cycle oscillations are due to the nonlinear effects of quantization ( and overflow ) in the recursive section of a digital filter. The amplitude of these limit cycles may be large and therefore they must be controlled or eliminated.

If practical digital filter implementations were linear systems then the choice of a particular filter structure would be based only on the number of components required. However, every different digital filter structure has a different non-linear behavior which must be accounted for in any cost versus performance comparison.

## DESIGN OF WEIGHTED-CHEBYSHEV NONRECURSIVE DIGITAL FILTERS

A. Antoniou  
Department of Electrical Engineering  
University of Victoria  
Victoria, British Columbia  
Canada V8W 2Y2

One of the most important methods for the design of nonrecursive digital filters is the weighted-Chebyshev method proposed by Rabiner, McClellan and Parks. This is essentially a multivariable optimization technique in which the maxima of the error function are minimized using the Remez exchange algorithm.

This is a very versatile design method and it can be used to obtain optimal equiripple designs for most types of nonrecursive filters like lowpass, highpass, bandpass, and bandstop filters, Hilbert transformers, and digital differentiators. Unfortunately, however, it entails a considerable amount of computation. If  $N$  is the number of samples in the impulse response, at least  $8(N-1)$  function evaluations are required per Remez iteration, where a function evaluation entails  $N-1$  additions,  $(N+1)/2$  multiplications, and  $(N+1)/2$  divisions. A Remez optimization usually requires four to eight iterations for lowpass or highpass filters, six to ten iterations for bandpass filters, and eight to twelve iterations for bandstop filters. Further, if prescribed specifications are to be achieved and the appropriate value of  $N$  is unknown, two to four Remez optimizations have to be performed. For example, if  $N=101$ , Remez optimizations=4, iterations per optimization=6, function evaluations per iteration= $8(N-1)$ , the design would entail 24 iterations, 19,200 function evaluations, 1,920,000 additions, 979,000 multiplications, and 979,000 divisions. Further, a significant amount of overhead computation would be required for each iteration.

In this paper, the Rabiner, McClellan, and Parks method is described and the source of the considerable amount of required computation is identified. Then several techniques are described which reduce the amount of required computation by as much as 87 percent, without degrading the robustness of the method. This improvement renders the design of high-order filters possible on small computers and workstations.

## PROLATE SPHEROIDAL DIGITAL FILTERING

B.P. Sinha and V. Neelakantan  
 Faculty of Engineering  
 Memorial University of Newfoundland  
 St. John's, Nfld., Canada A1B 3X5

**Abstract:** The use of Digital Prolate Spheroidal Wave Functions (DPSWF) in the field of digital filtering has increased steadily during the past decade. The unique property; that DPSWF provide maximum concentration of signal energy in the passband of a low-pass filter has been the basis of most of the work done in the area of digital filter design involving prolate functions. The maximization of energy corresponds to the largest eigenvalue  $\lambda_0$  which belongs to the lowest order ( $k=0$ ) of the eigen function  $U_k$  satisfying the eigen function equation (D. Slepian, Bell Sys. Tech. J., 57, 1371-1429, 1978)

$$\int_{-W}^W \frac{\sin N \pi (f-f')}{\sin \pi (f-f')} U_k(N,W; f') df' = \lambda_k(N,W) U_k(N,W; f),$$

$k = 0, 1, 2, \dots, N-1$  and  $-\infty < f < \infty$ , where  $N$  = the order of the filter,  $W$  = normalized bandwidth. The eigen values  $\lambda_k$  are such that  $\lambda_0 > \lambda_1 > \lambda_2, \dots > \lambda_{N-1}$ .

It is however, desirable to investigate the effect of higher order eigen functions in addition to the lowest order one on the filter characteristics and performance. This paper is the outcome of such investigations. A suitably weighted linear combination of those DPSWF which are even functions of frequency is made to approximate an ideal low-pass characteristic in the minimum mean squared error (MMSE) sense.

Results employing various numbers of even prolate functions are obtained and compared with each other and with the maximum energy concentration case. It is very satisfying to note that the flatness of the passband of a low-pass filter is greatly improved with the number of even prolate functions while maintaining a tolerable loss of energy in the passband.



## URSI COMMISSION E - SESSION E1

**Radio Noise Measurements  
and Modeling**

8:30 - 12:00

LAW 178

**Mesure et modélisation  
des bruits radio-électriques**Chairperson/Président: **A.D. Spaulding**, Institute for Telecommunications Sciences, Boudler, CO, USA

- 1 DEVELOPMENT OF A MINICOMPUTER 1 MHz ATMOSPHERIC NOISE MODEL IN LOCAL TIME. **D.B. Sailors**, Naval Ocean Systems Center, Ocean and Atmospheric Sciences Division, San Diego, CA, USA
- 2 THEORETICAL PREDICTION OF IMPULSIVENESS RATIO IN AN EXPANDED BANDWIDTH. **A.A. Giordano, G.P. Brefini, P. Lusardi**, GTE Government Systems Corporation, Communication Systems Division, Needham Heights, MA, USA
- 3 ON THE DIFFERENCES BETWEEN STATISTICAL MOMENTS OF REAL NOISE AND HALL MODEL NOISE. **J.R. Herman, X. DeAngelis**, GTE Government Systems Corporation, Strategic Systems Division, Westborough, MA, USA
- 4 A NEW MODEL FOR AUTO-IGNITION NOISE IN MOBILE DATA CHANNEL. **A.U.H. Sheikh, H. El-Damhoughy**, Carleton University, Dept. of Systems and Computer Engineering, Ottawa, ON
- 5 ELF EFFECTIVE NOISE MEASUREMENTS. **P.R. Bannister**, Naval Underwater Systems Center, System Analysis Branch, New London, CT, USA
- 6 TIME BEHAVIOR OF 160 KHz ATMOSPHERIC NOISE. **S.H. Knowles**, Naval Research Laboratory, E.O. Hulbert Center for Space Research, Washington, DC
- 7 THE NEAR-SPACE RFI ENVIRONMENT AS OBSERVED USING VHF LUNAR REFLECTIONS. **W.T. Sullivan III**, University of Washington, Dept. of Astronomy, Seattle, WA, USA; **S.H. Knowles**, Naval Research Laboratory, E.O. Huebert Center for Space Research, Washington, DC, USA
- 8 SWEEPERS IN THE HF/VHF BANDS. **A.K. Sen, S.K. Trehan, S. Shekhar De**, University of Calcutta, Institute of Radio Physics and Electronics, Calcutta, India; **J. Das, D.Dutta Majumder**, Indian Statistical Institute, Calcutta, India; **J.S. Sehra, S.K. Das**, Dept. of Electronics and Govt. of India, India

## E-1-1

### DEVELOPMENT OF A MINICOMPUTER 1 MHZ ATMOSPHERIC NOISE MODEL IN LOCAL TIME

D. B. Sailors  
Ocean and Atmospheric Sciences Division  
Naval Ocean Systems Center  
San Diego, CA 92152-5000

A practical but simplified atmospheric noise model in 1-MHz  $F_{am}$ , median value of the hourly values in a time block of the effective antenna noise-factor  $F_a$ , mapped in local time is presented. It is usable in estimating system signal-to-noise ratios in microminicomputer-based HF propagation prediction systems. Numerical mapping techniques like those used to represent worldwide atmospheric noise in universal time (D. B. Sailors and R. P. Brown, Radio Science, 18, 625-637, 1983) were modified to produce numerical maps in local time. In local time the gradients of atmospheric noise as a function of longitude are much smaller than those in universal time. In each and every case the local time numerical map has a lower rms error than the corresponding universal time map. However, the local time Lucas and Harper model (D. L. Lucas and J. D. Harper, Jr., NBS Tech. Note 318, 1965) is not always more accurate than the universal time Zacharisen and Jones model (D. H. Zacharisen and W. B. Jones, OT/ITS Research Report 2, 1970).

**THEORETICAL PREDICTION OF IMPULSIVENESS RATIO  
IN AN EXPANDED BANDWIDTH**

Arthur A. Giordano, Gary P. Brefini, Paul Lusardi

GTE Government Systems Corporation  
Communication Systems Division  
77 "A" Street  
Needham Heights, Massachusetts 02194

$V_d$ , the rms to average envelope ratio, is a single parameter measure of the impulsiveness of atmospheric noise. Accurate knowledge of  $V_d$  in the bandwidth of interest is essential for determining system performance in a digital communication system. The variability of this parameter with bandwidth changes has been previously investigated by theoretical analysis and by use of measured medium frequency data recorded in a 100 KHz bandwidth. Here a theoretical result, based on a truncated Hall model, yields a set of curves for  $V_d$  in a wide bandwidth as a function of  $V_d$  in a narrow bandwidth and the bandwidth expansion ratio. This theoretical bandwidth expansion result is then compared to data extracted from CCIR Report 322 and from the available measured data. The results indicate that the slopes of the curves are less than those obtained in CCIR Report 322 but greater than those obtained from measured data.

## E-1-3

### ON THE DIFFERENCES BETWEEN STATISTICAL MOMENTS OF REAL NOISE AND HALL MODEL NOISE

John R. Herman and Xavier DeAngelis

GTE Government Systems, Strategic Systems Division, 1 Research Drive,  
Westborough, MA 01570

The Hall model of atmospheric radio noise has gained wide acceptance since its introduction in 1966, for it gives a generally reasonable representation of impulsive noise. However, in comparing it to medium frequency (MF) measured atmospheric noise a number of interesting differences appear. Analysis software developed by GTE has been utilized to obtain the statistical characteristics of measured atmospheric radio noise as described at previous USNC/URSI National Radio Science Meetings. Recently, Hall noise was played through the same software to obtain crossing rates and pulse statistics to determine how well the model approximates the higher order statistical behavior of real atmospheric noise. The pulse spacing and duration distributions for Hall noise follow a Poisson distribution, as expected, and are in contrast to the distributions found for measured noise. A depiction of pulse repetitions shows graphically the burst-like, grouped character of MF measured noise pulses which leads to the peculiar tail on the spacing distribution. Errors in digital data streams recorded by communications receivers operating in the presence of atmospheric noise are expected to follow the burst patterns of the noise itself.

## A NEW MODEL FOR AUTO-IGNITION NOISE IN MOBILE DATA CHANNEL

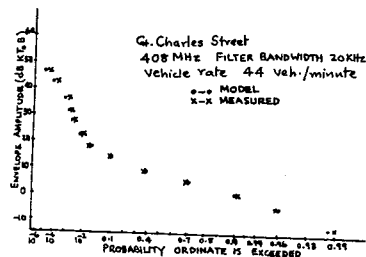
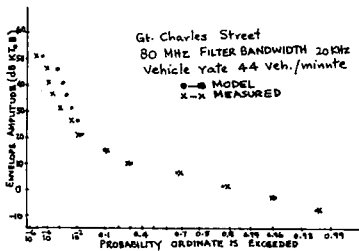
A.U.H. Sheikh and H. El-Damhoughy  
 Department of Systems and Computer Engineering,  
 Carleton University, Ottawa, Canada K1S 5B6

Abstract: Increased interests have been shown, recently, in implementation of digital transmission over mobile radio channels. In this paper we will be concerned only with mobile channel impulsive noise characterization. The presence of impulsive noise produces bursts of errors. We propose, a simple model for first order noise statistics (APD) to be used in prediction of error rates.

Noise Model: The composite noise at the receiver input is given by  $n(t) = \sum_{i=0}^K n_i(t)$ , where  $n_0(t)$  is background noise and  $n_i(t)$ ,  $i \neq 0$  are the impulsive noise components emitted by a number  $K$  (bounded by a low value  $\leq 5$ ) of sources. These sources can be assumed to be entering a zone of influence at a certain speed with Poisson arrival times. The victim receiver is affected by the sources in manner definable in terms of a queueing (M/M/k) model. The probability distribution of the composite noise is given by

$$f_I(x) = P_0 f_G(x) + P_1 f_G(x) * f_1(x) + \dots + P_K f_G(x) * f_1(x) * \dots * f_1(x)$$

where  $f_G(x)$  is the APD of background noise  $f_1(x)$  is the APD of a single car noise. The service time is related to the time for which a certain vehicle remains in the zone of influence and arrival times are considered to be Poisson distributed. From the receiver sensitivity point of view, the radius of the zone of influence is taken to be 100 feet and at a given average speed, there is a maximum of 3 cars affecting the receiver at any time. From these considerations and noting that convolution of Rayleigh and log normal distributions is given by a Rayleigh distribution at low levels and log normal at high levels, we can calculate the APD. The APD was calculated for given environmental conditions using the proposed model and compared with the measured results. The K-S test for goodness of fit, was applied, and a confidence factor in excess of 86% was obtained. It was thus concluded that this model is acceptable from the applications point of view.



## E-1-5

### ELF EFFECTIVE NOISE MEASUREMENTS

Peter R. Bannister  
Naval Underwater Systems Center  
New London, CT 06320

In the ELF (30 to 300 Hz) and VF (300 Hz to 3 kHz) bands, atmospheric noise is the limiting factor to receiver performance under most operating conditions. The dominant source of atmospheric noise is radiation induced by lightning. Owing to the low attenuation rate of ELF radio waves, which makes long range communication possible in this band, noise characteristics are affected not only by local thunderstorms, but also by storms megameters away. The effect of local thunderstorms is to produce large spikes, while the effect of distant storms is a background noise with occasional spikes. Even in relatively quiet parts of the world, spikes attributed to individual lightning strokes are evident, making the noise distinctly non-Gaussian.

The non-Gaussian nature of the atmospheric noise has an important effect on receiver design and on system performance. With Gaussian noise, the optimum receiver is a linear processor whose performance can be determined by measuring the noise spectra. However, with non-Gaussian noise, the performance of a linear processor can be much worse than is suggested by the noise spectra. Furthermore, with an appropriate (nonlinear) processor, the performance can be much better than with Gaussian noise of the same spectral level.

To optimize a communication receiver for operation in a non-Gaussian noise environment, it is desirable to place a controlled nonlinearity in the receiver at a stage of wide signal-plus-noise bandwidth to remove the high amplitude spikes. Various experiments with recorded ELF noise have concluded that a simple clipper, adjusted adaptively to clip between 10 and 40 percent of the time, provides near-optimum performance.

From 1976 to 1978 and 1982 to 1984, ELF field strength and effective noise measurements were taken continuously in Connecticut and sporadically at other land and sea sites. (The effective noise spectrum level is defined as the spectrum level of ELF noise at the signal frequency divided by the improvement, in signal-to-noise ratio, using nonlinear processing.) In this presentation, we will summarize the effective noise measurements taken at both land and sea locations during these periods.

## TIME BEHAVIOR OF 160 KHz ATMOSPHERIC NOISE

S. H. Knowles  
Naval Research Laboratory  
E.O. Hulburt Center for Space Research  
Space Science Division, Ionospheric Effects Branch  
Washington, DC 20375-5000

A reasonably extensive sample of 160 KHz atmospheric noise has recently been obtained near Washington, DC (S.H. Knowles, F.J. Kelly, S. Odenwald, and W.B. Waltman, Radio Science, in press). This data was recorded in fully coherent form, which enabled post-analysis of its statistical characteristics. Analysis of these characteristics has now been made, with emphasis on thorough treatment of the time behavior of the noise. Samples of time-behavior are presented, including strong thunderstorm activity. In addition to the customary time probability distribution statistics, other statistics are presented which may offer a fuller insight into the noise time behavior. These include auto-correlation and power spectra, as well as typical energy profiles. Comparison with C.C.I.R. parameterization will be made. It is found that time behavior statistics are not stationary, and that bursts lasting a large fraction of a second can occur during typical thunderstorm conditions. Brief comments will be made on the applicability of this analysis to modem design.

## E-1-7

### THE NEAR-SPACE RFI ENVIRONMENT AS OBSERVED USING VHF LUNAR REFLECTIONS

Woodruff T. Sullivan, III (Univ. Washington)  
and

Stephen H. Knowles (Naval Research Lab)

Manned terrestrial radio leakage as reflected off the moon has been observed with the 305 meter Arecibo antenna. The nature and intensity of this leakage gives one some indication of the radio-frequency interference environment for operations in space in the 150-500 MHz range. As predicted in the model of Sullivan et al. (1978, Science 199, 377), we find that military radars and television transmitters are main contributors.

The experiment consisted of observing both on the moon and on a nearby patch of blank sky (as a way to identify local interference) for three nights using a 1008 channel 10 MHz autocorrelation spectrometer at a variety of VHF frequencies. Television video carriers for a wide variety of international frequency allocations were observed, along with various narrowband signals which could not be identified. In addition, a synoptic series of 182-192 MHz spectra revealed the expected intensity variations as the earth's rotation caused transmitters on different regions of the globe to sweep across the moon.

The moon, like the earth, is remarkably bright at radio frequencies. The present brief study lends experimental support to the basic model of Sullivan et al.: the earth indeed is revealing itself to any interstellar eavesdropper who uses the equivalent of an Arecibo antenna at distances up to 30 light years, or who uses a Cyclops system (1000 100 meter dishes) up to fifteen times farther away.

Further details are now in press for IEEE Trans. EMC.

## SWEEPERS IN THE HF/VHF BANDS

A.K. Sen, S.K. Trehan, S. Shekhar De  
Institute of Radio Physics and Electronics  
University of Calcutta, India

J. Das and D. Dutta Majumder  
Indian Statistical Institute  
Calcutta, India

J.S. Sehra and S.K. Das  
Department of Electronics and Govt. of India

A sweeper is a peculiar radio noise in the form of a swept frequency carrier modulated by a repetitive pulse waveform, observed in Calcutta, India (A.K. Sen and S.K. Trehan, Ind. J. Radio and Space Physics, 6,117-119, 1977). The sweepers occur in the H F band between 25-30 MHz as well as at the VHF harmonic bands. The diurnal and seasonal variations of the sweepers indicate some ionospheric control of the rate and intensity of sweepers. Such a control is also evidenced during a solar flare as well as during a solar eclipse. Besides the observations at Calcutta the sweepers have been noticed also in Delhi, Bombay and even in U.K. from which it appears that it is a worldwide phenomena. All the parameters of a sweeper, such as the rate of sweep, duration and repetition, rate of the pulse modulation, exhibit random variability. This suggests a geophysical origin of the sweepers. Whatever might be the origin of the sweepers, the intensity to which a sweeper builds up and its continuity of occurrence at least for the last 7 years during which it was observed appears to call for a revision of the radio noise data in the HF-VHF bands in which a sweeper is noticeable. In particular the pulse modulations of a sweeper have got a sizeable annoyance value, as the peak to average level of the modulation is appreciable. Some of the interesting characteristics of the sweepers observed in Calcutta is presented in this paper. The probably sources of origin of the sweepers are also discussed.



## URSI COMMISSION E - SESSION E2

Receiver Performance  
in Radio Noise1:30 - 5:00  
LAW 178Performance des récepteurs  
en présence de bruits  
radio-électriquesChairperson/Président: **J.M. Morris**, Howard University, Washington, DC, USA

- 1 ERROR CONTROL AND SYNCHRONIZATION ON RAYLEIGH FADING CHANNELS. **P.F. Driessen**, MDI Mobile Data International Inc., Vancouver, BC
- 2 SIMULATION OF BIT ERROR PATTERNS AND PULSE STATISTICS OF PSK AND MSK RECEIVER MODELS IN ATMOSPHERIC RADIO NOISE. **P.D. Stynes**, GTE Government Systems, Strategic Systems Division, Westborough, MA, USA
- 3 CONVOLUTIONAL CODE PERFORMANCE IN IMPULSIVE OR BURST NOISE CHANNELS. **J.W. Modestino, K.R. Matis**, Rensselaer Polytechnic Institute, Dept. of Electrical, Computer and Systems Engineering, Troy, NY, USA
- 4 PERFORMANCE ANALYSIS OF DS/SSMA RECEIVERS IN NON-GAUSSIAN NOISE. **B. Aazhang, H. V. Poor**, University of Illinois at Urbana-Champaign, Coordinated Science Laboratory, Urbana, IL, USA
- 5 ON HARD-LIMITING IN SAMPLED BINARY DATA SYSTEMS. **N.C. Beaulieu, C. Leung**, University of British Columbia, Dept. of Electrical Engineering, Vancouver, BC
- 6 ACTUAL VERSUS THEORETICAL PERFORMANCE OF LOCALLY OPTIMUM AND SUB-OPTIMUM DETECTOR PERFORMANCE IN NON-GAUSSIAN INTERFERENCE ENVIRONMENTS. **A.D. Spaulding**, National Telecommunications and Information Administration, Institute for Telecommunication Sciences, Boulder, CO, USA
- 7 DETECTION OF NARROWBAND SIGNALS IN NON-GAUSSIAN NOISE. **S.A. Kassam**, University of Pennsylvania, Dept. of Electrical Engineering, Philadelphia, PA, USA
- 8 A SUBOPTIMAL RANDOM-THRESHOLD, MULTISAMPLE DECISION RULE AGAINST KNOWN SIGNALS WITH ADDITIVE AMPLITUDE-BOUNDED RANDOM INTERFERENCE. **J.M. Morris, N.E. Dennis**, Howard University, Electrical Engineering Dept., Washington, DC, USA

## E-2-1

### ERROR CONTROL AND SYNCHRONIZATION ON RAYLEIGH FADING CHANNELS

Peter F. Driessen  
MDI Mobile Data International Inc.  
Vancouver, B.C. Canada

In the design of synchronization and error control schemes for fading mobile radio channels, it is important to know both the mean and the distribution of the fade lengths which must be accommodated.

The mean fade length  $\bar{\tau}$  for a Rayleigh fading channel is given in terms of the Doppler frequency  $f_d$  and the signal level  $\rho$  below the mean signal level at which a fade is deemed to occur (W.C. Jakes Microwave Mobile Communications, Wiley, 1974). The distribution of the fade lengths  $\tau$  about  $\bar{\tau}$  is approximated by an exponential law

$$p(\tau \geq n\bar{\tau}) = 10^{-n/2} \text{ for } n \geq 2$$

The validity of this approximation is verified by comparison with previous results (G.A. Arrendondo, J.I. Smith, IEEE Trans. VT-26, 88-93, 1977)(M.R. Karim, IEEE Trans. VT-31, 1-6, 1982) for an SNR of 10-15 dB and  $n \leq 8$ .

If a hypothetical modem has a bit error rate which is approximated to be zero for SNR greater than  $\rho$  and 0.5 for SNR less than  $\rho$  (i.e. a rectangular instead of an exponential BER vs SNR curve), then the burst error length distribution is equivalent to the fade length distribution. For a real modem with an exponential BER vs SNR curve, the burst error length distribution at a given SNR will be similar to the fade length distribution for  $\rho$  somewhat greater than the SNR. The smaller the difference ( $\rho - \text{SNR}$ ) the better the performance of the modem. This result is verified by simulation for two different continuous-phase FSK modulation formats. Thus the rectangular approximation to the exponential BER vs SNR curve is valid and the fade length distribution can be used to predict the distribution of burst error lengths.

The successful message probability for various synchronization and error-correcting codes on Rayleigh fading channels is calculated using the burst error length distribution.

Tradeoffs in choosing block size and the ratio of information bits to total bits are discussed.

**Simulation of Bit Error Patterns and Pulse  
Statistics of PSK and MSK Receiver Models  
in Atmospheric Radio Noise**

**Peter D. Stynes**

GTE Government Systems  
Strategic Systems Division  
One Research Drive  
Westborough, MA 01581

Digitized samples of experimentally recorded atmospheric noise have been combined in a computer simulation with PSK and MSK signalling to represent a radio communications link. Appropriate computer models of several receiver types terminated the link. Bit error streams from this link were monitored, for various signal to noise levels. Error pulse duration and spacing statistics were collected.

Such error pulse statistics are useful in the efficient design of error correction coding schemes to use with atmospheric noise. They also partially illuminate the higher order time statistics of the noise itself, which are tracked by the simpler error statistics of the modulations. Further, they offer a test for the partial validation of noise models. Each of these topics are discussed in this paper.

The noise samples were collected in the MF band by previous experimenters. They were gathered in a 100 KHz bandwidth about a 450 KHz center frequency: as a part of the present work they were filtered to a 2 KHz bandwidth. Two segments of noise have been used, each about 30 seconds duration, one at a high and one at a moderate level of impulsiveness as indicated by  $V_d$ .

Convolutional Code Performance in Impulsive  
or Burst Noise Channels

J. W. Modestino and K. R. Matis  
Electrical, Computer and Systems Engineering Department  
Rensselaer Polytechnic Institute  
Troy, New York 12181

## Abstract

We consider the performance of short constraint-length convolutional codes in conjunction with coherent BPSK modulation in impulsive or burst noise channels when an imperfect erasure mechanism is used to exorcise symbols contaminated by noise hits. The erasure mechanism is a simple hole-puncher operating on the sampled matched filter outputs and is characterized by a fixed false alarm probability  $P_F$  and a miss probability  $P_M$ . This scheme is representative of a large number of erasure declaration strategies. Some general conclusions are drawn on the basis of cutoff rate arguments under an idealized channel modeling assumption. For short constraint-length convolutional codes we provide tight upper bounds on bit error probability performance under the same idealized channel modeling assumptions. These bounds compare favorably with simulation results for both randomly occurring and periodic noise hits. Departures from idealized channel modeling assumptions are investigated through simulation. Results indicate an important distinction between the case of random and periodic noise hits and has implications for the use of interleaving in impulsive or burst noise channels. The significance of these results to real-world channels is described through consideration of a particular physical impulsive noise channel exhibiting many of the properties of the idealized channel model. It is expected that the results are applicable to more general interference channels exhibiting burst characteristics.

**PERFORMANCE ANALYSIS OF DS/SSMA RECEIVERS IN NON-GAUSSIAN NOISE**

by

Behnaam Aazhang and H. Vincent Poor  
Coordinated Science Laboratory  
University of Illinois at Urbana-Champaign  
1101 W. Springfield Ave.  
Urbana, IL 61801

Performance of DS/SSMA receivers is studied in a multi-user environment. Data transmission is over a non-Gaussian channel. The contribution of the non-Gaussian noise is examined by modeling the samples of noise after front-end filtering. The multi-user interference is accounted for by considering  $K$  users transmitting over the channel using the binary PSK direct-sequence SSMA technique. Computationally simple method for evaluating the average error probability of the linear correlation receiver is suggested when the length of the signature sequence is large. Some asymptotic results are obtained when infinitely long sequences are used.

## E-2-5

### ON HARD-LIMITING IN SAMPLED BINARY DATA SYSTEMS

Norman C. Beaulieu and Cyril Leung  
Dept. of Electrical Engineering  
The University of British Columbia  
Vancouver, B.C. V6T 1W5

The optimum detection procedure for a number of hard-limited independent samples in a binary data system is derived. The processing is characterized by a set of optimal weights. The optimal weights are derived for an arbitrary noise environment. The relation of the optimum weights to some weighting functions previously proposed in the literature is described. In particular, examples of when previous weighting functions are optimal and suboptimal are given.

The loss of optimality incurred as a result of hard-limiting in a binary system with gaussian noise is investigated. The penalty, which is defined in the signal detectability sense, is expressed as a function of the signal-to-noise ratio of the input samples for some specific sample sizes. Explicit formulae for the loss as a function of the number of samples are presented for the cases of high and low signal-to-noise ratio.

ACTUAL VERSUS THEORETICAL PERFORMANCE OF LOCALLY  
OPTIMUM AND SUB-OPTIMUM DETECTOR PERFORMANCE IN  
NON-GAUSSIAN INTERFERENCE ENVIRONMENTS

A. D. Spaulding

National Telecommunications and Information  
Administration, Institute for Telecommunication  
Sciences

Boulder, Colorado 80303

Since the normally assumed white Gaussian noise is the most destructive in terms of minimizing channel capacity, substantial improvement in system performance can usually be obtained if the real-world interference environment (highly non-Gaussian) is properly taken into account in the design of the detector structure. Here the performances of the locally optimum Bayes detector (LOBD) and various ad-hoc non-linear detectors are compared both theoretically and "measured" from computer simulation of the detectors and interference processes. Two classes of interference are considered; Class A, characteristic of collections of narrowband interfering signals and coherent pulse trains, and Class B, characteristic of broadband impulsive noise. It is demonstrated that the standard theoretical results can be misleading because of the assumptions that are required in order to analytically derive them. The critical assumptions of "sufficiently" small signal level and large number of samples (large time-bandwidth product so that the Central Limit Theorem applies) may not be appropriate in actual physical situations. Extensive sets of results for the coherent phase shift keying (CPSK) system are given as an example. One result is that there are situations where the band-pass limiter (sub-optimum), for example, outperforms the LOBD (locally optimum) as the signal level increases. Another example shows situations where the LOBD becomes drastically (even inferior to a linear detector) sub-optimum.

## DETECTION OF NARROWBAND SIGNALS IN NON-GAUSSIAN NOISE

Saleem A. Kassam  
Department of Electrical Engineering  
University of Pennsylvania  
Philadelphia, PA 19104

It is well-known that in many communication systems the corrupting noise arising from sources such as atmospheric disturbances, and from man-made sources, is non-Gaussian. In particular, such noise is generally characterized by probability density functions which are much more heavy-tailed than the Gaussian density. While much attention has previously been focused on the design of optimum detection systems for Gaussian noise environments, more recently there has been increasing interest in the study of detectors for signals in such non-Gaussian noise.

In this paper we will present the results of recent work on the general structure of detectors for narrowband signals in non-Gaussian narrowband noise. For situations where the non-Gaussian noise is in addition only incompletely characterized, we consider the use of nonparametric hard-limiting schemes and also robust non-linear detectors for improved stability of performance. Both the coherent and non-coherent case of narrowband signals are considered, and detectors are examined which may be described as being of the generalized-narrowband-correlator types. Some considerations of quantization and extension of the results to the random signal case are also discussed.

The primary criterion of performance is the relative efficiency in the asymptotic case, which is particularly relevant in the case of weak-signal detection. It is shown that the non-linear schemes can provide a very considerable degree of performance improvements over linear schemes when non-Gaussian noise is present.

A SUBOPTIMAL RANDOM-THRESHOLD, MULTISAMPLE DECISION RULE AGAINST KNOWN SIGNALS WITH ADDITIVE AMPLITUDE-BOUNDED RANDOM INTERFERENCE

Joel M. Morris & Neville E. Dennis  
Electrical Engineering Department  
Howard University  
Washington, D.C. 20059

A random-threshold multi-sample decision rule against known signals with additive, unknown-mean, amplitude-bounded, random interference is proposed as an extension to a single-sample robust (minimax) decision rule ([1]). Simulated probability-of-error ( $P_e$ ) performance results are presented for a variety of non-Gaussian noise models: (1) Middleton's Class A canonical model ([2]); (2) El-Sawy's least favorable noise model [3]; (3) the sum of two Gaussians; and (4) the Rayleigh. The results show that a lower bound on the performance is determined by the related single-sample robust decision rule result; and is achieved by zero-mean symmetrical-density noise models. This lower bound is shown to be given by:

$$P_e(\lambda) = \frac{1}{2} \left[ \sum_{k=0}^{\lambda-1} \binom{M}{k} \left( \frac{N+1}{2N} \right)^k \left( \frac{N-1}{2N} \right)^{M-k} + \sum_{k=\lambda}^M \binom{M}{k} \left( \frac{N-1}{2N} \right)^k \left( \frac{N+1}{2N} \right)^{M-k} \right]$$

where  $\lambda$  is the optimal integer fixed threshold,  $N$  is the number of thresholds, and  $M$  is the number of samples accumulated before making a decision.

The performance of this decision rule is compared with, and shown to be better than, that of the sign detector, which is a non-parametric decision rule against symmetrical-density noise. The performance comparisons are depicted in terms of theoretical and simulated  $P_e$  vs  $M$  curves parameterized by  $N$  ([4]).

#### References

- [1] J.M. Morris, "On Single-Sample Robust Detection of Known Signals with Additive Unknown-Mean Amplitude-Bounded Random Interference - Part II: The Randomized Decision Rule Solution", IEEE Trans. Inform. Theory, Vol. IT-27, no. 1, pp. 132-136, Jan., 1981.
- [2] D. Middleton, "Canonical non-Gaussian noise models: Their implications for measurement and for prediction of receiver performance," IEEE Trans. Electromagn. Compat., Vol. EMC-21, pp. 209-220, Aug. 1979.
- [3] A.H. El-Sawy, V. David Vandelinde, "Robust Detection of Known Signals", IEEE Transactions on Information Theory, Vol. IT-23, No. 6, pp. 722-727.
- [4] N.E. Dennis, "Simulation of Suboptimal Multisample Decision Rule", Master's Thesis, Electrical Engineering Department, Howard University Washington, D.C., Sum. 84.



## URSI COMMISSION F - SESSION F1

## Scattering Theory

8:30 - 12:00

## Théorie de la diffusion

LAW 101

Chairperson/Président: **J. Kong**, Massachusetts Institute of Technology, Cambridge, MA, USA

- 1 TRANSFER FUNCTIONS OF SCATTERING POINTS. **S.M. Sherman**, Cherry Hill, NJ, USA
- 2 THE COHERENT EFFECTIVE FIELD IN A DENSELY POPULATED, CORRELATED MEDIUM. **M.A. Karam, A.K. Fung**, University of Texas at Arlington, College of Engineering, Arlington, TX, USA
- 3 BISTATIC SCATTERING FROM METAL CUBES: THEORY AND EXPERIMENT. **R.V. McGahan**, Rome Air Development Center, Electromagnetic Sciences Division, Hanscom AFB, MA, USA
- 4 THE CONTRIBUTION TO DOPPLER SPECTRUM WIDTH BY A SCANNING RADAR. **P.J. Eccles**, MITRE Corporation, Transportation Systems Engineering Division, McLean, VA, USA
- 5 A THEORETICAL STUDY OF DIFFUSE GROUND SCATTERING IN EARTH-SATELLITE COMMUNICATION LINKS. **V. Jamnejad**, California Institute of Technology, Jet Propulsion Laboratory, Pasadena, CA, USA
- 6 A ROUGH SURFACE SCATTERING MODEL FOR THE ENTIRE FREQUENCY RANGE. **A.K. Fung, G.W. Pan**, University of Texas at Arlington, College of Engineering, Arlington, TX, USA
- 7 A NUMERICAL STUDY OF THE REGIONS OF VALIDITY OF THE KIRCHHOFF AND SMALL PERTURBATION THEORIES IN ROUGH SURFACE SCATTERING. **A.K. Fung, M.F. Chen**, University of Texas at Arlington, College of Engineering, Arlington, TX, USA
- 8 PROBING OF SUBSURFACE CONDUCTORS WITH ELECTROCHEMICAL BOUNDARY CONDITIONS. **J.R. Wait**, University of Arizona, ECE, Tucson, AZ, USA
- 9 ANALYSIS OF A PARTIALLY BURIED CYLINDER. **X.-B. Xu, C.M. Butler**, University of Houston, Dept. of Electrical Engineering, Houston, TX, USA
- 10 MICROWAVE IMAGING OF TWO-DIMENSIONAL BURIED INHOMOGENEITIES. **L. Chommeloux, Ch. Pichot, J. Ch. Bolomey**, C.N.R.S.-E.S.E., Laboratoire des Signaux et Systèmes, Gif-sur-Yvette, France

## F-1-1

### TRANSFER FUNCTIONS OF SCATTERING POINTS

Samuel M. Sherman  
Consultant

In the physical-optics method of electromagnetic backscattering analysis, the echo from a radar target can be decomposed into contributions from discrete scattering points. With sufficient pulse bandwidth, the individual scattering points can be resolved in range. Even when they are not resolved, there is often an advantage in calculating their individual echo contributions and summing them (with due attention to time displacements and relative phases) rather than dealing with the entire body. This approach gives insight into the scattering mechanism and sometimes simplifies the calculations.

Each scattering point is characterized by a transfer function having magnitude and phase, as in circuit theory, defined so that the square of the magnitude equals the radar cross-section of the scattering point. The fact that the transfer function also includes a phase characteristic (over and above the phase due to distance from the radar) is often overlooked. The phase has important effects on the characteristics of echo pulses from resolved as well as unresolved scattering points. To derive the transfer function for a specified aspect, the body geometry is first expressed in the form of projected area vs. range for that aspect. Each discontinuity in this "area function" or in any of its derivatives, including the discontinuity at the leading edge of the body, produces a scattering point, which is represented as being due to an "incremental area function" originating at that point, superimposed on the continuation of the preceding area function. A Laplace transformation of the incremental area function yields the transfer function. Examples are given for various body shapes. Transfer functions are particularly simple to derive when the incremental area functions can be expressed as polynomials.

Given the incident pulse waveform and the transfer function of the scattering point, one can calculate the echo pulse waveform. Computer-generated examples are given. A simple approximate method has also been developed, which describes the changes in the pulse upon reflection in terms of a time shift (in addition to the propagation time delay), a phase shift of the carrier relative to the envelope, and a shift in instantaneous frequency.

**THE COHERENT EFFECTIVE FIELD IN A DENSELY  
POPULATED, CORRELATED MEDIUM**

Karam M.A. and A.K. Fung  
Wave Scattering Research Center  
Box 19016, College of Engineering  
University of Texas at Arlington  
Arlington, Texas 76019

The coherent effective field in densely populated media containing randomly oriented scatterers is formulated. In this formulation, the scatterer orientation, the three particle correlation and the multiple scattering among pair of scatterers are taken into consideration.

Numerical results illustrating the extinction coefficient for a dense medium with Markovian distribution are shown. The difference between this formulation and Lax formulation is also demonstrated.

BISTATIC SCATTERING FROM METAL CUBES:  
THEORY AND EXPERIMENT

Robert V. McGahan  
Electromagnetic Sciences Division  
Rome Air Development Center  
Hanscom Air Force Base, MA 01731

The backscattering cross section of the perfectly conducting cube, for broadside, planewave incidence, has a resonant maximum at  $4s/\lambda \approx 1$  and a null at  $4s/\lambda \approx 1.5$ , where  $s$  is the cube side length and  $\lambda$  is the wavelength (Yaghjian and McGahan, *IEEE Trans. Ant. Prop.*, Vol AP-33(3), 1985). In the present paper we have computed the bistatic scattering from cubes at the resonant point ( $4s/\lambda \approx 1$ ) and at the null ( $4s/\lambda \approx 1.5$ ) in the H-plane, using the Magnetic Field Integral Equation (MFIE). In addition we have made bistatic scattering measurements on two metal cubes, at  $4s/\lambda = 1$  ( $s=7\text{mm}$ ,  $f=10.71\text{GHz}$ ) and  $4s/\lambda = 1.5$  ( $s=12\text{mm}$ ,  $f=9.37\text{GHz}$ ), over the range  $15^\circ < \theta < 155^\circ$  and compared them with the theoretical values previously computed. The measured values agree with theory to within  $\pm 0.5$  dB except at the  $30^\circ$  point on the curve for  $4s/\lambda = 1.5$ . The variation of bistatic scattering with angle is a maximum at this point and it is not clear if the discrepancy is due to measurement error or positioning error. Figure 1 shows the bistatic scattering from a metal cube of size  $4s/\lambda = 1.5$ . It is interesting to note that even though there is a backscatter null, there is considerable scatter at other angles.

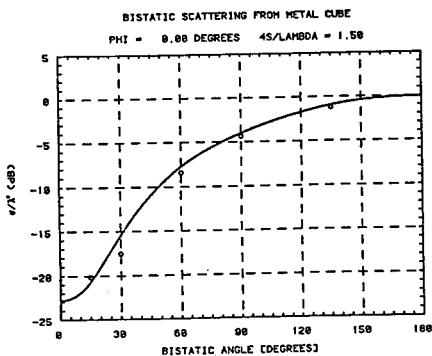


Figure 1. Bistatic scattering from a metal cube of side length 12 mm at 9.37 GHz. Theory ---, Measured o o o.

THE CONTRIBUTION TO DOPPLER SPECTRUM WIDTH BY A SCANNING RADAR

PETER J. ECCLES  
MITRE CORPORATION #

A computer model of a completely uniform reflectivity stationary storm containing stationary particles shows that the number of independent samples obtainable per pulse-volume by a scanning radar is a minimum of about 5.5. This is universal for such radars and is independent of any radar parameters: wavelength, P.R.F., scanning speed, beamwidth or dish size. It is due to the total effect of two parts, (a) averaging which occurs when the main-lobe "window" sweeps by a meteorological target, and (b) averaging which occurs when the pulse-window sweeps past the meteorological targets in range. However, the radar must take many samples per pulse width as well as many samples per beamwidth to achieve both effects, which provide an equivalent Doppler variance to which the Doppler variance within the scanned volume may be added.

Fortuitously, Hamidi and Zrnich (Considerations -- for Weather Radars, Preprints 20 Conf. Radar Met., AMS Boston, pp 319-326, 1981), called H-Z below, found that an S-band radar of .8° one-way beamwidth scanning at 10°/s gave a distributed ground clutter spectrum width of .26 m/s. Distributed ground clutter behaves like meteorological targets and is defined by (1) for a radar which samples once per pulse width:

$$\sigma_{Ca} = .108 \times 2.35 \times 10 / (4 \pi \cdot 8) = .252 \text{ m/s} \quad (1)$$

where  $\lambda = .108 \text{ m}$ ,  $10^\circ/\text{s}$  is the scanning speed,  $.8^\circ$  is the one-way beamwidth for that radar and  $2.35 = \sqrt{5.5}$  (azimuth averaging only). This result is plotted on the H-Z results in Fig. 1 above.

This confirms the results from the computer model, and shows that the H-Z theoretical value of .17 m/s is  $\sqrt{2}$  too low.

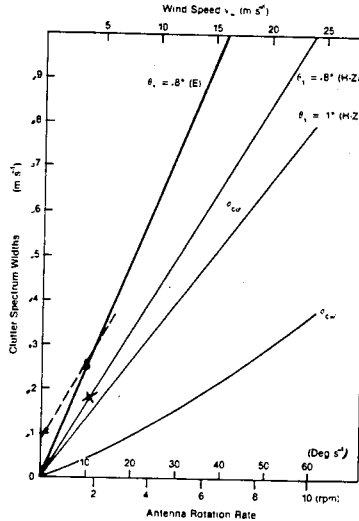


Figure 1. Shown, after H-Z, are Doppler spectrum widths of ground clutter,  $\sigma_{Ca}$  due to antenna rotation (scale on the lower axis) and  $\sigma_{Cw}$  due to wind speed (upper axis). The dashed line is through two experimental points of H-Z. The new value of  $\sigma_{Ca}$  for the NSSL radars rotating at  $10^\circ \text{ s}^{-1}$ , obtained by multiplying the H-Z computed spectrum broadening by  $\sqrt{2}$ , is near .25 m/s, very close to their experimental value of .26 m/s. The thick line gives the spectrum width for those radars due to any rotation rate as computed from (1).

# Mail Stop W280, 1820 Dolley Madison Boulevard, McLean, VA, 22102

A THEORETICAL STUDY OF DIFFUSE GROUND SCATTERING  
IN EARTH-SATELLITE COMMUNICATION LINKS

Vahraz Jamnejad  
Jet Propulsion Laboratory  
California Institute of Technology  
Pasadena, CA 91109

Evaluation of the incoherent diffuse scattering from rough surfaces and its contribution to the multipath in satellite-to-ground links is a rather complicated process. In most cases reliance is made on the experimentally available data, although some theoretical guidelines based primarily on the seminal works of Beckmann and Spizzichino is also available.

Here an attempt is made to study parametrically the contribution of the diffuse scattering at the ground receive antenna due to the incident field from a high-orbit satellite antenna. A random surface with a Gaussian distribution is assumed. First the contribution from an element of surface is formulated in a simple but approximate manner, valid for all ranges of values of the rms surface roughness. A general formulation of the magnitude and polarization (both linear and circular) of the total diffuse component, integrated over the "glistening" region (contributing to the diffuse component) is then given.

Some computed results indicating the relative variation of the magnitude of the diffuse component as a function of the elevation angle, receive antenna height, rms height and correlation length of surface irregularities, and antenna gain pattern variations will be presented. Finally assuming additional simplifications an example is worked out for a proposed future Ocean Topography Experiment (TOPEX) which uses the TRANET ground antennas in a precision orbit determination scheme.

A ROUGH SURFACE SCATTERING MODEL FOR  
THE ENTIRE FREQUENCY RANGE

A.K.Fung and G.W.Pan  
Wave Scattering Research Center  
Box 19016, College of Engineering  
University of Texas at Arlington  
Arlington, TX 76019

The standard integral equation for surface current was solved on a perfectly conducting random surface. The far zone scattered field and the average backscattered power were then computed using this current estimate. Simple and explicit expressions were obtained for the backscattering coefficients. It was shown that in the low frequency limit the results agreed with those of the first-order small perturbation for both horizontal and vertical polarizations. In the high frequency limit the same expressions for the backscattering coefficients reduced to that of the geometrical optics. The explicit forms of the backscattering coefficients were shown to contain three significant terms and the difference between the horizontal and vertical polarizations was just the sign in one of the terms.

Numerical illustrations were provided in which comparisons were shown between the results of the present theory and those of the Kirchhoff and the first-order small perturbation for a variety of surface parameter values. A comparison was also shown with measurements from a known man-made random surface. Results indicate that the difference between the horizontal and vertical polarization is at its maximum in the low frequency limit where the small perturbation theory is applicable. This difference gradually decreases as frequency increases. Thus, measured data may appear to have polarization characteristics similar to those of the small perturbation theory in frequency regions where the perturbation theory is no longer valid.

A NUMERICAL STUDY OF THE REGIONS OF VALIDITY OF THE  
KIRCHHOFF AND SMALL PERTURBATION THEORIES IN  
ROUGH SURFACE SCATTERING

A.K.Fung and M.F.Chen  
Wave Scattering Research Center  
College of Engineering  
University of Texas at Arlington  
Arlington, TX 76019

The regions of validity of the common rough surface scattering models, namely, the Kirchhoff and the first-order perturbation models are studied by numerical simulation. The procedure is to generate a one dimensional perfectly conducting random surface on the digital computer, compute the induced surface current on the surface due to an impinging plane wave by the moment method, and then calculate the far zone backscattered field and power. This procedure is repeated at least forty times or more and the results averaged to obtain the average scattered power. Many so called Kirchhoff model involve simplifying assumptions in addition to the Kirchhoff approximation. To avoid confusion the Kirchhoff model here uses only the Kirchhoff approximation for the surface current and the far zone scattered field and power are evaluated numerically to avoid the use of additional approximations. Comparisons between the approximate models and the numerical calculations are made for various values of the standard deviation of surface heights and the surface correlation length both normalized with respect to the incident wave number denoted by  $k_0$  and  $k_1$  respectively. By using these two normalized surface parameters to form a two dimensional space the approximate regions of validity are then established.

It is found that due to the inclusion of the coherent scattering component the Kirchhoff model continues to provide good agreement near vertical incidence when  $k_1$  is less than 6 and  $k_0$  is less than 1. It is also found that the usual requirement of small slope in the small perturbation model is inadequate. This condition should be replaced by requiring  $k_1$  to be small.

PROBING OF SUBSURFACE CONDUCTORS WITH  
ELECTROCHEMICAL BOUNDARY CONDITIONS

James R. Wait, ECE, University of Arizona, Tucson, AZ 85721

It is now well known that the effective conductivity and permittivity of earth materials in situ are strong functions of frequency. This is particularly true at ELF and VLF. The physical mechanisms are not clearly understood but it is clear that change of conduction from electronic to electrolytic in the case of disseminated mineralization is a major source of the dispersion. A simple phenomenological model that has met with success is the ensemble of coated metallic spheres or spheroids. The interface impedance is then fitted into the boundary value problem in a straight-forward fashion ( e. g. Chap. 2 in GeoElectromagnetism by J. R. Wait, Academic Press, 1982). Assuming more realistic electrochemical descriptions of the metal-electrolyte interface and non-spherical particle shapes, the dependence on volume loading, particle orientation, and texture can be examined. We also consider a model for dispersion in clay like media where the influence of bound ions on the particle surface can be modelled as a conductive sheath which, in general, may be complex and highly dispersive. Finally we consider a general particle model where the sheath effects can be treated as a combined interface impedance and interface admittance. In the context of potential theory this model allows for the simultaneous discontinuity of potential and normal current flow at the surface of the particle. Such effective electrochemical boundary conditions can be further generalized to include the electromagnetic surface impedance that plays a role when the problem is no longer quasi-static in nature. Such an example is a long metal conductor buried in the earth. Then the induced eddy currents add their share of the overall dispersion as seen by an external observer. ( e. g — see M. S. theses by P. W. Flanagan and J. T. Williams, University of Arizona, 1983 and abstracts from Commission B meeting of URSI in Houston May, 1983) Some of the analytical details of this type of boundary problem are described in Electromagnetic Wave Theory ( by J. R. Wait, Harper and Row, 1984).

**ANALYSIS OF A PARTIALLY BURIED CYLINDER**

Xu, Xiao-Bang and Chalmers M. Butler  
Department of Electrical Engineering  
University of Houston  
Houston, Texas 77004, USA

The current induced by an incident plane wave on a conducting cylinder which resides partially in one half space and partially in another is determined. The cylinder is of uniform cross section and of infinite length and its axis is parallel to the planar media interface. The semi-infinite half spaces contain different materials and are homogeneous. The excitation is (1) transverse magnetic and (2) transverse electric to the cylinder axis and is invariant in this axial direction. Integral equations for the structure are presented and discussed. Numerical methods for solving the equations are described and special analytical features of the solution procedures are investigated in some detail. The induced current is presented graphically as a function of the various parameters of the problem. From the data presented, one can see that known conditions at media interfaces are exhibited by the current and its derivative. Also, far-zone scattered field patterns are presented and discussed.

MICROWAVE IMAGING OF TWO-DIMENSIONAL  
BURIED INHOMOGENEITIES

L. CHOMMELOUX, Ch. PICHOT, J.Ch. BOLOMEY

Groupe d'Electromagnétisme  
Laboratoire des Signaux et Systèmes  
C.N.R.S. - E.S.E.  
Plateau du Moulon  
91190 GIF-sur-YVETTE, FRANCE

Many diagnostic problems in Geophysics and Civil Engineering are characterized by interaction of electromagnetic waves with objects buried in homogeneous or stratified media. Most of the investigations which have been done in this domain, concern the detection of buried objects but few papers have dealt with the problem of identifying the objects (canalizations, tunnels, etc.).

The proposed method is based on the integral representation for a plane wave incident on a lossy half-space containing a cylindrical object of arbitrary cross section and electrical properties (Fig. 1). The induced current distribution in the object is obtained from the backscattered field measurement in amplitude and phase. In order to improve the spatial resolution in the image, the scattered field is measured for different plane wave incidences and various frequencies. A large number of numerical simulations concerning the shape, the size and the position of the object have been carried out for different values of soil and object electromagnetic parameters.

In order to obtain more realistic results, we also considered the effects of a layer (water, ice, snow, etc.) on the quality of the reconstruction. Simulations show that an isotropic resolution can be obtained so that :  $\delta_x = \delta_y = \frac{\lambda_1}{2}$  ( $\lambda_1$  : wavelength in vacuum). An example of our results, for a  $\frac{\lambda_1}{2}$  cylinder with rectangular section is shown in Fig. 2 at 3 GHz.

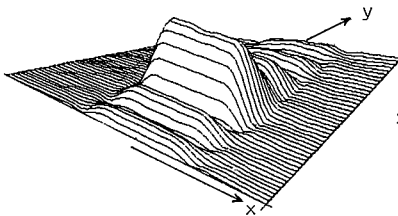


Figure 2

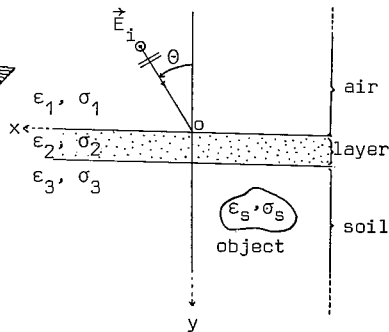


Figure 1



## URSI COMMISSION F - SESSION F2

**Mobile Radio and  
Urban Propagation**

8:30 - 12:00  
LAW 102

**Radio mobile et  
propagation urbaine**

Chairperson/Président: **D.C. Cox**, Bell Communications Research, Red Bank, NJ, USA

- 1 (8:40) LAND MOBILE RADIO PROPAGATION MEASUREMENTS AT 869 and 1501 MHz. **W.J. Vogel**, University of Texas at Austin, Electrical Engineering Research Laboratory, Austin, TX, USA
- 2 (9:10) PROPAGATION MEASUREMENTS IN NEW YORK CITY AT 850 MHz. **S.B. Rhee**, AT&T Bell Laboratories, Whippany, NJ, USA
- 3 (9:40) TIME DELAY SPREAD MEASUREMENTS OF WIDEBAND RADIO SIGNALS IN BUILDINGS. **D.M.J. Devasirvatham**, Bell Communications Research, Radio and Satellite Systems Research Division, Holmdel, NJ, USA
- 4 (10:10) RF POWER SPECTRUM MEASUREMENTS IN THE MOBILE RADIO ENVIRONMENT. **R.L. Campbell**, Michigan Technological University, Dept. of Electrical Engineering, Houghton, MI, USA
- 5 (10:40) MEASURED CHARACTERISTICS OF 800/900 MHz RADIO CHANNELS WITH HIGH ANGLE PROPAGATION THROUGH MODERATELY DENSE FOLIAGE. **R.J.C. Bultitude**, Department of Communications, Communications Research Centre, Ottawa, ON
- 6 (11:10) MACROSCOPIC DIVERSITY IN THE PORTABLE RADIOCOMMUNICATION ENVIRONMENT. **H.W. Arnold, R.R. Murray, D.C. Cox**, Bell Communications Research, Holmdel, NJ, USA

LAND MOBILE RADIO PROPAGATION MEASUREMENTS  
AT 869 AND 1501 MHZ

Wolfhard J. Vogel  
Electrical Engineering Research Laboratory  
The University of Texas at Austin  
10100 Burnet Road  
Austin, TX 78758

In order to design a satellite system which would provide vehicles travelling through rural areas in the continental United States with mobile access to the telephone network, one requires a quantitative knowledge of the signal characteristics produced by typical propagation scenarios.

An experiment is described in which measurements of the amplitude and phase of continuous wave radio signals were made in a van while driving through East Texas, Louisiana, Mississippi, and into Alabama. Two circularly polarized transmitters, at 869 and 1501 MHz, were carried for some 20 hours by a stratospheric balloon at an altitude of 33 km in simulation of a satellite link. Measurements were made at elevation angles from 20 to near 90 degrees. Road types encountered ranged from paved rural two-lane to interstate highways. Vegetation blockage of the line of sight, when present, was caused by the deciduous and coniferous trees typical to the south-eastern states. At 869 MHz, in addition to the drooping dipole receiving antenna, measurements were made with azimuth steerable microstrip and helix antennas to assess their ability of rejecting ground reflections. Results of the statistics and spectra of the received power and phase at the two frequencies and under a variety of conditions will be presented.

Propagation Measurements in New York City  
at 850 MHz

S. B. Rhee

AT&T Bell Laboratories  
Whippany, NJ 07981

Abstract

This paper describes the results of propagation measurements performed in the heavily built-up urban areas of New York city at 800 MHz cellular mobile frequency band. In the measurements, four base station transmitters located in New Jersey near Newark, NJ have been used to transmit signals at four discrete frequencies. Mobile receivers on-board a specially instrumented vehicle, the AT&T Bell Laboratories Mobile Communications Laboratory (MCL), have been used to monitor and record four signals simultaneously as the MCL traveled on the streets of Manhattan.

This paper will describe the measurement configuration, data processing and organization as well as the results of the measurements in detail. Also discussed will be how the results of these measurements compare against some earlier measurement results in other urban areas.

## F-2-3

### TIME DELAY SPREAD MEASUREMENTS OF WIDEBAND RADIO SIGNALS IN BUILDINGS

Daniel M. J. Devasirvatham  
Bell Communications Research  
Radio and Satellite Systems Research Division  
HOH Room L-175  
Holmdel-Keyport Road  
Holmdel, NJ 07733

Propagation of radio waves in buildings is characterized by strong multipath effects, which cause different rays of the signal to reach the receiver at slightly different times. The resulting time smear could cause inter-symbol interference which limits the usable signalling rate of digital radio communications systems operating in buildings.

An experiment to measure the time delay spread of a wideband radio signal was implemented. The method uses the correlation properties of maximal length pseudo-random noise codes to reduce data acquisition rates, while effectively probing the medium with a narrow pulse. Measurements were made at 850 MHz using bi-phase modulation at 40 Mbits per second.

Measurement sites varied from a large office building to private residences. The results indicate that root mean square time delay spreads of several hundred nanoseconds can occur. Therefore, signalling rates of a few hundred kilobits per second may be supported by digital communications systems in buildings.

Note: Current address will change in spring of 1985 to:  
Bell Communications Research  
331 Newman Springs Road, NVC 3X-343  
Red Bank, NJ 07701

RF POWER SPECTRUM MEASUREMENTS  
IN THE MOBILE RADIO ENVIRONMENT

Richard L. Campbell  
Department of Electrical Engineering  
Michigan Technological University  
Houghton, Michigan 49931

Measurements were made of the Doppler spread signal at a receiver moving through a residential area of Seattle at 144, 432 and 1296 MHz. The CW transmitting antenna was mounted on the roof of one of the houses. The receiver moved in a straight line at a constant velocity of about 4 m/s along residential streets at right angles to the direct transmitter-receiver path. Measurements were made at transmitter-receiver distances of approximately 470 m and 1570 m. The signal was simultaneously received on co and cross polarized antennas on the vehicle roof, amplified and linearly translated to a low frequency IF and digitally signal processed. Power spectra were averaged over 320 m of vehicle travel with a frequency resolution of 0.1 to 0.4 Hz. Total received intensities relative to free space are -43 to -52 dB at 144 MHz, -21 to -45 dB at 432 MHz and -57 to -74 dB at 1296 MHz. Cross polarized total intensities are 2 to 4 dB lower than copolarized total intensities at 144 MHz, about 6 dB lower at 432 MHz and 0 to 2 dB lower at 1296 MHz. The experiment geometry allows conversion of the Doppler power spectrum to a signal arrival angle spectrum. Further signal processing, using the known direct path arrival angle as a function of time, allows separation of the received signal intensity into coherent and incoherent parts. The shape of the incoherent power spectrum at all frequencies, distances and polarizations is consistent with the assumptions that the scattered signals are equally likely to arrive at any angle in the horizontal plane and that the strongest signals arrive from the scatterers near the receiver. The coherent contribution to the total intensity is found to be significant at all frequencies and distances, and for both co and cross polarizations. For copolarized signals at 1570 m distance at both 144 MHz and 432 MHz, the total intensity has nearly equal coherent and incoherent parts.

MEASURED CHARACTERISTICS OF 800/900 MHZ RADIO  
CHANNELS WITH HIGH ANGLE PROPAGATION  
THROUGH MODERATELY DENSE FOLIAGE

Robert J.C. Bultitude  
Communications Research Centre  
Department of Communications  
Ottawa, Canada

The digital transmission capacity of randomly fading multipath radio channels is limited to that capacity at which the bandwidth of transmission is much less than the coherence bandwidth ( $B_c$ ) of the channel. It is therefore of interest for system design purposes to determine  $B_c$  in propagation environments where the use of digital radio systems is planned.

One channel on which fading is expected due to multipath propagation and terminal motion is that of a geostationary satellite link to a mobile terrestrial receiver. A mobile digital communication system of this type is being planned by the Canadian Government for operation in the 800/900 Mhz band. Since this system is planned for operation in rural environments, trees bordering roadways are expected to be the major and most consistent cause of multipath interference. For the purpose of predicting capacity limitations on the planned channels, experiments were therefore conducted to determine the fading statistics and frequency correlation characteristics of 800/900 MHz channels over which propagation is at high angles ( $20^\circ$ ) through moderately dense foliage.

The paper to be presented details the results of experiments that were conducted to simulate conditions on the planned satellite channels by operating a pseudo-noise channel probe from a 210 ft. tower through deciduous trees to a receiver at close range. Measurement results include: channel impulse response estimates, Doppler/angle of arrival analyses, envelope fading statistics and double sided frequency correlation plots. Comparisons are made between channel characteristics during the summertime, and during the autumn when the leaves have fallen from the trees. Estimates of digital channel capacity limitations are also given.

## MACROSCOPIC DIVERSITY IN THE PORTABLE RADIOCOMMUNICATION ENVIRONMENT

H. W. Arnold, R. R. Murray, and D. C. Cox  
Bell Communications Research  
Holmdel, NJ 07733

Microwave propagation into and around buildings is subject to severe spatial fluctuations in path loss. Multipath propagation produces rapid fluctuations on a scale of one wavelength. Larger-scale fluctuation, often called shadow fading, is produced by buildings and other large geographical features. This shadow fading is typically log-normally distributed, with a standard deviation in excess of 10 dB (Cox, et. al., AT&T BLTJ, 63, 921-954, 1984). This shadow fading restricts the reliable coverage range of a low-power portable radiocommunication system.

In a dense radio network with many fixed nodes, portable users may potentially be served by more than one fixed node. If the shadow fading between a portable and several fixed nodes is independent, reliability at coverage extremes can be improved by selecting the node with the lowest average path loss. This technique will be termed macroscopic diversity.

Propagation measurements at 816 MHz have been conducted in and around eight houses from several fixed locations distributed around each house. Geometric path lengths were below 2300 feet in all cases. Data were reduced to estimate the shadow fading component of the path loss between each fixed location and several locations in and around each house. Significant reliability improvements were obtained by selecting, from randomly-chosen pairs and triples of fixed locations, that path with the lowest value of shadow fading at every portable location. The additional improvements obtainable from other choices of fixed locations will be discussed.



## URSI COMMISSION F - SESSION F3

**Microwave Meteorological  
Measurements**

8:30 - 12:00  
LAW 101

**Mesures météorologiques  
par micro-ondes**

Chairperson/Président: **R.K. Moore**, University of Kansas, Lawrence, KS, USA

- 1 FINESTRUCTURE STABLE LAYERS OBSERVED BY SOUNDER AND IN-SITU TOWER SENSORS. **E.E. Gossard**, University of Colorado, Cooperative Institute for Research in the Environmental Sciences, Boulder, CO, USA; **J.E. Gaynor**, NOAA/ERL/Wave Propagation Laboratory, Boulder, CO, USA
- 2 MODEL GRAVITY WAVE SPECTRA FOR COMPARISON WITH SPECTRA OBSERVED BY DOPPLER BOUNDING SYSTEMS. **T.E. VanZandt**, National Oceanic and Atmospheric Administration, Aeronomy Laboratory, Boulder, CO, USA
- 3 THE PROPOSED FLATLAND ST RADAR. **J.L. Green**, **T.E. VanZandt**, **K.S. Gage**, National Oceanic and Atmospheric Administration, Aeronomy Laboratory, Boulder, CO, USA; **G.D. Nastrom**, Control Data Corporation, Minneapolis, MN, USA
- 4 VARIABILITY IN DOPPLER RADAR MEASUREMENT OF HORIZONTAL WIND. **A.T. Waterman Jr.**, Stanford University, STAR Laboratory, Stanford, CA, USA
- 5 COMPUTATION OF BACKSCATTER AND PROPAGATION EFFECTS IN SEVERE CONVECTIVE STORMS: COMPARISON WITH DUAL-POLARIZED RADAR OBSERVATIONS AT S- AND X-BANDS. **J. Vivekanandan**, **V.N. Bringi**, **V. Chandrasekar**, Colorado State University, Dept. of Electrical Engineering, Ft. Collins, CO, USA
- 6 ESTIMATION OF EDDY DISSIPATION RATES IN A STORM FROM DOPPLER RADAR DATA. **D.S. Zrnic**, National Oceanic and Atmospheric Administration, National Severe Storms Laboratory, Norman, OK, USA; **K.A. Brewster**, Program for Regional Observing and Forcasting Services Boulder, CO, USA
- 7 MID-LATITUDE MICROWAVE MEASUREMENTS OF MESOSPHERIC MOISTURE. **C.L. Croskey**, **L.C. Hale**, Pennsylvania State University, Dept. Electrical Engineering, University Park, PA, USA; **R.G. Joiner**, Office of Naval Research, Arlington, VA, USA; **P.J. Moser**, Bloomsburg University of Pennsylvania, Dept. of Physics, Bloomsburg, PA, USA; **J.J. Olivero**, **J.-J. Tsou**, Pennsylvania State University, Dept. of Meteorology, University Park, PA, USA
- 8 POLARIZATION EFFECTS IN MICROWAVE RADIOMETRY SUBJECT TO WET REFLECTORS. **D.C. Hogg**, **M.D. Jacobson**, National Oceanic and Atmospheric Administration, Wave Propagation Laboratory, Boulder, CO, USA
- 9 EXPENDABLE TOTAL POWER RADIOMETER TARGET DETECTORS AT Ku-Ka BANDS. **M. Friedman Axler**, **H.K. Wolfe, Jr.**, AAI Corporation, Baltimore, MD, USA

FINESTRUCTURE STABLE LAYERS OBSERVED BY  
SOUNDER AND IN-SITU TOWER SENSORS

E.E. Gossard

Cooperative Institute for Research in the Environmental Sciences

University of Colorado

Boulder, Colorado 80303

J.E. Gaynor

NOAA/ERL/Wave Propagation Laboratory

Boulder, Colorado 80303

A study of the finestructure within elevated stable atmospheric layers is described. The observational program consisted of measurements made with fast-response turbulence sensors on a carriage traversing a 300 m tower and comparison of the carriage data with acoustic and radar echo sounders. Some supporting observations using a free-balloon-borne sensor of  $C_T$  are also shown. The layers studied were found to be composed of sheets and layers in temperature, humidity and wind reminiscent of the sheet and layer structures often reported in lakes, estuaries and the oceans. The distributions of turbulence properties through the layered structures are described, and some implications for models are discussed. A quite general ratio of sheet-to-layer thickness is proposed toward which the process of step formation proceeds. A model of specular reflection is compared with a Bragg backscatter model, and it is concluded that specular contributions from the observed gradients can exceed the Bragg return if radar wavelengths greater than a few meters are used. It is found that atmospheric turbulence may be highly anisotropic even for scales smaller than a meter in very stable zones or in convectively unstable layers.

MODEL GRAVITY WAVE SPECTRA FOR COMPARISON WITH  
SPECTRA OBSERVED BY DOPPLER BOUNDING SYSTEMS

T.E. VanZandt, Aeronomy Laboratory, NOAA,  
325 Broadway, Boulder, CO 80303

Doppler remote sensing techniques (radar, lidar, and sodar in the atmosphere, Doppler sonar in the ocean) measure the radial velocity versus time and radial range. From such measurements, the power spectra of the radial velocity fluctuations versus frequency and radial wavenumber can be calculated. One objective of such measurements is to assess the process or processes that cause the velocity fluctuations by comparing the observed spectra with model spectra based on physical descriptions of the proposed processes. A likely process is internal gravity waves. But comparison of observed spectra with model gravity wave spectra is not straightforward, since model gravity wave spectra are usually described in terms of horizontal or vertical wavenumber and frequency, not radial wavenumber and frequency. Because of the particular properties of gravity wave, conversion from horizontal or vertical wavenumber to radial wavenumber is not simple.

In this paper, model gravity wave spectra versus radial wavenumber and frequency are calculated from the formalism that Pinkel (Deep-Sea Res., 28A, 269-289, 1981) developed for Doppler sonar. A Garrett and Munk (J. Geophys. Res., 80, 291-297, 1975) two-dimensional gravity spectrum, which has been shown to be at least a fair approximation to observed atmospheric spectra (VanZandt, Geophys. Res. Lett., 9, 575-578, 1982), is used as input. The resulting model spectra are discussed as a function of the parameters of the input model (spectral slopes and wavenumber bandwidth), buoyancy frequency, averaging time, zenith angle, etc.

The use of such model spectra will be illustrated by comparison with observed spectra of wind fluctuations in the summer mesosphere obtained by the MST radar technique.

## F-3-3

### THE PROPOSED FLATLAND ST RADAR

J. L. Green, T.E. VanZandt, K.S. Gage, and G.D. Nastrom<sup>\*</sup>  
NOAA, Aeronomy Lab, 325 Broadway, Boulder, CO 80303

It has been demonstrated by Nastrom et al., (Monthly Weather Rev., in press, 1985) that the small vertical velocities of the atmosphere associated with synoptic scale meteorology can be measured by an ST radar when orographic effects are not present. At present all ST radars are located in or near mountains.

To study the measurement of vertical velocity, the Aeronomy Laboratory of NOAA plans to build a VHF ST radar near Urbana, Illinois, where the surrounding terrain is extremely flat and far from any mountains. Such a radar will also be extremely useful for studying frontal passages, gravity waves and jet streams, etc.

The design of the proposed radar will be based on that of the Sunset Radar (located near Boulder, Colorado). It will have a wavelength of 7.4m and a 60m x 60m steerable array antenna. With the steerable antenna beam it should be possible to check the consistency between the vertical velocity measured with the vertical beam and that inferred from beams in several oblique directions using the continuity equation.

<sup>\*</sup>Control Data Corp., P.O. Box 1249, Minneapolis, MN 55440

VARIABILITY IN DOPPLER RADAR MEASUREMENT  
OF HORIZONTAL WIND

A. T. Waterman, Jr.  
STAR Laboratory  
Stanford University

There are an increasing number of radars capable of obtaining echoes from the clear air and using them to measure wind in the height range below 20 km. Of the various wind-measuring techniques, that utilizing the Doppler frequency shift of the return signal is common. To measure the vector wind at any given altitude, the radar beam must be pointed in at least three non-coplanar directions. For a single monostatic radar this means that the components of the vector wind are obtained using data from different locations in the atmosphere, and sometimes also from different times. The question then arises as to how much accuracy is lost.

The present paper, while not attempting to answer this question adequately, nevertheless does present data that are relevant to the problem. Using the SOUSY 47 MHz radar in the 300m-diameter antenna at Arecibo, measurements were made at seven different zenith angles, and repeated at two different azimuths. For each azimuth, zenith angles were chosen in pairs, and the horizontal and vertical wind components were computed from the data for each pair, for a given height. The results were then compared for consistency. Examples will be shown of these results and the variability found.

## F-3-5

### COMPUTATION OF BACKSCATTER AND PROPAGATION EFFECTS IN SEVERE CONVECTIVE STORMS: COMPARISON WITH DUAL-POLARIZED RADAR OBSERVATIONS AT S- AND X-BANDS

J. Vivekanandan, V. N. Bringi and V. Chandrasekar  
Department of Electrical Engineering  
Colorado State University  
Ft. Collins, CO

A theoretical backscatter and propagation model is described for application to hydrometeors present in severe convective storms. The hydrometeors to be modelled are oblate raindrops, conical graupel and oblate hailstones which are assumed to be exponentially distributed with size and possess a Gaussian distribution of canting angles. Aircraft 2D PMS probe observations are used to model the shape and size distributions of raindrops and graupel. Computations of differential reflectivity (ZDR) at S-band and linear depolarization (LDR) at X-band are shown to be consistent with radar measurements in convective storms obtained using the National Center for Atmospheric Research CP-2 radar in June 1984 in the vicinity of Boulder, CO.

ESTIMATION OF EDDY DISSIPATION RATES IN A STORM FROM  
DOPPLER RADAR DATA

Dusan S. Zrnic<sup>1</sup>  
National Severe Storms Laboratory, NOAA  
1313 Halley Circle, Norman, OK 73069

Keith A. Brewster  
Program for Regional Observing and  
Forecasting Services  
325 Broadway, Boulder, CO 80303

Doppler radars offer unique data from which it is possible to estimate turbulent eddy dissipation rates,  $\epsilon$ . If the inertial subrange extends to lengths longer than the resolution volume size,  $\epsilon$  can be obtained from the Doppler spectrum width. Spatial spectra of mean Doppler velocities can also yield  $\epsilon$  estimates but only if a significant portion of the analysis length is contained within the inertial subrange. We compare dissipation rate estimates obtained with the two independent measurements. At close range and vertical incidence agreement between the two independent estimates of  $\epsilon$  is within 10%. Furthermore, the slope of the spatial energy densities is very close to  $-5/3$ , predicted by Kolmogorov. The energy input is mainly from buoyancy-driven updrafts, and the transition wavelength between the input scale and the inertial subrange is therefore somewhat smaller than the updraft-downdraft circulation cell, which has a diameter of about 10 km. For a more distant storm at a range of 60 km, the filtering of mean velocities by the resolution volume precludes precise estimation of  $\epsilon$  from spatial spectra of mean velocities. Kinetic energy development during the growth phase of this storm is examined using wind fields obtained from two Doppler radars and Doppler spectrum width data. The kinetic energy grew exponentially before becoming nearly steady-state. Energy exchanges are most vigorous within and in the vicinity of the updraft region. When summed over the entire storm volume, eddy dissipation and production from vertical shear of the mean wind are also important.

## F-3-7

### MID-LATITUDE MICROWAVE MEASUREMENTS OF MESOSPHERIC MOISTURE

C. L. Croskey and L. C. Hale  
Communications and Space Sciences Laboratory  
Department of Electrical Engineering  
The Pennsylvania State University  
University Park, PA 16802

R. G. Joiner  
Office of Naval Research  
Arlington, VA 22217

P. J. Moser  
Department of Physics  
Bloomsburg University of Pennsylvania  
Bloomsburg, PA 17815

J. J. Olivero and J.-J. Tsou  
Communications and Space Sciences Laboratory  
and Department of Meteorology  
The Pennsylvania State University  
University Park, PA 16802

Over a period of several years, ground based remote measurements have been made of water vapor in the mesosphere using microwave radiometry techniques from University Park, PA. Initially these measurements utilized absorption of solar radiation at the 1.35 cm H<sub>2</sub>O line and subsequently they were converted to observing emission of this line with a low noise MASER receiver. These data are systematically studied for secular and seasonal structure, and for correlations with other measurements, including radio wave propagation.

## POLARIZATION EFFECTS IN MICROWAVE RADIOMETRY SUBJECT TO WET REFLECTORS

D. C. Hogg and M. D. Jacobson

Wave Propagation Laboratory, Environmental Research Laboratories, NOAA  
Boulder, CO 80303

In many applications, microwave radiometers are required to operate under all weather conditions; these include those under which the exposed element of the antenna system becomes wetted by rain. Here we discuss the special case of a wetted flat reflector with energy at 20.6 and 31.6 GHz, linearly and orthogonally polarized, incident at an angle of  $45^\circ$ . The brightness temperatures of the wet reflector are computed from conventional theory, and are measured, for various thicknesses of water layer. The impact of these results on design of radiometers for research and operational application is discussed.

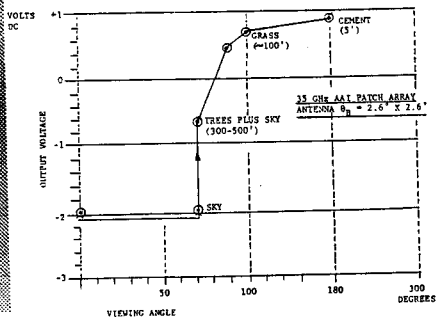
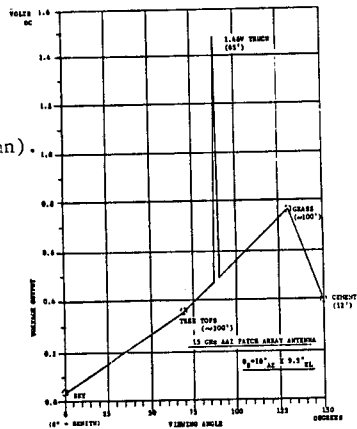
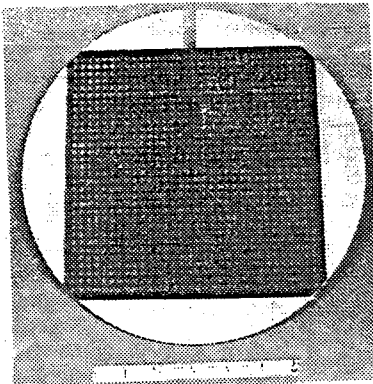
# F-3-9

## EXPENDABLE TOTAL POWER RADIOMETER TARGET DETECTORS AT Ku-Ka BANDS

M. Friedman Axler and H. K. Wolfe, Jr.; AAI Corporation

Low cost total power radiometers for application in airborne vehicles as target detectors are demonstrated employing AAI developed conformal patch array antennas with receivers tuned to Ku- and Ka-bands. Effects of component/signal processing circuitry parameters and viewing angles on detection sensitivity are illustrated. The 35 GHz radiometer conformal antenna shown in the figure is composed of a square array of a 32 x 32 element matrix linearly polarized with a total of 1024 patch elements. A corporate reactive tee microstrip feed insures equal amplitude and phase distribution to each element. Target detection data taken with engineering models is shown in the figures at 15 and 35 GHz. The 35 GHz engineering model is centered with a single waveguide to microstrip transition that results in a length of 7.3" of microstrip line to each patch. The antenna gain is 28 dB; beamwidths 2.6° x 2.6°. A new feed system has been developed using waveguide with three H plane reactive power divider junctions with reduced microstrip line lengths of 3.65" to each patch.

Low VSWR waveguide to microstrip transition designed to feed each of four 256 patch arrays provides antenna gain of 32 dB nom. with input VSWR of 1.3:1; beamwidths 2.5° x 2.5°; -20 dB sidelobes, (acknowledgement is made to C. R. Mann). The patch elements are printed on 10 mil. duroid 5880 backed by 1/16" aluminum plate. Waveguide T-junctions and input section are mounted on the back. Target detection data collected with the higher gain 35 GHz antenna is also shown.



## URSI COMMISSION F - SESSION F4

Clear Air  
Propagation I

1:30 - 5:00  
LAW 101

Propagation en  
temps clair I

Chairperson/Président: **D.C. Hogg**, NOAA, Boulder, CO, USA

- 1 ACCURATE COMPUTATION OF DIFFRACTION LOSS IN VHF LINKS. **H.A. Kalhor, A.M. Riazi**, Shiraz University, Electrical Engineering Dept., Shiraz, Iran
- 2 VHF AND UHF RADIO PROPAGATION IN THE NORTHWEST PASSAGE. **R.S. Butler**, Department of Communications, Communications Research Centre, Ottawa, ON
- 3 METEOROLOGICAL PROPERTIES OF THE NOCTURNAL BOUNDARY LAYER DURING MULTIPATH PROPAGATION. **J. Claverie, C. Klapisz, M. Sylvain**, CNET/PAB/RPE, Issy les Moulineaux, France
- 4 MICROWAVE MULTIPATH POWER AND ANGLE-OF-ARRIVAL SPECTRA USING FFT SIGNAL ANALYZERS. **R.L. Campbell**, Michigan Technological University, Dept. of Electrical Engineering, Houghton, MI, USA; **W.J. Helms**, University of Washington, Dept. of Electrical Engineering, Seattle, WA, USA
- 5 AMPLITUDES AND ANGLES-OF-ARRIVAL OF TROPOSPHERIC MULTIPATH MICROWAVE SIGNALS USING A WIDE APERTURE ARRAY. **A.R. Webster, A.M. Scott**, University of Western Ontario, Centre for Radio Science, London, ON
- 6 LINE-OF-SIGHT MULTIPATH DEPENDENCE ON OBSERVED AND MODELED REFRACTIVITY STRUCTURE. **U.H.W. Lammers, R.A. Marr**, Rome Air Development Center, Hanscom AFB, MA, USA
- 7 INTERFERENCE DUE TO TERRAIN SCATTERING IN MICROWAVE RADIO RELAY SYSTEMS. **P.E. Butzien, A.J. Giger**, AT&T Bell Laboratories, North Andover, MA, USA
- 8 DISTRIBUTIONS OF THE CROSS-POLARIZATION DISCRIMINATION AND THE CO-POLARIZED ATTENUATION DUE TO MULTIPATH IN CLEAR-AIR. **H. Jin**, China Research Institute of Radiowave Propagation, Xinxiang, China

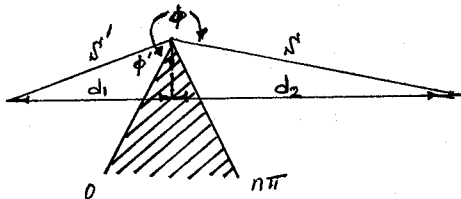
# F-4-1

## ACCURATE COMPUTATION OF DIFFRACTION LOSS IN VHF LINKS

H. A. Kalhor & A. M. Riazi  
Department of Electrical Engineering, Shiraz University  
Shiraz, Iran

Bullington's diffraction loss formula (K. Bullington, IRE, 35, 1124-1136, 1947) has been the basis for VHF link design. Recently, some discrepancies have been observed between computation and actual field strength measurement results. The discrepancies disappear when obstructions approach ideal knife edges and become appreciable when obstacles depart significantly from knife edges.

A new computation method based on geometrical theory of diffraction (R. G. Kouyoumjian and P. Pathak, Proc. IEEE, 62, 1448-1461, 1974) has been employed and results have been found to agree closely with actual experimental results.



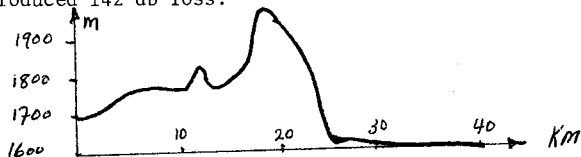
In the new approach an obstacle, as shown above, is treated as follows:

$$E_{GTD} = E_0 \frac{\exp(-jkS')}{S'} \cdot D \sqrt{\frac{S'}{S(S'+S)}} \cdot \exp(-jkS)$$

for perfectly conducting obstacle and vertically polarized wave:

$$D = \frac{\exp[-j\pi/4 \sin(\frac{\pi}{n})]}{n \sqrt{2\pi k}} \left[ \frac{1}{\cos(\frac{\pi}{n}) - \cos(\frac{\phi - \phi'}{n})} + \frac{1}{\cos(\frac{\pi}{n}) - \cos(\frac{\phi + \phi'}{n})} \right]$$

For the path shown below Bullington's method gives a total path loss of 117 db and the new procedure yields 145 db whereas actual measurement at 170 MH produced 142 db loss.



*Withdrawn*

**F-4-2**

VHF AND UHF RADIO PROPAGATION  
IN THE NORTHWEST PASSAGE

R.S. Butler  
Communications Research Centre  
Department of Communications  
Ottawa, Canada

A radio propagation experiment is being conducted in the region of the Northwest Passage, at latitude 75°N, to assess the performance of maritime mobile communications with shore stations in this area. Four UHF radio paths which have both ends elevated are included, as well as six VHF paths each having one end elevated and the other near sea level, and three VHF paths with both ends near sea level. These combinations provide information on the reliability of both point-to-point and ship-to-shore links, and on the interference which may occur between equipments on different ships. The UHF paths have obstruction clearances which range from grazing to almost one Fresnel zone; the VHF paths range from grazing to deep within the diffraction propagation region. Path lengths are in the range 60 to 100 km.

Because of the unique climate of this region the statistics of signal fading and enhancement are quite different than those normally observed in the temperate maritime environment. Signal variation statistics will be presented and qualitatively interpreted on the basis of these climatic differences.

## F-4-3

### METEOROLOGICAL PROPERTIES OF THE NOCTURNAL BOUNDARY LAYER DURING MULTIPATH PROPAGATION

J. CLAVERIE, C. KLAPISZ and M. SYLVAIN

CNET/PAB/RPE - 38-40, rue du Général Leclerc  
92131 ISSY LES MOULINEAUX (France)

Multipath propagation, as it is a major source of impairments for line of sight radio-links, is a great research theme for radio-communication engineers. Many studies have been accomplished, aiming at the understanding of frequency selective fading effects on high rate data transmissions.

Multipath fading occurs mainly during nighttime and is caused by strong negative gradients in air refractivity  $N$ .  $N$  being a function of temperature, air pressure, water vapor pressure (BEAN and DUTTON, Radiometeorology, NBS Monograph 92), its variations are generally associated with the existence of the nocturnal inversion layer.

Theoretical work, concerning the description of the nocturnal boundary layer is commonly based on simple hypothesis, such as horizontal homogeneity. Recent progress in computation techniques permits more realistic models, including various parameters such as the terrain slope (BROST and WYNGAARD, Journal of Atmospheric Sciences, Vol 35, August 78), but there is still a lack of studies dealing with radiometeorological properties of multipath fading.

The PACEM I experiment (M. SYLVAIN et al, Proc. URSI commission F 1983, Symposium, Louvain, Belgium, June 1983) took place in France near Paris during the summer 1982, and associated fading measurements (using a Microwave Link Analyser) with the collection of a complete set of meteorological data. From these data we deduce refractive index profiles and use them in a ray-tracing program, and as noticed before (MON and MAYRARGUE, IEEE Intern. Conf. on Comm. 68-6, Denver, 1981) we show that acoustic soundings give an helpful sight of the low atmosphere dynamical behaviour. The period studied is too short to derive significant statistical properties of the propagation medium, but showed some different physical situations resulting in various time scales for the fading observed. It also seems, that these situations can be classified using general climatic conditions described by daytime temperature, wind direction ...

The results of the PACEM II experiment, which is planned to last about three years should provide more accurate conclusions.

MICROWAVE MULTIPATH POWER AND  
ANGLE-OF-ARRIVAL SPECTRA  
USING FFT SIGNAL ANALYZERS

Richard L. Campbell  
Department of Electrical Engineering  
Michigan Technological University  
Houghton, Michigan 49931

Ward J. Helms  
Department of Electrical Engineering  
University of Washington  
Seattle, Washington 98195

Microwave signals received via multiple paths fluctuate in time if the source, receiver or scattering medium is moving. The period of these fluctuations ranges from minutes for tropospheric paths to milliseconds for mobile radio signals in cities. In recent years small, stand alone digital FFT signal analyzers have been used in the millihertz to tens of kilohertz range for studies of geophysical, mechanical and acoustic systems. Studies of microwave multipath fluctuations may be easily conducted by using a frequency stable cw transmitter and a frequency stable down converter as a front end to an FFT signal analyzer. This paper describes a measurement apparatus used for studies of the received RF power spectrum and angle-of-arrival spectrum in the urban mobile radio environment. The vehicle mounted apparatus consists of a half-wave dipole antenna, stable down-converter and tape recorder for recording the IF signals for later processing. At 1296 MHz a power spectrum resolution of 0.3 HZ, angle-of-arrival resolution of 1.9 degrees, and receiver sensitivity of -197 dBw were obtained.

## F-4-5

### AMPLITUDES AND ANGLES-OF-ARRIVAL OF TROPOSPHERIC MULTIPATH MICROWAVE SIGNALS USING A WIDE APERTURE ARRAY

A.R. Webster and A.M. Scott  
Centre for Radio Science  
University of Western Ontario  
London, Ontario CANADA

A system consisting of a wide aperture vertical receiving array, operating at a frequency of 16.65 GHz, has been developed to investigate tropospheric microwave propagation under various, especially multipath, conditions. Sampling of the complex amplitude across the array leads directly, by way of the Fourier Transform, to a measure of the amplitude and angle-of-arrival (AOA) of the various rays arriving at the receiver.

The system itself consists of 12 horns (20 dB gain) spaced at intervals of 51 wavelengths, a reference antenna (37 dB gain paraboloid) to provide a phase reference, and the associated receiver; the transmitter is a simple c.w. source connected to a similar paraboloid. Sampling of the whole array is accomplished in less than 50 ms and repeated once a second. An unambiguous range in AOA of 1.2 deg. is covered with a resolution of 0.1-0.15 deg. depending on the weighting applied before Fourier transforming; a 30 dB Dolph-Tchebyshev weight is used routinely.

The system was operated during the late summer/early fall of 1984 on a 35 km link in S-W Ontario. It is observed that on occasions when multipath occurs, often 3 distinct paths are in evidence; typical separations of 0.2 deg. are measured, well within the system resolution. On occasion, more than 3 paths emerge with some evidence of a single path splitting into two distinct and separate paths.

Relatively long periods ( $\sim 1$  hour) occur when the AOA of the separate components changes but little. At the same time, significant variations in ray amplitude are observed over periods ranging from one to several seconds.

LINE-OF-SIGHT MULTIPATH DEPENDENCE  
ON OBSERVED AND MODELED REFRACTIVITY STRUCTURE

U. H. W. Lammers and R. A. Marr  
Rome Air Development Center, Hanscom AFB, MA 01731

Despite their sometimes profound effect on wideband communication systems, line-of-sight multipath ray parameters are difficult to measure individually because of the high resolution required in elevation angle and delay. Likewise, they are not amenable to accurate modeling because of generally limited information on the refractivity structure of the propagation medium.

We compare experimental data of multiple-wavefront arrival angles and delays obtained on two long New England links with modeled data. The latter are based on the assumption of stratified ducting layers. Since stratification in the atmosphere is actually of limited extent, required minimum layer dimensions are determined to explain observed phenomena.

Multipath effects as revealed by experimental elevation angle and delay scans are approximated by simulated scans whose ray parameters are selected for a best fit. We investigate the manifestations of component rays unresolvable by the experimental hardware. Some statistical aspects of the observed multipath effects will be discussed.

F-4-7

INTERFERENCE DUE TO TERRAIN SCATTERING IN  
MICROWAVE RADIO RELAY SYSTEMS

Paul E. Butzien  
Adolf J. Giger  
AT&T Bell Laboratories  
1600 Osgood St.  
North Andover, MA 01845

A major source of microwave interference has been found to be scattering from the terrain where the antenna beams of two radio hops cross or converge. Recent measurements are compared to calculations and results using digital terrain maps are presented. Models used in early calculations (A. J. Giger and J. Shapira, ICC '83 Conference Record, June 1983, pp 1254-1261) have been extended and modified to give more accurate estimates of interference levels for specific types of scattering environments.

DISTRIBUTIONS OF THE CROSS-POLARIZATION  
DISCRIMINATION AND THE CO-POLARIZED  
ATTENUATION DUE TO MULTIPATH IN CLEAR-AIR

Jin Huiqun  
China Research Institute of Radiowave Propagation  
P.O. Box 138  
Xinxiang, Henan Province, China

The theoretical formulae for the statistic distributions of the cross-polarization discrimination XPD and the co-polarized attenuation CPA are presented.

The XPD is described as a function of the phase difference between the direct and multipath rays reflected from a layer, the arrival-angles of rays and the parameters of co-polar and cross-polar pattern of antenna. On the assumption of spherical-stratified atmosphere, the formula of the phase difference is obtained, which is dependent on the frequency, the path length, the refractive index gradient, the height of the layer and the height difference between receiving and transmitting antennas. The formula of the arrival-angle is also derived. When the curvature of spherical surface tends to zero, the above representations reduce to the current formulae for plane-stratified atmosphere.

According to the distribution of refractive index gradient the theoretical formulae for statistic distributions of XPD and CPA are derived by means of the representations of the phase difference and arrival-angle for spherical-stratified atmosphere. They are both simple and accurate for applications. A linear equi-probability relation between XPD and CPA is also obtained using the above statistic distributions. The distributions of XPD and CPA and the constant of the relation are dependent on the frequency, the path length, parameters of weather and antenna cross-polarization pattern which can be obtained from the statistic distribution of refractive index gradient and fitting the measured antenna pattern respectively. These dependences coincide with the conclusions from experiments in most countries.

The probability of XPD and CPA and the constant in the equi-probability relation can be predicted using the above presentations derived for a given path. The predicted results agree with the empirical relations of CPA in CCIR report 338-4 and the measured data of XPD in China, Japan, Canada and the United States.



## URSI COMMISSION F - SESSION F5

Radar Remote Sensing I

1:30 - 5:00  
LAW 101

Téledétection par radar I

Chairperson/Président: **A. Hendry**, National Research Council of Canada, Ottawa, ON

- 1 BROAD-BAND BACKSCATTER MEASUREMENTS FROM THE OCEAN. **R. Lawner, R.K. Moore, S. Gogineni, A.H. Chaudhry**, University of Kansas Center for Research, Inc., Remote Sensing Laboratory, Lawrence, KS, USA
- 2 STATISTICS OF LOW-GRAZING ANGLE RADAR SEA SCATTER. **D.B. Trizna**, Naval Research Laboratory, Radar Division, Washington, DC, USA
- 3 MEASUREMENT OF THE OCEAN RADAR CROSS SECTION AT 5.3 GHz. **W.C. Keller**, US Naval Research Laboratory, Washington, DC, USA; **F. Feindt, V. Wisman, W. Alpers**, Max-Planck-Institut für Meteorologie, Hamburg, FRG
- 4 RADAR BACKSCATTER FROM SPLASHING RAINDROPS. **J.P. Hansen, I.B. Wetzel, S.R. Laxpati**, Department of the Navy, Naval Research Laboratory, Washington, DC, USA
- 5 NEW ALGORITHMS FOR THE DEPENDENCE OF THE SEA SURFACE RADAR CROSS SECTION ON WIND SPEED, THE WAVE SLOPE AND AIR-SEA TEMPERATURE. **D.E. Weismann**, Hofstra University, Dept. of Engineering, Hempstead, NY, USA; **M.H. Freilich**, California Institute of Technology, Jet Propulsion Laboratory, Pasadena, CA, USA
- 6 THE EFFECT OF ATMOSPHERIC STABILITY ON THE MODULATION OF MICROWAVE BACKSCATTER. **G.R. Valenzuela, D.T. Chen**, Naval Research Laboratory, Washington, DC, USA
- 7 MODULATION TRANSFER FUNCTIONS FOR RADAR BACKSCATTER FROM THE OCEAN. **V. Hesany, S. Gogineni, A.H. Chaudhry, R.K. Moore**, University of Kansas Center for Research, Inc., Remote Sensing Laboratory, Lawrence, KS, USA
- 8 MICROWAVE BRAGG SCATTERING AND THE MEASUREMENT OF OCEAN SURFACE CURRENTS. **W.J. Plant, W.C. Keller**, US Naval Research Laboratory, Washington, DC, USA
- 9 MICROWAVE MEASUREMENTS OF THE SURFACE EFFECTS OF INTERNAL WAVES IN THE OCEAN. **D.L. Schuler**, US Naval Research Laboratory, Washington, DC, USA
- 10 PERTURBATION OF THE SURFACE-WAVE HEIGHT SPECTRUM DUE TO THE PRESENCE OF SURFACE CURRENT FEATURES. **D.R. Thompson**, The Johns Hopkins University, Applied Physics Laboratory, Laurel, MD, USA

BROAD-BAND BACKSCATTER MEASUREMENTS FROM THE OCEAN

R. Lawner, R.K. Moore, S. Gogineni and A.H. Chaudhry  
Remote Sensing Laboratory  
University of Kansas Center for Research, Inc.  
Lawrence, Kansas 66045-2969

Measurements of radar backscatter from the ocean surface were made during January and February 1984, using an FM-CW radar system located on the Nordsee tower off the coast of Germany. These measurements were made at frequencies between 4.5 and 17 GHz, incidence angles from  $18^\circ$  to  $75^\circ$ , and with either VV or HH polarization. The windspeed varied from 6 to 22 m/sec during the experiment and most of the measurements were made in either the upwind or the downwind direction.

This paper presents the dependence of the scattering coefficient on the incidence angle as well as on windspeed. Selected radar backscattering measurements at frequencies ranging from 4.5 to 17 GHz, and incidence angles from  $45^\circ$  to  $65^\circ$  were used to calculate the apparent ripple spectra at various windspeeds. The results are compared with the semi-empirical model proposed by Fung and Lee [1982]. The agreement between the experimental and theoretical results is fairly good.

Reference:

Fung, A.K. and K.K. Lee, "A semi-empirical sea-spectrum model for scattering coefficient estimation," IEEE J. Oceanic Engr., vol. OE-7, pp. 166-176, October 1982.

## STATISTICS OF LOW-GRAZING ANGLE RADAR SEA SCATTER

Dennis B. Trizna  
Propagation Staff, Radar Division  
Naval Research Laboratory  
Washington, D.C. 20375

Shipboard radar sea scatter measurements have been made using a high resolution X-band marine navigation radar using horizontal polarization. Results indicate that a two-parameter distribution function is necessary to describe the statistics of the pulse-to-pulse normalized radar cross section (NRCS) of the sea scatter. Thus, the mean or median value of the NRCS used in scatterometry for high grazing angles is not a sufficient descriptor of the statistics, since the distribution is not a single parameter Rayleigh distribution for the low grazing angle case. We present a comparison of different two-parameter models for the NRCS statistics, and find that the scatter typically requires two Weibull distributions to describe the behavior of the data. Some suggestions are made regarding modeling the scatterers responsible for these two distributions.

## F-5-3

### MEASUREMENT OF THE OCEAN RADAR CROSS SECTION AT 5.3 GHZ

W. C. Keller  
U.S. Naval Research Laboratory  
Washington, DC 20375-5000

F. Feindt, V. Wisman and W. Alpers  
Max-Planck-Institut Fur Meteorologie  
2000 Hamburg 13, FRG

Measurements of the normalized radar cross section (NRCS) at 5.3 GHz (C-band) of the sea surface as a function of wind speed and direction are presented. The data were obtained by a coherent scatterometer mounted on a small twin-engine airplane performing circle flights over the Bay of Biscay.

Our data show that the wind speed exponent at 5.3 GHz is typically 20 percent smaller than at 13.9 GHz (Ku-band). Furthermore, the upwind/crosswind and the upwind/downwind ratios of the NRCS are typically 20 percent and 30 percent, respectively, smaller at C-band than at Ku-band. Preliminary results indicate that the relative direction between wind and swell can effect the directional distribution.

The aircraft measurements were supplemented by those from a second scatterometer operated from the ocean research tower, Nordsee, located in the German Bight area of the North Sea. This provided long term averages with high quality environmental data, thus permitting better isolation of certain parameters.

## RADAR BACKSCATTER FROM SPLASHING RAINDROPS

James P. Hansen  
Lewis B. Wetzel  
Sharadbabu R. Laxpati  
Naval Research Laboratory  
Washington, D.C. 20375-5000

While it is well recognized that sea surface features such as wind blown ripples and breaking waves contribute to near grazing radar backscatter, little work has focused on the physical disturbance produced by falling rain. This paper presents results from a recent experimental measurement program which indicate that splashing raindrops also produce unique surface features which can contribute to radar backscatter.

Measurements have been performed with several 3.2 cm wavelength pulsed radar systems. In one field experiment, a radar situated on a cliff overlooking the Chesapeake Bay was used to observe low grazing angle surface backscatter with both horizontal and vertical linear polarizations. Additional experiments were conducted with a high resolution radar illuminating the surface of a water filled test tank. Backscatter was measured before, during and after several rainstorms and for a variety of wind conditions. These experiments have shown that with an initially calm surface, splashing raindrops can greatly increase the radar backscatter. This splash effect was observed to be dependent on rainfall rate, surface conditions, and radar polarization.

The experimental measurements have led to an examination of the surface features produced by a splashing raindrop and how these features might produce some of the observed scattering phenomena. Photographic measurements in typical rainstorms have shown that the solid water spout of a raindrop splash can reach heights in excess of 3 cm. In addition, outwardly propagating circular ripples are of comparable size to wind blown capillary waves. An analytical model has been developed which examines the time dependent radar backscatter which could be produced from the many phases of a single splash formation. This model has also been extended to the radar backscatter which would occur from a surface containing many such splashes in various stages of development. The backscatter characteristics evidenced in the experimental measurements and represented by this model suggest that the presence of rainfall must be considered in both the interpretation of remote sensing information and the estimation of potential sea clutter levels.

NEW ALGORITHMS FOR THE DEPENDENCE OF THE SEA  
SURFACE RADAR CROSS SECTION ON WIND SPEED,  
THE WAVE SLOPE AND AIR-SEA TEMPERATURE

D.E. Weissman  
Hofstra University  
Hempstead, New York 11550

M.H. Freilich  
Jet Propulsion Laboratory  
California Institute of Technology  
Pasadena, California 91109

The effect of ocean surface winds, air-sea temperatures and long wave slopes on microwave backscatter has been measured and analyzed to create new algorithms for remote sensing applications. A statistical study of experimental data has addressed the problem of creating explicit functions between the X-band radar cross section and these other quantities (for a vertically polarized and 45° incidence angle configuration). The results show that the magnitude of the root-mean-square long ocean wave slope is comparable in importance to the ocean surface wind in controlling the backscatter cross section under stable conditions. Under unstable conditions, the air-sea temperature difference (through the Monin-Obhukov length) becomes a parameter in the functional form for the RCS. The experimental data consists of observations conducted in the Gulf of Mexico (Keller, Plant and Weissman, J. Geophys. Res., 90, 1019-1029, Jan. 1985). The results here utilize this processed and organized data, and use statistical regression analysis methods to test and evaluate algebraic functions that can best fit the data. For the stable condition data a function that includes wave slope in addition to the wind speed gives a significantly smaller mean square error to the data than one which depends only on wind speed. The characteristics of each data point (radar parameters, averaging time, etc.) have been discussed in the above reference. For stable conditions 77 data points (20 minute averages) are used. The unstable data set is 135 points. The results for this condition yield closed form expressions that depend strongly on wind speed and the Monin-Obhukov term. The role of the slope under unstable conditions is not strong, and is still under investigation. These results indicate the environmental parameters that need to be measured for additional studies with larger data sets, over wider ranges of conditions from airborne platforms.

THE EFFECT OF ATMOSPHERIC STABILITY ON  
THE MODULATION OF MICROWAVE BACKSCATTER

G. R. Valenzuela and D. T. Chen  
Naval Research Laboratory  
Washington, DC 20375-5000

Unusually large modulations of microwave backscatter power at L- and X-band (over 20 dB) were recorded in the 1982 NRL Phelps Bank Experiment, Nantucket Shoals (Valenzuela et al., EOS Trans. Am. Geophys. Un., 64, 618-619, 1983) for winds less than 7 m/s. Further study of the microwave measurements in combination with the extensive in-situ data collected reveals that the highly stable atmospheric conditions prevailing during the experiment (the air was as much as 8°C warmer than the water) may be the reason for the anomalous large modulations. In this paper theoretical and experimental evidence will be presented on how the atmospheric stability (air-sea temperature difference) affects the modulations of microwave backscatter power.

MODULATION TRANSFER FUNCTIONS FOR RADAR BACKSCATTER  
FROM THE OCEAN

V. Hesany, S. Gogineni, A.H. Chaudhry and R.K. Moore  
Remote Sensing Laboratory  
University of Kansas Center for Research, Inc.  
Lawrence, Kansas 66045-2969

Capillary and short-gravity waves are modulated by the longer ocean waves. These ripples are the primary source of radar backscatter from the sea. The radar signal intensity is modulated both by the slope variation and the modulation of ripple amplitudes. Radar backscatter measurements have been made from towers in 1979 off the Dutch coast and in 1984 off the German coast using an FM-CW radar that allows simultaneous measurement of signal strength and surface elevation at the centroid of the beam.

Modulation transfer functions are typically used to relate the long-ocean-wave properties to the radar backscatter. These are calculated on the assumption that the relationships are linear so that Fourier-transform theory can be used. The MTF is, in essence, the ratio of the cross-spectrum between microwave signal and waveheight to the autospectrum of the waveheight.

Here we show that the modulation of the signal due to slopes of the long waves is highly nonlinear for realistic slope values encountered with moderate wave heights. In this case the widely used MTF is, at best, a linear approximation (in the least-squares sense) to the actual relationship. Hence it should be used with caution.

Another problem is the non-stationarity of the ocean surface. One wishes to obtain many degrees of freedom for estimating the spectra, but non-stationarity of the ocean conditions can severely limit the number of degrees of freedom available, as shown here with an example from the 1984 measurements.

Cross-correlations and MTFs are presented here for several sample conditions and compared with those obtained previously by other investigators.

MICROWAVE BRAGG SCATTERING AND THE MEASUREMENT  
OF OCEAN SURFACE CURRENTS

William J. Plant  
William C. Keller  
U.S. Naval Research Laboratory  
Washington, D.C. 20375

An L-Band, CW microwave system has been mounted on the pier operated by the Coastal Engineering Research Center at Duck, North Carolina to measure longshore surface currents. Doppler spectra of backscattered sea return from this system often show peaks due to advancing and receding Bragg waves even at fairly high wind speeds. The critical factor in whether or not these peaks are observed seems to be long wave orbital velocity, not wind speed. The advective effects of the orbital velocity broaden the advancing and receding Bragg lines so that a single, broad, skewed peak is observed. In either of these situations, the mean Doppler shift is found to vary depending on the surface current and wind direction. The effect of wind direction may be removed by subtracting the product of the cosine of the wind/antenna angle and the Bragg wave's intrinsic phase speed from the raw system output. The output then yields a measurement of longshore current speed just below the interface. Comparison of these radar-derived current speeds with those measured using drifting dye packets shows that the two measurements track each other quite well. A bias is noted in some cases, however, which may indicate that the dye packet is significantly influenced by the airflow just above the surface.

**MICROWAVE MEASUREMENTS OF THE SURFACE EFFECTS  
OF INTERNAL WAVES IN THE OCEAN**

Dale L. Schuler  
U. S. Naval Research Laboratory  
Washington, DC 20375-5000

Microwave measurements were made during the period 27 August - 7 September 1984 of changes in radar backscatter cross-section caused by the presence of internal wave packets generated at the continental shelf edge south of Long Island. Continuous, interleaved measurements were obtained at both X- and L-bands in order to study the effects of internal waves on 1.6 and 11.7 cm surface Bragg waves during passes of the research vessel USNS Bartlett through the packet locations. The measurements were collocated using bore-sighted antennas and made with identical bandwidths. Frequency-agility techniques were utilized to increase the number of degrees of freedom in the samples and, thus, to reduce sample variability. Data was acquired for 1) a wide range of incidence angles  $\theta$  ( $20^\circ \leq \theta \leq 70^\circ$ ), 2) both horizontal and vertical polarization, 3) look-angles (relative to the packet propagation direction) of approximately  $0^\circ$  or  $180^\circ$ , and 4) a variety of wind/wave conditions. Supporting measurements of surface winds, currents, long wave conditions, and fathometer scattering events were made. This data set will be presented and comparisons will be made between backscattering cross-sections obtained at X- and L-bands for a variety of configurations and conditions. Spatial correlations between backscatter returns and measured surface current perturbations will be presented and discussed utilizing recent theoretical predictions.

PERTURBATION OF THE SURFACE-WAVE HEIGHT  
SPECTRUM DUE TO THE PRESENCE OF  
SURFACE CURRENT FEATURES

Donald R. Thompson  
The Johns Hopkins University  
Applied Physics Laboratory  
Laurel, Maryland 20707

During the past decade or so, rapid advances in the field of remote sensing have made it possible to examine many interesting properties of the ocean surface. In particular, the development of Synthetic Aperture Radar (SAR) has provided a very extensive and rich data base which may be used to study a wide variety of oceanographic phenomena. A nice description of these phenomena is given in (R. C. Beal, et al, Spaceborne Synthetic Aperture Radar, The Johns Hopkins University Press, Baltimore, 1981) along with images showing such features as major current boundaries, warm and cold water eddies, and surface manifestations of bathymetry.

Due to the large number of uncontrollable and unmeasured parameters during the SAR overflight, it has not always been possible to determine which of many possible mechanisms is responsible for rendering these features visible in the SAR images. One likely candidate, especially where surface current features are present, is the perturbation of the surface-wave spectrum by the interaction of the surface waves with the local current field. If this perturbation has a large enough effect on the Bragg region of the surface-wave spectrum, a contrast in the radar cross section between the current and non-current regions will result. It is the purpose of this study to investigate quantitatively the properties of this wave-current interaction for typical surface current fields.

We present in this paper a brief discussion of the physics which governs the wave-current interaction process. In particular, we show how energy-transport equations which describe the interaction can be formulated in terms of the wave-action spectral density. We use these equations with measured surface current fields as input to predict the expected modulation in the Bragg region of the surface-wave spectrum. Our predictions are compared with measured spectral perturbations as a function of location in the current field. With the assumption of a simple Bragg scattering model, we also compare our predicted modulations with those observed in SAR images of surface current features of known strength. It is found that the predicted modulations agree reasonably well with the measured perturbations.



## URSI COMMISSION F - SESSION F6

Clear Air  
Propagation II

8:30 - 12:00  
LAW 101

Propagation en  
temps clair II

Chairperson/Président: **A.R. Webster**, University of Western Ontario, London, ON

- 1 AN EVALUATION OF NEW TROPOSCATTER MODELS - PRELIMINARY RESULTS. **A. Neuburger, P.J. Freyheit, G. Leroux, D.C. Livingston**, The MITRE Corporation, Bedford, MA, USA
- 2 PRELIMINARY OBSERVATIONS ON SPACE/SPACE QUAD DIVERSITY TROPOSCATTER LINKS. **M.J. Brown, A. Fejfar**, The MITRE Corporation, Bedford, MA, USA
- 3 PRELIMINARY OBSERVATIONS ON VERTICAL DIVERSITY TROPOSCATTER LINKS. **M.J. Brown, A. Fejfar, J.A. Wick**, The MITRE Corporation, Bedford, MA, USA
- 4 ATMOSPHERIC REFRACTIVITY STRUCTURE AND THE PERFORMANCE OF DIGITAL TROPO SCATTER RADIO. **O.R. Coté, J.F. Morrissey, Y. Izumi**, Air Force Geophysics Laboratory, Hanscom AFB, MA, USA
- 5 EXPERIMENTAL CONFIRMATION OF THE MILLIMETER WAVE PROPAGATION CODE MPM FOR CLEAR AIR. **H.J. Liebe, G.R. Hand, K.C. Allen**, National Telecommunications and Information Administration, Institute for Telecommunication Sciences, Boulder, CO, USA
- 6 AN EHF TELECOMMUNICATION PERFORMANCE PREDICTION MODEL. **K.C. Allen**, National Telecommunications and Information Administration, Institute for Telecommunication Sciences, Boulder, CO, USA
- 7 MILLIMETER WAVE TELEMETRY LINK TESTS. **Y.-K. Wu**, The MITRE Corporation, McLean, VA, USA

AN EVALUATION OF NEW TROPOSCATTER MODELS -  
PRELIMINARY RESULTS

A. Neuburger, P. J. Freyheit,  
G. Leroux, D. C. Livingston, The MITRE Corp.,  
Bedford, MA 01730

Existing validated troposcatter prediction models do not predict both path loss and multipath spread. The deployment of the AN/TRC-170 C-band digital troposcatter system has created a need for such a validated model if the adaptive modem contained in this terminal is to be used to its maximum effectiveness.

In response to this need, the Electronic Systems Division of the United States Air Force and The MITRE Corporation have undertaken a program to evaluate several new prediction models that predict both path attenuation and multipath delay spread. This program, currently half way through the data acquisition phase, utilizes path loss and multipath spread data collected on troposcatter links, with geometries typical of those used for tactical communications, for comparison with parameters predicted by the models. The field data spans a variety of climatic conditions and seasonal variations and includes, in addition to the radio data, radiosonde and air-borne refractometer meteorological observations.

This paper provides a description of the propagation models considered, the measurement program, and the methodology of model validation. Presented also are some preliminary results of the model evaluation activity. Summary statistics of measured path loss and multipath spread are presented for the first test links evaluated in the program.

PRELIMINARY OBSERVATIONS ON SPACE/SPACE QUAD  
DIVERSITY TROPOSCATTER LINKS

Monty J. Brown and Adolph Fejfar, MITRE Corporation, Bedford, MA

Analysis on four 4.5 GHz single frequency space/space quad troposcatter links indicate that usable values of zero-time shift correlation are obtainable from the crossed path pair. Existing data leaves the subject open to much conjecture. One article written shows the viability of space diversity on short troposcatter links (<300 km) to be unacceptable for all beamwidths. (R. Larsen, Space Polarization in Troposcatter Systems, Paper 7, 1980, AFCEA Conference.)

Real time data was taken four times an hour, for three minutes each time. The data for each period consists of samples taken at a rate of 400 per second on each channel. The samples are then quantized to one of 255 discrete levels, and analyzed on a Digital PDP-11/34 computer system. The measurements show first, that although the parallel path correlation is slightly better in performance than the crossed path pair, acceptable values are obtainable. Previous work shows acceptable correlation values need to be less than 0.6. The maximum mean values obtained on the parallel paths, and the crossed paths were 0.087 and .253, respectively. Secondly, a comparison of the crossed and parallel correlations indicate that changes in one branch are reflected in the other.

The results of this paper and the companion paper, "Preliminary Observations of Vertical Diversity", suggest that the troposphere is different at 5 GHz than it is at 2 GHz and below. Because of the shorter wavelength, layers in the atmosphere become transparent, and the scattering in the common volume becomes random, regardless of the angles of incidence into it.

Tests to date indicate that where only a single operating frequency is obtainable, the use of space/space quad diversity would provide the user with quad diversity gain.

## F-6-3

### PRELIMINARY OBSERVATIONS ON VERTICAL DIVERSITY TROPOSCATTER LINKS

Monty J. Brown, A. Fejfar, J. A. Wick, MITRE Corp., Bedford, MA

Testing on five 4.5 GHz vertical space diversity test links has shown that vertical space diversity on a tactical link is possible. The measurements for these tests compare the correlations between a pair of antennas horizontally spaced 119 wavelengths, and a pair of antennas vertically spaced 91 wavelengths. The links tested to date are considered to be typical of those encountered in the tactical world.

For troposcatter propagation, it was found that fading was less correlated on the horizontal pair than on the vertical by about 0.10, and a maximum value of 0.277 was measured on one link. As noted in a reference article, useful diversity gain is obtainable for signal correlations as high as 0.6. Data from one link in the diffraction mode showed correlations greater than this on both the horizontal and vertical pairs. In diffraction, the signal is much stronger and fade depths are less than 10 dB so that diversity gain is not required. These tests indicate that even though the signals travel through essentially the same common volume, the phase disturbances due to scatters provides for two largely independent paths.

The value of a vertical diversity system is obvious in a wooded region where a usable takeoff angle is not obtainable on the normal support structure. Erecting one tower to support two antennas is normally easier and more cost effective than erecting two towers.

Atmospheric Refractivity Structure and the Performance  
of Digital Troposcatter Radio

by

O.R. Cote, J.F. Morrissey and Y. Izumi  
Air Force Geophysics Laboratory  
Hanscom AFB, Massachusetts 01731

The AN/TRC-170 is a tactical digital radio for multi-channel troposcatter communications developed by Raytheon for the Air Force Systems Command. It employs a adaptive digital modem to counter the inherent multipath dispersion of a troposcatter channel in which the data rate is variable from .256 to 4.096 MBPS. Projected path lengths for radio deployment are 50 to 250 miles.

During the past two years of performance testing of the TRC-170 in Arizona, Florida, and across the North Sea, atmospheric refractivity measurements have been made within the test path. Both portable radiosonde balloons and an airborne refractometer were used. The measured vertical profiles of mean refractivity were used in conjunction with ray tracing techniques to determine the change in scattering angle within the common volume. The refractometer allowed  $C_N^2$ , the refractivity structure function to be determined. Low altitude ducting layers are observed to lead to pronounced signal enhancements. Ray tracing for these conditions suggests that such signal enhancements are related to scattering angle reduction by the duct effect on the transmitter beam.

Multiple ducting levels within the altitude zone of the common volume lead to large delay spreads. Thunderstorms have on a few occasions produced dramatic increases in the delay spread. The path loss data for March 1983 to March 1984 for the path across the North Sea shows a dramatic correlation between high path loss and frontal rain storms crossing the link. The complex relationship between the lengths of a troposcatter path, the common volume geometry, and atmospheric boundary layer refractivity structure and their influence on path performance can be successfully studied with a ray trace technique specifically adapted to the troposcatter case.

## F-6-5

### EXPERIMENTAL CONFIRMATION OF THE MILLIMETER WAVE PROPAGATION CODE MPM FOR CLEAR AIR

H. J. Liebe, G. R. Hand, and K. C. Allen  
National Telecommunications and Information  
Administration, Institute for Telecommunication  
Sciences  
Boulder, Colorado 80303

Questions concerning atmospheric effects upon millimeter wave system performance are answered best analytically. Based on meteorological variables, the computer efficient code MPM (H. Liebe, NTIA Report 83-137, December 1983) predicts attenuation, delay, and noise properties of a radio path over frequency and height ranges from 1 to 1000 GHz and 0 to 30 (100) km, respectively. The clear air part of the code MPM has been updated with improved spectroscopic information for dry air and water vapor absorption and tested with high quality experimental data, recently available from field experiments. These efforts employed (a) horizontal line-of-sight links (path length: 0.8 to 27 km; temperature: -18 to 40°C; water vapor concentration: 1 to 25 g/m<sup>3</sup>) operating at test frequencies between 28 and 430 GHz (10 cases) and (b) vertical (zenith) paths to outer space (starting height: 0 to 3.8 km; integrated water vapor: 1 to 75 mm) at frequencies between 2.5 and 215 GHz (12 cases). With very few exceptions, excellent agreement between experimental and model data is obtained and discussed.

AN EHF TELECOMMUNICATION PERFORMANCE PREDICTION MODEL  
K. C. Allen  
National Telecommunications and Information Administration,  
Institute for Telecommunication Sciences,  
Boulder, Colorado 80303

An EHF Telecommunication System Engineering Model (ETSEM) has been developed as an aid in the design of line-of-sight communication systems from 10 to 100 GHz. ETSEM has been implemented on a desk-top computer. The computer code provides tabulations of path geometry parameters and analyzes ray-path and Fresnel zone clearances to help in the path design. ETSEM also predicts the performance (availability) of both digital and analog systems based on recently developed EHF propagation models and equipment specifications. Attenuation by rain, clear-air absorption, and multipath are modeled. These effects are expected to essentially determine the statistics of link availability as limited by propagation impairments. Performance may be predicted for any interval of months of the year. A climatological data base for North America and Europe provides parameters for the propagation models or the parameters may be hand entered. The computer code is written so that selected link specifications can be easily changed and the resulting change in predicted performance examined. This allows the design engineer to determine the cost effectiveness of different means of improving link performance. Weaknesses and limitations as well as envisioned improvements in ETSEM are discussed. ETSEM was developed for the United States Army Communications Electronics Engineering Installation Agency (USACEEIA).

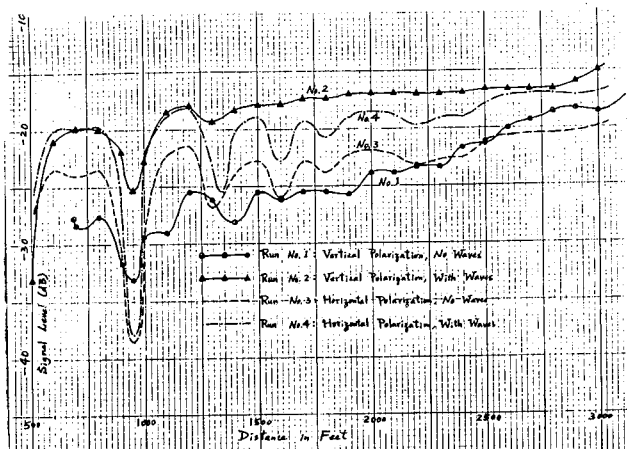
## MILLIMETER WAVE TELEMETRY LINK TESTS

Yung-Kuang Wu  
The MITRE Corporation

Millimeter wave propagation tests were performed inside an enclosed test basin on top of a straight water channel, in order to provide design data for a millimeter wave telemetry link. The test link consists of a stationary antenna and a moving antenna separated by a straight water channel of a maximum distance one kilometer. Two similar antennas were chosen operating at 35 GHz. By selecting antenna height at 10' above water line, no significant multipath effects should be expected until beyond 2,296 ft separation distance.

The test results are summarized in the following Figure. The deepest multipath fadings were observed at about 950 ft from the far end, which corresponds to the separation distance of 2,330 ft. Maximum variations of signals for all four runs were less than 20 dB, which is much less than 60 dB variation as predicted from free space calculation. This difference seems to be due to signal saturation effect inside the receiver mixer-preamp package.

Stronger multipath fadings were measured with horizontally polarized waves than with vertically polarized waves. Smoother signals with less variations were observed with waves than without waves, which should be expected since one to two-foot waves far exceed the Rayleigh Criterion for smooth surface. Thus, we should experience less specular reflections from the wavy water surface.



## URSI COMMISSION F - SESSION F7

Radar Remote Sensing II

1:30 - 5:00

Téledétection par radar II

LAW 101

Chairperson/Président: C.T. Swift, University of Massachusetts, Amherst, MA, USA

- 1 RADAR BACKSCATTER FROM SEA ICE DURING SUMMER. S. Gogineni, R.G. Onstott, R.K. Moore, *University of Kansas Center for Research, Inc., Remote Sensing Laboratory, Lawrence, KS, USA*
- 2 MODELLING THE DETECTABILITY OF ICEBERGS ON A MARINE RADAR. B.R. Dawe, *NORDCO Limited, St. John's, NF*
- 3 MULTIFREQUENCY, MULTIPOLARIZATION BACKSCATTER MEASUREMENTS OF RESONANT VEGETATION STRUCTURES. A.J. Blanchard, D.F. Zook, *University of Texas at Arlington, Dept. of Electrical Engineering, Arlington, TX, USA*
- 4 TERRAIN CROSS SECTION MEASUREMENTS. K.V.N. Rao, J.W. Coffey, *Rome Air Development Center, Electromagnetic Sciences Division, Hanscom AFB, MI, USA*
- 5 DETERMINATION OF BACKSCATTERING SOURCES IN TALL PRAIRIE GRASS OF THE KONZA PRAIRIE AT 10 GHz. R. Zoughi, R.K. Moore, L.K. Wu, *University of Kansas Center for Research, Inc., Remote Sensing Laboratory, Lawrence, KS, USA*
- 6 ANALYSIS OF SYNTHETIC APERTURE RADAR SYSTEM INDUCED DEPOLARIZATION EFFECTS. A.J. Blanchard, D. Luckert, *University of Texas at Arlington, Dept. Electrical Engineering, Arlington, TX, USA*
- 7 REMOTE SENSING OF THE STRUCTURE OF PRECIPITATION USING SEQUENTIAL CIRCULAR AND LINEAR RADAR POLARIZATIONS. A. Hendry, Y.M.M. Antar, *National Research Council, Division of Electrical Engineering, Ottawa, ON*
- 8 RADAR AND MICROPHYSICAL STUDIES OF THE CONVECTIVE MELTING TRANSITION: IMPLICATIONS FOR ATTENUATION MODELLING. V.N. Bringi, J. Vivenkanandan, *Colorado State University, Dept. of Electrical Engineering, Ft. Collins, CO, USA*; R.M. Rasmussen, *National Center for Atmospheric Research, Convective Storms Division, Boulder, CO, USA*
- 9 RAIN RATE MEASUREMENT TECHNIQUES FOR EVALUATION OF RADAR ALTIMETERS. R.F. Russell, J.S. Cole, R.A. Lane, D.P. Gaines, *US Army Missile Command, Advanced Sensors Directorate, Redstone Arsenal, AL, USA*

RADAR BACKSCATTER FROM SEA ICE DURING SUMMER

S. Gogineni, R.G. Onstott and R.K. Moore  
Remote Sensing Laboratory  
University of Kansas Center for Research, Inc.  
Lawrence, Kansas 66045-2969

Although the utility of radar for sea-ice study has been well established in the last 15 years, most of the radars used were not optimized for sea-ice studies. Radar return from sea ice depends on its electrical and physical properties and the system parameters. Optimum radar parameters for sea ice can be selected only by understanding the behavior of sea ice when illuminated with microwaves. This necessitates measurement of backscatter from sea ice during different seasons at various locations, and the subsequent development of theoretical or empirical models to explain the backscatter mechanism.

Physical and electrical properties of sea ice undergo a rapid change in a short time during summer. Most of the experimental as well as theoretical studies reported to date have been on the winter sea ice. Radar backscatter measurements were made by the University of Kansas from summer sea ice near Mould Bay, N.W.T., Canada, during June-July 1982. This paper summarizes the results of that experiment.

The results indicate that in early summer a reversal of contrast occurs between first-year (FYI) and multiyear (MYI) ice; during this period, there is higher backscatter from FYI as opposed to a lower value during winter. The contrasts between FYI and MYI disappear for a short period during summer, but reappear during late summer with higher backscatter from MYI than from FYI. On the strength of backscatter alone, it may not be possible to discriminate MYI from FYI over a short period during summer, but it may be possible to use texture and shape to make the distinction.

The backscatter difference between FYI and MYI increases with decreasing frequency during late summer. The contrast at L-band is 2.5 and 4 dB higher than that at C- and X-Ku-bands, respectively, but is much lower during winter.

## MODELLING THE DETECTABILITY OF ICEBERGS ON A MARINE RADAR

Byron R. Dawe  
NORDCO Limited  
St. John's, Newfoundland, Canada

Despite a number of extensive field measurement programs over the last 40 years up to now a quantitative assessment of the detectability of icebergs on marine radar has not been derived. A key factor limiting the ability to make accurate predictions of the radar signal return from icebergs and hence derive the probability of detection has been a lack of a suitable radar cross section model. Such a model has now been developed and is shown to give excellent agreement with past data when compared on the basis of measured signal return, and that derived using a comprehensive computer based model. Applying probability of detection theory the detectability versus range is shown to fall off in the far range due to a decreasing signal-to-noise ratio and in the near range due to a decreasing signal-to-clutter ratio, for growlers, bergy bits and small icebergs. This results in an annulus at some range from the radar in which detection is reliable. It is shown that even in low to moderate sea states some small targets may be rendered totally undetectable, while in high sea states even large targets may not be detected. The effect of antenna height is seen to be dramatic with the lower antenna providing much greater detection reliability in clutter. The ability to obtain quantitative probability of detection data greatly improves the capability to perform more reliable risk analyses for ships and drilling platforms operating in iceberg infested waters. It can also be used to optimize future installations.

## F-7-3

### Multifrequency, Multipolarization Backscatter Measurements of Resonant Vegetation Structures

A. J. Blanchard and D. F. Zook  
Wave Scattering Research Center  
Electrical Engineering Department  
University of Texas at Arlington  
Arlington, Texas USA 76019

There has been a great deal of interest in the response of radar systems to vegetation. Recent research has indicated a sensitivity of radar backscatter to vegetation type and growth stage at certain frequencies, polarizations, and incident angles. The understanding of this target/energy interaction is also of interest in military applications (clutter suppression, masking, etc.) and in other remote sensing application where vegetation may act as a confusion factor. Recently acquired SAR imagery has been analysed and an unusual radar/vegetation response was identified. Imagery from SeaSat and SIRA both indicate the response. These studies show an increase in the radar backscatter to vegetation with a stalk type structure. The increase occurs when the nodal length of the stalk is one wavelength and more importantly only when the moisture in the plant concentrates in the nodes of the stalk. Prior to the observation most vegetation scattering processes were thought of and modeled as the interaction of energy with the random scatterers that comprise the canopy. There is reason to believe that because of structural coherency of the vegetation layer, a resonant interaction process may be responsible for the unusual backscatter behavior.

This paper reports the results of a series of backscatter measurements designed to investigate the nature of this phenomenon. The measurements were made at two transmit frequencies (1.6 and 4.75 Ghz) and four linear transmit/receive polarization combinations (HH,VV,HV,VH). The system is a truck mounted radar scatterometer, using pulse compression (50ns compressed pulse) and a digital IF receiver with relatively narrow band width (20Mhz). Measurements were made at incident angles from 0 to 30 degrees. Spatial averaging was used to minimize the fading characteristics of the recovered signature.

In an effort to isolate the nature of the scattering process, the measurements were made from an artificial target designed to mimic the salient properties of the real vegetation. The stalks were constructed from PVC pipe and nodes were simulated using metal rings. Nodal seperation could be varied in this manner. Physical properties were as close to the actual plant as possible. Measurements were made at three row spacings to simulate variations in plant density and at three stalk nodal seperations (.8,1.0,1.2 wavelengths at 1.6 Ghz.). The results from the measurement sets and speculations on the nature of the scattering process are presented.

TERRAIN CROSS SECTION MEASUREMENTS

K.V.N. Rao  
James W. Coffey

Electromagnetic Techniques Branch  
Electromagnetic Sciences Division  
Rome Air Development Center  
Hanscom AFB, MA 01731

An S-band pseudo-noise channel probe described earlier (K.V.N. Rao, James W. Coffey and John Austin, URSI meeting at Boulder, CO., January 1984 paper B2-7) was modified and used to measure the backscatter clutter cross section of various types of terrain. This channel probe relies on its ability to discriminate the echoes arriving from clutter cells separated in range by at least 5 feet. In order to obtain the backscatter cross section measurements, the transmit and receive antennas of the channel probe were co-located on the roof of a mobile van. Microwave absorbing material was placed between the two antennas to reduce the mutual coupling. We will describe the techniques of calibrating the channel probe, antenna pattern effects on determining the terrain cross section and the results obtained from two types of terrain.

The channel probe's receiver was calibrated by measuring its response when signals of known amplitude were injected into it. In addition to this method, the receiver's response was calibrated by measuring the amplitudes of the echoes returned from standard calibrating targets located in a clutter free environment in the far-field regions of the antennas. The backscatter cross section of these targets, mostly conducting spheres and corner reflectors varied from  $-20$  dBsm to  $+2$  dBsm.

We will discuss the errors associated with estimating the clutter cross section from the channel probe receiver's response. These errors include the effects of (a) background noise (b) antenna positioning and (c) estimate of radar footprint from antenna patterns.

The average backscatter cross section from sandy soil which has irregularly spaced ridges and troughs was measured to be  $-19.2$  dB at incidence angle of less than 4 degrees. The distribution of the surface heights of the soil in the radar's footprint was also measured by standard surveying techniques. Results on the backscatter cross section and temporal statistics of the echo amplitude obtained from pine trees will be described.

## F-7-5

### DETERMINATION OF BACKSCATTERING SOURCES IN TALL PRAIRIE GRASS OF THE KONZA PRAIRIE AT 10 GHZ

R. Zoughi, R.K. Moore and L.K. Wu  
Remote Sensing Laboratory  
University of Kansas Center for Research, Inc.  
Lawrence, Kansas 66045-2969

Fine-resolution measurements of the radar backscattering characteristics of tall prairie grass at 10 GHz were conducted during the summer of 1983. The main objective of these measurements was to determine the major backscattering sources. Two different sites on the Konza prairie, located in northeast Kansas were studied. One site was of undisturbed grass with about 10 cm of dead material from the previous year on top of the soil. The other site had intentionally been burnt before the growing season, so no dead-grass residue existed on top of the soil. Hence, soil moisture at the burnt site was appreciably less than at the natural site. Burning the residue is a common practice to enhance prairie productivity.

Each site was observed three times: (a) in a natural setting, (b) soil/root combination (grass cut and removed), and (c) cut grass laying on top of the soil. Observations were made at 30° and 50° incidence angles, and the lack of soil moisture in the burnt site was evident in the measurements. For both sites in the natural setting, a 15-cm-thick volume of grass about 25 cm above the soil was the major source of backscatter.

This research was performed in collaboration with agronomists at Kansas State University, Manhattan, Kansas.

ANALYSIS OF SYNTHETIC APERTURE RADAR  
SYSTEM INDUCED DEPOLARIZATION EFFECTS

A. J. BLANCHARD & D. LUCKERT  
Wave Scattering Research Center  
Electrical Engineering Department  
The University of Texas at Arlington  
Arlington, Texas USA 76019

The use of depolarized radar cross section measurements is advantageous in a number of remote sensing areas. The measurement contains information that is otherwise not available in other cross-section measurements. The scattering is in general a second order effect and weak (magnitude) when compared to the more robust scattering processes. Care must be exercised when attempting to recover the depolarized scattering cross-section in the presence of the like-polarized measurements. System effects have been identified (Blanchard et al, GRS-S, GE-21, 1, 113-117, 83) which may seriously affect the quality of the required depolarization measurements. Analyses have been conducted using real beam radar system to illustrate how system parameters may compromise the quality of scattering measurements. The isolation between the polarization status of both the transmit and receive antenna is critical to making high quality depolarization measurements. Recent results indicate that boresite isolation may not be adequate in specifying antenna polarization performance. Because the system is used to measure the scattering cross section of targets that are area extensive, a more appropriate parameter of integrated polarization isolation must be used. That part of the beam width which acquires information must be included in the integration. For non-doppler real aperture system this generally means first null to first null beam width. Adequate measurements can be made if the integrated isolation is 16dB above the difference between like and cross polarized scattering coefficients.

The other system induced artifact results from a mismatch between the polarization states of the antenna and those defined by the target surface normal and direction of propagation to the target. Studies have shown that for real apertures severe errors can occur for certain antenna orientation and target scattering cross sections. Generally, the effect is most severe near nadir, although significant error can be induced throughout the spectrum of incident angles. These analyses were all performed for real aperture non imaging systems. Since most applications will require the use of imaging systems, and in many cases synthetic aperture images, we wish to know how the system induced effects apply.

This paper presents the results of similar analyses except they apply to synthetic aperture imaging systems. Results are presented for various system constraints including beam width, in both azimuth and elevation, doppler band width, phase variations due to range, etc. Criteria for adequate recovery of depolarized scattering cross sections are presented.

## F-7-7

### REMOTE SENSING OF THE STRUCTURE OF PRECIPITATION USING SEQUENTIAL CIRCULAR AND LINEAR RADAR POLARIZATIONS

A. Hendry and Y.M.M. Antar  
Division of Electrical Engineering  
National Research Council of Canada  
Montreal Road, Ottawa, Ontario, Canada  
K1A 0R8

Remote sensing of the micro-physical properties of precipitation by two-channel polarization diversity radars is enhanced if data taken with opposite-sense circular polarizations are complemented by data taken sequentially using orthogonal linear polarizations. For example, the combination of data from these two different polarization base vectors permits separation of particle shape factors from the effects of preferred orientation.

The technique for these measurements involves measurement of the complex cross-correlation between the opposite sense components of the echoes with a circularly polarized radar, followed by measurement of the variation, with direction of polarization, of the co-polar and cross-polar components of the echoes obtained when linearly polarized transmissions are used. This technique, which is feasible when the precipitation is steady, has been applied to stratiform rain, snow, and the melting layer.

The paper reports measurements of the micro-physical properties of the melting layer made with a 3.1 cm dual-channel polarization diversity radar.

RADAR AND MICROPHYSICAL STUDIES OF THE CONVECTIVE MELTING  
TRANSITION: IMPLICATIONS FOR ATTENUATION MODELLING

V. N. Bringi & J. Vivekanandan  
Department of Electrical Engineering  
Colorado State University  
Ft. Collins, CO

and

R. M. Rasmussen  
Convective Storms Division  
National Center for Atmospheric Research  
Boulder, CO

Vertical profiles of dual-polarized radar observables in convective storms often show enhanced values of linear depolarization (LDR) during the melting of graupel with strongly positive values of differential reflectivity ( $Z_{DR}$ ) in the rain layer below. A detailed one dimensional microphysical melting model initiated using aircraft measurements has been used to calculate the profiles of  $Z_{DR}$  and LDR through the melting layer. Based on wind tunnel data, melting graupel is modelled as conical in shape with an inner ice core, and a distribution of canting angles. Implications of these observations for prediction of attenuation and differential attenuation at horizontal and vertical polarizations through the convective melting transition are discussed.

**RAIN RATE MEASUREMENT TECHNIQUES FOR  
EVALUATION OF RADAR ALTIMETERS**

Robert F. Russell, John S. Cole,  
Richard A. Lane, and David P. Gaines  
Advanced Sensors Directorate  
US Army Missile Command  
Redstone Arsenal, AL 35898

Performance of a KU band radar utilized as an altimeter is determined under various rainfall rate conditions. Details of a unique rate device used in the data collection are presented to allow meaningful correlation between measured rain rate and radar return. Rain models, test site selection, and test procedures are also addressed.

## URSI COMMISSION F - SESSION F8

Rain Attenuation

8:30 - 12:00  
LAW 101

Atténuation de la pluie

Chairperson/Président: **D. Zrenic**, NOAA, Norman, OK, USA

- 1 FADE RATES AT 13 GHz ON EARTH-SPACE PATHS IN CANADA. **R.V. Webber, J.J. Schlesak**, Department of Communications, Communications Research Centre, Ottawa, ON
- 2 SITE DIVERSITY GAIN CONCEPTS AND MEASUREMENTS. **K.T. Lin, C.A. Levis**, Ohio State University ElectroScience Laboratory, Columbus, OH, USA
- 3 COMPUTER SIMULATION OF SITE DIVERSITY SYSTEM OPERATION. **R.G. Wallace, J.L. Carr**, ORI, Inc., Rockville, MD, USA
- 4 ON THE "MEAN" TEMPERATURE  $T_m$  FOR INFERRING ATMOSPHERIC ATTENUATION FROM RADIOMETRIC MEASUREMENTS. **R.E. Leonard, C.A. Levis, K.T. Lin, C.W. Wang**, Ohio State University ElectroScience Laboratory, Dept. of Electrical Engineering, Columbus, OH, USA
- 5 MICROWAVE RAIN ATTENUATION MODEL FOR SHORT TERRESTRIAL PATHS. **S.H. Lin, M.V. Pursley**, Bell Communications Research, West Long Branch, NJ, USA
- 6 EXTRAPOLATION OF POINT RAIN-RATE DISTRIBUTIONS. **T.S. Chu, J.A. Schecker**, AT&T Bell Laboratories, Crawford Hill Laboratory, Holmdel, NJ, USA
- 7 SPATIAL CORRELATION FUNCTION OF RAINFALL RATE IN EUROPE INFERRED FROM STATISTICS OF POINT RAINFALL RATE AND RAIN ATTENUATION. **T. Manabe, T. Ihara, S. Uratsuka, Y. Furuhashi**, Radio Research Laboratories, Tokyo, Japan; **H. Kobayashi**, Chuo University, Faculty of Science and Engineering, Tokyo, Japan
- 8 RADAR DERIVED TWO DIMENSIONAL RAIN CELL STATISTICS. **J. Goldhirsh, B. Musiani**, The Johns Hopkins University, Applied Physics Laboratory, Laurel, MD, USA

*Withdrawn*

F-8-1

FADE RATES AT 13 GHz ON  
EARTH-SPACE PATHS IN CANADA

R.V. Webber and J.J. Schlesak  
Communications Research Centre  
Department of Communications  
Ottawa, Canada

From 15 station-years of radiometer data recorded at six locations in Canada, fade rate statistics have been compiled for 13 GHz signals on earth-space paths for attenuations up to about 9.0 dB. Attenuation statistics that were derived from these data have already been reported (R.V. Webber, J.I. Strickland and J.J. Schlesak, URSI Commission F. Symposium, Louvain-la-Neuve, Belgium, 1983, 127-133).

Among the six stations a fade rate of 0.04 dB/sec was exceeded for up to 2.5 hours per year, 0.20 dB/sec for up to 1.5 minutes per year and 0.40 dB/sec for up to about ten seconds per year. At four stations there was a clear tendency for high fade rates to occur when the attenuation was also high. However, this was not so for the fifth station and at the sixth there were too few high fade rates to justify any conclusions.

Fade rate distributions for selected threshold attenuations and fade rate duration distributions are presented for each station.

These fade rate statistics show little dependence on either the latitude of the radiometer site or the annual rainfall accumulation. It is concluded that, as with the attenuation statistics, fade rate statistics depend mainly on the local climate.

## SITE DIVERSITY GAIN CONCEPTS AND MEASUREMENTS

K. T. Lin and C. A. Levis  
ElectroScience Laboratory  
The Ohio State University  
Department of Electrical Engineering  
Columbus, Ohio

Site diversity is usually defined as the equivalent gain realized on a statistical basis by switching always to the best of the signals received from several antennas (D. B. Hodge, Rad. Sci. 17, 1393-99, 1982). In many cases other methods, e.g., maximal-ratio linear combination can produce better results (Schwartz, Bennet, Stein, Communications Systems and Techniques, Ch. 10, 1966).

This paper describes an experiment at 28.6 GHz from which the statistical propagation information is presented in the form of a conditional probability matrix. This contains all the available information, some of which would be lost in the traditional diversity-gain presentation. The performance of any proposed diversity system can be calculated from the matrix. The performance of two-antenna switched and maximal-ratio diversity systems are compared in this manner for an Earth-satellite path.

## F-8-3

### COMPUTER SIMULATION OF SITE DIVERSITY SYSTEM OPERATION

Ronald G. Wallace  
James L. Carr

ORI, Inc.  
1375 Piccard Drive  
Rockville, Maryland 20850

Site diversity, as applied to satellite communications Earth stations, capitalizes on the spatial inhomogeneity of heavy rainfall to reduce the link outage time due to rain attenuation. This improvement is gained by switching between the two Earth station sites in a manner that results in using the path that is least faded, most of the time. Switching an uplink from one antenna to another cannot help but cause amplitude, phase, and timing discontinuities, and the resulting transients can disrupt communication. It is desirable, then, to limit the frequency of switches between diversity sites to the minimum required to maintain the link. In an operational system, switching would presumably be automatic, controlled by an algorithm that decided on the basis of path attenuation measurements whether or not to switch. One would expect the design of the decision algorithm to have some bearing on the relationship between the site switching rate and the system availability. A computer simulation was performed to investigate the relation between switching rate and system availability, and see how the decision algorithm affects it.

The stochastic dynamic model for rain attenuation proposed by Maseng and Bakken (IEEE Trans. Com., COM-29, No. 5, May 1981) was used in the simulation. A program incorporating this model was written to create time functions representing simultaneous rain attenuation at two diversity sites, and various algorithms were employed to decide which simulated site to use and when to switch between them. For each algorithm, cumulative outage statistics were collected for many simulated hours of rainfall. The results showed a clear trade-off between the system outage time and site switching rate, that varied with the algorithm used. Based on the results, it appears possible to devise site switching algorithms that jointly minimize outage time and site switching frequency in a way that is consistent with the impact of the switching transients on channel performance.

ON THE "MEAN" TEMPERATURE  $T_m$  FOR INFERRING  
ATMOSPHERIC ATTENUATION FROM RADIOMETRIC MEASUREMENTS

R. E. Leonard, C. A. Levis, K. T. Lin, and C. W. Wang  
ElectroScience Laboratory  
The Ohio State University  
Department of Electrical Engineering  
Columbus, Ohio

In the absence of suitable signal sources, millimeter-wave attenuation through the atmosphere is often calculated from radiometric data by means of

$$A = 10 \log_{10} \frac{T_m - T_s}{T_m} \text{ dB}, \quad (1)$$

where the "mean" temperature  $T_m$  is given by an empirical formula or an estimated constant value (Altshuler, Falcone, & Wulfsberg, IEEE Spectrum, July 1968, 83-90). In this paper it is shown rigorously that under suitable assumptions regarding scattering  $T_m$  is a function of the true attenuation, the ground temperature, and the distributions of absorption and temperature along the paths. Explicit relationships are presented for various temperature and absorption profiles. In general the dependence on total attenuation is strongest, that on attenuation distribution is next, and that on temperature distribution is of least importance.

These relationships can be used to obtain improved estimates of  $T_m$  and, consequently, attenuation. The greatest improvement is obtained when the spatial profiles are known, but significant improvement is also possible on the basis of the attenuation dependence alone when reasonable profiles are assumed. Examples of these improvements are given at 28.6 GHz for a data period during which satellite-beacon signal strength at the ground, radiometric sky brightness, and radar reflectivity were measured simultaneously.

## F-8-5

### MICROWAVE RAIN ATTENUATION MODEL FOR SHORT TERRESTRIAL PATHS

S. H. Lin and M. V. Pursley  
Bell Communications Research  
West Long Branch, New Jersey 07764

Recently many telephone and communications companies have become interested in using digital radio systems operating at 18 GHz or at higher frequencies on short terrestrial paths in large metropolitan areas to interconnect locations of customers having need to transport large volumes of data. These new systems known as subscriber radio systems or digital termination systems intensify the need for reliable estimates of rain attenuation on short terrestrial paths. This paper presents a method for calculating microwave rain attenuation distributions on terrestrial paths which are less than 10 km long. The method is derived from Lin's model which was originally published in 1977 and used extensively since then to estimate rain outage for systems operating in the 11 GHz common carrier band where path lengths usually exceed 10 km. For shorter paths however the estimates tend to be optimistic, and, based on short path rain attenuation data, the modified approach improves the accuracy of the calculated rain attenuation distributions.

Lin's model, as modified for short path applications, coupled with long term (20 years or greater) rain rate statistics for 300 U.S. cities previously compiled by Lin permit accurate path engineering of subscriber radio systems in practically any major U.S. metropolitan area.

## EXTRAPOLATION OF POINT RAIN-RATE DISTRIBUTIONS

T. S. Chu and J. A. Schecker\*  
AT&T Bell Laboratories  
Crawford Hill Laboratory  
Holmdel, New Jersey 07733

Design of radio communication systems above 10 GHz needs rain-rate distributions to predict rain fading statistics. The trends toward higher microwave frequency give rise to the interest in light rain statistics. Measured statistics at light rain rates are not readily available and those at very heavy rain rates are often unstable, whereas there are plentiful stable statistics at moderately heavy rain rates. The purpose of this paper is to explore the possibility of using a log-normal approximation for extrapolating the available rain-rate distributions to lower and higher rain rates.

It was demonstrated that both rain-rate and rain-attenuation distributions are approximately log-normal (S. H. Lin, BSTJ, 54, 1051-1086, 1975). However, a major shortcoming of the log-normal representation is the uncertainty of the parameter  $P_0$ , which is the expected fraction of time that rain falls at the location. The arbitrary definition of when it is raining implies the ambiguity of measured raining time. We carried out a numerical experiment to test the sensitivity of the log-normal approximation to  $P_0$  in extrapolating point rain-rate distributions for 19 U.S. cities. The predicted probabilities at extrapolated rain rates are shown to be relatively insensitive at each location for an order of magnitude change in raining probability,  $P_0$ . In most cases the range of estimated probabilities<sup>0</sup> is only of the order of 10%. These uncertainties are much smaller than variations from year to year.

\*Now with State University of New York at Stony Brook.

SPATIAL CORRELATION FUNCTION OF RAINFALL RATE  
IN EUROPE INFERRED FROM STATISTICS OF  
POINT RAINFALL RATE AND RAIN ATTENUATION

T. Manabe, H. Kobayashi\*, T. Ihara, S. Uratsuka, and Y. Furuhashi  
Radio Research Laboratories  
Koganei, Tokyo 184, Japan  
\*Faculty of Science and Engineering, Chuo University  
Bunkyo-ku, Tokyo 112, Japan

Radio waves at frequencies above 10 GHz are subject to serious attenuation due to rain. In designing reliable radio communication links at these frequencies, it is necessary to predict the rain attenuation. Several methods have been proposed for predicting rain attenuation statistically from rainfall rate measured near the propagation path. Since the measurement of rainfall rate for a given path is generally performed at a fixed point, some model taking account of the spatial inhomogeneity of rainfall along the propagation path must be employed.

To take account of the spatial inhomogeneity, Morita and Higuti [Trans IECE Japan, E61, 425, 1978] proposed a method in which the spatial correlation function of rainfall rate whose functional dependence on distance  $d$  is given by  $\exp(-\alpha\sqrt{d})$  is employed and the log-normal distributions are assumed for both cumulative distributions of rainfall rate and attenuation. Their method was successfully applied to Japanese climate.

Considering possible variability of the spatial structure of rainfall from one locality to another, the form of the spatial correlation function is considered to be dependent on climatic condition. In this paper, the functional dependence of the spatial correlation function on distance is examined by applying their method to terrestrial paths in 8 localities across Europe where the reliable statistics of rainfall rate and attenuation are available [F. Fedi, Alta Freq., 48, 167, 1979]. In addition to the correlation function given by  $\exp(-\alpha\sqrt{d})$ , another type of correlation function given by  $\exp(-\beta d)$  is examined. The parameter  $\alpha$  or  $\beta$  for each locality is so determined as to give the best fit prediction of cumulative distribution of attenuation.

Although there are several propagation path in each locality, the variance of the inferred parameter  $\beta$  is smaller than that of the inferred parameter  $\alpha$  within each locality. This fact implies that the correlation function given by  $\exp(-\beta d)$  is more appropriate to the spatial structure of rainfall in Europe than that given by  $\exp(-\alpha\sqrt{d})$ . It is also found that the values of the parameter  $\beta$  for different localities within a particular climatic region (CCIR Rep. 563) are close to each other, while those for different climatic regions differ significantly between different climatic regions. This shows that the parameter  $\beta$  depends considerably on the climatic region.

RADAR DERIVED TWO DIMENSIONAL RAIN  
CELL STATISTICS

Julius Goldhirsh and Bert Musiani  
The Johns Hopkins University  
Applied Physics Laboratory  
Johns Hopkins Road  
Laurel, Maryland 20707

Two dimensional contours of equi-rain intensity levels,  $R$  (mm/hr) have been derived employing a multi-year radar data base of the rain reflectivity structure. An S Band radar (SPANDAR) located at the NASA/Goddard Space Flight Center, Wallops Flight Facility at Wallops Island, Virginia was used to acquire the rain reflectivity data. The rain rate intensities examined range from a few mm/hr up to 150 mm/hr and their contours were derived from low elevation azimuthal  $360^\circ$  radar scans (PPIs) of the rain environment and simultaneously acquired disdrometer data.

Backscatter power levels of the rain environment were recorded for adjacent range bins from 10 to 100 km with a resolution of 150 m (pulse width = 1  $\mu$ sec), at azimuthal intervals of  $1^\circ$ ). These power levels were initially converted to radar reflectivity factor levels,  $Z$  ( $\text{mm}^6/\text{m}^3$ ). Simultaneous with each rain period, drop size spectra data were obtained with a near-by disdrometer. These disdrometer data were analyzed for each rain period and a best fit  $R = aZ^b$  power law relationship was derived for each rain day. The radar reflectivity levels were converted to rain intensities by utilizing the appropriate  $R$ - $Z$  relationship for the rain period in question. In this way, planes of  $Z$  were converted to planes of  $R$  structure for each PPI.

An algorithm was developed enabling the determination of contours for defined narrow intervals of rain rate intensities. The actual areas and diameters of the equi-circular areas of these contours were subsequently derived. Statistics for both the actual areas as well as the equi-circular diameters were determined and these results are presented. Cell size comparisons are made with those derived by other investigators.

These results are useful for rain attenuation modeling and rain scatter interference problems and should provide an important data base to the International Radio Consultative Committee (CCIR).



## URSI COMMISSION G - SESSION G1

HF Propagation

8:30 - 12:00

Propagation HF

LAW 201

Chairperson/Président: **H. Soicher**, US Army Communications Electronics Command, Fort Monmouth, NJ, USA

- 1 HIGH-FREQUENCY RADIO PATHS IN MODEL IONOSPHERIC LAYERS WITH HORIZONTAL GRADIENTS. **K. Davies**, National Oceanic and Atmospheric Administration, Environmental Research Laboratories, Boulder, CO, USA
- 2 COMPARISON OF THE FOPPIANO AND VONDRAK AURORAL LOSS MODELS. **G.H. Millman, K.H. Rex**, General Electric Company, Military Electronic Systems Operations, Syracuse, NY, USA
- 3 AN IMPROVED MUF ALGORITHM FOR MICROCOMPUTER APPLICATIONS. **R.A. Sprague, D.B. Sailors**, Naval Ocean Systems Center, Ocean and Atmospheric Sciences Division, San Diego, CA, USA
- 4 UPDATE OF SKYWAVE TRANSMISSION CURVES TO MATCH MULTIPLE LAYER PROPAGATION PREDICTIONS FOR REAL TIME OVER-THE-HORIZON RADAR AND COMMUNICATION SYSTEM OPERATIONS. **R.D. Chaney, D.B. Odom, N.P. Viens**, Raytheon Company, Equipment Division, Wayland, MA, USA
- 5 USE OF A GLOBAL EFFECTIVE SUNSPOT NUMBER (IG) FOR LONG-TERM IONOSPHERIC PREDICTIONS. **R. Liu, K. Liu, Y. Zhou**, China Research Institute of Radiowave Propagation, Xixiang, China
- 6 EXPERIMENTAL VERIFICATION OF A REAL-TIME HF FREQUENCY MANAGEMENT TECHNIQUE. **C.M. Rush**, National Telecommunications and Information Administration, Institute for Telecommunication Sciences, Boulder, CO, USA; **J. Perry**, DoD, Washington, DC, USA; **P. Argo**, LANL, Los Alamos, NM, USA; **R. Conkright**, NOAA/EDIS, Boulder, CO, USA; **A. Paul**, NOSC, San Diego, CA, USA; **B. Reinisch**, University of Lowell, Lowell, MA, USA
- 7 DAY-TO-DAY VARIATIONS OF FIELD STRENGTH ON HF TRANSMISSION LINKS. **T. Damboldt**, Forschungsinstitut der Deutschen Bundespost, Darmstadt, FRG
- 8 SPORADIC-E MEASUREMENTS USING A HIGH TIME RESOLUTION HF CHANNEL PROBE. **L.S. Wagner**, Naval Research Laboratory, Information Technology Division, Washington, DC, USA
- 9 ANGLE OF ARRIVAL OF ECHOS REFLECTED FROM SPORADIC E-LAYERS. **A.K. Paul**, Naval Ocean Systems Center, Ocean and Atmospheric Sciences Division, San Diego, CA, USA
- 10 A THREE-NODE TRANSATLANTIC DIGITAL HF EXPERIMENT. **M. Ahmed**, GTE Government Systems Corporation, Communication Systems Division, Needham Heights, MA, USA; **B.W. Reinisch**, University of Lowell, Center for Atmospheric Research, Lowell, MA, USA; **J.C. Jodogne**, Institut Royal Meteorologique, Bruxelles, Belgium; **J. Gilbert**, Rutherford Appleton Laboratory, Didcot, U.K.

## G-1-1

High-frequency radio paths in model ionospheric layers with horizontal gradients.

by

Kenneth Davies

Horizontal gradients of electron density can play an important role in the determination of radio ray paths as they produce errors in radio location based on measurements of angles of elevation and azimuth. Large gradients are known to occur regularly in such areas as: the equatorial anomaly, the sub-auroral trough, the sunrise terminator, travelling ionospheric disturbances etc. Using parabolic models of vertical electron density with linear variations in the horizontal direction, the three-dimensional ray paths are expressed by analytical formulas. Using gradients of  $N_{max}F_2$  observed in Europe, it has been found that errors of 50 to 100 km are possible in the apparent location of a source with ranges of the order of 300 km. When the horizontal gradients are sufficiently large, horizontal reflection occurs and the ray can be reflected back along itself as is the case with "vertical" sounding using ionosondes.

## COMPARISON OF THE FOPPIANO AND VONDRAK AURORAL LOSS MODELS

GEORGE H. MILLMAN  
KENNETH H. REX  
GENERAL ELECTRIC COMPANY  
SYRACUSE, NEW YORK 13221

The auroral loss model developed by Foppiano and the one proposed by Vondrak, which is a modified version of the Foppiano model, are compared. Both models were incorporated into the IONCAP ionospheric prediction computer program developed by the Institute for Telecommunication Sciences.

The comparison of the auroral losses predicted by the two models for a location in the Northeastern United States was based on HF oblique propagation paths specified as a function of skip distance, bearing, time of day, season, magnetic activity and sunspot number.

An examination of the computed data reveals that, for high magnetic activity, Vondrak's auroral absorption is higher than the Foppiano results. Under some conditions, the difference could be as large as 10 dB. For low magnetic activity, Foppiano's estimates are slightly higher than the Vondrak predictions, the maximum difference being on the order of 2 dB.

## G-1-3

### AN IMPROVED MUF ALGORITHM FOR MICROCOMPUTER APPLICATIONS

R. A. Sprague and D. B. Sailors  
Ocean and Atmospheric Sciences Division  
Naval Ocean Systems Center  
San Diego, CA 92152-5000

An improved version of MINIMUF-3.5 was developed to predict accurate maximum usable frequencies (MUFs) under conditions of anomalously high sunspot numbers, to predict foF2 values suitable for ray-tracing applications, and to predict M3000 factor values usable for determining the mirror height of reflection for oblique incidence propagation. This version includes sunspot number dependence in both the foF2 and the M factor calculations and provides a natural saturation in the MUF vs sunspot number curve, reducing the error in predicted MUF values under very high sunspot number conditions.

The improvement in the prediction of the foF2 values was made by comparing the predicted foF2 values against 480 path months of foF2 data measured at 30 sites. The data at each site covered the low, medium, high, and very high sunspot ranges for one month of each season of the year. The sunspot number variation previously used in MINIMUF 3.5 was deleted and the constant 58.0 called  $A_1$  in MINIMUF-3.5 was replaced by a linear equation. The constants in the equation were chosen to minimize the bias in predicted foF2 as a function of sunspot number.

The M factor portion of the algorithm was modified to include sunspot number, seasonal, and diurnal variations using over 7200 observed oblique sounder medium MOFs measured on 39 paths. A linear variation in sunspot number with negative slope was found that minimized the bias in the predicted MUFs. A sixth-order Fourier series was fit to the bias of the predicted MUFs for each month of the year to determine the seasonal dependence. The diurnal dependence was determined by first fitting a linear equation to the daytime values of the bias in the predicted MUFs and then fitting a sixth-order Fourier series to the nighttime values of the bias in the predicted MUFs. The resulting M factor portion of the algorithm can be used to predict M3000 factors for obtaining mirror heights of reflection for oblique incidence propagation (M. Lockwood, Proc. IEE, 131, 117-124, 1984).

UPDATE OF SKYWAVE TRANSMISSION CURVES TO MATCH MULTIPLE  
LAYER PROPAGATION PREDICTIONS FOR REAL TIME OVER-THE-  
HORIZON RADAR AND COMMUNICATION SYSTEM OPERATIONS

R.D. Chaney, D.B. Odom and N.P. Viens  
Raytheon Company, Equipment Division  
Wayland, Massachusetts 01778

One of the problems frequently encountered when analyzing the processing time-line of over-the-horizon (OTH) radar and communication systems is the inability to accurately estimate as well as supply the computer resources required to support a real time raypath analysis through a realistic ionospheric model. To overcome this problem a procedure has been developed which provides an update to the presently used Smith Transmission Curves as adapted by Wieder (Smith, N., 1939, Wieder, B., 1955 and Davis K., 1965) which allows the transmissions curves to more accurately predict the propagation conditions which would apply to realistic multiple layer profiles that are characteristic of both quiet and disturbed conditions.

The advantages provided by this procedure are twofold: 1) The observed ionospheric profile can be updated in real time by manually tracing the local ionospheric sounding obtained at the HF radar and communication sites or use can be made of an automatic ionospheric digitizing procedure such as that developed at the University of Lowell (Reinisch, B.W., 1983). 2) The use of the updated transmission curve relationships to predict, in real time, the ionospheric propagation conditions which are present in the region of the ionospheric sounder substantially reduces the raypath analysis requirement placed upon the system processor and allows realistic estimates of a much reduced computational load to be made.

This paper reviews the analytical procedures used to update the transmission curve predictions and provides a comparison with ray-trace calculations performed through both Chapman and multiple parabolic layers for both day and nighttime conditions for a mid-latitude site location. The physical relationship of this new transmission curve function to the variation in the scale height as a function of altitude is discussed. This transmission function is constrained to have the propagation parameters match those which result when Chapman profiles are used to model the region of the skip ray. A comparison between the results obtained using the Smith curves and those derived from the new propagation modeling procedure is provided along with an estimate of the computational load to be addressed during real time communication system and radar operations.

## G-1-5

### USE OF A GLOBAL EFFECTIVE SUNSPOT NUMBER (IG) FOR LONG-TERM IONOSPHERIC PREDICTIONS

Liu Ruiyuan, Liu Kefeng and Zhou Yuzhi  
China Research Institute of  
Radiowave Propagation  
P. O. Box 138  
Xinxiang, Henan Province  
China

A new index of solar activity called the global effective sunspot number (IG) has been developed ( Liu et al., Telecomm. J., Vol. 50, 8, 408-414, 1983 ). The present work is based on Chinese vertical incidence sounding stations' data in order to investigate the possibility of the use of  $IG_{12}$ , the 12-month running mean of IG, for long-term ionospheric predictions. It is shown that the correlation coefficients between the ionosphericly-derived index ( $IG_{12}$ ) and ionospheric characteristics ( $f_0F_2$  and  $F_2(3000)MUF$ ) are higher than those between sunspot number  $R_{12}$  and ionospheric characteristics.

The efficacy of the use of  $IG_{12}$  for predicting  $f_0F_2$ ,  $M(3000)F_2$  and  $F_2(4000)MUF$  has been evaluated, using CCIR Report 340, by comparison with  $R_{12}$  in current use. The evidence presented shows that the use of  $IG_{12}$  instead of  $R_{12}$  in the CCIR prediction scheme yields more accurate values of  $f_0F_2$  and  $F_2(4000)MUF$ . In the predictions of  $f_0F_2$  and  $F_2(4000)MUF$  12-month in advance, the average improvements in accuracy are about 18% and 10% respectively. Other advantages arising from the use of the IG index are discussed.

EXPERIMENTAL VERIFICATION OF A REAL-TIME  
HF FREQUENCY MANAGEMENT TECHNIQUE

Charles M. Rush, NTIA/ITS, Boulder, CO 80303, Jane Perry, DoD, Washington, D.C. 20755, Paul Argo, LANL, Los Alamos, N.M. 87545, Ray Conkright, NOAA/EDIS, Boulder, CO 80303, Adolf Paul, NOSC, San Diego, CA 92152, and Bodo Reinisch, University of Lowell, Lowell, MA 01854

A high frequency (HF) experiment was conducted in October 1984 to test the concept of employing cooperative beacons to improve the accuracy of HF time-difference-of-arrival geolocation systems. The experiment involved continuous transmission of HF signals from 10 transmitter sites (taken 2 at a time) to 5 receiver sites. The path length of the circuits that were studied varied from less than 50 km to nearly 1600 km. Vertical incidence ionosondes were operated at Boulder, Colorado; Los Alamos, New Mexico; and Salina, Utah; and the observations were used to provide real-time information about the ionospheric structure in the vicinity of the experiment. The ionosonde information was used, along with propagation predictions obtained from the IONCAP program, to provide quasi-real frequency management for all the circuits in the experiment. Communication, i.e., hearability, was achieved for over 90 percent of the time during the experiment.

In this paper we will describe the experimental setup, the ionosonde operation, and the frequency management methods that were used to achieve the observed high level of hearability. In addition, the procedures used to update the IONCAP prediction program with the ionosonde data will be described. Results will be presented illustrating how well the circuits performed under a variety of conditions--day/night, dawn/dusk, short distance/long distance, quiet magnetic conditions/disturbed conditions.

## G-1-7

### Day-to-day variations of field strength on HF transmission links

by

Thomas Damboldt

Forschungsinstitut der Deutschen Bundespost  
D-6100 Darmstadt

Continuous field-strength recordings of distant HF transmitters have been made since 1969 by the Research Institute of the Deutsche Bundespost. The AGC voltages of the receivers, which are a measure for the input voltages, are recorded on strip-chart recorders. The strip charts are evaluated such that hourly medians are determined. At present 24 transmitters are recorded (i.e. 576 hourly (median) values per day). This yields about 17,000 values per month from which the monthly (hourly) medians, quartiles and deciles are obtained. The complete set of data collected so far consists of about 40,000 of each of these values. A comparison of medians and quartiles (or deciles), i.e. an estimation of the day-to-day variation, yields differences of up to  $\pm 50$  dB. A more detailed analysis reveals that the day-to-day variation is largest near the critical frequency. It is almost independent of path length, solar activity, season, geographical latitude of the path midpoint and of time of day.

## Sporadic-E Measurements Using a High Time Resolution HF Channel Probe

L. S. Wagner  
Naval Research Laboratory

Observation of sporadic-E with a high resolution ( $1\mu\text{s}$ ), coherent, coded-pulse, oblique sounder reveals interesting structural details unresolved by lower resolution sounders. Measurements were made on a 126 km baseline mid-latitude path. Results will be presented showing the pulse response for a variety of forms of sporadic-E. In all cases, the time evolution of the sporadic-E return is monitored over an extended time and frequency interval with a revisit time, at a given frequency, of approximately 10 seconds. In selected cases, the pulse response at a given frequency is monitored every 0.5 second over an interval of approximately 1 minute. This mode of operation is useful for examining fast fluctuation phenomena. Doppler analysis and examination of the coherent pulse response helps in distinguishing between signals refracted in a more or less conventional manner and those scattered by an extended cloud of irregularities.

## G-1-9

### ANGLE OF ARRIVAL OF ECHOS REFLECTED FROM SPORADIC E-LAYERS

Adolf K. Paul

Ocean and Atmospheric Sciences Division  
Naval Ocean Systems Center San Diego, California 92152-5000

Ionograms recorded with the NOAA digital ionosonde at four receiving antennas include the information for angle of arrival computation. Recordings taken between August 1980 and January 1981 near Brighton, Colorado were analyzed to study tilts of sporadic E-layers. It was found that tilts of  $10^\circ$  or more are quite frequent and can be as large as  $30^\circ$ . In some cases where apparently two layers at different virtual heights were observed it was found that the echos were reflected at approximately equal heights from two different locations. The observations imply that characteristic dimensions of sporadic E-layers are frequently less than 50 km. The limited number of samples available give no clear indication whether sporadic E-layers have a wavelike or patchy structure, both types may exist. The consequences of these results for HF-propagation will be discussed.

## A THREE-NODE TRANSATLANTIC DIGITAL HF EXPERIMENT

Mukhtar Ahmed  
Communication Systems Division  
GTE Government Systems Corporation  
Needham Heights, MA 02194

Bodo W. Reinisch  
University of Lowell Center for Atmospheric Research  
Lowell, MA 01854

Jean Claude Jodogne  
Institut Royal Meteorologique  
1180 Bruxelles, Belgique

John Gilbert  
Rutherford Appleton Laboratory  
Chilton, Didcot, Oxfordshire, OX11 0QX, England

Reported here are the results of bidirectional transatlantic soundings conducted during September 16-19, 1984 with identical Digisonde 256 sounders at Needham, USA, Slough, UK, and Dourbes, Belgium. Each sounder was operated simultaneously in the vertical monostatic and oblique bistatic modes transmitting 10 KW pulses at a repetition rate of 100 Hz.

Bidirectional soundings at each node were performed by simultaneous transmission to and reception of signals from the other two nodes. A typical transmission cycle consists of a 5-minute swept frequency ionogram incremented every 0.1 MHz in the range 4-26 MHz followed by a fixed frequency ionogram for the same length of time. In the swept frequency ionograms recorded at Needham starting at 4.0 MHz the even and odd increments of 0.1 MHz represent signals from Slough and Dourbes respectively. The fixed frequency ionograms show signals from Slough and Dourbes alternating in the first and second 2.56 period.

The four-day experiment encompassed a very quiet period of geomagnetic activity followed by a highly disturbed phase ( $K_p = 8$ ) at high latitudes. Significant variations in the SNR and varying multi-mode structures reflect highly variable propagation conditions. Criteria are presented for Real Time Channel Evaluations during day/night and benign/stressed propagation conditions. Cross correlation and power spectral analyses of ionograms show spatial diversity, and different fading and Doppler characteristics of signals from Slough and Dourbes.



## URSI COMMISSION G - SESSION G2

**Modeling and Dynamics  
of the Ionosphere**1:30 - 5:00  
LAW 157**Modélisation et  
dynamique de l'ionosphère**Chairperson/Président: **R.T. Tsunoda**, SRI International, Menlo Park, CA, USA

- 1 (1:40) A MODEL OF THE GLOBAL IONOSPHERE. **R.W. Schunk, J.J. Sojka**, Utah State University, Center for Atmospheric and Space Sciences, Logan, UT, USA
- 2 (2:20) THE IMPORTANCE OF INCOHERENT SCATTER DATA FOR THE URSI-COSPAR 'INTERNATIONAL REFERENCE IONOSPHERE'. **K. Rawer, D. Bilitza**, Albert-Ludwigs-Universität, Freiburg, FRG
- 3 (2:40) ON LONG-TERM TRENDS OF IONOSPHERIC CHARACTERISTICS. **P. Dominici, B. Zolesi**, Istituto Nazionale di Geofisica, Ionospheric Dept., Rome, Italy
- 4 (3:00) ON "LOCAL" IONOSPHERIC MODELS. **P. Dominici, B. Zolesi**, Istituto Nazionale di Geofisica, Ionospheric Dept., Rome, Italy
- 5 (3:20) DYNAMIC INTERACTION BETWEEN THE IONOSPHERE AND THERMOSPHERE. **R.G. Roble**, National Center for Atmosphere Research, Boulder, CO, USA
- 6 (4:00) CALCULATED RAYLEIGH-TAYLOR INSTABILITY GROWTH RATES FOR SOLAR MINIMUM AND SOLAR MAXIMUM CONDITIONS. **D.N. Anderson**, Air Force Geophysics Laboratory, Hanscom AFB, MA, USA
- 7 (4:20) SOURCES OF F-REGION IONIZATION ENHANCEMENTS IN THE NIGHTTIME AURORAL ZONE. **R.M. Robinson**, Lockheed Palo Alto Research Laboratory, Space Sciences Laboratory, Palo Alto, CA, USA; **R.T. Tsunoda, J.F. Vickrey**, SRI International, Radio Physics Laboratory, Menlo Park, CA, USA
- 8 (4:40) F-REGION IONOSPHERIC IRREGULARITIES - A REVIEW. **J.F. Vickrey**, SRI International, Menlo Park, CA, USA

## G-2-1

### A MODEL OF THE GLOBAL IONOSPHERE

R. W. Schunk and J. J. Sojka, Center for Atmospheric and Space Sciences, Utah State University, Logan, Utah 84322, USA

We constructed a time-dependent, 3-dimensional, multi-ion model of the global ionosphere at E and F-region altitudes. The model is based on a numerical solution of the coupled continuity, momentum, and energy equations for electrons and six ions ( $\text{NO}^+$ ,  $\text{O}_2^+$ ,  $\text{NO}^+$ ,  $\text{O}^+$ ,  $\text{N}^+$ ,  $\text{He}^+$ ). The model takes account of magnetospheric and equatorial electric fields, auroral precipitation, a global thermospheric wind, and the displacement between the geographic and geomagnetic poles. Our initial model studies indicate that the ionosphere displays a marked variation with altitude, latitude, longitude, universal time, season, solar cycle and geomagnetic activity, which is in agreement with the extensive body of data that has been collected over the last two decades. Depending on the conditions, the model produces a number of interesting ionospheric features, including ionospheric hot spots, drifting plasma blobs, localized ionization troughs, a tongue of ionization in the polar caps, mid-latitude troughs, Appleton ionization peaks, and an equatorial fountain. These features all display a significant UT variation owing to the offset between the geomagnetic and geographic poles. Also, at a given instant of time,  $N F_2$  can vary by almost three orders of magnitude over the globe. These and other results will be reviewed.

THE IMPORTANCE OF INCOHERENT SCATTER DATA FOR THE  
URSI-COSPAR 'INTERNATIONAL REFERENCE IONOSPHERE'

Karl RAWER and Dieter BILITZA

Albert-Ludwigs-Universität Freiburg (Br.), FRG

The International Reference Ionosphere (IRI) has for task to produce vertical profiles of the main ionospheric parameters depending on space and time coordinates. The chosen parameters are: plasma (electron) density, electron and ion temperature and chemical composition of the major ions. Ground and space based data have been and are considered to this end.

Specific contributions obtained by incoherent scatter techniques (inc. sc.) are most important in certain altitude ranges for the plasma density, and at all altitudes for the temperature profiles. As for the ion composition, inc. sc. technique can give valuable complementary information. In general, the station-bound inc. sc. data are particularly useful when they can be combined with world-wide data as obtained by satellites. They are quite often needed for checking such data, and as a primary source of information in height ranges which are only accessible to rockets, not satellites. A few problems have been encountered in the past when combining data of different techniques and sources. Some desiderata are indicated, concerning the kind and rhythm of inc. sc. measurements in view of the IRI project.

In the future, IRI plasma motions are also to be described at least provisionally. The combination of inc. sc. results with those of other techniques needs yet some discussion.

## G-2-3

### ON LONG-TERM TRENDS OF IONOSPHERIC CHARACTERISTICS

P. Dominici and B. Zolesi  
Ionospheric Department  
Istituto Nazionale di Geofisica, Roma, Italy

The measurement of ionospheric characteristics by systematic vertical radio soundings began some tens of years ago and now it is possible to study long series of data for many stations of the world ionospheric network: for instance, in order to put in evidence long-term trends, as it happens for the elements of the geomagnetic field.

The data carried out from about 1948 at the ionospheric station of Rome (41.8°N, 12.5°E) have been statistically analysed from this particular point of view.

The results seem to confirm the existence of some long-term trends, but further studies are necessary, in particular for what concerns the independence of some data from measuremental facts.

ON "LOCAL" IONOSPHERIC MODELS

P.Dominici and B.Zolesi  
Ionospheric Department  
Istituto Nazionale di Geofisica, Roma, Italy

For studies and applications regarding a not large area it is convenient to use local ionospheric models from the data of the ionospheric stations in that zone, which are more accurate than general models. The criteria for such models especially for that concerns the predictions for the ionospheric HF radio propagation are briefly discussed.

A model of this kind for the central Mediterranean area is shown.

## Dynamic Interaction between the Ionosphere and Thermosphere

Raymond G. Roble  
National Center for Atmosphere Research\*  
P.O. Box 3000  
Boulder, Colorado 80307

Ion drag has a strong influence on the dynamic structure of the Earth's thermosphere. At high magnetic latitudes the ion drag associated with magnetospheric plasma convection derives a largely rotational, nondivergent, double-vortex wind system at F-region altitudes that can attain velocities greater than  $500 \text{ ms}^{-1}$  during moderate levels of geomagnetic activity. This wind system has been observed by instruments on board the Dynamics Explorer-2 satellite and also from various ground-based observatories. At mid-latitudes the thermospheric winds are primarily driven by solar EUV and UV radiation during geomagnetic quiet periods but they are strongly influenced by electric fields penetrating equatorward from the auroral zone during geomagnetic disturbed periods. At low-latitudes ion drag variations associated with equatorial  $\bar{E} \times \bar{B}$  plasma drifts also influence the dynamic structure of the thermosphere. The observational evidence describing these large-scale dynamic interactions will be reviewed. The results of numerical simulations made with the NCAR thermospheric general circulation model (TGCM) to examine these dynamic interactions will also be presented.

CALCULATED RAYLEIGH-TAYLOR INSTABILITY GROWTH RATES FOR  
SOLAR MINIMUM AND SOLAR MAXIMUM CONDITIONS

David N. Anderson  
Air Force Geophysics Laboratory  
Hanscom AFB, MA 01731-5000

There is strong evidence that the post-sunset formation of equatorial plasma depleted regions or "bubbles" has a solar cycle dependence with the largest occurrence frequency coming at solar maximum and the smallest at solar minimum periods. An essential ingredient in creating the ambient ionospheric conditions which lead to the growth of plasma instabilities is the post-sunset enhancement in upward  $E \times B$  drift. This is a common feature during solar maximum years, but is essentially absent at solar minimum. To quantitatively study Raleigh-Taylor instability growth rates and how they compare with the dissipating process of chemical loss rates, the time-dependent plasma continuity equation is solved numerically to give electron density profiles as a function of latitude and local time. Calculated ambient ionospheric conditions at 1900 LT for equinox, solar cycle maximum and solar cycle minimum periods are presented. It is found that under solar maximum conditions, the calculated "time constants" for instability growth and chemical loss are 17 min. and 151 min. respectively, implying that depleted regions grow much faster than they are dissipated. In contrast, during solar minimum period, chemical loss dissipation occurs in 27 minutes compared to a growth time constant of 52 minutes. The importance of the chemical loss rate is discussed in the light of a recent suggestion that neutral winds may play an important role in accounting for the seasonal/ longitudinal variation in the observed occurrence of equatorial "bubbles" and scintillation activity.

## G-2-7

### SOURCES OF F-REGION IONIZATION ENHANCEMENTS IN THE NIGHTTIME AURORAL ZONE

- R. M. Robinson (Space Sciences Laboratory, Lockheed Palo Alto Research Laboratory, Palo Alto, Ca. 94304)  
R. T. Tsunoda and J. F. Vickrey (Radio Physics Laboratory, SRI International, Menlo Park, Ca. 94025)

Data obtained during elevations scans with the Chatanika incoherent-scatter radar have revealed the presence of ionization enhancements in the nightside auroral F-region with scale sizes ranging from tens of kilometers (medium-scale) to hundreds of kilometers (large-scale). These ionization enhancements are typically found in the midnight local time sector and extend longitudinally in the evening and morning sectors near the equatorward boundary of the auroral oval. We show the results of two models which demonstrate that these ionization enhancements are produced by a combination of local production by precipitating particles and transport. By combining various source distributions with a high latitude convection pattern, we were able to examine the effectiveness of a given source in producing the observed distributions. The results show that the Harang discontinuity near midnight is an important source region for F-region ionization enhancements. However, we also show that the equatorward edge of the oval is a preferred location for ionization enhancements transported from the polar cap into the auroral zone. In convecting from midnight toward dawn and dusk, large-scale ionization enhancements become extended longitudinally so their latitudinal scale sizes decrease.

## F-REGION IONOSPHERIC IRREGULARITIES--A REVIEW

James F. Vickrey  
SRI International  
333 Ravenswood  
Menlo Park, CA 94025

The study of ionospheric structure has traditionally concentrated on fluctuations in electron concentration. Recent results indicate, however, that a full understanding of density structure requires knowledge of structure in electrodynamics, neutral winds and waves, and plasma temperature and composition as well. Ionospheric structure can exist over scale sizes ranging from global scales to centimeters. The sources of this structure vary with location. At the equator, for example, nighttime F region structure results from instabilities that can dominate the plasma motion. At high latitudes, plasma instabilities are accompanied by structured particle precipitation, strong and highly structured magnetospheric convection electric fields and field-aligned currents, all of which can produce variations in ion concentration.

The ultimate spectrum of fluctuations in ion concentration that is observed experimentally is a balance between the strength and scale size dependencies of the sources and sinks of structure. In this review, recent progress in modelling the sources and sinks of structure will be emphasized. In addition, experimental observations for comparison to theory, and for establishing a hierarchy of sources and sinks will be presented.



## URSI COMMISSION G - SESSION G3

**Ionospheric Studies  
Using Radio Waves**

8:30 - 12:00  
LAW 201

**Études ionosphériques au moyen  
des ondes radio-électriques**

Chairperson/Président: **S. Basu**, Emmanuel College, Boston, MA, USA

- 1 WHAT IS THERE LEFT TO STUDY IN IONOSPHERIC RADIO PROPAGATION?. **J. Aarons**, Boston University, Dept. of Astronomy, Boston, MA, USA
- 2 USE OF SCINTILLATION THEORY TO UNDERSTAND FREQUENCY-SPREAD ON F-REGION IONOGRAMS AND FADING ON HF IONOSPHERIC COMMUNICATION-LINKS. **H.G. Booker, P.K. Pasricha, W.J. Powers**, University of California at San Diego, Dept. of Electrical Engineering and Computer Sciences, La Jolla, CA, USA
- 3 SIMULATION OF HF WAVE PROPAGATION AT OBLIQUE INCIDENCE IN A STRATIFIED IRREGULAR IONOSPHERE. **J.-F. Wagen, K.C. Yeh**, University of Illinois at Urbana-Champaign, Dept. of Electrical and Computer Engineering, Urbana, IL, USA
- 4 THE SPECTRAL CHARACTERISTICS OF HIGH-LATITUDE F-REGION IRREGULARITIES DEDUCED FROM HILAT SATELLITE PHASE SCINTILLATION DATA. **C.L. Rino**, SRI International, Radio Physics Laboratory, Menlo Park, CA, USA
- 5 IRREGULARITY SHAPES OBSERVED VIA HILAT. **E.J. Fremouw**, Physical Dynamics, Inc., Bellevue, WA, USA
- 6 EFFECTS OF IONOSPHERIC IRREGULARITIES ON COHERENT MICROWAVE SYSTEMS. **W.D. Brown**, Sandia National Laboratories, Systems Research Division, Albuquerque, NM, USA
- 7 TRANSIONOSPHERIC RADIOWAVE PROPAGATION EFFECTS IN THE IONOSPHERE. **J.A. Klobuchar, G. Bishop, E. Weber, P. Fougere**, Air Force Geophysics Laboratory, Ionospheric Effects Branch, Hanscom AFB, MA, USA, **P.H. Doherty**, Emmanuel College, Physics Research Division, Boston, MA, USA
- 8 VARIABILITY OF TOTAL ELECTRON CONTENT AT HIGH LATITUDES NEAR SOLAR MINIMUM. **H. Soicher**, US Army Communications-Electronics Command, Center for Communications Systems, Fort Monmouth, NJ, US
- 9 MEM AND FFT ANALYSIS OF HIGH-LATITUDE SPACED-RECEIVER MEASUREMENTS. **E. Costa**, Emmanuel College, Physics Research Division, Boston, MA, USA; **P.F. Fougere**, Air Force Geophysics Laboratory, Ionospheric Physics Division, Hanscom Air Force Base, MA, USA
- 10 COMPUTER SIMULATION OF SPACE-TIME VARIATIONS OF IONOSPHERIC IRREGULARITIES AND SCINTILLATION. **S.J. Franke, C.H. Liu**, University of Illinois, Ionosphere Radio Laboratory, Urbana, IL, USA

## G-3-1

### WHAT IS THERE LEFT TO STUDY IN IONOSPHERIC RADIO PROPAGATION?

Dr. Jules Aarons  
Dept. of Astronomy  
Boston University, Boston, MA 02215

The technical demands for studies of ionospheric radio propagation have two sources. In one stream the ionosphere is studied because it is a component black box in the electronic system. Low frequency navigation and communication systems and HF communication and radar systems are examples. The other often silent group of system operators and designers studies the ionosphere reluctantly wishing the ionosphere wasn't there; then the system wouldn't have to correct for ionospheric delays or wouldn't be bothered by fading problems at equatorial and high latitudes. Both streams of technical needs are generating new demands on ionospheric radio propagation research. The demands include higher accuracy in navigation systems, greater percentage of probability of detection for OTH radars, new methods of detecting objects from space and from the ground, high error-free data rates, and new uses of the UHF band for satellite communications and navigation. It is of interest to note that the demands for HF communications are increasing.

On the science side there are new demands on ionospheric research. What are the roles of various instability mechanisms in creating irregularities at high latitudes? What is the morphology of electron density parameters in the polar region? What are the relationships of magnetosphere and high latitude effects to equatorial parameters? What are the triggering mechanisms for the plumes or patches of irregularities? Why can't we as yet forecast the presence on any night of patches? What is the connection between the plasmopause irregularities and the auroral and polar regions? There are many other questions which abound in ionospheric physics which are not answered.

The new demands of technology and the unanswered questions of science will lead us to a continuing technical study of ionospheric radio propagation and a study of the physics of the ionosphere. There is much left to study in the field.

withdrawn

G-3-2

USE OF SCINTILLATION THEORY TO UNDERSTAND FREQUENCY-SPREAD ON  
F-REGION IONOGRAMS AND FADING ON HF IONOSPHERIC COMMUNICATION-LINKS

Henry G. Booker, Pradeep K. Pasricha\* and William J. Powers  
Department of Electrical Engineering and Computer Sciences  
University of California, San Diego,  
La Jolla, CA 92093, USA

Frequency-spread on F region ionograms is to be explained primarily with the aid of large-scale irregularities of ionization density in the F-region of the ionosphere. Large-scale irregularities are ones whose sizes extend from the Fresnel scale up to the outer scale. This means scales ranging from about two kilometres up to some tens of kilometres, or wavelengths ranging from about ten kilometres up to several hundred kilometres. Irregularities of scale in excess of the Fresnel scale cause refractive scintillation of a vertically incident wave on its upward journey through the F-region and on its return journey. Irregularities also cause the critical surface separating underdense ionization from overdense ionization to be rough. Irregularity-scales from the Fresnel scale up to the outer scale cause reflection from this surface to take the form of glints. However, this mechanism by itself does not produce enough frequency-spread to explain satisfactorily the more extensive forms of spread-F. In these circumstances refractive scattering of a wave on its upward journey into the F-region ceases to be small-angle scattering before the reflecting stratum is reached. Return of energy to the ionosonde becomes possible by multiple refractive scattering alone. This is diffuse scattering by irregularities of ionization density with scales ranging from the Fresnel scale up to the outer scale. The mathematical theory of scintillation needs to be extended so as to cover large-angle multiple refractive scattering.

### G-3-3

#### SIMULATION OF HF WAVE PROPAGATION AT OBLIQUE INCIDENCE IN A STRATIFIED IRREGULAR IONOSPHERE

J.-F. Wagen and K. C. Yeh  
Department of Electrical and Computer Engineering  
University of Illinois at Urbana-Champaign

The phase screen-diffraction layer method is a powerful tool to study the signal scintillation of a wave propagating in a turbulent, stratified medium. Under the forward scattering approximation, the complex amplitude is shown to satisfy a parabolic equation which describes effects arising from phase changes due to irregularities and diffraction due to phase mixing. Below the turning point, these two effects can be computed sequentially. Stepping in altitude phase changes are imbedded into each phase-screen; it is then followed by diffraction between phase-screens using FFT techniques. This method is equivalent to the split-step algorithm known in ocean acoustics but generalized to the case of oblique incidence.

Near the turning point, the diffraction effects are assumed negligible due to the small vertical thickness of the considered region. The deterministic part of the wave fields is taken to be proportional to the Airy functions. This allows a more accurate evaluation of the phase change near the turning point than the WKB solutions. The coupling between the ascending and descending waves is discussed.

The simulation model is described and, as an example, results for a linearly stratified turbulent ionosphere are given.

THE SPECTRAL CHARACTERISTICS OF HIGH-LATITUDE  
F-REGION IRREGULARITIES DEDUCED FROM HILAT  
SATELLITE PHASE SCINTILLATION DATA: C. L. Rino,  
Radio Physics Laboratory, SRI International,  
333 Ravenswood Avenue, Menlo Park, CA 94025

The HILAT satellite has been collecting auroral-zone and polar cap scintillation, energetic electron spectrometer, particle density, particle drift, and magnetometer data since November, 1983. In this paper we shall review the average spectral characteristics of intermediate scale F-region irregularities, which are primarily responsible for radiowave scintillation, and their relation to known auroral morphological features as inferred from the other instrumentation. An analysis procedure has been developed that allows us to measure power-law spectral segments and breakpoints independently. The data confirm the generally accepted morphology of high-latitude irregularities, but allow us to quantify the average structure levels in the medium and intermediate scale regimes.

The results are reviewed within the context of a unified model proposed originally by Kelley and Vickrey (1983) in which particle-produced and solar EUV ionization on the day-side provide a source function of large-scale structure that is convected away from the source regions and cascaded to smaller scale sizes through convective instabilities and then dissipated through diffusion at small scale sizes.

## G-3-5

### IRREGULARITY SHAPES OBSERVED VIA HILAT

E.J. Fremouw  
Physical Dynamics, Inc.  
Bellevue, WA 98009 USA

The HiLat Satellite is returning data on high-latitude ionospheric irregularities via a complement of five instruments: a VHF/UHF coherent beacon with an L-band phase reference, an *in-situ* plasma monitor consisting of a retarding potential analyzer and an ion drift meter, a three-axis magnetometer, an energetic electron spectrometer, and two visual-wavelength photometers. Data are being collected at five ground stations ranging in latitude from the plasmapause to the polar cusp. Processing includes spectral analysis of VHF and UHF phase scintillation recordings and power-law fits to the resulting spectra. The best-fit power spectral density,  $T$ , at a fixed fluctuation frequency (1 Hz) is used as an index of phase-scintillation strength. This paper will describe the behavior of  $T$  as a function of the orientation of the radio ray relative to the local magnetic meridian and L shell at the ray's F-layer (350-km) penetration point. The behavior presented will be interpreted in terms of the statistical shape (anisotropy) of scintillation-producing irregularities.

Effects of Ionospheric Irregularities  
on Coherent Microwave Systems

Warren D. Brown  
Systems Research Division, 0314  
Sandia National Laboratories  
Albuquerque, NM 87185

Propagation of RF signals through the electron density irregularities in the ionosphere can produce random variations (scintillations) in the amplitude and phase. The effects of these scintillations on frequency and phase modulated communications systems are briefly reviewed. These effects are dependent primarily on modulation scheme (e.g., CPSK), modulation parameter values (e.g., phase lock loop bandwidth) and the specifics of modem design. The phase scintillation can degrade the performance of a variety of coherent microwave systems such as synthetic aperture radars and geopositioners. For these coherent systems, the spectral index of the phase scintillation spectrum and the ratio of the irregularity outer scale size to a characteristic aperture length are the critical parameters in determining the severity and character of the degradations. Critical issues are identified and recommendations are made for system design which allows successful operation through the disturbed ionosphere.

## G-3-7

### TRANSIONOSPHERIC RADIOWAVE PROPAGATION EFFECTS IN THE IONOSPHERE

J.A. Klobuchar, G. Bishop, E. Weber, P. Fougere  
Ionospheric Effects Branch  
Air Force Geophysics Laboratory  
Hanscom AFB, MA 01731

P.H. Doherty  
Physics Research Division  
Emmanuel College  
Boston, MA 02115

The first measurements of the effects of the polar cap ionosphere on L-band radio waves were obtained early in 1984 from a ground station at Thule, Greenland, 76.5°N., 86° Corrected Geomagnetic Latitude. The spectrum of the satellite L-band transmissions allowed us to measure 1) differential carrier phase advance, which yields accurate information on relative TEC changes, both long and short term, from which phase scintillation can be determined; 2) absolute group delay, proportional to Total Electron Content (TEC) and which can be used to provide an absolute calibration for the highly accurate, but relative, differential carrier phase advance, and 3) carrier amplitudes for measuring amplitude scintillation.

The diurnal maximum values of TEC at times exceeded those of the mid-latitude ionosphere. These diurnal maximum values were due to large TEC enhancements having periods as short as a few minutes moving across the polar cap ionosphere. The TEC enhancements were also seen optically by means of all-sky imaging which showed regions of enhanced 6300A airglow emissions (F-region ionization patches) moving in the anti-sunward direction with velocities of up to 1 km/sec. These large enhancements in TEC occurred mainly during the late afternoon and evening hours. On one occasion during a two hour interval there were several quasi-periodic TEC enhancements of greater than a factor of two which occurred within a period of approximately 10 minutes. During other times the background ionosphere was generally quiet with relatively low values of TEC which likely represented the solar produced component of ionization. Associated with some of the TEC enhancements were short periods of weak, but clearly observable, amplitude scintillation having values of  $S_4$  up to 0.2. Using a high pass detrend time of 150 seconds we observed phase scintillations up to  $\pm 5$  radians peak to peak, referenced to a standard single frequency of 1 GHz, with corresponding smaller peak phase changes with shorter detrend times.

VARIABILITY OF TOTAL ELECTRON CONTENT  
AT HIGH LATITUDES NEAR SOLAR MINIMUM

HAIM SOICHER  
CENTER FOR COMMUNICATIONS SYSTEMS  
US ARMY COMMUNICATIONS-ELECTRONICS COMMAND  
FORT MONMOUTH, NEW JERSEY 07703-5000

Faraday observations were conducted at Anchorage, Alaska ( $61.04^{\circ}\text{N}$ ,  $149.75^{\circ}\text{W}$ ) utilizing beacon transmissions from a geostationary satellite during the period just following the minimum phase of solar cycle 21.

Average maximum monthly values of total electron content (TEC) were below  $15 \times 10^{16} \text{ el/m}^2$ , while individual daily maximum values never exceeded  $20 \times 10^{16} \text{ el/m}^2$ . Seasonal and day-to-day variabilities were observed.

Unique representation of the data has permitted the study of day-to-day variability of TEC. For example, during all seasons the TEC structure appears uniform from day to day during the buildup and decay phases of the local ionosphere. During the maximum and minimum of the diurnal phase, the TEC structure variability is seasonally dependent.

During periods of magnetic sudden commencements, which rarely occurred in the observation period, significant positive phase response of TEC did not materialize.

## G-3-9

### MEM AND FFT ANALYSIS OF HIGH-LATITUDE SPACED-RECEIVER MEASUREMENTS

Emanoel Costa  
Physics Research Division  
Emmanuel College  
400 The Fenway  
Boston, MA. 02115

Paul F. Fougere  
Ionospheric Physics Division  
Air Force Geophysics Laboratory  
Hanscom Air Force Base, MA 10731

The maximum entropy method (MEM) for the estimation of power spectral densities (PSD) of discretely sampled stochastic processes was introduced about twenty years ago. It has been shown that MEM possesses some advantages over the more traditional approach of the periodogram spectral estimate, obtained as the squared magnitudes of the output values of an FFT performed directly on the data set (whether windows, zero-padding and/or smoothing are used or not) that make it attractive for geophysical applications. MEM has also been shown to produce a smoother spectrum with higher resolution than the FFT-based techniques, particularly when applied to short data sets.

MEM was originally applied to seismological studies. Recently, it has been used in the study of geomagnetic micropulsations, in the prediction of Zurich sunspot numbers and in the estimation of power spectra of ionospheric scintillation data.

In this contribution, both MEM and FFT will be applied to the processing of data from spaced-receiver measurements of UHF radio waves. A correlation function analysis of HILAT satellite data recorded at Tromsø, Norway (69.7°N, 19.0°E) at 413 MHz will be performed by both techniques in order to characterize the parameters (anisotropy and velocity) of the moving diffraction patterns. A comparative analysis of the results yielded by each technique will be presented, together with examples to illustrate their respective advantages and shortcomings. The results from this analysis will then be interpreted in terms of anisotropies and drifts of high-latitude irregularities, using a single-scattering phase-screen model.

COMPUTER SIMULATION OF SPACE-TIME VARIATIONS  
OF IONOSPHERIC IRREGULARITIES AND SCINTILLATION

S. J. Franke and C. H. Liu  
Ionosphere Radio Laboratory  
University of Illinois, Urbana, IL 61801

We will discuss a numerically efficient simulation technique for generating realizations of space-time random fields and the application of the simulation to spaced receiver measurements of ionospheric scintillation. The random fields are generated using the "random motion" model that was recently proposed by D. A. de Wolf. In this model, the random field is generated by superposing a number of distinct "eddies" that have a gaussian profile. The scale size of the individual eddies can take on a range of values; by appropriately adjusting the number of eddies with a given size, we are able to generate a random field with a prescribed power spectral density. By allowing each eddy to move with a different pseudo-random velocity, the temporal variation of the random field can be included in the model. Examples of random space-time fields (in one space dimension) will be presented, and the statistics of the generated fields will be compared to theoretical models.

Examples of numerical propagation simulations will also be discussed. The goal of the propagation simulation is to investigate the space-time statistics of strongly scintillating signals that have encountered a "deep" phase screen. In these simulations, a space-time random field is generated and used to represent a time varying phase-screen. Numerical computations are used to obtain the complex-signal in the reception plane at a number of spaced receiver sites. Our initial studies are directed toward assessing the applicability of conventional spaced-receiver analysis techniques to cases where the scintillation is strong. Thus, the "apparent velocity" and "characteristic random velocity" of the scintillation patterns are of interest and will be discussed.



## URSI COMMISSION G - SESSION G4

High Latitude  
Ionosphere1:30 - 5:00  
LAW 201Ionosphère aux  
latitudes élevéesChairperson/Président: **P.A. Forsyth**, University of Western Ontario, London, ON

- 1 THEORETICAL STUDY OF THE PRODUCTION AND DECAY OF LOCALIZED ELECTRON DENSITY ENHANCEMENTS IN THE POLAR IONOSPHERE. **J.J. Sojka, R.W. Schunk**, Utah State University, Center for Atmospheric and Space Sciences, Logan, UT, USA
- 2 POLAR IONOSPHERIC IRREGULARITIES AND POSSIBLE SOURCE MECHANISMS. **M.C. Lee**, Massachusetts Institute of Technology, Research Laboratory of Electronics, Cambridge, MA, USA; **J. Buchau, H.C. Carlson Jr., J.A. Klobuchar, E.J. Weber**, Air Force Geophysics Laboratory, Ionospheric Physics Division, Hanscom AFB, MA, USA
- 3 SPECTRAL CHARACTERISTICS OF HIGH LATITUDE IRREGULARITIES FROM DE-2 AND SCINTILLATION MEASUREMENTS. **Sunanda Basu, Santimay Basu**, Emmanuel College, Physics Research Division, Boston, MA, USA; **W.R. Coley, R.A. Heelis**, University of Texas at Dallas, Richardson, TX, USA; **M. Sugiura**, NASA/GSFC, Greenbelt, MD, USA; **C.S. Lin, J.D. Winningham**, Southwest Research Institute, San Antonio, TX, USA
- 4 POLAR CAP E-REGION DOPPLER RADAR OBSERVATIONS NEAR THE CLEFT. **M.J. McKibben, G.J. Sofko, J.A. Koehler**, University of Saskatchewan, Institute of Space and Atmospheric Studies, Saskatoon, SK
- 5 "TYPE 3" DOPPLER SPECTRA FROM TWO 50 MHz CW AURORAL BISTATIC RADARS. **P. Prikryl, G. Sofko, J. Koehler**, University of Saskatchewan, Institute of Space and Atmospheric Studies, Saskatoon, SK
- 6 SPACED ANTENNA HF DOPPLER OBSERVATIONS OF F-REGION DRIFTS IN THE POLAR CAP AND THE AURORAL ZONE. **B.W. Reinisch, C. Dozois, K. Bibl**, University of Lowell, Center for Atmospheric Research, Lowell, MA, USA; **J. Buchan, E.J. Weber**, Air Force Geophysics Laboratory, Hanscom AFB, MA, USA
- 7 VHF DOPPLER RADAR "BREAKUP" SIGNATURE OF AURORAL SUBSTORMS. **G. Sofko, J. Koehler, P. Prikryl**, University of Saskatchewan, Institute of Space and Atmospheric Physics, Saskatoon, SK
- 8 NEARLY SIMULTANEOUS MEASUREMENTS OF RADIO-AURORAL HEIGHTS AND DOPPLER VELOCITIES AT 398 MHz. **D.R. Moorcroft, J.M. Ruohoniemi**, University of Western Ontario, Dept. of Physics and Centre for Radio Science, London, ON
- 9 AURORAL PLASMA MEASUREMENTS WITH THE BARS DOPPLER RADAR SYSTEM. **A.G. McNamara**, National Research Council of Canada, Herzberg Institute of Astrophysics, Ottawa, ON
- 10 ON WEAK STRIATED ECHOES IN THE MORNING SECTOR OF VHF RADAR AURORA. **C. Haldoupis, E. Nielsen**, Max-Planck-Institut für Aeronomie, Lindau, FRG; **G. Sofko**, University of Saskatchewan, Physics Dept., Saskatoon, SK

## G-4-1

### THEORETICAL STUDY OF THE PRODUCTION AND DECAY OF LOCALIZED ELECTRON DENSITY ENHANCEMENTS IN THE POLAR IONOSPHERE

J. J. Sojka and R. W. Schunk, Center for Atmospheric and Space Sciences, Utah State University, Logan, Utah 84322, USA

The origins, transport and decay of large scale ( $> 10$  km) F-region density irregularities was theoretically studied using our High Latitude Time Dependent ionospheric model (HLTD). Such density irregularities (blobs) have been found both in the polar cap and the auroral zone. Our model studies show that observed precipitation energy flux magnitudes can readily give rise to the blob densities if a plasma flux tube is exposed to them for 5-10 minutes. Furthermore once transported away from the source the F-region profile recovers its shape on a time scale of 10-20 minutes. Hence whether the production was caused by soft or hard precipitation is no longer discernable from the profile shape. Once created a blob will maintain its relative size for many hours since it decays at the same rate as the adjacent non-blob plasma. Blobs are removed by being transported into a region of high production where the new density exceeds the old blob density, (i.e., sunlight). The high  $h'F_2$ 's observed with some blobs need not necessarily imply soft precipitation, induced upward plasma drifts from neutral winds or  $\text{ExB}$  convection can readily account for them. Since the high latitude ionosphere is filled with discrete structured auroral forms both in the oval and polar cap and plasma is continually convecting through these regions blobs are the rule rather than the exception.

## POLAR IONOSPHERIC IRREGULARITIES AND POSSIBLE SOURCE MECHANISMS

M.C. Lee

Research Laboratory of Electronics  
Massachusetts Institute of Technology

J. Buchau, H.C. Carlson, Jr., J.A. Klobuchar, E.J. Weber

Ionospheric Physics Division  
Air Force Geophysics Laboratory

Coordinated experiments using optical and radio waves (digital ionosonde, satellite phase and amplitude scintillation, total electron content, incoherent scatter radar) and in situ measurements have been conducted over the past five years to investigate the large scale structures and dynamics of the polar ionosphere, and the relation of these to ionospheric irregularities. F layer arcs and ionization patches (i.e. large scale plasma enhancement) have previously been reported as the dominant ionospheric structures in the polar cap. Both of these features are subject to plasma instability processes which lead to ionospheric irregularities. These cause amplitude and phase scintillations of trans-ionospheric radio propagation. Plasma instabilities such as the E x B, current convective, and thermal instabilities will be examined as possible source mechanisms for exciting polar ionospheric irregularities. Factors such as precipitating electrons, horizontal transport, and relative ion-neutral velocities within ionospheric structures will be considered. In particular, various thermal effects that can contribute to the occurrence of irregularities in the polar ionosphere will be discussed.

## G-4-3

### SPECTRAL CHARACTERISTICS OF HIGH LATITUDE IRREGULARITIES FROM DE-2 AND SCINTILLATION MEASUREMENTS

Sunanda Basu and Santimay Basu  
Emmanuel College  
Boston MA 02115

W.R. Coley and R.A. Heelis  
University of Texas at Dallas  
Richardson TX 75080

M. Sugiura  
NASA/GSFC  
Greenbelt MD 20771

C.S. Lin and J.D. Winningham  
Southwest Research Institute  
San Antonio TX 78284

Characteristics of small scale ( $\sim 10$  km and smaller) density irregularities in the various domains of the high latitude F-region in the winter (i.e., dark) hemisphere are examined with the help of multiple sensor data on Dynamics Explorer-2. For the first time it has been possible to study simultaneously on a systematic basis the spectral characteristics of not only the density irregularities but of the velocity irregularities, as well. It is generally found that the largest amplitude ( $\sim 30$  percent) irregularities are associated with the low-energy precipitation, field aligned current and drift structure in the dayside cusp. The spectra of both density and velocity fluctuations have similar slopes in such regions. Discrete irregularity structures in the polar cap, convected out of the dayside cusp, have somewhat lower irregularity amplitudes (10-20 percent) and different spectral characteristics for their density and velocity spectra. In general, the velocity spectra in the convected structures seems to have little power at scale lengths  $< 1$  km. The nightside auroral oval again seems to be characterized by similar density and velocity spectra. The varying characteristics of the density and velocity spectra in the polar cap and auroral regions are related to the forms of scintillation spectra observed on satellite to ground communication links in such regions.

## Polar Cap E-Region Doppler Radar Observations Near the Cleft

M.J. McKibben, G.J. Sofko and J.A. Koehler

Institute of Space and Atmospheric Studies  
University of Saskatchewan  
Saskatoon, Sask. S7N 0W0

In July 1982, a 50 MHz bistatic radar campaign in the Canadian Arctic measured E-region drifts near the polar cap - auroral zone interface. The ionosphere above Sachs Harbour ( $\sim 77.1^{\circ}\text{N}$ ,  $77.3^{\circ}\text{W}$  geomagnetic, based upon the MGST 5/80 model) was illuminated by two transmitters, one at Inuvik and one at Cambridge Bay. The obliquely scattered signals were received at Fort Franklin. As a consequence of this geometry, Doppler shifts were measured along roughly the magnetic north-south and east-west directions (the bisectors were  $20.5^{\circ}$  E of S for the Inuvik - Fort Franklin path, and  $10.0^{\circ}$  S of E for the Cambridge Bay - Fort Franklin path). During a 4 hour period of strong scatter near magnetic noon, on the disturbed day ( $\Sigma Kp = 37$ ) of July 16, the Doppler spectra and magnetometer data showed strong evidence that flows coming from the throat region passed over Sachs Harbour. The Doppler signature associated with this flow is discussed in detail, using a movie to show the temporal development of the spectra.

## G-4-5

### 'Type 3' Doppler Spectra From Two 50 MHz CW Auroral Bistatic Radars

P. Prikryl, G. Sofko and J. Koehler

Institute of Space and Atmospheric Studies  
University of Saskatchewan  
Saskatoon, Sask. S7N 0W0

In the summer of 1983 two 50 MHz CW bistatic radars with bisectors roughly in the magnetic north-south and east-west directions were operated so as to observe a common region of aurora above Southend, Saskatchewan ( $56.3^{\circ}\text{N}$ ,  $103.5^{\circ}\text{W}$  geographic;  $64.0^{\circ}\text{N}$ ,  $36.0^{\circ}\text{W}$  geomagnetic). Narrow spectral peaks at about  $\pm 50$  Hz were a characteristic feature of the strong echoes from the westward electrojet.

The Doppler radars were supported by a set of ground-based experiments at Southend - namely a meridian-scanning photometer, an all-sky camera, a magnetometer and an ionosonde. In this paper, we compare the data from these instruments at the time of 'Type 3' radar echoes, in order to determine the auroral conditions during which these echoes occur, and hence to understand the exact nature of the scattering process. In particular, consideration is given to the suggestion by Fejer et al. [1984] that these echoes are due to electrostatic ion cyclotron (EIC) waves.

SPACED ANTENNA HF DOPPLER OBSERVATIONS OF F-REGION  
DRIFTS IN THE POLAR CAP AND THE AURORA ZONE

Bodo W. Reinisch, C. G. Dozois, K. Bibl, ULCAR,  
Lowell, MA 01854, J. Buchau and E. J. Weber,  
AFGL, Hanscom AFB, MA 01731

Spaced antenna Doppler drift observations of the winter time F-region were conducted at Goose Bay, Labrador (65° CGL) and Thule (86° CGL). The Digisonde calculates the discrete Fourier transforms of the ionospheric HF echo signals received on each of the four receiving antennas. Cross-correlation of the spectra leads to skymaps displaying the reflection points for the existing Doppler components. A least-squares procedure determines the three-dimensional velocity vector for the plasma bulk motion.

Analysis of data from Goose Bay and Thule shows that the two-cell polar cap plasma convection can be monitored with the SADD technique. A number of 24-hour measurements show a fast change in the drift direction from west to east at local magnetic midnight for the subauroral station, and an almost linearly rotating drift direction for the polar cap station. The magnitude of the drift velocities is 300 to 900 m/s in the polar cap, and 50-300 m/s in the subauroral F-region. Optical observations with an all sky imaging photometer on 6300A confirm the HF measurements.

## G-4-7

### VHF Doppler Radar "Breakup" Signature of Auroral Substorms

G. Sofko, J. Koehler and P. Prikryl

Institute of Space and Atmospheric Studies  
University of Saskatchewan  
Saskatoon, Sask. S7N 0W0

In the summer of 1983, a common volume of aurora over Southend, Sask. ( $56.3^{\circ}\text{N}$ ,  $103.5^{\circ}\text{W}$  geographic;  $64.0^{\circ}\text{N}$ ,  $36.0^{\circ}\text{W}$  geomagnetic) was illuminated by remote 50 MHz radars, so that Doppler velocity components in approximately the magnetic east-west and north-south directions could be measured. In addition, scanning photometer and magnetometer data were taken at Southend. A very striking Doppler signature of the breakup phase was observed. This signature consisted of rapid, marked broadening of the north-south Doppler spectra. At the same time, the east-west spectra are characterized by narrow spectral peaks near zero shift and/or the expected range for ion-acoustic and ion cyclotron scatter. Virtually no evidence of the north-south broadening appears on the east-west spectra. These spectral characteristics will be discussed in relation to several models of the auroral plasma dynamics at breakup.

NEARLY SIMULTANEOUS MEASUREMENTS OF RADIO-AURORAL  
HEIGHTS AND DOPPLER VELOCITIES AT 398 MHZ

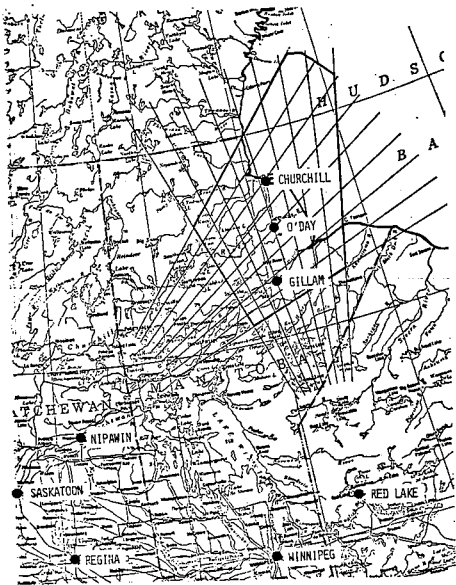
D. R. Moorcroft and J. M. Ruohoniemi  
Department of Physics and Centre for Radio Science  
University of Western Ontario, London, Ontario N6B 2A3

Data were obtained in 1976 and 1978 using the 398 MHz phased-array radar operated by SRI International at Homer, Alaska (no longer in operation). During some periods, different modes of operation were interleaved on a time scale of one or two minutes, so that nearly simultaneous measurements of radio-auroral heights and doppler velocities have been obtained. Although the analysis is complicated by effects on echo heights due to aspect angle and variations in the E-region electron density, at times the heights appear to depend in a systematic way on the doppler velocity. These results will be presented and compared with theoretical predictions.

## AURORAL PLASMA MEASUREMENTS WITH THE BARS DOPPLER RADAR SYSTEM

A.G. McNamara  
Herzberg Institute of Astrophysics  
National Research Council of Canada  
Ottawa, Canada, K1A 0R6

A new radar system called BARS, consisting of two pulsed 48 MHz Doppler radars located at Nipawin, Sask. and Red Lake, Ont., is due to come on-line in April 1985. Digitally-formed multiple beams overlap in 200,000 km<sup>2</sup> area of the auroral ionosphere, spanning geomagnetic latitudes from 67 to 73°. The radar signals are processed on-site and the data transmitted in real time to a central data network node in Ottawa for immediate merging to produce vector velocities over the common area. This paper reviews the characteristics of the BARS system and presents preliminary data obtained from aurora.



ON WEAK STRIATED ECHOES IN THE MORNING SECTOR OF VHF  
RADAR AURORAC. Haldoupis<sup>1,2,\*</sup>, E. Nielsen<sup>1</sup>, and G. Sofko<sup>2</sup>

- 1: Max-Planck Institut für Aeronomie, Katlenburg-Lindau, F.R.G.
- 2: University of Saskatchewan, Physics Department, Saskatoon, Saskatchewan, Canada.

In a recent paper, E. Nielsen G. Sofko and W. I. Axford (Nature, Vol. 299, p.238, 1982) reported a new type of radio auroral echoes which appear as a series of striations on the STARE RTI records and last for about one to two hours. The average characteristics of signal intensity and mean Doppler velocity for these echoes differ significantly as compared to the commonly observed backscatter associated with typical auroral electrojet activity.

In this paper we present further evidence on the striated echoes based on crossed-beam Doppler spectrum measurements made with the STARE system. Our findings are summarized as follows: 1) The Doppler spectra are mainly centered at sub-ion acoustic velocities and are very narrow in contrast with the broad spectra of typical auroral backscatter. 2) The mean radial Doppler drift follows a cosine law dependence. 3) The signal strength and spectrum width are strictly isotropic in the observing plane perpendicular to the earth's magnetic field. 4) The spectrum width tends to increase with drift velocity magnitude. 5) The observed motions are confined about the bisector of the north-east quadrant.

Our observations seem to exclude that these echoes are due to primary plasma waves generated by the two stream instability. Also the observation of very narrow spectra near zero Doppler shifts contradicts the notion of secondary plasma wave turbulence generated by the gradient drift instability. Finally, we discuss the possibility that these irregularities are associated with neutral gas turbulence driven by a wind shear mechanism similar to that proposed for sporadic E-layers.

\*Permanent affiliation: Physics Department, University of Crete, Iraklion, Crete, Greece.



## URSI COMMISSION G - SESSION G5

**Wave Propagation -  
Simulation and Experiments**

8:30 - 12:00  
LAW 201

**Propagation des ondes -  
simulation et expériences**

Chairperson/Président: **K.C. Yeh**, University of Illinois, Urbana, IL, USA

- 1 MINIMUM DISTANCE TO THE FAR FIELD FOR A FINITE SOURCE IN A MAGNETIZED PLASMA. **C.E. Rasmussen, P.M. Banks, K. Harker**, Utah State University, Center for Atmospheric and Space Sciences, Logan, UT, USA
- 2 THE OBSERVATION OF THE IONOSPHERIC EQUATORIAL ANOMALY BY MEANS OF SATELLITE DIFFERENTIAL DOPPLER MEASUREMENTS. **Y.-J. Tzeng**, Ministry of Communication, Telecommunication Laboratories, Taiwan, China
- 3 STUDIES OF TROPICAL IONOSPHERIC F-REGION PLASMA MOTIONS USING SPACED VHF POLARIMETERS. **M.A. Abdu, Y. Nakamura, J.H.A. Sobral, I.S. Batista, E.R. de Paula, I.J. Kantor**, INPE, Instituto de Pesquisas Espaciais, São Paulo, Brazil
- 4 LOCALISATION ET SUIVI DE FRONTS MÉTÉOROLOGIQUES AVEC LE RADAR TRANSHORIZON DE VALENTOLE. **J. Parent, E.E.R.M.**, Boulogne Billancourt, France
- 5 MOVING RANDOM SURFACES AND CORRELATION ANALYSIS. **M.J. Burke**, Department of Communications, Communications Research Centre, Ottawa, ON
- 6 ELECTRIC FIELDS IN THE HIGH LATITUDE IONOSPHERE. **J. MacDougall**, University of Western Ontario, London, ON
- 7 STUDIES OF TID SOURCES IN WESTERN QUEBEC WITH RAPID-RUN IONOSONDES, FAN-BEAM RIOMETERS, AND THE MILLSTONE HILL RADAR. **M.G. Morgan**, Dartmouth College, Thayer School of Engineering, Hanover, NH, USA
- 8 THE CONJUGATE SOURCE LOCATIONS OF LARGE-SCALE TID'S. **L.A. Hajkowicz**, University of Queensland, Physics Dept., St. Lucia, Australia; **R.D. Hunsucker**, University of Alaska, Geophysical Institute, Fairbanks, AK, USA
- 9 OBSERVATIONS OF TIDS WITH THE NOAA HF RADAR. **P.E. Argo**, Los Alamos National Laboratory, Los Alamos, NM, USA

## G-5-1

### MINIMUM DISTANCE TO THE FAR FIELD FOR A FINITE SOURCE IN A MAGNETIZED PLASMA

C. E. Rasmussen, P. M. Banks and K. Harker, Center for Atmospheric and Space Sciences, Utah State University, Logan, Utah 84322, USA

Although the distance to the far-field zone from a source is well known if the source is operating in free space, the far-field distance is not as completely understood if the same source is operating in an anisotropic medium such as a magnetized plasma. In spite of the fact that substantial changes occur to the wave field if the source is placed in an anisotropic medium, many authors use the free space results as an approximation to far-field distance in a magnetized plasma. In this paper we derive the conditions that allow one to obtain the distance to the far field in an anisotropic medium and apply them to magnetohydrodynamic radiation in the near-earth environment. It is found, for sources whose size is greater than a few meters, that the free space results grossly underestimate the distance to the far-field zone.

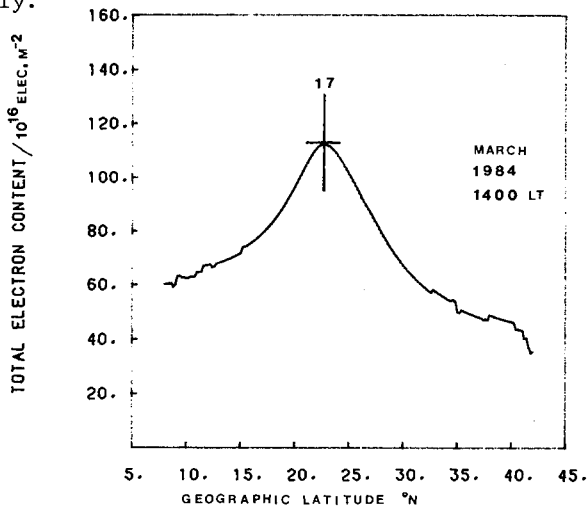
THE OBSERVATION OF THE IONOSPHERIC EQUATORIAL ANOMALY  
BY MEANS OF SATELLITE DIFFERENTIAL DOPPLER MEASUREMENTS

Yih-Jer Tzeng

Telecommunication Laboratories, M. O. C.  
Chung-Li P.O. Box 71, Taiwan, ROC

The signals of the NNSS satellites (Navy Navigational Satellite System) have been used to derive Differential Doppler from the coherent beacons with frequencies 150 MHz and 400 MHz at Lunping Observatory (25.00 N; 121.17 E) since March 1984. The observatory observes simultaneously NNSS Differential Doppler and the Fraday effect on three beacon signals from three geostationary satellites, SIRIO, ETS-2, and AtS-1, respectively. By means of Fraday data from one or two geostationary satellite, the latitudinal variations of ionospheric total electron content (TEC) were determined.

The flowing figure shows a monthly mean latitudinal variation of ionospheric total electron content. In this report, the time and latitude depence of ionospheric electron content were investigated, the results show that the ionospheric equatorial anomaly started devolping between 0900 hr and 1000 hr, and devolped competely between 1300 and 1600 hr local time. Changes in the position of the north crests of the ionospheric equatorial anomaly also were studied. On 1347 LT March 30, 1984, the position of the north equatorial anomaly crest moved to 27.2 N. All the Differential Doppler data have been used to study the devolpment of ionospheric equatorial anomaly.



STUDIES OF TROPICAL IONOSPHERIC F-REGION PLASMA  
MOTIONS USING SPACED VHF POLARIMETERS

M.A. Abdu, Y. Nakamura, J.H.A. Sobral, I.S. Batista  
E.R. de Paula and I.J. Kantor  
Instituto de Pesquisas Espaciais, INPE  
12200 - São José dos Campos, SP, Brazil

Tropical F-region nighttime plasma zonal flow is investigated using polarimeter measurements of geostationary satellite beacon carried out in low geomagnetic latitude locations in Brazil. Trans-equatorial plasma bubbles, (or ionization depleted regions), are used as tracers of the ambient plasma motion, since the flux tube aligned, vertically extended and east-west drifting developed structures of such bubbles could modulate the total electron content of the ionosphere (TEC) in the satellite-earth propagation path to a degree that the resulting changes in the Faraday rotation angle of the satellite VHF beacon could be within the detection sensitivity of polarimeters operating at low geomagnetic latitude ( $-28^\circ$  dip, in the present case). The correlation times of the bubble induced TEC fluctuations at two locations, separated by 110km in magnetically east-west direction, are thus used to obtain the zonal velocities as a function of local time. The results of the measurements carried out during the last four years are compared with the plasma bubble irregularity, and bulk plasma, zonal motions obtained by other workers for other equatorial and low latitude locations using radio as well as optical techniques, which seems to suggest the existence of a latitudinal variation in the zonal plasma flow. Our results from radio measurements are compared with results of the plasma bubble zonal motion obtained from an east-west scan 6300 Å airglow photometer operated simultaneously at one of the polarimeter locations. The radio technique is found to yield velocities consistently higher than those obtained from optical technique which might suggest the existence of a velocity shear between the two height regions sensitive to the two techniques. The vertical velocity shear and the latitudinal velocity gradient are discussed in the light of the wellknown models of tropical ionospheric electrodynamic processes. Further, marked decrease in the plasma zonal flow is observed with the decreasing solar activity that characterized our present series of measurements.

LOCALISATION ET SUIVI DE FRONTS METEOROLOGIQUES  
AVEC LE RADAR TRANSHORIZON DE VALENSOLE

par

J.Parent

E.E.R.M.

77 rue de Sèvres  
92106 Boulogne Billancourt

L'installation de rétrodiffusion ionosphérique HF de Valensole est décrite ainsi que le principe de la détermination de la direction du vent à partir du rapport entre les amplitudes des raies du 1er ordre dans le spectre de l'onde rétrodiffusée.

Les résultats d'une campagne de mesure, dont le but était une première évaluation des possibilités de cartographie automatique en temps réel de la direction du vent, sont décrits. Lors de cette campagne, l'intervention de l'opérateur se limitait au choix des fréquences de travail à partir des ionogrammes verticaux obtenus à la station.

Des phénomènes météorologiques bien marqués (fronts froids), qui ont eu lieu pendant cette période, ont pu être localisés et on décrit leur évolution. Ces données sont comparées à des cartes fournies par le modèle de prévision du vent à maille fine du centre Européen de Reading.

Le problème de la correction de l'écart entre la distance de groupe et la distance réelle au sol est abordé. Une méthode simple est décrite dont l'efficacité est testée grâce aux références sol nombreuses en Mer du Nord.

MOVING RANDOM SURFACES AND CORRELATION ANALYSIS

by  
M.J. BURKE

Communications Research Center  
Box 11490, Station H  
Ottawa, Ontario, K2H-8S2

SUMMARY

Three models of moving random surfaces with known velocity and known correlation function are described. The random surfaces are formed from an infinite set of plane waves with decorrelation arising from random temporal and spatial changes. It is shown that, if there are random spatial changes in the direction of motion, then speeds derived by the full correlation method of Briggs et.al.(Proc. Phys. Soc., B63: 106-121, 1950) will be less than the true speed of the surface. Random spatial changes at right angles to the direction of motion are necessary if the axial ratio of the correlation ellipse is to be finite. From modeling of a multi-antenna array, it is shown that the correlation ellipse is the average of the various shapes within the surface as argued by Burke(Radio Science, 10: 1035-1036, 1975). If temporal-series based on the various models are subjected to a high-pass filter before correlation analysis, the correlation speeds increase in value.

Temporal correlation functions from one of the models, Model 2, fail the requirements for full correlation analysis because the half-width of the cross-correlation function is greater than the half-width of the auto-correlation function. However, from a survey of experimental ionospheric drift measurements, it is argued that radio interference patterns appear to have the form of this model. For Model 2, correlation speeds increase with increasing antenna spacing and the correlation ellipse tends to line up with that antenna pair with the greatest spacing(Golley and Rossiter, J. Atmos. Terr. Phys., 32: 1215-1233, 1970), the straight line of the straight-line method of Briggs et.al., will not be straight(Sales and Bowhill, J. Atmos. Terr. Phys., 24:451-465, 1962) and, as stated above, the speeds will be low(Wright and Fedor, Space Research VII, North-Holland Pub. Co. Amsterdam, 67-72, 1967; Sprenger and Schminder, J. Atmos. Terr. Phys., 31:1085-1098, 1969).

It is shown that the similar-fades method(Variant 2 of Sprenger and Schminder) gives a better estimate of the surface speed than does the correlation method.

## ELECTRIC FIELDS IN THE HIGH LATITUDE IONOSPHERE

John Mac Dougall  
University of Western Ontario  
London, Ont., CANADA N6A 3K7

The high latitude ionosphere is set into convective motion by electric fields conducted down from the magnetospheric dynamo. This paper will discuss these electric fields from the standpoints of;

(a) The 'picture' of the convection based on winter and summer measurements using the 'long-line-system' in the polar cap region.

(b) The magnetospheric model which could be responsible for the observed electric fields.

## G-5-7

### STUDIES OF TID SOURCES IN WESTERN QUEBEC WITH RAPID-RUN IONOSONDES, FAN-BEAM RIOMETERS, AND THE MILLSTONE HILL RADAR

M. G. Morgan, Radiophysics Laboratory, Thayer School of Engineering,  
Dartmouth College, Hanover, N.H. 03755, U.S.A.

This paper is a sequel to the paper "Locating TID sources with a north-south chain of rapid-run ionosondes in western Quebec" (Morgan, Radio Science, 18, 1066, 1983). Referring to Figure 3 of that paper, the network has been reconfigured with a close-spaced triangle of ionosondes, 50 km on a side, at Chibougamau (CH,  $L \approx 4.5$ ) and retaining the ionosonde at La Grande (LA,  $L \approx 6$ ). The ionosonde at Rapide Blanc (RA,  $L \approx 4$ ) has been replaced with a riometer with a fan beam, narrow in the north-south direction and wide in the east-west direction; and a similar riometer is being placed at Gouin, between Rapide Blanc and Chibougamau. Observation of the lower ionosphere over the riometer sites, with the Millstone Hill radar, is planned. With these new observations, it should be possible to explore much more convincingly the findings in the previous paper that the sources of post-dawn morning TID's, seen by the ionosonde network in northern New England, lie near  $L = 4$  and produce northward traveling TID's as well as southward traveling TID's. At the required abstract submission date (1985 Jan 4), observations have just begun and results are not yet available. Substantial results are expected to be available for presentation at the meeting in June.

## THE CONJUGATE SOURCE LOCATIONS OF LARGE-SCALE TID'S

L. A. Hajkowicz\* and R. D. Hunsucker  
Geophysical Institute  
University of Alaska/Fairbanks, Alaska 99701

## ABSTRACT

Thirty-two sudden auroral absorption increases (SAI events) were analyzed for southern and northern (Macquarie Island - Alaska) magneto-conjugate areas during 1971 - 1981, using data from seven standard riometer stations displaced in latitude. The hard particle precipitation belts at the onset of SAI events, as inferred from riometer, magnetometer, all-sky camera and the satellite auroral imagery data, were largely limited in latitude to a shell positioned between L-values 5 - 6 but extending over 70 degrees in longitude west of Alaska. The occurrence of SAI events in the conjugate areas, centered close to local midnight at College, Alaska, preceded the presence of sequential enhancements in ionospheric parameters characteristic of the F-region: virtual height ( $h'F$ ) and range spread-F ( $Sr$ ). The enhancements were consistently observed by two chains of 10 vertical-incidence standard ionosondes, operating at 15-minute intervals and displaced mainly in latitude in the Australian and Japanese meridional sectors.

The sequential ionospheric disturbances were consistent with the presence of two separate trains of large-scale TID's (LS TID's) in both hemispheres, generated at the onset of SAI events in the conjugate areas, and propagating equatorwards with a typical velocity of 600-800 m/sec. The long range of propagation of LS TID's, from auroral to equatorial latitudes, appears to indicate that line rather than point sources are involved in the generation of these disturbances in both auroral zones. The line source characteristic is also consistent with the riometer (and other high-latitude instruments) observations of the particle precipitation belts.

\*Permanent Address:  
Physics Department  
University of Queensland  
St. Lucia, Queensland  
Australia

**OBSERVATIONS OF TIDS WITH THE NOAA HF RADAR**

Paul E. Argo, Los Alamos National Laboratory, Los Alamos, NM

During several days of ionospheric measurements with the HF Radar (October, 1984), instances of acoustic gravity wave passages were recorded. In a few cases the ionograms evidenced both the medium scale trough and "blob" characteristics described by Lobb and Titheridge (J. Atmos. and Terr. Phys., 39, 129, 1977). In these cases the causative wave is seen to have a single enhancement and depletion. Using the echo-location capabilities of the HF Radar the waves are tracked as they move across the sky. Scale sizes, velocities, and direction of travel can be deduced from the single station measurements. Where possible these will be compared to measurements using three separated locations (of which the radar at Los Alamos was one). Large scale TIDS, which are primarily observed by slow changes in the virtual heights of reflection will also be examined and discussed.

## URSI COMMISSION G - SESSION G6

**Incoherent Scatter**1:30 - 5:00  
LAW 201**Diffusion-non cohérente**Chairperson/Président: **A. Richmond**, National Center for Atmospheric Research, Boulder, CO, USA

- 1 PLASMA ENHANCEMENTS AND EAST-WEST ELECTRIC FIELDS IN THE HIGH-LATITUDE F-REGION IONOSPHERE. **R.T. Tsunoda, T.M. Dabbs, J.D. Kelly**, SRI International, Radio Physics Laboratory, Menlo Park, CA, USA
- 2 COMPARISON OF SIMULTANEOUS CHATANIKA AND MILLSTONE HILL OBSERVATIONS WITH IONOSPHERIC MODEL PREDICTIONS. **C.E. Rasmussen, R.W. Schunk, J.J. Sojka, V.B. Wickwar, O. de la Beaujardiere, J. Foster, J. Holt, D. Evans**, Utah State University, Center for Atmospheric and Space Sciences, Logan, UT, USA
- 3 INCOHERENT SCATTER OBSERVATIONS OF THE LATITUDINAL STRUCTURE OF NEUTRAL ATOMIC OXYGEN DENSITIES. **W.L. Oliver**, Massachusetts Institute of Technology, Haystack Observatory, Westford, MA, USA
- 4 F REGION ION DRIFT AND VELOCITY OF SMALL SCALE IRREGULARITIES USING HF BACKSCATTER: A EISCAT-EDIA PRELIMINARY COMPARISON. **A. Bourdillon**, Université P.M. Curie, LPE, Paris, France; **D. Fontaine**, CRPE/CNET, Saint Maur des Fossés, France
- 5 IONIZATION AND OPTICAL EMISSIONS DETECTED BY THE CHATANIKA RADAR AND THE DE-1 SPIN-SCAN AURORAL IMAGER. **R.M. Robinson, R.R. Vondrak**, Lockheed Palo Alto Research Laboratory, Space Sciences Laboratory, Palo Alto, CA, USA; **J.D. Craven, L.A. Frank**, University of Iowa, Dept. of Physics and Astronomy, Iowa City, IA, USA; **K.L. Miller**, Utah State University, Center for Atmospheric and Space Sciences, Logan, UT, USA
- 6 THEORETICAL STUDY OF ANOMALOUSLY HIGH F-REGION PEAK ALTITUDES IN THE POLAR IONOSPHERE. **J.J. Sojka, R.W. Schunk**, Utah State University, Center for Atmospheric and Space Sciences, Logan, UT, USA
- 7 IMPROVED F-REGION ACF MEASUREMENTS AT ARECIBO. **M.P. Sulzer**, National Astronomy and Ionosphere Center, Arecibo, PR, USA
- 8 THE CODED LONG PULSE TECHNIQUE. **M.P. Sulzer**, National Astronomy and Ionosphere Center, Arecibo, PR, USA
- 9 A STUDY OF THE EFFECT OF COLLISIONS ON THE INCOHERENT SCATTER SPECTRUM. **T. Fla**, EISCAT Scientific Association, Ramfjordbotn, Norway

## G-6-1

### PLASMA ENHANCEMENTS AND EAST-WEST ELECTRIC FIELDS IN THE HIGH-LATITUDE F-REGION IONOSPHERE

Roland T. Tsunoda, Teri M. Dabbs, and John D. Kelly  
Radio Physics Laboratory  
SRI International  
Menlo Park, California 94025

We investigate the relationship of F-region plasma enhancements to east-west electric fields in the high-latitude ionosphere. We have compiled a data base using Sondrestrom incoherent-scatter radar measurements made during elevation scans in the magnetic meridian. The data base includes all elevation scan data obtained with the radar during the period June 1983 through December 1984. We use the data base to investigate (1) the existence and occurrence frequency of a convection "throat" region, (2) the transport of plasma "patches" of solar-produced F-region plasma from the dayside ionosphere into the dark polar cap, and (3) the development of F-region polarization electric fields in response to the presence of localized plasma enhancements (or "blobs").

COMPARISON OF SIMULTANEOUS CHATANIKA AND MILLSTONE HILL  
OBSERVATIONS WITH IONOSPHERIC MODEL PREDICTIONS

C. E. Rasmussen, R. W. Schunk, J. J. Sojka, V. B. Wickwar, O. de la Beaujardiere, J. Foster, J. Holt and D. Evans, Center for Atmospheric and Space Sciences, Utah State University, Logan, Utah 84322, USA

As part of the MITHRAS program, the Chatanika and Millstone Hill incoherent-scatter radars made coordinated observations of the polar ionosphere on June 27 and 28, 1981. We compare these data with predictions made by a high-latitude ionospheric model. Qualitatively, the same features are evident in both the model and the radar data: fairly constant densities on the dayside with a mid-latitude trough forming poleward of 65 degrees around 1900 MLT (magnetic local time). This trough is seen to extend equatorward with increasing MLT, such that the minimum densities occurring in the trough appear just after midnight around 60 degrees dipole latitude. These features are primarily understood in terms of the different regions of convection, further influenced by photoionization and vertical transport. The only areas of major disagreement between the measurements and model are noted in the auroral oval and at a portion of the times during which substorms occurred. Quantitatively, equally good agreement is obtained. The densities predicted by the model are usually within 25% of those measured by the radars, although appreciable differences occur in some regions of the ionosphere at certain times.

## G-6-3

### INCOHERENT SCATTER OBSERVATIONS OF THE LATITUDINAL STRUCTURE OF NEUTRAL ATOMIC OXYGEN DENSITIES

W. L. Oliver, MIT Haystack Observatory  
Westford, Massachusetts 01886 U.S.A.

The steerable 150-foot antenna at the Millstone Hill incoherent scatter radar facility has been employed in elevation scans along the meridian to monitor the latitudinal structure of the ionosphere/upper-atmosphere system. By lowering the elevation angle to 4 degrees to the north and south the latitude span 25-60 degrees north (at an altitude of 500 km) can be observed (Oliver, Geophys. Res. Lett., 11, 915-918, 1984). Antenna cycle time for these measurements is about 30 minutes, and continuous observing periods for up to 7 days have been achieved.

The atomic oxygen density and neutral temperature results for three multi-day elevation-scan experiments are presented, a summer solstice (June 1984), a fall equinox (September 1984), and a winter solstice (January 1985) period. Analysis of the summer period shows a mostly uniform latitudinal profile of atomic oxygen density during the magnetically quieter periods. After a period of a sustained moderate level of magnetic activity, increases in both temperature and oxygen density were observed with particularly large density increases (by a factor of about 3) occurring at the lower latitudes. The equinox period covered one week and experienced varying levels of magnetic activity with the A index ranging from 2 to 76. Atomic oxygen densities at midlatitudes did not react strongly to low and moderate levels of magnetic activity during this period (up to A=28) but decreased by a factor of nearly 3 on the day with A=76. These density variations are discussed in terms of high-latitude dynamics and the global circulation response. The latitudinal-seasonal and diurnal structures of the density data are also discussed.

This technique represents a means of monitoring simultaneously the spatial and temporal structure of upper atmosphere densities and temperatures. Latitudinal coverage from the polar cap to the equator and studies of the global response to high-latitude energy inputs are possible through use of the entire incoherent scatter Radar Chain. This technique could prove very useful for monitoring the upper atmosphere during the current period of scant satellite coverage.

F REGION ION DRIFT AND VELOCITY OF SMALL SCALE  
IRREGULARITIES USING HF BACKSCATTER:  
A EISCAT-EDIA PRELIMINARY COMPARISON

A. Bourdillon<sup>1</sup> and D. Fontaine<sup>2</sup>

1 LPE, Université P.M. Curie, 4 place Jussieu,  
75230 Paris Cédex, France

2 CRPE/CNET, 4 avenue de Neptune, 94107  
Saint Maur des Fossés Cédex, France

Abstract: On February 6-7, 1984 the EISCAT incoherent scatter facility was operated in a meridian scan mode extended toward sub-auroral latitudes. Simultaneously the EDIA experiment, which is conducted with two HF coherent radars looking at a common scattering volume located approximately 15° West of the EISCAT field of view, was measuring the velocity of sub-auroral F region irregularities. Using the two components of the phase velocity of the irregularities we computed the northward and the westward velocities in a plane perpendicular to the geomagnetic field. In this paper we compare ion drift velocity with the phase velocity of the irregularities and we discuss uncertainties and discrepancies in the data and especially the large velocities measured by EDIA in the early of the night.

## G-6-5

### IONIZATION AND OPTICAL EMISSIONS DETECTED BY THE CHATANIKA RADAR AND THE DE-1 SPIN-SCAN AURORAL IMAGER

- R. M. Robinson and R. R. Vondrak (Space Sciences Laboratory,  
Lockheed Palo Alto Research Laboratory, Palo Alto, CA 94304)  
J. D. Craven and L. A. Frank (Department of Physics and Astronomy,  
University of Iowa, Iowa City, Iowa 52242)  
K. L. Miller (Center for Atmospheric and Space Sciences, Utah  
State University, Logan, Utah 84322)

Electron density measurements made by the Chatanika incoherent scatter radar and simultaneous imagery obtained with the Dynamics Explorer-1 (DE-1) spin-scan auroral imager have been compared to relate optical emissions to ionization in the auroral zones. The Chatanika radar data were obtained in an elevation scan mode so that electron density was measured as a function of altitude and latitude in the magnetic meridian plane. The DE-1 images used in the initial phase of this study were obtained using two filters. One accepted visible emissions at 557.7 nm; the other accepted ultraviolet (UV) emissions at wavelengths between 123.0 and 155.0 nm. Each image was constructed from 12-minutes of measurements during times when the satellite was near apogee over the northern hemisphere. Times were chosen when Alaska was near the center of the DE-1 image so that the instrument was nearly nadir-viewing when detecting emissions from the ionosphere above the radar. Data obtained in the early evening sector in October and November 1981 are presented, and these include examples of diffuse and discrete aurora. There is good agreement between the location of aurorally-produced E region ionization and the UV and visible emissions detected by the DE-1 imager. In the diffuse aurora where E region peak densities of  $10^5 \text{ cm}^{-3}$  are observed, both the UV and 557.7 nm emissions were approximately  $5 \text{ kR}_3$ . In bright arcs with typical E region peak densities of  $5 \times 10^5 \text{ cm}^{-3}$ , the 557.7 nm intensity was about 20 kR, while the UV intensities were somewhat less. These data are used to quantify the relation between the optical emissions and aurorally-produced E-region ionization and to evaluate the effects of ground-albedo, absorption, and scattering on space-based sensors for ionospheric remote sensing.

THEORETICAL STUDY OF ANOMALOUSLY HIGH F-REGION  
PEAK ALTITUDES IN THE POLAR IONOSPHERE

J. J. Sojka and R. W. Schunk, Center for Atmospheric and Space Sciences, Utah State University, Logan, Utah 84322, USA

During the last solar maximum period several observations of anomalously high F-region peak altitudes have been made by the high latitude incoherent scatter radars. The observations indicate that there are several distinctive features associated with these high  $h'F_2$  ionospheric profiles; (a) they are observed near midnight with the plasma flowing out of the polar cap, (b)  $N F_2$  ranges from  $10^5$  to  $10^6$   $\text{cm}^{-3}$ , (c)  $h'F_2$  ranges from 400 to 500  $\text{km}$ , (d) below 300 km the profile is devoid of ionization, and (e) the observations are for solar maximum conditions. In an effort to explain these radar observations, a time-dependent high latitude ionospheric model was used to study transport effects for a wide range of solar cycle, seasonal, magnetic activity, and neutral wind conditions. The model results indicate that high  $h'F_2$  values in the midnight sector of the polar region can be generated without the need for ionization due to auroral precipitation. For solar maximum, all of the observed features of the high  $h'F_2$  density profiles are reproduced by the model if the neutral wind across the polar cap is greater than 400 m/s. Such wind speeds have been frequently measured during the last solar maximum period.

The study also shows general results for the influence of transport in the polar cap for different seasonal and solar cycle conditions.  $N F_2$  and  $h'F_2$  are lower for solar minimum than solar maximum. However, the seasonal dependences are strongly coupled with both the strength of the convection and the neutral wind speed.

G-6-7

IMPROVED F-REGION ACF MEASUREMENTS AT ARECIBO

Michael P. Sulzer  
National Astronomy and Ionosphere Center  
Box 995.  
Arecibo, PR 00613  
USA

A description of a new technique for improving F-region autocorrelation (ACF) measurements at Arecibo is given. The technique can be used whenever the signal to noise ratio (SNR) in normal long pulse measurements is substantially greater than unity. As is well known, backscatter measurements do not significantly improve as the SNR is increased much above unity. Normal practice is to trade away SNR for an increased number of independent measurements. This new technique achieves this by turning the single radar into a number of sub-radars each operating simultaneously on a slightly different frequency. This is done with no new hardware using binary phase coding techniques. Codes have been developed which allow the radar signal spectrum to be split into a number of lines with nearly equal power in each and other lines with much less power so that the amount of wasted power is small. A single receiver is used covering the bandwidth of all the sub-radars, and all the ACF's are computed and combined using numerical techniques. At present Arecibo lacks the processing power to take full advantage of this technique, but the necessary computing equipment should be available in the next year.

## THE CODED LONG PULSE TECHNIQUE

Michael P. Sulzer  
National Astronomy and Ionosphere Center  
Box 995.  
Arecibo, PR 00613  
USA

The coded long pulse technique is described and evaluated. This technique is used for measuring incoherent backscatter spectra or autocorrelation functions (ACF's) when the required range resolution is smaller than the longest lag in the ACF. It consists of transmitting a binary phase coded pulse where the code is random and is changed frequently during the integration period. The technique is intended for use in the same applications as the standard multiple pulse technique, but the new technique can be used in situations with lower electron density since the average transmitted power is higher. Thus it has application to E-region measurements and might allow measurements to extend further into the evening and begin earlier in the morning. Under high signal to noise conditions the integration time is determined by random clutter as in the multiple pulse technique.

Computational techniques for implementing the technique are discussed, and some HF induced enhanced plasma line measurements are described.

*Withdrawn*

## G-6-9

A STUDY OF THE EFFECT OF COLLISIONS ON THE INCOHERENT  
SCATTER SPECTRUM

T. Fla  
EISCAT Scientific Association,  
N-9027 Ramfjordbotn, Norway.

A parameter study of the influence of collisions on the incoherent scatter spectrum is presented for different values of the electron to ion temperature ratio and normalised ion neutral collision frequency. The incoherent scatter spectra for the BGK collision frequency operator and the Brownian motion model of Hagfors and Brockelman(1971) are compared. The study shows that the incoherent scatter spectrum is model dependent when the ion neutral collision frequency is comparable to the width of ion line. Some care must therefore be taken in the analysis of collision frequencies and electron temperatures.

## URSI COMMISSION GH - SESSION GH1

**Ionospheric  
Modification  
and Heating - I**

1:30 - 5:00  
LAW 201

**Échauffement et modification  
de l'ionosphère au moyen  
des ondes radio-électriques I**

Chairperson/Président: **R.E. Horita**, University of Victoria, Victoria, BC

- 1 EFFECTS OF ENERGETIC ELECTRON PRODUCTION DUE TO RESONANT ABSORPTION DURING HIGH POWER HF IRRADIATION OF THE IONOSPHERE. **M. Shoucri, G.J. Morales, J.E. Maggs**, University of California at Los Angeles, Dept. of Physics, Los Angeles, CA, USA
- 2 OBSERVATIONS OF NONLINEAR PHENOMENA DURING IONOSPHERIC MODIFICATION. **J.P. Sheerin, D.R. Nicholson, G.L. Payne**, University of Iowa, Dept. of Physics and Astronomy, Iowa City, IA, USA; **L.M. Duncan**, Los Alamos National Laboratory, Los Alamos, NM, USA
- 3 EXTERNAL CONTROL OF HIGH LATITUDE IONOSPHERIC IRREGULARITIES BY POWERFUL RADIO WAVES. **P.K. Chaturvedi**, Science Applications International Corporation, McLean, VA, USA; **M.J. Keskinen**, Naval Research Laboratory, Geophysical and Plasma Dynamics Branch, Washington, DC, USA; **S.L. Ossakow**, Naval Research Laboratory, Plasma Physics Division, Washington, DC, USA
- 4 GENERATION OF E-REGION DENSITY IRREGULARITIES BY THERMAL PLASMA INSTABILITIES. **M.C. Lee**, Massachusetts Institute of Technology, Research Laboratory of Electronics, Cambridge, MA, USA; **S.P. Kuo**, Polytechnic Institute of New York, Farmingdale, NY, USA
- 5 NONLINEAR SIMULATIONS OF HF-INDUCED SHORT-SCALE IONOSPHERIC IRREGULARITIES. **A.L. Newman**, The Aerospace Corporation, Space Sciences Laboratory, Los Angeles, CA, USA
- 6 A THEORETICAL MODEL OF ARTIFICIAL SPREAD F ECHOES. **S.P. Kuo, S.C. Kuo**, Polytechnic Institute of New York, Farmingdale, NY, USA; **M.C. Lee**, Massachusetts Institute of Technology, Research Laboratory of Electronics, Cambridge, MA, USA
- 7 PHASE SCREEN SIMULATION OF SPACE-BASED SYNTHETIC APERTURE RADAR IN THE PRESENCE OF IONOSPHERIC STRIATIONS. **B.M. Lamb, G. St.-Cyr, M.K. Grover, R. Manasse**, R&D Associates, Marina del Rey, CA, USA
- 8 IONOSPHERIC ANOMALY SIMULTANEOUS WITH THE 1984 MORGAN HILL, CALIFORNIA, EARTHQUAKE. **R.L. Showen, V.R. Frank**, SRI International, Remote Measurements Laboratory, Menlo Park, CA, USA

## GH-1-1

### EFFECTS OF ENERGETIC ELECTRON PRODUCTION DUE TO RESONANT ABSORPTION DURING HIGH POWER HF IRRADIATION OF THE IONOSPHERE

M. Shoucri, G.J. Morales, and J.E. Maggs  
University of California at Los Angeles  
Los Angeles, California 90024, U.S.A.

A theoretical analysis is presented of the effects of energetic tails in the electron distribution function that result from the resonant absorption of electrostatic waves excited near the layer  $\omega_{pe}(z) = \omega$ , when an external HF signal at frequency  $\omega$  is used to irradiate an overdense ionosphere. Special attention is given to the slowing down and absorption of the tail electrons as well as the possible production of wave fields. Unique signatures of the presence of fast electrons are explored in the context of present HF heating experiments.

OBSERVATIONS OF NONLINEAR PHENOMENA  
DURING IONOSPHERIC MODIFICATION

J. P. Sheerin, D. R. Nicholson, and G. L. Payne  
Department of Physics and Astronomy  
University of Iowa  
Iowa City, IA 52242 USA

L. M. Duncan  
M.S. D466  
Los Alamos National Laboratory  
Los Alamos, NM 87545 USA

Ionospheric modification by high-power radio waves reveals a complex tapestry of nonlinear effects (e.g., filamentation, self-focusing, heated electrons, profile modification, parametric instabilities, soliton collapse and more). Several theories have been proposed to explain various features observed in the experimental data. We have made very high resolution (temporal and spatial) radar measurements of the HF interaction region. This technique complements spectral studies previously made and together they may provide a means of testing at least some of the features of the various theoretical models proposed. Results from a recent series of tests performed at Arecibo Observatory will be presented and compared with past experiments and existing theories. Theoretical developments aimed at refining experimental tests of theory will also be detailed.

EXTERNAL CONTROL OF HIGH LATITUDE  
IONOSPHERIC IRREGULARITIES BY POWERFUL  
RADIO WAVES

P.K. Chaturvedi, Science Applications International  
Corporation, McLean, VA 22102  
M.J. Keskinen<sup>(a)</sup> and S.L. Ossakow<sup>(b)</sup>, Naval Research  
Laboratory, Washington, D.C. 20375

We investigate the possibility of externally generating or suppressing naturally occurring ionospheric irregularities in the high latitude ionosphere using powerful ground-launched electromagnetic waves. Earlier studies are generalized to include the effects of finite pump wavelength. Threshold power requirements for the pump wave are computed and compared with that attainable using existing heaters.

GENERATION OF E-REGION DENSITY IRREGULARITIES  
BY THERMAL PLASMA INSTABILITIES

M.C. Lee

Research Laboratory of Electronics  
Massachusetts Institute of Technology  
Cambridge, MA 02139

S.P. Kuo

Polytechnic Institute of New York  
Long Island Center  
Farmingdale, NY 11735

Large electron-neutral collisions in the ionospheric E region may provide potential thermal sources for plasma instabilities to create density irregularities in the following two cases. (I) When the ionospheric E region is illuminated continuously by powerful radio waves, the ohmic dissipation of EM wave energy may become the driving source of thermal instabilities. The conditions for the excitation of ionospheric density irregularities and possibly earth's magnetic field fluctuations depend upon the radio wave frequencies and intensities. (II) Intense electrojet current may heat the E region through electron-neutral collisions and effectively excite ionospheric density irregularities via a thermal instability. These E region plasma instabilities driven by thermal source mechanisms can cause relatively large-scale irregular structures. The common feature characteristic of these thermal instabilities is that ohmic heating of electrons by AC (case I) or DC (case II) fields produces a thermal pressure force as the key nonlinearity of the instabilities.

**NONLINEAR SIMULATIONS OF HF-INDUCED SHORT-SCALE  
IONOSPHERIC IRREGULARITIES**

Alice L. Newman  
Space Sciences Laboratory  
The Aerospace Corporation, P. O. Box 92957  
Los Angeles, California 90009, U.S.A.

Mid-latitude ionospheric modification experiments have been simulated computationally to examine highly nonlinear interactions between transmitted high-power HF (3-12 MHz) radio waves and the natural ionosphere. Recent experiments by Djuth and others at Arecibo, Puerto Rico have provided a comprehensive data base describing the generation of short-scale irregularities and simultaneous phenomena in the heated region. Multidiagnostics were employed to distinguish between various nonlinear physical processes occurring on somewhat different time scales.

Two-dimensional nonlinear simulations have been performed to test our understanding of physical mechanisms effective during the process of HF ionospheric modification, and to examine their interaction over a range of time scales. Parametric and resonant processes, Brillouin scattering, self-focusing instabilities, and secondary processes will be discussed in the context of computational experiments which duplicate the functions of the observed diagnostics in the terrestrial geomericional plane. Specific simulations analogous to the Arecibo experiments will be described in detail, providing the time evolution of density and temperature irregularities, the nature of nonlinear mode coupling, and the frequency spectra associated with late-time stationary or saturation states. Estimates of instability thresholds, rise and decay times, and saturation amplitudes will be compared with the Arecibo observations. By tracing evolutionary variations in the amplitude and effect of various terms in the equations, it is possible to examine competing mechanisms as each becomes dominant in driving highly nonlinear field-plasma interactions.

## A THEORETICAL MODEL OF ARTIFICIAL SPREAD F ECHOES

S.P. Kuo  
Polytechnic Institute of New York, Long Island Center  
Farmingdale, NY 11735

M.C. Lee  
Research Laboratory of Electronics  
Massachusetts Institute of Technology  
Cambridge, MA 02139

S.C. Kuo  
Polytechnic Institute of New York, Long Island Center  
Farmingdale, NY 11735

Four invariants of the ray trajectory are found for a ray propagating in a horizontally stratified ionosphere under the density perturbation of HF wave-induced field-aligned irregularities. The reflection height of the ray can then be determined with the aid of those invariants. The results show that the reflection height of the ray varies drastically (namely, strong spread F echoes) in the presence of irregularities that polarize in the magnetic meridian plane. By contrast, the reflection height is not affected (namely, no spread F echoes) by those irregularities that polarize in the direction perpendicular to the meridian plane. Spread F is quite insensitive to the magnetic dip angle  $\theta_0$  in the region from  $20^\circ$  to  $70^\circ$ . The dependence of spread F on the scale length of the irregularity has also been examined. It is found that spread F is not caused by irregularities with scale lengths less than about 100 meters.

## GH-1-7

### PHASE SCREEN SIMULATION OF SPACE-BASED SYNTHETIC APERTURE RADAR IN THE PRESENCE OF IONOSPHERIC STRIATIONS

B. M. Lamb, G. St-Cyr, M. K. Grover and R. Manasse  
R & D Associates  
Post Office Box 9695  
4640 Admiralty Way  
Marina del Rey, CA 90295

Synthetic aperture radars (SARs) can produce high-resolution images through phase-coherent processing of signals transmitted and received at different times and platform locations. SAR image quality can be degraded by random perturbations of signal phase. For space-based SARs, one possible source of random phase errors is the signal propagation through a structured, or "striated," ionosphere. Ionospheric striations occur naturally, and can also be artificially generated by high-altitude chemical releases, high-power ionospheric heaters, and nuclear explosions. We have developed models for simulating space-based SAR performance in the presence of ionospheric striations. The SAR simulation has been keyed to the JPL SEASAT experiment. Degradation of SAR image quality has been evaluated as a function of various parameters describing the SAR design and the ionospheric striations. A variety of mitigation techniques have also been evaluated, e.g., increasing carrier frequency, optimization of synthetic aperture length, optimization of SAR orbital and viewing geometry, and adaptive refocusing during the phase-coherent signal processing. The adaptive refocusing techniques use information in the return signals to derive an estimate of the propagation-induced signal phase perturbations. Limited comparisons with actual SEASAT SAR data have also been made.

IONOSPHERIC ANOMALY SIMULTANEOUS WITH THE 1984  
MORGAN HILL, CALIFORNIA, EARTHQUAKERobert L. Showen and Victor R. Frank  
SRI International  
Menlo Park, California 94025

An ionosonde anomaly was observed simultaneously with a magnitude 6.2 earthquake near Morgan Hill, California on 24 April 1984. The anomaly consists of loops appearing in an ionogram record in the F<sub>1</sub>-region within 15 seconds of the onset of the earthquake. The loops are not seen on ionograms taken 10 minutes before or after the earthquake. If these loops are caused by the earthquake, the prompt response of the ionosphere means that acoustic waves produced by the ground motion cannot be the cause. Loops are rarely observed on ionograms and are associated with ionospheric tilts. A mechanism to produce ionospheric tilts by earthquakes is postulated based on a charge build-up at the epicenter which may accompany earthquakes. The evidence for the charge build-up comes from the phenomenon of earthquake lights, where charges produced by friction during ground motion ionize the atmosphere. We postulate that a charge at the epicenter creates an electric field in the ionosphere large enough to cause significant  $\vec{E} \times \vec{B}$  drifts resulting in tilts which produce the temporary loops.



## URSI COMMISSION GH - SESSION GH2

**Alouette-ISIS**

8:30 - 5:00

**Programme****Program I**

LAW 169

**Alouette-ISIS I**Chairperson/Président: **H.G. James**, Department of Communications, Ottawa, ON

- 1 (8:40) A QUANTITATIVE ANALYSIS OF THE SUCCESS OF THE ALOUETTE-ISIS PROGRAM. **J.E. Jackson**, NASA/GSFC, National Space Science Data Center, Greenbelt, MD, USA
- 2 (9:20) THE IMPACT ON CANADIAN INDUSTRY OF THE ALOUETTE - ISIS PROGRAM. **F.J.F. Osborne**, Spar Aerospace Limited, Satellite and Aerospace Systems Division, Ste-Anne-de-Bellevue, PQ
- 3 (10:00) ALOUETTE-ISIS OBSERVATION OF ELECTROSTATIC RESONANCES. **D.B. Muldrew**, Department of Communications, Communications Research Centre, Ottawa, ON
- 4 (10:40) PROTON CYCLOTRON ECHOES AND SPURS OBSERVED ON ALOUETTE II AND ISIS II. **R.E. Horita**, University of Victoria, Dept. of Physics, Victoria, BC
- 5 (11:00) SOLAR AND GEOMAGNETIC ACTIVITY DEPENDENCE OF TRANS-EQUATORIAL ION WHISTLER. **S. Watanabe**, **T. Ondoh**, Ministry of Posts and Telecommunications, Radio Research Laboratories, Tokyo, Japan
- 6 (11:20) CHARACTERISTICS OF RISER EMISSIONS OBSERVED BY ISIS SATELLITES. **T. Ondoh**, Ministry of Posts and Telecommunications, Radio Research Laboratories, Tokyo, Japan

## GH-2-1

### A QUANTITATIVE ANALYSIS OF THE SUCCESS OF THE ALOUETTE-ISIS PROGRAM

J. E. Jackson  
National Space Science Data Center  
NASA/GSFC, Greenbelt, Maryland 20771

The resources and documentation of the National Space Science Data Center (NSSDC) have made it possible to prepare a comprehensive assessment of the success of the Alouette-ISIS program. Since its very beginning NSSDC has shown a considerable interest in the data and results of the Alouette-ISIS program. Approximately 100 Alouette-ISIS data sets are available at NSSDC. One can convey some idea of the magnitude of these data holdings by pointing out that the one million Alouette 1 ionograms constitute only one data set. Also available at NSSDC is a computerized file containing bibliographical entries related to space experiments. This file contains about 1000 citations based upon the Alouette-ISIS program. The citations can be searched by spacecraft, investigations, authors, titles, journals, publication dates, etc. and organized accordingly. Several extensive NSSDC reports, either already published or under preparation, have been either entirely or substantially based upon the Alouette-ISIS program. The present paper is based upon information compiled for these reports.

THE IMPACT ON CANADIAN INDUSTRY  
OF THE ALOUETTE - ISIS PROGRAM

Dr. F. J. F. Osborne  
Satellite and Aerospace Systems Division  
Spar Aerospace Limited

With the launch in 1961 of the Alouette spacecraft Canada entered the space age, becoming the third nation in the world to build and operate a satellite. With the ensuing phases of the four satellite Alouette-ISIS program, Canada became a major contributor in the space sciences, particularly the ionospheric-magnetospheric disciplines which had been and are traditional Canadian scientific strengths.

In the course of the Alouette-ISIS program, under the dual forces of the natural interest and declared government policy, Canadian industry increased its involvement from a relatively minor participation as a hardware supplier to a proven prime contracting capability in the management and technological aspects of a multi-faceted program of considerable scientific and engineering complexity.

The ISIS spacecraft involved several major organizations as interfaces, including the Defence Research Telecommunications Establishment (later the Communications Research Center), NASA and the launch vehicle supplier, as well as experimenters from Canadian and US establishments and universities. Some of the management techniques developed for the ISIS program to service these interfaces were applied in other major US programs.

The fact that many of the spacecraft payloads involved were highly interactive with the space environment and/or each other required special consideration of experiment sequences, sampling rates etc., as well as laboratory simulation of many of the anticipated phenomena.

Because of the overall complexity of the equipments and mission, special emphasis was placed on the techniques used in spacecraft level check-out, leading to new approaches now used extensively in spacecraft and programs of all types.

ALOUETTE-ISIS OBSERVATION OF  
ELECTROSTATIC RESONANCES

D.B. Muldrew  
Communications Research Centre  
Department of Communications  
Ottawa, Ontario K2H 8S2

Electrostatic resonances are manifest on topside ionograms by narrowband signals stimulated by the transmitter and persisting up to many milliseconds. At frequencies near the plasma frequency  $f_N$ , the upper hybrid frequency  $f_{UH}$ , and harmonics of the gyrofrequency  $nf_H$ ,  $n \geq 2$ , electrostatic waves of slightly different frequencies generated by the transmitter pulse, propagate in the ionospheric plasma, become reflected at distances of several hundred meters from the satellite, and return to the satellite producing a continuous receiver response. At frequencies near the gyrofrequency  $f_H$ , and the maximum frequency of the Bernstein modes  $f_{QB}$ , the electrostatic waves can propagate so that their direction of energy flow is along the moving antenna, again producing a continuous response. The fundamental resonance,  $f_H$ , is still not well understood. Under the assumption of homogeneous plane waves, the refractive index for electrostatic propagation near  $f_H$  is complex and heavy damping would be expected. However, if inhomogeneous waves are assumed, it appears possible to have undamped propagation.

PROTON CYCLOTRON ECHOES AND SPURS OBSERVED ON ALOUETTE II AND  
ISIS II

R. E. Horita

Department of Physics, University of Victoria, Victoria, B. C.,  
Canada V8W 2Y2

Proton cyclotron echoes and spurs observed on the topside-sounder ionograms on the Canadian Alouette II and ISIS II satellites are phenomena related to the proton cyclotron frequency. They appear on the ionograms at apparent ranges which lead to a frequency close to the proton cyclotron frequency; the frequency is calculated by taking the reciprocal of the time elapsed between the transmission of the sounder pulse and the reception of the signal at the satellite.

Over 1000 ionograms exhibiting proton cyclotron echoes and/or spurs were examined and were classified depending on apparent range, frequency range (horizontal extent on the ionogram), and shape of the echoes or spurs. Echoes and spurs often occur alone but echoes and spurs occur together approximately as frequently. Most proton cyclotron echoes and spurs occur at frequencies below the electron plasma frequency,  $f_N$ , however one type of spur occurs at frequencies above  $f_N$ . The echoes occur predominantly at frequencies slightly above the electron cyclotron frequency,  $f_H$ , while the spurs occur predominantly when a harmonic of  $f_H$  is near  $f_N$ . Details of the classification and occurrence features  $N$  will be presented.

## GH-2-5

### SOLAR AND GEOMAGNETIC ACTIVITY DEPENDENCE OF TRANS-EQUATORIAL ION WHISTLER

S.Watanabe and T.Ondoh (Radio Research Labs., Ministry of Posts.  
& Telecom., Tokyo 184 Japan)

We have investigated occurrence probabilities and patterns of trans-equatorial proton (TEP) and deuteron (TED) whistler from the ISIS-2 satellite in time compressed dynamic spectra. It is shown that the TEP whistlers have high occurrence probability in an active solar period, while the TED whistler has low occurrence probability. In a quiet solar period, the TEP whistler has a relatively lower occurrence probability than the TED whistler. The TEP whistler in a quiet solar period shows a strong seasonal variation. That is a higher occurrence probability in winter than in the summer in the Northern Hemisphere at Japanese longitude. These phenomena seem to be explained by using the bouncing surface diagram of multi-component and inhomogeneous plasmas with various proton density. The spectral pattern of trans-equatorial ion whistlers and calculation of an approximate equation with regard to deuteron effect show that relative proton densities to electrons  $N_p/N_e$  decrease with increasing solar activity.

Several ion whistlers were observed by ISIS-1,-2 during geomagnetic storms associated with large solar flare in 1982. It seemed that the proton density ratio to electrons  $N_p/N_e$  deduced from the crossover frequency of the trans-equatorial ion whistlers observed at low latitude during the main phase of the geomagnetic storm on July 14th 1982 was lower than the density ratio  $N_p/N_e$  during quiet period. An abnormal pattern seen on the time-compressed dynamic spectra for September 6th 1982 suggests existence of strong effect by the component ( $M/Q=3$ )  $^3\text{He}^+$  in quite small amount.

## CHARACTERISTICS OF RISER EMISSIONS OBSERVED BY ISIS SATELLITES

T. Ondoh

Radio Research Laboratories, Tokyo, 184

Riser emissions and VLF hisses with fine rising structures are observed in the mid-latitude topside ionosphere. The giant riser emissions, whose frequency rises from about 8 kHz to 15 kHz or more in a few seconds occur often at geomagnetically invariant latitudes from  $47^{\circ}$  to  $60^{\circ}$  in the recovery phase of geomagnetic substorms. The giant riser emission may be interpreted by the Doppler-shifted cyclotron radiations emitted forward from energetic protons of 10 keV in the plasmasphere.

Groups of the normal riser emissions, whose frequency rises from about 5 kHz to about 10 kHz in 1.5 seconds, were repeatedly observed in a period of 26 - 27 seconds at geomagnetically invariant latitudes from  $56.5^{\circ}$  to  $61.9^{\circ}$  by the ISIS-2 on March 10, 1981. Geomagnetic pulsations of Pc 3 were also observed simultaneously with the periodic appearance of the normal riser emissions at Memambetsu (geomag. lat.  $34.1^{\circ}$ N, long.  $208.8^{\circ}$ E). The periodic occurrence of the riser emission may be explained by the periodic modulation of riser emission growth-rate which results from the particle precipitations modulated by the geomagnetic pulsations of Pc 3.



## URSI COMMISSION GH - SESSION GH3

**Alouette-ISIS  
Program II**

1:30 - 500  
LAW 169

**Programme  
Alouette-ISIS II**

Chairperson/Président: **R.F. Benson**, NASA/Goddard Space Flight Center, Greenbelt, MD, USA

- 1 (1:40) JAPANESE ACTIVITIES IN THE ALOUETTE/ISIS PROGRAM. **N. Matuura**, **K. Aikyo**, Ministry of Posts and Telecommunications, Radio Research Laboratories, Tokyo, Japan
- 2 (2:20) BANDWIDTH AND AMPLITUDE INCREASES OF VLF TRANSMITTER SIGNALS DURING TRANSIONOSPHERIC PROPAGATION. **T.F. Bell**, **U.S. Inan**, **J.P. Katsuftrakis**, STAR Laboratory, Stanford, CA, USA; **H.G. James**, Department of Communications, Communications Research Centre, Ottawa, ON
- 3 (2:40) Z-MODE DUCTING. **W. Calvert**, University of Iowa, Dept. of Physics and Astronomy, Iowa City, IO, USA
- 4 (3:00) Z-MODE DUCTS OBSERVED BY ALOUETTE 2 AT LOW LATITUDES. **S.H. Gross**, Polytechnic Institute of New York, Dept. of Electrical Engineering, Farmingdale, NY, USA; **D.B. Muldrew**, Department of Communications, Communications Research Centre, Ottawa, ON; **W. Calvert**, University of Iowa, Iowa City, IA, USA
- 5 (3:20) ISIS 1 OBSERVATIONS OF AURORAL KILOMETRIC RADIATION. **R.F. Benson**, NASA/Goddard Space Flight Center, Laboratory for Extraterrestrial Physics, Greenbelt, MD, USA
- 6 (3:40) EXCITATION OF 2 MHz RADIO NOISE BY THE CYCLOTRON MASER INSTABILITY IN THE LOW ALTITUDE AURORAL REGION. **H.K. Wong**, NASA/Goddard Space Flight Center, Laboratory for Extraterrestrial Physics, Greenbelt, MD, USA
- 7 (4:00) SOME CHARACTERISTICS AND PROPAGATION OF AURORAL Z-MODE RADIATION OBSERVED ABOVE THE ANTARCTIC REGION WITH ISIS-1. **K. Aikyo**, **T. Ondoh**, **R. Nishizaki**, Ministry of Posts and Telecommunications, Radio Research Laboratories, Tokyo, Japan
- 8 (4:20) PANEL DISCUSSION/TABLE RONDE.

## **GH-3-1**

### **JAPANESE ACTIVITIES IN THE ALOUETTE/ISIS PROGRAM**

**N. MATUURA and K. AIKYO (Radio Research Labs., Ministry of Posts and Telecom., Tokyo 184 Japan)**

A review on the past activities in the Alouette/ISIS program in Japan, mainly in RRL (Radio Research Laboratories, Ministry of Posts & Telecommunications, Japan) will be given with regard to ground operations and scientific research. A preview on future plan about ISIS program will also be mentioned.

RRL joined the ISIS Working Group on the fifth meeting at London in 1965 and began to acquire the topside sounding data in August 1966 and VLF data in July 1971 from Alouette-1 and -2 by RRL working group consisting of data acquisition group at Kashima Space Station, RRL and data reduction and analyses group at Koganei, Tokyo, HQ RRL. Acquisition of the data from ISIS-1 and ISIS-2 at Kashima Station started respectively in January 1970 and May 1971. Furthermore, telemetry-only operation for ISIS satellites at Syowa Station (69°00.4'S, 39°35.4'E) Antarctica with command support by French Stations through CRC has been carried out since April 1976 in cooperation with NIPR (National Institute of Polar Research, Ministry of Education, Japan). The topside ionograms processed at RRL have been distributed to CRC, NSSDC at GSFC, WDC-A at NOAA and Rutherford Appleton Lab. since 1973. After the cease of ISIS operations by CRC in March 1984, the operations have been transferred to RRL on the basis of an agreement between CRC and RRL and acquisition of ISIS data at both Kashima and Syowa will be continued at least until March 1986.

Scientific research in Alouette/ISIS program in Japan has been put forward mainly by using data from topside sounders and VLF receivers. The result from analyses of the topside sounder data concerns the structure of the topside ionosphere in quiet and disturbed conditions seen by the electron density distributions given from resonance frequencies, critical frequencies, and N(h) reduction and also concerns the various kinds of radio phenomena such as ducted echoes, proton cyclotron echoes, diffuse resonance, cosmic radio noises, solar radio bursts and dayside AKR. The data books on the topside electron density distribution over Japan have been so far published in six volumes by RRL.

The result from analyses of the VLF data concerns the spectral characteristics and latitudinal variation of ELF hiss and whistler ducts in the low and midlatitudes and also concerns the deuterium whistler and trans-equatorial propagation of ion whistlers. The works relating to the polar region includes study of source of VLF saucer, relation of VLF saucer and quasi-periodic VLF/ELF emissions to the auroral activity. The ISIS data on narrow band multifrequency noise have been contained in Radio and Space Data Vol. 1-15, RRL.

## Bandwidth and Amplitude Increases of VLF Transmitter Signals During Transionospheric Propagation

T. F. BELL, U. S. INAN, J. P. KATSUFRAKIS

*STAR Laboratory, Stanford, California, 94305*

H. G. JAMES

*Communications Research Centre, Shirley Bay, Ottawa, Ontario, Canada K2H8S2*

VLF/ELF wave electric field data acquired on the ISIS-1, ISIS-2, ISEE-1, and DE-1 spacecraft demonstrate the existence of a new phenomenon in which initially narrowband ( $\sim 1$  Hz) signals from ground-based VLF transmitters undergo a significant increase in bandwidth as they propagate through the ionosphere up to altitudes in the range 600-4000 km. For transmitter signals in the range 3-20 kHz the bandwidth increase can be as high as 20% of the nominal frequency of the input signal.

The bandwidth increases occur only in the presence of impulsive VLF/ELF hiss and/or a lower hybrid resonance (LHR) noise band with an irregular lower cutoff frequency, and only for signals whose frequency exceeds the LHR frequency at the satellite location. For transmitter pulses propagating within the plasmasphere, all portions of the pulse show a bandwidth increase but little amplitude change. However, for pulses propagating poleward of the plasmopause the bandwidth increases are sometimes impulsive in nature and are accompanied by amplitude increases of up to 20 dB. The impulsive bandwidth increases typically endure for 100 msec and often the sidebands are symmetric about the nominal carrier frequency. The effect is most pronounced when the transmitter pulses lie close to the lower border of an impulsive hiss band near 3 kHz.

Comparison of wave electric and magnetic fields indicates that the bandwidth increases are present only in the wave electric field component. This finding suggests that the sideband waves are quasi-electrostatic in nature and propagate with their wave normals close to the whistler mode resonance cone.

Since impulsive VLF hiss and irregular LHR noise bands have been linked to energetic ( $< 1$  Kev) electron precipitation in the past, it is conjectured that the bandwidth and amplitude increases are produced in a process driven by precipitating electrons.

## Z-MODE DUCTING

W. Calvert, Department of Physics and Astronomy  
The University of Iowa, Iowa City, Iowa 52242

Wave ducting, exemplified by the guiding of light within optical fibers, involves the guidance of waves by relative maxima of the wave refractive index. In a magnetoplasma, such maxima can arise from variations of the plasma density. Since natural density variations usually extend along the ambient magnetic field, this produces ducting in that direction, known as 'field-aligned' ducting. The ordinary and extraordinary magnetoionic wave modes (occurring for  $X < 1$  and  $X < 1 - Y$ , respectively, in Ratcliffe's notation) are both always ducted by density depletions, or 'troughs'. The Z-mode (which occupies  $1 + Y > X > 1 - Y^2$ ) exhibits more varied ducting because of its more complex anisotropic refractive index. At frequencies just above cutoff ( $X = 1 + Y$ ), Z-mode ducting occurs in troughs, having ducted wave normals which oscillate between opposite sides of the duct axis. Beyond a 'curvature reversal' frequency, given by  $X = (1 + Y)/(1 + Y/2)$  and corresponding to the development of a dimple along the axis in the Z-mode refractive index, this ducting continues in troughs, but now with its wave normals remaining on one side of the axis (like the similar whistler-mode trough ducting below half the cyclotron frequency). Also at the curvature reversal frequency, Z-mode 'crest' ducting begins within density enhancements, and it co-exists with the trough ducting up to the plasma frequency, where both kinds of ducting cease. An additional, but separate region of Z-mode crest ducting can also occur between the plasma and cyclotron frequencies ( $X = 1$  to  $Y = 1$ ), whenever the latter frequency is greater. Only the trough ducting, however, should produce topside ducted echoes, since neither region of Z-mode crest ducting would be continuous to the wave reflection level. No field-aligned Z-mode ducting is possible above the greater of the plasma or cyclotron frequency, there being no refractive index extremum in the direction of the duct.

Z-MODE DUCTS OBSERVED BY ALOUETTE 2  
AT LOW LATITUDES

S. H. Gross, Polytechnic Institute of New York, Farmingdale, New York; D. B. Muldrew, Communications Research Centre, Ottawa, Ontario; W. Calvert, University of Iowa, Iowa City, Iowa.

Z-mode ducted traces are observed in Alouette 2 ionograms. We have studied these traces on ionograms for low latitude passes of the satellite. It is found that the vertical Z-mode trace extends from the Z-mode cutoff at the satellite through the plasma frequency to  $fZI$ , the frequency of infinite apparent range. The Z-mode ducted trace starts from the Z-mode cutoff at the satellite and terminates at the plasma frequency. Other traces are apparent in the frequency range above the plasma frequency to  $fZI$  that are believed to be combination mode Z traces due to waves that start off vertically from the satellite and enter ducts below where the plasma frequency is greater than the wave frequency. These traces are not the oblique Z traces. Conjugate Z mode ducts are also observed. The duct traces appear to be in accordance with the theory of Z mode ducting. X-mode multiple ducted traces are also observed on the same ionograms, and it is likely that these X-mode ducts are part of the same structure causing the Z-mode ducts. Examples will be shown including interpretations by means of ray tracings.

## GH-3-5

### ISIS 1 OBSERVATIONS OF AURORAL KILOMETRIC RADIATION

Robert F. Benson  
NASA/Goddard Space Flight Center  
Laboratory for Extraterrestrial Physics  
Greenbelt, MD 20771

Auroral kilometric radiation (AKR) is an intense electromagnetic emission associated with discrete auroral arcs. The investigation of AKR has been extensive (nearly 100 scientific publications in the last decade), partly because of its relevance to other astrophysical radiation phenomena. AKR is commonly observed on ISIS 1 nighttime apogee auroral-zone ionograms. The ISIS 1 topside sounder provides reliable ambient and remote measurements of the plasma frequency  $f_N$  and the ambient electron cyclotron frequency  $f_H$ . The resulting  $f_N/f_H$  values in the AKR source region have been of fundamental importance to AKR theories. The received signal intensities and the relative strengths of the various wave modes are dependent on the ambient plasma parameter  $f_N/f_H$ . (Wave mode identifications are based on comparisons of the observed natural AKR signals with sounder-generated cutoff and resonance phenomena.) AKR is observed in the extraordinary, ordinary, Z and whistler modes. The fundamental AKR in each of these modes is confined to frequencies below 900 kHz. Intense signals at higher frequencies are also observed which are identified either with AKR harmonics or intense low altitude (< 1000 km) emissions near 2 MHz and 4 MHz. These observations, and their significance to the various theoretical mechanisms proposed to explain AKR, will be reviewed.

EXCITATION OF 2 MHz RADIO NOISE BY THE CYCLOTRON MASER  
INSTABILITY IN THE LOW ALTITUDE AURORAL REGION

H. K. Wong  
NASA/Goddard Space Flight Center  
Laboratory for Extraterrestrial Physics  
Greenbelt, MD 20771

Radio noise of frequency about 2 MHz at auroral latitudes has been reported by James et al. (AGARD Conference Proceedings No. 138, 1974). It was suggested by these authors that the electromagnetic radiation was generated by the conversion of electrostatic upper hybrid waves into electromagnetic ordinary waves through a wave-wave interaction process. Here we propose that the observed radiation can also be explained by a direct generation mechanism, i.e., the radiation is excited directly as an electromagnetic extraordinary wave at twice the gyrofrequency in the source region by the cyclotron maser instability. One distinct feature of this mechanism is the direct transfer of energy from the particles to the radiation. Thus it should be a more efficient mechanism than the wave-wave interaction process.

## GH-3-7

### SOME CHARACTERISTICS AND PROPAGATION OF AURORAL Z-MODE RADIATION OBSERVED ABOVE THE ANTARCTIC REGION WITH ISIS-1

K. AIKYO, T. ONDOH and R. NISHIZAKI (Radio Research Labs., Ministry of Posts & Telecom., Tokyo 184 Japan)

Various types of plasma wave emissions can be seen on the ISIS-1 topside ionograms obtained over the auroral zone and the polar cap. Among the emissions the broadband Z-mode radiation is examined in detail with respect to propagation using ray tracing technique. This type of radiation detected by ISIS-1 is characterized by 1) sharp frequency cutoff near electron gyrofrequency,  $f_H$  and 2) relatively stable structure of spectrum with maximum intensity near 300 kHz over the polar region where the plasma frequency,  $f_N \ll f_H$ . Observation is limited in the radial distance of about  $1.5 R_E$  (earth radii). Similar radiation has been observed in the higher altitudes ( $\geq 2 R_E$ ) with DE-1 (Gurnett, D.A. et al., J. Geophys. Res., 88, 329, 1983)

On the basis of the spin modulated signals on chains of the fixed frequency frames (0.25 MHz) in 'Swept frequency mode', the orientation of antenna at the instant when the radiation exhibits minimum level are determined to reduce the angle of direction of arrival with the simple fitting procedure. The similar technique was used to derive the wave vector angle of R-X mode AKR (James, H.G., J. Geophys. Res., 85, 3367, 1980). Application of simplified geometry with respect to wave electric field plane, local geomagnetic field and wave vector and the antenna orientation determined results in the wave normal angle ranging about  $95^\circ$  to  $110^\circ$  with respect to the local geomagnetic field depending on the local  $f_N$  from 0.05 to 0.1 MHz. This implies that the direction of propagation is upward provided that radiation comes from low latitude side.

The computation of the ray paths is made to locate the source region for auroral Z-mode radiation using plausible model magnetosphere allowed for the steep gradient near the plasmopause, indicating that trapping and reflection along and near the plasmopause after nearly horizontal propagation of long distance affect the ray paths with wide extent for the initial wave normal angles. Thus the inclusion of the plasmopause effect is essential in the source geometry and propagation for Z-mode radiation proposed by Gurnett et al. (1983).

## URSI COMMISSION GH - SESSION GH4

**Ionospheric  
Modification  
and Heating II**8:30 - 12:00  
LAW 201**Échauffement et modification  
de l'ionosphère au moyen  
des ondes radio-électriques II**Chairperson/Président: **D.B. Muldrew**, Department of Communications, Ottawa, ON

- 1 (8:40) IONOSPHERIC MODIFICATION EXPERIMENTS AT ARECIBO. **J.A. Fejer**, University of Illinois at Urbana-Champaign, Dept. of Electrical and Computer Engineering, Urbana, IL, USA
- 2 (9:20) STIMULATED ELECTROMAGNETIC EMISSION IN IONOSPHERIC HF MODIFICATION EXPERIMENTS. **B. Thidé**, Uppsala Ionospheric Observatory, Uppsala, Sweden
- 3 (10:00) HF-INDUCED PLASMA INSTABILITIES IN THE E REGION. **F.T. Djuth**, The Aerospace Corporation, Space Sciences Laboratory, Los Angeles, CA, USA
- 4 (10:40) PHASE AND INTENSITY SCINTILLATIONS INDUCED BY HF HEATING OF THE DAYTIME SUB-AURORAL IONOSPHERE. **Santimay Basu, Sunanda Basu**, Emmanuel College, Physics Research Division, Boston, MA, USA; **P. Stubbe, H. Kopka**, Max Planck Institut für Aeronomie, Lindau, FRG, **H.C. Carlson**, Air Force Geophysics Laboratory, Hanscom AFB, MA, USA
- 5 (11:00) STANDING WAVE PATTERN OF HF RADIO WAVES IN THE IONOSPHERIC REFLECTION REGION. **B. Thidé, B. Lundborg**, Uppsala Ionospheric Observatory, Uppsala, Sweden
- 6 (11:20) INJECTION OF ELF/VLF INTO THE EARTH-IONOSPHERIC WAVEGUIDE GENERATED BY MODULATING THE DYNAMO CURRENT SYSTEM FROM HF HEATING. **K. Carroll, A.J. Ferraro**, The Pennsylvania State University, Communications and Space Sciences Laboratory, University Park, PA, USA
- 7 (11:40) AN IONIZATION DUCT EXPLANATION OF PLASMA-LINE OBSERVATIONS WITH A 46.8-MHz RADAR. **D.B. Muldrew**, Department of Communications, Communications Research Centre, Ottawa, ON

GH-4-1

IONOSPHERIC MODIFICATION EXPERIMENTS AT ARECIBO

J. A. Fejer  
Department of Electrical and Computer Engineering  
University of Illinois at Urbana-Champaign  
1406 West Green Street  
Urbana, IL 61801

Recent experimental results obtained using the Arecibo heating facility are reviewed and their relation to existing theories is discussed. Among the new experimental results are the first observations of the time history of the appearance and disappearance of a flux of accelerated electrons as the heater is cycled on and off, the first experimental demonstration of the plasma line spectrum below threshold, the first measurements of the width of the "growing mode line" (20-60Hz), the use of such narrow lines for accurate measurements of the electron drift velocity, and the discovery of a radical qualitative change in the spectrum as the HF power is increased.

**STIMULATED ELECTROMAGNETIC EMISSION IN  
IONOSPHERIC HF MODIFICATION EXPERIMENTS**

Bo Thidé  
Uppsala Ionospheric Observatory  
S-75590 Uppsala, Sweden

Abstract not available at time of printing/  
Le résumé n'était pas disponible lors de l'impression

## HF-INDUCED PLASMA INSTABILITIES IN THE E REGION

Frank T. Djuth  
Space Sciences Laboratory  
The Aerospace Corporation, P. O. Box 92957  
Los Angeles CA 90009, U.S.A.

High-power radio waves reflecting in the F region of the ionosphere are known to excite several different types of plasma instabilities. These instabilities are responsible for a variety of effects, which include the production of large-scale ( $\geq 100$  m) and short-scale (1 - 10 m) density irregularities, the generation of plasma turbulence, the acceleration of electrons, enhanced electron temperatures and the formation of a plasma bulge across the HF beam. This paper focuses upon several of these phenomena that have also been observed at E-region heights. Particular attention is paid to the production of plasma turbulence and the formation of short-scale, field-aligned irregularities (FAIs) in the E region. E-region results are compared with observations made in the F region.

The ambient E-region plasma contrasts markedly with the plasma environment found in the F region. Notable differences are found with respect to electron temperatures, ion composition, collision frequencies and vertical electron density gradients. Differences in electron density gradients are most pronounced when one compares the vertical scale lengths in sporadic E (0.1 - 1.0 km) with those encountered at F-region heights (30 - 60 km). This introduces several interesting effects. For example, in sporadic E the vertical extent of the instability region is compressed to several tens of meters (compared to 5 - 10 km in the F region). Not surprisingly, the response of the sporadic-E plasma to the abrupt turn-on of the HF beam is not the same as that found in the F region. The so-called plasma line overshoot observed in the F region is characterized by a quick ( $\leq 50$  msec) growth in HF-induced turbulence followed by a significant reduction in the turbulence level over time scales of seconds. Plasma line overshoot is also observed in sporadic E but the growth and decay phases take place within a few milliseconds. In general, the spectral signatures and the dynamic behavior of the HF-enhanced plasma lines and FAI backscatter exhibit striking differences in the normal daytime E region, sporadic E, and the F region. The emphasis of this presentation will be on providing a consistent interpretation of HF-induced phenomena observed in the various ionospheric regions and at different geomagnetic latitudes.

PHASE AND INTENSITY SCINTILLATIONS INDUCED BY HF HEATING  
OF THE DAYTIME SUB-AURORAL IONOSPHERE

Santimay Basu and Sunanda Basu  
Emmanuel College  
Boston MA 02115

P. Stubbe and H. Kopka  
Max Planck Institut für Aeronomie  
D-2411 Katlenburg  
Lindau, W. Germany

H.C. Carlson  
Air Force Geophysics Laboratory  
Hanscom AFB MA 01731

During March, 1984 the high power HF heating facility located at Ramfjordmoen (69.6°N, 19.2°E geographic) was used to modify the ionospheric F-region and an experiment was performed to study the generation of artificial F-region irregularities in the daytime sub-auroral environment. For the experiment, 250 MHz transmissions from a near stationary satellite were received at the Tromso telemetry station at an ionospheric zenith angle of 17° and a magnetic azimuth of 75° and the heater beam was tilted to intercept the ionospheric intersection of the propagation path from the satellite to the receiver. The satellite signal intensity and phase were recorded by the computer controlled phase lock receiver and the fluctuations of intensity and phase were analyzed to detect the presence of the irregularities of F-region electron density generated by the heater. It was found that it is indeed possible to excite F-region irregularities in the daytime sub-auroral environment causing 3 dB fluctuations of signal intensity at 250 MHz. The spectra of intensity and phase scintillations indicate maximum power spectral density (psd) within a narrow range of characteristic scales of about 200-400 m with very steep high frequency spectral index ( $n \sim -8$ ) which is followed by a gentle roll-off with a spectral index of about -1.5. The stable excitation of a narrow band of scale sizes throughout the period when the heater is on suggests that the linear stage of self-focusing instability is operative. The slow high frequency roll-off at a much lower psd is indicative of a weak cascading towards shorter scales. The decay time of the artificial irregularities is found to be rather short being of the order of a minute in contrast to the lifetime of tens of minutes for natural irregularities.

**GH-4-5**

**STANDING WAVE PATTERN OF HF RADIO WAVES  
IN THE IONOSPHERIC REFLECTION REGION**

Bo Thidé and Bengt Lundborg  
Uppsala Ionospheric Observatory  
S-75590 Uppsala, Sweden

General analytical formulas for the field strength near the height of reflection of an electromagnetic wave in the ionosphere have been derived within a uniform approximation which, unlike the related WKB approximation, does not break down at the reflection point. The formulas are valid for general, smooth plasma profiles where the density either increases monotonically or exhibits a local maximum. The usefulness of the method is illustrated by application to physically realistic situations encountered in ionospheric modification experiments.

**INJECTION OF ELF/VLF INTO THE EARTH-IONOSPHERIC WAVEGUIDE  
GENERATED BY MODULATING THE DYNAMO CURRENT SYSTEM FROM  
HF HEATING**

**K. Carroll and A. J. Ferraro  
Communications and Space Sciences Laboratory  
316 Electrical Engineering East  
The Pennsylvania State University  
University Park, PA 16802**

ELF/VLF signals have been successfully generated by modulating the dynamo current system using the high power heating facility of the Arecibo Observatory.

The source of the ELF/VLF radiation originates in the D and lower E regions of the ionosphere, and the electromagnetic energy is injected into the earth-ionosphere waveguide. This paper presents a theoretical analysis of the injection in order to predict ELF/VLF field strengths at ground-based receivers and compare the latitude dependence of the efficiency of injection. Results are presented for generation of ELF/VLF by heating facilities located in the polar, equatorial, and mid-latitudes.

Comparison with experiments conducted over the path of Arecibo to University Park, PA are presented.

## **GH-4-7**

### **AN IONIZATION DUCT EXPLANATION OF PLASMA-LINE OBSERVATIONS WITH A 46.8-MHZ RADAR**

D.B. Muldrew  
Communications Research Centre  
Department of Communications  
Ottawa, Ontario K2H 8S2

Recently published HF-enhanced plasma-line observations (Fejer et al., J. Geophys. Res., 88, 2083, 1983) using a 46.8-MHz radar show that the upshifted decay line is absent. The upshifted spectrum consists of a single line ('growing line') within a few hertz of 51.9 MHz (46.8 MHz plus the heating wave frequency of 5.1 MHz). The downshifted line is obscured by interference. Fejer et al. explain their observations by considering Langmuir wave propagation in the electron density depression generated by the ponderomotive force of the heating wave near reflection. Another approach is to consider Langmuir wave propagation in magnetic field-aligned ionization ducts which are generated by the HF heating wave. This latter approach appears to yield a more satisfactory explanation of the observations.

## URSI COMMISSION H - SESSION H1

**Active Experiments  
Using Space Vehicles I**

8:30 - 12:00  
LAW 169

**Expériences actives  
avec des véhicules spatiaux I**

Chairperson/Président: **B.A. Whalen**, National Research Council of Canada, Ottawa, ON

- 1 (8:40) WISP/HF: THE NEXT GENERATION OF ACTIVE HIGH-FREQUENCY EXPERIMENTS INSIDE THE IONOSPHERE. **H.G. James**, Department of Communications, Communications Research Centre, Ottawa, ON; **C.H. Hersom**, Canadian Astronautics Limited, Ottawa, ON
- 2 (9:20) PROPAGATION OF SHEATH-WAVES ALONG A LINEAR ANTENNA IMMERSSED IN A PLASMA. **M. Le Blanc**, **M. Nachman**, **S. Prevost**, École Polytechnique of Montreal, Dept. of Electrical Engineering, Montreal, PQ
- 3 (9:40) SHEATH WAVES ON VERY LONG ANTENNAS IN PLASMA. **G.A. Morin**, **K.G. Balmain**, University of Toronto, Dept. of Electrical Engineering, Toronto, ON
- 4 (10:00) SHEATH WAVES ON AN INFINITE METAL PLATE IN A WARM PLASMA. **M.M. Reeves**, **K.G. Balmain**, **G.A. Morin**, University of Toronto, Dept. of Electrical Engineering, Toronto, ON
- 5 (10:20) LOW-FREQUENCY SHEATH ADMITTANCE OF A SPHERE IN A COLLISIONLESS PLASMA. **R. Godard**, Royal Military College of Canada, Kingston, ON; **J.G. Laframboise**, York University, Physics Department and Centre for Research in Experimental Space Science, Toronto, ON
- 6 (10:40) NUMERICAL SIMULATION OF TIME-DEPENDENT SHEATH AROUND ELECTRODES IN COLLISIONLESS PLASMA. **A.C. Calder**, **J.G. Laframboise**, York University, Centre for Research in Experimental Space Science and Physics Dept., Toronto, ON
- 7 (11:00) NONLINEAR BEHAVIOR OF THE WISP ANTENNA. **R.R.J. Gagné**, Laval University, Dept. of Electrical Engineering, Québec, PQ
- 8 (11:20) VELOCITY SPACE PLASMA INSTABILITIES EXCITED BY BARIUM RELEASES FROM CRRES. **M.B. Pongratz**, Los Alamos National Laboratory, Space Plasma Group, Los Alamos, CA, USA

## H-1-1

### WISP/HF: THE NEXT GENERATION OF ACTIVE HIGH-FREQUENCY EXPERIMENTS INSIDE THE IONOSPHERE

H.G. James  
Communications Research Centre  
Department of Communications  
Ottawa, Ontario K2H 8S2

C.H. Hersom  
Canadian Astronautics Limited  
1050 Morrison Drive  
Ottawa, Ontario K2H 8K7

The scientific requirements of the Waves-In-Space-Plasmas (WISP) experiment (R.W. Fredricks, Plenary Session paper, this meeting) have inspired a number of novel features in the WISP High Frequency Sounder System (HFSS). In response to a need for coherence, flexibility and agility in the frequency domain, the instrument's transmitter has two phase-locked-loop frequency synthesizers. These also allow two-frequency transmissions. The measurement of the direction of arrival of electromagnetic waves in sounding or radar experiments and of the wave number of electrostatic waves will be achieved by the doppler detection capability of the receiver. To permit the study of the onset of plasma nonlinearities, the transmitter's pulse shape and power output are variable. A widely perceived need for improved understanding of radiation and propagation throughout all scale lengths has led to the bistatic geometry: the transmitter on the Shuttle will be synchronized with a receiver on a subsatellite. As befits a plasma laboratory in space, human direction of experiments is planned in real time. Adjustment by the Shuttle crew of the HFSS operating frequency, typically when it is based on the local plasma frequency, will be made following on-board display of swept-frequency data. Shuttle crew and scientists on the ground also will have the option of interrupting and redirecting experiments in response to unanticipated opportunities. Faced with an ongoing requirement for a series of missions with evolving scientific goals, WISP designers have implemented a digitally controlled HFSS coordinated by programmable microprocessors.

## PROPAGATION OF SHEATH-WAVES ALONG A LINEAR ANTENNA IMMERSIED IN A PLASMA

MARIO LE BLANC, MANFRED NACHMAN\* AND SYLVAIN PREVOST

Dept. of Electrical Engineering, Ecole Polytechnique of Montreal

ABSTRACT: A conductor immersed in a plasma is surrounded by an electron-depleted sheath, separating it from the plasma. Due to the presence of the sheath, guided surface waves (so-called sheath-waves) may exist along a cylindrical antenna in a plasma. For an antenna of finite length ( $L$ ) a standing-wave pattern results, leading to a family of resonances in the reflection coefficient versus frequency plot (J. Marec and G. Mourier, C.R. Acad. Sci. Paris, 271, 367-3070, 1970).

A detailed experimental study of these resonances at frequencies below the plasma frequency is presented here for a short cylindrical antenna immersed in an isotropic argon plasma. The antenna consisted of the extension of the inner conductor of a coaxial cable. D.C. potentials could be applied independently to the antenna and the outer conductor. The reflection coefficient ( $\Gamma$ ) of the antenna was measured over a frequency range extending from  $10^9$  to  $8 \times 10^9$  Hz and its admittance was computed from the experimental values of  $\Gamma$ .

The effect on the resonance frequencies of plasma density and antenna bias and radius were investigated for two different antenna lengths. An increase in plasma density or antenna bias, or a reduction in antenna radius resulted in a shift of the resonances towards higher frequencies. From the data on the resonance frequencies the dispersion curve of the sheath-waves could be obtained.

Several configurations of the transmission line to antenna transition were studied and an impedance transformer insuring optimum R.F.-energy coupling to the sheath-waves was designed. Experiments with a dielectric-coated antenna yielded results similar to those of a negatively biased monopole, however the positions of the resonances were less sensitive to changes in antenna-bias.

Our data are in good agreement with those derived from the dispersion equation for sheath-waves (P. Meyer et al., J. Appl. Phys., 45, 700-706, 1974). By fitting the experimental points with the theoretical curves representing the dependence of the resonance frequencies on sheath radius, the sheath thickness could be determined.

-----  
\* Author to whom correspondence should be addressed.

## H-1-3

### SHEATH WAVES ON VERY LONG ANTENNAS IN PLASMA

Gilbert A. Morin, Keith G. Balmain,  
Dept. of Electrical Engineering, Univ. of Toronto,  
Toronto, Ontario, Canada.

A wire immersed in an ionized-gas plasma is surrounded by an ion sheath which can carry waves called "sheath waves" at frequencies under the electron plasma frequency (J.J. Marec, G. Mourier, C.R. Aca. Sc. Paris, t. 271, pp 367-70, 10 aout 1970, Serie B). Due to their expected importance to the WISP/HF Space Shuttle experiment, we have studied these waves in a 20 litre plasma chamber. For dc bias less than floating potential, the wave attenuation was found to be small enough so that very long wires could be used to observe reflections off the end of the wire. The dispersion relation of the sheath waves was obtained from the measurements and the losses were estimated. Because of the limited size of the laboratory plasma, helical antennas were used to fit more wire into the available space. Since sheath waves are non-radiative and their fields do not extend farther than few Debye lengths from the wire surface, a helix behaves essentially as a straight wire.

It was found that sheath wave losses increased strongly with positively increasing dc bias. One loss mechanism is surface absorption of the electrons by the wire (M.M. Reeves et al., to be presented at this meeting). Using hydrodynamic theory these losses have been calculated and comparison was made with our measurements. In order to be able to estimate the effects of sheath waves on more complex structures, a cold plasma model with a lossy sheath was used in a general purpose antenna program (J.H. Richmond, Ohio State Univ., NASA report CR-2396, 1974). The results compare well with experiments and show the usefulness of this approach.

In order to increase our understanding of sheath wave losses, two other antenna structures were studied. A glass-coated wire was found to behave in the same way as a bare wire with high negative bias, which supports the validity of the vacuum sheath model often used in this case. Also, sheath-wave effects were observed readily in helical antennas which were wound so tightly as to exclude plasma from the interior of the helix.

## SHEATH WAVES ON AN INFINITE METAL PLATE IN A WARM PLASMA

Margarida M. Reeves, Keith G. Balmain, and Gilbert A. Morin  
Dept. of Electrical Engineering, Univ. of Toronto  
Toronto, Ontario, Canada

A better understanding of the radio-frequency behaviour of long antennas in plasma is required for the planned WISP/HF Space Shuttle experiment. For the case in which the cylindrical dipole antenna in that experiment has a radius appreciably greater than a Debye length, some aspects of wave propagation along the antenna may be studied by assuming the metal antenna surface to be a flat plate. Adjacent to the metal plate is the ion sheath, an electron-depleted region a few Debye lengths thick, and trapped waves which are essentially confined to the sheath region can propagate at frequencies below the electron plasma frequency. The propagation of these sheath waves, especially on wires, has been studied (for example, P. Meyer et al., Jour. Appl. Phys., Vol.45, 1974, pp.700-706), and non-collisional sheath losses have been studied insofar as their effects on short antennas are concerned (N. Meyer-Vernet, Doctoral thesis, University of Paris VII, France, 1976). Little is known about the attenuation of sheath waves, especially that part of the total attenuation which must be caused by charged-particle absorption at the metal surface.

In order to investigate this aspect of sheath-wave propagation, an analytical model was developed using hydrodynamic theory. The sheath region was modelled as a warm plasma with a uniform density considerably lower than the homogeneous surrounding plasma. At the interface between the two regions--sheath and surrounding plasma--continuity of electric and magnetic fields, continuity of particle flux and continuity of power flux were imposed, implying that there will be no charge accumulation and no power dissipation at the interface. At the metal-to-sheath boundary, the continuity of electric and magnetic fields and an absorptive boundary condition were used. A dispersion relation was developed, from which the values for the propagation and attenuation constants were obtained. It was found that, for frequencies below plasma frequency, as frequency increases both propagation and attenuation constants increase. For frequencies above plasma frequency the propagation constant approaches the electron-acoustic wave value and the attenuation drops rapidly after reaching a maximum just below the plasma frequency. An increase in sheath plasma density caused a pronounced increase in the attenuation. As the metal-surface absorption coefficient was increased from zero to one the attenuation increased considerably, showing that the surface absorption of electrons by the metal plate is the main loss mechanism in this model. The collision frequency contributed little to the attenuation constant, in comparison with the surface absorption. However, the collision frequency effect became more noticeable for a sheath plasma with a low density. It was also found that as sheath thickness is varied the propagation constant shifted in accordance with measurement (see G.A. Morin and K.G. Balmain, paper presented at this meeting).

## H-1-5

### LOW-FREQUENCY SHEATH ADMITTANCE OF A SPHERE IN A COLLISIONLESS PLASMA

R. Godard<sup>+</sup> and J.G. Laframboise\*

<sup>+</sup>Royal Military College of Canada, Kingston, Ontario K7L 2W3

\*Physics Department and Centre for Research in Experimental Space  
Science, York University, Toronto, Canada M3J 1P3

A systematic theoretical study of the low-frequency sheath admittance of a spherical electrode immersed in a collisionless, nonflowing, Maxwellian plasma with no magnetic field is done for the following ranges of plasma parameters: nondimensional electrode DC bias potential  $-25 \leq e\phi_p/kT_e \leq 25$ , ion to electron temperature ratio  $0 \leq T_i/T_e \leq 1$ , electrode radius to Debye length ratio  $0 \leq r_p/\lambda_D \leq 200$ . A surprising feature of the results is the existence of double and triple peaks in the sheath capacitance as a function of DC bias potential at certain values of  $r_p/\lambda_D$ . The sheath capacitance also shows discontinuous behaviour when the DC bias passes through space potential, suggesting a method for measuring space potential.

NUMERICAL SIMULATION OF TIME-DEPENDENT  
SHEATH AROUND ELECTRODES IN COLLISIONLESS PLASMA

A.C. Calder and J.G. Laframboise  
Centre for Research in Experimental Space Science  
and Physics Department, York University, Toronto, Canada

We have developed a computer code for the simulation of spherical or cylindrical RF electrodes in isotropic collisionless plasmas. The velocity distribution of the plasma surrounding the electrode is approximated by a multiple water bag distribution. The instantaneous response of the plasma to a sinusoidal potential applied to the electrode is calculated in the electrostatic approximation. Transient and nonlinear effects can be modelled in this way. Data produced by the code include the instantaneous particle flux and electric field at the electrode surface, from which the RF admittance is calculated. We present model current and admittance characteristics in the frequency range  $0.1\omega_{pe}$  to  $2\omega_{pe}$  for spherical electrodes of radius 5 and  $10\lambda_D$ . Comparison is made between small signal cases (RF amplitude  $0.1kT/e$ ) and large signal cases (RF amplitude 2 or  $3kT/e$ ). Negative conductance is seen in some cases.

We have also undertaken modifications of this code to model constant current RF signals as well as constant voltage RF signals. Preliminary results from this work will be discussed.

## H-1-7

### NONLINEAR BEHAVIOR OF THE WISP ANTENNA

Réal R. J. Gagné,  
Elect. Eng. Dept., Laval University, Québec, Qué., Canada.

The behavior of the antenna during the Waves In Space Plasma experiment raises several questions, one of which is the problem of nonlinearity. Although amplitude and phase of the voltage and current at the input of each feed line (one for each arm) will be monitored and that the two waveforms will be sampled at  $v-l-f$ , these measurements, as will be shown, will not be easy to interpret if significant nonlinearity exists.

For frequencies below the plasma frequency, the ionospheric plasma will appear resistive. Also, each arm of the antenna will behave like a cylindrical diode where the arm is the anode and the plasma is the cathode. During transmission, for a voltage larger than the break-point voltage, the junction will present a low impedance during the positive half cycle of the waveform and a high impedance during the negative half cycle. The issuing consequences can be illustrated by considering a length of transmission line which is driven by a sine-wave generator and terminated by an ideal diode. The diode will present a short circuit during the positive part of the incident voltage waveform and an open circuit during the negative part. As a result, both the voltage waveform and the current waveform at the input of the line will differ from that at the output, and the lack of similitude will be severe if the line is not electrically short at the applied frequency. A situation similar to that which has just been discussed exists not only with respect to the feed line but, also, with respect to the antenna itself. In effect, considering that each arm behaves like a cylindrical diode and also has transmission line properties, the current waveform and the voltage waveform observed at the input of each arm will not be easily related to the current and the voltage waveforms existing along the arm. The overall situation is further complicated by the fact that currents will circulate, through the conductive plasma, from one arm of the antenna to the other and from the arms to the shuttle surface where nonlinear effects and charging of the non-conductive surfaces (insulating tiles) will also occur.

It is realized that current and voltage waveforms, even if observed directly at the antenna terminals, will not yield easily interpretable information if nonlinearity significantly affects these waveforms. Clearly, a study is needed to at least establish the relative importance of the nonlinear effects with respect to the linear properties of the antenna. A study applicable at low frequencies, where all dimensions would be negligible with respect to wavelength, would yield such an information.

VELOCITY SPACE PLASMA INSTABILITIES EXCITED BY  
BARIUM RELEASES FROM CRRES

Morris B. Pongratz  
Space Plasma Physics Group, ESS-8  
Los Alamos National Laboratory, MS D438  
Los Alamos, New Mexico 87545

The NASA-sponsored CRRES (Combined Release and Radiation Effects Satellite) mission provides an opportunity to study fundamental plasma instability processes using space as a laboratory without walls. Thermite barium releases at orbital velocity result in barium ion velocity space distributions with free energy available for conversion to wave energy. These distributions vary from unmagnetized counterstreaming beams to ring-shaped configurations with positive  $df/dv$ . The wave modes amplified by these unstable distributions vary in frequency from  $\omega_{ci}$  to the lower hybrid resonance frequency. They are generally electrostatic but some electromagnetic modes may grow close to the release at early times when the kinetic beta exceeds unity. Diagnostics onboard the CRRES vehicle will permit in situ measurement of relevant plasma and wave parameters. Remote optical, HF and VHF measurements can be planned over special ground-based facilities not normally accessible to sounding rockets. This paper will present configuration- and velocity-space distributions of barium ions as a function of time and space following a CRRES release from low earth orbit. The effects of collisions, photoionization, magnetic mirror force and gravity will be presented. Growth rates and wavelength of maximum growth for the various waves will also be discussed.



## URSI COMMISSION H - SESSION H2

**Active Experiments  
Using Space Vehicles II**

1:30 - 5:00  
LAW 169

**Expériences actives  
avec des véhicules spatiaux II**

Chairperson/Président: **K.J. Harker**, Stanford University, Stanford, CA, USA

- 1 (1:40) BEAM-PLASMA INTERACTIONS - LABORATORY EXPERIMENTS AND THEORY. **W. Bernstein**, Rice University, Dept. of Space Physics and Astronomy, Houston, TX, USA; **A. Konradi**, NASA/Johnson Space Center, Solar System Exploration Division, Houston, TX, USA
- 2 (2:20) RESPONSE OF IONOSPHERIC PLASMA AND ATMOSPHERE TO ELECTRON AND PLASMA BEAM INJECTION IN SEPAC/SPACELAB 1. **T. Obayashi**, **N. Kawashima**, **S. Sasaki**, **M. Yanagisawa**, **K. Kuriki**, The Institute of Space & Astronautical Science, Tokyo, Japan
- 3 (2:40) SOUNDER-ACCELERATED IONS OBSERVED ON ISIS-2. **H.G. James**, Department of Communications, Communications Research Centre, Ottawa, ON
- 4 (3:00) PERTURBATIONS OF THE IONOSPHERE BY AN ARGON ION BEAM. **L.J. Cahill Jr.**, University of Minnesota, School of Physics and Astronomy, Minneapolis, MN, USA; **R.L. Arnoldy**, University of New Hampshire, Dept. of Physics, Durham, NH, USA
- 5 (3:20) PLASMA DEPLETION IN IONOSPHERIC MODIFICATION EXPERIMENTS. **A.W. Yau**, **B.A. Whalen**, National Research Council of Canada, Herzberg Institute of Astrophysics, Ottawa, ON
- 6 (3:40) WATERHOLE, AURORA MODIFICATION EXPERIMENTS. **B.A. Whalen**, **A.W. Yau**, National Research Council of Canada, Herzberg Institute of Astrophysics, Ottawa, ON; **M.B. Pongratz**, Los Alamos National Laboratory, Los Alamos, NM, USA
- 7 (4:00) OPTICAL OBSERVATIONS OF THE AMPTE ION RELEASES FROM NEW MEXICO. **P.A. Bernhardt**, **M.B. Pongratz**, **J.H. Wolcott**, **R.A. Rousell-Dupre**, Los Alamos National Laboratory, Earth and Space Sciences Division, Los Alamos, NM, USA; **D.E. Beatty**, **R.C. Ramsey**, **R.L. Ireland**, MIT Lincoln Laboratory, Space Surveillance Group, Stallion Range Center, Socorro, NM, USA
- 8 (4:20) EMISSIONS FROM ATOMIC OXYGEN STIMULATED BY CHEMICAL RELEASES INTO THE IONOSPHERE. **P.A. Bernhardt**, Los Alamos National Laboratory, Earth and Space Sciences Division, Los Alamos, NM, USA

## H-2-1

### BEAM-PLASMA INTERACTIONS - LABORATORY EXPERIMENTS AND THEORY

W. Bernstein  
Dept. of Space Physics and Astronomy  
Rice University  
Houston, TX 77251 U.S.A.

A. Konradi  
Solar System Exploration Division  
NASA/Johnson Space Center  
Houston, TX 77058 U.S.A.

This talk will describe several laboratory experiments and supporting theory intended to provide a good physical understanding of the behavior of energetic electron beams injected into the ionosphere-atmosphere system. Among the subjects to be discussed are:

- 1) The convective and/or absolute nature of the interaction and, in particular, the occurrence of the absolute instability when the plasma frequency exceeds the cyclotron frequency.
- 2) The threshold nature of the absolute instability as manifested in a critical beam current, neutral density, magnetic field strength, and pathlength to provide empirical scaling laws for different experimental conditions.
- 3) Signatures of the interaction, including severe energy diffusion of beam electrons, but without significant pitch angle scattering, heating of ambient electrons, production of superthermal electrons, and the generation of intense Langmuir waves.
- 4) Conditions for ignition of the beam plasma discharge (BPD) and its steady state characteristics.

The relevance of these results to the flight experiments will be discussed.

RESPONSE OF IONOSPHERIC PLASMA AND ATMOSPHERE TO ELECTRON AND  
PLASMA BEAM INJECTION IN SEPAC/SPACELAB 1

T.Obayashi, N. Kawashima, S. Sasaki, M. Yanagisawa  
and K. Kuriki  
The Institute of Space & Astronautical Science  
Tokyo, Japan

Spacelab-1 SEPAC electron beam and plasma beam injection experiment was performed from November 30 to December 6, 1983. Electron beam up to 5 keV and 0.3 A and MPD arcjet plasma were injected into the ionosphere along the orbit of an inclination of 57. Diagnostics were plasma probes(Langmuir probe and floating probe), wave detectors(HF/VLF), electron energy analyser, photometer, vacuum gauge and high sensitivity TV camera. The shuttle charge-up due to the electron beam emission were detected by Langmuir probe, floating probe and energy analyser. The shuttle charge-up shows a strong dependence on the shuttle attitude with respect to the velocity vector. it has been revealed that not only the surface of the main nozzles(largest conductive surface on the shuttle) but also a cluster of small conductive segments over the payload bay are effective for the collection of the returning electrons from the ionospheric plasma. when the charge-up of the shuttle is large. The charge-up neutralization experiment using MPD arcjet was successfully performed and the dependence of the charge-up neutralization effect on various experimental parameters has been studied. A strong wave emission associated with the vehicle charging and the charge-up neutralization was also observed in VLF range and HF range. An anomalous increase of ambient plasma density was observed associated with a neutral gas ejection experiment and its relationship with critical ionization velocity phenomena will be discussed.

## H-2-3

### SOUNDER-ACCELERATED IONS OBSERVED ON ISIS-2

H.G. James  
Communications Research Centre  
Department of Communications  
Ottawa, Ontario K2H 8S2

Fluxes of ions with energies up to about 100 eV have been widely observed with the Soft Particle Spectrometer (SPS) on the ISIS-2 spacecraft. This energization is attributed to the negative potential induced on the spacecraft body by the rf pulses from the topside sounder, operating between 0.1 and 20 MHz. When the 3-rpm spin vector of the spacecraft is nearly perpendicular to the satellite's orbital plane, the SPS samples a wide range of  $\alpha$ , the angle between the SPS axis and the flow velocity (wake) direction. At the highest observed ion energies, the SPS detects ions only near  $\alpha = 0^\circ$  for a given energy. The  $\alpha$ -peak is narrower when the oxygen density in the ambient plasma is much greater than the hydrogen density. For decreasing ion energies, ions are detected in increasingly wider ranges of  $\alpha$ . At the lowest energies with  $O^+$  dominant, peaks are obtained at  $\alpha$  near both  $0^\circ$  and  $180^\circ$ ; with  $H^+$  dominant, the  $\alpha$ -distribution is uniformly spread with a rather flat upper limit of flux. The form of the  $\alpha$ -distributions suggests that ions are subject to a quasi-central force field on the front side of the spacecraft, but that they enter the SPS from a turbulent region inside a Mach cone on the wake side.

## PERTURBATIONS OF THE IONOSPHERE BY AN ARGON ION BEAM

L.J. Cahill, Jr.

School of Physics and Astronomy, University of Minnesota

R.L. Arnoldy

Physics Department, University of New Hampshire

Two argon ion beam flights have been made in the auroral ionosphere. The argon beam carried a current of argon ions of order 100 ma with beam energy of order 30 volts. The results of the flights were quite different. In the first flight over a weak intermittent aurora, strong effects on electrons were noted. In this flight the gun remained attached to the main diagnostic payload. Two new populations of electrons appeared with each gun operation: 1) an isotropic population with peak energy near 400 eV 2) a field aligned population below 100eV. Intense wave generation accompanied each gun operation. Broad band noise .1 to 6 kHz was observed as well as broad band noise 1-10 MHz. In the second flight over several bright auroral arcs, the electron effects were less apparent. Argon ions were detected several hundred meters from the gun. An intense band of waves at 6 to 7 kHz was observed during gun operations where the gun has separated from the main payload. After the first gun operation several narrow lines were noted, independent of gun operation, in the range .1 to 3 kHz.

## H-2-5

### PLASMA DEPLETION IN IONOSPHERIC MODIFICATION EXPERIMENTS

A.W. Yau and B.A. Whalen  
Herzberg Institute of Astrophysics  
National Research Council of Canada  
Ottawa, Ontario K1A 0R6 Canada

In ionospheric depletion experiments where chemically reactive vapors such as water and carbon dioxide are injected into the F-region to accelerate the plasma recombination rate and to reduce the plasma density, the ion composition in the depleted region is modified and photometric emissions are produced. In this paper, we compare in-situ ion composition, density and photometric observations from a number of ionospheric depletion experiments with predictions from model simulations. We discuss the implications of our observational and simulation results on current concepts of ionospheric depletion experiments.

**WATERHOLE, AURORA MODIFICATION EXPERIMENTS**

B.A. Whalen, A.W. Yau  
Herzberg Institute of Astrophysics  
National Research Council of Canada  
Ottawa, Ontario K1A 0R6 Canada

M.B. Pongratz  
Los Alamos National Laboratory  
Los Alamos, NM 87545 U.S.A.

A series of perturbation experiments in which "holes" were created in the F region ionosphere by explosive releases of large quantities of water vapour, have been conducted to test theories of the electrodynamic structure of auroral arcs. The water vapour releases created large (~50 km diameter) "holes" in the ionosphere in and near structured pre-midnight auroral arcs. It was anticipated that these "holes" would interrupt or perturb the ionospheric current systems associated with the arcs and that this perturbation would in turn affect the acceleration mechanism responsible for the aurora. Results from the successful rocket flights are presented and it is shown that significant modifications of the energetic electron precipitation patterns were induced by all releases. Various models and theories for the perturbation mechanism will be discussed.

OPTICAL OBSERVATIONS OF THE AMPTE ION  
RELEASES FROM NEW MEXICO

P.A. Bernhardt, M.B. Pongratz, J.H. Wolcott, R.A. Roussel-Dupre  
Earth and Space Sciences Division  
Los Alamos National Observatory, Los Alamos, NM 87545

D.E. Beatty, R.C. Ramsey, R.L. Ireland  
Space Surveillance Group, MIT Lincoln Laboratory  
Stallion Range Center, Socorro, NM 87801

In support of the Active Magnetospheric Particle Tracer Explorer (AMPTE) program, high-resolution, low-light-level optical stations were operated at three widely separated locations in New Mexico. The releases occurred at geocentric distances of 12 to 18 earth radii. Long-focal-length tracking telescopes were used in conjunction with intensified, filtered cameras to trace the motion of the barium, lithium, and europium expelled from the AMPTE Ion Release Module (IRM). The optical stations were located at Los Alamos National Laboratory, at the MIT/LL Experimental Test Site, and at the southern end of the White Sands Missile Range. The typical telescope had a 5 meter focal length with a 0.42 meter aperture, yielding a 0.5 degree field of view. Electrostatic and microchannel-plate intensifiers with gains between 1000 and 50,000 were mounted between the telescopes and the image recording instruments. Televisions were used for real time tracking of the events. Film and CCD image cameras provided permanent records for analysis. Narrow band interference filters were placed in front of the intensifiers to isolate the images of fluorescent neutral or ion species. Preliminary analysis of images from the barium release into the solar wind and from the barium or lithium/europium releases into the magnetotail will be presented.

EMISSIONS FROM ATOMIC OXYGEN STIMULATED  
BY CHEMICAL RELEASES INTO THE IONOSPHERE

Paul A. Bernhardt  
Atmospheric Sciences Group  
Earth and Space Sciences Division  
Los Alamos National Laboratory  
Los Alamos, NM 87545

Every chemical release which depletes the F-layer of ions and electrons produces an enhancement in airglow from atomic oxygen. During the ionospheric depletion process, the atomic oxygen ions and electrons in the ionosphere are combined to form monatomic oxygen atoms in electronically excited states. Depending on the substance released, the chemical reactions may involve ion-molecule charge exchange, positive- and negative-ion mutual neutralization, ion-electron recombination and/or electron attachment. Each of these processes subtract part of the energy from the final excited state of the oxygen atom. The airglow emission wavelength is an indication of the excited state of the oxygen and, consequently, provides information about the chemical reactions involved in the ionospheric depletion processes.

Examples of airglow stimulated by chemical releases are taken from experiments involving sounding rocket payloads, from rocket and shuttle exhaust vapors and from potential experiments involving the Combined Release and Radiation Effects Satellite (CRRES). The released species considered include  $H_2$ ,  $CO_2$ ,  $H_2O$  and  $SF_6$ . Each species produces a unique airglow signature at wavelengths ranging from ultraviolet (130.4 nm, 135.6 nm) through visible (553.5 nm, 630.0 nm) to near infrared (777.4 nm, 844.6 nm).



## URSI COMMISSION H - SESSION H3

**Wave-Induced Particle  
Precipitation Effects I**

8:30 - 12:00  
LAW 169

**Effets des précipitations  
de particules induites par  
des ondes I**

Chairperson/Président: **R.A. Goldberg**, NASA/Goddard Space Flight Center, Greenbelt, MA, USA

- 1 (8:40) WAVE INDUCED PARTICLE PRECIPITATION: AN OVERVIEW OF RECENT RESULTS. **U.S. Inan**, Stanford University, STAR Laboratory, Stanford, CA, USA
- 2 (9:20) THE SPECTRAL AND TEMPORAL CHARACTERISTICS OF RF RADIATION FROM LIGHTNING. **D.M. Le Vine**, Goddard Space Flight Center, Greenbelt, MD, USA
- 3 (9:40) IONOSPHERIC ELECTRIC FIELD MEASUREMENTS OF LIGHTNING SPHERICS AND ASSOCIATED WHISTLERS. **C.L. Siefring, M.C. Kelley**, Cornell University, School of Electrical Engineering, Ithaca, NY, USA
- 4 (10:00) THE PRECIPITATION OF RADIATION BELT ELECTRONS BY VLF TRANSMITTERS, BY PLASMASPHERIC HISS, AND BY LIGHTNING WHISTLERS. **W.L. Imhof, H.D. Voss, M. Walt, E.E. Gaines, J. Mobilia, D.W. Datlowe**, Lockheed Palo Alto Research Laboratory, Palo Alto, CA, USA
- 5 (10:20) SATELLITE OBSERVATION OF LIGHTNING-INDUCED ELECTRON PRECIPITATION. **H.D. Voss, W.L. Imhof, M. Walt, J. Mobilia, Y.T. Chiu, E.E. Gaines, D.W. Datlowe**, Lockheed Palo Alto Research Laboratory, Palo Alto, CA, USA
- 6 (10:40) DIRECT OBSERVATION OF MAGNETOSPHERIC ELECTRON PRECIPITATION STIMULATED BY LIGHTNING. **R.A. Goldberg, S.A. Curtis**, NASA/Goddard Space Flight Center, Laboratory for Extraterrestrial Physics, Greenbelt, MD, USA; **J.R. Barcus**, University of Denver, Dept. of Physics, Denver, CO, USA; **L.C. Hale**, Pennsylvania State University, Dept. of Electrical Engineering-CSSL, University Park, PA, USA
- 7 (11:00) WAVE-PARTICLE INTERACTIONS AND THE DETAILED STRUCTURE OF LIGHTNING INDUCED ELECTRON PRECIPITATION. **S.A. Curtis, R.A. Goldberg**, NASA/Goddard Space Flight Center, Laboratory for Extraterrestrial Physics, Greenbelt, MD, USA; **J.R. Barcus**, University of Denver, Dept. of Physics, Denver, CO, USA; **L.C. Hale**, Pennsylvania State University, Dept. of Electrical Engineering-CSSL, University Park, PA, USA

### WAVE INDUCED PARTICLE PRECIPITATION: AN OVERVIEW OF RECENT RESULTS

U. S. Inan  
STAR Lab, Stanford University, Stanford, CA

In recent years, the phenomenon of wave-induced precipitation of energetic radiation belt particles and its associated magnetospheric and ionospheric effects have received increased attention. The pitch angle scattering of the particles is believed to be a result of resonant interactions with various kinds of magnetospheric waves, including lightning-generated whistlers, spontaneous and triggered emissions and signals from man-made sources such as VLF transmitters and power lines. Recent experimental results include the direct satellite observation of electrons precipitated by man-made signals as well as whistlers, observations of subionospheric signal perturbations caused by whistler-induced precipitation, observations of correlations between microbursts and VLF chorus, detection of correlations between VLF emission bursts and photoemissions and X ray bursts, and associations between ELF/VLF emissions and ULF magnetic impulses. Theoretical modeling of the wave-induced scattering process has advanced to a point where detailed dynamic energy spectrum of precipitation flux induced by waves with known spectral characteristics can be estimated. Comparisons of theory and recent satellite observations have enabled us to calibrate our models so that they can be better applied to interpret experimental data. In this paper, we present a brief overview of the topic, including the characteristics of magnetospheric waves that are believed to interact with and precipitate the energetic particles, the highlights of recent experimental and theoretical results and future opportunities for advancing our understanding of the scattering mechanisms and its implications in terms of the dynamics of the radiation belt particles and the coupling of the ionosphere and the magnetosphere.

THE SPECTRAL AND TEMPORAL CHARACTERISTICS OF  
RF RADIATION FROM LIGHTNING

D. M. Le Vine  
Goddard Space Flight Center  
Greenbelt, Maryland 20771

A single lightning flash is a composite of many individual events each of which radiates over a wide band of frequencies from a few kilohertz to hundreds of MHz. Some of these events, such as return strokes, have been studied in detail, but most are discharges of an incompletely understood nature occurring within the cloud. Early research has shown that the spectrum of radiation from the composite of these events peaks near 10 kHz and then decays roughly as (frequency)<sup>-1</sup>. Recent research has focussed on identifying the spectrum of the individual events in the flash. The spectrum of return strokes also appears to peak near 10 kHz and to decay inversely with frequency, although some controversy exists regarding the high frequency behavior.

A review will be given of the temporal and spectral structure of radiation from lightning using examples from the author's measurements for illustration. Then it will be shown that many of the spectral characteristics of the radiation can be explained with a conventional transmission line model for the discharge (current pulse propagating along the channel) as long as channel tortuosity is taken into account.

## H-3-3

### IONOSPHERIC ELECTRIC FIELD MEASUREMENTS OF LIGHTNING SPHERICS AND ASSOCIATED WHISTLERS

C. L. Siefring and M. C. Kelley  
School of Electrical Engineering  
Cornell University, Ithaca, New York 14850

On August 9, 1981 two sounding rockets performed simultaneous electric field measurements over an active nighttime thunderstorm. One rocket made measurements on the ionosphere (apogee 154 km) and the other rocket made measurements in the mesosphere (apogee 89 km). No whistlers were detected by the instruments on the mesospheric payload although numerous whistlers were detected by the ionospheric payload. It is considered normal for unducted whistlers to be detected above but not below the ionosphere. However, similarities between ducted whistlers detected at Palma, Anartica (Carpenter, private communication 1983) just minutes before the rocket launches, indicate these whistlers are indeed ducted events.

In this experiment we can directly compare the electric field intensity of a lightning spheric (in the ionosphere) to that of the whistler it creates. Furthermore, we can do this at virtually the same altitude and (therefore) in virtually the same plasma conditions. Such a comparison reveals that the signal strengths are similar (often within ten db over the entire frequency range) even though the whistler wave packet has travelled some 30,000 km. A crude path loss model indicates that a 30-40 db amplification has occurred along the path.

It is also possible to compare the amplitude of the lightning induced VLF with the VLF signals from the Annapolis (NAA) transmitter. In the ionosphere, the NAA transmitter signal had an amplitude of  $\sim 1$  mV/m while the lightning induced VLF (spherics) varied greatly in amplitude from 1-10 mV/m over the frequency range below 24 KHz. This and the fact that stimulated emissions were associated with the returning whistlers strongly indicates that particle precipitation was induced by these events.

These whistler and spheric observations suggest a new model for the generation of whistlers in situ above a thunderstorm cell. The interpretation we present here is that the area of the ionosphere above an active thunderstorm can be viewed as an aperture antenna. The spatial and temporal variations in the electric field on the aperture are prescribed by the penetrating transient electric fields from the lightning discharges. This antenna generates waves which propagate in the whistler mode with a variety of wave normal angles. If a duct is illuminated at the base of the protonosphere it will trap some of the energy, guide it to the other hemisphere and provide a return path for the signal. The returning signal is in the whistler mode and hence, due to its relatively short wavelength, will not be readily transmitted across the base of the ionosphere.

THE PRECIPITATION OF RADIATION BELT ELECTRONS  
BY VLF TRANSMITTERS, BY PLASMASPHERIC HISS,  
AND BY LIGHTNING WHISTLERS

W. L. Imhof, H. D. Voss, M. Walt, E. E. Gaines, J. Mobilia,  
and D. W. Datlowe

Lockheed Palo Alto Research Laboratory  
Palo Alto, California 94304

The frequency of occurrence of the various processes by which VLF waves precipitate geomagnetic electrons can be studied by the characteristic energy spectra of the precipitated electrons. In the inner radiation belt and the slot region it has been clearly demonstrated that ground-based transmitters precipitate electrons with narrowly peaked spectra, and that the energy of the peaks decreases rapidly with increasing L. In the slot region electrons are often precipitated by wave bands associated with plasmaspheric hiss and lightning whistlers. The resulting energy spectra of the precipitated electrons have broad peaks with a similar L-dependence to those associated with transmitters. Using data from electron spectrometers on two low altitude satellites, we will show spectra attributed to each of these processes. The data provide a measure of the relative importance of the various loss mechanisms as a function of L, local time and geomagnetic activity.

## H-3-5

### SATELLITE OBSERVATION OF LIGHTNING-INDUCED ELECTRON PRECIPITATION

H. D. Voss, W. L. Imhof, M. Walt, J. Mobilia, Y. T. Chiu,  
E. E. Gaines, and D. W. Datlowe  
Lockheed Palo Alto Research Laboratory  
Palo Alto, California 94304

Energetic electron precipitation bursts ( $100 \leq E \leq 1000$  keV) from the earth's radiation belts have been observed with the low-altitude S81-1 satellite in association with terrestrial lightning flashes. The measured energy deposition ( $\sim 10^{-3}$  ergs  $\text{cm}^{-2}$ ) of a single Lightning-induced Electron Precipitation (LEP) burst represents a reduction of 0.01 - .001% of the radiation belt population at  $L = 2.3$  in the region covered by the burst magnetic field lines. A strong correlation is found between thunderstorm lightning flash events observed with the S81-1 391.4 nm photometer and the LEP bursts. A one-to-one correlation is found between whistlers observed at Palmer, Antarctica and LEP bursts observed on the satellite. In one case, a precipitation-induced subionospheric VLF signal perturbation observed at Palmer is correlated with an LEP event observed 2000 km away in longitude at the S81-1 satellite (Voss et al., Nature, 312, 740-742, 1984).

Whistler waves (1-6 kHz) that undergo cyclotron resonance with radiation-belt electrons are believed to cause the first electron precipitation pulse of the LEP event. This pulse has a broadly peaked energy spectrum ( $100 < E < 200$  keV at  $L = 2.3$ ) and at 200 km altitude a narrow pitch angle distribution near  $90^\circ$ . Subsequent reflections and backscatterings in the northern and southern hemisphere produce a train of pulses ( $\sim 320$  ms period) of diminishing intensity which make up the individual LEP event.

The observed LEP peak resonance energies decrease with increasing  $L$  consistent with the variation in the equatorial cold plasma density in accordance with cyclotron resonance as well as the radiation-belt spectra. A study of the latitude variation of LEP events over North America indicates a maximum occurrence frequency near  $L = 2.3$  with a rather sharp equatorward cutoff at  $L = 2$ . This  $L$ -shell region of frequently observed LEP burst is found to be similar to the radiation belt slot region, the midlatitude electron zone and the region of efficient VLF transmitter-induced electron precipitation.

In addition to the satellite observation of optical lightning flashes and LEP bursts in the vicinity of thunderstorms the satellite plasma probe also observed associated F-region irregularities, TID variations ( $\lambda \sim 200$  km) and transient displacement currents that are thought to be induced by the transient lightning-induced electromagnetic electric field. The lightning associated transient electric fields are observed to have rise times faster than the instrument resolution of 64 msec and recovery times of several seconds.

DIRECT OBSERVATION OF MAGNETOSPHERIC ELECTRON PRECIPITATION  
STIMULATED BY LIGHTNINGR. A. Goldberg<sup>1</sup>, J. R. Barcus<sup>2</sup>, L. C. Hale<sup>3</sup>, and S. A. Curtis<sup>1</sup><sup>1</sup>Laboratory for Extraterrestrial Physics, NASA/Goddard Space Flight Center, Greenbelt, Maryland 20771, USA<sup>2</sup>Department of Physics, University of Denver, Denver, Colorado 80208, USA<sup>3</sup>Department of Electrical Engineering-CSSL, The Pennsylvania State University, University Park, Pennsylvania 16802, USA

Magnetospheric electron precipitation stimulated by observed lightning flashes has been studied using rocket techniques. Simultaneous effects caused by the NSS VLF transmitter in Annapolis, Maryland were measured during the same experiment. The observations were conducted aboard a Nike Orion Rocket flight (NASA 31.042) launched from Wallops Island, Virginia, on August 23, 1984 at 0911 UT. The payload, which was released for a parachute-borne descent near 100 km apogee, carried instrumentation to detect electrons, x-rays, electric fields, and VLF signals caused by lightning and/or the VLF transmitter. Payload aspect was monitored with a three axis magnetometer. The payload was launched during a period when thunderstorms were in progress over an extensive area covering the coastal regions of Virginia and North Carolina. Several lightning flashes have been identified during the first 50 seconds following deployment, at which time the payload was located above 90 km in the domain where energetic electrons could arrive with minimal atmospheric absorption. The first and strongest of the flashes was also observed by the East Coast Lightning Detection Network, which established it to be a cloud-to-ground stroke at 236.4 km range and 166.3 degrees south-east of Wallops Island. A sequence of electron pulses was observed to occur following each identified lightning flash. Electrons with energy thresholds of >40 and >135 keV were independently measured with Geiger tube and x-ray scintillator detectors, permitting comparison of measured delay times for the first pulse arrival with those expected theoretically in both energy ranges. Good agreement is found if ion-cyclotron resonance conditions were met near the magnetic equator. The NSS VLF transmitter was also operating in a pulsed mode (3 seconds "on," 2 seconds "off") during the first 9 minutes of the flight, when the payload was above 40 km. Using superposed epoch analysis, x-ray data show the occurrence of weak electron precipitations associated with the transmitter at lower energies than those associated with lightning. This is not unexpected since the NSS frequency (21.4 kHz) is well above that for the predominant VLF spectral peaks of lightning (<10 kHz).

## H-3-7

### WAVE-PARTICLE INTERACTIONS AND THE DETAILED STRUCTURE OF LIGHTNING INDUCED ELECTRON PRECIPITATION

S. A. Curtis<sup>1</sup>, R. A. Goldberg<sup>1</sup>, J. R. Barcus<sup>2</sup>, and L. C. Hale<sup>3</sup>

<sup>1</sup>Laboratory for Extraterrestrial Physics, NASA/Goddard Space Flight Center, Greenbelt, Maryland 20771, USA

<sup>2</sup>Department of Physics, University of Denver, Denver, Colorado 80208, USA

<sup>3</sup>Department of Electrical Engineering-CSSL, The Pennsylvania State University, University Park, Pennsylvania 16802, USA

A detailed study of the magnetospheric electron precipitation stimulated by observed lightning flashes, as recorded by a Nike Orion rocket flight launched from Wallops Island, Virginia on August 23, 1984 at 0911 UT, has been performed. This study has revealed a periodic structure in the electron precipitation flux through the use of fast-fourier transform filtering of the data. Specifically, the first precipitation peak occurred at a time delay after the observed lightning-induced spheric, equal to the computed whistler propagation time to the magnetic equator plus one quarter of the electron bounce period. Afterward, there were a series of 3 or 4 later peaks at time spacings equal to the full electron bounce period. This train of precipitation peaks was observed to follow each of the large lightning-induced spherics recorded during the rocket flight, and in two distinguishable electron energy ranges (>40 and >135 keV). The periodicity requires that the wave-particle interaction region be confined close to the magnetic equator. The results of an analysis of the peak amplitudes as a function of the number of bounce periods from the primary peak and of the energy dispersion of the peaks are presented. A comparison is made with earlier observations reported by Rycroft. It is concluded that after the initial wave-particle interaction in the equatorial plasmasphere and its associated precipitation, later precipitation peaks are the result of atmospheric backscatter of loss cone electrons. Since the observations are found to be dominated by the kinematics of electron and whistler flight times, it is not possible to exclude either collective effects due to plasma instabilities or single particle-wave type interactions induced by spheric-driven whistlers.

## URSI COMMISSION H - SESSION H4(a)

Wave-Induced Particle  
Precipitation Effects II

1:30 - 3:00  
LAW 169

Effets des précipitations  
de particules induites par  
des ondes II

Chairperson/Président: **R.A. Goldberg**, NASA/Goddard Space Flight Center, Greenbelt, MA, USA

- 1 ENERGY-DEPENDENT ELECTRON PRECIPITATION IN THE SLOT. **A.L. Vampola**, The Aerospace Corporation, Los Angeles, CA, USA
- 2 OBSERVATIONS AND MODELING OF WAVE-INDUCED PARTICLE PRECIPITATION. **T.J. Rosenberg**, University of Maryland, Institute for Physical Science and Technology, College Park, MD, USA
- 3 PRELIMINARY OBSERVATIONS OF TRIMPI EVENTS FROM ITHACA, N.Y.. **P.M. Kintner, J. Labelle, C. Siefving**, Cornell University, School of Electrical Engineering, Ithaca, NY, USA
- 4 MODELING THE EFFECTS OF ELECTRON PRECIPITATION ON VLF SUBIONOSPHERIC WAVE PROPAGATION. **A. Tolstoy**, Naval Research Laboratory, Washington, DC, USA; **T.J. Rosenberg**, University of Maryland, Institute for Physical Science and Technology, College Park, MD, USA

## H-4(a)-1

### ENERGY-DEPENDENT ELECTRON PRECIPITATION IN THE SLOT

A. L. Vampola  
The Aerospace Corporation  
P. O. Box 92957, Los Angeles, CA 90009

Energy-dependent precipitation of energetic (~200 keV) electrons in the slot region of the radiation belts, which is interpreted as evidence of resonant interaction between the electrons and nonducted waves from VLF transmitters, has been studied using data from the S3-3 satellite. Deconvolution of pitch-angle data permits determination of the longitude of the last interaction of the distribution with the atmosphere with relatively good accuracy ( $< 2^\circ$  in longitude). The majority of events are associated with the location of powerful VLF transmitters. The rest of the events have an equatorial pitch-angle cutoff equal to either the local atmospheric loss-cone angle or to the "mid-longitude anomaly" atmospheric loss-cone angle and cannot be traced back to the point of their origin. When statistical accuracy is sufficient, the high angular resolution of the S3-3 data permits an evaluation of the longitudinal distribution of the original precipitation event and thereby provides a measurement of the longitudinal distribution of field intensity above the ionosphere due to a given transmitter (under the assumption that the intensity of precipitation is proportional to the strength of the VLF waves in the interaction region).

OBSERVATIONS AND MODELING OF WAVE-INDUCED  
PARTICLE PRECIPITATION

T. J. Rosenberg  
Institute for Physical Science and Technology  
University of Maryland  
College Park, MD 20742

Wave-induced bursts of energetic electrons precipitated into the atmosphere have been detected with a variety of techniques. Our observations are of burst precipitation effects; e.g., bremsstrahlung x-rays, cosmic radio noise absorption, produced in the lower ionosphere by electrons with energies in excess of 10-20 keV. In one study (conducted jointly with Dr. U. S. Inan, Stanford University) energy-time features of x-ray microbursts were examined and compared with test particle simulations of burst precipitation arising from the pitch angle scattering of trapped energetic electrons undergoing cyclotron resonance interactions with VLF chorus. Simulations of the flux- and energy-time profiles of direct and mirrored burst precipitation were obtained for reasonable plasma, energetic particle, and wave parameters. The observed spectrum variation within microbursts (softer spectrum at the peak energy influx) and the time duration of the bursts compare favorably with the characteristic signatures imparted to the precipitated electron pulse by the wave-particle interaction and the particle travel time from a near-equatorial interaction region.

The characteristics of ionospheric absorption impulses arising from wave-induced particle precipitation and model computations of the effects of such precipitation on the subionospheric propagation of VLF radiowaves will also be discussed.

## H-4(a)-3

### PRELIMINARY OBSERVATIONS OF TRIMPI EVENTS FROM ITHACA, N.Y.

P. M. Kintner, J. Labelle, C. Siefring  
School of Electrical Engineering  
Cornell University, Ithaca, N.Y.

"Trimpi" events are the name given to a phenomena where a receiver monitoring a VLF transmitter records a sudden change in signal amplitude (approximately 1 sec) followed by a slower (a few 10's of sec) exponential recovery to the original signal amplitude. Trimpi events have been observed for over an decade and they may be explained by a model where lightning initiates a whistler which propagates into the deep magnetosphere. Somewhere near the magnetic equator the whistler resonates with electrons whose energy is the order of 10keV to a few 100keV and whose velocity is opposite to the whistler phase velocity. The resonant electrons then precipitate into the lower ionosphere near the original lightning stroke and change the shape of the D-region. This changes the phase path of a VLF signal which may be reaching a receiver by two or more phase paths. The receiver then sees a sudden amplitude perturbation which may be either positive or negative followed by a slow recovery as the D-region returns to its predisturbance profile.

We have been observing Trimpi events on baselines between Ithaca and Annapolis, Maryland (21.4kHz and 88kHz) and Ithaca and Cutler, Maine (24.0kHz). This configuration is unique since the Ithaca-Annapolis baseline is only 380km compared to the shortest baseline previously reported of 1800km. Our preliminary conclusions are that the Ithaca-Annapolis baseline is much more active than the Ithaca-Cutler baseline and that Trimpi events can be commonly observed 2 to 3 times per week. The 21.4kHz transmitter was monitored on 23 nights and Trimpi events were observed on 7 nights. The 88kHz transmitter was monitored on 13 nights and Trimpi events were observed on 3 nights, all of them simultaneous with the 21.4kHz Trimpi events. The 24.0kHz transmitter was monitored on 14 nights but Trimpi events were observed on only 1 night. We are in the process of installing a digital data acquisition system so we soon expect to have a better statistical picture of Trimpi events on the eastern seaboard of the US.

MODELING THE EFFECTS OF ELECTRON PRECIPITATION  
ON VLF SUBIONOSPHERIC WAVE PROPAGATION

A. Tolstoy  
Naval Research Laboratory, Code 5120  
Washington, D.C. 20375

T. J. Rosenberg  
Institute for Physical Science and Technology  
University of Maryland  
College Park, MD 20742

In this paper we will first discuss the capabilities and limitations of the two-dimensional Budden-Wait-Pappert sub-ionospheric VLF wave propagation model. Next we shall present results on applications of the model to situations for which VLF phase and amplitude changes have been observed to occur coincidentally with whistler activity, i.e., for Trimpri events. These events are believed to be the consequence of short-lived whistler-induced electron precipitation resulting in ionospheric density enhancement regions located primarily near the receivers. Early calculations with the model suggested the additional sometime presence of longer-term transmitter-induced precipitation. Consequently, both such effects have been included in the analysis and will be discussed. Finally, we shall propose extensions to the propagation model to treat the problem in three dimensions and subsequently allow for its application to the larger class of ionospheric situations now believed to be appropriate for the Trimpri effect.



URSI COMMISSION H - SESSION H4(b)

**Sources of Waves  
in Space Plasmas I**

3:10 - 5:00  
LAW 169

**Sources d'ondes dans  
les plasmas spatiaux I**

Chairperson/Président: **R.L. Dowden**, University of Otago, Dunedin, New Zealand

- 1 (3:20) RADIO LASING AT THE EARTH AND JUPITER. **W. Calvert**, University of Iowa, Dept. of Physics and Astronomy, Iowa City, IO, USA
- 2 (4:00) THE EFFECT OF DIFFERENT DISTRIBUTION FUNCTIONS ON THE CYCLOTRON MASER INSTABILITY WITH APPLICATIONS TO AURORAL KILOMETRIC RADIATION. **H.K. Wong**, NASA/Goddard Space Flight Center, Laboratory for Extraterrestrial Physics, Greenbelt, MD, USA

## H-4(b)-1

### RADIO LASING AT THE EARTH AND JUPITER

W. Calvert, Department of Physics and Astronomy  
The University of Iowa, Iowa City, Iowa 52242

'Lasing' implies the sustained oscillation of wave systems and the consequent emission of intense coherent beams. Aside from its intrinsic interest, evidence for lasing in nature could be crucial to explaining certain observed radiations. An inherent property of lasing, common to all oscillators and virtually independent of its causative stimulated emission, is the production of discrete spectra. The Earth's auroral kilometric radiation ('AKR', extending from about 50 to 600 kHz) and Jupiter's famous decametric radio emissions ('DAM', between about 0.5 and 40 MHz) both exhibit discrete spectra, the latter in the well-known 'S' or 'millisecond' bursts. Both spectra, moreover, tend to show the equal spacings which would be expected for adjacent longitudinal laser modes. Although previously attributed to resonant emission by bunched electrons, such discreteness of the AKR and DAM more likely implies that both of these planetary cyclotron emissions originate from lasing, albeit at radio rather than optical wavelengths.

THE EFFECT OF DIFFERENT DISTRIBUTION FUNCTIONS ON THE  
CYCLOTRON MASER INSTABILITY WITH APPLICATIONS  
TO AURORAL KILOMETRIC RADIATION

H. K. Wong  
NASA/Goddard Space Flight Center  
Laboratory for Extraterrestrial Physics  
Greenbelt, MD 20771

In recent years, motivated by the study of auroral kilometric radiation (AKR), considerable work has been done calculating the growth rates of different wave modes excited by the cyclotron maser instability. Most of these calculations are performed using particular forms of distribution functions that suit specific purposes. However, at least three different free energy sources have been identified in the AKR source regions: the upward loss cone, the ring distribution, and the hole distribution. It is important to determine how each free energy source contributes to the diversified AKR phenomena observed. In this study, growth rates of different wave modes are calculated using different distribution functions. Our results indicate that the growth rates are very sensitive to the form of distribution function chosen. We believe that many AKR observations can be explained by assuming multiple free energy sources rather than the upward loss cone alone.



## URSI COMMISSION H - SESSION H5

Sources of Waves  
in Space Plasmas II1:30 - 5:00  
LAW 169Sources d'ondes dans  
les plasmas spatiaux IIChairperson/Président: **R.L. Dowden** University of Otago, Dunedin, New Zealand

- 1 (1:40) EXPERIMENTS ON VLF WAVE GENERATION MECHANISMS IN THE MAGNETOSPHERE. **R.A. Helliwell**, Stanford University, Space, Telecommunications and Radioscience Laboratory, Stanford, CA, USA
- 2 (2:20) VLF HISS SOURCE LOCATION BY MULTIPLE OBSERVATIONS ON LONG-LIFE BALLOONS. **R.L. Dowden**, University of Otago, Physics Dept., Dunedin, New Zealand; **R.H. Holzworth**, University of Washington, Geophysics Dept., Seattle, WA, USA
- 3 (2:40) IMPULSIVE ELECTRON PRECIPITATION CAUSING AURORAL PULSATIONS. **R.N. Singh**, Banaras Hindu University, Dept. of Applied Physics, Varanasi, India
- 4 (3:00) ELECTRON ACCELERATION BY MODE CONVERTING WHISTLER WAVES. **J.E. Maggs**, **G.J. Morales**, **A. Baños**, **M. Shoucri**, University of California at Los Angeles, Los Angeles, CA, USA
- 5 (3:20) A TWO SATELLITE STUDY OF A LONG DURATION PULSATION EVENT. **J.F. Fennell**, **D. Croley Jr.**, The Aerospace Corporation, Space Sciences Laboratory, Los Angeles, CA, USA; **A. Korth**, Max-Planck-Institut für Aeronomie, Lindau, FRG; **B. Ledley**, Goddard Space Flight Center, Greenbelt, MD, USA
- 6 (3:40) THE POLARIZATION OF ULF WAVES AT THE POLAR CUSP. **J.V. Olson**, University of Alaska, Geophysical Institute, Fairbanks, AK, USA
- 7 (4:00) GENERATION OF ELECTROSTATIC NOISE IN THE PLASMA SHEET BOUNDARY. **P.B. Dusenbery**, University of Colorado, Dept. of Astrophysical, Planetary and Atmospheric Sciences, Boulder, CO, USA; **L.R. Lyons**, The Aerospace Corporation, Los Angeles, CA, USA
- 8 (4:20) A NEW SOURCE FOR EXCITATION OF KINETIC WAVES IN A MAGNETOPLASMA WITH A NONUNIFORM ELECTRIC FIELD. **G. Ganguli**, **Y.C. Lee**, Science Applications International Corporation, McLean, VA, USA; **P. Palmadesso**, Naval Research Laboratory, Plasma Physics Division, Washington, DC, USA

EXPERIMENTS ON VLF WAVE GENERATION  
MECHANISMS IN THE MAGNETOSPHERE

R. A. Helliwell

Space, Telecommunications, and Radioscience Laboratory  
Stanford University, Stanford, California 94305

Experiments using the VLF transmitter at Siple Station, Antarctica have shown that coherent VLF signals can be amplified 30-50 dB in the magnetosphere and can trigger strong emissions. However, when the input signal is modulated in frequency or amplitude the output tends to be reduced and new frequencies may be generated. Two new modulation experiments reveal effects that may help to explain several features of the natural noise background, including VLF hiss and chorus.

In the first experiment two carriers are transmitted through magnetospheric ducts to Roberval, Quebec, with spacings of  $\Delta f = 5-45$  Hz. Sidebands up to 7th order often are generated and they may exceed the intensity of either input signal. The sidebands are attributed to triggering of an emission by each beat and suppression of that emission by the following beat. An interesting feature of this experiment is an almost total absence of growth of the input frequencies, indicating that nearly all of the emission energy is confined to the sidebands. The amount of sideband energy created in this way can exceed the energy in the input signals.

In the second experiment the frequency of an approximately constant-amplitude carrier is randomly changed every 10 ms over a frequency band limited centered on a frequency of, typically, 4 kHz and limited to a range of 400 Hz or less. This sequence of frequencies is repeated every second. Dispersion in the magnetosphere mixes the phases and group delays of these 10 ms elementary wave trains causing the spectrum to approximate band-limited hiss. From time-to-time short sequences of 3 or 4 of the 10 ms elements appear to link together in a chain that may extend well beyond the last element. The resulting emission resembles a typical chorus element. Each such chain usually repeats over many cycles of the one second random sequence. Chains are attributed to favorable relative phasing and group delays of the component elements that make the input pulse sequence look approximately like a frequency ramp. Changing dispersion, due probably to duct drift, alters these relations causing particular sequences to die out and be replaced by others.

These two experiments taken together suggest an interesting connection between mid-latitude hiss and chorus. Hiss elements consist of chorus-like emissions that overlap one another in time, as in the sideband mechanism of the first experiment. Chorus elements are created from the serial linkage of hiss elements having favorable phase relations. When these chains grow beyond the triggering threshold new emissions are generated. The process repeats when echoing is present. Thus the commonly observed mixture of mid-latitude hiss and chorus in the same band can be understood and the same coherent-wave mechanism can be employed to explain both.

VLF HISS SOURCE LOCATION BY MULTIPLE  
OBSERVATIONS ON LONG-LIFE BALLOONS

R.L.Dowden, Physics Department, University of Otago  
Dunedin, New Zealand

R.H.Holzworth, Geophysics AK-50, University of Washington  
Seattle, WA 98195, U.S.A.

VLF Hiss recorders were flown in six high-altitude (25 km), super pressure balloons which remained aloft for several weeks drifting some ten thousand kilometres westward of the launch site at Christchurch, New Zealand. All longitudes and latitudes of 35°S to 80°S were scanned. Simultaneous observations on several balloons and ground stations enabled location of the predominant regions in which VLF hiss enters the earth-ionosphere wave guide.

## H-5-3

### IMPULSIVE ELECTRON PRECIPITATION CAUSING AURORAL PULSATIONS

R.N. Singh

Applied Physics, Institute of Technology  
Banaras Hindu University, Varanasi-221005, India

Reported features of auroral pulsations and various simultaneous wave phenomena in the auroral region, their conjugate point and along the connecting geomagnetic field lines have been reviewed. The simultaneity of recorded intensity variations of VLF waves, optical intensity emitted by excitations of atoms and molecules and influx of precipitating electrons seem to establish the interaction of gyrating electrons and their periodic energization due to the presence of magnetospheric VLF waves. Accounting for relativistic variation of electronic mass, it is shown that the electron motion in the presence of whistler mode VLF waves conforms to a motion in the pseudo-potential trough. The interacting electron in the presence of magnetospheric VLF waves thus gives rise to a periodic energization of electrons (C.S. Roberts and S.J. Buchsbaum, *Phy. Rev.*, 135, 381, 1964). The electron-wave resonance condition once established continues for the major part of the gyrating electron trajectory. The oscillatory energized electron fluxes are produced almost all along the entire geomagnetic field lines. The pitch angle scattering of electrons in the presence of magnetospheric waves may only alter the flux of oscillating energetic electrons. The period of this energy oscillation is found to depend on the strength of the VLF waves, plasma density and geomagnetic field strength in the interaction region of the magnetosphere. It is shown that the non-linear wave-particle interaction is capable of explaining the observed features of auroral flickers and auroral pulsations.

The precipitating energetic electrons give rise to rich optical emissions and their intensities also change accordingly. Recent reports establish the correlation of optical emission intensity and VLF wave intensity in the conjugate region (J.H. Doolittle and D.L. Carpenter, *Geophys. Res. Letters*, 10, 611, 1983). The localised instability mechanisms of intensity variations of auroral emissions seem to play a less important role and under suitable conditions these mechanisms at best may play the secondary role of decreasing or increasing the frequency and intensity of auroral pulsations.

ELECTRON ACCELERATION BY  
MODE CONVERTING WHISTLER WAVES

J.E. Maggs, G.J. Morales, A. Baños and M. Shoucri  
University of California at Los Angeles  
Los Angeles, California 90024, U.S.A.

The structure of electrostatic waves near plasma resonance is analyzed for a plasma with a longitudinal density gradient. The fourth order differential equation governing their behavior is obtained by retaining thermal corrections in the parallel component of the dielectric tensor. It is found that waves with frequencies less than the electron gyrofrequency (i.e. electrostatic whistler waves) launched from inside the plasma mode convert at plasma resonance entirely into short wave length thermal modes. The detailed structure of the electric field of the mode converting whistler wave near plasma resonance is obtained analytically. The acceleration of thermal electrons by the large electric fields produced near plasma resonance in the mode conversion process is studied numerically. Mode conversion of electrostatic whistler waves can create energetic tails in the electron distribution.

## H-5-5

### A TWO SATELLITE STUDY OF A LONG DURATION PULSATION EVENT

J. F. Fennell<sup>1</sup>, A. Korth<sup>2</sup>, D. Croley, Jr.<sup>1</sup>  
and B. Ledley<sup>3</sup>

Space Sciences Laboratory, THE AEROSPACE CORPORATION  
P. O. Box 92957, Los Angeles, CA 90009

<sup>2</sup>Max Planck Institut fuer Aeronomie,  
D-3411 Katlenburg-Lindau 3, West Germany

<sup>3</sup>Goddard Space Flight Center  
Greenbelt, MD 20771

This paper emphasizes the B field and particle observations made by the GEOS-2 and SCATHA spacecraft during the 14 November 1979 pulsation event. GEOS-2 and SCATHA were 90° apart in longitude. SCATHA and GEOS-2 both observed the pulsation starting at ~0600 UT on 14 November with GEOS-2 near 9 MLT and SCATHA near 17 MLT. The B field oscillations disappeared at SCATHA after 1.5 hours near 18.6 MLT and then reappeared at 1500 UT when SCATHA entered the morning local time region. They were then observed by SCATHA for the next ~12 hours. The pulsation was seen continuously at GEOS-2 until ~1800 UT near 20 MLT. The pulsation observed at GEOS-2 on the morning side had nearly pure transverse B field oscillations ( $\Delta B_H \sim 2.8$  nT,  $\Delta B_D \sim \Delta B_Y \sim 11.2$  nT) with a frequency of 1.8-2.0 mHz while  $B_H$  showed significant amplitude at ~1.8 mHz and ~3.6 mHz. At GEOS-2 the pulsation amplitude became small and the frequency doubled near 1500 UT about 3 hours before they terminated. The amplitudes of the B field oscillations measured early at SCATHA were very small with a frequency near 2.0 mHz. On the morning side SCATHA observed compressional oscillations with a frequency of 1.6-2.0 mHz. At both satellites the energetic particle flux oscillations were generally out of phase with the B field oscillations ( $J_{max}$  at  $B_{min}$ ). The electron and ion oscillations were in phase. At GEOS-2 the particle oscillations had a frequency of ~3.6 mHz but the peak to minimum flux difference was smaller every other period, indicative of a lower frequency component. In the SCATHA data weak energy dependent phase lag is apparent between the particles and B field. There is also evidence for a higher frequency component of 3.2-4.0 mHz. While many features of the event are consistent with a drift mirror instability for producing the waves observed by SCATHA, calculations using the ion angular distributions and covering the energy range from ~70 eV to 300 keV indicate the instability criterion is not met. The Kelvin-Helmholtz instability criterion was also considered for this event and ruled out by Higbie, et al. (*J. Geophys. Res.*, **87**, 2337, 1982.) These and other features of the event will be discussed in detail.

## The Polarization of ULF waves at the Polar Cusp

John V. Olson  
Geophysical Institute  
University of Alaska  
Fairbanks, Alaska 99701

In the fall of 1982 digital pulsation stations were placed in operation at Cape Parry (MLAT = 73.8) and Mould Bay (MLAT = 79.3) Canada by the University of Alaska. The stations are instrumented with fluxgate and induction coil magnetometers and riometers. At Cape Parry, nearly every day, a broad band of ULF pulsations are observed near local noon. We believe this spectrum is associated with the polar cusp. The pulsation spectrum shows broad maxima near 5 mHz and 40 mHz. We are investigating the polarization states of the dominant signals in these bands. We believe the 40 mHz band probably represents direct transmission of part of the turbulent magnetosheath spectrum to the ground. The lower frequency band probably reflects magnetopause boundary phenomena including surface waves and flux transfer events.

GENERATION OF ELECTROSTATIC NOISE IN  
THE PLASMA SHEET BOUNDARY

P.B. DUSENBERY (Dept. of Astrophysical, Planetary, and Atmospheric Sciences, Univ. of Colo., Boulder, CO 80309)

L.R. LYONS (The Aerospace Corp., P.O. Box 92957, Los Angeles, CA 90009)

The acceleration of current sheet ions in the geomagnetic tail results in distributions of ions, highly peaked in energy at several keV, streaming earthward on the outer edge of the plasma sheet. The earthward streaming ions outside the loss cone will mirror and return towards the neutral sheet. Counter-streaming ion beams may therefore be present. The dominant current sheet ions are hot  $H^+$  and  $He^{++}$  ions. During times of geomagnetic activity the ionosphere is an important source of magnetospheric ions. Observations of cold (10-50eV), streaming (<1keV) ionospheric ions have been made in the plasma sheet boundary layer. The dominant ions of ionospheric origin are cold  $H^+$  and  $O^+$  ions.

The major wave dispersion branches of the electrostatic mode are: the ion acoustic, the whistler, and the upper hybrid. Results of a comprehensive study modeling the generation of electrostatic noise in this region of geospace will be presented with particular emphasis on the role the ionosphere plays.

Observations of broad band electrostatic noise will be shown to be a result of a negative energy slow beam acoustic mode instability excited by cold, streaming ionospheric ions. Heating rates for both electron and current sheet ion populations will be given. The formation of the hot central plasma sheet may be a result of the diffusion of ions and electrons resonant with the slow beam acoustic mode.

A NEW SOURCE FOR EXCITATION  
OF KINETIC WAVES IN A MAGNETOPLASMA  
WITH A NONUNIFORM ELECTRIC FIELD

G. Ganguli, Y.C. Lee\*, Science Applications International Corporation, McLean, VA 22102,  
P. Palmadesso, Plasma Physics Division, Naval Research Laboratory, Washington, D.C. 20375

We discuss a new source to excite kinetic waves (ion Cyclotron, Lower hybrid, etc) in a magnetoplasma with a localized electric field perpendicular to the external magnetic field. In the absence of the electric field the mode energy is positive while in the presence of a uniform electric field perpendicular to the magnetic field the wave energy can be negative. However, when the electric field is nonuniform, it is possible for a finite region of space (over which the electric field is localized) to be of negative wave energy density surrounded by regions of positive wave energy density. A nonlocal wave packet couples the two regions so that a flow of energy from the region of negative wave energy to the region of positive wave energy will cause the mode to grow. This gives rise to the instability.

This work is supported by the Office of Naval Research and NASA.

\*Permanent address: University of Maryland, College Park, MD 20740



## URSI COMMISSION J - SESSION J1

Very Long Baseline  
Interferometry

1:30 - 5:00  
LAW 157

Interférométrie à très  
longue ligne de base

Chairperson/Président: J.L. Yen, University of Toronto, Toronto, ON

- 1 A WATER VAPOR RADIOMETER FOR VLBI CALIBRATION. A.K. Wu, I.F. Diegal, W.M. Golding, *Bendix Field Engineering Corporation, Columbia, MD, USA*
- 2 MILLIMETER WAVELENGTH VLBI. A.C.S. Readhead, A.T. Moffet, C.R. Masson, *California Institute of Technology, Owens Valley Radio Observatory, Pasadena, CA, USA*; D.C. Backer, M. Wright, R. Plambeck, *University of California, Radio Astronomy Laboratory, Berkeley, CA, USA*; J.M. Moran, *Harvard-Smithsonian Center for Astrophysics, Cambridge, MA, USA*; A.E.E. Rogers, *Haystack Observatory, Westford, MA, USA*; C.R. Predmore, *University of Massachusetts, Amherst, MA, USA*
- 3 APERTURE SYNTHESIS USING ORBITING TELESCOPES. T.B.H. Kuiper, S.P. Synnott, R.P. Linfield, G.M. Resch, E.F. Tubbs, *California Institute of Technology, Jet Propulsion Laboratory, Pasadena, CA, USA*
- 4 QUASAT. B.F. Burke, *MIT, Dept. of Physics, Cambridge, MA, USA*; A.C.S. Readhead, A.T. Moffet, *California Inst. of Technology, Owens Valley Radio Observ., Pasadena, CA, USA*; F. Jordan, R.A. Preston, *California Inst. of Technology, Jet Propulsion Lab., Pasadena, CA, USA*; K.J.J. Johnston, *Naval Research Lab., Washington, DC, USA*; K.I.K. Kellerman, *National Radio Astronomy Observ. Green Bank, WV*; J.D. Rommey, *Max-Planck Inst. für Radiostronomie, Bonn, FRG*; D.C. Backer, *University of California, Radio Astronomy Lab., Berkeley, CA, USA*; M.J. Reid, *Harvard-Smithsonian Ctr. for Astrophys., Cambridge, MA, USA*
- 5 A PROGRESS REPORT ON THE VERY LONG BASELINE ARRAY. P. Napier, *National Radio Astronomy Observatory, Socorro, NM, USA*

## J-1-1

### A WATER VAPOR RADIOMETER FOR VLBI CALIBRATION

Albert K. Wu, Irvin F. Diegel, William M. Golding  
Bendix Field Engineering Corporation  
One Bendix Road  
Columbia, Maryland 21045

A dual channel water vapor radiometer operating at 20.7 and 31.4 Ghz has been developed under contract to the NASA Crustal Dynamics Project for use as a VLBI calibration source. This instrument allows both the water vapor and liquid water content of the atmosphere to be estimated along the path of interest. This measurement of water content may then be converted to an excess propagation delay which affects the VLBI observables. Typical excess zenith path delays range from 60 psec to over 600 psec and are highly variable with site, season and meteorological conditions.

The first of these instruments is currently undergoing field tests at the Mojave Base Station at Goldstone, California. We will present engineering results from these tests as well as recovered path delays. Preliminary tests and laboratory measurements have indicated that the WVR has a sensitivity limit of 0.7 deg. K. The hot loads are stable to a few millidegrees per day while the outside temperature ranges from -30 C to +50 C. System temperatures are near 500 deg. K. in each channel. Algorithms for accurate delay corrections are currently being developed for NASA by another contractor.

The WVR microwave package is mounted on a two axis, servo-controlled mount. This package is temperature controlled with a thermal isolation factor of greater than 60. The control electronics, power supplies and control microcomputer are packaged in a rack which may be located in any convenient indoor location.

Three additional WVRs are expected to be delivered to the Crustal Dynamics Project during the first half of 1985. These instruments will be deployed at selected VLBI sites in support of project observing activities.

## MILLIMETER VLBI

D. Backer (UC Berkeley), C. Masson (Caltech), A. Moffet (Caltech), J. Moran (CfA), R. Plambeck (UC Berkeley), R. Predmore (UMass), A. Readhead (Caltech), A. Rogers (Haystack), M. Wright (UC Berkeley)

Interferometry at 90 GHz with intercontinental baselines provides a new probe of active galactic nuclei capable of subparsec resolution. Our October 1981 experiment detected one object, 3C84, on one baseline with  $0.001''$  resolution. Our April 1983 experiment detected four sources, 3C84, 3C273, OJ287 and OV-236, on three baselines with maximum resolution of  $0.005''$ . In April 1984, 3C273 was detected on Massachusetts to California baselines with  $0.0002''$  resolution. Scientific and technical achievements from these past experiments and the March 1985 run will be summarized.

## APERTURE SYNTHESIS USING ORBITING TELESCOPES

T. B. H. Kuiper, S. P. Synnott, R. P. Linfield,  
G. M. Resch, E. F. Tubbs  
Jet Propulsion Laboratory  
California Institute of Technology

A study was carried out to determine the feasibility, with current technology, of performing aperture synthesis using two telescopes in coordinated Earth orbits separated by  $\sim 10$  m to 1 km. The objective was to determine whether there is a practical alternative to a very large deployed servo-controlled submillimeter telescope (i.e. the Large Deployable Reflector--LDR) for obtaining high resolution submillimeter images of astronomical sources. We find that suitable classes of orbits exist which can provide good UV coverage over the entire sky.

In many cases, a constant difference in one or more of the orbital parameters combined with apsidal precession can give complete UV coverage out to a maximum baseline length. In the case of circular orbits, a linear increase in the mean anomaly difference between the two spacecraft, achieved by a single thrust, can fill the UV plane in a relatively short period of time. An exponential spiral coverage can be achieved by a very low level constant thrust.

The most difficult task appears to be the real-time determination of the orientation of the baseline vector in a stable coordinate system. We have identified a plausible scheme for the determination of an arbitrary direction to within  $0''.003$  in the astrometric coordinate system to be established by the planned HIPPARCOS mission. A cluster of high-precision star trackers would track selected HIPPARCOS stars, while one cluster member would record the motion of the distant spacecraft. The relative position of the spacecraft tracker would be calibrated against a HIPPARCOS star before the spacecraft passes through the field-of-view. This scheme not only makes submillimeter interferometric image reconstruction possible, but should have numerous other applications.

The most practical scheme for correlation of the wide-band signals appears to be to do it in space, returning the correlation coefficients to Earth for further processing. A hybrid filter-bank/auto-correlator and an acousto-optic correlator appear to be possible with the current state-of-the-art.

QUASAT

B.F. Burke, MIT, Dept. of Physics, Cambridge, MA, USA

A.C.S. Readhead, A.T. Moffet, California Inst. of Technology,  
Owens Valley Radio Observ., Pasadena, CA, USA

F. Jordan, R.A. Preston, California Inst. of Technology,  
Jet Propulsion Lab., Pasadena, CA, USA

K.J.J. Johnston, Naval Research Lab., Washington, DC, USA

K.I.K. Kellerman, National Radio Astronomy Observ.,  
Green Bank, WV, USA

J.D. Rommey, Max-Planck Inst. für Radioastronomie, Bonn, FRG

D.C. Backer, University of California,  
Radio Astronomy Lab., Berkeley, CA, USA

M.J. Reid, Harvard-Smithsonia Ctr. for Astrophys.,  
Cambridge, MA, USA

Abstract not available at time of printing/  
Le résumé n'était pas disponible lors de l'impression

## J-1-5

### A PROGRESS REPORT ON THE VERY LONG BASELINE ARRAY PROJECT

Peter J. Napier  
National Radio Astronomy Observatory  
Socorro, New Mexico, USA

The Very Long Baseline Array (VLBA) radio telescope, whose construction is scheduled to begin in April 1985, is an array of ten antennas separated by distances up to 8300 km. The antennas will be located in Puerto Rico, near Haystack (Massachusetts), North Liberty (Iowa), Fort Davis (Texas), Los Alamos (New Mexico), Pie Town (New Mexico), Kitt Peak (Arizona), Oroville (Washington), Owens Valley (California) and on the Island of Hawaii. The reflector surfaces of the 25m diameter antennas will be sufficiently accurate so as to be usable at frequencies up to 86 GHz.

The receiver and feed design will allow observations in eleven bands centered on the frequencies 327 MHz, 610 MHz, 1.55 GHz, 2.3 GHz, 4.8 GHz, 6.1 GHz, 8.4 GHz, 10.7 GHz, 14.9 GHz, 23 GHz and 43 GHz, although not all of these receivers will be built during the initial construction project. Accurate time will be provided at each antenna by a hydrogen maser clock. The signals received by the antennas will be recorded on longitudinal tape recorders capable of recording 100 Mbit/sec for 12 hours without a tape change. The correlator used to combine together the signals from the antennas will be capable of producing 512 spectral channels for each of the 45 interferometer baselines available from 10 antennas or 128 spectral channels for the 190 baselines available with 20 antennas.

During the talk an overview of the current design of the VLBA will be presented and the current schedule for the project will be discussed.

## URSI COMMISSION J - SESSION J2

**Radiotelescope  
Feeds**8:30 - 12:00  
LAW 157**Sources primaires  
de radiotélescope**Chairperson/Président: **W.J. Welch**, University of California, Berkeley, CA, USA

- 1 NEAR-MILLIMETER WAVE IMAGING ARRAYS. **D.B. Rutledge, C.E. Zah**, California Institute of Technology, Division of Engineering and Applied Science, Pasadena, CA, USA; **N.C. Luhmann Jr.**, University of California, Dept. of Electrical Sciences, Los Angeles, CA, USA
- 2 APERTURE EFFICIENCY ENHANCEMENT IN A CASSEGRAIN SYSTEM BY MEANS OF A DIELECTRIC LENS. **J.A. Hudson**, University of California, Radio Astronomy Laboratory, Berkeley, CA, USA
- 3 ANTENNA EFFICIENCY IMPROVEMENTS AT GREENBANK. **J.R. Fisher**, National Radio Astronomy Observatory, Greenbank, WV, USA
- 4 DIFFRACTION ANALYSIS OF A PROPOSED NEW DUAL-REFLECTOR FEED FOR THE SPHERICAL REFLECTOR ANTENNA IN ARECIBO. **P.-S. Kildal**, Norwegian Institute of Technology, Electronics Research Laboratory, Trondheim, Norway
- 5 EXPERIMENTS ON PHASED ARRAY FEEDS. **S. Dmitrevsky, J.L. Yen**, University of Toronto, Toronto, ON

NEAR-MILLIMETER WAVE IMAGING ARRAYS

D.B Rutledge, C.E. Zah and N.C. Luhmann, Jr.

D.B Rutledge and C.E. Zah are with the Division of Engineering and Applied Science, California Institute of Technology, Pasadena, CA. N.C. Luhmann, Jr. is with the Department of Electrical Sciences, University of California, Los Angeles, CA.

Near-millimeter wave imaging arrays show much promise for plasma diagnostics, military applications, and radio astronomy. The idea is that an image is focused onto an array of antennas, each with its own detector, and the signal received by the antennas is interpolated to form an imaging. These systems have potential advantages over mechanically scanned systems that may either be too slow to see a fast event or require a integration time that is too long. This approach is particularly suited for submillimeter and millimeter wavelengths, where the antennas in the array may be made as thin-film metal patterns and may be integrated monolithically with the detectors.

Several different arrays for frequencies ranging from 90 GHz to 3000 GHz have been developed. These arrays have demonstrated diffraction-limited resolution and system efficiencies of 50 per cent. Polarimeter arrays that image polarization as well as intensity have also been demonstrated, as well as interferometers that generate realtime phase holograms of tokamak plasmas. The arrays have been integrated with microbolometer detectors at the higher frequencies and GaAs Schottky diodes at the lower frequencies. Recent results by others with superconducting tunnel junction receivers indicate that it should be possible to make submillimeter-wave imaging arrays with the sensitivity that is needed for radio astronomy.

APERTURE EFFICIENCY ENHANCEMENT IN A CASSEGRAIN SYSTEM  
BY MEANS OF A DIELECTRIC LENSJerome A. Hudson  
Radio Astronomy Laboratory, University of California, Berkeley

For Cassegrain radio antenna systems with equivalent focal ratios  $\sim f:3.0$ , illuminated with Gaussian or  $\cos^n \theta$  feed patterns, it is possible to achieve a boost in aperture efficiency from  $\sim 55\%$  to better than  $90\%$  by means of a dielectric lens. The lens, of weak optical power, but strongly aspherical figure, is placed a short distance in front of the feed. The aberrations (defocussing and spherical) introduced by the lens are balanced by displacing the secondary mirror. The wavefront at the secondary is rendered more uniform in amplitude, with fairly sharp cutoff at the edges. There is some ( $\sim 3\%$ ) spillover. The design method used by the author employs a fast algorithm (using FFT) for evaluating the scalar diffraction integral.

J-2-3

**ANTENNA EFFICIENCY IMPROVEMENTS AT GREENBANK**

J.R. Fisher  
National Radio Astronomy Observatory  
Greenbank, WV, USA

Abstract not available at time of printing/  
Le résumé n'était pas disponible lors de l'impression

**DIFFRACTION ANALYSIS OF A PROPOSED NEW DUAL-REFLECTOR FEED FOR THE SPHERICAL REFLECTOR ANTENNA IN ARECIBO\***

Per-Simon Kildal  
Electronics Research Laboratory (ELAB)  
Norwegian Institute of Technology (NTH)  
N-7034 Trondheim-NTH, Norway

The existing line feeds for the 1000 ft diameter spherical reflector antenna of the Arecibo observatory have very narrow frequency bandwidth. This can be improved by replacing the line feeds with a proposed new dual-reflector feed system. This consists of horn antennas plus two shaped feed reflectors which correct for the aberrations introduced by the spherical reflector. The beam of the Arecibo antenna is steered by moving the feed so that it illuminates different regions of the 1000 ft spherical reflector. This beam steering is limited because of the additional pick-up of ground noise when the illuminated aperture starts to spill over the spherical reflector. The maximum beam steering is larger the smaller the area of the illuminated aperture is. This compromise between steering and gain can be improved by using an elliptical illumination of the spherical reflector rather than the circular one obtained with the line feeds. The elliptical illumination can be realized with the new dual-reflector feed system by shaping of the reflectors. Furthermore, the dual-reflector feed system have much smaller ohmic losses than the line feeds. Altogether this means that the dual-reflector feed system can provide an almost 3 dB improvement of the sensitivity of the telescope.

The performance of the dual-reflector feed system will be reduced at low frequencies due to diffraction. The purpose of this paper is to present introductory calculations of these diffraction effects. These calculations are needed for optimization of the reflector geometries and for determination of the lower frequency limit. For these calculations a new secondary asymptotic diffraction theory is developed. By this theory secondary diffraction results like increased spillover and reduction in aperture efficiency can be found, without knowing the exact shapes of the reflectors and without time-consuming numerical integration of diffracted fields over the reflectors. The theory is also applied to the existing line feeds, in order to justify the accuracy of the theory by comparison with straight forward numerical integration.

\*This work was supported by the National Astronomy and Ionospheric Center, USA, and by scholarship from the Norwegian Council for Scientific and Industrial Research.

**J-2-5**

**EXPERIMENTS ON PHASED ARRAY FEEDS**

S. Dmitrevsky, J.L. Yen  
University of Toronto  
Toronto, ON

Abstract not available at time of printing/  
Le résumé n'était pas disponible lors de l'impression

## URSI COMMISSION J - SESSION J3

**Radar and Radio  
Astronomy**

1:30 - 5:00  
LAW 157

**Radar et  
radioastronomie**

Chairperson/Président: **A.T. Moffet**, California Institute of Technology, Pasadena, CA, USA

- 1 RADAR OBSERVATIONS OF THE RINGS OF SATURN. **R.M. Goldstein, R.F. Jurgens**, Jet Propulsion Laboratory, Pasadena, CA, USA
- 2 COMPUTED SCINTILLATION SPECTRA FOR STRONG SCATTERING DURING ATMOSPHERIC OCCULTATIONS. **D.P. Hinson**, Stanford University, Center for Radar Astronomy, Stanford, CA, USA
- 3 OBSERVATIONS OF INTERPLANETARY DISTURBANCES USING SPACECRAFT DOPPLER SCINTILLATIONS. **R. Woo**, California Institute of Technology, Jet Propulsion Laboratory, Pasadena, CA, USA
- 4 INTERFERENCE TO RADIO ASTRONOMY FROM SATELLITE SYSTEMS. **V. Pankonin**, National Science Foundation, Washington, DC, USA
- 5 RADIO MONITORING OF THE MILKY WAY. **W.T. Sullivan III**, University of Washington, Dept. of Astronomy, Seattle, WA, USA; **M.J. Klein**, Jet Propulsion Laboratory, Pasadena, CA, USA
- 6 MULTIFREQUENCY LIGHT CURVES AT LOW-FREQUENCY FOR EXTRAGALACTIC RADIO SOURCES. **J.J. Broderick, K.J. Mitchell, B.K. Dennison, S.L. O'Dell**, Virginia Polytechnic Institute and State University, Blacksburg, VA, USA; **D.R. Altschuler**, MPIfR and UPR; **H.E. Payne, J.J. Condon**, NRAO
- 7 PRELIMINARY RESULTS FROM SETI FIELD TESTS AT GOLDSTONE. **S. Gulkis**, California Institute of Technology, Jet Propulsion Laboratory, Pasadena, CA, USA; **J. Tarter**, University of California at Berkeley, Berkeley, CA, USA

**J-3-1**

RADAR OBSERVATIONS OF THE RINGS OF SATURN

R. M. Goldstein and R. F. Jurgens  
Jet Propulsion Laboratory  
4800 Oak Grove Drive  
Pasadena, California 91109

Radar observations of Saturn's rings have been made with the ring plane only  $6^\circ$  from edge-on. The normalized radar cross section has not dropped appreciably with angle. This result, coupled with earlier data and computer simulations, shows that the radar detected ring particles must be much larger than the wavelength - on the order of a meter or larger. Polarization results require the particles to be of irregular, jagged shape.

COMPUTED SCINTILLATION SPECTRA FOR STRONG SCATTERING  
DURING ATMOSPHERIC OCCULTATIONS

D. P. Hinson  
Center for Radar Astronomy  
Stanford University, CA 94305

Atmospheric dynamics, such as turbulence or buoyancy waves, can modulate the quiescent refractive index and cause radio-wave scattering during spacecraft occultations by planetary atmospheres. The resulting rapid signal fluctuations are a common feature observed during radio occultation experiments, especially in the outer solar system. By applying an appropriate scattering theory, it is possible in principle to study the underlying atmospheric dynamics through analysis of the scintillation data. However, in the past, the absence of a theory that accounts for strong scattering during atmospheric occultations has obstructed progress in this area, and has limited data analysis to the weak-scattering regime. Recently, we have removed this restriction. Through use of a technique described by Haugstad (Radio Sci., 17, 565-573, 1982) in conjunction with earlier results by Rumsey (Radio Sci., 10, 107-114, 1975), we derived a generalized theoretical expression for the spatial spectrum of intensity fluctuations caused by scattering from a thin screen. The result remains valid for strong scintillations even when the phase screen includes a gradient in the quiescent refractive index -- a unique and essential feature of this expression. In the model phase screen, the refractive irregularities are anisotropic in shape, with a size distribution that follows a power law. The strength, axial ratio, orientation, and power-law exponent that characterize the irregularities, as well as the "scale height" of the inhomogeneous phase screen, are included in the theory as free parameters.

This new expression for the intensity spectrum involves integrals that cannot be solved analytically at present. To overcome this difficulty, we developed an algorithm for numerical integration, and verified the accuracy of the computations through comparisons with earlier results for certain limiting cases (Marians, Radio Sci., 10, 115-120, 1975; Rino, Radio Sci., 15, 41-47, 1980), and through comparisons with asymptotic forms for both weak and strong scattering. A more interesting test of the theory was obtained using data from the dual-frequency radio occultation of Voyager 1 by Jupiter. Shortly after immersion, the propagation path from spacecraft to earth passed through Jupiter's topside ionosphere but remained above the neutral atmosphere; at this time, Jupiter's ionospheric irregularities caused weak scattering at X-band (8415 MHz), accompanied by strong scattering at S-band (2295 MHz). We applied the conventional weak-scattering theory to interpret the former, and used the new theory described above to interpret the latter. The results were found to be mutually consistent, supporting both the accuracy of the calculations and the validity of the scattering model.

OBSERVATIONS OF INTERPLANETARY DISTURBANCES  
USING SPACECRAFT DOPPLER SCINTILLATIONS

Richard Woo

Jet Propulsion Laboratory, California Institute of Technology  
Pasadena, CA 91109, USA

The scintillation of celestial radio sources due to electron density irregularities along lines of sight through the interplanetary medium has provided a convenient ground-based method for monitoring disturbances in interplanetary space (see e.g. Rickett, Solar Phys. 43,237, 1975; Gapper et al., Nature, 296, 633 1982). Daily observations of interplanetary scintillations have revealed enhancements related to corotating high-speed streams and flare-associated shock waves. Although these observations have been very useful for studying the shape and extent of the interplanetary disturbances in three dimensions, they have been carried out at meter wavelengths, and have therefore provided little information inside 0.5 AU. Also, because the observations are conducted at meridian transit, each radio source is tracked for at most only a couple of hours per day, and the temporal resolution is generally poor.

In contrast, spacecraft radio signals are at centimeter wavelengths and are ideally suited for observing the near-sun region that has so far been inaccessible to direct spacecraft measurement. Equally important is the fact that the spacecraft radio signals are coherent so that phase or Doppler scintillations can be observed in addition to intensity scintillations. Compared with intensity scintillations, the virtues of Doppler scintillations are: (1) they do not saturate when strong, consequently, they have a large dynamic range and can be observed over a wide range of heliocentric distances, (2) their sensitivity for detecting interplanetary shocks and other fast-moving speed in addition to density fluctuations, and (3) their temporal resolution is much improved over intensity scintillations measured at single-site observations because the NASA Deep Space Network permits continuous tracking of single spacecraft.

In this paper, the advantages of Doppler scintillations will be demonstrated with recent observations of interplanetary shocks made by the Pioneer and Voyager spacecraft.

## INTERFERENCE TO RADIO ASTRONOMY FROM SATELLITE SYSTEMS

Vernon Pankonin  
National Science Foundation, Washington, DC 20550

Up to the present time radio frequency interference due to satellite systems could generally be considered an irritation to radio astronomy operations. The occasional interference was usually temporary. That situation is rapidly evolving to the point where satellite systems could soon pose a serious and continuous impediment to radio astronomy research in certain frequency bands. The worst case scenarios are associated with geostationary satellite orbits and with large numbers of low orbiting satellites which are elements of a single system. This paper examines the expected satellite interference environment for radio astronomy. The frequency bands which are used by radio astronomers that are most likely to be impacted by satellite transmissions are identified, and the technical standards which apply to satellite transmitters are noted. Specific satellite systems such as GLONASS, GPS, GEOSTAR, and MOBILSAT, which may impact radio astronomy, are described. Several courses of action should be pursued to minimize problems with satellite interference. Astronomers must provide input on the requirements for radio astronomy at the planning phase of satellite systems to try and avoid an interference situation. If such a situation is unavoidable, astronomers will have to make adjustments in their equipment and data analysis routines, such as adding filters, designing software to recognize and deal with interfering signals, and continuously monitoring certain frequency bands for man-made transmissions.

RADIO MONITORING OF THE MILKY WAY

Woodruff T. Sullivan, III (Univ. Washington)  
and  
Michael J. Klein (Jet Propulsion Lab)

Strong arguments can be made that if a new radio source as strong as Cassiopeia A (or even the sun) were to appear in the sky tonight and last for only one month, the world's radio astronomers would never find it (Sullivan 1982, Pub. Astron. Soc. Pacific 94, 901). A program is therefore being developed to conduct a semi-automatic monthly monitoring of a large fraction of the Milky Way at microwavelengths in order to search for transient galactic radio sources which would otherwise with high probability remain undiscovered. Such sources might be young supernovae in our Galaxy analogous to those now being studied in other galaxies, a class of less luminous supernovae not yet discovered, or any other completely new class of object.

We plan to operate at a wavelength of 13 cm using one of the 26 or 34 meter antennas in NASA's Deep Space Network. A five-hour period each month will be spent sweeping at a rate of  $10^{\circ}/\text{min}$  across a band of  $120^{\circ}$  by  $2^{\circ}$  centered on the galactic center; this covers the directions to ~50% of all the stars in the Galaxy. The sensitivity to any changes in the intensity of unresolved sources is expected to be in the range of 0.2 to 1.0 Jy, dependent on the complexity of any particular region.

We will present the results of test observations and discuss various algorithms for inter-comparison of the monthly maps.

MULTIFREQUENCY LIGHT CURVES AT  
LOW-FREQUENCY FOR EXTRAGALACTIC RADIO SOURCES

J. J. Broderick (VPI&SU), K. J. Mitchell (VPI&SU), B. K. Dennison (OSO and VPI&SU), D. R. Aitschuler (MPIFR and UPR), H. E. Payne (NRAO), J. J. Condon (NRAO) and S. L. O'Dell (VPI&SU).

We present "light-curves" on a four year time-baseline from a multifrequency flux-density monitoring program in which we observed a complete sample of 30 low-frequency-variable extragalactic radio sources about 6 times a year. These observations were made at frequencies of 318, 430, 606, 880 and 1400 MHz using the 305 m telescope of NAIC's Arecibo Observatory and the 92 m telescope of NRAO at Green Bank.

Preliminary Results from SETI Field Tests at Goldstone

by

Sam Gulakis  
Jet Propulsion Laboratory

and

Jill Tarter  
University of California Berkeley and the SETI Institute

Over the past few months we have been assisting our colleagues to verify the performance of prototype instrumentation constructed for NASA's program to Search for Extraterrestrial Intelligence (SETI). This prototype was constructed by a collaborative effort of JPL, Stanford University and NASA Ames Research Center. It consists of a downconverter, 4-bit A/D converter, in phase and quadrature mixers feeding a multichannel spectrum analyzer (MCSA) producing 74000 channels of complex spectral information that are analyzed in pseudo-real-time by a series of virtually concurrent software processes residing in a VAX 11/750 and a SUN graphics workstation. The architecture that yields the extreme output frequency resolution of the MCSA is not a correlator as is typical for many radio astronomical applications, but is in fact a Fourier transform spectrometer. This is implemented by cascading 2 layers of finite impulse response digital filters ahead of a selectable collection of discrete prime factor Fourier transform processors. The resulting hardware is capable of providing instantaneous ( $B\tau=1$ ) complex samples of the spectral density function with intrinsic resolutions of 1 KHz, 32 Hz or 1Hz. The software resident on the VAX and SUN systems attempts to analyze the resultant data streams to recognize the presence of drifting or stationary CW and narrowband pulsed signals.

In this paper we recount the experience gained from our first series of field tests using DSS13 (26m antenna) at Goldstone, CA. The instrumentation was tested in the laboratory at Stanford University in order to verify its design. The field tests were primarily concerned with the system performance in the real world of astrophysical sources, RFI surrounding or over-flying the site, and the ensemble of discrete digital signals inherent to the processing equipment within the observatory itself.

## HF RADAR TECHNIQUES - SPECIAL SESSION SS1

<b>Overview of HF Radar Systems and Skywave Applications</b>	8:30 - 12:00 LAW 102	<b>Vue d'ensemble des systèmes radar HF et des applications des ondes ionosphériques</b>
--	-------------------------	--

Chairperson/Président: **P.H. LeBlond**, University of British Columbia, Vancouver, BC

- 1 (8:40) REVIEW OF HF OCEAN REMOTE SENSING IN NORTH AMERICA. **D.E. Barrick**, Ocean Surface Research, Boulder, CO, USA
- 2 (9:20) REMOTE SENSING OF SEA-STATE BY HF RADAR - DIRECTIONS FOR RESEARCH. **E.D.R. Shearman**, University of Birmingham, Dept. of Electronic and Electrical Engineering, Birmingham, UK
- 3 (10:00) PROPAGATION PREDICTIONS FOR HF RADAR SYSTEM PLANNING. **R.S. Gill, R.N. Herring, S.P. Kingsley, J.D. Milsom, J.M. Pielou, S. Rotheram**, GEC, Research Laboratories, Marconi Research Centre, Chelmsford, UK
- 4 (10:20) AN ESTIMATE OF THE COVERAGE EFFICIENCY OF HF SKYWAVE RADAR FOR MAPPING OCEAN WINDS AND WAVES. **J.W. Maresca Jr.**, Vista Research Inc., Palo Alto, CA, USA; **T.M. Georges, J.P. Riley**, NOAA/ERL, Boulder, CO, USA; **C.T. Carlson**, Sohio Petroleum, Dallas, TX, USA
- 5 (10:40) SHIP DETECTION WITH HIGH RESOLUTION HF SKYWAVE RADAR. **J.R. Barnum**, SRI International, Remote Measurements Laboratory, Menlo Park, CA, USA
- 6 (11:00) AN EXPERIMENTAL INVESTIGATION OF SKYWAVE SEA-STATE RADAR TECHNIQUES AT A LATITUDE NEAR THE AURORAL ZONE. **E.L. Winacott**, Department of Communications, Communications Research Centre, Ottawa, ON
- 7 (11:20) REMOTE SENSING WITH THE JINDALEE SKYWAVE RADAR. **S.J. Anderson**, Defence Research Centre-Salisbury, Electronics Research Laboratory, Adelaide, South Australia
- 8 (11:40) FREQUENCY MANAGEMENT SUPPORT FOR REMOTE SEA-STATE SENSING USING THE JINDALEE SKYWAVE RADAR. **G.F. Earl, B.D. Ward**, Defence Research Centre-Salisbury, Electronics Research Laboratory, Adelaide, South Australia

REVIEW OF HF OCEAN REMOTE SENSING IN NORTH AMERICA

D. E. Barrick  
Ocean Surface Research  
Boulder, Colorado 80303

The past two years have seen considerable changes in activities involving HF radar for ocean remote sensing; the direction of these changes is toward overall acceptance of the technology, and its integration into operational applications. Canadian activities have expanded in St. John's, Newfoundland to include three groups jointly pursuing CODAR and other HF ocean monitoring projects: C-CORE, Memorial University of Newfoundland, and Instrumar, Ltd; over-the-horizon (OTH) investigations from the Ottawa antenna facility are continuing. The U.S. NOAA Wave Propagation Laboratory terminated HF remote sensing research activities as three companies were formed that are advancing the technology developed there into operational contexts: Codar Technology, Inc., Ocean Surface Research, and CODAR Systems Incorporated. In addition, NOAA, the U.S. Army Corps of Engineers, U.S. Coast Guard, and U.S. Navy have all begun programs integrating CODAR into their operations. Two major oil companies have begun using CODAR for offshore and Arctic observations. Finally, government sponsorship of OTH research and development for ocean surface observations continues at SRI International, based around their WARF antenna array.

Major efforts in both countries have focussed on understanding the limitations of, and optimizing methods for, the extraction of surface directional information using compact antenna systems. In this context, CODAR has begun operating from offshore platforms, and methods to handle antenna pattern distortions caused by the metal of the nearby rig structure have been developed. Objective, automatic, analysis methods to extract current and wave information from the sea echo, as well as ice/water drift from transponders, have been introduced. Research on models for propagation over ice and scatter from it continues at Memorial University of Newfoundland. The major observational advance of the period, however, appears to be the HF detection by of icebergs off Newfoundland by C-CORE last summer, and the simultaneous CODAR detection and mapping of pack-ice velocities from the ice echo in Prudhoe Bay by the U.S. CODAR team.

REMOTE SENSING OF SEA-STATE BY HF RADAR - DIRECTIONS FOR RESEARCH

Prof. E.D.R. Shearman

Department of Electronic &amp; Electrical Engineering, University of Birmingham, . .K.

Current HF ground-wave radar remote sensing technique for measuring ocean waveheight, wave-period and directional wave-spectrum centres on the use of second-order features of the received Doppler-spectrum from a patch on the sea. First-order interaction only yields information about approaching and receding waves and requires inconveniently low frequencies to sense swell.

For directional wave-spectrum observations, a steerable radar beam is useful in an area where a homogeneous sea can be assumed, such as around a platform. However, for longer range work, such as the current European interest for wave mapping in the Southern North Sea with its complex bottom topography by long range sensing from the sea coast, this approach is not useful.

Work in the U.K. is, therefore, focussed on developing radars with ranges of 100km or more and capable of yielding data on directional wave spectrum from a chosen patch of sea.

Such ranges imply the use of frequencies in the 5-15MHz band with consequent need to operate in a congested HF radio spectrum. Optimum strategies for radar technique in this environment are discussed. Experiments at the University of Birmingham have indicated the need for Bragg line to noise floor ratio of 40dB or more, to obtain useful signal second-order echoes.

To extract significant waveheight and first-moment wave-period data, short algorithms usable in near real time, have been developed, as described by L.R. Wyatt et al in a companion paper. The technology for such measurements thus appears to be available now.

For the more difficult problem of deriving the low frequency directional spectrum or the complete directional spectrum including wind-waves, more elaborate integral inversion or model-fitting approaches are required, as described by L.R. Wyatt et al. The use of two radars, with different look directions at a given sea area, may possibly be required and the processing is likely to require an array-processor for on-site analysis.

To obtain Doppler spectra of adequate signal-to-noise ratio, beam forming antenna systems and averaging over a period of 30 minutes, are required. To make measurements over a useful sector, parallel processing of the data from, say, 4 beams, appears to be desirable. Current studies of achievable directional patterns on practical coastal sites are reported.

Finally, some recent results on the Doppler characteristics of skywave propagation, relevant to long range skywave sea-state sensing, are reported.

## SS-1-3

### Propagation predictions for HF radar system planning

by

R. S. Gill, R. N. Herring, S. P. Kingsley, J. D. Milsom,  
J. M. Pielou, S. Rotheram.

In recent years, the authors have developed and implemented several propagation prediction algorithms which are proving useful in the design of HF radar systems. The algorithms are concerned with sky-wave and ground-wave propagation characteristics, clutter from meteor trail reflections and clutter associated with backscatter from a sea surface.

A sky-wave prediction method is described which incorporates a raytracing procedure, propagation loss factors, external noise estimates and a radar equation. The prediction scheme is described and some example results are presented for a hypothetical radar site in Southern England.

Three different ground-wave path loss prediction methods are in use. These are:- (a) Ott's integral equation method which can deal with terrain which varies in conductivity, dielectric constant, height and slope. (b) Furutsu's method which caters for ground with sections of different height and electrical properties. (c) Rotheram's method for a homogeneous ground but with an exponential atmosphere refractive index profile. In this third case Barrick's sea-state losses are also included. Example results are presented for each class of terrain.

Backscattered energy from meteor trails may confuse target detection processes. In sufficient numbers, the meteor echoes represent a source of Doppler spread clutter. A method of estimating the meteor trail detection rate for an h.f. radar is described and some example predictions are presented.

Finally, Lipa and Barrick's model of the first and second order Bragg backscattering spectrum of the sea surface has been extended to incorporate broad antenna beams, moving radar platforms and finite spectral resolution. Some example results are presented and compared with measured spectra.

**AN ESTIMATE OF THE COVERAGE EFFICIENCY OF  
HF SKYWAVE RADAR FOR MAPPING OCEAN WINDS AND WAVES**

J.W. Maresca, Jr., Vista Research, Inc.  
3600 W. Bayshore Rd., Palo Alto, CA, USA

T.M. Georges, J.P. Riley, NOAA/ERL  
325 S. Broadway, Boulder, CO, USA

C.T. Carlson, Sohio Petroleum  
5420 LBJ Freeway, Dallas, TX, USA

The operational utility of an HF skywave radar for monitoring ocean winds and waves depends on how frequently space-time-frequency windows with low ionospheric distortion can be found. The results of two radar experiments designed to make a first estimate of the coverage efficiency expected for a skywave radar operating under F-layer ionospheric conditions will be described. Both large-area and on-demand small-area mapping operations were tested over 3 days and 4 days, respectively. For wave measurements, the operational coverage efficiency, defined as the number of locations where high-confidence radar measurements were found divided by the total number of measurements attempted, was over 80%. Wind maps, covering the entire  $4 \times 10^6 \text{ km}^2$  radar coverage, were routinely produced in about an hour.

## SS-1-5

### SHIP DETECTION WITH HIGH RESOLUTION HF SKYWAVE RADAR

James R. Barnum  
Remote Measurements Laboratory  
SRI International  
Menlo Park, California

Ships can be detected at long ranges by high-frequency (HF) skywave backscatter radars that employ sufficient resolution in the radar spatial and Doppler frequency domains. The HF sea backscatter Doppler spectrum limits the target signal-to-clutter ratio (SCR), as a function of the ocean wave height distribution, wind direction, and radio frequency (Maresca and Barnum, IEEE AP, 30, 837-845, 1982). The SCR equals the ratio of mean target radar cross-section (RCS) to the mean sea clutter RCS, which is a sensitive function of Doppler frequency. A typical ship RCS for vertical polarization is 40 dBsm, which includes the target's ocean image. Within each radar spatial resolution cell, the sea clutter RCS can exceed 50 dBsm at the spectral line frequencies arising from first-order Bragg resonance.

Experimental data recorded at the ONR/SRI Wide Aperture Research Facility (WARF) over-the-horizon radar (OTHR) in central California demonstrate reliable detection of routine merchant shipping in the NE Pacific Ocean. WARF is a bistatic radar, transmitting approximately one MW average effective radiated power, and receiving with a 2.55-km broadside array of vertical monopole element pairs. The beamwidth is 0.5 deg at 15 MHz. The radar uses a linear frequency-modulated continuous wave (FMCW) waveform, that is typically swept over a 20-kHz bandwidth at a 5-Hz repetition rate. Swept bandwidths as high as 200 kHz have also been employed. Sufficient spectral resolution is achieved with a coherent integration time (CIT) of 12.8 s. Longer CITs, or the use of an autoregressive spectral analysis technique such as Marple's algorithm, can be employed to enhance Doppler resolution.

AN EXPERIMENTAL INVESTIGATION OF SKYWAVE SEA-STATE RADAR  
TECHNIQUES AT A LATITUDE NEAR THE AURORAL ZONE

E. Lloyd Winacott  
Communications Research Centre  
Department of Communications, Ottawa, Canada

In 1980 the Communications Research Centre (CRC) undertook a limited experimental programme to investigate the feasibility of measuring sea-state characteristics off the east coast of Canada by means of high-frequency skywave radar. The propagation path, from the radar receiver at Ottawa to the observation area east of Newfoundland and Labrador, was tangent to the auroral zone, at times within and at best only a few degrees of latitude south of the auroral absorption zone. The experiment was conducted on a number of occasions between October, 1980, and April, 1982, for a period of about six hours at midday on each occasion.

Several agencies were involved: CRC personnel designed and conducted the experiment, using the Sampled Aperture Receiving Array (SARA) facility, and carried out the bulk of the analysis; transmissions were provided from Ava, New York, by the Rome Air Development Center; the Centre for Cold Ocean Resources Engineering (C-CORE), at Memorial University in Newfoundland, assembled ground-truth maps, operated a transponder, and developed an algorithm for automatic derivation of wave direction.

CRC analysis techniques relied heavily upon computer-aided manual selection and interpretation of the Doppler spectra. Early attempts to construct automatic algorithms for the extraction of waveheight statistics encountered intractable problems, although the C-CORE wave-direction algorithm did meet with some success.

Under quiet ionospheric conditions it was found that waveheights frequently could be measured with acceptable accuracy, although accurate measurement was difficult when waveheights were low (2 metres). On the other hand, wave direction was easily derived; it emerged as a by-product of the waveheight analysis even when waveheights could not be measured accurately.

The project demonstrated that a skywave radar could function at northern latitudes, but the limitations of the experimental facilities left practicability still in question. Considerable improvement would be expected, however, if unlimited freedom of choice of operating frequency was permitted, if the transmitter signal was focussed to increase the power density in the target area, if the receiving array was more comprehensive, i.e., designed specifically for the task, and if the radar was located near the east coast, to move the ionospheric reflection area as much as possible out of the auroral absorption zone.

REMOTE SENSING WITH THE JINDALEE SKYWAVE RADAR

S.J. Anderson  
Electronics Research Laboratory  
Defence Research Centre Salisbury  
South Australia

The JINDALEE skywave radar is being developed primarily for defence surveillance of Australia's EEZ but its remote sensing potential has long been recognised. Studies which commenced in 1974 led to successful measurements of sea state and inferred surface wind fields in 1977/78 using a prototype radar; the current radar has been observing the Eastern Indian Ocean region since 1982.

The JINDALEE radar is now linked to the Australian Bureau of Meteorology regional forecasting centres by a facsimile transmission network. Wind maps surveying over a million square kilometres of ocean can be produced automatically in near real-time at the radar facility and transmitted directly to forecasters. This capability, which became operational in January 1985, is supported by active research programs directed at improving the scope and accuracy of the measurements as well as investigating a variety of meteorological and oceanographic phenomena.

This paper will present an overview of the JINDALEE remote sensing program with emphasis on the characteristics and performance of the operational system.

FREQUENCY MANAGEMENT SUPPORT FOR REMOTE SEA-STATE SENSING  
USING THE JINDALEE SKYWAVE RADAR

G.F. Earl and B.D. Ward  
Electronics Research Laboratory  
Defence Research Centre Salisbury  
South Australia

Successful operation of a skywave (over-the-horizon) radar in a remote sea-state sensing mode is critically dependent upon the application of comprehensive frequency management techniques. In addition to the problem of selecting a frequency yielding adequate signal-to-noise ratio in the geographical area under investigation, attention must be paid to the minimisation of ionospheric multimode and other phenomena capable of distorting or convoluting the sea backscatter.

This paper describes the manner in which these problems have been addressed in the JINDALEE skywave radar. Subsystems include backscatter and oblique-incidence sounding, HF spectral surveillance, and a low-powered frequency-agile "mini" radar capable of operating in a backscatter or oblique mode.



## HF RADAR TECHNIQUES - SPECIAL SESSION SS2

HF Radar and Ocean

1:30 - 5:00

Radar HF et mesures

Measurements: Currents

LAW 102

océaniques: courants

Chairperson/Président: **J.F.R. Gower**, Institute of Ocean Sciences, Sidney, BC

- 1 HF COASTAL OCEAN SURFACE RADAR OBSERVATIONS OF SURFACE CURRENTS. **M.L. Heron**, James Cook University, Physics Dept., Townsville, Australia
- 2 SOME LIMITATIONS ON THE APPLICATION OF HF OCEAN RADAR TO CURRENTS AND WIND DIRECTIONS. **M.L. Heron**, James Cook University, Physics Dept., Townsville, Australia
- 3 THE PERFORMANCE OF THE RAL OCEAN SURFACE CURRENT RADAR SYSTEM. **D. Eccles**, **F.D.G. Bennett**, **G.M. Howes**, **K. Slater**, Rutherford Appleton Laboratory, Didcot, UK
- 4 EVALUATION OF HF GROUNDWAVE RADAR ON THE NOVA SCOTIAN SHELF. **D.J. Lawrence**, **P.C. Smith**, Bedford Institute of Oceanography, Dept. of Fisheries and Oceans, Dartmouth, NS
- 5 SURFACE CURRENTS STUDIES USING HF RADARS. **P. Broche**, Université de Toulon, Lab. de Sondages Electromagnétiques de l'Environnement Terrestre, Toulon, France
- 6 ENVIRONMENTAL CONSIDERATIONS FOR CODAR CURRENT MEASUREMENTS. **P.H. LeBlond**, University of British Columbia, Dept. of Oceanography, Vancouver, BC
- 7 SURFACE CIRCULATION IN THE DELAWARE BAY OBTAINED FROM CODAR SEA ECHO AND TRANSPONDER TRACKING. **J.M. Hubertz**, US Army Corps of Engineers/CERC, Vicksburg, MI, USA; **R.G. Williams**, NOAA/NOS, US Dept. of Commerce, Rockville, MD, USA; **D.E. Barrick**, **B.J. Lipa**, Ocean Surface Research, Boulder, CO, USA
- 8 CODAR MEASUREMENTS FOR A SEMI-SUBMERSIBLE DRILLING VESSEL. **M.W. Spillane**, Gulf Oil Exploration and Production Company, Houston, TX, USA; **B. Braennstroem**, Saga Petroleum, Hovik, Norway
- 9 MULTIFREQUENCY HF RADAR OBSERVATIONS OF CURRENTS AND CURRENT SHEARS. **C.C. Teague**, Stanford University, Stanford, CA, USA
- 10 FOUR-ELEMENT CODAR BEAMFORMING. **P.K. Jeans**, C-CORE, St. John's, NF; **R. Donnelly**, Carleton University, Ottawa, ON

## SS-2-1

### HF COASTAL OCEAN SURFACE RADAR OBSERVATIONS OF SURFACE CURRENTS

M.L. Heron, Physics Department, James Cook University, Townsville,  
Australia

An HF coastal ocean surface radar was deployed in an experiment off Western Australia along with a current meter drogue tracking and wind stations. The radar was a two-station configuration, running simultaneously on 30 MHz to observe surface currents and wind directions.

During a 28-hour continuous radar run a weak meteorological cold front passed across the network with embedded strong winds backing through nearly 300°.

The surface currents respond quickly to the changing wind while the deeper water (12m deep) is essentially unaffected. By incorporating current observations from a collocated current meter and drogue tracking at various depths we can construct a working model for the shear layer thickness between the wind-driven surface layer and the deep water.

The radar-observed currents follow the formation of a residual eddy within the mapped field during the 28-hour period. Lagrangian trajectories calculated from half-hourly current maps show how an oceanic front (slick line) is formed.

The surface current maps provided by the radar are of good quality and are on time and space scales which would be very expensive by conventional methods. These results are unique for coastal engineering and in the study of the mobility of surface pollutants and nutrients.

This work was done under the auspices of Centre for Water Research, University of Western Australia.

SOME LIMITATIONS ON THE APPLICATION OF HF OCEAN RADAR  
TO CURRENTS AND WIND DIRECTIONS

M.L. Heron, Physics Department, James Cook University, Townsville,  
Australia

A 30 MHz coherent pulsed radar with a beam-forming antenna array has been deployed in several locations in Australia in experiments with other oceanographic and meteorological instruments. The radar results have provided unique and useful input to the larger scale experiments. However the supporting observations help to reveal some apparent limitations to the radar technique in three areas.

- (1) Wind directions are obtained using the  $\cos^2\theta/2$  algorithm. Commonly used S values (e.g. Tyler et al., Deep Sea Res., 21, 989-1016, 1974; Mitsuyasu et al., J. Phys. Oceanog., 5, 750-760, 1975) do not work at short fetches and/or at low wind speeds. There is evidence that under some conditions the form of the algorithm itself is not a good model.
- (2) Line broadening or even splitting of the first-order lines sometimes occur in the backscatter spectra. This occurs when the surface current vector field is not uniform across the target cell and reduces the reliability of the technique.
- (3) Currents derived from the radar are surface currents. The surface layer is stressed by momentum transfer from the wind as well as from the deeper water. Care needs to be exercised in interpreting the radar-observed currents in terms of mass transport of water.

These limitations do not negate the value of the radar observations in coastal engineering and management but they are a part of the operational experience required. Examples of these effects are given and strategies suggested for extracting useful geophysical data. In some cases the apparent limitation can be turned to advantage in providing further information about the flow structure.

## SS-2-3

### THE PERFORMANCE OF THE RAL OCEAN SURFACE CURRENT RADAR SYSTEM

D Eccles, F D G Bennett, G M Howes, and K Slater

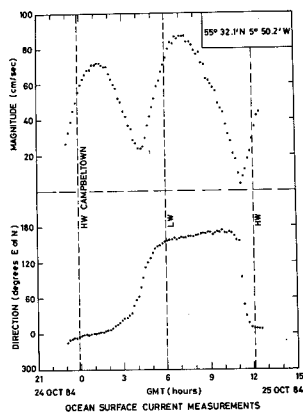
Rutherford Appleton Laboratory, Chilton, Didcot, Oxon, OX11 0QX,  
UK

The Ocean Surface Current Radar (OSCR) system developed at the Rutherford Appleton Laboratory has undergone a series of trials. These have demonstrated that the system can yield values of surface current which are extremely self consistent in both time and space out to a maximum range of 40 km.

The system consists of two HF radars, spaced approximately 20 km apart, each having a beam-forming receive antenna, which enables the radar signals back-scattered from the sea surface to be acquired from 16 different directions by each radar. Thus, in principle, vector current measurements can be made at the 256 points where the radar beams intersect. The radar receivers are identical to those used in the CODAR system, but by adopting the beam-forming approach, the need to rely on the direction-finding technique, employed in the CODAR system, is eliminated. It is believed that the high quality of the data obtained (see figure) is due, partly to the fact that there is no uncertainty in determining the direction of the radar returns, and partly as a result of the signal processing techniques used. OSCR has been shown to perform satisfactorily on a variety of sites; these have included sites located on a cliff top, behind a rocky foreshore, and near the high-tide mark on an ordinary beach.

The radars are computer controlled, and can be programmed to automatically collect and process the signals received, to produce radial current information from any 6 of the 16 available beams, each half hour, for a period lasting up to several days. The data from both sites are subsequently combined and displayed in the form of, (a) tidal plots of the current magnitude/direction and (b) surface current maps.

It is concluded from comparisons made with current meters, and also from the self consistency of the data obtained, that the OSCR system is capable of measuring currents to an accuracy of one or two cm/sec. The trials have proved that the system is transportable, and can be used to obtain detailed information about the flow of water in regions where the influence of coastal topography on the current patterns is pronounced.



## EVALUATION OF HF GROUNDWAVE RADAR ON THE NOVA SCOTIAN SHELF

D.J. Lawrence and P.C. Smith  
Atlantic Oceanographic Laboratory  
Department of Fisheries & Oceans  
Bedford Institute of Oceanography  
Nova Scotia, Canada B2Y 4A2

A surface current measurement and intercomparison experiment was conducted off southwest Nova Scotia, 14-26 November 1984. Remotely-sensed currents collected by a two-site HF Groundwave Radar (CODAR) will be compared to: a) direct Eulerian current measurements which were made with a surface mooring having an electromagnetic current meter at 1 m depth and a vector measuring current meter at 1.5 m and b) Lagrangian drifters of various effective depths tracked acoustically and by aerial photography. To assist in the evaluation of all current measurements, the wind field was measured from the ship and the directional wave spectrum from a moored buoy. The site, at the entrance of the Bay Fundy-Gulf Maine system, is dominated by strong tides (100 cm/s). Comparisons will be done with a nearby long term (1 year) current meter mooring and with the barotropic numerical model of the system.

## SURFACE CURRENTS STUDIES USING HF RADARS

P. Broche

Laboratoire de Sondages Electromagnétiques de l'Environnement Terrestre, Université de Toulon, 639 Bd des Armaris, 83100 Toulon, FRANCE

Measurements of surface coastal currents have been performed for a few years by using simultaneously, over the same area, two HF Doppler radars with directional antennae, the beam of which can be electronically scanned. First, the processes used to combine measurements of radial velocity performed by the two radars to obtain a bidimensional map of current velocity vector ( linear interpolations) are described with a special attention devoted to estimation of experimental inaccuracies and their propagation along all the computations. Both a theoretical and a direct estimate of intrinsic accuracy lead to the same order of magnitude ( 2 to 5 cm/s, at a radar frequency of 10 MHz, and in the actual conditions of measurements), and the final accuracy on each cartesian component of the current may reach a ten of cm/s in the same conditions.

Examples of results are then given, concerning:

-a study of the tidal circulation in the western part of Baie de Seine ( part of the Channel). Radar measurements, due to their high spatial density, have been used for a comprehensive validation of a numerical model of tides in this area, driven by independant water level estimates on the open border of the Baie.

-a study of surface wind-driven currents ( following an experiment on the French Mediterranean coast). Measurements have been obtained at two different radar frequencies, i.e. in fact at two different depths ( respectively 1 and 2 meters), and the observed currents have been compared together and with the wind speed on the shore. Original informations about the nature and the parameters of the wind-current relationship that can be inferred from this comparison are discussed.

One of the limitations of HF technique is in its relatively limited space-discrimination ( of the order of one kilometer), which decreases its potential interest for the very littoral areas ( in the range 0-10 km from the shore) where the space-scale of the phenomena may be shorter. For this prospect, a tentative use of a higher frequency radar ( in fact, a meteorological radar, operating near 50 MHz), which uses shorter pulses ( a few microseconds, corresponding to a few hundreds of meters) is now investigated ( indeed, its maximum range is shorter). Preliminary results of a first experiment performed in Etang de Berre, near Marseille, are described.

## ENVIRONMENTAL CONSIDERATIONS FOR CODAR CURRENT MEASUREMENTS

Paul H. LeBlond  
Department of Oceanography  
University of British Columbia

A review of environmental considerations relating to CODAR (Coastal Ocean Dynamics Application Radar) ocean current measurements has been conducted in order to arrive at **operational** guidelines for this system. Hydrodynamic **effects** considered included the directional spread of ocean waves, departures from linear phase speed and near surface shears. A review of field measurements and of comparisons with in-situ sensors was also carried out. It is suggested that CODAR current measurements would be most accurate under moderate sea states when the wavelength of the peak of the spectrum is near that for first order Bragg scattering of the radar signal. For 25.4 MHz radar this would correspond to wind waves with spectral peak wavelength in the range  $4.0 \text{ m} < \lambda < 7.5 \text{ m}$ . Spatial and temporal averaging or radar return echoes also limit measurements to currents of sufficiently slow variation in space and time; good results have been obtained for tidal and inertial flows. Flow speeds measured should also exceed about 25 cm/s for errors inherent in the system (at best  $\approx 5 \text{ cm/s}$ ) to remain relatively small.

SURFACE CIRCULATION IN THE DELAWARE BAY OBTAINED FROM  
CODAR SEA ECHO AND TRANSPONDER TRACKING

J.M. Hubertz  
U.S. Army Corps of  
Engineers/CERC  
Vicksburg, MI 39810

R.G. Williams  
NOAA/NOS  
U.S. Dept. of Commerce  
Rockville, MD 20852

D.E. Barrick  
B.J. Lipa  
Ocean Surface Research  
Boulder, CO 80303

In conjunction with NOAA's circulation survey of the Delaware Bay in Summer/Autumn, 1984, two CODAR sites were located on the Southwestern shore. Taking sea-echo data every 1.5 hours for a month, the system produced real-time map files of surface-current vectors and their uncertainties over the broad expanse and mouth of the bay. The spatial detail and temporal continuity of these CODAR surface-current maps will aid in developing and improving 3-dimensional circulation models for the bay; presently existing, vertically-integrated models are known to be most inaccurate near the surface. CODAR maps show semi-diurnal, tidal-dominated circulation, on which is superposed surface flow that follows the wind; interesting features such as gyres at slack tide seem to form at the mouth and propagate inward with the group speed of the tidal surge.

In addition, three drifters (drogued to the upper 1 meter) equipped with HF transponders were released near the center of the bay and allowed to drift for five days. Every 1.5 hours, the CODAR obtained their positions and velocities, concurrent with surface current mapping done from the sea echo. The drifters provide both Lagrangian tracks and instantaneous Eulerian velocities at their interrogated locations. These are compared with CODAR surface current data extracted from sea echo, and both are compared to simultaneous current measurements made by a bottom-mounted acoustic profiler.

## Codar Measurements for a Semi-submersible Drilling Vessel

M. W. Spillane\* and B. Braennstroem\*\*

- \* Senior Project Engineer, Gulf Oil Exploration and Production Company, Frontier Technology Department, P. O. Box 36506, Houston, Texas 77236
- \*\* Vice President, Saga Petroleum, a.s., Maries Vei 20, P. O. Box 9, 1322 Hovik, Norway

In 1982, Gulf Oil Exploration and Production Company initiated a development program to adapt the CODAR HF-Radar System for deployment from floating drilling vessels, for real-time measurement of surface currents, directional wave spectra and wind. The final test phase of the program was begun in the Spring of 1984. In cooperation with Saga Petroleum a.s., a CODAR system was installed aboard the "Treasure Saga" semi-submersible, drilling in the Norwegian sector of the North Sea. The principle objectives of the test were to verify the ability of CODAR to operate from a moving platform, and to implement the real-time processing software.

The CODAR crossed-loop antenna was mounted at the top of the derrick, 80 meters above the waterline, to minimize pattern distortion due to the vessel superstructure, and to eliminate any interference with marine VHF communication equipment. The antenna differed from an earlier version used offshore in the Gulf of Mexico, since it was designed to operate at either 25.4 MHz or 6.8 MHz, depending on the sea-state and vessel motion.

Results that will be presented include:

- A review of the Gulf/CODAR project field tests in the Gulf of Mexico and Northern California;
- CODAR measurement of surface currents in the Troll and Snorre fields offshore Norway.

**MULTIFREQUENCY HF RADAR OBSERVATIONS  
OF CURRENTS AND CURRENT SHEARS**

Calvin C. Teague  
Stanford University

Techniques have been developed for using high-frequency (HF) surface-wave radar to measure ocean currents and vertical current shears in the upper one or two metres of the ocean surface. An HF radar can precisely measure the phase velocity and direction of propagation of ocean waves whose wavelength is one-half the radar wavelength. In the absence of a current, the speed of the waves is given by the still-water dispersion relation. An underlying current will modify this speed. The radar measures the actual phase velocity through a Doppler shift, and the wavelength of the ocean wave is known through the first-order Bragg scattering relation, so a difference between observed and theoretical still-water phase velocity can be calculated. In addition, longer ocean waves are affected by currents at deeper depths than are shorter ocean waves. By measuring the phase velocity at several different wavelengths, it is possible to measure a vertical current shear in the top one or two metres of the ocean surface. This is a measurement that is very difficult to make by any other means.

A portable coherent, pulsed-Doppler HF radar system was developed at Stanford and used in several experiments, both on land on the California coast and on board a ship during the JASIN experiment. The land-based experiments demonstrated that a current could be measured by an HF radar, and that its value agreed well with that measured by *in-situ* drifting spar buoys. In addition, there was evidence of a vertical current shear, both from the radar measurements and from the buoy measurements. The JASIN experiment was an attempt to apply these techniques to the measurement of surface current and current shear in the open ocean. The radar system was installed on board a ship, along with a receiving antenna consisting of a steerable phased array of eight wideband loops. The steerable antenna was quite rugged and performed as expected. It produced antenna patterns consistent with the physical aperture of the array. The wind velocity during the JASIN experiment was quite low, so wind- and wave-generated currents were quite small. Nevertheless, there is some evidence of a current shear. Its magnitude is small and near the resolution limit of the radar, but it appears to be about 50% higher than what would be expected from the wind and wave conditions present at the time of the experiments.

FOUR-ELEMENT CODAR BEAMFORMING

by P.K. Jeans; C-CORE, St. John's, Nfld.  
R. Donnelly; Ph.D student, Carlton Univ., Ottawa, ON.

An high frequency groundwave radar called CODAR (Coastal Ocean Dynamics Application Radar) is presently being used in several forms to measure ocean surface parameters. The original version was developed at NOAA (National Oceanic and Atmospheric Administration) and utilizes a small four-element receive array as compared to its wavelength. The array consists of four equally spaced elements arranged on a circle of  $0.2151$  wavelengths (at 25 Mhz.). It was designed to measure ocean currents using direction finding techniques based on an extension to a simple two-element interferometer. The problem of determining the bearing of a radiating source can be readily shown to be equivalent to that incurred in spectral estimation. In an attempt to improve upon the processing of existing data, modern nonlinear spectral estimation techniques are applied in a beamforming bearing estimation procedure and compared against several direction finding algorithms. Enhancement of bearing estimators via analysis of the eigenstructure of a spatial correlation matrix is included. Antenna response patterns are calculated and used to investigate properties of direction finding algorithms. Both real and simulated data are used for a comparison of direction finding and beamforming. The asymmetrical bias of each method is investigated to determine its effect on the error in estimating the angle of arrival of a radar target.



## HF RADAR TECHNIQUES SPECIAL SESSION SS3

HF Radar and Ocean  
Measurements: Waves and Ice

8:30 - 12:00  
LAW 102

Radar HF et mesures  
océaniques: vagues et glace

Chairperson/Président: **M.L. Heron**, James Cook University, Townsville, Australia

- 1 RIJKSWATERSTAAT'S INTEREST IN THE H.F. RADAR. **J. van Heteren**, Directorate for Water Management and Hydraulic Research, Rijkswaterstaat, Hellevoetsluis, The Netherlands
- 2 HF RADAR MEASUREMENTS OF OCEAN WAVE PARAMETERS DURING NURWEC. **L.R. Wyatt, J. Venn, M.D. Moorehead, G.D. Burrows, A.M. Ponsford**, Birmingham University, Dept. of Electronic and Electrical Engineering, Birmingham, UK; **J. van Heteren**, Rijkswaterstaat, The Netherlands
- 3 USE OF NARROW-BEAM HF SURFACE-WAVE RADARS FROM THE NETHERLANDS COAST FOR NORTH SEA WAVE MONITORING. **J.W. Maresca Jr.**, Vista Research, Palo Alto, CA, USA; **D.E. Barrick**, CODAR Systems Inc., Longmont, CO, USA; **J. van Heteren**, Rijkswaterstaat, Hellevoetsluis, The Netherlands
- 4 ANALYSIS METHODS FOR NARROW BEAM HIGH-FREQUENCY RADAR SEA ECHO. **B.J. Lipa, D.E. Barrick**, NOAA Tech Rep., Wave Propagation Lab., Boulder, CO, USA
- 5 CODAR MEASUREMENT OF THE OCEAN WAVEHEIGHT DIRECTIONAL SPECTRUM. **B.J. Lipa, D.E. Barrick**, Ocean Surface Research, Woodside, CA, USA
- 6 MEASURING SEA ICE MOTION WITH HF CODAR DOPPLER TRANSPONDERS. **R.D. Crissman**, Gulf Oil Exploration and Production Company, Frontier Technology Dept., Houston, TX, USA; **M.W. Evans**, Codar Technology Inc., Longmont, CO, USA
- 7 MAPPING ARCTIC PACK-ICE BREAKUP FROM DIRECT ICE ECHOES. **M.W. Evans, B.J. Lipa, D.E. Barrick**, CODAR Systems Inc., Longmont, CO, USA; **R.D. Crissman**, Gulf Oil Exploration and Production Company, Frontier Technology Dept., Houston, TX, USA
- 8 REMOTE SENSING OF ICEBERGS BY HF GROUND WAVE DOPPLER RADAR. **J. Walsh, S.K. Srivastava, B.J. Dawe**, Memorial University of Newfoundland, St. John's, NF
- 9 AN ANALYTICAL MODEL FOR THE HF BACKSCATTERED DOPPLER SPECTRUM FOR THE OCEAN SURFACE. **S.K. Srivastava, J. Walsh**, Memorial University of Newfoundland, St. John's, NF
- 10 UNDERSTANDING AND DEALING WITH ANTENNA PATTERN DISTORTIONS IN CODAR SYSTEMS. **D.E. Barrick, B.J. Lipa**, Ocean Surface Research, Boulder, CO, USA

RIJKSWATERSTAAT'S INTEREST IN THE H.F. RADAR

J. van Heteren, Directorate for Water Management and Hydraulic Research, Coastal and Maritime District Hellevoetsluis Division

Rijkswaterstaat (RWS), one of the departments of the Ministry of Transport and Public Works in the Netherlands, is responsible for water management and protection of the land against the sea. To the safety of the Dutch Coast wave information is of vital importance. However, not only safety but also economical reasons play a role in the need of wave information.

To monitor the wave movement wave measuring networks are used consisting of a large number of wave measuring stations located at the North Sea. The data are transmitted using a datacommunication system to a center, where the data are analysed to give the information required. However, in spite of the high density of wave measuring stations the total wave information from such a large area as the North Sea is rather limited. Other disadvantages are the uncertainty with respect to the representativity for a wider area, the high costs for attachment and maintenance of sensors and data transmission systems, etc. Therefore, RWS is very interested in ground wave narrow beam H.F. radar systems, which would provide us with far more information of a very large area. A first necessity is to get knowledge on this radar system.

A nice opportunity was a cooperation with the University of Birmingham, which has been involved in the development of such a radar. This cooperation moulded into a joint experiment near Pembroke, called NURWEC (=Netherlands United Kingdom Radar Wave buoy Experimental Comparison). During NURWEC the WAVEC, a pitch and roll buoy provided by RWS, was deployed at one fixed position, in the center of the nearest radar cell, boresight of the radar. It is intended that the results of this experiment will be presented by prof. E.D.R. Shearman of the Birmingham University at the Re URSI meeting on H.F. radar.

Since the results of this experiment are promising RWS examines the possibility to instal a three-site ground wave narrow beam H.F. radar system in the Netherlands. Dr. J.W. Maresca, Jr. and Dr. D.E. Barrick prepared a proposal for a design study of a North Sea H.F. radar wave measurement system which is being studied by RWS. Dr. Barrick intends to present the design study at the Re URSI meeting on H.F. radar.

The present paper is meant as an introduction to those of Prof. Shearman and Dr. Barrick.

HF RADAR MEASUREMENTS OF OCEAN WAVE PARAMETERS  
DURING NURWEC (Netherlands/UK Radar, Wavebuoy Experimental Comparison)

L.R.Wyatt, J.Venn, M.D.Moorhead, G.D.Burrows, A.M.Ponsford  
DEPT. OF ELECTRONIC AND ELECTRICAL ENGINEERING  
BIRMINGHAM UNIVERSITY

J. van Heteren  
RIJKSWATERSTAAT, NETHERLANDS

The HF ground-wave technique has now evolved to the stage at which it is capable of yielding measurements of surface current, significant wave-height, mean wave period, non-directional and directional wave spectra. These measurements are deduced from the Doppler spectrum of the radar echoes from a selected patch of the sea.

The University of Birmingham (with the support of the UK Science and Engineering Council) has concentrated on the development of an HF radar optimised for wave measurement and surveying an area of sea some 100km in radius by 90deg in azimuth. This radar is operating at the University's field station at Angle, Pembroke in south-west Wales.

The processes which enable the radar to "see" the ocean surface wave spectrum are highly non-linear and the accuracy of methods that have been developed to extract wave information can only be quantitatively assessed by comparing results directly with alternative wave measuring instruments. Such a comparison should also help to improve the existing extraction algorithms or suggest alternative approaches. The main aim of the Nurwec experiment was to provide a data set for this comparison covering as wide a range of meteorological and oceanographic conditions as possible. The principle source of "sea truth" data was provided by a Datawell WAVEC buoy deployed 30km offshore by the Dutch Rijkswaterstaat with help from the Institute of Oceanographic Sciences. The experiment ran from 17th October to 10th December 1983 during which time over 110 hours of good quality radar data were collected and archived.

These data have been processed to yield estimates of significant waveheight and mean period for up to eight radar resolution cells from 15.0 to 67.5km offshore. The data in the 30km cell are highly correlated with the WAVEC estimates with mean differences of less than 0.7 secs (11.5%) in mean period and of about 26% in significant waveheight. A positive bias of about 20% was found for the radar estimates of waveheight which is attributed to uncertainties in the first order part of the Doppler spectrum. This is under study and we hope to improve the accuracy by increasing the frequency resolution in the Doppler spectrum.

SS-3-3

**USE OF NARROW-BEAM HF SURFACE-WAVE RADARS FROM THE  
NETHERLANDS COAST FOR NORTH SEA WAVE MONITORING**

J.W. Maresca, Jr.                      D.E. Barrick                      J. van Heteren  
Vista Research      CODAR Systems Incorporated      Rijkswaterstaat  
Palo Alto, CA 94303      Longmont, CO 80501      Hellevoetsluis, Netherlands

Because of its vulnerability to storm waves from the North Sea, the Netherlands has undertaken extensive programs for observing, modelling, and predicting wave conditions at its coasts and harbors. Under consideration for real-time monitoring of the waveheight directional spectrum is a network of narrow-beam HF surface-wave backscatter radars. Considerable analysis is involved in trading off the system cost with the performance necessary to meet the required observational objectives and accuracies.

By operating at a lower frequency (e.g., 6-12 MHz), distances of 150-200 km can be achieved, allowing land-to-land coverage across the channel. Lower frequencies circumvent the "saturation effect" as well, whereby higher waves produce little change to the second-order echo from which information is extracted. Three such sites could provide real-time monitoring around the entire Netherlands coasts. In addition, the ability of at least two sites to observe the same ocean area increases the directional accuracy for waveheight spectral inversion from the second-order Doppler echo, over that possible with single-site operation. With multiple-site narrow-beam operation, no assumptions need be made about wavefield homogeneity over the coverage area.

**ANALYSIS METHODS FOR NARROW BEAM HIGH-FREQUENCY  
RADAR SEA ECHO**

B.J. Lipa, D.E. Barrick  
NOAA Tech Rep., ERL 420-WPL 56  
Wave Propagation Lab.  
Boulder, CO, USA

A model fitting technique has been developed to extract the longwave directional spectrum from the Doppler spectrum of the received signal. This technique is an extension of one developed by Lipa and Barrick(1982) and extends the ocean wave frequency range that can be measured using radar frequencies in the low HF range (6-18MHz). All the NURWEC data with signal to noise greater than 40dB has been analysed in this way and compared with the Wavec measurements. The results will be presented to demonstrate the accuracy and the many limitations of the techniques. Work in progress aimed at extending the model fitting technique to have more general application will be discussed.

## SS-3-5

### CODAR MEASUREMENT OF THE OCEAN WAVEHEIGHT DIRECTIONAL SPECTRUM

B.J.Lipa and D.E.Barrick  
Ocean Surface Research  
165 Harcross Rd., Woodside, CA 94062

The use of CODAR for the automatic real-time measurement of ocean surface current maps is well established. We are at present developing a similar capability for the measurement of the ocean waveheight directional spectrum. In this paper, we describe the analytical methods on which the software is based: the inversion of an integral equation expressing the second-order radar sea-echo in terms of the directional spectrum and the surface current field in water of arbitrary depth. The surface current field is obtained from the first-order radar spectrum and substituted in the integral equation which is then inverted to give estimates of the directional spectrum. These methods are illustrated by application to data taken during the ARSLOE experiment and results compared with data measured by the NOAA data buoy XERB. A future experiment is planned for the California coast next winter with detailed comparisons between real-time CODAR wave measurements and surface truth.

## SS-3-6

### Measuring Sea Ice Motion with HF CODAR Doppler Transponders

Randy D. Crissman\* and Michael W. Evans\*\*

- \* Project Engineer, Gulf Oil Exploration and Production Company, Frontier Technology Department, P. O. Box 36506, Houston, Texas 77236
- \*\* President, Codar Technology, Inc., 1428 Florida Avenue, Longmont, Colorado 80501

Gulf Oil Exploration and Production Company completed two major phases in the development of a high frequency (HF) CODAR Doppler transponder system for measuring sea ice motion in 1983 and 1984. The system measures positions and instantaneous velocities of transponders deployed on the ice with accuracies of  $\pm 160$  ft. ( $\pm 50$  m) and  $\pm 0.003$  ft./sec. ( $\pm 0.001$  m/sec.), respectively, at ranges up to 38 miles (60 km). Each phase of the development involved a field deployment of the system in the Beaufort Sea, Alaska. The 1983 field program assessed the basic concept of using the system to measure ice motion. Based on the encouraging results of the 1983 program, Gulf committed to a major field demonstration of the system in 1984. The 1984 program demonstrated the capability of the system to accurately measure real-time velocities and positions of up to 25 transponders deployed on sea ice. Such data is considered to be valuable in developing reliable design, construction, and operation criteria for Arctic offshore structures and systems.

MAPPING ARCTIC PACK-ICE BREAKUP FROM DIRECT ICE ECHOES

M.W. Evans  
B.J. Lipa  
D.E. Barrick  
CODAR Systems Incorporated  
Longmont, CO 80501

R.D. Crissman  
Gulf Oil Exploration and  
Production Company  
Frontier Technology Department  
Houston, TX 77236

During June-July, 1984, two CODAR stations were deployed on islands in Prudhoe Bay (Alaska) to observe the summer pack-ice movement and breakup. Although normal ice operations rely on HF transponders embedded in the ice to record movement, the systems also observe and record echoes from other scatterers in the radar cells. These scatterers must be moving in order to identify and separate their echoes in Doppler shift from the carrier frequency that is always present in the received signals. During breakup, the solid ice cover on the Beaufort that extends down to the Alaskan coast most of the year begins to melt and move more rapidly, giving rise to mixed coverage conditions which include areas of open water along with low-profile pack ice. These separate surface regions in an annular CODAR resolution cell could be expected to produce echoes from both the moving ice pieces as well as from the Bragg scattering waves in the open sea areas.

Quite strong, direct echoes from moving ice during these periods were observed and processed to give maps of ice velocity vectors; the Bragg scatter echoes from the short sea waves were processed in the usual way to give surface-current maps for the open water regions. The normalized backscatter radar cross section per unit area for pack ice at 25 MHz is estimated from the data, along with density of ice coverage. The latter is compared to optical and SLAR maps of ice cover made from aircraft during the same period. Ice velocities from the direct echoes correlate with those measured by the transponders, and both follow the wind quite closely.

REMOTE SENSING OF ICEBERGS BY HF GROUND WAVE  
DOPPLER RADAR

John Walsh\*, Satish K. Srivastava\*, and Barry J. Dawe\*\*

\* Faculty of Engineering and Applied Science

\*\* Centre for Cold Ocean Resource Engineering  
Memorial University of Newfoundland  
St. John's, Newfoundland, Canada, A1B 3X5

An analytical technique has been developed for estimating the forward propagated and backscattered EM fields for mixed paths with discontinuities. The approach is based on the concept of generalized functions instead of classical methods and it is open to any finite source. The technique has been applied to the remote sensing of icebergs by predicting the backscattered cross-section for assumed iceberg models. The source used for these estimates is an elementary vertical electric dipole, located close to the surface. The resulting cross-sections are found to be dependant on the shape, size, and orientation of the modelled icebergs, which is expected physically. A similar technique has also been used to estimate the backscattered Doppler spectrum from the ocean surface. A model for EM propagation over a spherical earth, based on classical methods, has been used to predict forward and reverse transmission losses. However, this model includes a modified surface impedance, which accounts for layering and surface roughness effects. Based on the above results a software model for the detection of icebergs using HF Doppler radars has been developed. The model also accounts for the standard atmospheric and man-made noise estimates.

An experiment was designed to test the validity of the iceberg detection model. This experiment was recently conducted at Byron Bay, Labrador. The hardware used was an HF Doppler radar, operating at 25.40 MHz. The transmitting antenna was a three element yagi array and the receiving antenna was a 24 element, narrow beam, linear array. Data was recorded for a considerable number of icebergs at various ranges within the receiving beam pattern over a period of two weeks. Azimuth and range ground-truthing were provided by transit and marine radar. Aerial photography was used for shape and size estimation of the icebergs. The data is presently being analyzed for testing the validity of the above software model. The preliminary results are very encouraging and strongly suggest that HF radars are effective ice hazard remote sensors.

**AN ANALYTICAL MODEL FOR THE HF BACKSCATTERED  
DOPPLER SPECTRUM FOR THE OCEAN SURFACE**

Satish K. Srivastava and John Walsh  
Faculty of Engineering and Applied Science  
Memorial University of Newfoundland  
St. John's, Newfoundland, Canada, A1B 3X5

The classical Rayleigh-Rice perturbation method has been used by many investigators for the analysis of EM scattering from rough surfaces. By using an alternative approach the authors have developed an analytical technique for deriving the scattered EM field from rough surfaces. The technique is open to any finite source. An application of this method has yielded estimates for the average first and second order backscattered Doppler spectrum for an assumed model of the ocean surface (J.Walsh and S.K.Srivastava, Digest National Radio Science Meeting, Boston, pp 55, 1984). The source is assumed to be an elementary vertical electric dipole having a periodic, pulsed, sinusoidal excitation and the receiving antenna is assumed to have a narrow beam width. The first order represents single scattering at the primary ocean surface patch. The first term of the second order represents double scattering at the primary patch. These results are the same as those derived by other investigators using the above perturbation method, for a plane wave incident field. However, our second order result contains two additional terms. The first additional term represents first scattering at the source point and second scattering at the patch. The second additional term represents off the patch double scattering. The use of a dipole source accounts for these additional terms.

The above analysis has been extended for a wide beam or omnidirectional receiving antenna. For this antenna configuration two more contributions to the second order result have been identified. The first new term accounts for first scattering at the patch and the second scattering at the source point. The second new term accounts for first scattering at any point between the source and the patch and the second scattering occurring at a point in the opposite direction such that all the first and second order signals are received at the same time. Complete expressions for these terms are given. This constitutes a more complete model for HF scattering from the ocean surface, thus providing an improved estimation of the radar return when using an HF Doppler radar, for a general antenna configuration.

UNDERSTANDING AND DEALING WITH ANTENNA PATTERN  
DISTORTIONS IN CODAR SYSTEMS

Donald E. Barrick  
Belinda J. Lipa  
Ocean Surface Research  
Boulder, CO & Woodside CA

CODAR embodies the use of compact antennas at HF for directional information, rather than large phased arrays that are impractical in a host of coastal and offshore applications. Distortions from the ideal omnidirectional pattern of the vertical monopole/dipole, or the ideal cosine pattern of the small loop, will produce significant biases in the extraction of directional information from such systems. The use of MININEC, a widely available moment-method numerical electromagnetics computer code, has identified and quantified several sources of distortions: (i) mutual coupling among the four whips in the original CODAR square receiving array; (ii) interaction with metallic structures (such as the tower on an offshore oil rig) in the antenna near field; (iii) radiation from unbalanced feeder lines.

When the identified distortion cannot be eliminated, as in the case of CODAR operation from an offshore metal platform, it must be quantified by either applying the above computer code to solve for the pattern exactly, and/or by measuring the pattern. Then the actual, distorted patterns are used in the least-squares solutions for the desired ocean directional parameters (e.g., current vectors, wavefields, transponder-drifter tracks) and their uncertainties. Examples of distorted patterns measured for CODAR operating from an offshore rig in the North Sea are shown. The method described above is then applied to measured sea-echo data, and the extracted surface-current maps exhibit none of the chaotic nature they had when distortions were ignored.



## AP-S/URSI COMMISSION F - JOINT SESSION/SESSION JOINTE

<b>Wave Propagation/ Land Mobile</b>	1:30 - 5:00 IRC-3	<b>Propagation des ondes / systèmes mobiles</b>
--	----------------------	---

Chairperson/Président: **R.J. Bultitude**, Communications Research Centre, Ottawa, ON

- 1 "SPECTRAL" ANALYSIS OF THE CLASSICAL SOMMERFELD PROBLEM. **D.S. Gilliam**, Texas Tech University, Dept. of Mathematics, Lubbock, TX, USA; **J.R. Schulenberger**, ANAH Res. Corp., Tucson, AZ, USA
- 2 THE DETERMINATION OF ATMOSPHERIC PROPAGATION PARAMETERS AT OPTICAL AND MILLIMETER WAVELENGTHS VIA THE STATISTICAL FOURIER OPTICAL METHODS. **R.M. Manning, F.L. Merat**, Case Western Reserve University, Dept. of Electrical Engineering and Applied Physics, Cleveland, OH, USA
- 3 UHF-BAND RADIO PROPAGATION CHARACTERISTICS FOR LAND MOBILE SYSTEM USING LOW ANTENNA HEIGHT BASE STATIONS. **M. Kaji, A. Akeyama**, Nippon Telegraph and Telephone Public Corporation, Yokosuka Electrical Communication Laboratory, Kanagawa-ken, Japan
- 4 A MODEL FOR WAVE PROPAGATION IN AN ANISOTROPIC TURBULENT ATMOSPHERE. **R.M. Manning**, Case Western Reserve University, Dept. of Electrical Engineering, and Applied Physics, Cleveland, OH, USA
- 5 THE PRINCIPLE AND TECHNIQUE FOR LARGE OR SMALL DISPLACEMENT MEASUREMENT BY USING THE METHOD OF RANDOM COINCIDENCE IN THE TURBULENT ATMOSPHERE. **G.-L. Tan, G.-H. Feng, X.-D. Huang, J.-R. Lin, Q.-E. Zhao**, Wuhan University, Dept. of Physics, Wuhan, China; **P.-Y. Lu**, South and Central College for National Minorities
- 6 THE ELIMINATION-COMPENSATION-UTILIZATION TECHNIQUE OF THE TURBULENCE EFFECTS OF THE COLLIMATED LASER BEAM IN THE ATMOSPHERIC PROPAGATION - THE DISTRIBUTION AND COMPENSATION OF THE SPOT DANCE. **G.-L. Tan, P.-Y. Lu, G.-H. Feng, J.-R. Lin, Q.-E. Zhao, X.-D. Huang**, Wuhan University, Dept. of Physics, Wuhan, China
- 7 EXPERIMENTAL STUDY OF THE COVARIANCE FUNCTION OF THE FADING SIGNAL ENVELOPE IN THE 800 MHz BAND. **T. Knight, H.M. Hafez**, Carleton University, Dept. of Systems and Computer Engineering, Ottawa, ON
- 8 PROPAGATION MEASUREMENTS FOR LAND MOBILE SATELLITE SYSTEMS. **J.S. Butterworth**, Department of Communications, Communications Research Centre, Ottawa, ON
- 9 PROPAGATION EFFECTS ON LAND MOBILE SATELLITE COMMUNICATIONS. **W.L. Stutzman, W.S. Bradley**, Virginia Polytechnic Institute and State University, Dept. of Electrical Engineering, Blacksburg, VA, USA

Abstracts of paper nos. 3, 7, 8 and 9 appear in this volume while the digests of paper nos. 1, 2, 4, 5 and 6 appear in the AP-S volume

Les résumés des communications numéros 3, 7, 8 et 9 paraissent dans ce volume tandis que les condensés des communications 1, 2, 4, 5 et 6 paraissent dans le volume AP-S

## APS/URSI-F-3

### UHF-BAND RADIO PROPAGATION CHARACTERISTICS FOR LAND MOBILE SYSTEM USING LOW ANTENNA HEIGHT BASE STATIONS

Masatake KAJI and Akira AKEYAMA  
Yokosuka Electrical Communication Laboratory  
Nippon Telegraph and Telephone Public Corporation  
Yokosuka-shi, Kanagawa-ken, 238-03 Japan

An extremely small zone land mobile system (with radio zone radius less than 1 km) is most suitable for realizing low power portable radio communication services. However, many base stations must be constructed very closely, and the base station antenna height must be approximately 10 to 30 m to reduce co-channel interference and to decrease the construction cost. In the land mobile system, the path loss vitally depends on the base station antenna height, and when the base station antenna height is lower than building height the propagation mechanism may differ from that of the propagation mechanism using a high antenna base station.

When the base station antenna height is equal or lower than that of surrounding buildings, some waves diffract at the top of surrounding buildings and the other waves propagate along roads.

In this paper, waves which propagate over the tops of buildings are called "building diffracted waves" (BD waves), and waves which propagate along road paths are called "road guided waves" (RG waves).

BD waves propagate in all directions, while RG waves propagate in a linear fashion like plant roots. The total received power is the summation of received power from both BD waves and RG waves.

Strength of waves depends on factors such as base station antenna height, frequency, propagation distance and building distribution.

For RG waves, diffraction losses are large, but increase of path loss with distance is small.

For RG waves, path loss is very small when the road is straight, but increases abruptly at the corners of roads.

Therefore, RG waves are stronger than BD waves in areas near the transmitting antenna, and BD waves are stronger than RG waves in areas far from transmitting antenna.

The propagation test has been carried out to clarify the above model in high density building areas at 457 MHz, 920 MHz, 1.45 GHz and 2.2 GHz using half wave length dipole antennas.

Variations in path loss with distance is divided into three regions.

The first region is the nearest the base station; in this region, loss increases in distance exponentially by 2 - 3. In the second region, loss increases abruptly by 6 - 7. In the third region, loss increases by 3 - 4.

In the first region, RG waves are potent and road visibility is very good; thus loss increase gradient is small. In the second region, road visibility decreases at corners of roads; RG waves decreases rapidly. In the third region, BD waves becomes stronger than RG waves, so loss increase gradient becomes smaller than that of the second region.

The effectiveness of this propagation model consisting of two types of waves is supported by the data from various measurements.

It has been shown that total received power can be evaluated by superposing two types of received power.

EXPERIMENTAL STUDY OF THE COVARIANCE FUNCTION OF THE FADING  
SIGNAL ENVELOPE IN THE 800 MHZ BAND

by

T. Knight and H. M. Hafez  
Dept. of Systems and Computer Engineering,  
Carleton University,  
Ottawa, Ontario, Canada, K1S 5B6

The covariance function is essential for short term prediction of random signals. In land mobile channels, the envelope of the received signal fluctuates with time over wide dynamic range. For most applications, the envelope fluctuation is slow compared to the bandwidth of the transmitted signal, but fast enough to cause considerable disturbances to the demodulation process. Under these conditions knowledge of the covariance function of the process allows the receiver to track the envelope variation and adaptively correct it.

In this paper, we study the covariance function of the fading process in the 800 Mhz frequency band. The study is based on experiments conducted in various areas within the city of Ottawa, Canada. In these field measurements both the signal envelope and the vehicle speed were recorded simultaneously in areas representing urban, suburban and highway terrains. Details of the signal processing and statistical analysis of the signal envelope are presented.

The paper presents new and important results about the short term correlative behaviour of the received signals in land mobile communications systems. The results may be used in the application of adaptive mobile receivers.

# APS/URSI-F-8

## Propagation Measurements for Land Mobile Satellite Systems

John S. Butterworth

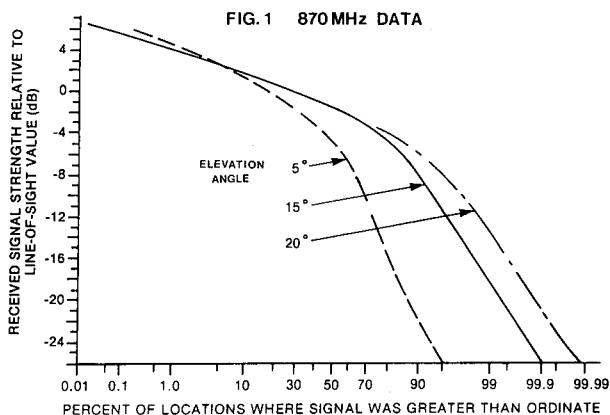
Communications Research Centre/Dept. of Communications

Box 11490, Station H, Ottawa, Canada K2H 8S2

Measurements of excess path-loss and polarization discrimination were made in support of the Dept. of Communications mobile-satellite program (MSAT). A helicopter carrying a transmitter and antenna was used to simulate an 870 MHz satellite signal source. During measurements, the helicopter flew above a road parallel to that followed by the test vehicle and moved along at the same speed, to keep a near-constant bearing and elevation from the test vehicle. The routes chosen for the measurements passed through a rural area which was 35% woodland, the rest being cleared land.

Data collected using an omni-azimuth receiving antenna in areas of open terrain had a multipath-to-constant-component ratio of about -11 dB. Measurements of the combined effects of fading and shadowing over 50 km of rural roads showed that the excess-loss margins above minimum quality of about 14 dB would be required to provide service to 99% of the locations at 20° elevation angle (Fig. 1). Fading and shadowing effects were simulated in the laboratory by using a modified version of previous simulators.

Measurements of polarization discrimination over the full test route showed that the median value of the co-polar/cross-polar ratio of the received signal for 20° elevation angle was about 3 dB. In completely open terrain, this figure rose to about 10 dB.



PROPAGATION EFFECTS ON  
LAND MOBILE SATELLITE COMMUNICATIONS

W. L. Stutzman  
W. S. Bradley  
Virginia Polytechnic Institute and State University  
Electrical Engineering Department  
Satellite Communications Group  
Blacksburg, Virginia 24061

Satellite systems are being planned for two-way communication with mobile vehicles using L-band frequencies. Of special concern in the system design are the characteristics of propagation in suburban and rural areas where fading occurs due to multipath effects and vegetative absorption.

This paper presents the results of a study on land mobile satellite communication propagation. First, available experimental data are examined, compared, and summarized. Next, the modeling of the fading statistics is discussed and model calculations are compared to experimental results. Finally, the impact of the propagation effects on digitally modulated systems is presented.



**AUTHOR INDEX / INDEX DES AUTEURS**



Aarons, J.	438	Belkasim, S.	124
Aas, J.A.	241	Bell, T.F.	501
Aazhang, B.	329	Bennett, F.D.G.	596
Abdu, M.A.	464	Benson, R.F.	504
Aboul-Atta, O.	154	Bentley, J.D.	294
Abouzahra, M.	277	Bernhardt, P.A.	532, 533
Abouzahra, M.D.	192	Bernstein, W.	526
Adey, W.R.	45	Besieris, I.M.	76
Agrawal, P.K.	10	Bevensee, R.M.	34
Ahmed, M.	425	Bhargava, V.K.	298
Aidarous, S.	286	Bibl, K.	455
Aikyo, K.	500, 506	Bilitz, D.	429
Akeyama, A.	618	Bishop, G.	444
Alanen, E.	106, 107	Blake, I.F.	305
Allan, L.E.	24	Blanchard, A.J.	398, 401
Allen, K.C.	392, 393	Boerner, W.-M.	273, 274
Alpers, W.	378	Bolomey, J. Ch.	345
Altintas, A.	216	Booker, H.G.	439
Altschuler, D.R.	581	Bornemann, W.	17
Anderson, D.N.	433	Bosisio, R.G.	37
Anderson, S.J.	590	Bourdillon, A.	475
Anderson, L.P. Jr.	20	Bracewell, R.N.	290
Angell, T.S.	270	Bradley, W.S.	621
Antar, Y.M.M.	24, 402	Braennstroem, B.	601
Antoniu, A.	312	Brand, J.C.	164
Argo, P.	421	Breakall, J.K.	34
Argo, P.E.	470	Brefini, G.P.	317
Arnold, H.W.	353	Brewster, K.A.	361
Arnold, J.M.	133, 225	Bridges, G.	154
Arnoldy, R.L.	529	Bringi, V.N.	360, 403
Arvas, E.	71	Broche, P.	598
Atkin, G.E.	305	Broderick, J.J.	581
Backer, D.C.	48, 49, 565, 567	Brown, M.G.	132
Bagby, J.S.	178	Brown, M.J.	389, 390
Bahar, E.	84	Brown, W.D.	443
Balanis, C.A.	294	Bruton, L.T.	308
Balling, P.	17	Buchan, J.	455
Balmain, K.G.	518, 519	Buchau, J.	451
Banks, P.M.	462	Bultitude, R.J.C.	352
Bannister, P.R.	320	Burke, B.F.	567
Baños, A.	557	Burke, G.J.	110, 160, 195
Bansal, R.	249	Burke, M.J.	287, 466
Barakat, M.A.	266	Burns, J.W.	233
Barcus, J.R.	541, 542	Burnside, W.D.	153
Barnes, F.S.	44	Burrows, G.D.	607
Barnum, J.R.	588	Butler, C.M.	23, 91, 206, 231, 344
Barrick, D.E.	584, 600, 608, 609, 610, 612, 615	Butler, R.S.	367
Barth, M.J.	160, 195	Butterworth, J.S.	620
Basu, Santimay	452, 511	Butzien, P.E.	372
Basu, Sunanda	452, 511	Buyukdura, O.M.	229
Batista, I.S.	464	Byus, C.V.	45
Beatty, D.E.	532	Cafarella, J.H.	292
Beaulieu, N.C.	330	Cahill, L.J. Jr.	529

Calder, A.C.	521	Craven, J.D.	476
Calvert, W.	502, 503, 550	Creamer, D.B.	78, 79
Campbell, R.L.	351, 369	Crissman, R.D.	611, 612
Candy, J.V.	34	Croley, D. Jr.	558
Carlson, C.T.	587	Croskey, C.L.	362
Carlson, H.C.	511	Curtis, S.A.	541, 542
Carlson Jr., H.C.	451	Cwik, T.	169
Carr, J.L.	408	Dabbs, T.M.	472
Carroll, K.	513	Dalmas, J.	136, 137
Casey, J.P.	249	Damaskos, N.J.	140
Castillo, S.P.	156	Damboldt, T.	422
Cavalcante, G.P.S.	109	Das, J.	323
Cha, A.G.	244	Das, S.K.	323
Chan, C.H.	102, 156	Datlowe, D.W.	539, 540
Chandra Mouly, M.C.	18	Davidovitz, M.	89
Chandrasekar, V.	360	Davies, K.	416
Chaney, R.D.	419	Davis, J.G.	139
Chang, D.C.	92, 144, 191, 212	Davis, M.M.	48
Chang, H-W.	276	Dawe, B.J.	613
Chaturvedi, P.K.	484	Dawe, B.R.	397
Chaudhry, A.H.	376, 382	de Hoop, A.T.	101
Chaudhuri, S.K.	150, 188, 273	de la Beaujardiere, O.	473
Chaya, F.	299	de Paula, E.R.	464
Chen, D.T.	381	de Pedro, H.E.	283
Chen, K.C.	108	de Wolf, D.A.	77
Chen, K.M.	250, 251	DeAngelis, X.	318
Chen, K.S.	291	Deleuil, R.	136, 137
Chen, M.F.	342	Demarest, K.R.	122
Cheng, U.	303, 306	Dennis, N.E.	333
Chew, W.C.	219, 220, 221	Dennison, B.K.	581
Chiu, Y.T.	540	DeSanto, J.A.	83
Chommeloux, L.	345	Devasirvatham, D.M.J.	350
Chow, Y.L.	188	Devi, N.R.	18
Christodoulou, C.G.	162, 164	Dianat, S.A.	30
Chu, C-M.	85	Diegal, I.F.	564
Chu, R.-S.	184	Djordjević, A.R.	157, 194
Chu, T.S.	411	Djuth, F.T.	510
Chuang, C.W.	263	Dmitrevsky, S.	574
Chuang, H.R.	251	Doherty, P.H.	444
Clark, G.A.	34	Dominek, A.K.	153
Claverie, J.	368	Dominici, P.	430, 431
Cloud, M.J.	180	Dong, T.L.	181
Codona, J.L.	78, 79	Donnelly, R.	603
Coffey, J.W.	399	Dowden, R.L.	555
Cole, J.S.	404	Dozois, C.	455
Coles, W.A.	80	Drachman, B.C.	180, 218
Coley, W.R.	452	Driessen, P.F.	326
Collin, R.E.	201, 239	Duchêne, A.	43
Condon, J.J.	581	Dudley, D.G.	100, 206, 258
Conkright, R.	421	Duncan, L.M.	483
Cook, C.E.	288	Dusenbery, P.B.	560
Costa, E.	446	Dutta Majumder, D.	323
Coté, O.R.	391	Earl, G.F.	591

Eccles, D.	596	Giordano, A.A.	317
Eccles, P.J.	339	Glisson, A.W.	66, 215
Eftimiu, C.	228	Godard, R.	520
Einzig, P.D.	204	Gogineni, S.	376, 382, 396
El-Damhoughy, H.	319	Goldberg, R.A.	541, 542
Elder, J.A.	42	Goldhirsh, J.	413
Elhakeem, A.	299	Golding, W.M.	564
Elsherbeni, A.Z.	205, 230	Goldstein, R.M.	576
Evans, D.	473	Gong, Zhengquan	66
Evans, M.W.	611, 612	Gossard, E.E.	356
Fan, G.	113	Graglia, R.D.	256
Feindt, F.	378	Green, C.	6
Fejer, J.A.	508	Green, J.L.	358
Fejfar, A.	389, 390	Gross, S.H.	503
Felsen, L.B.	130, 148, 224	Grover, M.K.	488
Fennell, J.F.	558	Gulkis, S.	582
Ferraro, A.J.	513	Guy, A.W.	40
Filice, J.P.	80	Habashy, T.M.	219
Fischer, J.H.	292	Haberman, S.A.	264
Fisher, J.R.	572	Haccoun, D.	296
Fla, T.	480	Hafez, H.M.	286, 619
Flatté, S.M.	78, 79	Hajkowicz, L.A.	469
Fontaine, D.	475	Haldoupis, C.	459
Fontana, T.P.	126	Hale, L.C.	362, 541, 542
Foo, B.-Y.	273	Hall, R.C.	168
Foster, J.	473	Hallidy, W.	142
Fougere, P.	444	Hamid, M.	60, 205, 230, 243, 279
Fougere, P.F.	446	Hand, G.R.	392
Frandsen, A.	5	Hansen, J.P.	379
Frank, L.A.	476	Hanson, D.F.	231
Frank, V.R.	489	Harker, K.	462
Franke, S.J.	447	Haroun, I.A.	189
Frehlich, R.G.	78, 79	Harrington, R.F.	71, 202
Freilich, M.H.	380	Harrison, C.A.	23
Fremouw, E.J.	442	Hartsgrove, G.W.	41
Freyheit, P.J.	388	Hau Lemanczyk, J.	3
Friedman Axler, M.	364	Havey, M.R.	254
Fung, A.K.	337, 341, 342	Hayes, J.F.	299
Furuhama, Y.	412	Heelis, R.A.	452
Gage, K.S.	358	Hellings, R.W.	48
Gagné, R.R.J.	522	Helliwell, R.A.	554
Gaines, D.P.	404	Helms, W.J.	369
Gaines, E.E.	539, 540	Hendry, A.	24, 402
Ganguli, G.	561	Henye, F.S.	78, 79
Gans, W.L.	33	Herd, J.S.	26
Gardioli, F.E.	186	Herman, J.R.	318
Gaynor, J.E.	356	Heron, M.L.	594, 595
Georges, T.M.	587	Herring, R.N.	586
Ghuniem, A.M.	82	Hersom, C.H.	516
Giger, A.J.	372	Hesany, V.	382
Gilbert, J.	425	Hess, D.W.	6
Gilbert, J.L.	248	Heyman, E.	94, 148
Gill, R.S.	586	Hinson, D.P.	577

Hogg, D.C.	363	Kassem, A.S.A.	114
Holm Larsen, F.	2, 3, 8	Kastner, R.	94, 165
Holt, J.	473	Katsufakis, J.P.	501
Holzworth, R.H.	555	Kauffman, J.F.	162, 164
Horita, R.E.	495	Kawashima, N.	527
Howes, G.M.	596	Kaye, M.	166
Hsiao, J.K.	27	Keller, W.C.	378, 383
Hubertz, J.M.	600	Kellerman, K.I.K.	567
Huddleston, P.L.	67, 228	Kelley, M.C.	538
Hudson, J.A.	571	Kelly, J.D.	472
Hunsucker, R.D.	469	Kent, B.M.	125
Hurd, R.A.	227	Keskinen, M.J.	484
Hurst, M.P.	196	Kildal, P.-S.	573
Huth, G.K.	303, 306	Kim, H.T.	155
Ibrahim, H.M.	267	King, R.J.	34
Ihara, T.	412	Kingsley, S.P.	586
Imhof, W.L.	539, 540	Kintner, P.M.	546
Inan, U.S.	501, 536	Klapisz, C.	368
Ireland, R.L.	532	Klein, M.J.	580
Ishimaru, A.	81, 275, 276	Kleinman, R.E.	270
Itoh, T.	179	Klobuchar, J.A.	444, 451
Izumi, Y.	391	Knight, T.	619
Jackson, J.E.	492	Knowles, S.H.	321, 322
Jacobson, M.D.	363	Kobayashi, H.	412
James, H.G.	501, 516, 528	Koberstein, D.R.	32
Jamnejad, V.	340	Koehler, J.	454, 456
Jeans, P.K.	603	Koehler, J.A.	453
Jensen, F.	4	Konradi, A.	526
Jin, H.	373	Kopka, H.	511
Jodogne, J.C.	425	Korth, A.	558
Johnk, R.	191	Koryu Ishii, T.	254
Johnston, A.	176	Kostinski, A.B.	274
Johnston, K.J.	50	Kotulski, J.D.	118
Johnston, K.J.J.	567	Kou, F.Y.	175
Joiner, R.G.	362	Kouyoumjian, R.G.	95, 96, 229
Jones, J.R.	6	Kraszewski, A.	41
Jordan, F.	567	Kuester, E.F.	92, 212, 213
Jost, R.J.	125	Kuga, Y.	275
Jouvie, F.	103, 364	Kuiper, T.B.H.	566
Jørgensen, R.	17	Kumar, A.	240
Jull, E.V.	151	Kuo, S.C.	487
Jurgens, R.F.	576	Kuo, S.P.	485, 487
Jurgens, T.G.	149	Kuriki, K.	527
Kahn, W.K.	172	Kuster, E.J.	69
Kahwa, T.J.	293	Kwan, B.W.	95, 96
Kaji, M.	618	Labelle, J.	546
Kalhor, H.A.	61, 366	Laframboise, J.G.	520, 521
Kaliouby, L.	37	LaHaie, I.J.	145
Kamm, D.H.	180	Lamb, B.M.	488
Kanda, M.	22	Lammers, U.H.W.	371
Kantor, I.J.	464	Lampariello, P.	57
Karam, M.A.	337	Lan, G.-L.	93
Kassam, S.A.	332	Lane, R.A.	404

Lang, R.H.	82, 271	Maa, H-F.	85
Langenberg, K.J.	131	MacDougall, J.	467
Lawner, R.	376	MacPhie, R.H.	136, 137
Lawrence, D.J.	597	Madsen, N.K.	167
Laxpati, S.R.	379	Maggs, J.E.	482, 557
Le Blanc, M.	517	Mallahzadeh, A.R.	61
Le Vine, D.M.	537	Manabe, T.	412
LeBlond, P.H.	599	Manara, G.	259
Ledley, B.	558	Manasse, R.	488
Lee, C.Q.	272	Mannersalo, K.	106
Lee, D.	134	Manshadi, F.	177
Lee, K.-M.	184	Maresca, J.W. Jr.	587, 608
Lee, M.C.	451, 485, 487	Marhefka, R.J.	119
Lee, S.W.	16	Marr, R.A.	371
Lee, Y.C.	561	Martin, L.C.	34
Leeper, W.	120, 121	Martinson, T.M.	92
Leonard, R.E.	409	Masson, C.R.	565
Leroux, G.	388	Matis, K.R.	328
Lesselier, D.	103	Mattison, E.M.	52
Leung, C.	297, 330	Matuura, N.	500
Levis, C.A.	285, 407, 409	Mautz, J.R.	71
Lewin, L.	192, 277	Mayes, P.E.	190, 253
Lewis, R.L.	13, 14, 15	McGahan, R.V.	338
Lian, H.X.	277	McKibben, M.J.	453
Liang, Y.Q.	250	McNamara, A.G.	458
Liebe, H.J.	392	Medgyesi-Mitschang, L.N.	64, 65, 67, 70
Lier, E.	241	Melson, B.	6
Lin, C.J.	251	Merrill, R.D.	160, 195
Lin, C.S.	452	Michalski, K.A.	23
Lin, J.L.	264	Mikhael, W.B.	310
Lin, K.T.	407, 409	Miller, E.K.	110, 160, 195
Lin, S.H.	410	Miller, K.L.	476
Lin, S.L.	220	Millman, G.H.	417
Lindell, I.V.	106, 107	Milsom, J.D.	586
Linfield, R.P.	566	Mitchell, K.J.	581
Ling, H.	245	Mitra, R.	68, 102, 156, 161, 168, 169, 196
Linscott, I.R.	291	Mobilia, J.	539, 540
Lipa, B.J.	600, 609, 610, 612, 615	Modestino, J.W.	328
Liu, C.H.	447	Moffatt, D.L.	155
Liu, K.	420	Moffet, A.T.	49, 51, 565, 567
Liu, R.	420	Monser, G.	260
Livingston, D.C.	388	Montgomery, J.P.	69
Lo, Y.T.	89	Moorcroft, D.R.	457
Loane, J.	16	Moore, R.K.	376, 382, 396, 400
Lovell, J.	221	Moorehead, M.D.	607
Luckert, D.	401	Morales, G.J.	482, 557
Ludwig, A.C.	2	Moran, J.M.	49, 565
Luhmann Jr., N.C.	570	Morgan, M.G.	468
Lundborg, B.	512	Morin, G.A.	518, 519
Lüneburg, E.	227	Morris, J.M.	333
Lusardi, P.	317	Morris, M.E.	58
Lyle, D.B.	45	Morrissey, J.F.	391
Lyons, L.R.	560	Moser, P.J.	112, 362

Mosig, J.R. . . . .	185, 186	Paul, A.K. . . . .	424
Muldrew, D.B. . . . .	494, 503, 514	Pavlasek, T.J.F. . . . .	238
Murray, R.R. . . . .	353	Payne, G.L. . . . .	483
Murthy, P.K. . . . .	166	Payne, H.E. . . . .	581
Musiani, B. . . . .	413	Pearson, L.W. . . . .	31, 123, 215, 252
Nachman, M. . . . .	517	Pelosi, G. . . . .	259
Nagl, A. . . . .	112	Peng, S.T. . . . .	181, 214
Naishadham, R. . . . .	123	Penno, R.P. . . . .	207
Nakamura, Y. . . . .	464	Perry, J. . . . .	421
Napier, P. . . . .	568	Peters, L. Jr. . . . .	153
Nasalski, W. . . . .	217	Peterson, A.M. . . . .	291
Nash, J.C. . . . .	167	Pichot, Ch. . . . .	345
Nastrom, G.D. . . . .	358	Pielou, J.M. . . . .	586
Natali, F.D. . . . .	302	Pinho, J.T. . . . .	109
Neelakantan, V. . . . .	313	Plambeck, R. . . . .	565
Neilson, G.B. . . . .	265, 266	Plant, W.J. . . . .	383
Nesenbergs, M. . . . .	282	Pogorzelski, R.J. . . . .	72
Neuburger, A. . . . .	388	Pokuls, R. . . . .	238
Nevels, R.D. . . . .	56	Polydoros, A. . . . .	304
Newell, A.C. . . . .	15	Pongratz, M.B. . . . .	523, 531, 532
Newman, A.L. . . . .	486	Ponsford, A.M. . . . .	607
Newman, E.H. . . . .	95, 96, 208	Poor, H. V. . . . .	329
Nicholson, D.R. . . . .	483	Powers, W.J. . . . .	439
Nielsen, E. . . . .	459	Pozar, D.M. . . . .	97
Nielson, D. . . . .	284	Predmore, C.R. . . . .	565
Nishizaki, R. . . . .	506	Preston, R.A. . . . .	567
Niver, E. . . . .	59	Prevost, S. . . . .	517
Nyquist, D.P. . . . .	180, 218	Prikryl, P. . . . .	454, 456
Nystrom, G.U. . . . .	52	Puc, A.B. . . . .	124
Obayashi, T. . . . .	527	Pursley, M.V. . . . .	410
O'Connor, S. . . . .	88	Putnam, J.M. . . . .	64, 67, 70
O'Dell, S.L. . . . .	581	Quazi, F.S. . . . .	213
Odom, D.B. . . . .	419	Ragheb, H.A. . . . .	243, 279
Oliner, A.A. . . . .	57	Rahmat-Samii, Y. . . . .	236
Oliver, W.L. . . . .	474	Rajaiah, K. . . . .	73
Olivero, J.J. . . . .	362	Ramsey, R.C. . . . .	532
Olson, J.V. . . . .	559	Randa, J. . . . .	22
Ondoh, T. . . . .	496, 497, 506	Rao, K.V.N. . . . .	399
Onstott, R.G. . . . .	396	Rao, S.M. . . . .	30, 163
Osborne, F.J.F. . . . .	493	Rasmussen, C.E. . . . .	462, 473
Ossakow, S.L. . . . .	484	Rasmussen, R.M. . . . .	403
Overfelt, P.L. . . . .	55	Rawer, K. . . . .	429
Paknys, J.R.J. . . . .	111	Rawle, W.D. . . . .	35
Palmadesso, P. . . . .	561	Ray, S.L. . . . .	167
Pan, G.W. . . . .	341	Raz, S. . . . .	204
Pankonin, V. . . . .	579	Readhead, A.C.S. . . . .	565, 567
Pantic, Z. . . . .	68	Rebollar, J.M. . . . .	242
Parent, J. . . . .	465	Reeves, M.M. . . . .	519
Pasricha, P.K. . . . .	439	Reid, M.J. . . . .	567
Patel, D.C. . . . .	261	Reinisch, B. . . . .	421
Pathak, P.H. . . . .	216, 259	Reinisch, B.W. . . . .	425, 455
Paul, A. . . . .	421	Rengarajan, S. . . . .	88

Resch, G.M.	566	Seshadri, S.R.	174
Rex, K.H.	417	Seshadri, T.K.	73
Rhee, S.B.	349	Seyed-Madani, M.S.	44
Riazi, A.M.	366	Shafai, L.	189, 265, 266
Richards, W.F.	90, 91	Shapira, M.	204
Riley, D.J.	54, 143	Shearman, E.D.R.	585
Riley, J.P.	587	Sheerin, J.P.	483
Rino, C.L.	441	Sheikh, A.U.H.	319
Riordon, S.	286	Shekhar De, S.	323
Ritt, R.K.	152	Sherman, G.C.	248
Roach, G.F.	270	Sherman, S.M.	336
Robinson, R.M.	434, 476	Shirai, H.	224
Roble, R.G.	432	Shoucri, M.	482, 557
Rogers, A.E.E.	49, 565	Showen, R.L.	489
Rogers, D.A.	109	Siefring, C.	546
Rojas, R.	259	Siefring, C.L.	538
Rojas, R.G.	138	Simpson, G.R.	125
Rommey, J.D.	567	Singh, R.N.	556
Rosenberg, T.J.	545, 547	Sinha, B.K.	73
Rotheram, S.	586	Sinha, B.P.	313
Rousell-Dupre, R.A.	532	Slater, K.	596
Ruohoniemi, J.M.	457	Sletten, C.J.	237
Rush, C.M.	421	Smith, C.E.	23, 31
Russell, R.F.	404	Smith, G.S.	36
Rutledge, D.B.	570	Smith, H.	59
Saad, S.M.S.	172	Smith, M.P.	290
Sabban, A.	94	Smith, P.C.	597
Sailors, D.B.	316, 418	Sobral, J.H.A.	464
Saleh, H.A.	271	Sockell, M.E.	76
Samaan, S.B.	31	Sofko, G.	454, 456, 459
Sandler, S.S.	255	Sofko, G.J.	453
Saoudy, S.	60	Soicher, H.	445
Sarkar, T.K.	30, 104, 127, 157, 163, 194	Sojka, J.J.	428, 450, 473, 477
Sasaki, S.	527	Spaulding, A.D.	331
Schaubert, D.H.	97	Spillane, M.W.	601
Schaug-Pettersen, T.	241	Sprague, R.A.	418
Schecker, J.A.	411	Srivastava, S.K.	613, 614
Schlesak, J.J.	406	St.-Cyr, G.	488
Schrote, M.R.	262	Standish, E.M.	48
Schuler, D.L.	384	Stone, W.R.	197
Schultz, D.M.	187	Stubbe, P.	511
Schunk, R.W.	428, 450, 473, 477	Stuchly, M.A.	41
Schwering, F.K.	214	Stuchly, S.S.	41
Scott, A.M.	370	Stutzman, W.L.	621
Scott, W.R. Jr.	36	Stynes, P.D.	327
Sedra, A.S.	309	Subramaniam, N.	115
Seely, G.A.	209	Suchy, K.	278
Sega, R.M.	25	Sugiura, M.	452
Séguin, G.	300	Sujata, K.	18
Sehra, J.S.	323	Sullivan, P.L.	97
Sen, A.K.	323	Sullivan, W.T. III	322, 580
Sengupta, D.L.	93	Sulzer, M.P.	478, 479
Senior, T.B.A.	226	Sylvain, M.	368

Synnott, S.P.	566	Wallace, R.G.	408
Taflove, A.	149, 150	Walsh, J.	613, 614
Tamir, T.	175	Walt, M.	539, 540
Tanir, O.	299	Walton, E.K.	32
Tanner, D.R.	190	Wang, C.W.	285, 409
Tarter, J.	582	Wang, D.-S.	65
Taylor, J.H.	48	Wang, H.	250
Teague, C.C.	602	Wang, N.	111, 155
Terzuoli, A.J.	125	Ward, B.D.	591
Thidé, B.	509, 512	Warne, L.K.	232
Thiele, G.A.	166	Watanabe, S.	496
Thompson, D.R.	385	Waterman, A.T. Jr.	359
Tiberio, R.	259	Webb, K.J.	161
Tolstoy, A.	547	Webber, R.V.	406
Trehan, S.K.	323	Weber, C.L.	303, 306
Trizna, D.B.	377	Weber, E.	444
Tsang, L.	81	Weber, E.J.	451, 455
Tseng, F.I.	127	Webster, A.R.	370
Tseng, F.-I.	30	Wegrowicz, L.	238
Tsou, J.-J.	362	Weisberg, J.M.	48
Tsunoda, R.T.	434, 472	Weissman, D.E.	380
Tubbs, E.F.	566	Wetlaufer, G.D.	25
Turner, L.E.	311	Wetzel, L.B.	379
Tzeng, Y.-J.	463	Whalen, B.A.	530, 531
Tzuang, C.	179	Wheeler, J.E.	56
Überall, H.	112	Whitman, G.	59
Umashankar, K.	149, 150	Wick, J.A.	390
Uratsuka, S.	412	Wickwar, V.B.	473
Uslenghi, P.L.E.	139, 140, 187, 256	Williams, J.T.	206
Uzunoglu, N.K.	173	Williams, R.G.	600
Valenzuela, G.R.	381	Winacott, E.L.	589
Vampola, A.L.	544	Winningham, J.D.	452
van den Berg, P.M.	101	Wisman, V.	378
van Heteren, J.	606, 607, 608	Wittmann, R.C.	12, 14, 19
Vani, N.V.	18	Wolcott, J.H.	532
VanZandt, T.E.	357, 358	Wolfe, H.K.	364
Venkataraman, J.	157	Wong, H.K.	505, 551
Venn, J.	607	Woo, R.	578
Vesecky, J.F.	290	Wood, P.J.	7
Vessot, R.F.C.	52	Wright, M.	565
Vickrey, J.F.	434, 435	Wu, A.K.	564
Viens, N.P.	419	Wu, D.	144
Viola, M.S.	218	Wu, L.K.	400
Vivekanandan, J.	360, 403	Wu, T.-K.	20
Vogel, W.J.	348	Wu, Y.-K.	394
Volakis, J.L.	226	Wyatt, L.R.	607
Vondrak, R.R.	476	Xu, S.J.	214
Voss, H.D.	539, 540	Xu, X.-B.	344
Vuillet-Laurent, D.	103	Yaghjian, A.D.	19
Wacker, P.F.	9	Yanagisawa, M.	527
Wagen, J.-F.	440	Yau, A.W.	530, 531
Wagner, L.S.	423	Yedlin, M.J.	151
Wait, J.R.	343	Yeh, C.	176

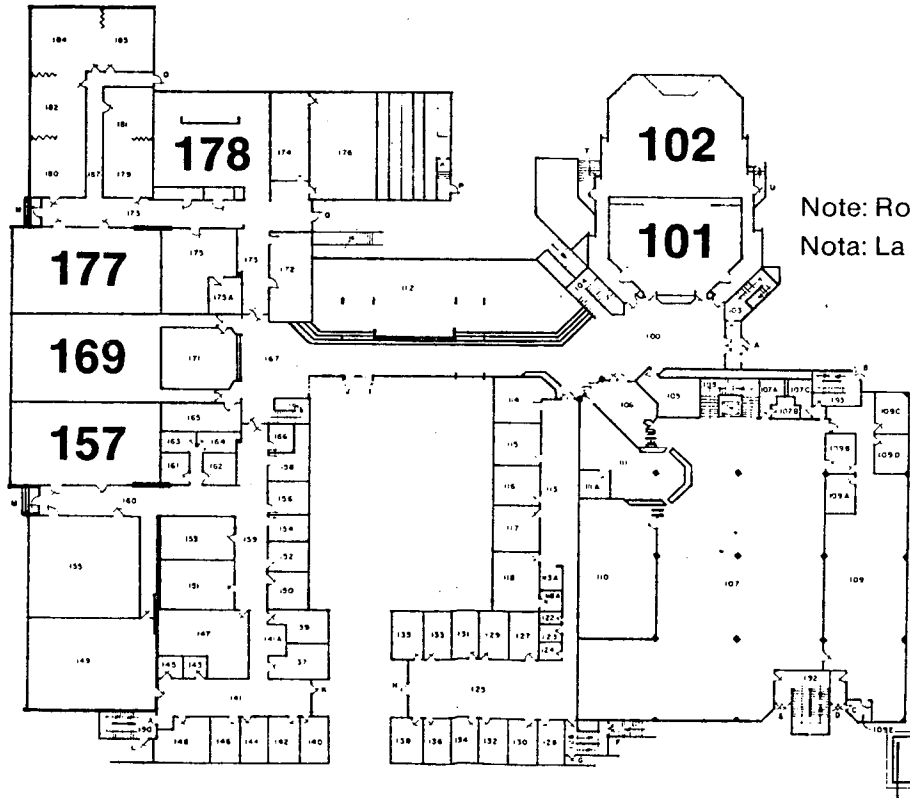
Yeh, C.W. . . . .	177
Yeh, K.C. . . . .	440
Yen, J.L. . . . .	574
Yip, G.L. . . . .	124
Yon, K.M. . . . .	126
Young, J.D. . . . .	119, 120
Yu, C.L. . . . .	141
Zah, C.E. . . . .	570
Zhou, Y. . . . .	420
Ziolkowski, R.W. . . . .	203
Zolesi, B. . . . .	430, 431
Zook, D.F. . . . .	398
Zoughi, R. . . . .	400
Zrnic, D.S. . . . .	361
Zucker, F.J. . . . .	200
Zürcher, J.-F. . . . .	185







# LAW



Note: Room 201 on floor above  
Nota: La salle 201 est au 2e plancher

GROUND FLOOR PLAN

